ATMOSPHERIC CORROSION OF METALS

Dean/Rhea, *editors*

ATMOSPHERIC CORROSION OF METALS

A symposium
sponsored by ASTM
Committee G-1 on
Corrosion of Metals
Denver, Colo., 19–20 May 1980

ASTM SPECIAL TECHNICAL PUBLICATION 767
S. W. Dean, Jr., Air Products and
Chemicals, Inc., and
E. C. Rhea, Reynolds Metals Co.
editors

ASTM Publication Code Number (PCN)
04-767000-27

1916 Race Street, Philadelphia, Pa. 19103

Library of Congress Catalog Card Number: 81-69768

NOTE

The Society is not responsible, as a body,
for the statements and opinions
advanced in this publication.

Printed in Baltimore, Md.
June 1982

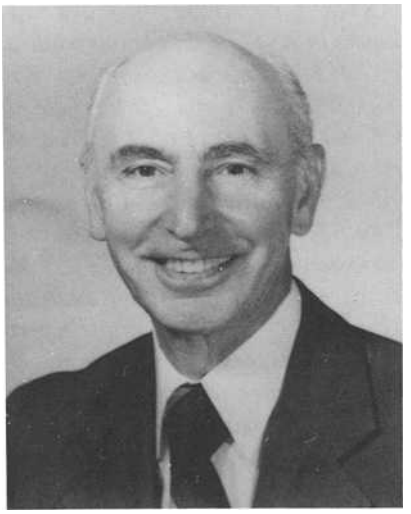

Anthony Gallaccio
13 February 1916 to 21 August 1980

Dedication

This volume is hereby dedicated as a living memorial to our professional friend—Anthony Gallaccio, President, Gallton Company and retired Chief, Materials Application Branch, Frankford Arsenal, Philadelphia, Pennsylvania, who passed away on 21 August 1980 at the age of 64 years.

Tony was born in Philadelphia, Pennsylvania and received his A.B. in Chemistry from Temple University. He began his career in the federal government in 1947 at Frankford Arsenal and retired some 30 years later in 1977. During this period, he became an international authority on corrosion and corrosion control, including such areas as high temperature oxidation, development of protective coatings systems, and environmental and accelerated corrosion testing. He has been granted five patents in the area of metals protection and has numerous publications in the area.

In addition to his managerial and research activities, Tony was active in numerous technical societies including ASTM, ACS, AOA, Electrochemical Society, Franklin Institute, NACE, and Scientific Research Society of Amer-

ica. Within ASTM, Tony has presented and had published a number of papers in ASTM publications while actively participating in G-1. He also was chairman of Subcommittee GO1.07 on Galvanic Corrosion. He has held numerous offices in NACE and was director of NACE Liberty Bell Corrosion Courses for over ten years. He has also chaired the following NACE committees: T9, Corrosion of Military Equipment; T9-B8, Finishes for Magnesium; and T9-A5, Galvanic Corrosion Test Methods. He has also been active in ASM's career development and education ventures. Numerous Government committees and panels saw Tony serve as a corrosion expert.

Tony was a life long resident of the Philadelphia area. He was married to Leonora Marotto on 12 November 1938. He leaves a married daughter, Maria Shire, three sisters, Anna Marotto, Frances Iaricci, and Catherine Pecca and two grandchildren, Nora and John Shire. An extremely energetic person, Tony found time, in addition to his work and technical society activities, to assist young musicians in the Youth Orchestra of Philadelphia, as President and Board Member. His hobbies included greenhouse gardening, ceramics, oil painting, classical music, Western history, as well as the piano.

Anthony Gallaccio, recognized corrosion authority, devoted husband, loving parent and grandparent, public servant, and aesthete will be sorely missed.

Foreword

The symposium on Atmospheric Corrosion of Metals was presented at Denver, Colorado, 19–20 May 1980. The symposium was sponsored by ASTM Committee G-1 on Corrosion of Metals in cooperation with the National Association of Corrosion Engineers. S. W. Dean, Jr., Air Products and Chemicals, Inc., and E. C. Rhea, Reynolds Metals, Co., are editors of this publication.

Related ASTM Publications

Underground Corrosion, STP 741 (1981), 04-741000-27

Electrochemical Corrosion Testing, STP 727 (1981), 04-727000-27

Sampling and Analysis of Toxic Organics in the Atmosphere, STP 721 (1980), 04-721000-19

Geothermal Scaling and Corrosion, STP 717 (1980), 04-717000-27

Corrosion of Reinforcing Steel in Concrete, STP 713 (1980), 04-713000-27

Corrosion and Degradation of Implant Materials, STP 684 (1979), 04-684000-27

Stress Corrosion Cracking—The Slow Strain-Rate Technique, STP 665 (1979), 04-665000-27

Atmospheric Factors Affecting the Corrosion of Engineering Metals, STP 646 (1978), 04-646000-27

A Note of Appreciation to Reviewers

This publication is made possible by the authors and, also, the unheralded efforts of the reviewers. This body of technical experts whose dedication, sacrifice of time and effort, and collective wisdom in reviewing the papers must be acknowledged. The quality level of ASTM publications is a direct function of their respected opinions. On behalf of ASTM we acknowledge with appreciation their contribution.

ASTM Committee on Publications

Editorial Staff

Contents

MODELING, CHARACTERIZATION, AND CORRELATIONS

Introduction

The American Society for Testing and Materials (ASTM) has been one of the most important sources of information on atmospheric corrosion technology in the 20th century. The leadership provided by ASTM has resulted from a need to develop performance data on metallic materials which are used in natural atmospheres. At the outset it was recognized that there was no satisfactory method for predicting the performance of materials in the atmosphere. Therefore it was necessary to run tests in the atmosphere to develop the data required to specify materials and design devices and structures for use in the atmosphere. As products entered the marketplace with systems designed to protect them from atmospheric corrosion, it became necessary to have standards which would accurately describe the performance of the systems. There was also a real need to understand the variables which affect atmospheric corrosion so that designers and engineers could work intelligently with the metallic materials in atmospheric service.

In the decade of the 1960's, Committee G-1 was formed for the purpose of bringing together and coordinating all standards-writing activities pertaining to metallic corrosion. As part of this work, Subcommittee GO1.04 was created to handle atmospheric corrosion. The decades of the 1960's and 1970's witnessed some subtle, but important, changes in the field of atmospheric corrosion. Environmentalists brought strong pressure to bear on society and industry in particular to minimize or eliminate pollution. This, coupled with the dramatic changes in costs of energy from various fossil fuels, has brought about a fundamental change in the types of atmosphere engineers have had to deal with. Industrial atmospheres could no longer be assumed to be heavily polluted with sulfur oxides. Another important change during this period was the development of sophisticated electronic instruments which allowed a wide variety of chemical and other types of measurements to be made. These instruments, together with digital computers, made possible a wide variety of correlations and other types of studies which heretofore were beyond the scope of laboratories involved in atmospheric corrosion work.

Earlier symposia held in 1973[1] and 1976[2] by Committee G-1 had papers

[1] *Corrosion in Natural Environments, ASTM STP 558,* American Society for Testing and Materials, 1974.

[2] *Atmospheric Factors Affecting the Corrosion of Engineering Metals, ASTM STP 646,* S. K. Coburn, Ed., American Society for Testing and Materials, 1978.

concerned with these various questions. Two Special Technical Publications (*STP*'s) have resulted from these symposia and provided a record of the earlier work on these questions. However, because atmospheric corrosion is a process requiring 10 to 20 years to become fully established, there is a real need to fortify these earlier studies with additional results as new data become available. Thus, the purpose of the 1980 symposium on atmospheric corrosion sponsored by Committee G-1 through Subcommittee GO1.04 was as follows:

1. To document how pollution control measures over the years have affected materials of construction and specifically various metallic materials used in the atmosphere.
2. To record information on the corrosion resistance of newer alloys and composites in the atmosphere in comparison with older, more traditional materials.
3. To discuss the mechanism of atmospheric corrosion and specifically the kinetics of atmospheric corrosion as determined by the variations of specific active species in the atmosphere.
4. To develop better systems for classifying the corrosivity of the atmospheres, including the use of electrochemical testing methods to characterize atmospheric corrosion behavior.
5. Finally, to show how laboratory tests can be used to simulate atmospheric corrosion.

The 1980 Atmospheric Corrosion of Metals Symposium met the objectives for which it was organized. A number of papers were presented on the behavior of engineering materials, including two on weathering steels, three on copper alloys, two on aluminum alloys, two on metals with metallic coatings, and one on zinc. In addition, two papers were presented on monitoring of atmospheric exposure sites using time of wetness or electrochemical corrosion monitoring systems. Two papers were also presented on laboratory tests and their correlation with atmospheric corrosion. Finally, there were papers concerned with characterizing atmospheric exposure sites and classifying the corrosivity of such sites, some work on the evaluation of microclimates and corrosion of metals, and the prediction of long-term corrosion rates of structural steels from short-term data.

This collection of papers should be very useful to engineers involved with designing and specifying materials for use in atmospheric applications, both in architectural structural and automotive applications. This publication should also be helpful to materials scientists interested in developing accelerated laboratory tests for predicting the long-term behavior of metallic materials in the atmosphere. The results herein should be useful to those planning new atmospheric corrosion exposures, both from the viewpoint of determin-

ing better monitoring methods for exposure sites and as a record of tests underway and recently completed. In addition, the data provided here should be of interest to those concerned with the economics of corrosion and how some of the newer alloy compositions behave.

In assembling the papers in this *STP* we have tried to provide a link between the past work and the future directions of ASTM in atmospheric corrosion testing, and specifically Committee G-1. There is no question that future symposia will be necessary, and we hope this volume will be an adequate progress report on the state of the art of atmospheric corrosion at the beginning of the decade of the 1980's.

S. W. Dean, Jr.
Air Products and Chemicals, Inc., Allentown, Pa. 18105; editor.

E. C. Rhea
Reynolds Metals Co., Richmond, Va. 23261; editor.

Outdoor Exposure Results

D. Knotková-Čermáková,[1] *J. Vlčková,*[1] *and J. Honzák,*[1]

Atmospheric Corrosion of Weathering Steels

REFERENCE: Knotková-Čermáková, D., Vlčková, J., and Honzák, J., **"Atmospheric Corrosion of Weathering Steels,"** *Atmospheric Corrosion of Metals, ASTM STP 767,* S. W. Dean, Jr., and E. C. Rhea, Eds., American Society for Testing Materials, 1982, pp. 7–44.

ABSTRACT: A general research program to study the corrosion behavior of weathering steels is being completed by the State Research Institute for Materials Protection. Three stages of research are discussed:

1. a description of the corrosion characteristics of these materials,
2. the corrosion behavior of weathering steels in structural service, and
3. the evaluation of the applicability of weathering steels for typical real structures.

The results of this program were used to formulate the corrosion section of the specification: Technical Direction for Application of Weathering Steels.

A comparison of the cost of construction using conventional paint coatings on steel versus the use of weathering steel is provided, including the protection and operation of construction.

KEY WORDS: atmospheric corrosion, weathering steel, corrosion tests on atmospheric sites, atmospheric pollution, outdoor and sheltered exposure, behavior of steel on structural elements, bolt joint, model crevice, patina rust layer, applicability on real objects, masts, industrial constructions, bridges, buildings

The corrosion of structural steels is a very serious technical problem. The volume of the steel constructions exposed to a corrosive environment is very high. The corrosivity of the atmosphere in which most steel structures are used is increasing and the application of the suitable protective systems is very complex and involved from both the raw material and energy points of view. In addition, the maintenance of the surface coatings on existing structures is laborious and expensive.

For these reasons, any system which allows the use of steel structures while minimizing cost during the service life is highly desirable. In addition, it is also desirable to obviate the need for both complex technological equipment for the production of the steel components in the structures and for labor for their maintenance in service. Thus, weathering steels which

[1] G. V. Akimov State Research Institute of Material Protection, Prague, Czechoslovakia (SVÚOM).

have an increased resistance to atmospheric corrosion and have been produced for many years under various commercial names—Cor-Ten, Mayari R, 10CHNDPŠ, Atmofix, etc.—enjoy an outstanding reputation in a wide range of applications.

These steels were manufactured in Czechoslovakia as early as before World War II, but a systematic regulation of their use occurred only in the late 1960's. At this time, extensive research programs were undertaken. The work started at that time had to yield, as quickly as possible, technical results sufficient for the state-aided application of these steels in practice. The research was, therefore, carried out as an extensive team effort which involved the collaboration of a number of the research institutes, for example, the Research Institute of Ferrous Metallurgy, Technically-Economic Research Institute of Metallurgy, the Research Institute of Steel Constructions, and the Welding Research Institute. This extensive research project was aimed at developing information concerning the metallurgy, corrosion resistance, fabrication techniques, and economics of weathering steels. The results of this research were used in the preparation of the very extensive and specific standard: "Czechoslovak Directions for the Application of Weathering Steels," published in December 1978 [*1*].[2]

The extent of the work carried out and the knowledge gained are much wider than reported earlier, and it is impossible to condense it in even one extensive publication. For this reason, only a section of our information on the atmospheric corrosion of weathering steels is discussed herein on the following three topics:

1. Description of the atmospheric corrosion characteristics.
2. Corrosion behavior of weathering steels on structural members in typical atmospheres.
3. Evaluation of the usability of weathering steels for real typical structures.

Atmospheric Corrosion Tests of Weathering Steels

Aim, Extent, and Method of Tests

The results of corrosion tests from the network of atmospheric testing stations forms a basis for establishing the corrosion performance of various materials. Such tests are carried out in a standardized mode and in well-defined conditions, and so the results for a particular material are comparable to results from other sources. However, the application of these results to an actual structure is neither simple nor unambiguous.

In the present study, three types have been used:

1. Tests at atmospheric exposure stations where the atmospheric condi-

[2] The italic numbers in brackets refer to the list of references appended to this paper.

tions are well known and the test technique has been standardized. Specifically, Location 1 involved in outdoor atmospheric exposure with specimens on stands, inclined 45 deg to the horizontal and facing south. Location 2 involved vertical specimens using a standard Stevenson screen.[3]

Most of the tests were carried out in the SVÚOM main atmospheric testing stations where conditions were monitored regularly and the corrosivity of the station atmosphere was measured periodically. The results of these corrosivity measurements are reported in Table 1. These tests were carried out over a 15-year period.

Tests also were performed, to a lesser extent, at single-purpose sites selected so that they could provide more detailed data on the corrosion behavior of selected steels in atmospheres having smaller variations in sulfur dioxide (SO_2) content for 5-year testing periods.

2. Tests at the single-purpose test stations, which are located in rural, urban, and industrial atmospheres in Category 2 exposures, that is, in sheds. Category 3 exposures involving indoor tests were also carried out. The present study required information on the effect of sheltering on the corrosion of these materials because most structural applications have some portions of the steel surface exposed in this mode. However, conventional station tests do not provide this information. These tests were carried out for 5 years on simple Novodur stands with actual construction geometries in exploitation microclimates.

3. Atmospheric exposures were carried out at test stations in specific locations to evaluate unusual and extreme effects. Three- to five-year exposures were made in various production plants to determine the corrosion behavior of these steels in specific industrial atmospheres. Such test results are not usually applicable to other environments.

4. Atmospheric exposures were carried out at test stations to evaluate special arrangements of the specimen, including the effect of orientation of the corroding surface, effect of specimen mass, and the individual corrosion rates of top and bottom sides of the specimens. The duration of these tests was 8–10 years.

Seven test programs of the type described under No. 1 of the foregoing have been initiated. Sixty different types of steels have been included in these tests.

Table 2 gives the compositions of the Atmofix type of Czechoslovakian commercial steels together with the composition of the comparison steel. The compositions of the other steels in these programs will be provided only when specific results are reported.

Only two types of steels were subjected to the tests described in Nos. 2 through 4 of the foregoing. These steels were the low-alloy Atmofix 52A steel

[3] The Stevenson screen is a louvered cabinet which shields specimens from direct exposure to the elements.

TABLE 1—*Characteristics of environment of atmospheric testing stations in which the verification tests of weathering steels were carried out.*

Data	Atmospheric Station			
	Prague Letňany	Ústí nad Labem	Hurbanovo	Kopisty
Geographical position altitude above sea level	275 m	186 m	115 m	240 m
East longitude	14°31′	14°82′	18°12′	17°38′
North latitude	58°08′	50°39′	47°52′	50°33′
Type of atmosphere	metropolitan	heavy polluted industrial, (specific chemical effects)	rural, changed over to urban	heavy polluted industrial, decisive effect of SO_2
Avg annual temperature, °C	8.35	9.8	10.35	9.1
Avg annual relative humidity, %	80.5	78.25	76	73
Duration of temperature intervals in % of total time below −10°C	0.15	0.29	0.19	0.42
−10 to −8°C	11.41	8.16	13.0	13.96
0.1 to +10°C	42.27	44.27	35.42	41.87
+10.1 to +20°C	37.94	34.86	38.75	34.33
+20.1 to +30°C	8.02	11.77	11.83	9.01
+30°C	0.21	0.65	0.81	0.41
Duration of humidity intervals in % of total time below 60% RH	12.25	10.0	17.83	19.84
60 to 80% RH	22.79	32.95	29.83	35.68
80 to 100% RH	64.98	57.05	52.34	44.48
Avg values of adsorption of SO_2, $mg \cdot m^{-2} \cdot d^{-1}$	85.75	132.6	40.95	128.95
Avg quantity of dusty fallout, $g \cdot m^{-2} \cdot d^{-1}$	0.28	0.63	0.32	0.85
Avg annual quantity of precipitations, mm	444	376	505	330

and the comparison steel, a standard structural carbon steel. The corrosion tests described under Nos. 2 and 3 were carried out in 55 different microclimates.

About 6000 specimens total were exposed after preparing their surface by blasting with cut wire. The surface roughness ranged from 6.3 to 12.3 μm. The results of these tests are presented as generalized results for typical environments rather than specific results for individual exposures. The extensive nature of this series of exposure programs makes possible this generalized approach, which, in turn, is more easily utilized.

TABLE 2—*Chemical composition of the Atmofix steels and comparison steel.*

Steel	Chemical Composition, %										
	C	Mn	Si	P	S	Cr	Ni	Cu	Nb	V	Al
15217—Atmofix 52A	max	0.30	0.25	0.07	max	0.50	0.30	0.30	. . .	. . .	min
	0.12	0.80	0.70	0.15	0.040	1.20	0.60	0.55	. . .	. . .	0.01
15127—Atmofix 52B	0.10	0.90	0.20	max	max	0.40	0.30	0.30	0.02	0.02	min
	0.17	1.20	0.45	0.040	0.040	0.80	0.60	0.55	0.06	0.06	0.01
15117—Atmofix 37	max	0.20	0.10	max	max	0.30	0.20	0.30	. . .	. . .	. . .
	0.12	0.55	0.35	0.045	0.040	0.60	0.40	0.50	. . .	. . .	. . .
15327—Atmofix 60	max	1.10	0.20	max	max	0.60	0.30	0.30	0.03	. . .	min
	0.16	1.50	0.40	0.050	0.040	1.00	0.50	0.50	0.08	. . .	0.01
11304—Comparison steel	max	0.40	. . .	0.025	0.025	. . .	. . .	. . .	. . .	. . .	. . .
	0.07	. . .	. . .	. . .	. . .	. . .	. . .	. . .	. . .	. . .	. . .

Corrosion Behavior in Various Outdoor Atmospheres

The natural atmospheres for which the corrosion performance of exterior architectural materials is normally specified include rural, urban, industrial, etc. In this study, we have departed a little from the limits of pollution specified in ST SEV 991-78, "Corrosion of Metals: Classification of Corrosivity of Atmospheres," for the various atmospheres. The atmospheres studied in this paper have been limited to ones with SO_2 contents nearer to the range of Czechoslovakian conditions, and the steels evaluated limited to alloys similar in composition to weathering steels. As a result, this study has been concerned mainly with the effects of pollution by SO_2, except for some specific microclimates.

It is well known qualitatively that many low-alloy steels form a sufficiently protective rust layer in exterior service as long as the pollution level is not too great. The contribution of this study is to provide detailed results on the corrosion behavior of weathering steels as a function of pollution level. Test results are provided for all materials with at least 5 years of exposure. The results on Atmofix 5A steel and steels of a similar composition were used in the generalized behavior plots. The bulk of the data were, of course, obtained from the SVÚOM atmospheric stations, but the results of the tests from single-purpose stations and on complex geometry specimens also were included so that the range of effects caused by SO_2 variations could be observed. After a preliminary evaluation, the results were divided into three groups. The data envelopes for the corrosion loss versus exposure time for the Atmofix and reference steels are presented in Figs. 1–3.

In rural and urban atmospheres with low levels of pollution, that is, SO_2 levels of about 40 mg/m^2/day or less, the conditions are suitable for the formation of a highly protective rust layer on low-alloy steels, resulting eventu-

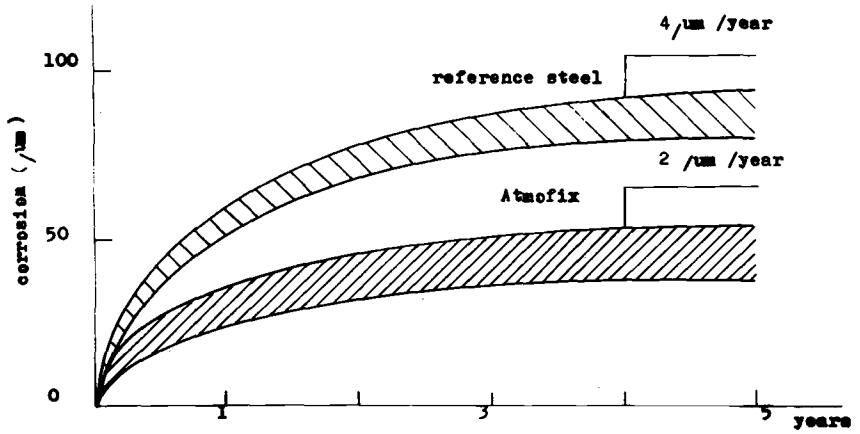

FIG. 1—*Corrosion losses of Atmofix 52A and the reference steels in the outdoor rural atmosphere.*

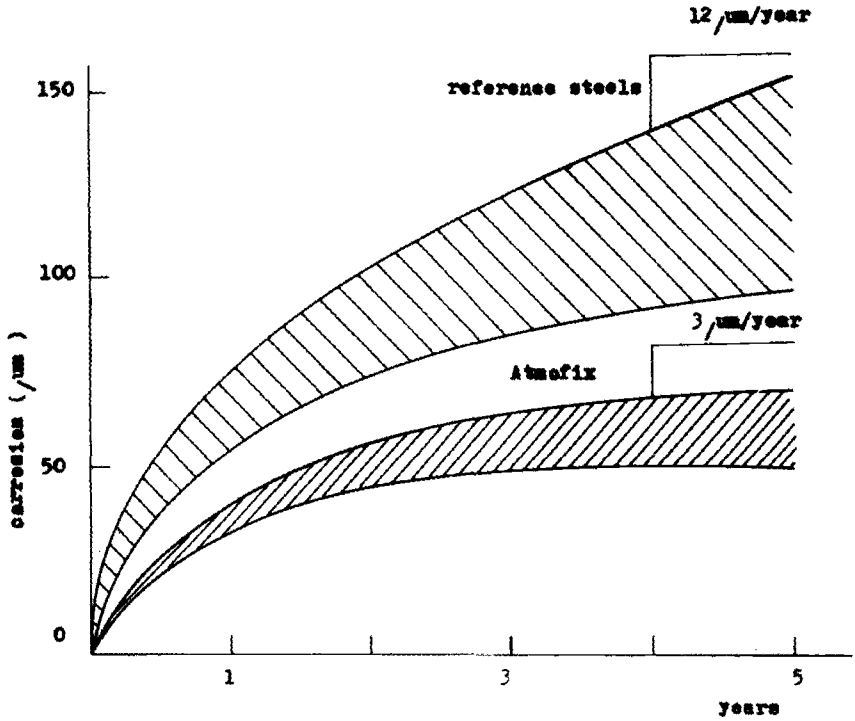

FIG. 2—*Corrosion losses of Atmofix 52A and the reference steels in the outdoor urban and weekly polluted industrial atmospheres (limit of SO_2 pollution is 90 mg/m²/day).*

ally in a relatively stable low rate of corrosion (see Fig. 1). The development of this low stable corrosion rate occurs after about 3 years of exposure and for practical purposes a zero rate may be assumed. The range of metal loss as shown by the envelope curves narrows considerably when this stable condition occurs, even for the reference steels. The reference steels do, however, show a higher corrosion rate initially and end up with a higher rate also. The time required to develop a stable corrosion rate is also longer in the case of reference steels, but the corrosion rate attained is still relatively low. The appearance of the rust layer on weathering steels is characterized by an attractive dark brown to violet color and a compact structure.

In more polluted urban and industrial atmospheres, when the annual average pollution level reaches 90 mg/m²/day, this increased SO_2 level causes a significant increase in the corrosion loss envelope curves, as seen in Fig. 2. The following conclusions may be drawn from this plot.

1. The corrosion loss envelope curves for the Atmofix steels are still narrow although higher than seen in Fig. 1. The rate of metal loss in this case does not become excessive and the alloy content functions to limit corrosion as before. However, the corrosion process initiates more rapidly.

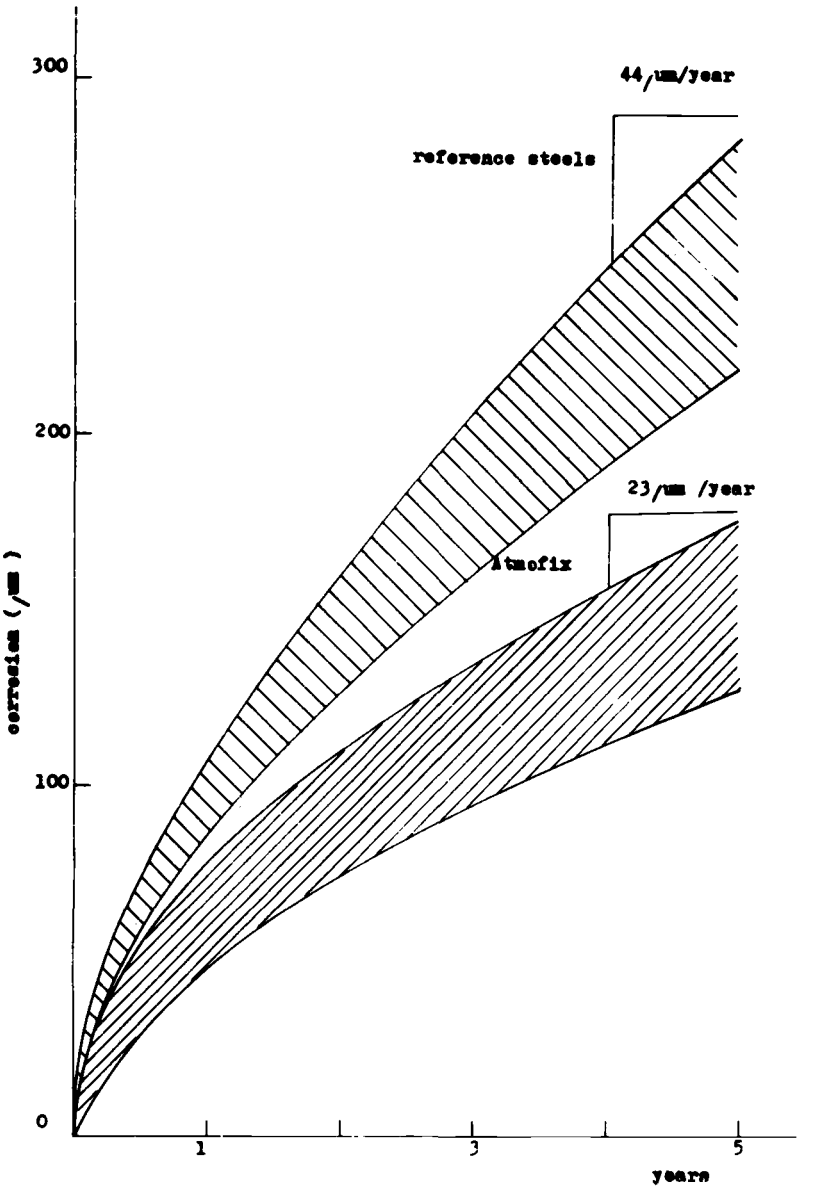

FIG. 3—*Corrosion losses of Atmofix 52A and the reference steels in the outdoor heavily polluted atmospheres.*

2. Very low values of the steady-state corrosion rate are attained so that, in principle, a zero rate can be assumed. This condition is attained a little later, however, usually between 3 and 5 years of exposure. A true zero corrosion rate did not occur in every case, as shown by the slope of the upper envelope curve.

3. The reference steel envelope curves are quite different in character, showing a fan-shaped pattern. These steels are apparently not capable of providing protection against the higher $SO_4^=$ concentrations resulting from the higher SO_2 contents. The greater spread in the data results from the larger variations in corrosivity of the atmospheres during the initial period.

4. The stable corrosion rates of the plain carbon reference steels are significantly higher than those of the weathering steels.

The rust layer formed on the weathering steels in these more polluted environments is again dark brown to violet, but its structure appears coarser than what was observed in rural atmospheres. It is likely that during certain seasons, the higher SO_2 content, coupled with higher humidity, causes local cracking and spalling of the rust layer and this requires that the layer reform in these areas.

For heavily polluted industrial atmospheres where the SO_2 level is high, the results shown in Fig. 3 indicate a higher corrosion rate than is generally seen on weathering steels with a stable rust layer. The zones bonded by the envelope curves for both weathering steels and the reference steels are fan shaped and the stabilized corrosion rates are significant. This indicates that the process of spalling and regrowth of the rust layer is occurring on both types of steel, both regularly and intensively. The appearance of the rust layer supports this contention. The weathering steels' performance is clearly separate and below the reference steels.

The corrosion of weathering steels must be a continuous function of SO_2 content, increasing as the SO_2 increases. For this reason, it is desirable to specify a maximum level of SO_2 in the atmosphere in which weathering steels may be used without protective coatings. A detailed analysis of the data set of long-term test results, supplemented by the results of the 3-year tests in the North Bohemian network of stations with more finely graduated levels of SO_2 content, was very helpful in defining more precisely the critical SO_2 level. The results of this analysis indicate a maximum limit of SO_2 content of 90 $mg/m^2/day$ annual average value. A summary plot showing this analysis is given in Fig. 4. However, it is apparent that this level is somewhat arbitrary because our understanding of the mechanism of rust formation does not suggest that there should be a sudden end to the protective nature of the rust layer at a specific pollution level.

The maximum limit of the SO_2 content represents the point where the process of periodic removal and regrowth of the rust layer becomes significant. As a result, the rust layer ceases to be protective and attractive at this point

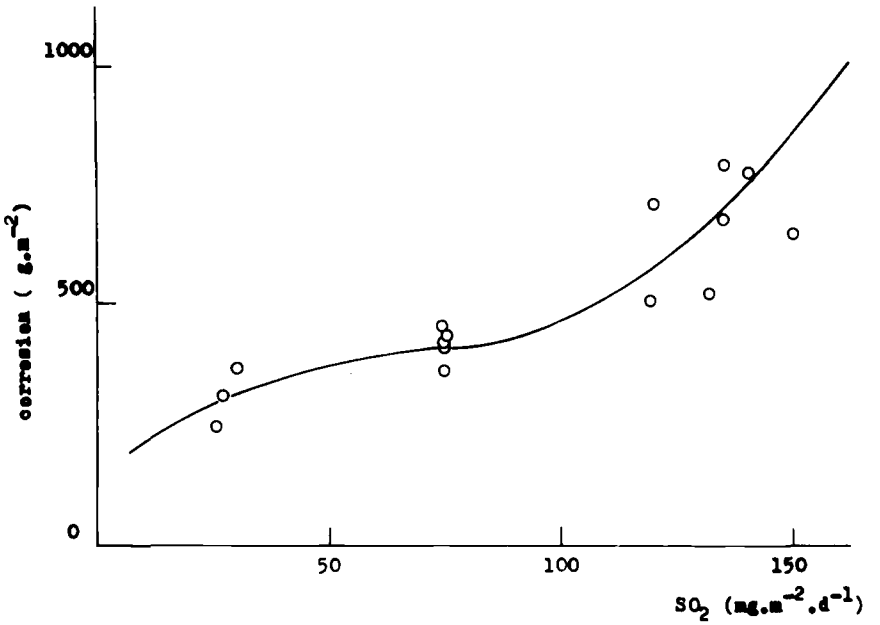

FIG. 4—*Corrosion of Atmofix 52A in the outdoor atmospheres with different levels of SO_2 pollution.*

and the metal loss rate which accompanies the rust formation process becomes important relative to this material's load-bearing function. Therefore, when weathering steels are used without protection in atmospheres exceeding this limit of SO_2 pollution, consideration must be given to the service life of the structure.

Our tests had to verify that the Czechoslovak Atmofix 52A steel is comparable, as far as its corrosion properties are concerned, with conventional steels of foreign manufacture with similar compositions and applications. The results plotted in Fig. 5 confirm the comparability of the corrosion properties, including the capability of forming an aesthetically pleasing rust layer.

Corrosion Behavior in Shed and Indoor Atmospheres

The results for shed and indoor exposures were obtained from 5-year tests on specimens of Atmofix 52A and reference steels, that is, standard structural carbon steels, after exposure in Stevenson screen enclosures in the SVÚOM exposure stations and in the actual microclimates of structures, including the lower deck of bridges, galleries in stadiums, loft spaces, storage houses, etc.

The results are plotted in Figs. 6 and 7 and these results are the basis of a number of important conclusions. Zero corrosion rates were not observed for either type of steel. There were not significant differences between the

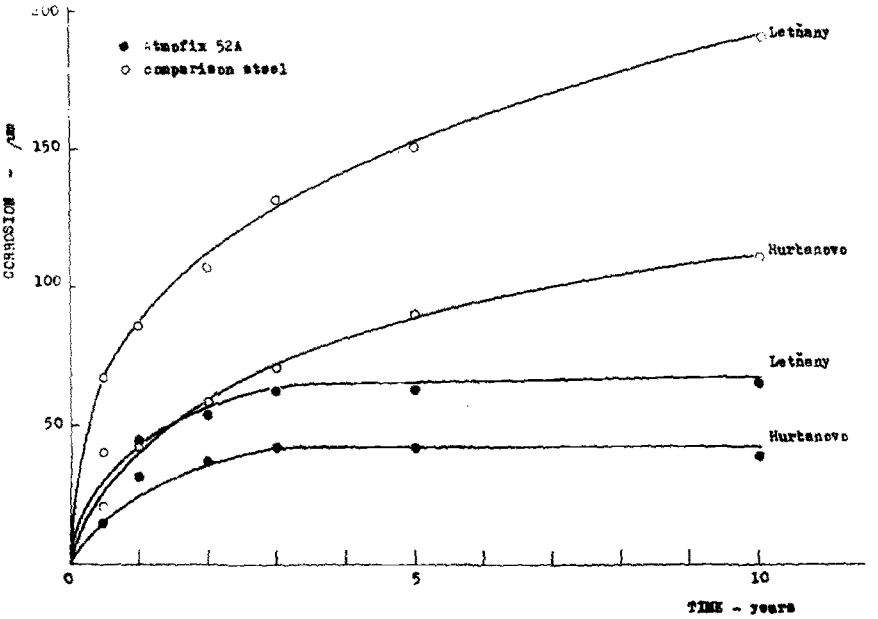

FIG. 5—*Corrosion properties of Atmofix 52A and comparison steel.*

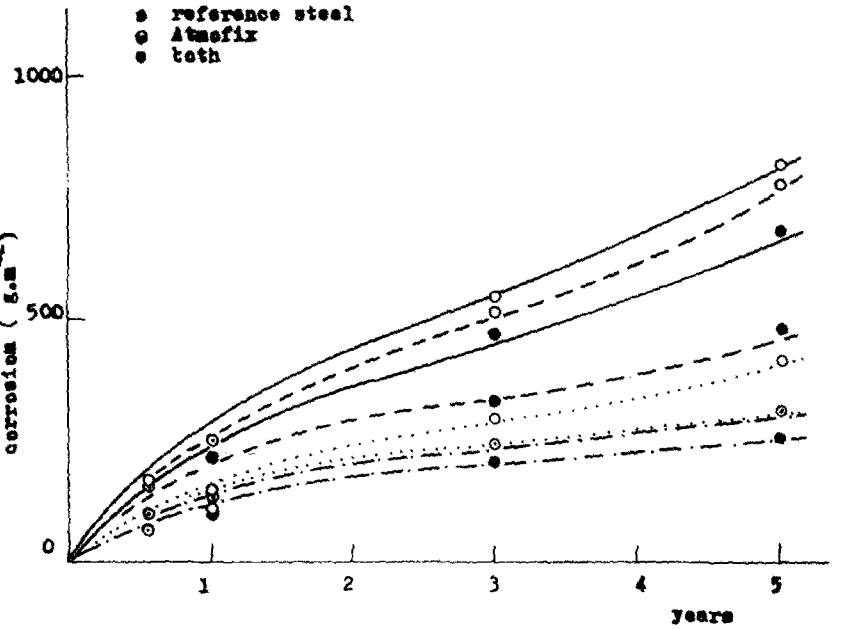

FIG. 6—*Corrosion of Atmofix 52A and the reference steel in ventilated microclimates in Location Category 2 (urban and weekly polluted industrial shed atmosphere). Lines of the same type (dotted, dot-and-dash) represent one exposition site.*

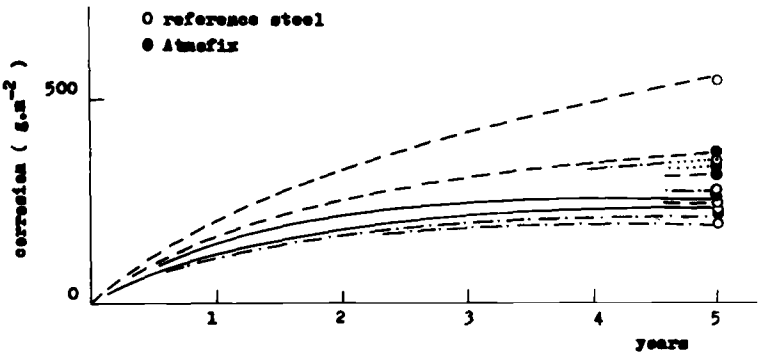

FIG. 7—*Corrosion of Atmofix 52A and the reference steel in indoor microclimates—Location Category 3 (urban type of atmosphere). Lines of the same type (dotted, dot-and-dash) represent one exposition site.*

corrosion performances of these two types of steel. True boundary envelopes of corrosion loss were not found for either atmosphere or steel. Certain different characteristics may be found when comparing the corrosion behavior of both kinds of steels in shed and indoor environments. The most favorable conclusions for the application of the Atmofix steel came from the urban shed exposures. The corrosion losses of the Atmofix steels at the same localities were lower than those of the comparison steels, and the locations with good ventilation proved to be especially favorable; for example, lower decks of bridges and open galleries. Even though the rust layers in these cases never had the typical appearance of exterior exposures, they were more compact and more adherent on the Atmofix steel than on the reference steel. The difference in steady-state corrosion rates is relatively low so that the final corrosion rates cannot be a motivation for using weathering steels instead of plain carbon steels.

TABLE 3—*Steady-state corrosion rates in some types of the shed and microclimates.*

Locality	Indoor Steady-State Corrosion Rate, μm/year	
	Comparison Steel	Atmofix 52A
Bridge, lower ceiling	7.72	5.66
Gallery exposure	9.17	6.27
Open storage exposure	16.93	8.70
Exposure in loft space	5.66	5.98
Exposure in textile finishing room (without chemical effects)	8.28	8.23

NOTES:

1. The results of the nonrecurring stipulations are mentioned.
2. The steady-state corrosion rates are derived by the straight-line regression of results of 5-year corrosion tests.

TABLE 4—*Comparison of corrosion losses in the open atmosphere and under a shed in industrial environments after a 10-year test.*

Station	Mode of Exposure	Corrosion Loss, $g \cdot m^{-2}$	
		Comparison Steel	Atmofix 52A
Letňany	open atmosphere	1488.6	518.0
	shed (Stevenson screen)	1274.3	1191.0
Ústí nad Labem	open atmosphere	3517.3	923.3
	shed (Stevenson screen)	1798.6	1110.3

The results of the indoor exposures in both rural and urban atmospheres show no systematic or consequential differences between the weathering and plain carbon steels. In some cases the weathering steels showed slightly less corrosion while in others the carbon steels were better, but the differences were not important in any case. The low corrosion rates observed in all of these exposures result from the low corrosivity of the environment and not from any alloying addition to the steel. Based on these results, there is no justification for specifying weathering steels for indoor atmospheres.

The steady-state corrosion rates for various microclimates calculated by a linear regression analysis of the results from the 5-year corrosion tests, including 1-year exposure results, are reported in Table 3. The results from shed exposures in highly polluted industrial atmospheres were not included because of the variability of these results. The rust layer which forms on weathering steels in shed exposures does not develop the protective quality which occurs in normal exposure to the weather. The data in Table 4 illustrate this behavior. In fact, the corrosion rates of weathering steels may be higher than that of plain carbon steels under these circumstances.

Corrosion Behavior in Manufacturing and Other Specific Microclimates

The corrosion behavior of these steels cannot be formulated in a generalized relationship which covers all environments. The results of this study must be considered on a case-by-case basis. Stanners [*4*] showed this in his extensive study several years ago and our tests have provided similar results.

We have tested Atmofix 52A steel and the reference steel in the microclimates of chemical plants, agricultural areas, metallurgical and textile production plants, as well as in automotive and streetcar environments. The results of these exposures, as illustrated by Fig. 8 and Table 5, show that weathering steels are generally not suited for such applications and their applicability must be established by experimental results in each specific case. One general conclusion from our studies is that unprotected Atmofix steel is not suitable in atmospheres containing chlorine. In microclimates where the major pollutant is SO_2, even in high concentrations, the Atmofix steel is significantly more resistant than the plain carbon reference steel. Consequently, there is a possible justification for using weathering steels in these applica-

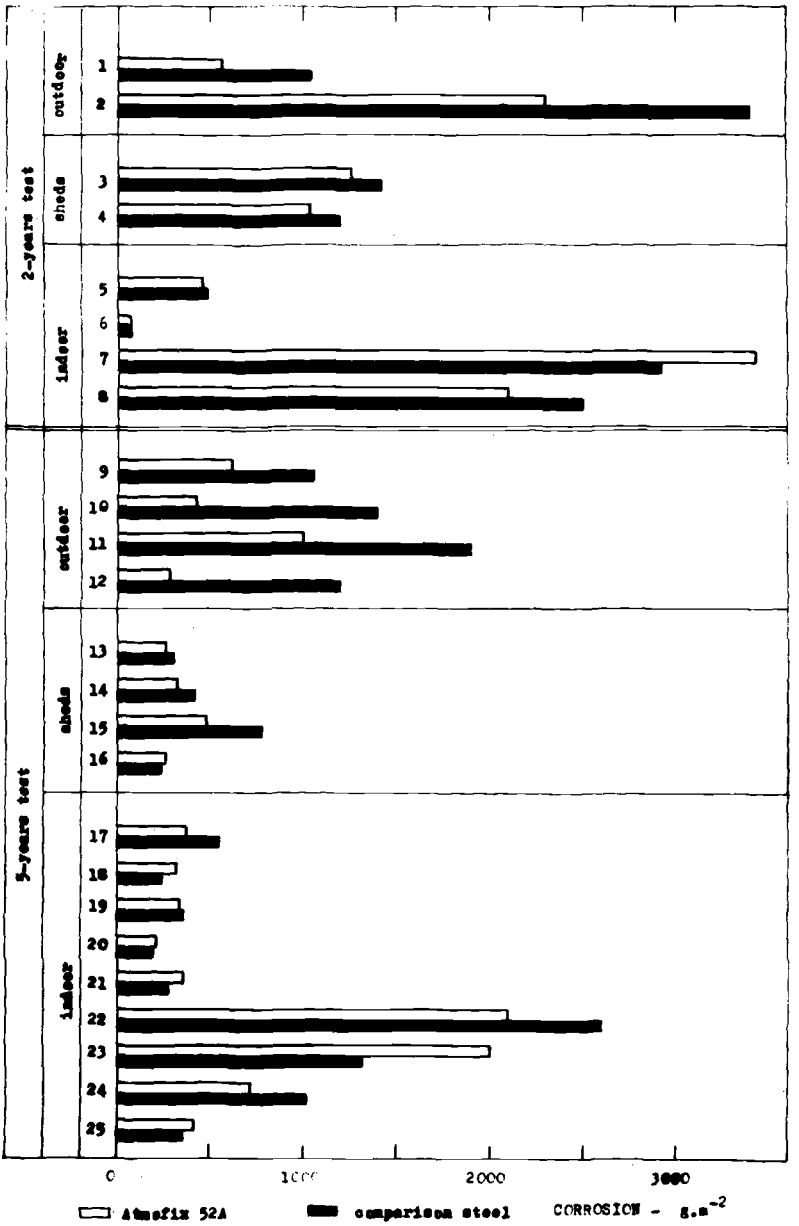

FIG. 8—*Corrosion behaviour of Atmofix 52A and the comparison steel in the productional specific microclimates:* 1—*production of Glauber salt;* 2—*production of* H_2SO_4; 3—*NaCl transporter;* 4—Cl_2 *bottling platform;* 5—*NaCl storehouse;* 6—*compressor room,* NH_3; 7—*electrolysis of NaCl;* 8—*liquefying of* Cl_2; 9—*atmospheric test station Letňany;* 10—*open-cut mining excavator;* 11—*overburden dumping machine;* 12—*separator of combustion products;* 13—*road bridge;* 14—*stadium;* 15—*storehouse of wood;* 16—*winter stadium;* 17—*greenhouse;* 18—*underground coal mine;* 19—*cowhouse—skylight;* 20—*cowhouse—loft;* 21—*little bull house—loft;* 22—*lead-coating workshop;* 23—*synthetic fertilizer storehouse;* 24—*textile dyeworks;* 25—*textile washing works.

TABLE 5—*Steady-state corrosion rate and corrosion losses in selected specific working microclimates.*

Locality	Comparison Steel		Atmofix 52A	
	A	B	A	B
1. Textile dyeworks	0.325	1018.71	0.333	718.31
2. Textile washing works	0.177	359.47	0.176	422.13
3. Lead coating workshop	3.692	2609.01	1.190	2097.13
4. Synthetic fertilizer storehouse	0.641	1323.02	1.111	2001.18
5. Cowhouse—skylight	0.013	356.80	0.175	338.1
6. Pighouse	0.478	623.3	0.421	537.0

NOTES:
A. Steady-state corrosion rate ($g/m^2 \cdot d$) calculated by the straight-line regression of the 5-year test results.
B. Corrosion loss during 5 years of the test (g/m^2).

tions. However, the corrosion behavior should be verified in such cases by a 3-year test in order to define the actual service life of the equipment in question.

In contrast to the approach of other authors [*5–9*], we have attempted to process the results of our tests in a generalized format for typical environments because we have considered such a presentation important for the use of weathering steels as a structural material. Some typical rust layers are shown in Fig. 9. The detailed results of our experiments are included in our comprehensive reports, especially in the final report [*2*]. These reports were partially published earlier [*10–13*].

Effect of Orientation on Corrosion Rate

It is apparent, even from the appearance of the rust layers on the steel specimens, that the amount of rain, sunshine, wind, etc. affects the corrosion process. The effects of panel orientation were studied for both weathering steels and plain carbon steels in the municipal atmospheres of the SVÚOM site at Jenerálka. The details of this study are given in Table 6.

Based on the appearance of the surfaces, the rust found on the specimens facing south, west, and east has an attractive fine texture and dark color and is comparable in all three orientations. The horizontal specimens were different in appearance. The weathering steel had a light-colored, coarse-textured but adherent rust layer while the rust on the plain carbon steel was flaking off locally. The gravimetric measurements shown in Table 6 reveal that the eastward exposure is the most aggressive. Moisture probably dries more slowly on the easterly facing specimens and this increases the time during which active corrosion occurs. The largest difference between weathering steel and carbon steel is seen in the south-facing specimens.

Based on these results, it is apparent that the southerly exposure represents the most favorable orientation for specimens of weathering steels subject to atmospheric corrosion.

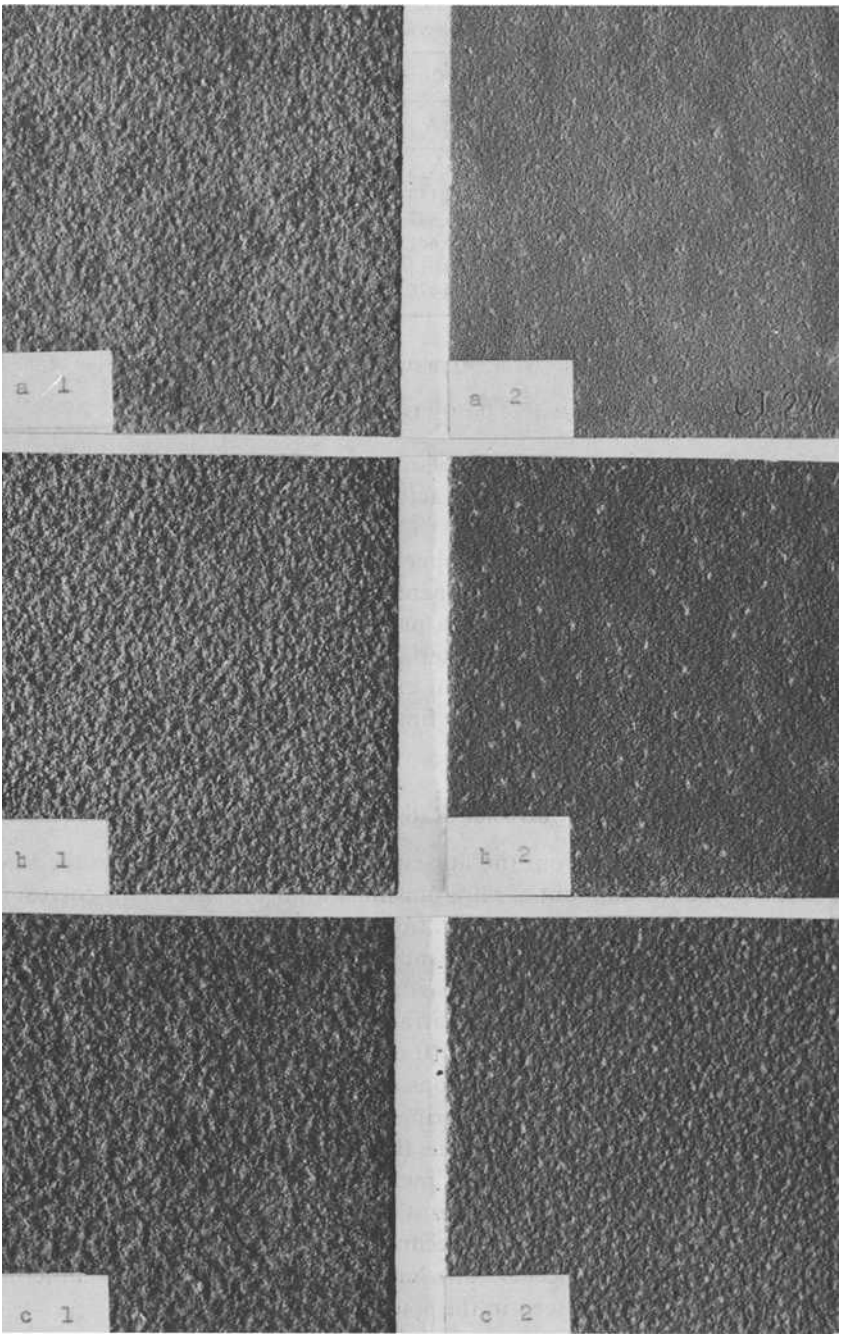
a 1
a 2
b 1
b 2
c 1
c 2

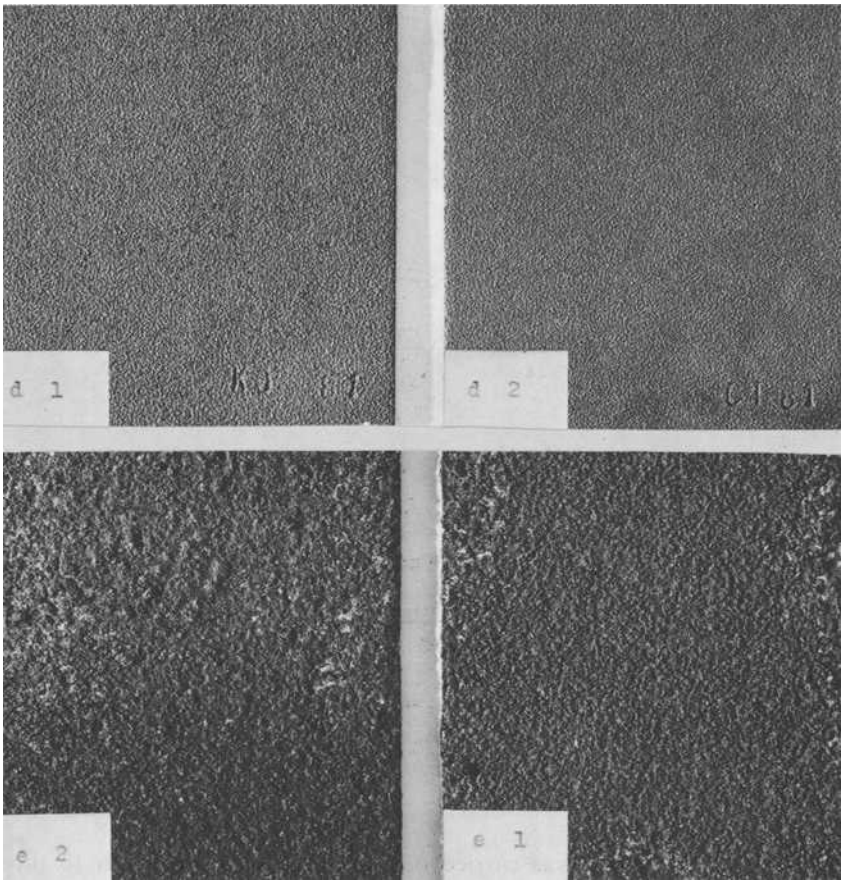

FIG. 9—*Appearance of rust layers after 10 years' exposure:* 1—*comparison steel;* 2—*Atmofix 52A;* a—*rural slightly polluted atmosphere (Hurbanovo) outdoor exposure;* b—*urban to industrial atmosphere (Letňany) outdoor exposure;* c—*heavy polluted atmosphere (Ústí nad Labem) outdoor exposure;* d—*urban to industrial atmosphere (Letňany) sheltered exposure;* e—*heavy polluted atmosphere (Ústí nad Labem) sheltered exposure.*

TABLE 6—*Comparison of corrosion loss* ($g \cdot m^{-2}$) *of weathering steel, 15 217, and plain carbon steel, 11 304, in dependence on the orientation of the corroding surface (3 years' exposure).*

	Steels	
Surface Orientation	15 217	11 304
Horizontal	419.63	649.24
East	572.79	818.30
West	476.48	723.80
South	312.26	677.76

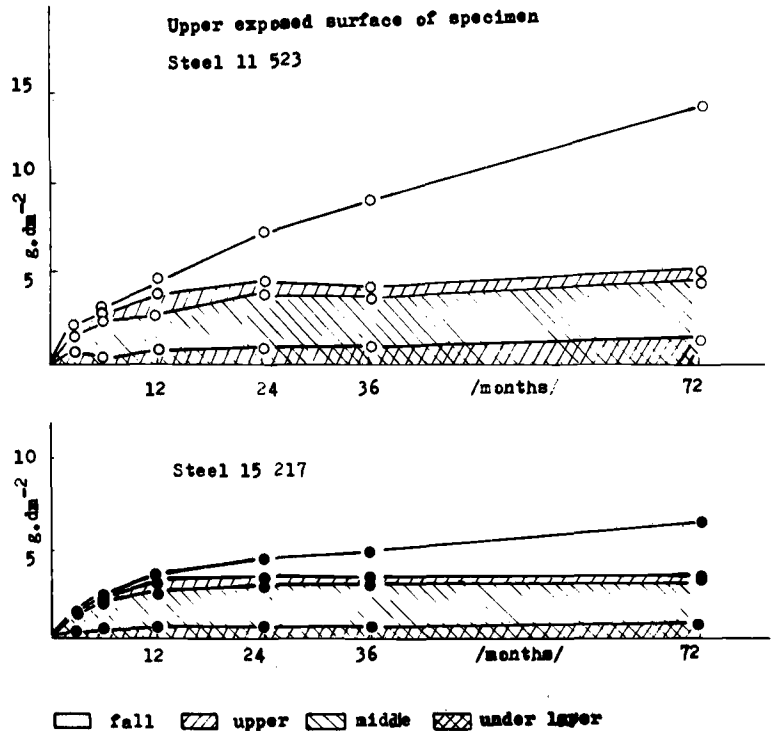

FIG. 10*a*—*Quantity of rust in the individual underlayers of Atmofix steel and comparison steel (upper exposed surface).*

Another experiment was carried out under conditions similar to those used in the orientation experiment. In this case, the corrosion rate was measured separately on the top and bottom sides of the specimens during their exposure in a southerly orientation at an exposure angle of 45 deg to the horizontal. The side of the specimen not exposed to the atmosphere was protected by a coating which was removed at the completion of the exposure, but before the weight loss measurement. The results are presented in Fig. 10. Both the quantity of iron in the individual rust layers and the total mass lost to corrosion are shown for both weathering steel and plain carbon steel. The 7-year results in Fig. 10 show a relative retardation of the corrosion process on the bottom sides of the plain carbon steel specimens. Although the iron lost from the surface is lower in the case of the downward-facing specimens, the total quantity of iron in the rust layer is comparable in the top and bottom layers. There are no fundamental differences in the corrosion reactions for the two surface orientations. Before further evaluation, however, it is not possible to claim that this conclusion applies to all exposures. In cases where large structures are exposed and the conditions of ventilation are different on

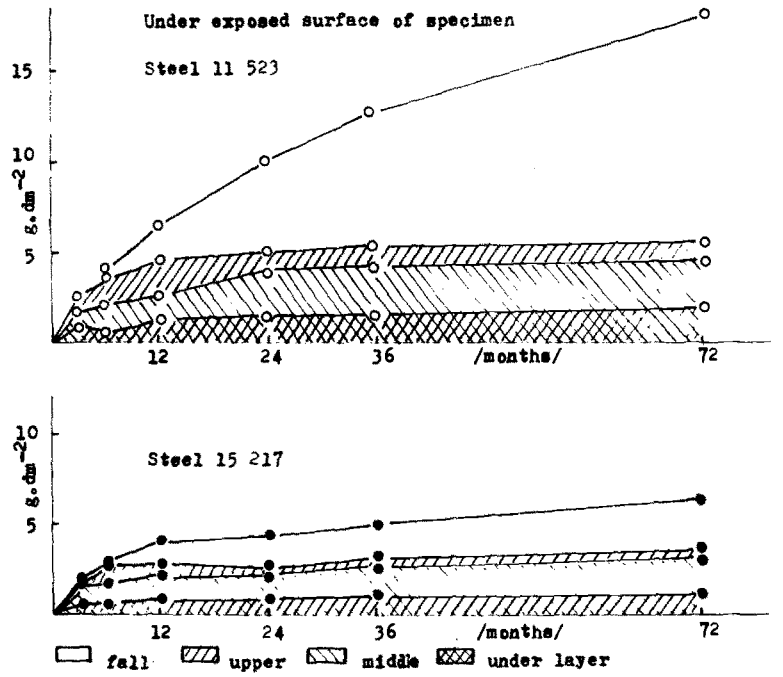

FIG. 10*b*—*Quantity of rust in the individual underlayers of Atmofix steel and comparison steel (under exposure surface).*

the downward-facing surfaces, the corrosion rates will be substantially different from those noted for standard panels in atmospheric exposure sites.

Properties of Rust Layers on Weathering Steels

The corrosion product layer formed on weathering steels during the process of atmospheric corrosion provides protection to the underlying steel without the need to coat the steel. It is necessary, therefore, to define the characteristic properties of this layer and the conditions which enable it to form successfully. This rust layer is not an homogeneous material and its protective properties are related to different structures and chemical components. The studies of the rust properties reported in the following were carried out with the cooperation of the Bergakademie Freiberg of the German Democratic Republic, and the Institute of Inorganic Chemistry AN of the Lithuanian Soviet Socialist Republic of the U.S.S.R. The detailed systematic evaluation of the properties of rust layers is being performed on steels with a range of compositions from various atmospheric exposures.

A portion of the results from these studies has been published [*15*] and the specific results on the Atmofix steels have been reported also [*16*]. The SVÚOM methods used for rust evaluation on weathering steels [*17,18*] are

concerned mainly with the analytical processes of examining the structure of the rust and the distribution of localized sulfate-rich areas, often referred to as "sulfate nests." An example of the structural difference between the reference carbon steel and the Atmofix steel is shown in Figs. 10*a* and 10*b*.

A combination of methods has been used to study the rust layer on weathering steels at various stages in the corrosion process, including metallographic evaluation of a cross section of the rust layer, microprobe analysis of the distribution of alloying elements, X-ray structural analysis, infrared analysis, radiochemical determination of sulfate nest distribution, and other methods described in the following. From these studies we have determined that protective corrosion product layers have the following characteristics:

1. optically visible layers characterized by dark gray stripes,
2. zones enriched by alloying elements, and
3. almost no frequency of sulfate nests (see Fig. 11).

Additional work based on layer macrostructure, visual evaluation, and gravimetric evaluation of the rust underlayers has led to the following conclusions about protective rust layers.

1. The color of the rust is a dark violet shade.
2. The structure appears to be a compact layer without peeling or flaking off of particles.
3. The maximum thickness of the layer is 200 μm.
4. The surface appears to be a composite of fine particles firmly attached to the underlying steel, whereas the carbon steel rust appears to be a layer of coarse particles which can easily be wiped off.

The successive disappearance of sulfate nests on the surfaces of corroding weathering steels is probably important in determining the corrosion rate of the steel. This disappearance of the sulfate nests is caused by the changes in the colloidal properties of the rust resulting from the alloying elements. A detailed discussion of this mechanism will be presented in a later publication.

Atmospheric Corrosion of Weathering Steel Structural Elements and Joints

Goals, Methods and Scope of Tests

The tests in this section represent a transition between standard panel tests and the testing of products and structures. The results of these larger-scale tests provide information on behavior of these steels in more practical situations and provide results which are not obtainable from standard panel tests. Therefore, these results are especially important for the use of weathering steels in real structures.

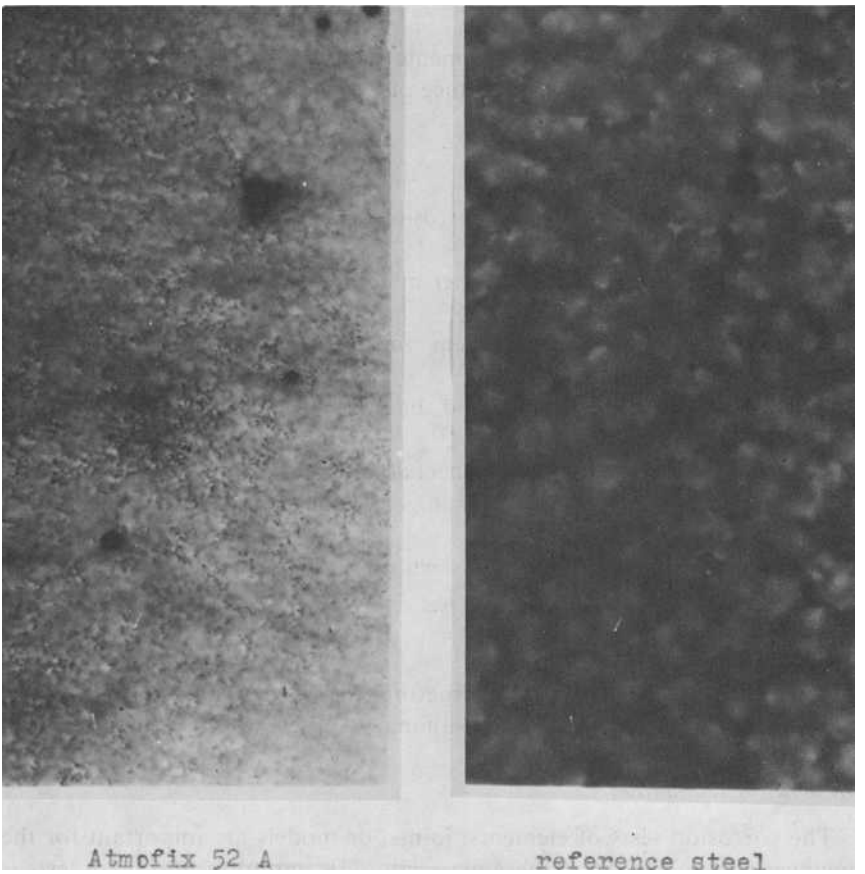

FIG. 11—*Decrease of amount of sulfate nests on Atmofix 52A compared with reference steel (radiochemical method, specimens from outdoor exposure, Hurbanovo, 10 years).*

These tests had to determine the behavior of weathering steels in selected structural configurations and to verify whether the corrosion followed the behavior established in panel tests in similar atmospheric conditions. The following types of tests were carried out.

1. Tests of selected types of structural elements and joints at atmospheric sites.
2. Tests of models of structural joints in accelerated laboratory tests and in exposure tests.
3. Tests of girder models exposed at actual construction sites.

Tests Performed

The tests of selected structural elements and joints were designed to provide basic information on the performance of weathering steels in the following applications:

- bolted joints,
- model crevice and galvanic corrosion,
- welds, and
- combinations of steel with other materials.

A brief description of the specimens and exposure conditions is given in Table 7.

The tests of models have included the following items:

- Tests of models of the facade sheet attachment to supporting structures, including accelerated laboratory testing of various types of construction versions of facade sheet attachments.
- The suspension of the facade sheet on a supporting structure with the test carried out on the entire unit.
- Tests of the steel girder models.

These tests were conducted on structures in service to allow all the microclimatic factors to operate. A brief summary of these tests is given in Table 8.

Methods of Evaluation

The corrosion tests of elements, joints, or models are important for the engineering application of these materials. The importance of these tests is apparent; however, the proper techniques of evaluating the results have not been completely worked out and this work has not been completed as yet. The evaluation based on appearance provides a sufficient, though only qualitative, approach. An evaluation based on mass loss is not possible because of the large size, weight, and complicated shapes of these specimens. Furthermore, techniques involving single-sided pickling of joint specimens result in a doubled number of exposure specimens.

The appearance evaluation was carried out in all tests. The following areas were evaluated for the selected structural elements and joints:

- external free area of surface beside joint,
- internal surfaces of joints limited by small top specimen, and
- both of the afore-mentioned surfaces after pickling.

In addition to the standard verbal description of the surfaces, we have at-

TABLE 7—*Survey of structural elements and joints of 5-year tests.*

Structural Element	Basic Material	Dimensions, mm	Connecting Material	Other Materials	Type of Atmosphere[a] 1	2	3
Bolted joints	weathering steel	150 × 100 × 3	bolts of weathering steel	. . .	X	X	X
			black galvanized steel				
Model crevice (0.5 mm) and contact corrosion	weathering steel plain carbon steel (class No. 11) and their combinations	150 × 100 × 1 80 × 50 × 4	bolts of structural steel insulated in the crevice	. . .	X	X	X
Welds (V-weld)	weathering steel	180 × 110 × 12	E-B204 electrode			X	X
Combination of materials	weathering steel	150 × 100 × 1		-tiles -plasters -coats of paint -aluminum -anodized aluminum -stainless steel			

[a] Atmosphere types:
1—Clean rural atmosphere.
2—Medium polluted urban atmosphere.
3—Heavy polluted industrial atmosphere.

TABLE 8—*Survey of façade sheet model tests.*

Structural Element Model	Basic Material	Connecting Material	Packing Material (Undercoating)	Exposure[a] 1	2	3
Bolted lapped joints	weathering steel -without coat -with coat	bolts of weathering steel	-asphaltic putty -flexible oil cement -two-component polyurethane sealing compound -minimum oil paint -Hydroban -Resistin	X		X
Models of façade sheet suspensions on supporting constructions	weathering steel	bolts of weathering steel	-distance rubber packing plates -undercoat; priming minimum coat of paint -two-component polyurethane sealing compound		X	
Suspension of façade sheet on the object supporting construction	sheet and supporting construction of weathering steel	self-cutting bolts of weathering steel				X

[a] Exposure:
1—Test in condensing chamber with SO_2 (ČSN 038 131 "B").
2—Test in condensing chamber with SO_2—cyclic.
3—Urban atmosphere.

tempted to characterize the surface according to the degree of attack and thereby quantify the evaluation.

The appearance of the pickled surface was also recorded and supplemented by a measurement of the surface roughness of the specimen. This approach is objective and can be used to characterize the extent of corrosion.

We also weighed the quantity of rust in a joint (the rust was conditioned at room temperature). This was carried out separately for the internal and external surfaces on a small specimen. This approach made possible the quantitative evaluation and comparison of the extent of corrosion for various types of joints in various environments.

The measurement of the sulfate content of corrosion products was carried out separately for external and internal surfaces of joints. These measurements were used to compare the corrosion processes on the internal and external surfaces and demonstrated the effects of atmospheric pollution on the corrosion within the joint.

Sulfate nest distribution evaluation was carried out for flat joints, bolted joints, crevice and galvanic specimens, and on the underside of a large specimen. This evaluation included the entire internal surface of the joint limited by the small top specimen and a part of the external free surface. The welded specimen was examined over the surface of the weld metal and the area immediately adjacent to the weld. This mode of evaluation provides a good measure of the rust layer quality and provides information on the corrosion process which occurs both inside a joint and outside.

Metallographic evaluation of the galvanic and crevice corrosion specimens and the welded specimens was also carried out.

Results

Bolted Joints—The results of the bolted joint tests can be summarized as follows:

1. When a bolted joint is sufficiently tightened, the joint internal surface becomes compressed during the course of the exposure and no unfavorable corrosion occurs, although the joint may be deformed by the process. This result was shown specifically in the bolted joints on the girder models where no significant corrosive attack occurred in the joints, even in highly aggressive environments.

2. The appearance and the quantity of rust in a joint is related to the location and time of exposure. The character of the external and internal joint surfaces after pickling shows no significant differences. In fact, the rate of corrosion within the joint is not excessive. Table 9 provides a brief summary of the results of the measurements of rust mass on the internal and external surfaces of the joint.

3. No significant accumulation of sulfate nests was found within the joints resulting from the exposure. Also, the quantity of sulfate in the rust shown in

TABLE 9—*Quantity of rust on the external and internal surfaces of a small specimen of a bolted joint after the 2-year exposure.*

Atmosphere	Quantity of Rust, g	
	External Surface	Internal Surface
Urban	1.00 to 1.40	0.93 to 0.99
Industrial	1.53 to 1.81	0.71 to 0.94

Table 10 provides further evidence for this fact. The most suitable bolting material for bolted joints was low-alloy steel. Chrome-plated high-strength bolts were less suitable, while standard structural steel bolts were least suitable. High-strength steel bolts provided the strongest and most rigid joints. However, weathering steel bolts should be used in cases where joint dissembly may be required.

4. Galvanized bolting is not suitable for joints of weathering steel and it is not recommended for use in heavily polluted atmospheres.

Galvanic and Crevice Corrosion—The following conclusions were based on the tests completed to date.

1. There is no acceleration of the corrosion of weathering steels from contact with standard structural steels. There is an increase in the corrosion of standard structural steels in relatively short exposure times from contact with weathering steels. This effect was seen in the metallographic examinations and should be verified by longer exposures.
2. No increase in the formation of sulfate nests was found in the rust in the crevices of weathering steel in contact with structural steel (see Fig. 12).
3. There was an increase in the formation of sulfate nests in the crevices as well as around them for standard structural steels in contact with weathering steels in heavily polluted industrial atmospheres (see Fig. 13).

Crevice corrosion is both very important and very complex in many applications. The results of these tests have shown that special attention must be given to crevices in the design and maintenance of real structures. The most

TABLE 10—*Content of sulfates in corrosion products from the external and internal surfaces of a small specimen bolted joint after the 2-year exposure.*

Atmosphere	Content of SO_4^{2-}, %	
	External Surface	Internal Surface
Urban	2.15 to 2.35	1.13 to 1.32
Industrial	1.12 to 1.96	1.14 to 1.40

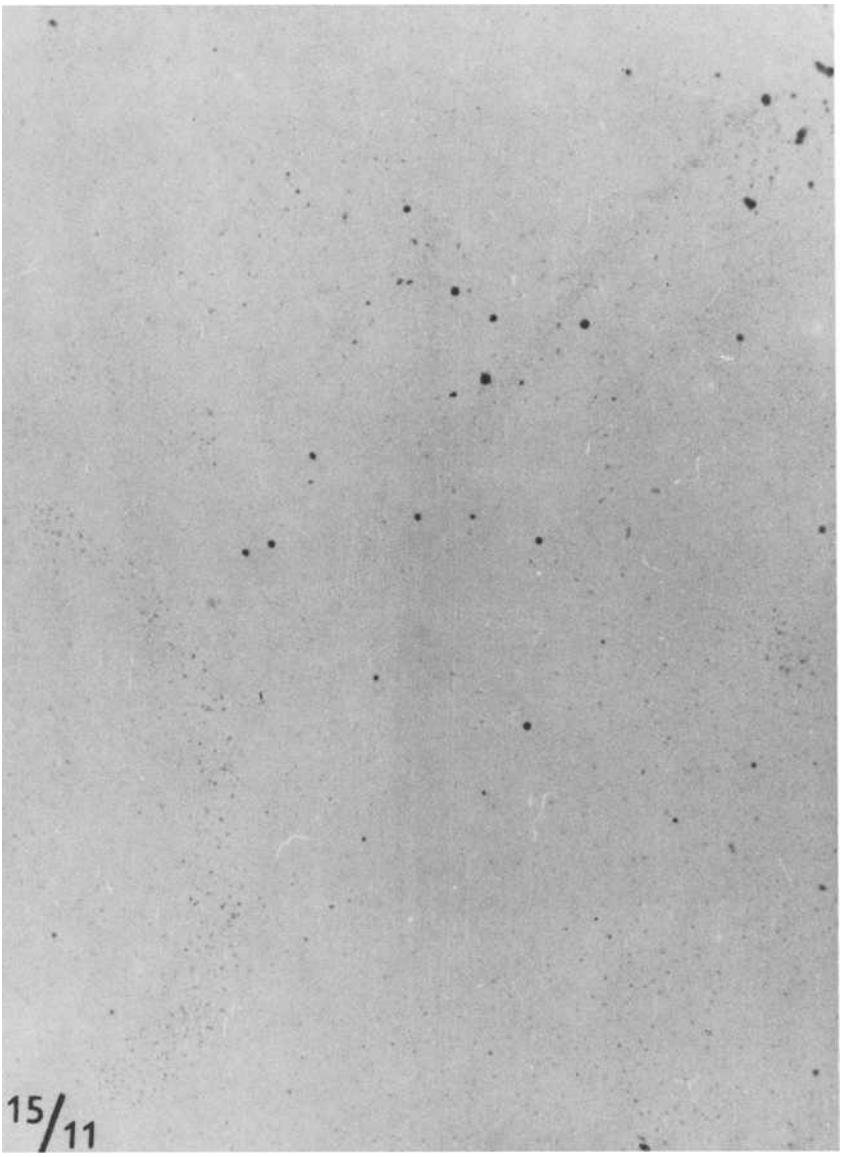

FIG. 12—*Distribution of sulfate nests in rust layer on Atmofix 52A in contact with structural steel after 3-year test in rural atmosphere (Hurbanovo).*

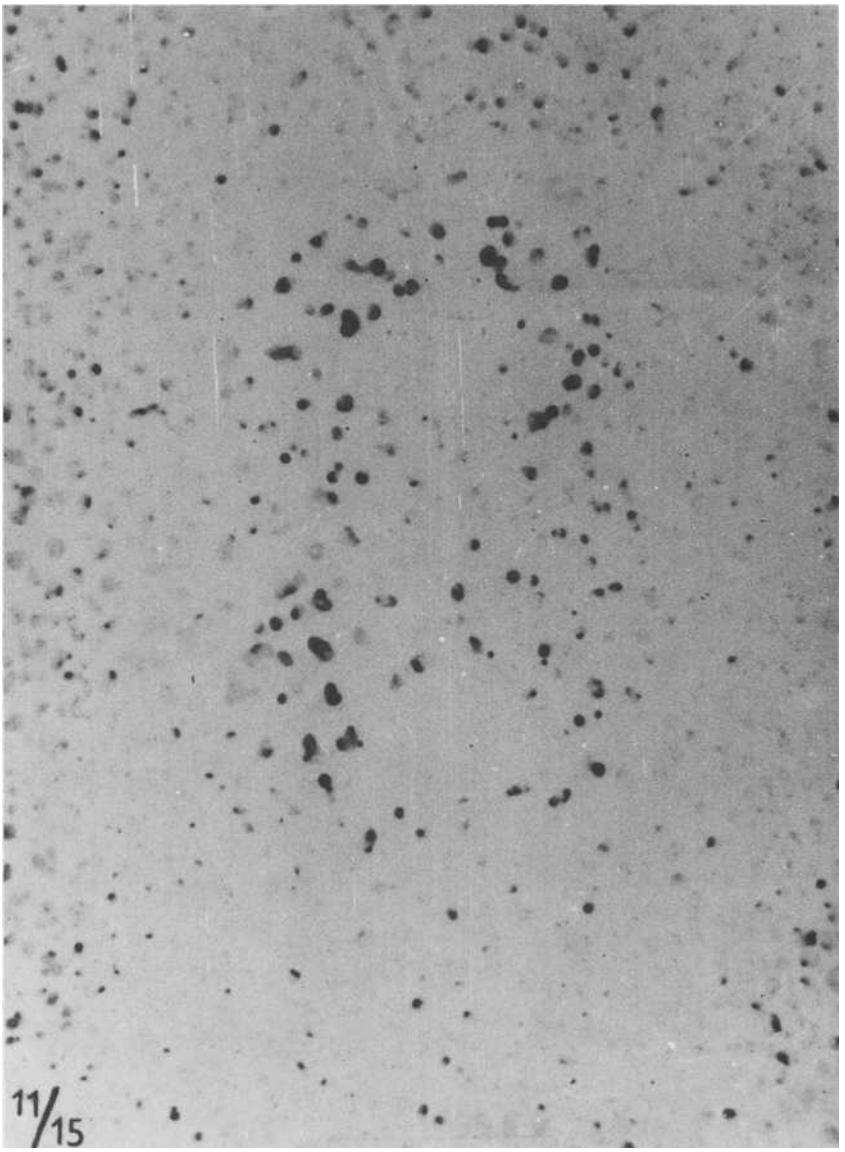

FIG. 13—*Distribution of sulfate nests in rust layer on Atmofix 52A in contact with structural steel after 3-year test in heavy polluted industrial atmosphere (Ústí nad Labem).*

significant results have come from both accelerated tests and atmospheric exposures on facade sheet attachments. Magnetite was found in the crevices during accelerated testing and this indicates insufficient drying during the cycles as well as insufficient transport of oxygen into the crevices.

Accelerated tests have also given essential information about the behavior of various types of joints between facade sheets and the supporting members. These tests have shown the need for caulkings and coatings for use in these crevices and have demonstrated the suitability of specific formulations of these materials.

The tests on models of facade sheet assemblies in the atmosphere showed that the development of rust on horizontal surfaces of supporting members together with the rust in the crevices acts as a moisture retainer. This moisture retention effect extends the time of active corrosion and consequently has an unfavorable influence. The corrosion products resulting from this process deformed the facade sheet and, as a result, opened up the crevice. Thus, an annular zone developed around each bolt in which corrosion occurred most rapidly, resulting in bulging and even perforation of the facade sheet. The most suitable arrangement for attaching thin sheets to supporting members has been to use a rubber packing piece applied or cemented to the sheet to seal the joint.

Welds—The tests already completed have shown that welds in weathering steels present no increased risk of corrosion. No significant differences were noted in the character of attack of either the weld metal or the basis metal nearby, using any of the evaluation techniques in the preceding described.

Combinations of Materials—The tests on various combinations of weathering steels with other building materials have not shown any unexpected results. Materials with smooth, nonporous surfaces, such as glazed ceramic materials, glass, aluminum, and stainless steel, can be used in contact with weathering steels. Materials with porous surfaces should not be used in contact with weathering steels.

Study of Atmofix Weathering Steel in Structures

The final stage in this program on the corrosion properties of weathering steels was the verification that the information already obtained was applicable to real structures. This stage of the program involved extensive collaboration with teams of engineers and designers interested in the technical properties of steels of this type. The corrosion engineers assisted with all the phases of construction during this study, including the formulation of instructions for designers, processing technology, materials handling, component storage and installation, and observation during the formation of a rust patina on the objects under study.

In order to achieve a wide application of the Atmofix steels in steel construction and other uses, a total of 50 different items were constructed of

TABLE 11—*Observed objects of feathering steels.*

Construction Type	Objects	Observed Effects	Direct Measurements Corrosion Tests	Elements of Risk	Knowledge, Experience
1	2	3	4	5	6
Towers (lattice steel towers)	TV transmission towers distribution substantion	atmosphere pollution construction arrangement of joint	measuring the atmosphere pollution by SO_2 corrosion tests of specimens on towers periodical measurement of selected point thicknesses (by ultrasound) quantity of free-bonded rust (periodical brushing-off) on selected towers rust structure (rust impressions on self-adhesive layer)	base corners horizontal surfaces crevices at joints	kind of a construction suitable for the application of low-alloy steels. Special attention must be paid to the bolted joints in highly contaminated atmospheres; galvanized bolts should not be used. Concrete footings should be of a sufficient inclination and it is recommended that they be protected by paint
Masts (19) (tubular construction)	lighting masts broadcasting, TV, communication masts	atmosphere pollution construction arrangement degree of sheltering	measuring the atmosphere pollution by SO_2 periodical ultrasonic measuring of thickness orientation corrosion tests of specimens in the TV transmitter body	base horizontal surfaces lower ceilings internal surfaces of bodies transitions of various diameters	construction type of a more complex shape than the lattice steel towers. Rust layer of a different appearance is formed on the transitions of various diameters, at the flanges. The larger the vertical tube diameter, the more apparent is the differentiation of the rust layer on the windward and the leeward sides. In the case of the horizontally situated tubes, an expressly unsuitable course of the rust layer formation occurs on the bottom sec-

					tions (water flowing down, deteriorated drying up). The base should always be of concrete, with a sufficient inclination, or should be protected by paint. It is unsuitable to imbed the foot foundations into gravel
Industrial constructions	outdoor crane run-ways, metallurgical production plants (project preparation)	atmosphere pollution	measuring the atmosphere pollution by SO_2 and Cl orientation corrosion tests of specimens on construction site	corner horizontal surfaces joints lower ceilings	
	open storage halls sheds	atmosphere pollution construction arrangement degree of joint sheltering combination of materials	measuring the atmosphere pollution by SO_2 corrosion tests of specimens on sheds rust structure (rust impression on self-adhesive layer)	lower ceilings base joints bottom parts of constructions material combinations	objects of the mentioned types are provided with no wall mantling or with a partial mantling only; the space is thus properly ventilated. The bottom sections of the roofs (lower ceilings) where condensations occur are problematical. Attention must be paid to the embedded elements, joints, and connecting material. Galvanized bolts inside the sheds show an excessive galvanic corrosion
Safety round barriers	selected test sections in various conditions	atmosphere pollution sprays abrasion stress	periodic measurement of thickness (ultrasonic) corrosion tests of specimens rust structure	horizontal surfaces rear averted side	this application represents an extreme use of low-alloy steel. The corrosion behavior can be appreciated only on the basis of the results of the direct corrosion tests of specimens at the selected points of the concerned sections under various service conditions
Road and railway bridges	walkways (industrial, cable, dam type) road bridges	atmosphere pollution construction arrangement degree of joint sheltering	measuring the atmospheric pollution by SO_2 periodic ultrasonic measurement of	corners horizontal surfaces lower ceilings material combinations	the bridge structures are extensive and typical applications of the low-alloy steels. They bring about more-complex problems from the corrosion point of view, that is, especially with

TABLE 11—(*Continued*)

Construction Type	Objects	Observed Effects	Direct Measurements Corrosion Tests	Elements of Risk	Knowledge, Experience
1	2	3	4	5	6
		material combinations permanently high moisture content (dams)	thicknesses at selected points corrosion tests of specimens/cable trays		regard to the fact that besides the typical and suitable outdoor exposures, the shed and internal exposures (box section bridges) are also involved. The construction design must take into the consideration the low-alloy steel properties and must, in advance, eliminate situations which could bring about any serious corrosion problems (horizontal surfaces; corners where rust fallout accumulates; moisture retained which results in an unfavorable source of corrosion; untight joints, crevices, and gaps). On large vertical areas the appearance defects occur on the rust layers (zones of the layer extraction) due to the water flowing down, water leaking in, and various time periods of the wetness. Attention must be paid also to the combinations with other materials (concrete, building materials) when their appearance depreciation results from the corrosion products of low-alloy steels
	web plate railway bridge/railway siding	as in case of preceding group	as in the case of the preceding group corrosion tests of specimens directly on the object, following		

			also the effects of weight and position (specimens bolted directly to various parts of the bridge structure)		
	box-type bridges (project preparation)	atmospheric pollution inside the boxes of existing bridges of alloy steel internal spaces and surfaces	measuring the atmospheric pollution by SO_2 inside the boxes corrosion tests of specimens inside the boxes	same as in the case of the preceding group internal surfaces	
Overground constructions (buildings)	external support structures of buildings	atmospheric pollution construction arrangement orientation of surfaces sheltering degree material combinations	measuring the atmospheric pollution by SO_2 periodic measuring (ultrasonic) of thicknesses at selected points	corners horizontal surfaces lower ceilings material combinations	the supporting projecting structures represent a suitable application. Special attention must be paid to the construction design with regard to the combinations with the other building and construction materials. It has been proved that it is necessary to select carefully the suitable design of windows, to avoid large horizontal surfaces and large continuous vertical surfaces for the reasons mentioned in the case of the bridge structures. The cladding of the buildings with regard to high demands made for appearance is a very pretentious application from the construction design point of view. Besides the principles mentioned in case of the support structures, special attention must be paid to the fixing of the façade sheets on support structures; overlapped and flat joints of thin-walled elements must be avoided (crevice corrosion). Should this not be possible, the contact surfaces must be

TABLE 11—(*Continued*)

Construction Type	Objects	Observed Effects	Direct Measurements Corrosion Tests	Elements of Risk	Knowledge, Experience
1	2	3	4	5	6
					protected (putties, paints) or removed a distance of 5 to 10 mm by means of spacers. Effective ventilation of space behind the mantle is necessary. Where water might occur behind the mantle, drains must be provided
	building cladding	as in case of the support structures fixing the sheets on support structures	as in the case of support structures, extensive testing program on the department store façade corrosion tests of specimens quantity of free-bonded rust at selected points sulfate nests measuring the time-of-wetness of the selected point	as in the case of the support structures slots joints rear sides of façade sheet flashing profiles	
Wagons (for loose materials)		mechanical and abrasion stress long-time effect of moisture orientation of surfaces	periodic measuring (ultrasonic) of thicknesses at selected points	floors corners	this application is being experimentally verified in operation. The long-time effects of moisture contained in transported materials and water accumulation on the floor are the problems of concern

these steels for testing. A maximum variation in the type of construction and the environment was chosen. This enabled us to obtain information on the performance of a full range of rolled stock. The cost of this program was partially covered by grants from the state. Also, the active participation of potential users in the verification of the suitability of the Atmofix steel was of substantial value. The bulk of the items examined in this study were metallic structures for above-ground use and structures of interest to civil engineers. However, there were some metallic structures used in mechanical and other technical applications. The methods for characterizing these objects, their environments, and the conditions of construction and operation have been carefully described in a uniform manner. The techniques for annual inspection have also been developed to provide for a uniform evaluation. Special test programs have been set up to verify the effects of construction arrangements on the corrosion behavior of Atmofix steel for a limited number of structures. A description of this study, including some of the results, is provided in Table 11.

The use of formed sections of thin sheets of steel for the construction of building walls, silos, storage bins, or as building siding has the most potential for weathering steels. The thickness of such material may be limited by corrosion of the steel and the need of such a structure to bear loads. There are a large number of exposure variations possible in such structures, including exposure orientation, inclination, contact with other materials, and modes of attachment on supporting members. It is difficult, therefore, to select a structure that would avoid areas which are not suitable for the use of weathering steels. The behavior of the facade of a building using thin sheets has been considered. In this case a department store under the actual conditions of exposure has been evaluated over a long period to determine the performance of the material from several viewpoints, namely:

1. The development of corrosion on a free area, depending on the position and orientation of the building.
2. The behavior of various types of interfaces and joints of steel with one another and with the supporting construction.
3. The effect of other materials adjacent to the facade, including the window glass and nearby concrete pavement.

The analyses of the corrosion behavior of one type of facade sheet attachment to the supporting structures is shown in Fig. 14. Vertical strips of formed sheet are attached by self-tapping screws in the horizontal beams of the supporting frame. The bolted joint was sufficiently strong, but there was an annular ring of 3 to 8 cm around the screwhead which suffered excessive corrosion, and the sheet was thinned in the crevice between the beam and the sheet. After about 5 years' exposure, perforation occurred at points above the bolt where a considerable quantity of rust accumulated on the horizontal surface

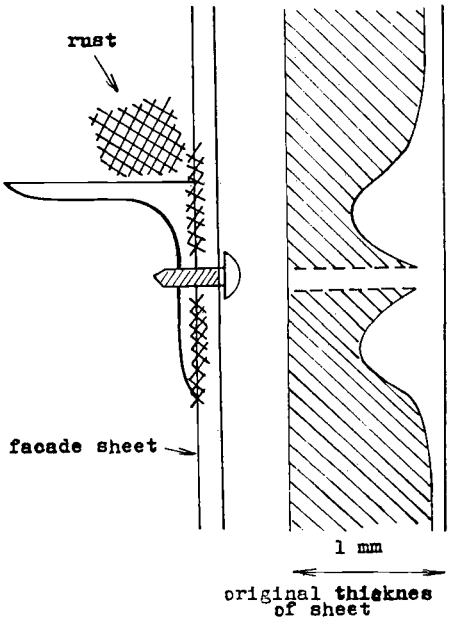

FIG. 14—*Corrosion behavior of the façade sheet attachment on the supporting structure.*

of the supporting element. This rust had retained moisture to the point where the crevice between the beam and the sheet was almost constantly wet. The crevice showed no evidence of being closed off by the corrosion products, but rather the sheet was deformed and bulging because of the pressure of the corrosion product formation.

This case has verified the undesirability of this type of joint and has demonstrated the deleterious effect of rust accumulations on horizontal surfaces with the acceleration of corrosion resulting on adjacent surfaces.

Conclusion

On the basis of the results of this study, a brochure entitled "Directions for the Use of Atmofix Steel" has been published. This brochure contains the detailed working concepts, verified in practice, to apply to the effective utilization of these steels together with both technical and economic information of interest to the users.

The material concepts selected have been compared with other ways of securing steel construction service life for different kinds of products and service environments. Suitable and economic areas of use for weathering steels have been defined from a corrosion performance point of view.

The costs of construction and maintenance of structures with conventional finishes compared with unprotected Atmofix steel have been presented for

typical applications. In some cases the economic evaluations are valid beyond the borders of Czechoslovakia.

The elimination of surface finishes, including the surface preparation prior to finishing, together with the subsequent maintenance of the finish, results in an average savings of 71 man-hours and 78 kg of paint per ton of construction when standard coating systems are applied to standard steel construction with a service life of 45 years. When the steel surface is protected by galvanizing, about 3 kg of zinc are necessary per ton of steel construction. When these data are applied to a 10 000-ton (metric) steel construction job, the following direct savings of man hours and materials may be achieved, assuming a service life of 45 years:

1. Initial coating system (during production): 103 960 h, that is, 58 workers for 1 year
2. Repainting after construction: 543 072 h, that is, 37 workers every fifth year (for 1 year)
3. Volume of paint—total: 826 tons

There are also savings in the area of energy consumption. The application of weathering steels also reduces air and water pollution which results from the production and application of paints as well as from the surface preparation steps necessary to ready the steel for painting.

This paper has provided a survey of the corrosion properties of weathering steels relative to their use in steel structures. A wide range of experimental results has been presented together with the experience gained in the field in these applications. Generalizations are provided relative to the use of these materials in the atmosphere and the types of construction suited to the use of weathering steels. The limitations of weathering steels in terms of economic and technical problems are also presented.

References

[1] "Directions for Use of Atmofix Steels, Technical and Economic Research Institute of Metallurgical Industry," Prague, C.S.S.R., Dec. 1978.
[2] Knotková, D. et al, "Corrosion Characteristics of Weathering Steels," State Research Institute for Material Protection, Final Report, SVÚOM 14, Prague, C.S.S.R., 1978.
[3] Madison, R.B., *Civil Engineering*, American Society of Civil Engineers, Feb. 1966, pp. 68–72.
[4] Stanners, J.F., *Journal of Applied Chemistry*, Vol. 10, Nov. 1960, p. 461.
[5] Copson, H.R. in *Proceedings*, American Society for Testing and Materials, Vol. 52, 1955, p. 1005.
[6] Larrabee, C. P. in *Proceedings*, First Congress on Metallic Corrosion, London 1961, p. 252.
[7] Hudson, J. C. and Stanners, J. F., *Journal of the Iron and Steel Institute*, July 1955, p. 271.
[8] Koschelev, G. G. and Klark, G. V., *Trudy Instituta Fizičeskoj Chimii*, Vol. 8, 1970, p. 84.
[9] Vedenkin, S. G., Special Publication, *Korrozija Metallov*, Moscow, 1952, p. 3.
[10] Knotková, D., Honzák, J., and Spanilý, J., *Koroze a Ochrana Materiálu*, Vol. 18, 1974, p. 5.
[11] Knotková, D., Spanilý, J., and Kuchyňka, D. in *Proceedings*, 2nd International CMEA Congress on Corrosion, Prague, Vol. 11, 1975, p. 1634.

[*12*] Knotková, D., Kupiliková, A., and Honzák, J., *Korrosion (ZKS)*, No. 2, 1975, p. 8.
[*13*] Knotková, D. and Marek, V., *Koroze a Ochrana Materiálu,* Vol. 19, No. 3, 1975, p. 45.
[*14*] Honzák, J., *British Corrosion Journal,* No. 8, 1973, p. 162.
[*15*] Kukurs, O. et al in *Proceedings,* 3rd International CMEA Congress on Corrosion, Warsaw, Vol. 4, 1980, p. 191.
[*16*] Knotková, D., Kuchyňka, D., Rössler, K., and Baum, H., *Neue Hütte,* Vol. 24, No. 1, Jan. 1979, p. 26.
[*17*] Honzák, J. and Kuchyňka, D., *Werkstoffe und Korrosion,* Vol. 21, 1940, p. 342.
[*18*] Honzák, J., "Corrosion Important Components of Rust," Ph.D. Dissertation, Prague, 1974.
[*19*] Brockenbrough, R. L. and Schmitt R. J. in *Proceedings,* Winter Meeting, Institute of Electrical and Electronic Engineers, New York, 27 Jan. 1975.
[*20*] Knotková, D., Honzák, J., Jírovský, I. in *Proceedings,* 6th European Congress on Corrosion, London, 1977, p. 663.

H. E. Townsend[1] *and J. C. Zoccola*[1]

Eight-Year Atmospheric Corrosion Performance of Weathering Steel in Industrial, Rural, and Marine Environments

REFERENCE: Townsend, H. E. and Zoccola, J. C., "**Eight-Year Atmospheric Corrosion Performance of Weathering Steel in Industrial, Rural, and Marine Environments,**" *Atmospheric Corrosion of Metals, ASTM STP 767*, S. W. Dean, Jr., and E. C. Rhea, Eds., American Society for Testing and Materials, 1982, pp. 45–59.

ABSTRACT: Weathering steel (ASTM A588, Grade B) and steels with 0.021 and 0.21 percent copper were tested for corrosion resistance in marine, rural, and two industrial environments. The results of these tests are represented well by kinetic equations of the form $C = At^B$, where C is the corrosion loss, t is time, and A and B are constants. On the basis of the time required to achieve a 250-μm (0.01 in.) thickness loss that is calculated using these equations, the weathering steel is 6 to 19 times more durable than the 0.021 percent copper steel and 2 to 10 times more durable than the 0.21 percent copper steel.

KEY WORDS: corrosion, corrosion tests, atmospheric corrosion, industrial environment, marine environment, rural environment, steels, weathering steel, kinetics, regression analysis, evaluation

The term weathering steel describes a class of steels that contain small amounts of alloying elements (generally less than about 3 percent) which promote formation of a protective rust layer during open exposure to the atmosphere. Owing to the ability of weathering steels to form a dense, adherent rust that acts as a self-healing barrier against further corrosion, these steels are widely used without paint or other protective coatings.

The ASTM Specification for High-Strength Low-Alloy Structural Steel with 50 000 psi Minimum Yield Point to 4 in. Thick (A588-77a) covers weathering steels that are characterized by weldability and high strength [yield strength greater than 345 MPa (50 000 psi)]. The combination of corrosion resistance and low maintenance costs with superior mechanical properties and weldability has led to the widespread use of A588 steels in a variety of structural applications, including buildings and bridges.

[1] Supervisor and engineer, respectively, Corrosion and Coatings Research Section, Research Department, Bethlehem Steel Corp., Bethlehem, Pa. 18016.

Specification A588-77a describes the atmospheric corrosion resistance of this steel as approximately twice that of carbon structural steel with copper. Carbon structural steels with copper contain greater than 0.2 percent copper and have an atmospheric corrosion resistance approximately twice that of carbon structural steel without copper (that is, steel with 0.02 percent maximum copper).

The purposes of this paper are (1) to present the results of long-term outdoor corrosion tests of A588 weathering steel in a variety of environments, and (2) to compare the performance of A588 with those of steels with copper contents of about 0.2 and 0.02 percent.

Materials and Test Procedures

Steels with the chemical compositions given in Table 1 were cut into panels approximately 150 by 100 by 2.5 mm (6 by 4 by 0.1 in.), grit-blasted, stamped with identifications, degreased, and weighed prior to atmospheric exposure.

The weathering steel is Bethlehem's ASTM A588, Grade B, commercially available as Mayari R-50. It was hot-rolled in our laboratories to the test thickness from plant-produced 38-mm-thick (1 1/2 in.) plate. The steel containing 0.21 percent copper was similarly prepared from plant-produced 5-mm (3/16 in.) plate. The steel containing 0.021 percent copper is a plant-produced cold-rolled and annealed 2.8-mm (0.11 in.) carbon steel sheet. The latter steel is similar to that used for purposes of determining the corrosiveness of various atmospheric test sites in an ASTM study [*1*].[2]

The steel panels were exposed at four test sites selected to represent a broad range of environmental conditions, as follows:

1. *Kure Beach, N.C.* is an internationally known marine test site located about 250 m (800 ft) from the open Atlantic Ocean that is operated by the International Nickel Co. (INCO).
2. *Saylorsburg, Pa.* is Bethlehem's rural test site located in the Pocono Mountains about 50 km (31 miles) north of Bethlehem.
3. *Bethlehem, Pa.* is our industrial test site located about 3 km (1.9 miles) from Bethlehem's integrated steelmaking facility.
4. *Newark, N.J.* is a site located atop a two-story building occupied by the New Jersey Department of Transportation and adjacent to heavily traveled expressways.

Test panels were exposed 30 deg from the horizontal, with skyward surfaces facing south. Duplicate specimens were removed after exposure intervals of 1, 2, 4, and 8 years, cleaned in a molten sodium hydroxide-hydride mixture to remove corrosion products, and reweighed in order to determine metal loss according to conventional procedures [ASTM Recommended

[2] The italic numbers in brackets refer to the list of references appended to this paper.

TABLE 1—*Composition of steels in the atmospheric corrosion tests.*

Steel	Composition, % by weight								
	C	Mn	P	S	Si	Ni	Cr	Cu	V
:athering steel, ASTM A588, Grade B	0.13	1.02	0.008	0.018	0.22	0.27	0.64	0.210	0.062
:1Cu steel	0.02	0.35	0.005	0.013	0.01	0.02	0.02	0.210	. . .
021Cu steel	0.07	0.35	0.009	0.020	<0.001	0.01	0.02	0.021	. . .

Practice for Preparing, Cleaning, and Evaluating Corrosion Test Specimens (G1-72)].

Results and Discussion

The results of our tests are considered in the following in terms of linear and logarithmic representations. Kinetic equations derived from the logarithmic representations are employed to facilitate a quantitative comparison of the three steels.

Linear Representation of Corrosion Test Results

Results of the corrosion tests are plotted as a linear function of time in Figs. 1–4. Each point represents the average of values from duplicate specimens. These plots show that the steels can be qualitatively ranked in terms of their corrosion resistance as follows: weathering steel >0.21Cu steel >0.021Cu steel. As discussed later, however, quantitative comparisons of the steels on the basis of these figures alone is not a straightforward matter.

Logarithmic Representation of Corrosion Test Results

When the atmospheric corrosion test results shown in Figs. 1–4 are replotted on logarithmic scales, Figs. 5–8, the data fit well to straight lines. This type of relationship has been observed for the corrosion of a variety of materials, including low-alloy steels, nonferrous metals, zinc-coated steels, aluminum-coated steels, and steels coated with aluminum-zinc alloy [*2,4–9*].

The straight-line relationships in Figs. 5–8 can be represented by equations in slope-intercept form as follows

$$\log C = \log A + B \log t \tag{1}$$

where

C = corrosion loss,
t = time, and
A and B = constants.

The constants obtained by linear regression analysis of these data along with the associated correlation coefficients, R, are summarized in Table 2.

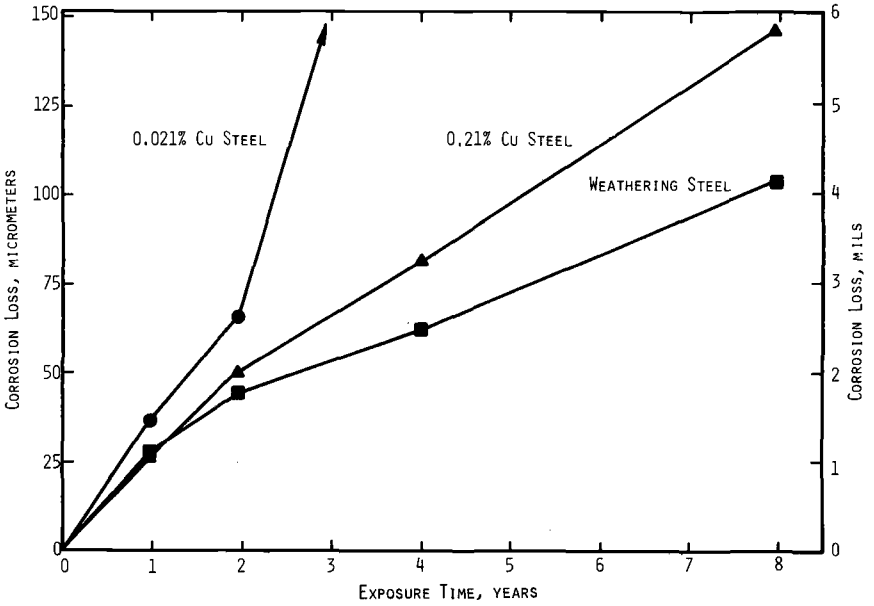

FIG. 1—*Corrosion performance of steels at Kure Beach, N. C.*

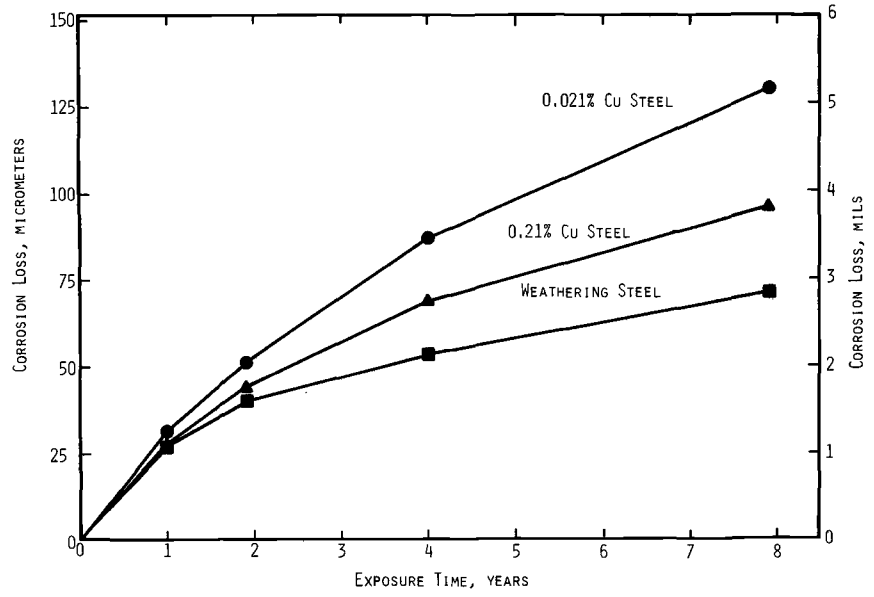

FIG. 2—*Corrosion performance of steels at Saylorsburg, Pa.*

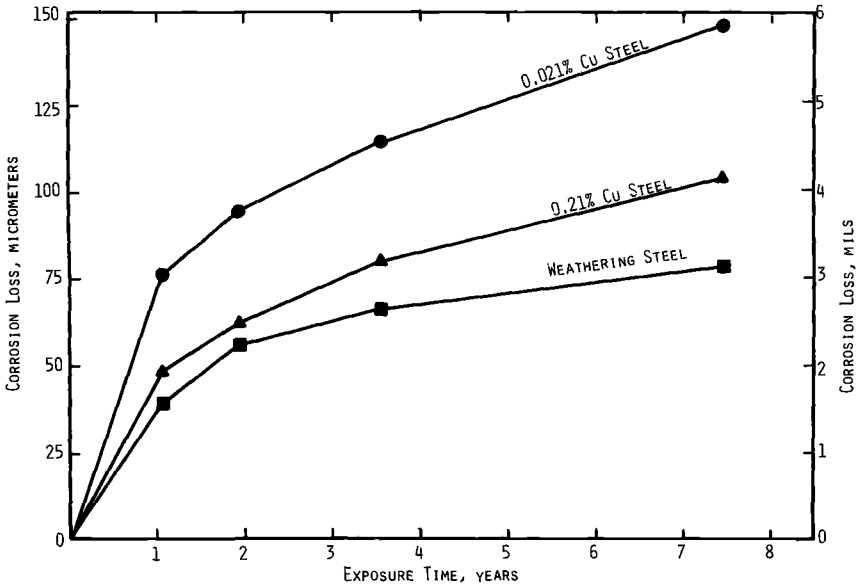

FIG. 3—*Corrosion performance of steels at Bethlehem, Pa.*

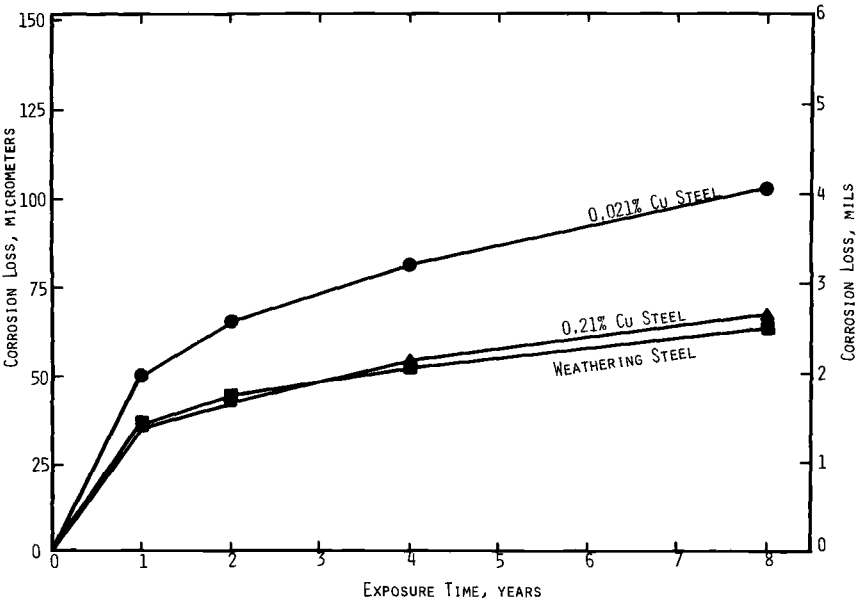

FIG. 4—*Corrosion performance of steels at Newark, N. J.*

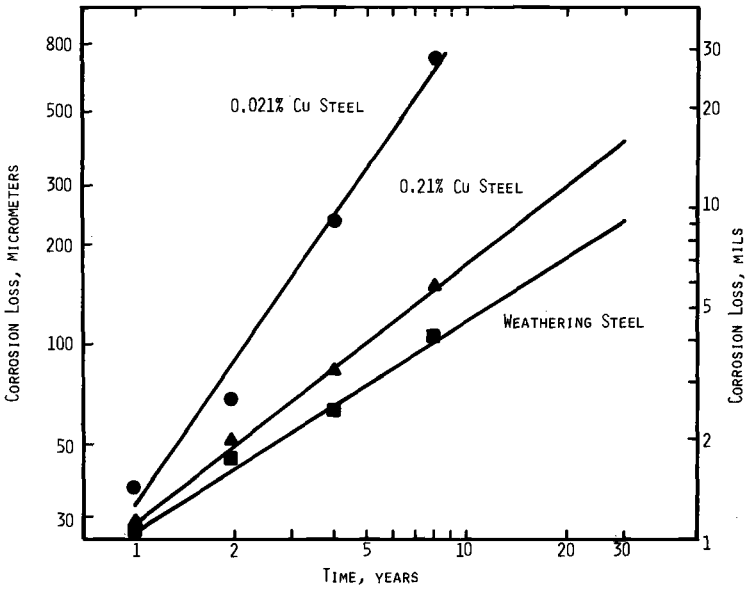

FIG. 5—*Logarithmic plot of corrosion performance at Kure Beach, N. C.*

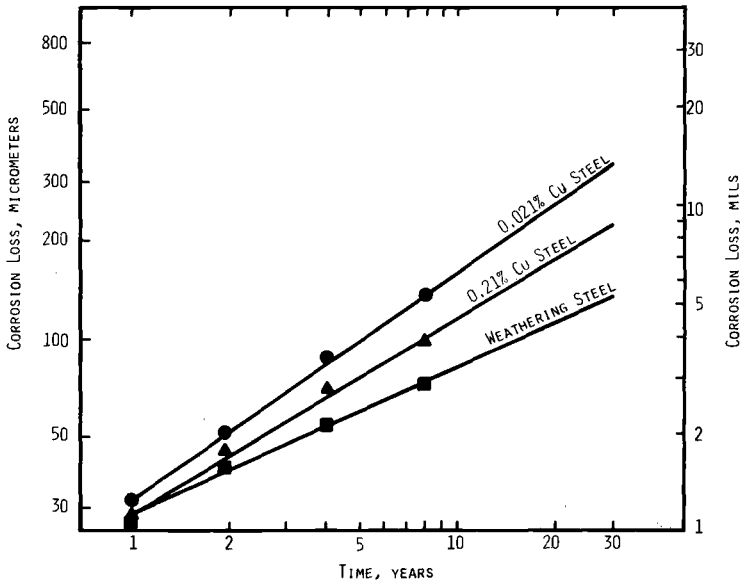

FIG. 6—*Logarithmic plot of corrosion performance at Saylorsburg, Pa.*

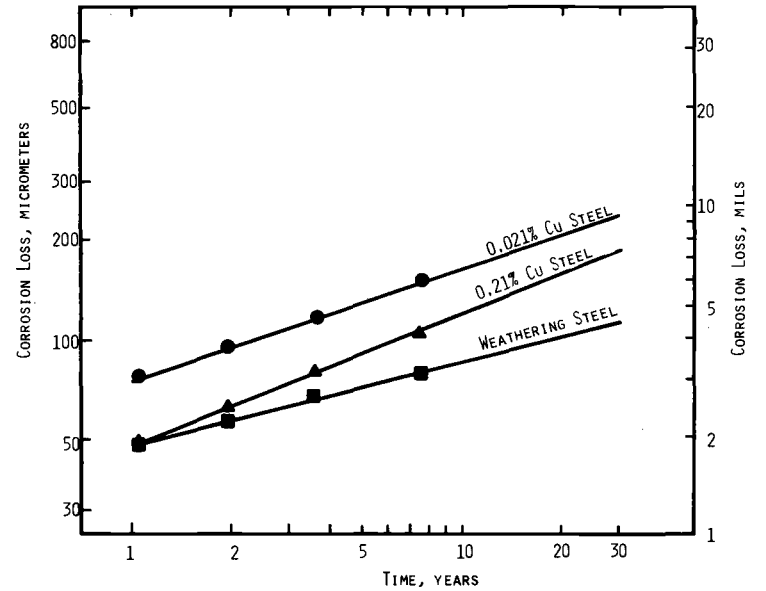

FIG. 7—*Logarithmic plot of corrosion performance at Bethlehem, Pa.*

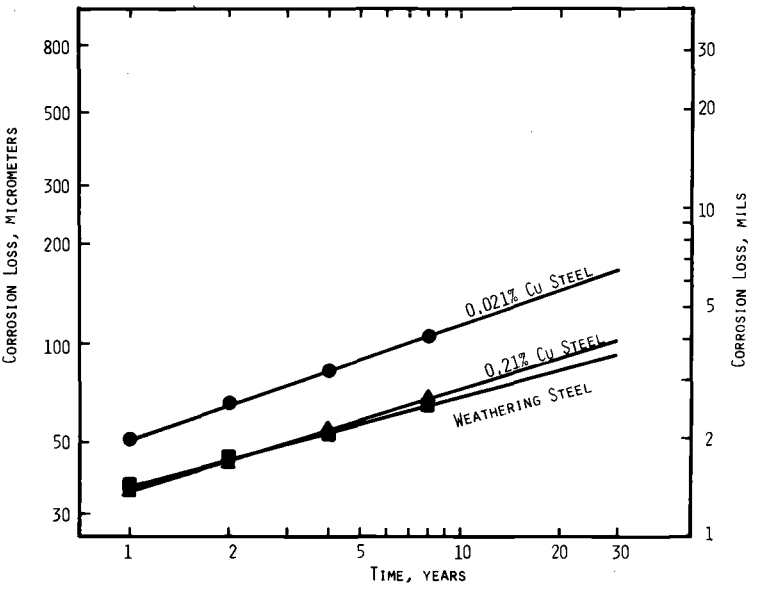

FIG. 8—*Logarithmic plot of corrosion performance at Newark, N. J.*

TABLE 2—*Least-squares coefficients for atmospheric corrosion data.*

Test Site	Weathering Steel			0.21Cu Steel			0.021Cu Steel		
	A	*B*	*R*	*A*	*B*	*R*	*A*	*B*	*R*
Kure Beach, N.C.	28.0	0.621	0.996	29.2	0.770	0.998	31.7	1.459	0.990
Saylorsburg, Pa.	28.5	0.456	0.994	28.8	0.602	0.996	31.9	0.697	0.998
Bethlehem, Pa.	47.2	0.258	0.959	47.0	0.403	0.998	74.8	0.339	0.999
Newark, N.J.	36.1	0.273	0.973	35.0	0.310	0.997	50.4	0.346	0.999

NOTES:

1. A and B are coefficients of the equation $C = At^B$, where C is the corrosion loss in micrometres and t the exposure time in years.
2. R is the correlation coefficient of the least-square regression of the logarithms.

The R-values are 0.96 or more in all cases and indicate generally good agreement with Eq. 1. In 10 of 12 cases, the R-value is 0.99 or greater and indicates that 98 percent (R^2) of the changes with time are accounted for by the kinetic equations.

Kinetic Equations

Taking antilogarithms of the terms in Eq 1 gives the following exponential expression

$$C = At^B \tag{2}$$

From Eq 2 it is clear that A is numerically equivalent to the corrosion loss when time is unity. Accordingly, A is generally considered to be a measure of the initial reactivity of the material with its environment prior to longer-term changes, such as the accumulation of corrosion products.

In contrast, the exponent B reflects changes that occur in corrosion loss with time. That is, from Eq 1

$$B = \frac{d \log C}{d \log t} \tag{3}$$

or

$$B = \lim_{\Delta C,\, \Delta t \to 0} \frac{\dfrac{\Delta C}{C}}{\dfrac{\Delta t}{t}} \tag{4}$$

or, in other words, B is numerically equal to the percent change in corrosion loss with percent in time.

In the absence of some change at the surface that would affect the rate of corrosion with time, B would be unity. For example, linear behavior reported for the groundward surfaces of aluminum-coated steel exposed at

Kure Beach was attributed to the formation of an initial corrosion product that rapidly grows to a limiting thickness and thereafter undergoes only negligible change [*8*].

Another value of B occurs when an adherent corrosion product is formed at the surface that acts as a diffusion barrier to hinder further reaction. When this happens, parabolic growth kinetics, $B = 1/2$, are observed as, for example, in the case of the oxidation of iron in the temperature range 250 to 1000°C (482 to 1832°F) [*10*].

By taking the time derivative of Eq 2 we obtain an expression for the corrosion rate, $\dot{C}$, as a function of time.

$$\dot{C} = ABt^{B-1} \tag{5}$$

Corrosion rates calculated from the Eq 5 are plotted in Figs. 9–12.

Alternatively, Eq 2 can be solved for t^*, the time required to reach a particular value of corrosion loss, C^*.

$$t^* = \left(\frac{C^*}{A}\right)^{1/B} \tag{6}$$

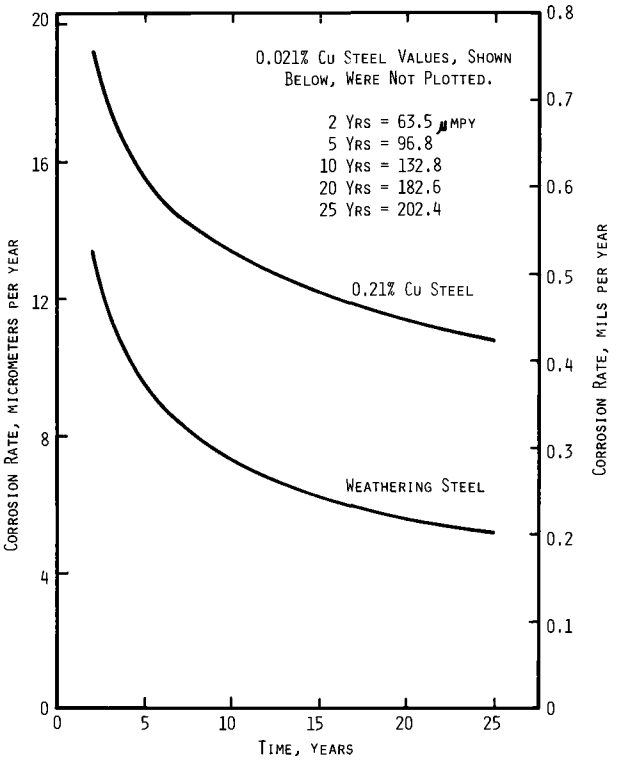

FIG. 9—*Corrosion rates at Kure Beach, N. C.*

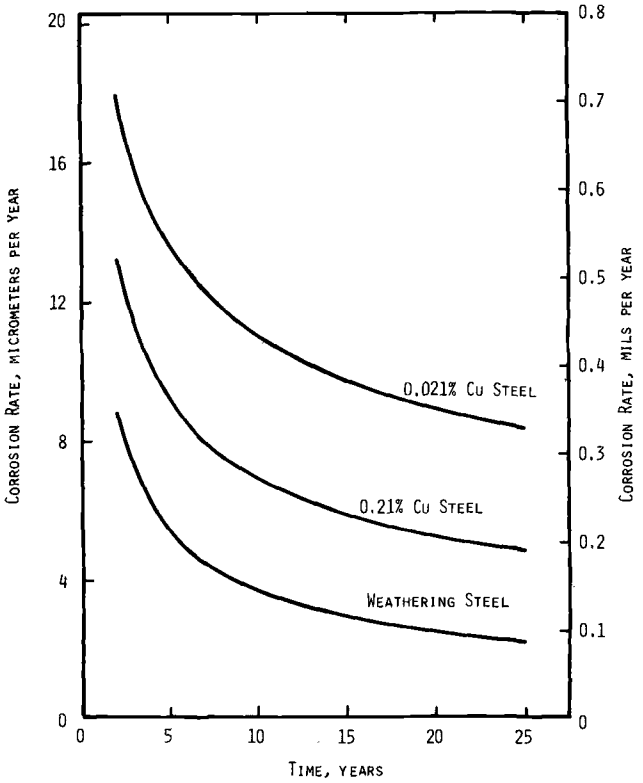

FIG. 10—*Corrosion rates at Saylorsburg, Pa.*

Quantitative Comparisons of the Corrosion Resistance of Steel

While comparing the corrosion resistance of different steels on the basis of a ratio of corrosion losses might seem attractive because of simplicity, closer examination reveals a serious shortcoming of this approach. The shortcoming arises because the loss ratio is time-dependent, as can be seen from Figs. 1–4, or from a ratio based on Eq 2 where subscripts 1 and 2 refer to the different steels, as follows

$$\frac{C_1}{C_2} = \frac{A_1}{A_2} t^{B_1 - B_2} \tag{7}$$

Arbitrary selection of a fixed time at which the ratio is calculated eliminates the time dependence. However, the selection of a fixed time leads to a paradoxical situation in which the advantages of the most corrosion-resistant material are understated in the least-corrosive environments within the time period of typical corrosion tests.

A ratio of corrosion rates might also be considered in comparing the per-

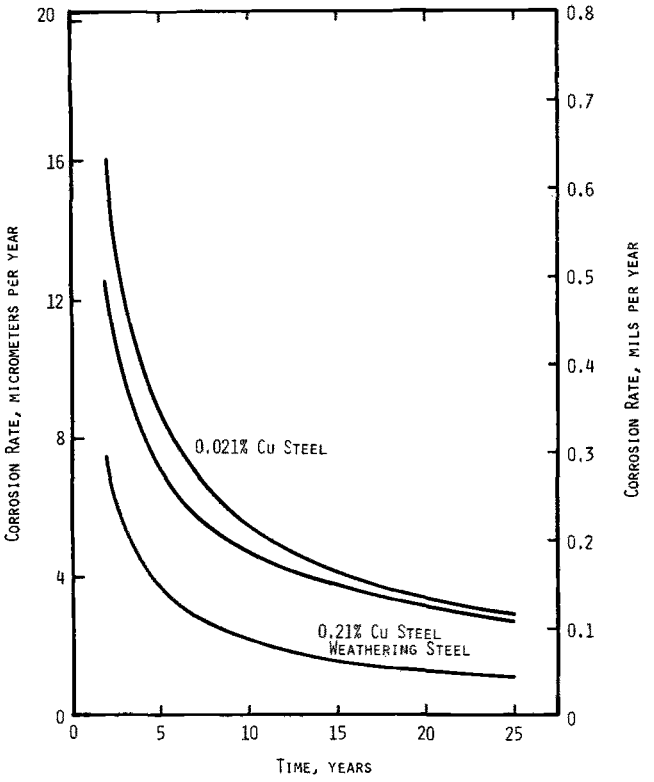

FIG. 11—*Corrosion rates at Bethlehem, Pa.*

formance of steels. However, as can be seen from such a ratio based on Eq. 5, where subscripts refer to Materials 1 and 2

$$\frac{C_1}{C_2} = \frac{A_1 B_1}{A_2 B_2} t^{B_1 - B_2} \tag{8}$$

the rate ratio has exactly the same time dependence as the loss ratio (see Eq 7). This time dependence again leads to the drawbacks discussed in the foregoing.

A third approach for comparing the corrosion resistance of steels is based on the ratio of times required to achieve a particular loss of thickness. This approach is attractive because it recognizes that the integrity of an engineering structure is affected by the absolute, rather than the relative, amount of corrosion loss. Although selection of a loss for computation of the time ratio is arbitrary, we believe the selection should meet the following requirements:

1. The loss should be large enough to permit enough corrosion to occur so that significant differences can be observed between materials.

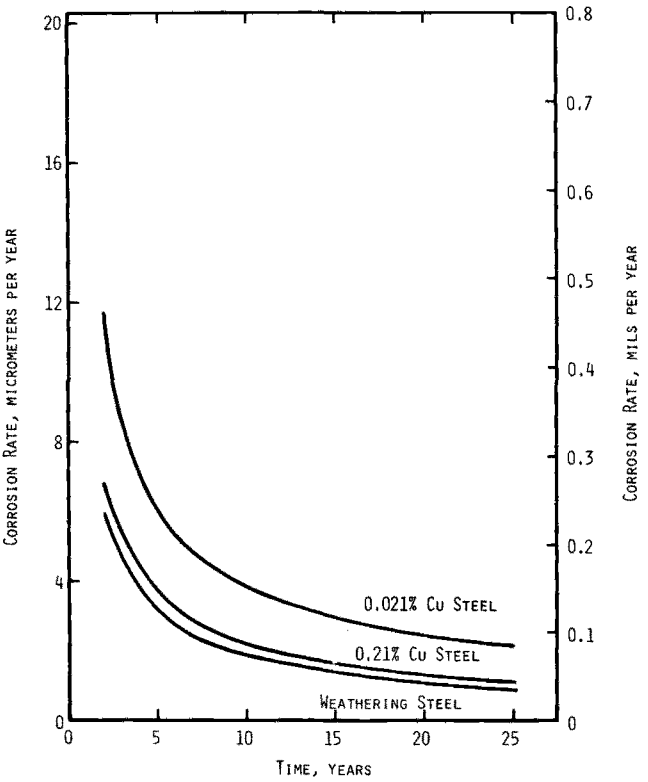

FIG. 12—*Corrosion rates at Newark, N. J.*

2. The loss should be small enough that the value can be achieved by the least corrosion-resistant material in corrosive environments within a reasonably short time.

3. The loss should also be small enough that it falls within the design allowances. That is, the loss should result in an insignificant reduction in load-bearing cross-sectional area.

Based on these considerations, we selected a loss of 250 μm (0.01 in.) for the calculation of time ratios. As can be seen in Table 3, the times to exhibit a 250-μm (0.01 in.) loss as calculated from Eq 6 and the constants in Table 2 conform to the first and second requirements. In practical applications of structural steels where members are generally 13 mm (1/2 in.) or greater, the 250-μm (0.01 in.) decrease [or 500-μm (0.02 in.) decrease if corrosion occurs from two sides] results in a loss of cross section of 4 percent or less. Thus, we conclude that the selection of a 250-μm (0.01 in.) loss provides a rational basis for computing time ratios.

Time ratios calculated (Table 3) for 0.21Cu steel relative to 0.021Cu steel

TABLE 3—*Time required to reach a thickness loss of 250 μm (0.01 in.).*

Test Site	Time, years			Ratio of Times		
	Weathering Steel	0.21Cu Steel	0.021Cu Steel	Weathering: 0.21Cu Steel	Weathering: 0.021Cu Steel	0.21Cu Steel: 0.021Cu Steel
Kure Beach, N.C.	34.8	16.6	4.2	2.1	8.3	4.0
Saylorsburg, Pa.	122	37.1	19.6	3.3	6.2	1.9
Bethlehem, Pa.	682	65.9	36.9	10.4	18.5	1.8
Newark, N.J.	1260	597	107	2.1	11.8	5.6

fall in the 1.8 to 5.6 range. This result is in reasonably good agreement with the statement that copper-bearing steel has approximately twice the corrosion resistance of structural steel without copper.

In the case of weathering steel, the time ratios in Table 3 indicate that it is 6 to 19 times more durable than with 0.021Cu steel and 2 to 10 times more durable than 0.21Cu steel.

From Table 3 we can rank the long-term corrosivity of the test environments in the following order (most corrosive to least corrosive): Kure Beach > Saylorsburg > Bethlehem > Newark. The greater corrosivity of the Kure Beach site can be attributed to the presence of airborne salt from the nearby ocean. Legault and Pearson [*2*] showed that the initial level of reactivity of steel with its environment increases as the distance from the ocean decreases.

The lower corrosivity of the industrial sites, Bethlehem and Newark, is probably due to airborne dust that becomes entrapped in the rust. In fact, Horton [*3,6*] found that dust particles from nearby industrial operations became enveloped in the outer layers of rust formed on weathering steels exposed at Pittsburgh. Trapped dust particles could increase the protective nature of rust layers by one or more of the following mechanisms: (1) increasing the thickness of the barrier, (2) decreasing its permeability, and (3) providing mechanical strengthening.

Conclusions

The main findings from an analysis of data provided by 8-year outdoor corrosion tests of weathering steel, 0.21Cu steel, and 0.021Cu steel are as follows:

1. In agreement with the results obtained by others for a variety of materials, the corrosion behavior of the steels tested in a broad range of environments is represented well by exponential kinetic equations readily derived by regression analyses of the data expressed in logarithmic form.
2. Meaningful comparisons of the corrosion resistance of steels can be made on the basis of a calculated time ratio to exhibit a 250-μm (0.01 in.) loss. Specifically, A588 Grade B weathering steel is 6 to 19 times more durable than the steel with 0.021 percent copper and 2 to 10 times more durable than the steel containing 0.21 percent copper.

Acknowledgment

The authors are indebted to the New Jersey Department of Transportation for allowing us to conduct tests at the Newark location, to J. B. Horton for encouraging this work, to E. L. Gehman and S. V. Jones for technical assistance, and to B. S. Mikofsky for editorial assistance.

References

[1] Coburn, S. K., Larrabee, C. P., Lawson, H. H., and Ellis, O. B. in *Metal Corrosion in the Atmosphere, STP 435*, American Society for Testing and Materials, 1968, pp. 360–391.
[2] Legault, R. A. and Pearson, V. P., *Corrosion*, Vol. 34, No. 12, 1978, p. 433.
[3] Horton, J. B., *The Rusting of Low-Alloy Steels in the Atmosphere*, Booklet 2385-A, Bethlehem Steel Corp., Bethlehem, Pa., 1971.
[4] Passano, R. F. in *Proceedings*, Symposium on the Outdoor Weathering of Metals and Metallic Coatings, Washington Regional Meeting of the American Society for Testing and Materials, March 1934.
[5] Pilling, N. B. and Wesley, W. A. in *Proceedings*, American Society for Testing and Materials, Vol. 40, 1940, p. 643.
[6] Horton, J. B., "The Composition, Structure, and Growth of Atmospheric Rust on Various Steels," Ph.D. Dissertation, Lehigh University, Bethlehem, Pa., 1964.
[7] Legault, R. A. and Pearson, V. P. in *Atmospheric Factors Affecting the Corrosion of Engineering Materials, ASTM STP 646*, S. K. Coburn, Ed., American Society for Testing and Materials, 1978, pp. 83–86.
[8] Legault, R. A. and Pearson, V. P., *Corrosion*, Vol. 34, No. 10, 1978, p. 344.
[9] Townsend, H. E. and Zoccola, J. C., *Materials Performance*, Vol. 18, No. 10, 1979, pp. 13–20.
[10] Scully, J. C., *The Fundamentals of Corrosion*, Pergamon Press, Oxford, U.K., 1966 pp. 13–14.

DISCUSSION

D. O. Sprowls[1] (*written discussion*)—Have you been able to ascribe significance to the constants, A and B, in relationship to type of alloy, or to type of environment?

H. E. Townsend and J. C. Zoccola (*authors' closure*)—From these and other studies, we observe in general that: (1) the initial reactivity of the steel (as reflected by coefficient A) is primarily determined by the corrosivity of the environment, and (2) the ability of the steel to form a protective rust layer (as reflected by coefficient B) is influenced mainly by alloy content, in particular, phosphorus, chromium, silicon, copper, and nickel.

[1] Alcoa Laboratories, Alcoa Center, Pa.

A. P. Castillo[1] *and J. M. Popplewell*[2]

General, Localized, and Stress-Corrosion Resistance of a Series of Copper Alloys in Natural Atmospheres

REFERENCE: Castillo, A. P. and Popplewell, J. M., **"General, Localized, and Stress-Corrosion Resistance of a Series of Copper Alloys in Natural Atmospheres,"** *Atmospheric Corrosion in Metals, ASTM STP 767,* S. W. Dean, Jr., and E. C. Rhea, Eds., American Society for Testing and Materials, 1982, pp. 60–84.

ABSTRACT: The general, localized, and stress-corrosion performance of a series of copper-base alloys exposed to marine, urban-industrial, and heavy-industrial environments is described after up to 12 years' exposure. The effect of alloying additions, test environment, and test parameters are reported versus corrosion susceptibility.

KEY WORDS: copper-base alloys, marine, urban-industrial and heavy-industrial environments, alloying additions, localized and stress-corrosion performance, corrosion susceptibility

One important phase of metals selection for use in natural environments is the acquisition of corrosion data obtained under a wide range of environmental conditions. Corrosion conditions for specific applications can often be simulated in the laboratory but general atmospheric corrosion data are difficult and expensive to determine under laboratory conditions using artificial atmospheres. Although standard accelerated laboratory test methods are useful during alloy development and for screening of new alloys, data obtained from these tests must be correlated and further supported by data obtained from long-term service.

In order to obtain such long-term atmospheric corrosion data, Olin Corp. utilizes three outdoor test sites at the present time: one in New Haven, Conn., a second at East Alton, Ill., and a third at the Battelle Marine Re-

[1] Formerly, senior research engineer, Olin Corp., Metals Research Laboratories, New Haven, Conn.; presently, director of research and development, Sandusky Foundry & Machine Co., P. O. Box 1281, Sandusky, Ohio 44870-0590.

[2] Formerly, associate research director, Olin Corp., Metals Research Laboratories, New Haven, Conn.; presently, director of product research, Olin Chemical and Consumer Group, 275 Winchester Ave., New Haven, Conn. 06511.

search Facility, Daytona Beach, Fla. A fourth site, located in Brooklyn, N. Y., was eliminated in 1974 as a result of security problems at this location. Short-term stress corrosion data only, as a result of exposure to this environment, are included in this report. These sites represent, respectively, an urban-industrial environment, an industrial environment, a marine environment, and a chloride-containing heavy industrial environment.

The original atmospheric corrosion program was designed to last only eight years with panel withdrawals at intermediate periods of 2 and 4 years. Atmospheric corrosion results of nine copper-base alloys, included in this report as a basis for comparison, were reported in 1973 and are part of a current ASTM publication [*1*].[3] Based upon the exposed panel corrosion results of 1973, obtained at two and four years, together with the anticipated increased service life of newer alloys placed into test more recently, the final withdrawal period of the atmospheric test program has been extended to 20 years.

A stress-corrosion phase of the atmospheric corrosion program called for inspection of stressed specimens biweekly or more frequently. A recent paper [*2*] reports the stress-corrosion resistance of copper-base alloys after short-term exposure. New copper alloys have been added to this phase of the program since its inception to provide additional stress-corrosion cracking (SCC) resistance data.

This paper summarizes the performance of 21 copper alloys evaluated as flat panels after 2 and 4 years' exposure. It further updates stress-corrosion resistance as a function of environment and longer times of exposure of 20 copper alloys. The data presented are interim results; however, planners, designers and engineers will find short-term atmospheric corrosion resistance information helpful since, in many applications, useful service life may be relatively short [*3,4*].

Experimental Procedures

Testing and Evaluation of Flat Panel Specimens

Table 1 is a listing of copper alloys evaluated in both phases of the atmospheric corrosion program, their nominal compositions, and commercial trade names with equivalent ASTM and Copper Development Association (CDA) designations.

Material "as received" from the mill was cut into panels 0.10 m (4 in.) by 0.20 m (8 in.) with the long edge in the rolling direction. The "as-received" material thickness ranged from 0.76 mm (0.030 in.) to 1.07 mm (0.042 in.). Initial longitudinal mechanical properties of materials to be evaluated were determined (Table 2). An identifying code was stamped on each specimen. The panels were degreased and cleaned in acid solution as outlined in the

[3] The italic numbers in brackets refer to the list of references appended to this paper.

TABLE 1—*Copper alloys evaluated, their nominal compositions, and commercial designations.*

ASTM Designation	Commercial Designation	Nominal Composition	CDA Designation
B370	oxygen free	99.95Cu	C10200
B152	electrolytic tough pitch	99.9Cu	C11000
B465	HSM[a]	97.5Cu-2.35Fe-0.12Zn-0.03P	C19400
	Strescon[a]	97.0Cu-1.5Fe-0.6Sn-0.1P-0.8Co	C19500
B36	commercial bronze, 90%	90.0Cu-10.0Zn	C22000
B36	red brass, 85%	85.0Cu-15.0Zn	C23000
B36	cartridge brass, 70%	70.0Cu-30.0Zn	C26000
B121	high leaded brass, 62%	62.0Cu-36.2Zn-1.8Pb	C35300
B591	Lubronze[a]	87.5Cu-11.4Zn-1.1Sn	C42200
B591	Lubaloy X[a]	88.0Cu-9.3Zn-2.2Sn	C42500
B171	Admiralty, arsenical	71.0Cu-27.5Zn-1.0Sn-0.06As	C44300
B103	phosphor bronze, 5%	94.8Cu-5.0Sn-0.2P	C51000
B103	phosphor bronze, 4%	96.0Cu-3.8Sn-0.06P	C51100
B103	phosphor bronze, 8%	91.8Cu-8.0Sn-0.2P	C52100
	Coronze[a]	95.0Cu-2.8Al-1.8Si-0.4Co	C63800
	Cobron[a]	84.5Cu-11.5Zn-1.5Fe-0.5Co	C66400
	Masiloy[a]	63.5Cu-24.5Zn-12.0Mn	C66900
B111	aluminum brass, arsenical	77.5Cu-20.0Zn-2.1Al-0.06As	C68700
	Alcoloy[a]	73.5Cu-22.7Zn-3.4Al-0.4Co	C68800
B432	copper nickel, 10%	88.2Cu-1.4Fe-10.0Ni	C70600
	copper nickel tin	88.2Cu-2.3Sn-9.5Ni	C72500
B122	nickel silver, 65-18	65Cu-17Zn-18Ni	C75200
B122	nickel silver, 59-12	59.0Cu-29.0Zn-12.0Ni	C76200
B122	nickel silver, 55-18	55.0Cu-27.0Zn-18.0Ni	C77000

[a] Registered trademark, Olin Corp.

ASTM Recommended Practice for Preparing, Cleaning, and Evaluating Corrosion Test Specimens (G 1-72). The test panels were measured to the nearest 0.1 mm (0.004 in.), and weighed to the nearest 0.1 mg. Control specimens of each alloy were retained in the laboratory to provide a means of detecting mechanical property changes not related to atmospheric corrosion.

Quadruplicate panels of each alloy were placed in test for each time period at each site. Specimens were placed in aluminum frame exposure racks, in turn bolted to an aluminum test stand on site. The specimens are held in place by edge contact with four neoprene grommets which electrically insulate them from the mounting hardware, preventing galvanic effects and providing some measure of susceptibility to crevice attack. Figure 1 shows a typical test site, including panels, stressed U-bend specimens, racks, and stands.

Upon removal from exposure, panels were evaluated "as corroded" for extent of patina, color, and texture of other oxides formed. Corrosion products (oxides) were removed from three of the four panels of each alloy as outlined in ASTM Method G 1-72. Weight losses were determined, followed by inspection for localized corrosion on cleaned panels. Gloves were continuously used in handling panels. Tension specimens were machined from cleaned panels and longitudinal mechanical properties determined. Longitudinal

TABLE 2—*Mechanical properties of copper alloys in atmospheric corrosion program.*

ASTM (CDA) Alloy Code	Temper (gage, mm)	Location[a]	Longitudinal Mechanical Properties								
			0.2% Offset Yield Strength, MN/m^2			Ultimate Tensile Strength, MN/m^2			% Elongation, in 0.05 m		
			Initial	2 Years	4 Years	Initial	2 Years	4 Years	Initial	2 Years	4 Years
B370	hard	MRL (C)	298	300	303	310	309	314	9.1	8.0	10.0
(C10200)	(0.76)	NH	. . .	299	300	. . .	309	310	. . .	8.3	8.3
		DB	. . .	298	298	. . .	308	310	. . .	7.9	7.6
		EA	. . .	298	297	. . .	309	308	. . .	8.2	8.3
B152	hard	MRL (C)	324	321	. . .	342	339	. . .	6.5	6.7	. . .
(C11000)	(1.02)	EA	. . .	323	. . .	. . .	340	. . .	. . .	6.8	. . .
B152	hard	MRL (C)	325	. . .	318	336	. . .	330	5.1	. . .	6.2
(C11000)	(0.76)	EA	. . .	. . .	316	. . .	. . .	328	. . .	. . .	5.8
B465	hard	MRL (C)	410	412	. . .	452	452	. . .	8.2	8.0	. . .
(C19400)	(0.99)	EA	. . .	413	. . .	. . .	452	. . .	. . .	8.1	. . .
B465	hard	MRL (C)	454	. . .	454	471	. . .	467	3.6	. . .	4.0
(C19400)	(0.76)	EA	. . .	. . .	452	. . .	. . .	463	. . .	. . .	4.0
(C19500)	spring-NK[b]	MRL (C)	634	656	. . .	662	670	. . .	3.0	4.2	. . .
	(0.91)	NH	. . .	644	. . .	. . .	657	. . .	. . .	4.0	. . .
		EA	. . .	644	. . .	. . .	661	. . .	. . .	3.4	. . .
(C19500)	spring-NK	MRL (C)	592	589	585	620	618	616	3.5	3.6	3.6
	(0.76)	NH	. . .	. . .	591	. . .	. . .	618	. . .	. . .	3.2
		DB	. . .	589	586	. . .	620	616	. . .	3.9	3.3
		EA	. . .	. . .	587	. . .	. . .	616	. . .	. . .	3.2
B36	hard	MRL (C)	419	416	418	436	430	432	4.3	4.7	5.2
(C22000)	(0.76)	NH	. . .	420	419	. . .	432	434	. . .	4.5	4.8
		DB	. . .	416	416	. . .	430	432	. . .	4.8	5.0
		EA	. . .	418	418	. . .	431	432	. . .	4.7	4.8
B36	hard	MRL (C)	444	450	. . .	478	474	. . .	5.5	5.5	. . .
(C23000)	(1.07)	EA	. . .	447	. . .	. . .	474	. . .	. . .	5.5	. . .
B36	hard	MRL (C)	445	. . .	445	469	. . .	470	6.0	. . .	6.0
(C23000)	(0.76)	EA	. . .	. . .	443	. . .	. . .	467	. . .	. . .	5.9

TABLE 2—*Continued.*

ASTM (CDA) Alloy Code	Temper (gage, mm)	Location[a]	Longitudinal Mechanical Properties: 0.2% Offset Yield Strength, MN/m^2 Initial	2 Years	4 Years	Ultimate Tensile Strength, MN/m^2 Initial	2 Years	4 Years	% Elongation, in 0.05 m Initial	2 Years	4 Years
B36	hard	MRL (C)	462	470	. . .	510	514	. . .	12.0	11.9	. . .
(C26000)	(1.02)	EA	. . .	472	. . .	. . .	516	. . .	. . .	11.2	. . .
B36	hard	MRL (C)	490	. . .	496	527	. . .	528	8.0	. . .	9.0
(C26000)	(0.76)	EA	. . .	. . .	486	. . .	. . .	518	. . .	. . .	8.2
B591	hard	MRL (C)	477	487	481	523	525	523	5.8	5.3	5.9
(C42200)	(1.02)	EA	. . .	483	482	. . .	520	523	. . .	5.2	5.8
B591	3/4 hard	MRL (C)	438	450	449	472	476	478	10.4	10.1	10.1
(C42500)	(0.89)	NH	. . .	445	447	. . .	472	474	. . .	10.1	9.6
		DB	. . .	446	447	. . .	473	473	. . .	10.0	9.6
		EA	. . .	444	442	. . .	470	470	. . .	9.6	10.1
B103	extra hard	MRL (C)	594	598	602	607	611	612	6.2	6.6	6.0
(C51000)	(0.99)	EA	. . .	601	591	. . .	610	603	. . .	6.3	6.5
B103	hard	MRL (C)	554	559	562	566	570	574	5.0	4.9	5.0
(C51100)	(0.76)	NH	. . .	557	561	. . .	570	572	. . .	4.9	5.0
		DB	. . .	560	561	. . .	568	572	. . .	4.8	4.8
		EA	. . .	565	556	. . .	574	566	. . .	5.0	5.0
B103	hard	MRL (C)	582	583	592	654	654	660	16.0	17.7	17.4
(C52100)	(0.76)	NH	. . .	587	584	. . .	658	656	. . .	17.1	17.0
		DB	. . .	581	588	. . .	654	659	. . .	17.3	16.4
		EA	. . .	584	578	. . .	652	652	. . .	17.5	17.5
(C63800)	hard	MRL (C)	694	616	. . .	854	819	. . .	6.0	6.8	. . .
	(0.99)	NH	. . .	625	. . .	. . .	818	. . .	. . .	6.7	. . .
		EA	. . .	621	. . .	. . .	820	. . .	. . .	6.5	. . .
(C63800)	3/4 hard	MRL (C)	614	646	640	782	790	793	5.7	5.3	5.2
	(0.76)	NH	. . .	. . .	633	. . .	. . .	789	. . .	. . .	5.3
		DB	. . .	639	642	. . .	792	796	. . .	5.4	5.0
		EA	. . .	. . .	633	. . .	. . .	787	. . .	. . .	5.3

(C66400)	hard	MRL (C)	568	571	572	609	605	612	4.1	4.7	4.2
	(0.86)	NH	. . .	572	574	. . .	605	616	. . .	4.2	4.1
		DB	. . .	570	567	. . .	599	604	. . .	4.3	4.2
		EA	. . .	564	564	. . .	600	601	. . .	4.2	4.2
(C66900)	hard	MRL (C)	596	610	. . .	618	626	. . .	3.0	2.9	. . .
	(0.76)	NH	. . .	594	. . .	. . .	610	. . .	. . .	2.3	. . .
		EA	. . .	599	. . .	. . .	615	. . .	. . .	2.7	. . .
(C66900)	hard	MRL (C)	607	618	622	647	656	656	2.9	2.8	2.8
	(0.76)	NH	. . .	. . .	610	. . .	. . .	635	. . .	. . .	1.9
		DB	. . .	598	582	. . .	632	613	. . .	2.2	2.0
		EA	. . .	. . .	583	. . .	. . .	607	. . .	. . .	1.9
(C68800)	1/2 hard	MRL (C)	588	650	. . .	683	701	. . .	5.5	5.0	. . .
	(1.02)	NH	. . .	640	. . .	. . .	690	. . .	. . .	5.1	. . .
		EA	. . .	650	. . .	. . .	700	. . .	. . .	4.7	. . .
(C68800)	1/2 hard	MRL (C)	636	648	645	769	774	776	4.1	4.4	4.3
	(0.76)	NH	. . .	. . .	650	. . .	. . .	779	. . .	. . .	4.2
		DB	. . .	653	651	. . .	776	778	. . .	4.0	4.0
		EA	. . .	. . .	647	. . .	. . .	771	. . .	. . .	3.9
B432	1/2 hard	MRL (C)	464	470	469	479	483	476	3.4	3.7	4.0
(C70600)	(0.76)	NH	. . .	466	458	. . .	483	479	. . .	3.5	3.8
		DB	. . .	461	460	. . .	476	480	. . .	3.7	3.5
		EA	. . .	458	462	. . .	478	478	. . .	3.7	3.7
(C72500)	hard	MRL (C)[e]	538	. . .	. . .	565	. . .	. . .	3.0	. . .	. . .
	(0.76)	NH	. . .	572	. . .	. . .	580	. . .	. . .	2.8	. . .
		EA	. . .	570	. . .	. . .	577	. . .	. . .	3.2	. . .
(C72500)	hard	MRL (C)	543	553	551	556	566	567	3.4	3.2	3.0
	(0.76)	NH	. . .	. . .	550	. . .	. . .	563	. . .	. . .	3.0
		DB	. . .	550	545	. . .	564	558	. . .	3.1	3.1
		EA	. . .	. . .	545	. . .	. . .	557	. . .	. . .	3.0
B122	spring	MRL (C)	659	650	. . .	670	663	. . .	2.0	1.9	. . .
(C75200)	(0.76)	NH	. . .	664	. . .	. . .	673	. . .	. . .	1.9	. . .
		DB	. . .	659	. . .	. . .	667	. . .	. . .	1.9	. . .
		EA	. . .	660	. . .	. . .	670	. . .	. . .	1.8	. . .
B122	hard	MRL (C)	573	580	578	597	601	598	3.0	2.7	3.0
(C75200)	(0.76)	NH	. . .	. . .	589	. . .	. . .	608	. . .	. . .	2.4
		DB	. . .	587	584	. . .	605	602	. . .	2.9	2.8
		EA	. . .	. . .	575	. . .	. . .	595	. . .	. . .	2.9

TABLE 2—*Continued.*

ASTM (CDA) Alloy Code	Temper (gage, mm)	Location[a]	Longitudinal Mechanical Properties: 0.2% Offset Yield Strength, MN/m^2 Initial	2 Years	4 Years	Ultimate Tensile Strength, MN/m^2 Initial	2 Years	4 Years	% Elongation, in 0.05 m Initial	2 Years	4 Years
B122	extra hard	MRL (C)	707	706	. . .	724	717	. . .	2.0	2.0	. . .
(C76200)	(0.76)	NH	. . .	705	. . .	. . .	719	. . .	. . .	2.0	. . .
		DB	. . .	705	. . .	. . .	733	. . .	. . .	2.0	. . .
		EA	. . .	715	. . .	. . .	730	. . .	. . .	2.0	. . .
B122	hard	MRL (C)	630	646	641	663	672	671	3.1	3.2	3.0
(C76200)	(0.76)	NH	. . .	. . .	647	. . .	. . .	670	. . .	. . .	3.0
		DB	. . .	649	652	. . .	670	674	. . .	3.3	3.1
		EA	. . .	. . .	640	. . .	. . .	666	. . .	. . .	3.2
B122	hard	MRL (C)	626	684	. . .	700	725	. . .	6.2	4.1	. . .
(C77000)	(1.04)	EA	. . .	692	. . .	. . .	724	. . .	. . .	4.0	. . .
B122	hard	MRL (C)	691	698	698	708	713	717	3.1	3.1	3.0
(C77000)	(0.76)	NH	. . .	. . .	662	. . .	. . .	678	. . .	. . .	1.9
		DB	. . .	696	692	. . .	713	710	. . .	3.1	3.0
		EA	. . .	. . .	649	. . .	. . .	664	. . .	. . .	1.8

[a] MRL (C) = retained control/NH = New Haven, Conn.; DB = Daytona Beach, Fla; EA = East Alton, Ill.
[b] Precipitation heat-treated and cold-work spring.
[c] Data unreported.

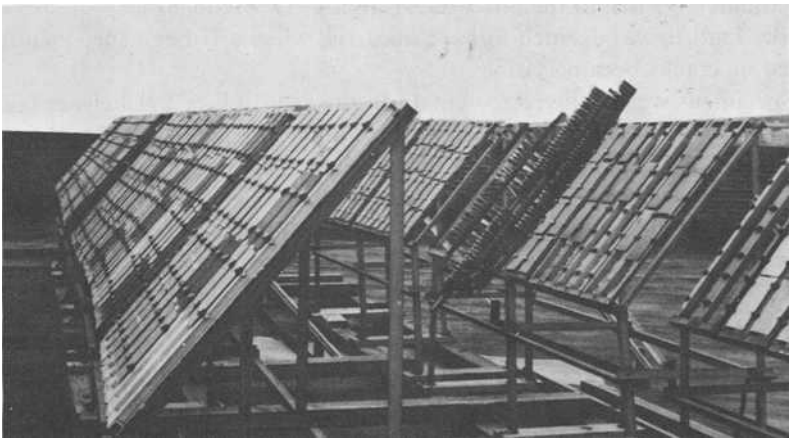

FIG. 1—*Typical atmospheric corrosion test facility, including mounted unstressed panels and stressed U-bends, aluminum racks, and stands.*

mechanical properties of control panels of each alloy, which had been retained in the laboratory, were determined initially as well as at the 2- and 4-year withdrawal periods (Table 2). The remaining exposed and uncleaned panel was carefully wrapped and stored to preserve the corrosion products. In this manner, oxide color comparisons can be accomplished and patina growth documented as a function of exposure time.

Stressed U-bend Specimen Testing Program

All alloys were exposed as preformed U-bend specimens 152 by 13 mm (6 by 1/2 in.) stressed in the long transverse direction (bad-way bend). The edges were carefully milled to produce a uniform edge finish. A permanent set of 90 deg was induced by bending around a 19.05-mm-diameter (3/4 in.) mandrel. The specimens were then acid-cleaned, as outlined in ASTM Method G 1-72, to remove surface oxides, and dried in methanol and acetone followed by storage in a desiccator. Gloves were continuously used in handing all stress U-Bends.

The legs of the specimens were sprung into micarta jigs at a spacing of 16.5 mm (0.66 in.) (that is, constant strain). The applied stress on each U-bend was therefore dependent on initial mechanical properties, the stronger materials in general having a higher level of stress. In addition, stress relaxation occurs as a function of time, the amount again being dependent on initial properties, alloy characteristics, and temperature achieved during exposure. A plastic pin inserted through the jig ensured that even on failure the U-bend would remain in the jig. The jigs, containing quintuplicate U-bends of each alloy, were then placed at the appropriate atmospheric sites with the apex of the U-bend specimen in tension facing skyward and the jig at an angle of ap-

proximately 45 deg to the horizontal (see Fig. 1). Frequent inspections were made. Failure was deemed to have occurred when a U-bend specimen fractured or cracks became visible.

Specimens were allowed to remain in the atmosphere until either failure occurred by SCC or sufficient stress relaxation occurred to drastically reduce the stress on the specimen. This was determined to have occurred when a specimen was observed to no longer be constrained by its holder. Metallographic sections to determine the existence of cracks or crack morphology were taken in every case whether cracks were visible or not.

Atmospheric Sites

The New Haven, Conn. site is characterized as urban-industrial. The rainwater and dew have a low pH and contain sulfates and nitrates typical of industrial atmospheres [*2*]. In addition, New Haven Harbor is approximately 3 km (2 miles) away and a minor amount of chloride is carried to the site by winds as sea salt. Additional chloride (such as sodium chloride) contamination from road salt may occur in winter due to the proximity of this location to several major highways. The New Haven site contains only minor levels of ammonia, unlike the other industrial environments. Test panels and U-bends are located in racks five stories above ground level.

The Brooklyn, N. Y. site is classified as a heavy industrial environment and is located adjacent to the East River (brackish water). Many major manufacturing facilities are located in the immediate vicinity of this site. The atmosphere contains large quantities of particulate matter. Ammonia (NH_3^+), sulfur dioxide (SO_2), hydrogen sulfide (H_2S), carbon dioxide (CO_2), nitrate (NO_3^-), and sulfate ($SO_4^=$) are present in this environment (from stacks and flue gases). Chloride contamination of the atmosphere, to some extent, is caused by proximity to the East River. In winter, road salt (containing chloride as sodium chloride) is also present as a result of numerous major highways in the area. Specimens were situated on the roof of a six-story building.

The East Alton, Ill. site is classified as an industrial environment. Specimens are situated on the roof of a four-story building. The atmosphere contains particulate matter, to a lesser extent than Brooklyn. The East Alton site contains corrosive agents in the atmosphere similar to those described for the Brooklyn site. Chloride contamination (as sodium chloride) of this environment is considered to be negligible.

The fourth site is located at Daytona Beach, Fla. The environment contains high levels of chloride with negligible industrial pollution. Sea salt spray is carried by the wind and falls directly onto all test specimens. The annual mean temperature of this site is somewhat higher than the industrial locations.

At the industrial sites, panels and stressed U-bend specimens face in a southeasterly direction at an angle of 45 deg from horizontal. At Daytona Beach,

all specimens are situated at ground level and face eastward (skyward surface buffeted by prevailing easterly winds). They are also mounted at an angle of 45 deg from horizontal.

Results

Table 2 is a listing of mechanical properties data of flat panels as a function of alloy, time and, atmospheric environment. Included in this table are the mechanical properties data of laboratory-retained controls, also as a function of time. Yield strength (0.2 percent offset) and ultimate tensile strength (specifically when comparing as-corroded to laboratory-retained control data, per withdrawal period) changed slightly irrespective of composition and environment. In certain materials, however, percent elongation was seen to be significantly affected by various forms of localized corrosion.

Table 3 lists the relative corrosion resistance of copper-base alloy panels to localized forms of corrosion after being exposed to industrial and marine environments for 2 and 4 years, respectively. Figure 2 typifies the combination of SCC and plug-type dealloying observed in (C66900). Crack morphology is predominately intergranular. Dealloying and transgranular SCC in the industrial environment for alloy B122 (C76200) is shown in Fig. 3. Figure 4 illustrates the transgranular crack morphology for alloy B122 (C77000) seen after 4 years' exposure in New Haven. In all cases of SCC, the direction of crack propagation was transverse to the rolling direction and originated at the indented regions of code numbers mechanically stamped on the panel surface where high residual stresses would be anticipated.

Table 4 lists the color of oxides formed as a function of alloy, time, and location and shows to what extent a patina developed after 4 years exposure at all sites. For aesthetic reasons, patina-forming copper alloy data are desired by architects and builders when considering these metals for applications in natural environments.

Table 5 lists weight loss versus time data and further indicates the degree of alloy, environment, and time-of-exposure dependence. B370 (C10200) and B103 (C52100) experienced the greatest losses in the marine environment equivalent to uniform penetration rates of 3.0 μm (0.12 mils) and 3.5 μm (0.14 mils) per year, respectively.

Table 6 lists the stress-corrosion resistance of 20 copper-base alloys which constitute the U-bend atmospheric stress-corrosion program. In the industrial environment, many of the alloys failed in relatively short times. These include cartridge brass B36 (C26000), leaded brass B121 (C35300), and the manganese modified brass (C66900). Crack morphology was predominately intergranular with the exception of B121 (C35300) and (C66900), where a mixed morphology was evident. Metallographic cross sections of B36 (C26000) and B121 (C35300), revealing typical intergranular and mixed crack morphologies, are shown in Figs. 5 and 6. The nickel-silvers B122

TABLE 3—*Susceptibility to localized corrosion of copper-base alloys in flat panel phase of atmospheric corrosion.*

ASTM (CDA) Alloy Code	Type of Localized Attack and Deepest Penetration, μm					
	New Haven		Daytona Beach		East Alton	
	2 Years	4 Years	2 Years	4 Years	2 Years	4 Years
B370 (C10200)	. . .	. . .	. . .	. . .	. . .	. . .
B152 (C11000)	. . .	. . .	. . .	. . .	. . .	. . .
B465 (C19400)	. . .	. . .	. . .	. . .	. . .	. . .
(C19500)	. . .	. . .	. . .	. . .	. . .	. . .
B36 (C22000)	. . .	. . .	. . .	slight dealloying	. . .	. . .
B36 (C23000)	. . .	. . .	. . .	slight dealloying	. . .	. . .
B36 (C26000)	. . .	moderate[b] dealloying	. . .	moderate[b] dealloying	. . .	slight dealloying
B591 (C42200)	. . .	. . .	. . .	. . .	. . .	. . .
B591 (C42500)	. . .	. . .	. . .	. . .	. . .	. . .

B103 (C51000)	. . .	. . .	. . .	. . .	pitting, 127	pitting, 127
B103 (C51100)	. . .	. . .	. . .	. . .	. . .	. . .
B103 (C52100)	. . .	pitting, 101.6	. . .	. . .	. . .	pitting, 76.2 crevice, 101.6
(C63800)	. . .	. . .	. . .	pitting, 76.2	. . .	. . .
(C66400)	. . .	. . .	. . .	crevice, 127.0	. . .	. . .
(C66900)	extensive dealloying	extensive dealloying (ISCC)[c]	extensive dealloying	extensive dealloying (ISCC)	slight dealloying	extensive dealloying (ISCC)
(C68800)	slight dealloying	slight dealloying	slight dealloying	slight dealloying	slight dealloying	slight dealloying
B432 (C70600)	. . .	. . .	. . .	. . .	. . .	. . .
(C72500)	. . .	. . .	. . .	. . .	. . .	. . .
B122 (C75200)	. . .	. . .	. . .	crevice, 101.6	. . .	. . .
B122 (C76200)	. . .	. . .	. . .	. . .	. . .	slight dealloying(TSCC)
B122 (C77000)	. . .	. . . (TSCC)[d]	. . .	pitting, 76.2 (TSCC)	. . .	pitting, 76.2 (TSCC)

[a] Signifies negligible pitting or crevice attack or both.
[b] Data previously reported.
[c] (ISSC) Intergranular stress corrosion cracking.
[d] (TSCC) Transgranular stress corrosion cracking.

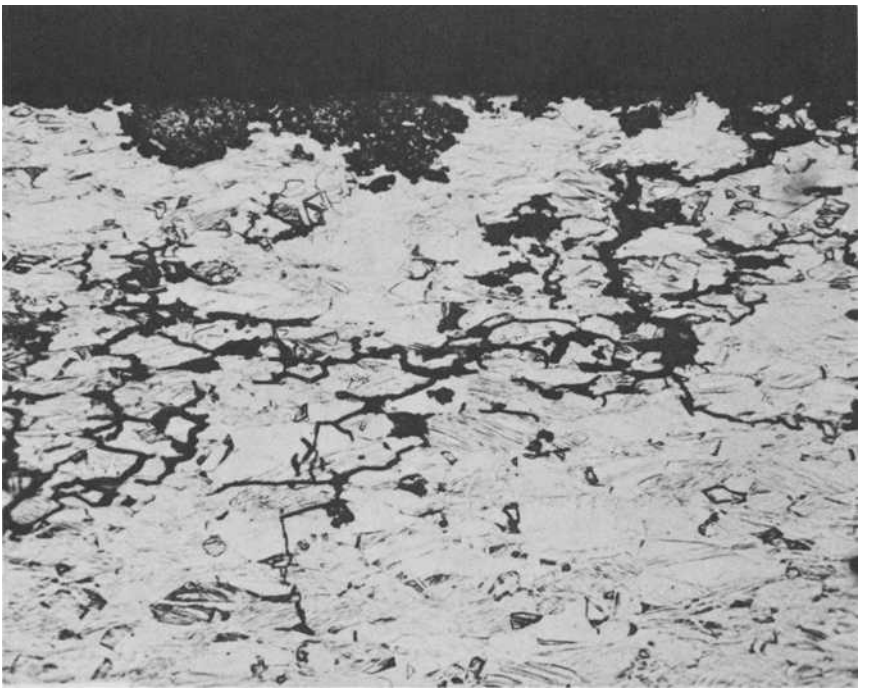

FIG. 2—*Alloy C66900; East Alton, 4 years; surface-initiated SCC with significant subsurface branching. Mixed crack morphology, primarily intergranular with slight transgranular behavior evident. Note extensive surface plug-type dealloying* (×200).

(C76200) and B122 (C77000) were also susceptible to stress corrosion in the industrial sites. However, crack morphology was exclusively transgranular. The aluminum brasses B111 (C68700) and (C68800) were also susceptible to SCC in the industrial atmospheres with transgranular crack morphology. However, failure times were much longer than for other failed materials. Admiralty brass B171 (C44300) also failed in the industrial environments with transgranular crack morphology.

In the marine environment, only two alloys, B122 (C77000) and (C66900), failed by stress-corrosion cracking. Crack morphologies were transgranular and mixed, respectively.

Discussion

Excluding the brasses at high zinc levels (≥15 percent), (C42200), (C68800), and the nickel-silver alloys, the marine environment produced the highest weight losses overall after 4 years' exposure (Table 5). Reproducibility of triplicate weight loss values, where applicable, was excellent and well

FIG. 3—*Alloy B122 (C76200); East Alton, 4 years; surface-initiated SCC with a transgranular morphology (×375).*

within the 10 percent of mean-value test criteria established for data rejection. Corresponding corrosion rate calculations based on weight loss data after 4 years' exposure reveal that, overall, the copper-base alloys were corroding at less than 25.4 μm/year [<1 mil per year (mpy)]. This would suggest that the copper oxides formed on all alloys were protective. However, as will be discussed shortly, this was not necessarily the case, since many alloys suffered from localized corrosion. Consequently, care should be exercised in using weight loss data alone. In addition to weight loss data, corresponding localized corrosion resistance data should be provided and utilized when considering metal usage in various atmospheric environments [*5*].

Reviewing the localized corrosion susceptibility results (Table 3) from the standpoint of alloying additions, the addition of zinc to copper appears to be

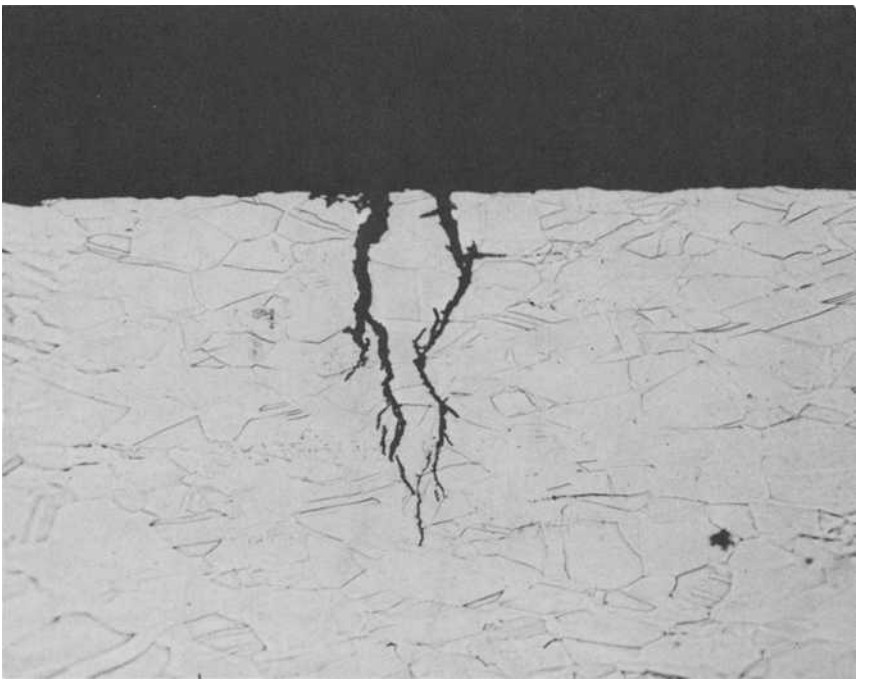

FIG. 4—*Alloy B122 (C77000); New Haven, 4 years; exposed surface-initiated SCC showing a transgranular morphology (×375).*

detrimental in that selective removal of zinc from the copper matrix is observed to occur in the marine (high chloride containing) environment even at low zinc levels (<15 percent). This attack is localized (plug type) and appears as small areas of copper on the yellow brass surfaces. Dezincification, as it is most commonly referred to and seen by previous investigators [*1,6,7*], was observed to increase in frequency with increasing zinc levels. In industrial environments, dezincification did not occur, however, until the level of zinc exceeded 15 weight percent. Additions of tin to a copper-phosphorous alloy (B103 series) in amounts exceeding 4 weight percent result in susceptibility to pitting and crevice attack in the industrial environments. Longer exposure times are required to determine whether pits will further propagate or initiate on those alloys not showing pitting attack to date.

Reduction of zinc to approximately 10 weight percent and addition of 1.5 weight percent iron and 0.5 weight percent cobalt (C66400) eliminated dealloying; however, slight pitting and crevice corrosion susceptibility were still seen in the marine environment. The addition of manganese to a 30 percent zinc alloy (C66900) significantly reduces the corrosion resistance. Severe

TABLE 4—*Corrosion product appearance as a function of time and location.*

ASTM (CDA) Alloy Designation	New Haven		Daytona Beach		East Alton	
	2 Years	4 Years	2 Years	4 Years	2 Years	4 Years
B370(C10200)	orange-brown	gray-brown	brown	brown	brown	white-spots-dark brown
B152(C11000)	red-brown[a]	green-brown[a,b]	red-brown[a]	green-red-brown[a,c]	brown	white spots-dark brown
B465(C19400)	. . .	brown[a]	brown[a]	red-brown[a,c]	dark brown	white spots-dark brown
(C19500)	dark brown	dark brown	brown	brown	brown	green-white spots-dark brown
B36(C22000)	brown	brown	brown	brown	brown	white spots-dark brown
B36(C23000)	brown[a]	yellow spots-brown[a]	green-brown[a,c]	green spots-brown[a,c]	brown	white spots-dark brown
B36(C26000)	dark brown[a]	dark brown[a]	gold[a]	gold-brown[a]	brown	white spots-dark brown
B591(C42200)	red-brown[a]	yellow spots-brown[a]	brown[a]	green-brown[a,c]	brown	white spots-dark brown
B591(C42500)	brown	white spots-brown	brown	green-brown[c]	green-dark brown	dark green-brown
B103(C51000)	red-brown[a]	green spots-brown[a,c]	red-brown[a]	green-red-brown[a,c]	dark green-brown	dark green-brown
B103(C51100)	orange-brown	brown	red-brown	green-red-brown[c]	green-brown[c]	white spots-dark brown
B103(C52100)	light green-brown[c]	light green-brown[c]	green-red-brown[b]	green-red-brown[c]	green-brown[c]	white spots-dark brown
(C63800)	light brown	white spots-yellow-brown	brown	brown	brown	white spots-dark brown
(C66400)	brown	white spots-brown	brown	brown	dark green-brown	dark green-brown
(C66900)	dark brown	white spots-dark brown	dark brown	dark brown	light brown	white spots-dark brown

TABLE 4—*Continued.*

ASTM (CDA) Alloy Designation	New Haven		Daytona Beach			
	2 Years	4 Years	2 Years	4 Years	2 Years	4 Years
(C68800)	light brown	light green-brown[c]	gold-brown	light gold	light brown	white spots-dark brown
B432(C70600)	brown	gray-brown	brown	red-brown near edges	green-brown[b]	white spots-brown
(C72500)	brown	gray-brown	brown	brown	brown	dark green-brown
B122(C75200)	light brown	white spots-brown	light brown	green-light brown[b]	dark brown	dark brown
B122(C76200)	brown	white spots-brown	light brown	green-light brown[b]	dark brown	white spots-brown
B122(C77000)	brown	white spots-brown	green-brown[a]	green[a,d]	dark brown	white spots-dark brown

[a] Data previously reported in *ASTM STP 558.*
[b] Slight degree of uniform patina.
[c] Spots of patina formation over exposed surface.
[d] Moderate degree of uniform patina.

TABLE 5—*Flat panel atmospheric corrosion program: average weight loss versus time (mg/cm^2), 2- and 4-year results at three locations.*

ASTM Designation	CDA Alloy	East Alton		New Haven		Daytona Beach	
		2 Years	4 Years	2 Years	4 Years	2 Years	4 Years
B370	C10200	3.1	5.0	2.0	4.5	5.6	11.1
B152	C11000	1.9	5.2	1.9[a,b]	3.8[a,b]	4.6[a,b]	8.0[a,b]
B465	C19400	2.0	5.4	1.7[a,b]	3.8[a,b]	3.4[a,b]	5.4[a,b]
	C19500	3.7	6.5	1.8	3.3	4.4	8.4
B36	C22000	2.9	5.0	1.5	3.4	3.1	5.8
B36	C23000	1.8	5.3	1.6[a,b]	3.7[a,b]	1.5[a,b]	2.3[a,b]
B36	C26000	1.7	5.3	2.2[a,b]	4.6[a,b]	0.7[a,b]	1.2[a,b]
B591	C42200	1.7[b]	5.2	1.8[a,b]	4.2[a,b]	2.4[a,b]	3.5[a,b]
B591	C42500	2.7	4.6	1.6	4.0	3.4	6.2
B103	C51000	1.9[b]	4.2	2.1[a,b]	4.6[a,b]	6.9[a,b]	9.7[a,b]
B103	C51100	3.5	6.2	1.6	3.9	6.8	9.1
B103	C52100	2.1	5.7	1.2	4.8	6.1	12.2
	C63800	1.4	4.3	1.4	2.8	2.7	4.7
	C66400	2.8	6.2	1.6	5.1	2.6	6.5
	C66900	1.8	5.5	2.3	2.9	4.0	7.6
	C68800	1.2[b]	4.1	1.2	2.1	0.9	1.9
B432	C70600	2.5	4.6	1.5	3.3	2.7	4.6
	C72500	1.9[b]	5.6	1.8	3.8	3.3	6.2
B122	C75200	1.8[b]	5.0	2.2[b]	3.4	1.1	2.1
B122	C76200	1.7	5.4	2.2[b]	3.7	1.1	2.4
B122	C77000	1.6[b]	5.2	2.4[a,b]	3.6	1.0	2.1

[a] Data previously reported in *ASTM STP 558.*
[b] Average of duplicate specimens only.

dealloying and SCC of (C69900) were observed in all environments. The silicon bronze alloy (C63800) shows some minor dealloying in all environments. The nickel-silver, B122 (C75200), was observed to be susceptible to crevice attack only in the marine environment, whereas B122 (C76200), with higher zinc and lower nickel levels, was susceptible to slight dealloying and SCC only in the industrial environment. The high-zinc high-nickel alloy, B122 (C77000), was susceptible to SCC in all environments and pitting in the marine and industrial atmospheres. It may be noted that SCC in susceptible alloys was related to residual stamping stresses as a result of applying identification marks and that not all alloys found susceptible in the U-bend program cracked in the atmospheric panel program. This was undoubtedly due to considerable variations in residual stresses due to differences in stamping techniques.

In most cases where localized corrosion was evident, elongation was significantly reduced [20 percent or greater (Table 2)]. The effect of localized forms of corrosion and changes in elongation has been discussed in previous work [*2*]. However, percent elongation is also affected by localized forms of corrosion, which, in some cases, cannot be seen with the naked eye [for ex-

TABLE 6—*Stress corrosion resistance of copper-base alloys as a function of time and atmospheric environment.*

ASTM (CDA) Alloy Code	Temper, % cold-rolled	Time to Failure, years (days)				Crack Morphology[a]			
		New Haven (NH)	Brooklyn (BR)	East Alton (EA)	Daytona (D)	NH	BR	EA	D
B152 (C11000)	37%	NF[b] 11.8	NF 9.2	NT[c]	NF 12.1	. . .	. . .	. . .	. . .
B152 (C11000)	extra hard	NF 5.9	NT	NF 5.9	NT	. . .	. . .	. . .	. . .
B465 (C19400)	37%	NF 11.8	NF 9.2	NT	NF 12.1	. . .	. . .	. . .	. . .
B465 (C19400)	extra hard	NF 5.9	NT	NF 5.9	NT	. . .	. . .	. . .	. . .
(C19500)	90%	NF 6.6	NF 3.9	NT	NF 6.5	. . .	. . .	. . .	. . .
B36 (C23000)	37%	NF 11.8	NF 9.2	NT	NF 12.1	. . .	. . .	. . .	. . .
B36 (C23000)	extra hard	NF 5.9	NT	NF 5.9	NT	. . .	. . .	. . .	. . .
B36 (C26000)	hard	(29–49)	(0–23)[d]	NT	NF 6.0	I	I	. . .	. . .
B36 (C26000)	extra hard	(14–44)[d]	NT	(19–29)[d]	NT	I	. . .	I	. . .
B121 (C35300)	50%	(51–136)[d]	(70–104)[d]	NT	NF 6.0	T + (I)	T + (I)	. . .	. . .
B591 (C42200)	37%	NF 11.8	NF 9.2	NT	NF 12.1	. . .	. . .	. . .	. . .
B591 (C42500)	extra hard	NF 7.0	NF 1.1	NT	NF 7.0	. . .	. . .	. . .	. . .
B591 (C42500)	extra hard	NF 6.9	NT	NF 5.9	NT	. . .	. . .	. . .	. . .
B171 (C44300)	10%	NF 6.0	NF 3.4	NT	NF 6.0	. . .	. . .	. . .	. . .
B171 (C44300)	40%	(51–95)[d]	(41–70)[d]	NT	NF 6.0	T	T	. . .	. . .

B171 (C44300)	40% + ordered[e]	(51–67)[d]	(33–49)[d]	NT	NF 6.0	T	T	. . .	. . .
B103 (C51000)	37%	NF 11.8	NF 9.2	NT	NF 12.1	. . .	. . .	. . .	. . .
B103 (C51000)	extra hard	NF 5.9	NT	NF 5.9	NT	. . .	. . .	. . .	. . .
B103 (C52100)	37%	NF 11.8	NF 9.2	NT	NF 12.1	. . .	. . .	. . .	. . .
B103 (C52100)	extra hard	NF 5.9	NT	NF 5.9	NT	. . .	. . .	. . .	. . .
(C63800)	50%	NF 9.1	NF 6.5	NT	NF 9.0	. . .	. . .	. . .	. . .
(C63800)	extra hard	NF 5.9	NT	NF 5.9	NT	. . .	. . .	. . .	. . .
(C66900)	annealed	(0–30)	(0–211)	NT	NF 6.5	I(T)	I(T)	. . .	. . .
(C66900)	extra hard	(0–7)	(0–19)	NT	(2–7)	I(T)	I(T)	. . .	I(T)
B111 (C68700)	10%	(517–540)[d]	2.3[d] NF 3.4	NT	NF 6.0	T	T	. . .	. . .
B111 (C68700)	40%	(221–495)[d]	(311–362)[d]	NT	NF 6.0	T	T	. . .	. . .
B111 (C68700)	40% + ordered[e]	(216–286)[d]	(143–297)[d]	NT	NF 6.0	T	T	. . .	. . .
(C68800)	10%	NF 6.0	NF 3.4	NT	NF 6.0	. . .	. . .	. . .	. . .
(C68800)	40%	4.7–NF 6.0	2.7 NF 3.4	NT	NF 6.0	T	T	. . .	. . .
(C68800)	40% + ordered[e]	3.6–3.7	NF 3.4	NT	NF 6.0	T	. . .	. . .	. . .
(C68800)	extra hard	NF 5.9	NT	(1484)	NT	. . .	. . .	T	. . .
B432 (C70600)	50%	NF 5.5	NF 3.1	NT	NF 5.5	. . .	. . .	. . .	. . .
B432 (C70600)	extra hard	NF 5.9	NT	NF 5.9	NT	. . .	. . .	. . .	. . .
(C72500)	40%	NF 5.5	NF 3.1	NT	NF 5.5	. . .	. . .	. . .	. . .
(C72500)	extra hard	NF 5.9	NT	NF 5.9	NT	. . .	. . .	. . .	. . .
B122 (C75200)	50%	NF 6.6	NF 3.9	NT	NF 6.5	. . .	. . .	. . .	. . .
B122 (76200)	50%	(142–270)[d]	(236–282)[d]	NT	NF 6.5	T	T	. . .	. . .
B122 (C76200)	extra hard	(378–396)	NT	(542–773)	NT	T	. . .	T	. . .

TABLE 6—*Continued.*

ASTM (CDA) Alloy Code	Temper, % cold-rolled	Time to Failure, years (days)				Crack Morphology[a]			
		New Haven (NH)	Brooklyn (BR)	East Alton (EA)	Daytona (D)	NH	BR	EA	D
B122 (C77000)	50%	(153–337)[d]	(489–540)[d]	NT	(692–970)[d]	T	T	. . .	T
B122 (C77000)	extra hard	(378–610)	NT	(542–636)	NT	T	. . .	T	. . .

[a] I = intergranular, T = transgranular. Parentheses indicate minor mode.
[b] NF = no failures in time specified.
[c] NT = not tested.
[d] Data previously reported.
[e] Heated @ 204°C (399°F) for 1/2 h.

FIG. 5—*Alloy B36(C26000); New Haven crack morphology is exclusively intergranular (×400).*

ample, B370 (C10200), and (C19500)]. Clearly seen is a correlation between localized corrosion susceptibility and reduction in percent elongation. Reinhart [*8*], in his corrosion studies of copper-base alloys in hydrospace after short-term exposure, concludes similarly that elongation is reduced greatly as a result of localized corrosion.

The degree of patination is alloy, time, and environment-specific [*1,6,9*]. The results show that 4 years, in general, is too short a time to effectively develop the normal green patina to any significant degree. However, other copper oxides formed (Table 4) produce a variety of colors and textures. It is not known whether longer exposure times will significantly change the appearance of the various alloys included in this atmospheric corrosion program. Under the present test duration criteria, we will be able to determine final oxide color(s) and protective nature after 20 years in two industrial and one marine environment. Oxide investigations, including chemical analyses, are being deferred until the 12- or 20-year withdrawal period.

Table 6 highlights the relative stress corrosion resistance of 20 copper-base alloys after exposure as preformed U-bends to three industrial and one marine environment for up to 12 years. The high-copper alloys, including the low-zinc-containing brass B36 (C23000), were not susceptible to SCC in any

FIG. 6—*Alloy B121 (C35300); Brooklyn crack morphology is primarily transgranular* (×*1675*).

environment up to 12.1 years' exposure. Some of the alloys were susceptible to SCC only in the industrial environments. Only two alloys were susceptible in the marine environment. Crack morphology was found to be more dependent on alloy composition than temper.

Atmospheric condition was also a factor but was of a second order when considering SCC susceptibility of the various alloys investigated. All alloys which failed contained zinc as a major alloying addition at levels greater than 20 weight percent. With this fact in mind, it is possible to assess with some degree of confidence the influence of other alloying additions to the copper-zinc system with respect to atmospheric stress-corrosion behavior.

Considering the industrial environments and zinc levels in copper of from 26 to 30 weight percent, the addition of nickel at high levels (that is, B122 alloys) is preferred. The addition of 1 weight percent tin B171 (C44300) appears to marginally improve SCC resistance. The addition of nickel and tin to the 30 weight percent zinc in copper alloy changed crack morphology from intergranular to transgranular. At a zinc level of 20 to 23 weight percent, additions of aluminum may be beneficial [for example, B111 (C68700) and (C68800)]. In all cases at low zinc levels or in alloys with tin and phosphorous additions (B103 alloys), no failures have been observed to date.

In the marine environment, the nickel-silver B122 (C77000) was suscepti-

ble to SCC with crack morphology being transgranular. The copper-zinc manganese alloy (C66900) was highly susceptible to SCC at the marine site. The effect of cold work is also quite evident with harder tempers having most rapid times-to-failure.

Some low-stacking-fault-energy alloys [for instance, B171 (C44300) and B111 (C68700)] had shorter times to failure in the industrial atmospheres after ordering at 204°C (399°F) for 30 min from an original 40 percent cold-work temper [*10*]. It is necessary to be particularly careful in selecting a suitable stress-relief annealing temperature in these materials. The majority of alloys tested were predominately single phase, with the exception of the aluminum brass (C68800) and the leaded brass [B121 (C35300)]. The presence of second-phase particles in (C68800) cannot be assessed. The lead particles in the leaded brass [B121 (C35300)] provided some increase in stress corrosion resistance when compared with the single-phase brass alloy B36 (C26000) at the same zinc level. This is probably due to the fact that second-phase particles in the grain boundaries act as barriers to crack propagation.

Those copper alloys subject to SCC in the panel portion of the atmospheric program were observed to have identical crack morphologies as the same metal exposed in the preformed U-bend condition. This was true also with respect to environment. Not all alloys subject to SCC susceptibility in the stressed portion of the program cracked as a result of exposure as a flat panel. Evidentally, stamping in these metals did not produce additional residual stress significant enough to induce SCC to date.

Current theories of SCC cannot be fully utilized to explain the atmospheric stress-corrosion results observed in this study. However, certain factors can be considered. A mechanism has been proposed recently [*11*] to explain SCC in brasses involving a stress-assisted dealloying mechanism. This would certainly appear to be a possibility in those environments where dealloying has been observed to occur. In addition, the protective properties of the copper oxide (Cu_2O) corrosion product film are important in determining whether cracking will initiate or propagate. It is known that minor elemental additions can significantly change the structure and properties of the resultant copper oxide which will influence corrosion performance [*12,13*]. Further, the atmospheric environment will play a role in determining whether alloys will form a protective film or can support a stress-assisted dealloying mechanism. It would appear that all environments are supportive of each or either of these mechanisms, depending on alloy composition.

Conclusions

1. Weight loss measurements alone do not reliably predict corrosion performance of copper-base alloys in natural atmospheres. Localized corrosion is more important and should be considered together with weight loss date.

2. Elongation is the only mechanical property sensitive to localized forms of corrosion after short-term atmospheric exposure.

3. The 4-year test period is not sufficient to predict long-term atmospheric corrosion behavior.

4. Very few of the alloys tested had developed the normally expected patina during 4 years' exposure to marine and industrial environments.

5. Corrosion performance is dependent on both alloy composition and environment.

6. The only alloys which were susceptible to stress corrosion cracking contained zinc levels in excess of 15 percent.

7. Industrial environments are much more severe than marine environments in causing stress-corrosion cracking. Only two alloys, a manganese-brass and a nickel-silver, cracked in the marine environment.

Acknowledgments

The authors wish to thank the Brass Group of Olin Corp. for permission to publish the results. The experimental work of M. Heine is also acknowledged. The authors are indebted to Messrs. J. Poulton and K. Farquharson for their metallographic and photographic endeavors.

References

[*1*] Herman, R. S. and Castillo, A. P. in *Corrosion in Natural Environments, ASTM STP 558*, American Society for Testing and Materials, 1975, pp. 82–96.

[*2*] Popplewell, J. M. and Gearing, T. V., *Corrosion*, Vol. 31, No. 8, Aug. 1975, pp. 279–286.

[*3*] Thompson, D. H. in *Metal Corrosion in the Atmosphere, ASTM STP 435*, American Society for Testing and Materials, June 1968, p. 140.

[*4*] Fontana, M. G. and Green, N. D., *Corrosion Engineering*, McGraw-Hill, New York, 1967, p. 125.

[*5*] Carter, V. E. in *Metal Corrosion in the Atmosphere, ASTM STP 435*, American Society for Testing and Materials, June 1968, p. 270.

[*6*] Mattsson, E. and Holm, R. in *Metal Corrosion in the Atmosphere, ASTM STP 435*, American Society for Testing and Materials, June 1968, p. 187 and p. 209.

[*7*] Vernon, W. H. J., *Transactions*, Faraday Society, Vol. 23, 1927, pp. 113–205.

[*8*] Reinhart, F. M. in *Corrosion in Natural Environments, ASTM STP 558*, American Society for Testing and Materials, August 1975, p. 169.

[*9*] Veron, W. H. J., *Journal of the Institute of Metals*, Vol. 49, 1932, pp. 153–166.

[*10*] Popplewell, J. M., Proctor, R. P. M., and Ford, J. A., *Corrosion Science*, Vol. 12, 1972, p. 193.

[*11*] Polan, N. W., Popplewell, J. M., and Pryor, M. J., *Journal of the Electrochemical Society*, Vol. 126, No. 7, July 1979, p. 1300.

[*12*] Popplewell, J. M., Hart, R. J., and Ford, J. A., *Corrosion Science*, Vol. 13, 1973, p. 295.

[*13*] Pryor, M. J. and North, R. F., *Corrosion Science*, Vol. 10, 1970, p. 297–311.

R. Holm[1] *and E. Mattsson*[2]

Atmospheric Corrosion Tests of Copper and Copper Alloys in Sweden—16-Year Results

REFERENCE: Holm, R. and Mattsson, E., **"Atmospheric Corrosion Tests of Copper and Copper Alloys in Sweden—16-Year Results,"** *Atmospheric Corrosion of Metals, ASTM STP 767,* S. W. Dean, Jr., and E. C. Rhea, Eds., American Society for Testing and Materials, 1982, pp. 85–105.

ABSTRACT: In 1958, exposure tests were started in rural, marine, and urban atmospheres in Sweden, covering 36 copper alloys in sheet or rod form. Test results after two and seven years' exposure have been reported earlier. This is the concluding report of the tests as completed after 16 years' exposure.

Greenish coatings had developed on most of the materials after six to seven years at the urban and marine sites. At the rural site, however, no distinct green coating had developed on any material after 16 years, only different shades of black or brown. The amount of patina retained increased substantially from 7 to 16 years of exposure. The patina was found to be more protective in the marine and rural atmospheres than in the urban one. The patina was also examined by X-ray analysis and scanning electron microscopy-EDX.

The average penetration (determined gravimetrically) during 16 years of exposure had stabilized at the following levels:

0.3 to 0.5 μm/year in rural atmosphere
0.5 to 0.9 μm/year in marine atmosphere
0.9 to 1.3 μm/year in urban atmosphere

The dezincification rate of brass had decreased somewhat during the period from 7 to 16 years. It was highest for brasses with an ($\alpha + \beta$)-phase structure, the maximum dezincification depth measured metallographically after 16 years being 90 to 215 μm, the loss in ultimate tensile strength 5 to 15 percent and the reduction in elongation up to 30 percent.

KEY WORDS: copper, copper alloys, atmospheric corrosion tests, field tests, patina coatings, dezincification

In 1958 the investigation reported herein was started. The aim was to gain knowledge of the behavior of a comprehensive selection of copper alloys under atmospheric conditions common in Sweden. It was also our particular

[1] Corrosion metallurgist, Gränges Metallverken, Research and Development, S-72188 Västerås, Sweden.
[2] Director, Swedish Corrosion Institute, Box 5607, S-11486 Stockholm, Sweden.

intention to study the surface coatings formed during exposure, with respec to color and composition in relation to the atmospheric conditions on the tes sites as recorded continuously during exposure. Results from two and sever years' exposure were reported in connection with an ASTM symposium.[3] This paper forms a concluding report covering results from the tests as completed after 16 years of exposure.

Materials

The investigation covered 36 alloys in sheet or rod form: 5 coppers, 20 brasses, 5 phosphor bronzes, 1 silicon bronze, 1 aluminum bronze, 1 cadmium bronze, 2 nickel silvers, and 1 free-cutting phosphor bronze. The composition of the alloys is given in Table 1.

The sheet specimens were cut from soft annealed sheet mainly from production runs, except for a few alloys which had been specially made in the laboratory (Table 1). The panels were vapor degreased in trichloroethylene, then pickled in bright dip (a mixture of equal volumes of concentrated nitric acid and concentrated sulfuric acid), and finally rinsed in deionized water. The rod specimens were also made of soft annealed material from production runs except for an experimental arsenical brass. After turning, the rod specimens were degreased and pickled in the same way as the panels. The specimens were stored indoors for four weeks in order to develop the naturally occurring invisible thin oxide film before exposure outdoors.

Exposure Conditions

Specimens of the alloys were exposed on three sites in Sweden, representing rural, marine, and urban atmospheres:

1. Erken in central Sweden, with a rural atmosphere.
2. Bohus Malmön on the west coast, with a marine atmosphere.
3. Stockholm, with an urban atmosphere.

The principal atmospheric contaminants on the sites, determined through continuous recording during the exposure, are given in Table 2.

The specimens were mounted by means of porcelain insulators on racks of galvanized steel at an inclination of 30 deg to the horizontal with a southward orientation. The sheet specimens had the dimensions 150 by 100 by 1 mm, while the shape and the dimensions of the rod specimens were as shown in our earlier paper (footnote 3).

Evaluation of Results

Exposed specimens have been taken in and examined in comparison with unexposed reference specimens of the same age on three occasions, that is,

[3] Mattsson, E. and Holm, R. in *Metal Corrosion in the Atmosphere, ASTM STP 435,* American Society for Testing and Materials, 1968, pp. 187–210.

TABLE 1—*Copper and copper alloys exposed.*

Type of Material	UNS[b]-Number	ISO[c]-Designation
Sheet		
electrolytic tough pitch copper	C11000	Cu-ETP
silver-bearing copper	(C11500)	CuAg(P)
phosphorized arsenical copper	C14200	Cu-DPA
tin-bearing copper	C50500	CuSn1
β-brass[a]	. . .	CuZn50
Muntz metal[a]	C28000	CuZn40
yellow brass	C27200	CuZn37
cartridge brass	(C26000)	CuZn28
red brass	C23000	CuZn15
commercial bronze	(C22000)	CuZn8
low-leaded brass	C33500	CuZn37Pb
arsenical aluminum brass	C68700	CuZn22Al2As
arsenical admiralty brass	C44300	CuZn28Sn1As
silicon bronze	C65500	CuSi3Mn1
phosphor bronze	C50900	CuSn3(P)
phosphor bronze[a]	C51000	CuSn5
phosphor bronze	C52100	CuSn7(P)
phosphor bronze	C52400	CuSn9(P)
phosphor bronze[a]	C52400	CuSn9
free-cutting phosphor bronze[a]	(C83600)	CuZn4Sn4Pb4
nickel silver	C75700	CuNi12Zn24
nickel silver	C75900	CuNi18Zn20
Rod		
leaded copper	C18700	CuPb1
leaded brass	C35000	CuZn38Pb1
free-cutting brass	C38590	CuZn40Pb3
architectural bronze	(C38000)	CuZn42AlPb
special brass	. . .	CuZn35Mn2Sn1AlFeNiPb
special brass	. . .	CuZn36Mn5.5Al3.5
special brass	. . .	CuZn30Al2Pb2Mn
special brass	C67000	CuZn24Al4.5Mn3.5Fe2
special brass	. . .	CuZn39Mn1.5Pb
special brass	. . .	CuZn39Si
special brass	. . .	CuZn36Pb2Sn1Fe
aluminum bronze	C63200	CuAl10Fe5Ni5
cadmium bronze	C16200	CuCd1
arsenical yellow brass[a]	. . .	CuZn37As

[a] Produced in the laboratory.
[b] UNS = Unified Numbering System for Metals and Alloys (ASTM, SAE).
[c] ISO = International Standardization Organization.

after 2 years (duplicate specimens), 7 years (triplicate specimens), and 16 years (triplicate specimens). The examination included the following steps:

1. Visual inspection.
2. Color determination and color photography (also performed at shorter intervals during the first year of exposure).
3. Analysis of corrosion products, including depth profile determinations for certain specimen surfaces.
4. Gravimetric determination of metal loss and amount of adhering cor-

TABLE 2—*Approximate annual mean values of principal atmospheric contaminants (sulfur oxides in the atmosphere, sulfate in the precipitation, all given as S, chloride as Cl) and pH-value of precipitation on the test sites during the period of exposure, that is, 1958 to 1974.*

Test Site	Contaminants				
	In Air, $\mu g/m^3$		By Precipitation, mg/m^2, year		pH-Value in Precipitation
	S	Cl	S	Cl	
Rural (Erken)	8	2	600	240	4.9
Marine (Bohus Malmön)	8	100	2200	9500	4.5
Urban (Stockholm)	75	3	1400	800	4.7

rosion products for sheet specimens (the corrosion products were removed by 10 percent sulfuric acid with mild brushing).

5. Metallographic examination of cross sections.

6. Determination of changes in ultimate tensile strength (UTS) and elongation.

Results

The most important effects of atmospheric corrosion on copper-base materials are patina formation, general corrosion, and dezincification of the high-zinc brasses.

Color Change

As for color changes, mainly the panels were observed. The appearance of the upper surfaces of the panels after 7 and 16 years' exposure is described in Table 3. During the first years of exposure, general darkening took place. In the urban and rural atmospheres the color of the copper gradually changed to black during the first year, more rapidly in the urban than in the rural atmosphere. In the marine atmosphere the copper acquired a brownish appearance during the first year. After the initial stage of darkening, a green patina appeared on some alloys, especially in the urban atmosphere.

As a general observation it should be added that the undersides of the panels exposed for 16 years have not developed a green patina, but show instead different shades of grayish brown to black.

Coppers—The surface appearance of copper and low-alloyed coppers after 16 years' exposure at the marine and urban sites shows no appreciable differences between the alloys; it is characterized by a uniform green patina with a bluish tinge. The surfaces at the rural site still show blackish shades with no definite signs of green, which also applies to the downsides of the sheet specimens at all three sites. As stated in our earlier paper (footnote 3) appreciable signs of green patina on coppers were observed after 6 to 7 years at the urban and marine sites.

Brasses—The brasses deviate in surface appearance from the coppers in

TABLE 3—*Appearance of panels after 7- and 16-years' exposure.*

Alloy		Type of atmosphere					
		Rural		Marine		Urban	
Type	ISO	7 years	16 years	7 years	16 years	7 years	16 years
Coppers	Cu - ETP	Uniform black	Uniform sparse gray on black	Uniform sparse grayish blue-green on brownish black	Brownish gray-white	Uniform dense grayish blue-green	Uniform white-green
	Cu Ag (P)						
	Cu - DPA				Sparse gray-green on black	Partly grayish blue-green, partly black	
Binary brasses	Cu Zn 8		Greenish black		Uniform gray-brown	Uniform grayish green	Uniform green
	Cu Zn 15		Uniform black	Nearly uniform sparse grayish green on brownish black		Unif. yellowish gray-green	Brownish green
	Cu Zn 28					Partly yellowish gray-green/black	
	Cu Zn 37				Sparse blue-green on black	Uniform black	Uniform black
	Cu Zn 40				Uniform gray-black	Partly grayish/reddish black	
	Cu Zn 50						
Special brasses	Cu Zn 37 Pb				Uniform gray-brown	Uniform sparse yellowish green on black	Brownish green
	Cu Zn 28 Sn 1 As			Nearly uniform grayish blue-green		Nearly uniform yellowish green	Uniform green
	Cu Zn 22 Al 2 As	Uniform brownish black	Uniform green-black	Nearly uniform brownish gray	Sparse green-white on brown	Uniform black	White-green
Nickel silvers	Cu Ni 12 Zn 24	Uniform brownish black	Uniform black	Uniform sparse grayish on brownish black	Uniform brown	Nearly uniform brownish gray-green	Uniform green green on black
	Cu Ni 18 Zn 20						
Phosph. bronzes	Cu Sn 1	Uniform black	Uniform sparse gray on black	Uniform sparse gray blue-green/brownish black	Sparse brown on grayish green	Uniform grayish green	Uniform green
	Cu Sn 3 (P)	Uniform brownish black	Sparse brown on gray	Uniform grayish blue-green		Nearly uniform black	
	Cu Sn 5		Gray-brown	Uniform sparse gray blue-green/brownish black		Partly grayish blue-green/black	
	Cu Sn 7 (P)	Uniform yellowish black	Brown	Uniform grayish blue-green		Uniform grayish green	Dense green
	Cu Sn 9 (P)		Light gray-brown			Uniform dense grayish green	Sparse white on dense green
	Cu Sn 9		Brown-green	Uniform sparse gray blue-green/brownish black	Grayish brown	Uniform black	Dense green
Other bronzes	Cu Zn 4 Sn Pb 94	Uniform	Uniform sparse gray on black	Uniform sparse grayish blue-green on brownish black	Sparse brown on grayish green	Nearly uniform grayish green	Uniform green
	Cu Si 3 Mn 1		Black		Grayish brown	Uniform sparse grayish green on black	Grayish green

showing brownish green tinges in the urban and more grayish ones in the marine atmosphere, the shade being darker for brasses with high zinc contents. In the rural atmosphere all brass surfaces have remained black.

Phosphor bronzes—The phosphor bronzes with 3 to 9 percent tin exposed at marine and urban sites show, in general, uniform, somewhat denser green patinas than plain copper, whereas they have remained dark with occasional grayish shades at the rural site.

Composition of Corrosion Products

The composition of the corrosion products after 7 years' exposure was determined by X-ray analysis (XRD) (footnote 3). The surface coatings formed

during exposure had in general copper oxide (Cu_2O) as a principal component. Further, basic copper salts were present, predominantly basic chloride [$Cu(OH)_{1.5}Cl_{0.5}$] and sulfate [$Cu(OH)_{1.5}(SO_4)_{0.25}$] in the marine, basic sulfate in the urban, and basic sulfate and nitrate [$Cu(OH)_{1.5}(NO_3)_{0.5}$] in the rural atmosphere. The basic carbonate [$CuOH(CO_3)_{0.5}$] occurred only rarely in the rural and urban atmospheres, but the corrosion products formed in the urban atmosphere in many cases contained carbon.

The adhering corrosion products on the copper alloys often consisted of compounds containing alloying constituents:

1. Zinc sulfate, in some cases basic zinc sulfate, on some of the brasses, especially in urban and marine atmospheres.
2. Lead sulfate, in some cases basic lead sulfate, on free-cutting phosphor bronze and on certain leaded brasses.
3. Silica on silicon bronze in the marine atmosphere.
4. Copper phosphate on some of the phosphor bronzes containing the higher percentage of phosphorus in the urban atmosphere.
5. Copper arsenate on arsenical copper and on some of the arsenical brasses.
6. Nickel sulfate on the nickel silvers in the urban atmosphere.

It should be kept in mind that XRD reveals only crystalline material. This may explain why tin oxide (SnO_2) was not detected on the phosphor bronzes, nor aluminum oxide (Al_2O_3) on the aluminum brasses.

Specimens taken in after 16 years' exposure were subjected to a (semi-quantitative) scanning electron microscopy (SEM) analysis. The results did not indicate any remarkable changes in corrosion product composition in comparison with the 7-year exposure results.

Depth profiles showing the surface layer composition as a function of depth from the surface were determined for sheet specimens of four copper materials exposed for 16 years: low-alloyed copper; α-brass, CuZn28; phosphor bronze, CuSn7(P); and nickel silver, CuNil2Zn24. The depth profiles have been determined mainly by SEM in combination with energy dispersive X-ray analysis (SEM-EDX: Philips PSEM 500 with a Kevex spectrometer), but in some cases also by Auger electron spectroscopy (AES). Profiles determined give percentage compositions in relation to the total substrate metal content. The percentages of other important elements such as carbon, oxygen, sulfur, and chlorine are also determined in relation to total substrate metal content. It should be noted that analysis for carbon and oxygen is not possible with the SEM-EDX device used.

The depth profiles generally confirmed results obtained by other means. The depth profile for phosphor bronze (Fig. 1), however, brought some additional information. The corrosion products on the skyward surface are apparently more depleted in copper than in tin, whereas on the downward sur-

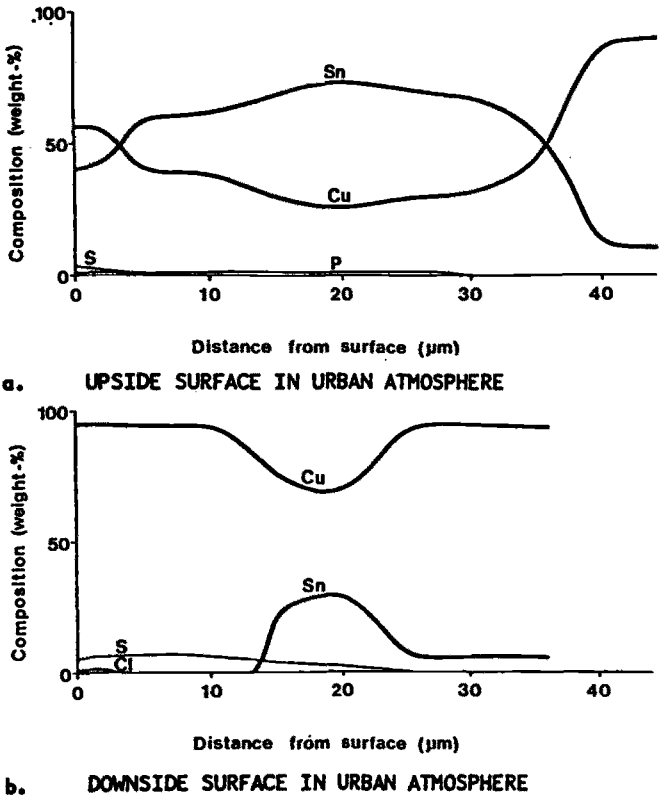

FIG. 1—*Depth profiles (SEM-EDX), representing surfaces of phosphor bronze, CuSn7(P), after 16 years' exposure.*

face an initial stage of tin corrosion (probably internal oxidation) is followed by the formation of copper corrosion products covering the initially formed tin oxide. This result indicates the usefulness of this technique, which might be more extensively used in future work.

Retention of Corrosion Products

The amounts of corrosion products adhering to sheet surfaces have been determined after 7 and 16 years' exposure, Fig. 2. Furthermore, comparisons of amounts of corrosion products related to alloying element content are given in Fig. 3 for the copper-zinc and the copper-tin series, respectively.

The amount has generally increased considerably during the last 9 years of exposure in all types of atmospheres (Fig. 2); in the rural atmosphere the amounts range between 20 and 60 g/m^2 (10 and 45 g/m^2 after 7 years), in the marine atmosphere between 45 and 80 g/m^2 (20 and 55 g/m^2 after 7 years), and in the urban atmosphere between 50 and 120 g/m^2 (25 and 70 g/m^2 after 7 years).

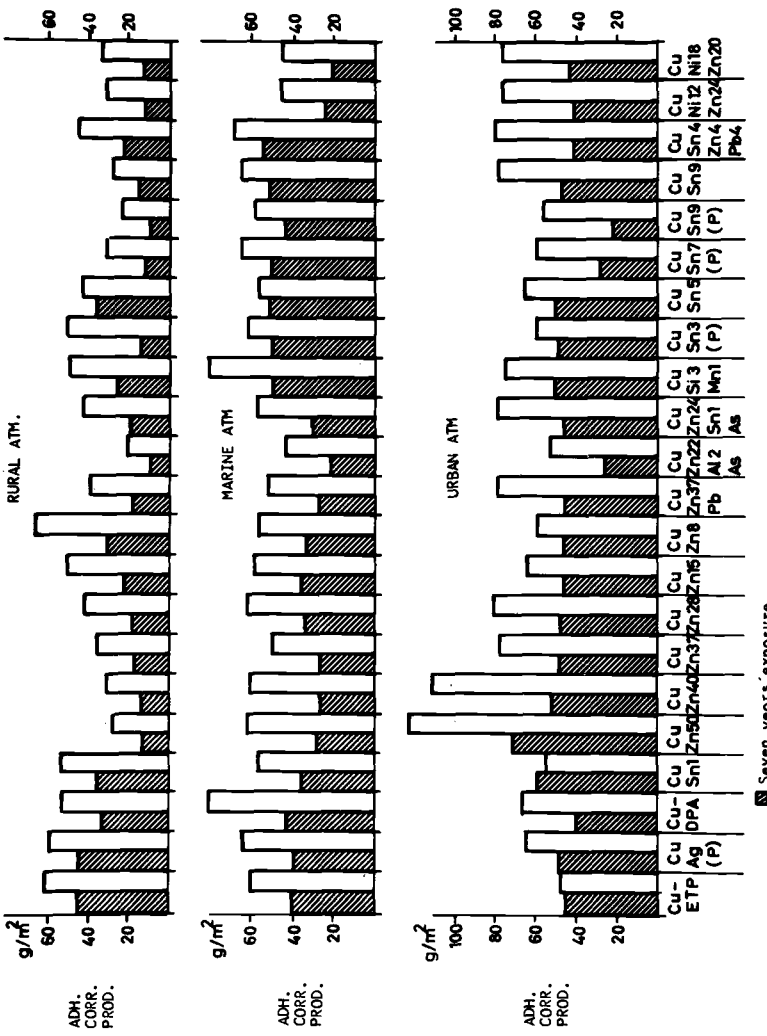

FIG. 2—*Amounts of adhering corrosion products on sheet specimens.*

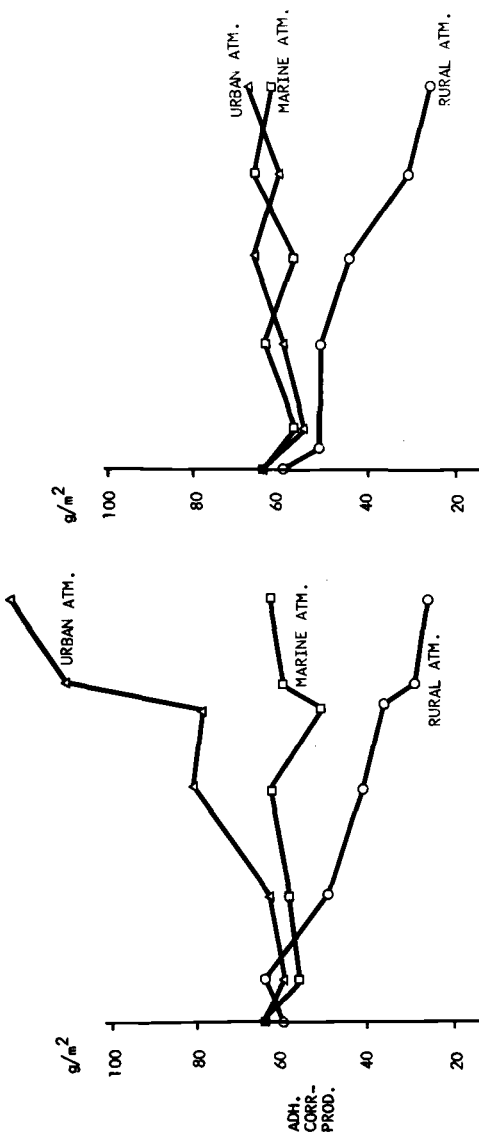

FIG. 3—*Amounts of adhering corrosion products in binary brasses and phosphor bronzes in relation to zinc and tin contents, respectively, after 16 years' exposure.*

The amounts of retained corrosion products on the *copper* panel surfaces (that is, the weight loss found after cleaning) do not differ much from a mean value of 60 g/m^2, that is, an increase of about 20 g/m^2 from the value after 7 years' exposure which applies for all three sites. The relation between retained amount of corrosion products and metal loss (that is, average penetration in g/m^2), however, proves to be lower in the urban atmosphere than in the marine and rural atmospheres. This indicates that the latter environments favor the development of relatively protective corrosion product coatings. The higher dissolution rate of copper observed in the urban atmosphere emphasizes the importance of measures to avoid the risk of blue water staining or microgalvanic corrosion on architectural objects in urban atmospheres.

In the binary *brass* series at the rural site the amounts of retained surface products (essentially corrosion products) increase with decreasing zinc content (from approximately 30 to 70 g/m^2). In the marine atmosphere the amounts are equal, independent of the zinc content (between 50 and 60 g/m^2), and in urban atmosphere they tend to decrease (from 120 to 60 g/m^2) with decreasing zinc content in the brasses, Fig. 3. An explanation could be that the sparingly soluble copper compounds dominate on low-zinc brass surfaces, giving values similar to those for copper surfaces. The zinc sulfate compounds in the corrosion products can be assumed to have a far lower solubility than zinc chloride compounds, which would account for a lower retention of corrosion products on the high-zinc brass surfaces in the marine atmosphere. In the rural atmosphere the zinc corrosion products formed seem to be easily soluble and readily washed away with rain water.

The amounts of corrosion products retained on *phosphor bronzes* decrease with increasing tin content at the rural site (from 50 to 25 g/m^2), but stay about the same (about 60 g/m^2) for different tin contents at the marine and the urban sites, Figs. 2 and 3. This would indicate that the corrosion-inhibitive effect of tin in copper is limited to mildly corrosive conditions.

Types of Corrosion

On the whole, the observations regarding types of corrosion after 16 years of exposure are in agreement with those made after 7 years; this applies to both sheet and rod specimens. The corrosion types are mainly general attack and, for the zinc-rich alloys, dezincification. A close metallographic examination of low-zinc brasses, nickel silvers, and arsenical special brasses has shown that the corrosion observed should be classified as general corrosion instead of dezincification as denoted at the inspection after 7 years of exposure. No signs of other types of corrosion have been observed.

General corrosion—The average penetration of panels has been determined gravimetrically. Unfortunately, however, the notes of the original weights of the panels before exposure have been lost. This has made it necessary to determine metal loss (average penetration) in relation to reference

panels of unexposed sheet from the same batch as the exposed panels and to cut the reference panels as closely as possible to the same size as the exposed panels. After a statistical judgment of the gravimetric accuracy achievable with these reference panels, the following materials were chosen for determination of the average penetration:

1. low-alloyed copper, CuAg(P),
2. α-brass, CuZn28,
3. phosphor bronze, CuSn7(P), and
4. nickel silver, CuNi12Zn24.

These materials represent the principal copper alloy types and their average penetrations are given in Fig. 4. A general observation for these materials is that the average penetration in no case exceeds 1.5 μm/year, and that it decreases in the order urban-marine-rural atmosphere as was also observed from the 7 years' exposure results. The corrosion rates seem to be about the same as or possibly slightly lower than those found after 7 years' exposure, and significantly lower than the rates obtained after 2 years of exposure. The range of rates seems not too wide for the various alloys on each site: 0.9 to 1.3 μm/year in the urban, 0.5 to 0.9 μm/year in the marine, and 0.3 to 0.5 μm/year in the rural atmosphere, the higher values holding for the brass and the lower values for the phosphor bronze and the nickel silver.

The corrosion rates determined in this investigation seem to be of about the same order as those reported in 1956 from a 20 years' test performed by ASTM at various sites in the United States[4] with corrosion rates ranging from 0.4 μm/year at the rural site up to about 2 μm/year at the industrial sites. Later 20-year exposure tests with copper materials in Great Britain reported by Scholes and Jacob in 1970[5] have shown an average penetration of somewhat less than 2 μm/year in industrial atmosphere and 0.7 to 1.5 μm/year in marine atmosphere.

Dezincification—The corrosion of copper alloys with relatively high zinc contents is predominantly of the dezincification type. Average and maximum dezincification depths measured in metallographic cross sections, representing upside and downside surfaces for sheet specimens, and the whole circumference for rod specimens, are given in Figs. 5*a*, 5*b*, and 5*c*. The extent of this type of attack corresponds well to losses in elongation, Fig. 6, and fairly well to losses in UTS, Fig. 7, but is not revealed by the weight loss figures for tested specimens.

The conclusion again emerges that the severity of attack in the various atmospheres decreases in the order urban-marine-rural atmosphere. For

[4] Tracy, A. W. in *Symposium on Atmospheric Corrosion of Non-Ferrous Metals, ASTM STP 175*, American Society for Testing and Materials, 1956, pp. 67–76.

[5] Scholes, I. R. and Jacob, W. R, in *Proceedings*, The Institute of Metals' International Symposium on Copper and Its Alloys, Amsterdam, 21–25 Sept. 1979.

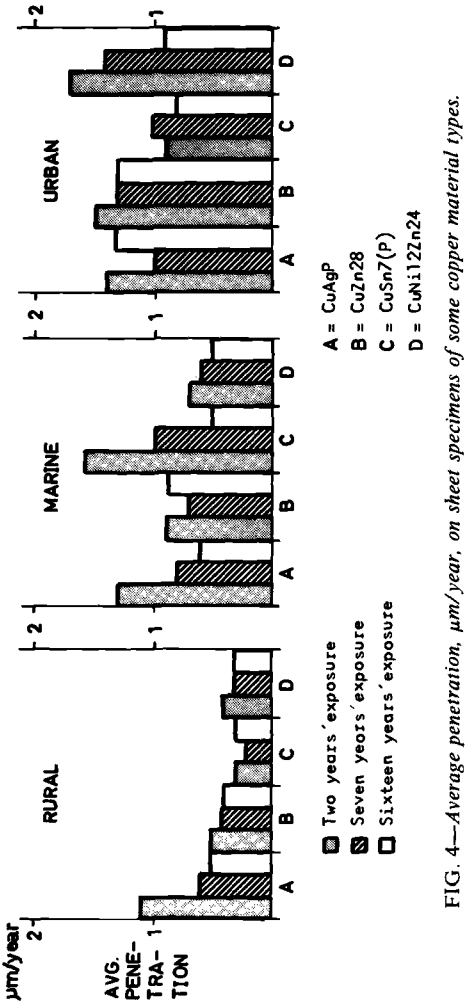

FIG. 4—*Average penetration, µm/year, on sheet specimens of some copper material types.*

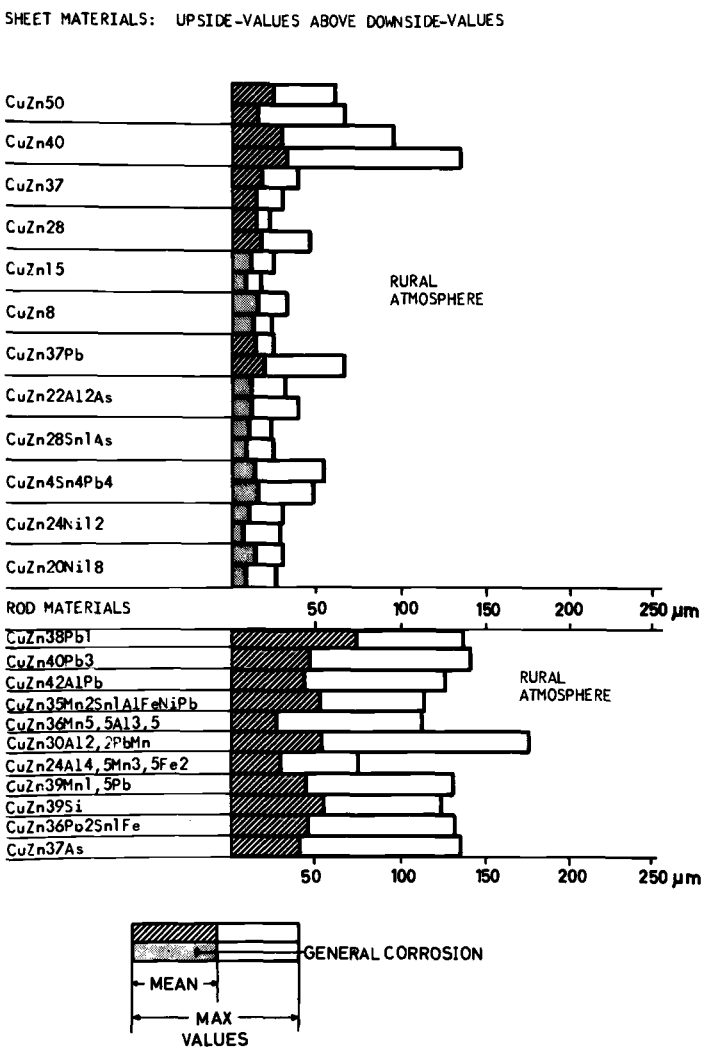

FIG. 5*a*—*Dezincification depth after 16 years' exposure.*

brasses with zinc content of 15 percent or less, for arsenical α-brasses, and for nickel silvers, no significant dezincification has been observed. The attack seems to be considerably retarded during the last half of the 16-year exposure period.

Interesting relations between the zinc content and the observed average and maximum dezincification depths in binary brasses are shown in Figs. 8*a* and 8*b*. The diagrams show deeper dezincification in the (α + β)-brass, mainly in the β-phase, as compared with both pure α- and pure β-brasses in

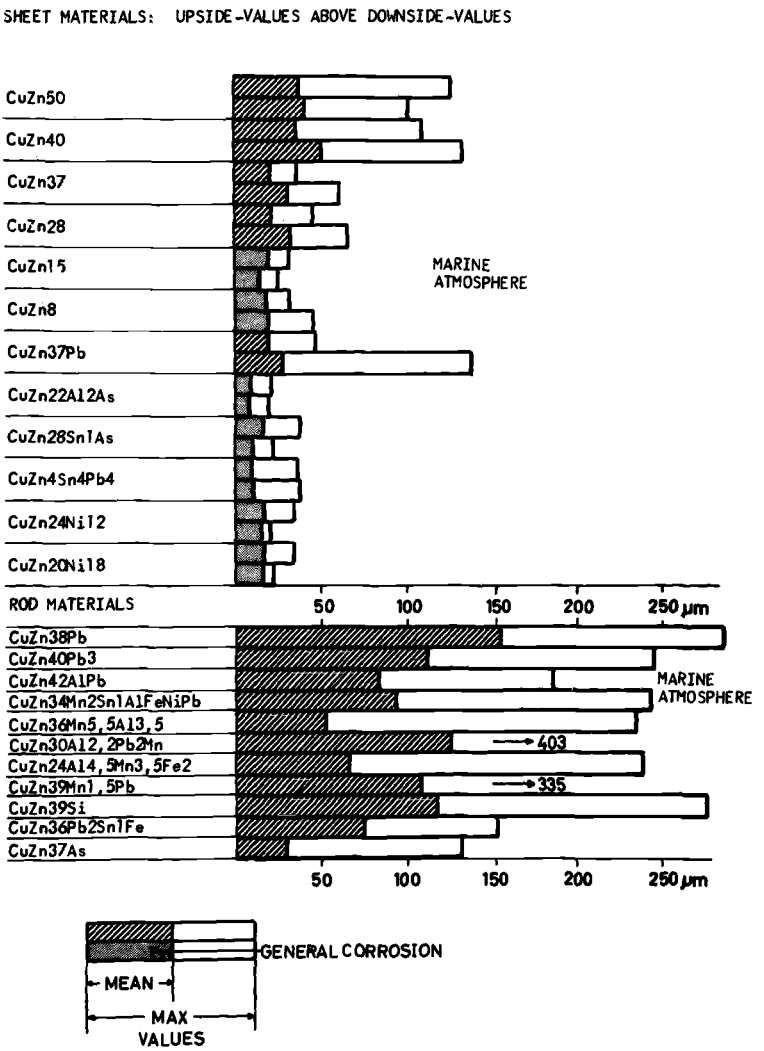

FIG. 5b—Dezincification depth after 16 years' exposure.

all three atmospheres and on both the upside and downside of the panels. This effect is probably due to local cell action when α- and β-phases occur together in the structure.

The depth of attack in the α-brasses does not show any significant decrease with decreasing zinc content, but the type of attack gradually changes from selective to general corrosion when the zinc content decreases below 15 percent. The diagrams also show that the attack tends to be deeper on the

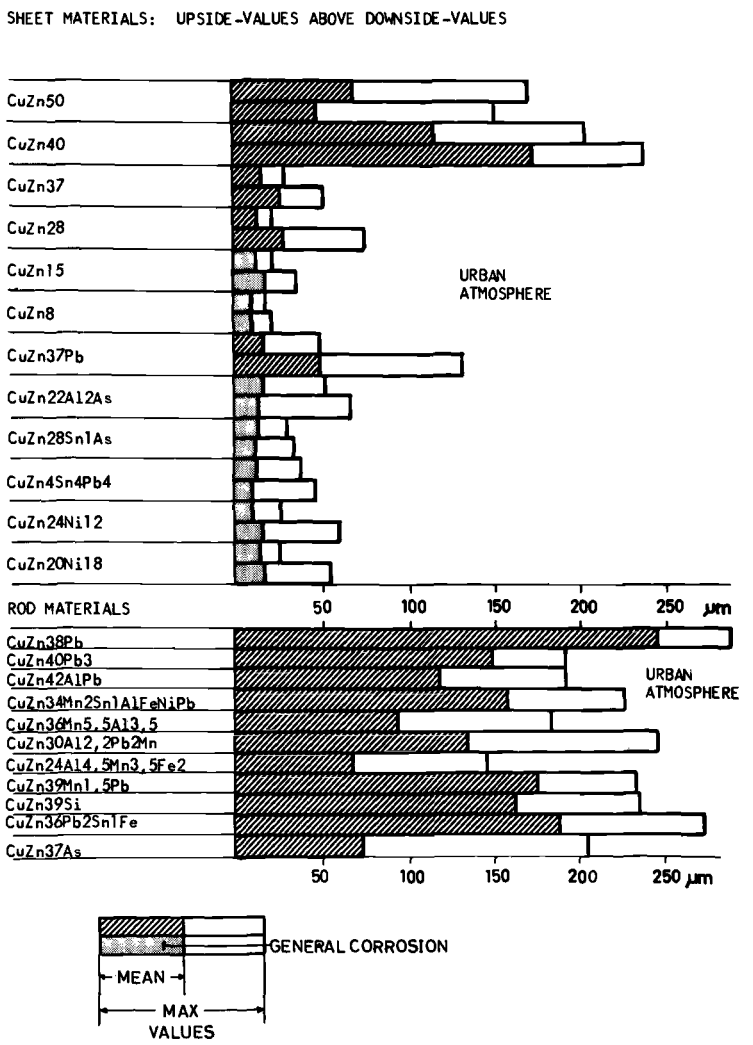

FIG. 5*c*—*Dezincification depth after 16 years' exposure.*

downside than on the upside of the panels, probably because the down-facing surfaces are not washed by rain.

A comparison of the dezincification of rod and sheet specimens of similar compositions (containing appreciable amounts of β-phase) shows better resistance for the rolled and annealed sheet specimens than for the machined rod specimens. For the rods the dezincification depth reaches average values of about 50 μm and maximum values up to about 150 μm in the rural atmosphere; in marine and urban atmospheres the average values for the ma-

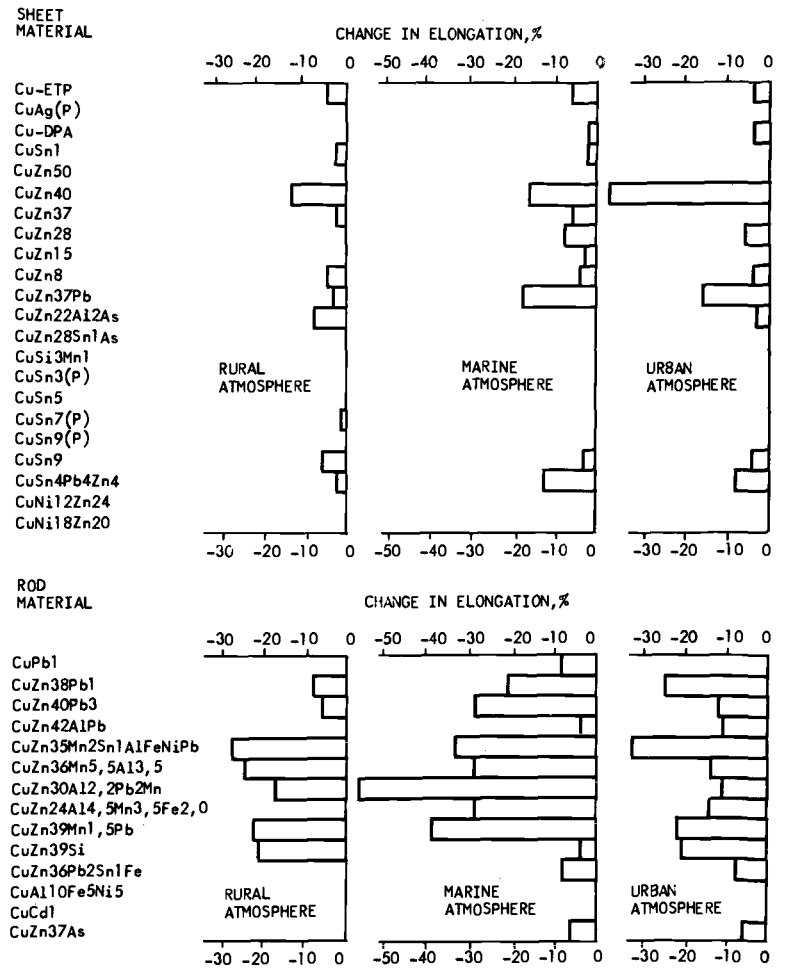

FIG. 6—*Changes in elongation of copper materials after 16 years' exposure.*

jority of brasses are 100 to 150 μm and the maximum values 200 to 300 μm. Among the more resistant of the (α + β)-brasses were the brasses alloyed with aluminum, tin, and arsenic and also the arsenical brass in which attack was restricted to the β-phase.

The dezincification observed is predominantly of the layer type, except for a few of the rod brasses with (α + β)-structure and for down-facing surfaces of brass sheet panels, which show a more localized attack.

Changes in Mechanical Properties

The changes in UTS were found to be less than 5 percent and the losses in elongation to be below 10 percent after 7 years' exposure for both sheet and

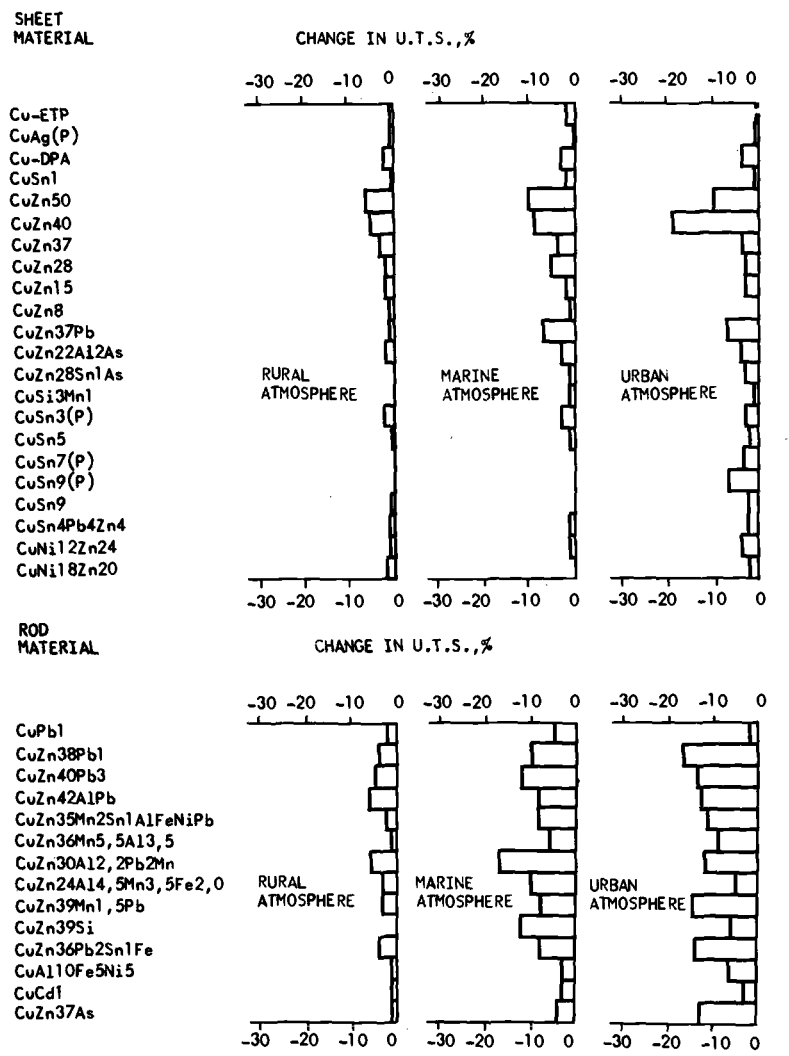

FIG. 7—*Changes in ultimate tensile strength of copper materials after 16 years' exposure.*

rod materials. The only exceptions were the brasses with a considerable content of β-phase, which was attacked by dezincification.

The results after 16 years' exposure are similar. A survey of the losses in mechanical properties of exposed materials as compared with reference material, stored indoors for 16 years, is given in Figs. 6 and 7.

For the majority of coppers and copper alloys the decrease in UTS does not exceed 5 percent and that in elongation does not exceed 10 percent for sheet or rod material from any test site. As before, an exception has to be

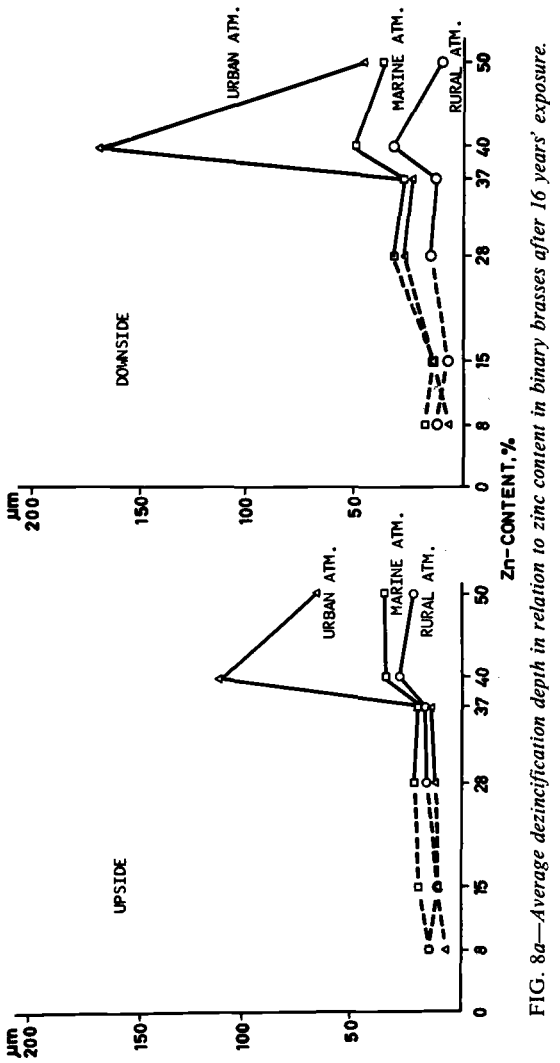

FIG. 8a—*Average dezincification depth in relation to zinc content in binary brasses after 16 years' exposure.*

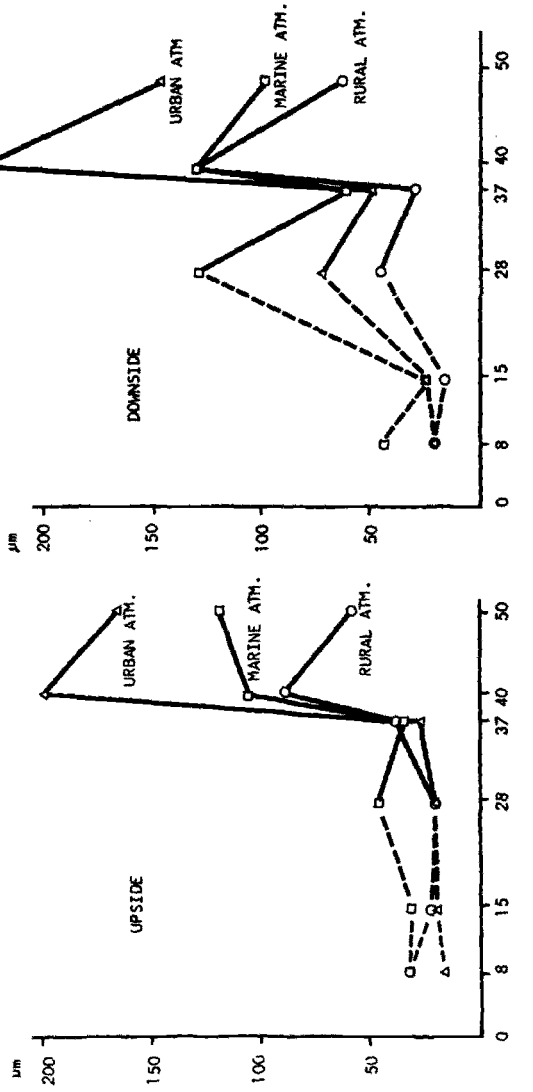

FIG. 8b—*Maximum dezincification depth in relation to zinc content in binary brasses after 16 years' exposure.*

made for the β-phase-containing brasses which show dezincification attack in this phase. In the urban and marine atmospheres these materials show losses of 10 to 15 percent in UTS and up to about 30 percent in elongation, the higher losses being in the marine atmosphere. In the rural atmosphere the corresponding losses amount to 5 percent and 10 to 20 percent, respectively.

Conclusions

The most important effects of atmospheric corrosion on the copper materials were found to be patina formation, general corrosion, and dezincification of zinc-rich alloys.

During the first years of atmospheric exposure the copper materials acquired a dark coating consisting mainly of Cu_2O but also containing basic copper salts and compounds of other alloy constituents, for example, amorphous SnO_2 and Al_2O_3 on alloys with tin and aluminum. In urban and marine atmospheres, signs of green patina appeared on copper after 6 to 7 years and on phosphor bronzes even sooner. The high-zinc brasses did not develop any attractive green patina. In the rural atmosphere no green patina had developed on any material after 16 years, only various shades of black or brown. The amount of corrosion products retained on the metal surface increased substantially from the 7th to the 16th year of exposure. The patina was found to be more protective in the marine and rural atmospheres than in the urban atmosphere.

The average penetration during the whole 16-year period was found to be about the same as during the first 7 years, but considerably lower than during the initial two years, that is

0.3 to 0.5 μm/year in rural atmosphere
0.5 to 0.9 μm/year in marine atmosphere
0.9 to 1.3 μm/year in urban atmosphere

The dezincification rate of the brasses had retarded somewhat during the last 9 years of exposure. It was highest for brasses with ($\alpha + \beta$)-structures, the effects of the 16 years' exposure being a maximum depth of 90 to 215 μm, a loss in UTS of 5 to 15 percent, and a reduction in elongation of up to 30 percent. Alloying with aluminum, tin, and arsenic improved the dezincification resistance of the ($\alpha + \beta$)-brasses.

The α-brasses with 15 percent zinc or less and arsenical α-brasses showed good resistance to dezincification.

Acknowledgment

The completion of this investigation, started by the Research Laboratory of Svenska Metallverken (now named Gränges Metallverken), Västerås, has been made possible by cooperation and financial support from the Swedish Corrosion Institute in Stockholm.

DISCUSSION

T. J. Summerson[1] (*written discussion*)—What explanation is offered for the relatively low pH of the precipitation at all three sites? Could this be related to the "acid rainfall" phenomenon?

R. Holm and E. Mattsson (*authors' closure*)—These pH-values are typical for the precipitation in Scandinavia and are actually somewhat higher than in most other European countries. The reason why the pH-value is so much below neutral is that the precipitation contains acid pollutants, mainly sulfur oxides, and has a very low buffering capacity.

[1] Kaiser Aluminum & Chemical Corp., Pleasanton, Calif.

L. P. Costas[1]

Atmospheric Corrosion of Copper Alloys Exposed for 15 to 20 Years

REFERENCE: Costas, L. P., "**Atmospheric Corrosion of Copper Alloys Exposed for 15 to 20 Years,**" *Atmospheric Corrosion of Metals, ASTM STP 767,* S. W. Dean, Jr., and E. C. Rhea, Eds., American Society for Testing and Materials, 1982, pp. 106–115.

ABSTRACT: Copper alloys were exposed for 15 to 20 years at two marine, one industrial, and one rural location. Based on average corrosion rates for 13 alloys, the industrial corrosion rate was 1.4 μm/year whereas the rate for the other sites was approximately 0.7 μm/year. As expected, alloying agents affected the corrosion rates by a factor of 2 to 3.

General attack was the predominant form of corrosion. Dezincification was positively identified in C260 alloy and intergranular attack was noted in C642. Pitting was not a factor for any alloy.

KEY WORDS: atmospheric corrosion tests, copper, copper alloys

This program was initiated in 1958 and a report[2] was written for the 2-year and 7-year exposures. The present data are for 15-year and 20-year exposures. The 15-year data are limited to the Point Reyes series because of vandalism.

Although the test details were given in the earlier paper, a brief description is in order. Triplicate panels of each alloy, at each site, and for each test period were exposed. These panels were approximately 10 by 20 by 0.13 cm (4 by 8 by 0.05 in.) and were mounted 30 deg to the horizontal. At the West Coast and East Coast marine locations (Point Reyes, Calif.) and Kure Beach, N. C.), respectively, they faced the water. At the industrial (Newark, N. J.) and the rural sites (State College, Pa.) they faced south. The composition of the alloys is listed in Table 1.

Originally 19 alloys were exposed but only 16 were returned for this evaluation. The three beryllium-bearing alloys were not included. Furthermore, the data sheets for two alloys were lost in the interim and all the initial weighings were erroneous in one case, so that complete data for the 2, 7, and 15- or

[1] Senior research metallurgist, Anaconda Industries, Brass Division, Research and Technical Center, P. O. Box 747, Waterbury, Conn. 06720.

[2] Thompson, D. H. in *Metal Corrosion in the Atmosphere, ASTM STP 435,* American Society for Testing and Materials, 1968, pp. 129–140.

TABLE 1—*Composition of alloys. Values are in weight percent.*

Alloy No.	Cu	Zn	Sn	P	Pb	Fe	Ni	Mn	Si	Other
65	98.71	< 0.10	1.18	0.11	. . .	. . .	. . .	. . .	. . .	. . .
66	88.23	0.10	. . .	. . .	<0.02	1.23	10.12	0.32	. . .	. . .
67	95.72	0.04	4.08	0.16	0.001	0.005	. . .	. . .	. . .	. . .
68	88.37	. . .	1.83	0.10	0.003	0.015	. . .	. . .	0.01	. . .
69	91.65	0.02	. . .	. . .	0.001	0.02	. . .	. . .	1.85	6.40 Al 0.06 As
70	84.71	15.25	<0.01	. . .	<0.05	0.02	. . .	. . .	. . .	. . .
71	70.60	29.38	<0.01	. . .	<0.05	0.014	< 0.01	. . .	. . .	. . .
72	64.58	24.46	. . .	. . .	0.01	0.01	10.53	0.41	. . .	. . .
73	65.14	15.87	. . .	. . .	0.01	0.02	18.56	0.40	. . .	. . .
74	99.94	. . .	. . .	. . .	. . .	. . .	. . .	. . .	. . .	0.042 O 0.003 S
75	97.99	. . .	. . .	. . .	. . .	0.03	1.85	0.02	. . .	. . .
76	93.73	. . .	. . .	. . .	. . .	0.01	6.34	0.01	. . .	. . .
77	90.35	. . .	. . .	. . .	. . .	0.18	9.16	0.27	. . .	. . .
78	77.18	. . .	. . .	. . .	. . .	0.04	22.76	0.01	. . .	. . .
79	55.38	. . .	. . .	. . .	. . .	0.30	42.75	1.67	. . .	. . .
80	82.62	. . .	. . .	. . .	. . .	0.20	4.13	12.83	. . .	. . .

NOTE—For a slightly more detailed list, see ASTM *Proceedings*, Vol. 59, 1959, p. 178.

20-year exposures exist for only 13 alloys. Also, it was painfully apparent that a considerable number of initial weight measurements were erroneous. In spite of the problems, however, which are almost inevitable over such a long time span where a few, if any, of the original personnel are still involved, considerable valuable information was gained.

Processing of Specimens

All specimens were first weighed with the corrosion products intact, using a single-pan digital readout balance that was checked and found accurate to within 0.01 g (0.00035 oz). The most typical upper surface of the triplicate specimens was photographed using color transparency film at a magnification of 1 to 4; this proved to be a good compromise between the overall appearance and resolution of some finer surface detail. X-ray diffraction specimens were then scraped from the upper surface.

Cleaning was done in two steps. The first involved immersion in a solution consisting of 500 ml (30 $in.^3$) of concentrated sulfuric acid (H_2SO_4) and 100 ml (60 $in.^3$) of concentrated hydrochloric acid (HCl) per litre. The second was a 30-s dip in 1:4 HCl, which in most cases was adequate to remove any remaining film.

The cleaning procedures were not altogether satisfactory, particularly with specimens from the industrial area because of the tendency to form copious amounts of a loosely attached, insoluble white material that was undoubtedly cuprous chloride. Also, there was a tendency to convert some copper oxide (Cu_2O) to metallic copper that plated onto the surface, which is, of course, an old problem with copper alloys.

The cleaned specimens were again weighed. The surfaces were examined for pits and none were found that were measurable by any mechanical means. Tension specimens were fabricated and pulled at a crosshead speed of 0.0002116 m/s (0.5 in./min). Finally, a metallographic study on transverse sections was made.

Corrosion Product Analysis

Specimens for X-ray diffraction were scraped from the topside of the panels by a knife blade using the stereomicroscope at ×10 to insure that all surface layers were removed. The resulting powder was then loaded into 0.3-mm-diameter (0.012 in.) capillaries and exposed to copper radiation filtered through nickel foil. A conscientious effort was made to include all layers, but some segregation may have occurred as the specimen dropped through the capillary.

X-ray specimens were taken from one sample of each triplicate series at every site with two exceptions (due to oversight). The results from each location are listed in the following.

Kure Beach (Eastern Marine)

In 14 of the 16 cases, both Cu_2O and $Cu_2Cl(OH)_3$, paratacamite, were identified. JCPDS No. 23-948 provided an excellent fit for the basic copper chloride pattern. Alloy 69 showed only paratacamite and Alloy 72 only Cu_2O. The pattern for Alloy 74 had a few weak lines for atacamite (23-947) as well, suggesting that a mixture of basic chlorides was present.

Newark (Industrial)

Eight of the 16 showed both Cu_2O and $Cu_4(OH)_6SO_4$, brochantite. Only Cu_2O was found with Alloys 69, 71, and 79 and only brochantite with Alloys 70, 74, 75, 78, and 80.

Point Reyes (Western Marine)

Alloy 73 was not received from this site and so the total number evaluated was 15. In 14 instances, both Cu_2O and paratacamite were found. In Alloy 69, only Cu_2O was noted and the strongest line for α-quartz was also detected. Whether the quartz was from the silicon in the alloy or from sand adhering to the surface could not be determined.

State College (Rural)

By oversight the corrosion product for Alloy 69 was omitted so that only 15 specimens were analyzed. In 10 cases both Cu_2O and brochantite were found. Alloy 72 yielded only Cu_2O and Alloys 70, 73, and 77 yielded only brochantite. Alloy 79 had no surface film.

In general, the alloys exposed to marine environments formed Cu_2O and paratacamite whereas those in urban or rural areas produced Cu_2O and brochantite, as expected.

Color

Only the topside of the specimens is described and given in Table 2.

The most striking feature is that only at the industrial site did the green or blue expected of weathered copper predominate. Even here, however, Alloys 66, 69, and 79 were brown or gray. Alloys 75, 76, and 80 were basically green, but a considerable amount of black, in the form of vertical streaks, was also present. At rural State College a blue or green hue was observed on 12 alloys, but not nearly to the same degree as at Newark.

At both marine sites blue or green appeared in only three or four of the 31 instances. Brown was the dominant color.

One specimen of each alloy from each site was photographed for future reference.

TABLE 2—*Color of upper surfaces of test panels.*

Alloy	Kure Beach Eastern Marine	Newark Industrial	Point Reyes Western Marine	State College Rural
65	RB	G	RB	G-GY
66	B	B	RB	B
67	RB	BG	B	B
68	RB	G	B	G-GY
69	RB	GY	B	RB
70	RB	G	B	GY
71	B	G	RB	G
72	GY	G	B	GY
73	GY	G	—	GY
74	B	G	B	GY
75	RB	G	B	G-GY
76	GY	G	B	G-GY
77	B	G	B	G-GY
78	B	G	B	G-GY
79	GY	B	B	B
80	B	G	B	GY

CODE: RB = red brown, B = brown, GY = gray, G = green, BG = blue green, G-GY = gray green.

Point Reyes exposure was for 15 years; all others were for 20.

Surface Layers

In general, reddish-brown cuprous oxide was present next to the metal at Kure Beach, Point Reyes, and State College. In 10 specimens from Newark, however, no positive visual evidence of Cu_2O was observed at ×10 during the sampling for X-ray diffraction although the X-ray results positively identified it in six cases. Possibly the Cu_2O was finely dispersed thoughout the brochantite.

The green brochantite found at Newark was relatively thick when compared with all other layers and ranged from adherent to so loosely held that the fingernail dislodged it. In the H_2SO_4-HCl cleaning solution, this green appeared to convert to a thick [estimated at 1-mm (0.04 in.)] white film which undoubtedly was cuprous chloride and was removable by wiping with a paper towel. This behavior is typical of Cu_2O rather than a cupric salt and further reinforces the idea that Cu_2O may be dispersed in the green rather than as an adherent layer next to the metal.

At both inland sites, vertical black streaks or splotches were observed, but only when a green surface layer was present; this occurred in seven cases at Newark and four at State College. This was also obvious with Alloy 80 at Kure Beach as well. These black areas were adherent and raised above the corrosion product surface slightly, but X-ray patterns from two different alloys failed to reveal any new crystalline phase. Oftentimes these were associated with scratches in the metal surface. No explanation for them is offered.

Corrosion Rates

Table 3 lists the corrosion rates. The data sheets containing the original specimen weights for Alloys 72 and 73 were lost so no calculations could be made. Also, numerous errors in the original weights of specimens in the replacements series for Point Reyes resulted in a loss of 10 individual corrosion rates. It is strongly suspected that the original weighing of Alloy 77 for Newark also was erroneous because of the exceptionally low corrosion rate calculated.

The "ratio" term of Table 3 is the ratio of maximum and minimum corrosion rates for the three (and occasionally two) specimens for the 15- and 20-year data; the closer the values are to 1.00, the less the scatter. It is apparent that some Point Reyes rates may be questionable.

Excluding the obviously erroneous or highly suspect data, the corrosion rates of all specimens from all sites vary from a maximum of 2.3 μm/year to a low of about 0.22 μm/year, a spread of approximately tenfold. No alloy proved to be the least corrosion resistant at all sites, but Alloy 69 with 2 percent silicon and 7 percent aluminum (C642) proved most resistant (in spite of a suspiciously low value of 0.22 at Point Reyes).

The spread of corrosion rates at each site is, of course, less than the tenfold just mentioned. These values in μm per year for Kure Beach, Newark, Point Reyes, and State College are, in order: 0.5 to 1.7, 1.2 to 2.3, 0.2 to 1.4, and 0.5 to 1.1.

Corrosion Product Retention

Mattsson and Holm[3] correlated the ratio of remaining weight of corrosion product to the metal lost and found the ratio decreased from rural to marine to urban.

The results for the present test, Table 4, show a somewhat different pattern. The two marine sites generally have the highest ratio, next is the rural, and finally the urban. Although no study was made, it appears that the reason for this behavior is that the marine sites form and retain greater amounts of Cu_2O than do the inland sites.

Corrosion Rate Trends with Time

The effect of time is obtainable for all sites except Point Reyes, where 7-year specimens were lost.

Using a criterion of greater than 0.1 μm/year as a measure of a significant corrosion rate change between the 7- and 20-year results, trends are evident, Table 5. The Eastern marine rates are decreasing with time, those at the industrial site have stabilized (possibly as early as two years), and in the rural environment the rates may be increasing.

[3] Mattsson, E. and Holm, R. in *Metal Corrosion in the Atmosphere, ASTM STP 435*, American Society for Testing and Materials, 1968, pp. 187–210.

TABLE 3—*Corrosion rates after 2, 7, and 15 or 20 years. Values are in μm/year.*

	Kure Beach Eastern Marine				Newark Industrial				Point Reyes Western Marine			State College Rural			
Alloy	2	7	20 Years	Ratio	2	7	20 Years	Ratio	2	15 Years	Ratio	2	7	20 Years	Ratio
65	2.1	1.8	1.1	1.8	1.7	1.6	1.4	1.0	1.1	0.38[b]	1.0	0.84	0.64	0.65	1.2
66	m[a]	m	1.4	1.1	m	m	2.3	1.0	m	0.97	1.4	m	m	1.1	1.3
67	3.8	2.5	1.7	1.2	1.4	1.9	2.0	1.2	2.2	0.75	1.1	0.56	0.56	0.70	1.2
68	1.5	0.61	0.53	1.1	1.7	1.7	1.7	1.1	1.1	0.52	3.2	0.58	0.76	0.80	1.2
69	0.43	0.43	0.46	1.2	1.1	1.3	1.2	1.1	0.23	0.22[b]	43	0.28	0.33	0.54	1.1
70	1.3	0.84	0.61	1.0	2.0	1.8	1.5	1.0	0.97	0.44	1.1	0.91	0.76	0.68	1.1
71	0.86	0.76	0.54	1.3	2.2	2.2	1.8	1.1	0.58	0.39[c]	. . .	0.81	0.81	0.91	1.3
72	0.76	0.61	m	. . .	2.3	2.0	m	. . .	0.51	m	. . .	0.76	0.64	m	. . .
73	0.76	0.53	m	. . .	2.8	2.0	m	. . .	0.51	m	. . .	0.76	0.61	m	. . .
74	1.8	1.7	1.1	1.4	1.9	1.4	1.3	1.1	1.7	0.43[b]	1.4	1.2	0.74	0.70	1.3
75	3.3	1.1	0.78	1.0	3.0	1.4	1.4	1.1	3.8	0.60	1.1	1.5	0.76	0.83	1.1
76	1.8	0.84	0.67	1.1	2.4	1.4	1.3	1.2	1.3	0.84[c]	. . .	1.2	0.64	0.80	1.6
77	1.3	0.94	0.74	1.2	1.7	1.5	0.04	1.5	0.99	1.4[c]	. . .	0.86	0.84	0.69	1.1
78	0.91	0.79	0.77	1.1	0.48	1.5	1.5	1.0	0.61	1.0	3.3	0.48	0.48	0.70	1.0
79	0.46	0.48	0.55	1.1	1.4	1.5	1.8	1.0	0.30	0.53[b]	1.3	0.38	0.25	0.53	1.0
80	1.5	0.91	0.72	1.1	1.7	1.6	1.7	1.1	1.2	1.1	1.6	0.76	0.64	0.69	1.0

[a] m denotes data or specimen missing.
[b] Based on two specimens.
[c] Based on one specimen only.

NOTE—Although three values were used in determining the 0.04 value for Alloy 77 after 20 years at Newark, the initial specimen weights are believed to be in error.

TABLE 4—*Retension of corrosion products after 15 or 20 years.*

Alloy	Ratio of Adhering Corrosion Product to Metal Loss			
	Kure Beach Eastern Marine	Newark Industrial	Point Reyes[a] Western Marine	State College Rural
65	0.96	0.27	0.91	0.68
66	0.33	0.18	0.37	0.25
67	0.51	0.24	0.97	0.59
68	0.79	0.27	0.68	0.72
69	0.55	0.21	0.81	0.40
70	0.71	0.30	0.90	0.56
71	0.72	0.38	0.83	0.57
72	. . .	. . .	. . .	. . .
73	. . .	. . .	. . .	. . .
74	1.01	0.31	0.69	0.67
75	0.75	0.36	0.91	0.82
76	0.80	0.35	0.41	0.75
77	0.73	8.9[b]	0.18	0.63
78	0.61	0.29	0.26	0.54
79	0.52	0.36	0.43	0.39
80	0.54	0.31	1.1	0.48

[a] Exposure at Point Reyes was for 15 years; all others were for 20.
[b] Probably in error due to incorrect initial weighing.
NOTE—Values are based on averages for the specimens available.

Metallographic Examination

A single specimen from each alloy from each site (64 total) was examined after mounting and polishing. Specimens were taken from the center of each panel and the length examined was approximately 2 cm (0.8 in.), a very small dimension from which to draw many firm conclusions. Furthermore, the panels had been cleaned prior to mounting, which further compromises the results. Acid pickling of copper alloys coated with Cu_2O, which nearly every panel had, almost always deposits copper metal onto the surface. Hence, the finding of copper during metallographic examination should be carefully interpreted. All too often dezincification is claimed when actually the copper noted is due to the cleaning process.

TABLE 5—*Corrosion rate trends with time.*

Corrosion Rates	Kure Beach Eastern Marine	Newark Industrial	State College Rural
Increasing	0	1	5
Static	4	8	7
Decreasing	9	3	1

NOTE—The above results are based on 7- and 20-year comparisons. Also, a rate change of greater than 0.1 μm/year from the 7-year values was used to define an increase or decrease in rate with time.

TABLE 6—*Evidence of copper on surface.*

Alloy 66—trace at Kure Beach only
Alloy 70—trace at Kure Beach, Point Reyes, and State College
Alloy 71—substantial at all sites
Alloy 73—trace at Newark and State College
Alloy 79—trace at Newark
Alloy 80—trace at Kure Beach and Point Reyes

NOTE—As mentioned in the text, it is conceivable that the trace copper levels observed may have originated from reaction of Cu_2O with acid during cleaning rather than a dezincification reaction in the field.

Table 6 lists the specimens which "showed" copper and hence could be suspected of dezincification. However, the only unquestionable instance of dezincification occurred with Alloy 71 (C260) and it appeared to be more severe on the bottom side at Newark, Point Reyes, and Kure Beach. The maximum depth of attack noted was 0.16 mm (0.0064 in.).

Intergranular attack was found on Alloy 69 (C642) except for the Point Reyes specimen. The maximum depth of attack measured was 0.05 mm (0.002 in.) Fig. 1. Four sections of unexposed Alloy 69 were examined and no evidence of intergranular attack was found, indicating that the original

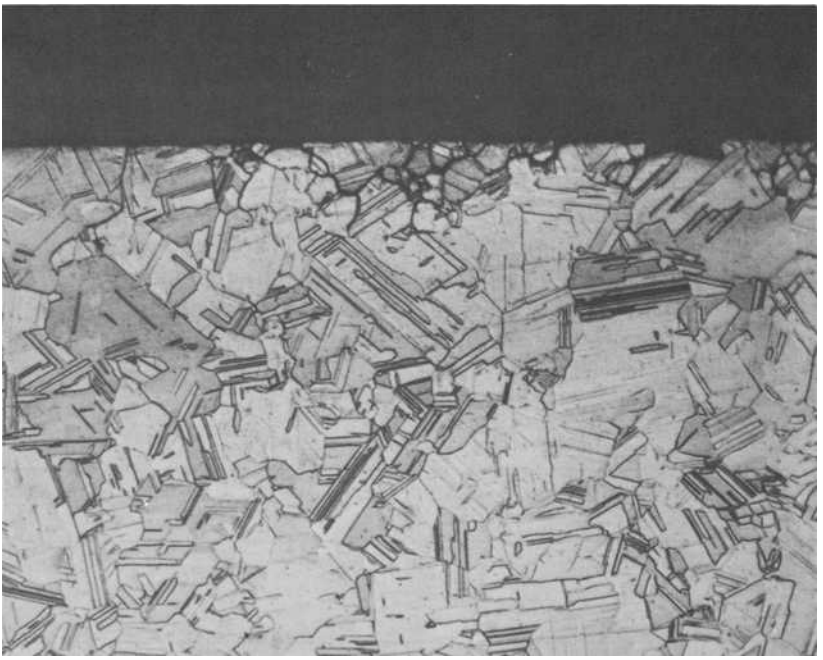

FIG. 1—*Intergranular attack. The intergranular penetration is only two or three grains deep, but it did occur on exposure rather than from a mill processing treatment* (×300).

material was sound and that the intergranular penetration observed occurred during exposure.

Tension Test Results

All specimens made from exposed panels broke within 5 percent of the ultimate tensile strength (UTS) of unexposed material with the single exception of one specimen of Alloy 69 at the industrial site, which gave a value of 5.85 percent less. In fact, except for five or six samples, all were within 2 percent.

The cross-sectional area was determined by measurement made on the cleaned specimens after exposure, not on the data taken prior to exposure. The reason for this was that the initial readings were listed to only two significant figures, which is rather crude.

At any rate, the tension tests revealed very little and, for the expenditure required, were hardly worthwhile. If alloys are intended for load-carrying purposes, then specimens under load should be exposed.

Conclusions

1. The corrosion rates of 14 copper and copper alloys at four locations after 15 to 20 years of exposure varied from a maximum of 2.3 μm/year [0.09 mils per year (mpy)] to a low of 0.22 μm/year (0.009 mpy).
2. The industrial site corrosion rate was approximately double that of the other three.
3. The green color associated with weathered copper was dominant only at the industrial site.
4. Cu_2O is commonly found on specimens at all locations. At the marine locations paratacamite is normally present whereas brochantite forms inland.
5. Dezincification was definitely noted in one alloy, C260, and intergranular attack was found in aluminum bronze C642.

Recommendations

1. Because of the importance of correct initial values, it is suggested that two independent laboratories weigh all specimens prior to exposure.
2. Consideration should be given to masking-off the bottom side of some panels so that a "topside only" corrosion rate can be separated from the overall rate based on total area.
3. Tension tests are time-consuming and, to date, have contributed little, if any, useful information; they should be terminated.
4. More effort should be given to metallographic study of sections taken from noncleaned specimens, particularly from the standpoint of corrosion product identification and morphology.

K. R. Wheeler,[1] *A. B. Johnson, Jr.,*[1] *and R. P. May*[1]

Aluminum Alloy Performance in Industrial Air-Cooled Applications

REFERENCE: Wheeler, K. R., Johnson, A. B., Jr., and May, R. P., "**Aluminum Alloy Performance in Industrial Air-Cooled Applications,**" *Atmospheric Corrosion of Metals, ASTM STP 767,* S. W. Dean, Jr., and E. C. Rhea, Eds., American Society for Testing and Materials, 1982, pp. 116–134.

ABSTRACT: Air-cooled equipment has an impressive record of performance in industrial cooling applications, particularly in rural–dry environments. At temperatures below the dew point, however, combinations of moisture and contaminants (particularly chlorides and some sulfur compounds) promote severe corrosion on aluminum. Washing the cooling surfaces with some commercial detergents provides a corrosive environment, particularly on areas where drainage collects. Coal dust deposits have caused corrosion of aluminum fins. Marine–humid–industrial locations have caused severe corrosion problems on aluminum air-cooled equipment, particularly when the coolers are at ambient temperatures for extended periods. The results of the domestic survey and available specimens have directed this study principally to aluminum. However, the foreign survey, which is summarized here, provided some insights into the behavior of galvanized steel cooling towers.

KEY WORDS: aluminum, galvanized steel, dry cooling, dew point, chloride, sulfur, coal dust, corrosion, pitting, detergents, airborne contamination

In many areas of the United States, water supplies are not adequate to meet the combined needs of agriculture, industry (including power production), and domestic use. As a result, large-scale allocation of water to central power stations for cooling purposes is becoming an increasing problem. Environmental restrictions, water costs, and diminishing availability of cooling water indicate that closed-cycle dry-cooled steam condensers may become attractive at some U.S. locations during this decade. The Department of Energy (DOE) and electrical utilities, through the Electric Power Research Institute (EPRI), are evaluating dry cooling for use in electric power plants. Battelle's Pacific Northwest Laboratory (PNL) is program manager of the DOE Dry-Cooling Tower Program.

In two surveys [*1,2*],[2] Battelle contacted suppliers and operators of a cross section of U.S. air-cooled equipment and made visits to several operating

[1] Battelle Memorial Institute, Pacific Northwest Laboratories, Richland, Wash.

[2] The italic numbers in brackets refer to the list of references appended to this paper.

dry-cooled power stations in Europe to discuss the current philosophy, methodology, and problems in dry-cooling technology.

The results of the surveys indicate that U.S. industrial air-cooled equipment functions with very few operational problems. Corrosion, while not a frequent problem, has resulted in shutdowns for major repair. Atmospheric corrosion is not the only consideration. Some corrosion failures have occurred from aggressive agents in process solutions being serviced by air-cooled equipment. This paper summarizes air-side corrosion data from operating air-cooled equipment, supported by corresponding laboratory studies. It includes results of metallographic examinations of fin specimens taken from operating industrial air-cooled heat exchangers (dry coolers) and from dry-cooling towers at central power stations. The equipment operated in a variety of environments in the United States and Europe.

Aluminum is one of the two predominant materials now used in dry-cooled power plants. Galvanized steel is also widely used, and some references to galvanized equipment performance are included. Both materials have generally performed satisfactorily for long periods. This paper examines both the scope of successful performance and the exceptions for air-side aluminum equipment, with the objective of defining environments and practices which should be avoided. Aluminum alloy fin specimens were collected from coolers and towers that were known to have corrosion problems; corrosion results reported here represent worst cases.

Procedures

The first level of assessment involved sending or taking a questionnaire to 16 major fabricators and operators of air-cooled equipment in the United States and Europe. The survey included visits to observe operating equipment. Air-cooled heat exchanger and dry-cooling tower sites chosen for the survey were classified by environment as rural–arid, rural–humid, industrial–arid, industrial–humid, and marine–humid. Cooling fin specimens were collected from several sites for metallographic examination of corrosion.

The majority of data and specimens collected in this survey were obtained from natural gas transmission companies operating gas compressor engines with air coolers because the temperature regime is similar to that in power station dry-cooling towers. The coolers have horizontal banks of finned tubes with forced-draft air flow. The tubes are either steel or copper alloys. In almost all cases the fins are aluminum.

As a second level of corrosion assessment, Battelle placed lengths of aluminum finned tubes on and around air-cooled gas compressors at two Gulf Coast industrial sites. The specimens seen in Fig. 1 consist of steel tubes covered by extruded alloy 6063 aluminum fins. The geometrical arrangement is typical of a tube-fin heat exchanger.

Fin specimens from the various tubes were taken after 1, 2, and 3 years.

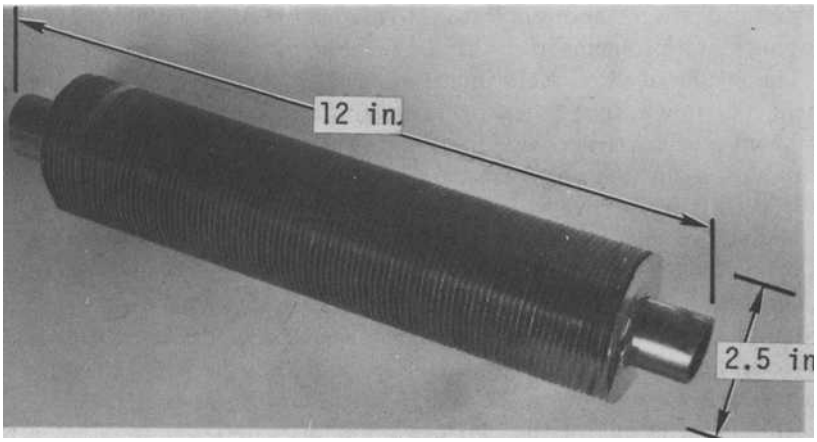

FIG. 1—*Tube specimen (aluminum fins, steel tube) similar to specimens installed at two Gulf Coast gas compressor stations (1 in. = 2.54 cm).*

One site is on the Gulf Coast in Louisiana; one site is about 9 km (6 miles) from the Gulf in Mississippi. Control specimens were exposed to ambient conditions at Richland, Wash. (rural-arid).

A third level of corrosion assessment involved investigation of aluminum corrosion under simulated dry-cooling tower conditions. Aluminum was exposed to selected contaminants in controlled environments in a Battelle laboratory. Coupons 1.9 cm (3/4 in.) square and 0.15 cm (1/16 in.) thick were cut from Alloy 1100-H14 aluminum sheet. Nine coupons were held at 58 to 63°C (136 to 145°F), which is above the dew point. Five coupons were held at room temperature [approximately 20°C (68°F)]. Five specimens were cycled between room temperature and operating temperature. All specimens were placed under a hood which provided flowing laboratory air. Ibbenbüren (Germany) and Salinas (Utah) coals, sulfur, and sodium chloride were the principal contaminants selected for the laboratory tests. All cooling fin and laboratory specimens analyzed in this study were examined visually, metallographically, and with the scanning electron microscope (SEM). Due to space limitations, only a brief cross section of the survey and laboratory results is given here. Details are available elsewhere [*1-3*].

Experimental Results

The scope of the survey of natural gas compressor engine coolers is summarized in Table 1. The survey included equipment operating in most geographic areas of the United States, from Florida to California, Texas to New York, and the Pacific Northwest [*2*]. Of the 219 stations covered in the survey, only two had experienced corrosion which required equipment replace-

TABLE 1—*Compressor engine air cooler survey.*[a]

Company	A	B	C	D	E	F	Total
No. of stations	60	22	36	52	40	9	219
No. of coolers	~360	77	313	261	410	121	1542
Avg age, years	20	15	17	22	20	17	. . .
Max age, years	26	19	25	25	28	>20	. . .
Locations:							
rural	90%	90%	96%	98%	most	79%	. . .
urban	5%	5%	5%	0	ND[b]	0	. . .
industrial	0	5%	0	2%	some	21%	. . .
marine	5%	0	0	0	0	0	. . .
Temperature in, °C	50 to 80	80	ND	ND	50 to 105	ND	. . .
Temperature out, °C	45 to 55	50	ND	ND	45 to 75	ND	. . .

[a] Responses through 1976.
[b] ND = not determined.

ment. The remaining stations indicated that corrosion had not begun to interfere with cooler performance during operation to 28 years (1976).

A second aspect of the survey addressed air cooler performance in petroleum refinery applications. One response included operation of 625 air coolers at 14 refineries in seven countries [*2*]. The predominant materials were aluminum fins on steel tubes. One cooler operated for more than 20 years; ten operated for 15 to 20 years; the remainder operated less than 15 years. Twenty-three coolers failed at ages from 1 to 12 years. One failure was due to freezing. The remainder occurred from the internal side, due to corrosion by aggressive process solutions. No failures occurred due to air-side corrosion.

Air-side corrosion was indicated as serious at one aluminum tower and noticeable at another aluminum tower. Two galvanized tower operators indicated that air-side corrosion was noticeable; one galvanized tower had moderate corrosion. One galvanized unit had noticeable condensate-side corrosion.

A major conclusion of the study was that corrosion was a minimal problem for both aluminum and galvanized towers. The unusual corrosion on Ibbenbüren and Rugeley towers is discussed later in the paper. The only dry-cooled central power station in the United States is sited at Wyodak, Wyoming. It has one aluminum-finned tower (1962 start-up) and two galvanized steel towers (1962 and 1978 start-ups). Air-side corrosion has not been significant on the three Wyodak towers [*4*].

At natural gas refinery sites with ~440 coolers, the principal materials were aluminum fins on steel or copper alloy tubes [*2*]. The sites could best be described as rural, arid, industrial. The older coolers had operated since 1952. Some corrosion problems occurred on early coolers having copper fins exposed to sulfide and sulfur oxide environments. Steel louvers have corroded, but the aluminum fins have performed well. Galvanized fins also have operated satisfactorily.

TABLE 2—*Summary of air-cooled equipment examinations.*

Plant/Location	Environment	Power Rating, MWe	Date On-Line	Materials	Evaluation Methods	Results of Fin Examinations	References
A. Wyodak, Gilette, Wyo.	rural-arid	3	1962	Adm[b] tubes Al[c] fins (wrapped)	visual	no significant corrosion after 10 and 13 years	[2,4]
B.	rural-arid	22	1969	steel tubes galvanized fins	visual	no significant corrosion after 6 years	[2]
C.	rural-arid	300	1978	steel tubes galvanized fins	N/A[a]	N/A	
D. Gas compressor, Plymouth, Wash.	rural-arid	N/A	1956	Adm tubes Al fins (soldered)	visual metallography	thin oxides and minor pitting after 18 years	[2,3]
E. Gas compressor, Gulf Coast, Mo.	rural-humid	N/A	1960	Adm tubes Al fins (wrapped)	visual metallography	thin oxides and minor pitting after 17 years	[3]
F. Gas compressor, Midland, Tex.	industrial-arid	N/A	1973	90-10 Cu-Ni tubes Al fins (wrapped)	visual metallography	thin oxides, no pitting	[3]
G.	industrial-arid	N/A	1953	Adm tubes Al fins (wrapped)	visual metallography	thin oxides, minor pitting	
H. Preussag, Ibbenbüren, Germany	industrial-humid	150	1967	Al tubes Al fins (plate type)	visual metallography	deep pitting under coal dust deposits (Figs. 2–4)	[1,3]
I. Rugeley, U. K.	industrial-humid	120	1962	Al tubes Al fins (plate type)	visual metallography	Al tube perforation in crevices (Fig. 5)	[1,3]
J. Gas compressor, Southern California Coast	marine-moist	N/A	1956	Tubes (unknown) Al fins	metallography	deep subsurface corrosion	[3]
K. Gas compressor, Louisiana Gulf Coast	marine-humid-industrial	N/A	1961/63	Adm tubes Al fins (soldered)	visual metallography	significant corrosion after 3 years, severe corrosion after 13 years (Fig. 6)	[2,3]

[a] N/A = not applicable—applies to coolers not associated with power plants. Thermal ratings were in the range 1×10^6 to 50×10^6 Btu/h.
[b] Adm = Admiralty brass—70–73Cu, ~1Sn, remainder zinc.
[c] Al = aluminum alloys—generally
1100: 0.2Cu, 0.6–0.8Fe, 0.8Si, remainder aluminum.
6061: 1.0Mg, 0.25Cu, 0.6Si, 0.2Cr, remainder aluminum.
6063: 0.6Mg, 0.4Si, remainder aluminum.

The European survey [*1*] included visits to 19 power plants: five with aluminum coolers (Heller), 13 with galvanized iron coolers (GEA), and one with a plastic cooler. Start-up dates were 1961 to 1973 for the aluminum units and 1956 to 1972 for the galvanized units.

Results of Air-Cooled Equipment Examinations

Specimens from several types of aluminum-finned air-cooled equipment were examined by visual inspection and metallography. Table 2 summarizes the scope and results of the examinations.

To summarize the results of the examinations:

1. Corrosion was minimal on aluminum fins exposed at the following locations: rural-arid (18 years); rural-humid (17 years); industrial-arid (22 years).
2. Corrosion was substantial on aluminum fins at an industrial-humid location (Ibbenbüren, Germany), but only at locations where coal dust was caked on the fins (see Figs. 2–4). There are indications that chloride and sulfur contaminants in the coal may have contributed to the corrosion. Galvanic effects under the coal dust poultice may also have been important.
3. At another industrial-humid site (Rugeley, United Kingdom) an unusual pitting attack occurred on aluminum tubes at crevices between the tubes, spacer collars, and fins (Fig. 5). The tower was subject to contaminants from a coal mine, an ash sintering plant, the city of Birmingham, and some salt transport from the sea coast; also, to drift from adjacent wet towers and to frequent rains. The principal corrosion factors appeared to be chlorides and other contaminants in the crevices when they were moist. Chloride ions are very corrosive to aluminum and its alloys [*5,6*]. The corrosion was estimated to be ~20 times faster when the tower was out of service, that is, at low temperatures, where moisture could penetrate the crevices.
4. At a marine-moist location on the Southern California coast, aluminum fins underwent substantial corrosion after 20 years. The cooler was located about 1.4 km (0.86 mile) from the shoreline, but was subject to frequent fogs, mists, and winds, which may have carried some chlorides. However, the most significant factor may be the fact that the cooler operated only about 25 percent of the time. However, the corrosion had caused significant reduction of cooler efficiency.
5. At a marine-humid industrial site, aluminum fins underwent severe corrosion, due to proximity to the Gulf Coast, also being downwind from a sulfur mine. Figures 6*a* and 6*b* show the appearance of cooling fins on the top and bottom bank of tubes after 13 years service. Gross corrosion is evident. Sulfur compounds combined with water provide a source of sulfuric acid generally regarded as corrosive to aluminum [*7*].

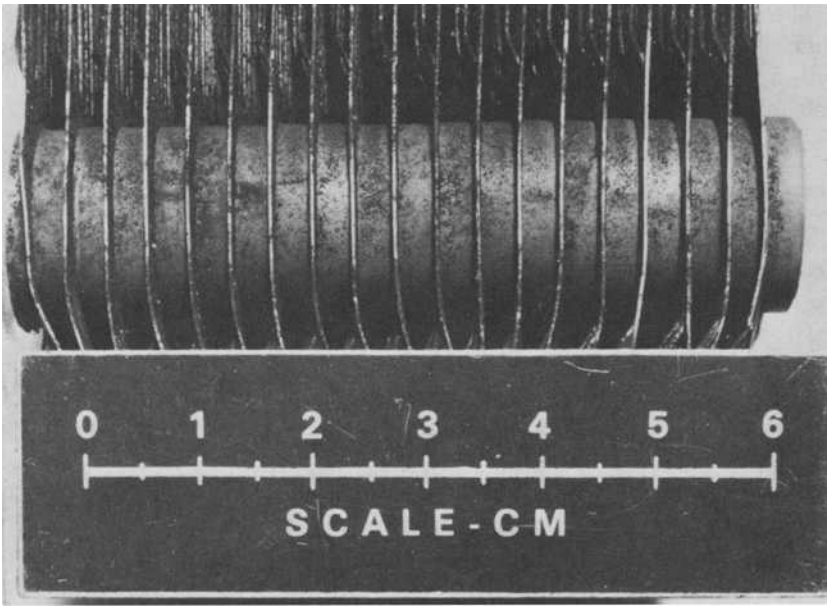

FIG. 2*a*—*Cooler section showing alternate layers of aluminum plates and spacers stacked around aluminum tubes. Note coal dust fouling (1 cm = 0.4 in.).*

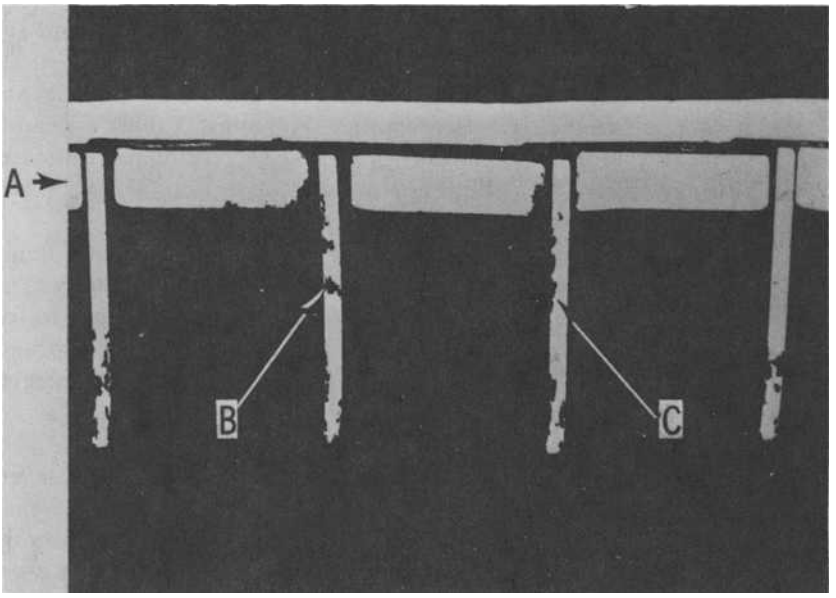

FIG. 2*b*—*Metallographic section through tube, spacer, and fin plate on section of aluminum cooling tower. Note severe corrosion on fins under coal dust and lack of corrosion on inner surfaces (Area A) where no coal dust was present. For B, refer to Fig. 3; for C, refer to Fig. 4.*

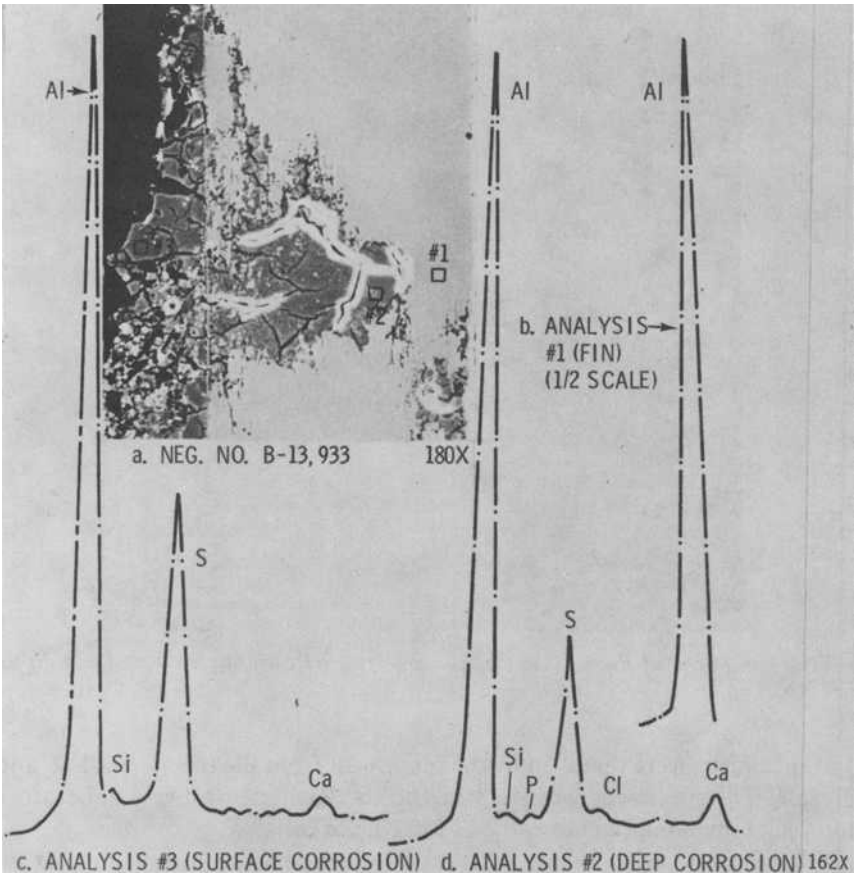

FIG. 3—(a) *SEM micrograph showing locations of microprobe analysis (Area of B of Fig. 2b).* (b) *Analysis No. 1 of fin metal.* (c) *Analysis No. 3 of corrosion product at surface.* (d) *Analysis No. 2 of deep corrosion product.*

Results of Examinations on Finned-Tube Specimens

Specimens Placed at Air-Cooled Sites—Battelle placed four 30-cm-long (1 ft) (Fig. 1) finned-tube sections at the site indicated as E in Table 2. Four specimens also were placed at the site indicated as K. In each case, specimens were placed

1. immediately above the upper bank of tubes, in the hot air steam (54°C) (130°F),
2. below the cooler in the cool incoming air (two specimens), and
3. at a point away from the cooler at ambient conditions.

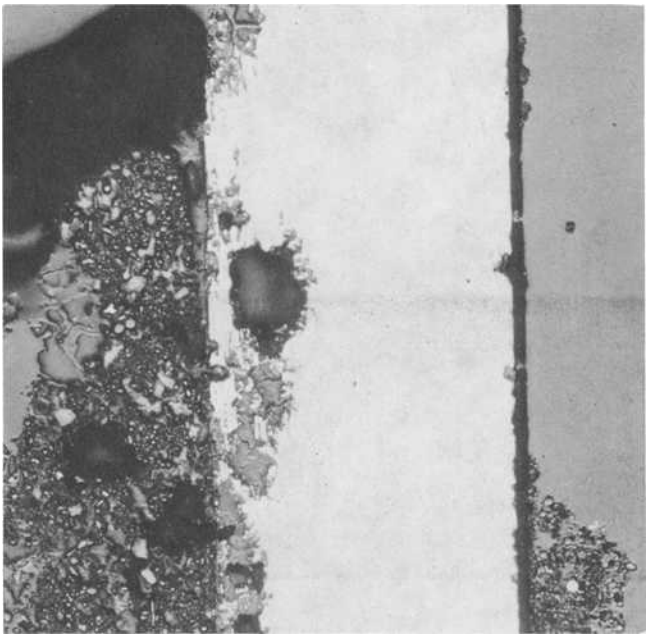

FIG. 4—*Close-up of Region C in Fig. 2b showing severe corrosion under coal dust deposit (×124).*

Fin specimens were removed by the plant staff from the tubes after 1, 2, and 3 years. The specimens were returned to the Pacific Northwest Laboratory for visual, metallographic, and SEM examinations.

Table 3 summarizes results of the aluminum-finned-tube specimen exposures at the two sites. (Figures 7 and 8 are referred to in this table.)

Results of Laboratory Specimen Corrosion Studies

Specimens of Alcoa 1100-H14 aluminum were exposed at Richland, Wash. (PNL) under three conditions:

1. continuously at 60°C (140°F) in humidified air,
2. cycled between 60 and 20°C (140 and 68°F) in humidified air, and
3. continuously at 20°C (68°F) in humidified air.

Selected specimens were exposed to contaminants: Ibbenbüren (Germany) or Salinas (Utah) coals[3]; elemental sulfur; sodium chloride; some combina-

[3] Salinas coal had 0.87 sulfur; 0.0028Cl, 0.0035F. Ibbenbüren coal had 2 percent sulfur; 0.15Cl; 0.37F percent by weight.

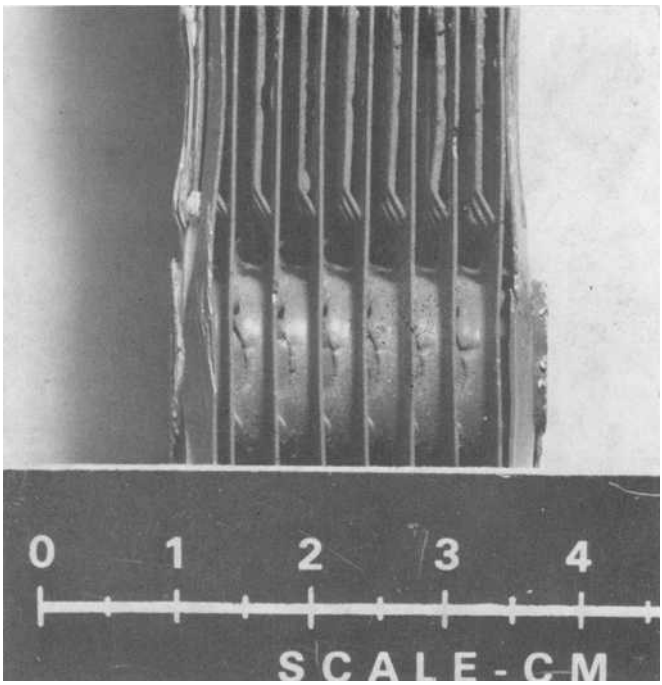

FIG. 5—*Close-up of crevice locations in heat exchanger at Rugeley where pinhole leaks were reported to have initiated (1 cm = 0.4 in.).*

tions. After 800 days the specimens were examined under the microscope. Those with evidence of corrosion were examined metallographically. The visual and metallographic examinations showed the following:

1. No corrosion on uncontaminated control 60°C (140°F).
2. No corrosion with elemental sulfur alone at 60 and 20°C (140 and 68°F); significant corrosion when cycled.
3. The coal with the higher chloride/flouride content promoted higher corrosion rates. Corrosion was mildly higher for the cycled specimens.
4. Sodium chloride caused substantial localized corrosion under all three conditions, in the following order of severity:

$$20°C > 60°C > 60 \fallingdotseq 20°C \ (68°F > 140°F > 140 \fallingdotseq 68°F)$$

5. Sodium chloride combined with elemental sulfur did not substantially alter the results for sodium chloride alone, although the cycled specimens had somewhat more severe corrosion.

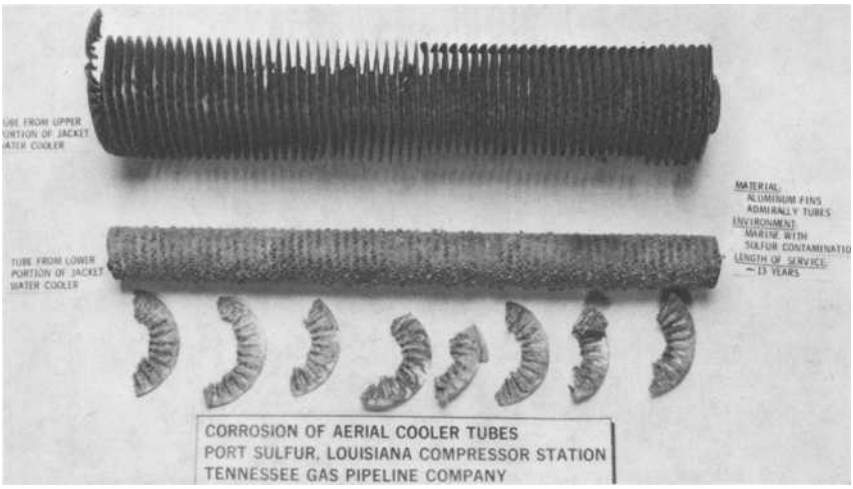

FIG.6a—*Aluminum fins after exposure for 13 years to a humid-marine environment (calcium carbonate, chlorine, and sulfur contamination). Fins detached from lower tube* (×25).

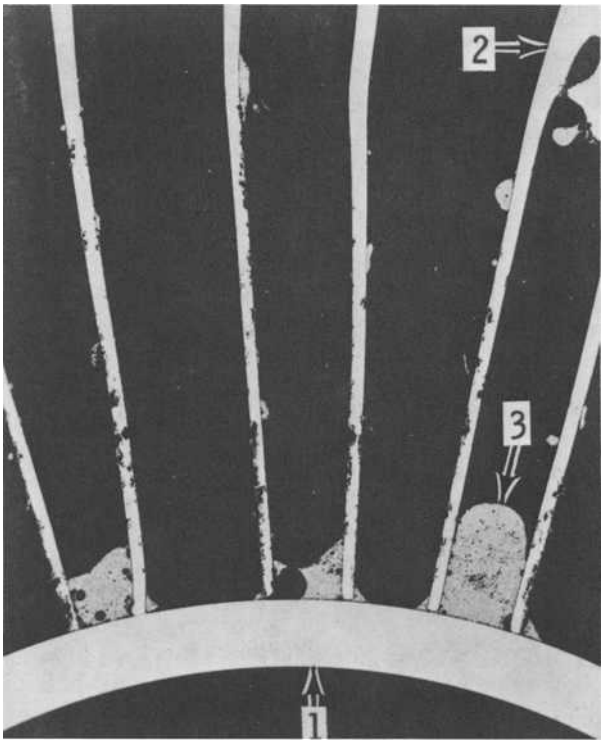

FIG. 6b—*Metallographic section through a tube from the upper bank; refer to Fig.* 6a. *Shows corrosion along the length of the fin and not associated with the solder* (1) *tube* (2) *fin* (3) *solder* (×6).

TABLE 3—*Summary of corrosion on aluminum alloy finned-tube specimens placed at two air-cooled sites.*

Tube No.	1		2		3		4	
	Site A[a]	Site B[b]	Site A	Site B	Site A	Site B	Site A	Site B
Location	above cooler	above cooler	below cooler[c]	below cooler	below cooler[d]	below cooler	site fence	headquarters building
Temperature	54°C (130°F)	54°C (130°F)	ambient	ambient	ambient	ambient	ambient	ambient
Contaminant deposition	slight	minor some S, Cl, Si	mild	moderate	mild	moderate	slight	moderate high S, minor Cl
Corrosion:								
1st year	slight	slight	minor	minor	mild	mild	slight	slight
2nd year	slight	slight	moderate some S, Cl	moderate high S, some Cl	severe high S, Cl	moderate high S, some Cl	minor some S, Cl	moderate high S, minor Cl
3rd year	slight (Fig. 7)	minor	moderate some S, Cl	moderate high S, some Cl	severe high S, Cl	moderate[e] high S, some Cl (Fig. 8)	minor some S, Cl	moderate high S, minor Cl
	slight < minor < mild < moderate < severe							

[a] Rural–humid site, 9.2 km (~6 miles) from Gulf Coast.
[b] Marine–humid industrial site, on Gulf Coast, downwind from sulfur mine.
[c] Not subject to detergent washing.
[d] Subject to detergent washing when air cooler coils are cleaned.
[e] In a 250-μm-thick (0.010 in.) fin, corrosion has penetrated 87.54 μm (0.0035 in.) inward from one surface and 31 μm (0.00125 in.) inward from the other in 3 years. This promotes total fin penetration in half time.

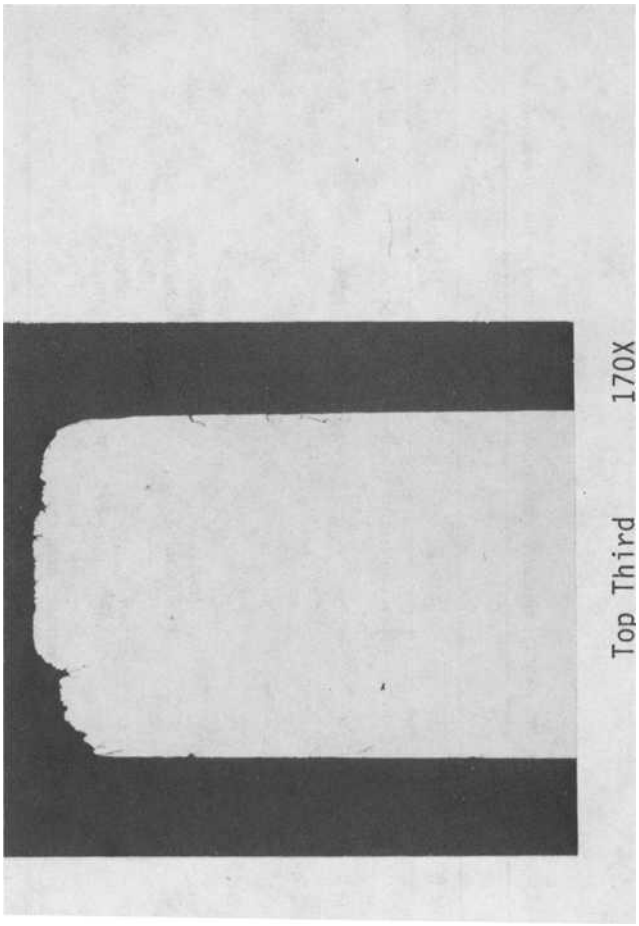
Top Third
170X

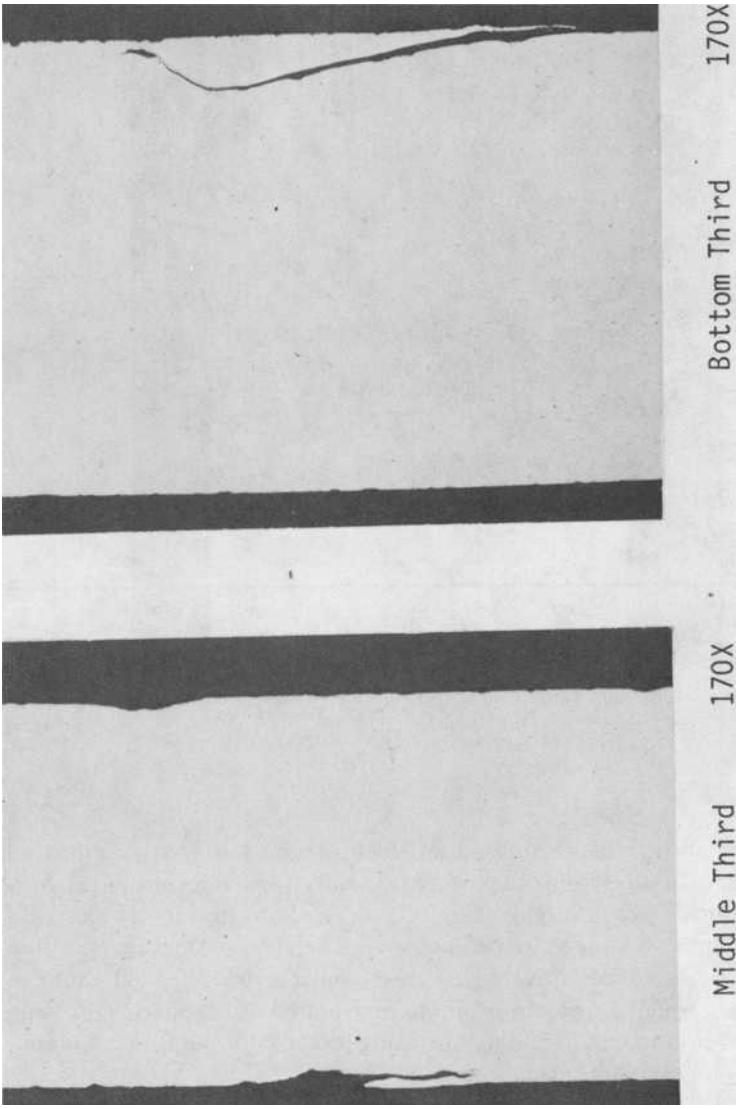

FIG. 7—*Top fin segment taken from tube located above cooler in hot [54°C (130°F)] flowing air.*

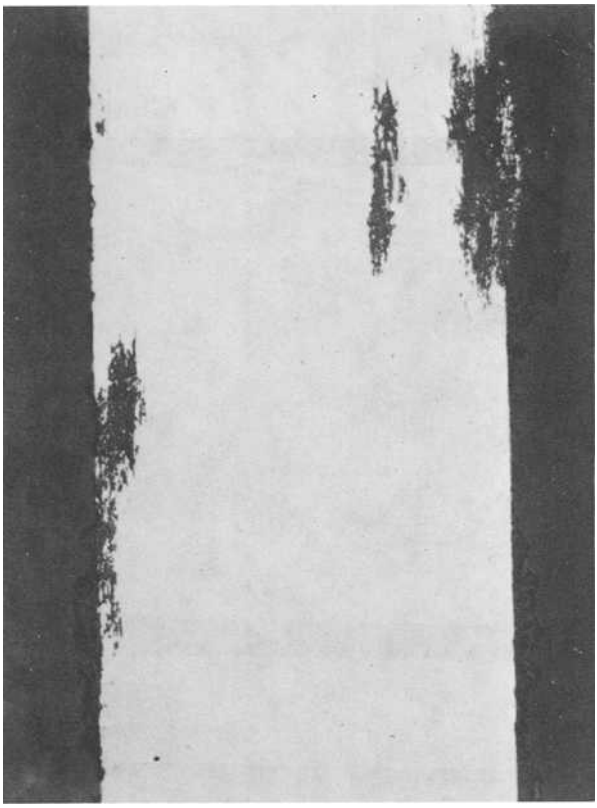

FIG. 8—*Corrosion penetration from both surfaces of aluminum alloy 6063 extruded fin* (×200).

Discussion

Aluminum alloys have performed satisfactorily in thousands of industrial air coolers in exposures up to 30 years, principally at rural locations [*2*]. Several aluminum-finned and galvanized-fin dry-cooling towers at electrical generating plants also appear to be functioning well [*1,2*]. At a small fraction of sites, however, substantial corrosion has occurred. We will examine briefly factors which appear to promote accelerated atmospheric corrosion of aluminum equipment, including operating mode, configuration, contaminants, and geographic location.

Operating Mode

Aluminum specimens placed at two industrial sites and exposed in the laboratory demonstrated that aluminum exposed at operating temperatures [50 to 70°C (120 to 150°F)] corroded less than corresponding specimens ex-

posed at ambient temperatures. The explanation lies in the concept of time-of-wetness [*8*]. Corrosion of aluminum at Rugeley was about 20 times higher during outages than during operation. Corrosion-prone metals, which are subject to periodic moisture condensation, generally undergo more attack than when they remain dry. Thus, exposures above the dew point are generally more favorable than exposures at lower temperatures where periodic wetting occurs. This suggests that corrosion during outages may be the most significant impact, particularly in moist, contaminated environments.

Configuration

Certain crevices were prone to corrosion on dry-cooled equipment at Rugeley. The crevices concentrated moisture and chlorides, causing local pitting. Other types of crevices, for example, on the corroding Ibbenbüren tower, did not show attack, presumably because impurities did not penetrate into the crevices.

Rows of tubes on the inlet side of the air flow tend to have the highest corrosion rates, presumably because they intercept a large fraction of airborne contaminants and debris.

Galvanic Factors

The performance of dry-cooling systems with dissimilar metals has been mixed. In aqueous circuits, there are instances where copper alloy components have appeared to cause accelerated corrosion of aluminum components. Operation of iron-base/aluminum-base aqueous circuits appears to be satisfactory with proper water chemistry control.

Air-side corrosion of aluminum fins on copper alloy tubes has been satisfactory in dry climates or where the cooler operates most of the time. Severe corrosion has occurred in copper-tube aluminum-fin crevices where moisture ingress had occurred.

Aluminum fins solder-bonded (for example, 80Pb-20Sn) to Admiralty tubes did not appear to corrode preferentially adjacent to the solder, including one plant where the aluminum corrosion was minor and one plant where the aluminum corrosion was severe.

Contaminants

Analysis of 6063 and 1100 aluminum alloy fin sections taken from U. S. and European cooling equipment indicates that chloride is generally associated with areas of severe aluminum corrosion. Acidic compounds containing sulfates or sulfites also corrode aluminum but less severely than chloride. There is some evidence that these two species combine with moisture to produce very aggressive local acid environments which readily attack aluminum. Minimum corrosion rates for aluminum are reported to occur in neu-

tral (pH 7) water depending on temperature and oxygen content. Corrosion rates increase as solution pH values increase or decrease from neutrality, but the rates depend on the species of acid or base responsible for the pH change.

Coal dust having high chloride, fluoride, and sulfur compounds promotes deep pitting in aluminum. Low halide in coal dust plus a chloride source (sodium chloride) is only moderately aggressive. Coal dust and other surface deposits may accentuate localized pitting by a poultice effect, concentrating the moisture and contaminants.

Severe corrosion of 6063 aluminum was observed on fins washed periodically by a commercial detergent. The washing effect is particularly evident on bottom edges of fins where detergent solution collected. The detergent is known to contain sulphates, chlorides, and phosphates and to have a saturated water solution pH 13, a condition known to be aggressive toward aluminum.

Geographic Location

Aluminum components exposed at rural–dry environments were least prone to corrosion attack. Rural–wet and industrial–dry locations were also mild in their corrosive effects on aluminum.

Instances of severe corrosion have occurred at a few humid, marine, and industrial sites. However, air-cooled equipment also has operated satisfactorily at some sites in these environmental categories. The principal factors influencing corrosion appear to be the amounts and species of contaminants and the amount of time the equipment is off-line. Corrosion is minimized when the equipment operates at temperatures above the dew point. When corrosive conditions are present, crevices and some galvanic couples have promoted corrosion in some cases.

Summary

1. Aluminum is an attractive choice for air-cooled heat exchangers because of its light weight, high thermal conductivity, corrosion resistance, fabricability, and low relative cost. However, aluminum is not suitable for extended use at some sites with high moisture and contamination levels, particularly where the equipment has extended downtime. Galvanized steel air-cooled equipment also has operated without substantial corrosion at most locations.

2. Aluminum alloy 6063 for condenser tubing has excellent corrosion resistance and high resistance to erosion compared with other aluminum alloys, but several other alloys have also functioned well, including 1100, 3003, 5052, 6061, and Alclad 3003.

3. Aluminum alloys can be expected to have lifetimes of 30 years or more at dry-cooling tower temperatures in clean environments. Many industrial air coolers with aluminum alloy fins also have had extended operation (a

decade or more) in some contaminated environments. Galvanized steel air-cooled equipment also has operated with minimal problems since 1956, according to one survey [*1*].

4. Effects of specific contaminants are not well defined at cooling tower temperatures, but chloride is clearly an aggressive agent on aluminum components, in agreement with extensively published evidence. Highly basic detergents used for washing are corrosive if not thoroughly removed by rinsing.

5. Corrosion is most severe at temperatures below the dew point, where moisture can participate in the attack. Severe corrosion seldom occurs at dry-cooling temperatures unless the plant is subject to considerable downtime; the implication is that high plant availabilities minimize corrosion. In aggressive environments, measures to minimize corrosion during extended outages are desirable.

6. The observation that caked coal dust promotes aluminum corrosion suggests that the relative siting of the cooling tower and the coal pile is an important consideration. The chloride content of the coal is an important aspect of its corrosive character. Equally important may be the poultice effect of the caked coal dust. The particulate layer traps impurities and promotes local concentration cells.

7. The importance of contaminants, materials selection, and siting of the dry-cooling equipment is evident. For relatively small units where 15- to 20-year lifetimes are acceptable, aggressive environments can be tolerated by aluminum alloys, particularly if plant downtime is to be minimal. A few environments where aluminum does not function satisfactorily need to be recognized and avoided. At potential power plant sites or other large installations, corrosion evaluations should be part of the plant site evaluation, both before and during plant operation. In our investigations, specimen studies correlated well with observed corrosion on operating equipment. Corrosive conditions at some sites became evident in one year on specimens placed at the sites, in visual and metallographic examinations.

8. Laboratory studies at dry-cooling tower temperatures and ambient temperatures induced corrosion similar to corrosion on similar plant specimens. The laboratory specimens emphasize the importance of moisture in the corrosion process and emphasize effects of certain contaminants in attacking aluminum (in this test, chlorides and coal dust containing halides and sulfur compounds).

Acknowledgments

The authors would like to thank B. M. Johnson, G. E. Zima, and D. R. Pratt for their technical contributions. We appreciate aluminum specimens supplied by ALCOA and Reynolds Co. and the fin-tube specimen fabrication by the Hudson Co. We are grateful to the numerous industrial organizations that provided discussions, metal specimens, and responses to the mate-

rials survey. Lastly, we wish to acknowledge funding support of the Electric Power Research Institute, Coal Combustion Systems Division, and the Department of Energy, Advanced Nuclear Systems and Projects Division, for this research.

References

[1] DeSteese, J. G. and Simhan, K., "European Dry Cooling Tower Operating Experience," BNWL-1995, Battelle Pacific Northwest Laboratories, Richland, Wash., March 1976.
[2] Johnson, A. B., Jr., Pratt, D. R., and Zima, G. E., "A Survey of Materials and Corrosion Performance in Dry Cooling Applications, BNWL-1958, Battelle Pacific Northwest Laboratories, Richland, Wash., March 1976.
[3] Johnson, A. B., Jr., Begej, S., Martini, M. W., and May, R. P., "Aluminum Alloy Performance Under Dry Cooling Tower Conditions," PNL-2392, Battelle Pacific Northwest Laboratories, Richland, Wash., Dec. 1977.
[4] Caruthers, W. H., "Corrosion Performance of Aluminum Finned Dry Cooling Tower Coils at Neil Simpson Station, Wyodak, Wyoming," Reynolds Metals Company, Richmond, Va., 1973.
[5] Wong, D. et al, "Study of Corrosion and Its Control in Aluminum Solar Collectors," COO/2934-6, U. S. Department of Energy, Washington, D. C., April 1978.
[6] Fontana, M. G. and Greene, N. D., *Corrosion Engineering,* McGraw-Hill Co., New York, 1978.
[7] Graedel, T. E. and Schwartz, N., *Materials Performance,* Vol. 16, No. 8, Aug. 1977, pp. 17-25.
[8] Sereda, P. J., in *Corrosion in Natural Environments, ASTM STP 558,* American Society for Testing and Materials, 1974, pp. 1-22.

DISCUSSION

H. E. Townsend[1] (*written discussion*)—What are the origins and significance of the calcium that is present in the corrosion products.

K. R. Wheeler (*authors' closure*)—Calcium was present as surface deposition from airborne dust. Calcium appears only to be indirectly related to the corrosion process by providing surface deposition (that is, calcium carbonate), which tends to trap and concentrate other corrosive impurities.

[1] Bethlehem Steel Corp., Bethlehem, Pa.

W. Showak[1] *and S. R. Dunbar*[1]

Effect of 1 Percent Copper Addition on Atmospheric Corrosion of Rolled Zinc After 20 Years' Exposure

REFERENCE: Showak, W. and Dunbar, S. R., **"Effect of 1 Percent Copper Addition on Atmospheric Corrosion of Rolled Zinc After 20 Years' Exposure,"** *Atmospheric Corrosion of Metals, ASTM STP 767,* S. W. Dean, Jr., and E. C. Rhea, Eds., American Society for Testing and Materials, 1982, pp. 135–162.

ABSTRACT: The atmospheric corrosion characteristics of a commercial rolled zinc alloy containing 1 percent copper and an unalloyed grade have been evaluated after 20 years' exposure under ASTM Committee B-3 (now G 01.04.04) 1957 test program on atmospheric corrosion of nonferrous metals. Corrosion damage was assessed by measurement of loss in weight, loss in mechanical properties, and depth of pitting. The 20-year corrosion rates are analyzed with respect to previous 2- and 7-year results. Comparisons are also made with the behavior of three unalloyed grades of rolled zinc investigated in the 20-year 1931 program by Committee B-3 using weight loss and tension test methods.

Weight loss method appears to be the most reliable way of determining the corrosion rates of zinc. Corrosion rates found for zinc in the 1931 and 1957 test programs are in good agreement. The corrosion rate of zinc is not significantly affected by variations in compositions investigated.

Local galvanic action is probably responsible for the pitting which occurs in the copper-containing zinc alloy. Pitting is most severe in the marine atmosphere in direct contact with salt spray. The pit-depth/total-penetration ratio tends to decrease with increasing total penetration. The net change in tensile strength after 20 years' exposure at all four test sites is equal to or less than that expected due to weight loss. Tensile elongation is found to be more sensitive to corrosion effects than tensile strength, although both alloys still possess considerable ductility after 20 years.

A better way of compensating for aging in zinc is needed if tension test results are to be useful in evaluating corrosion damage.

KEY WORDS: atmospheric corrosion testing, corrosivity of atmospheres, corrosion rates, rolled zinc, zinc-copper alloy, mechanical properties, tensile strength, elongation, aging (metallurgical)

In 1931, ASTM Committee B-3 on Corrosion of Non-Ferrous Metals and Alloys initiated a comprehensive test program to evaluate atmospheric corrosion effects on nonferrous metals. Included in that program were three

[1] Research associate and scientist (Ret.), Gulf + Western Natural Resources Group, Zerbe Research Center, Bethlehem, Pa.

grades of rolled zinc: Prime Western, High Grade, and Special High Grade. These three materials differ in composition basically with respect to their lead, iron, and cadmium contents. The intent of the work was to evaluate the metals under test and to simultaneously study two alternative test procedures, loss-in-weight and change-in-tensile properties, for evaluating the damage done by corrosion. The results on zinc in the 1931 program for 10- and 20-year exposure periods were reported on by Anderson [*1,2*][2] in 1946 and 1955.

In recognition of the value of that early data, the Committee initiated a 1957 test program to obtain atmospheric corrosion data on additional nonferrous alloys, with emphasis on newer alloys not tested in the 1931 program. A rolled zinc alloy containing 1 percent copper was included in the 1957 program. Corrosion results for exposure time periods of 2 and 7 years at four ASTM test sites were presented in 1967 by Dunbar [*3*]. The results from 20-year exposures are now available and this paper contains an analysis of all the data obtained in the 1957 test program for zinc.

Zinc Materials Tested

The analyzed chemical compositions of the two hot-rolled zinc alloys evaluated in the 1957 test program are given in Table 1. Composition data are also given for High Grade zinc material tested in the 1931 test program for which comparative data are presented in this paper. The other two alloys used in the 1931 program are listed to show the range of compositions evaluated.

Test panels 203.2 by 101.6 by 1.27 mm (8 by 4 by 0.050 in.) were cut from

TABLE 1—*Chemical analysis of zinc compositions.*

Metal or Alloy	Commercial Designation or ASTM Grade	Chemical Analysis, weight %						Rolling Practice
		Zn	Pb	Fe	Cd	Cu	As	
		1957 Test Program						
Alloy 61	High Grade zinc	[a]	0.058	0.007	0.009	. . .	. . .	hot rolled
Alloy 62	1Cu-Zn	[a]	0.093	0.012	0.004	0.79	. . .	hot rolled
		1931 Test Program						
AA	Prime Western[b]	[a]	0.84	0.012	0.20	. . .	0.0001	pack rolled
BB	High Grade[b]	[a]	0.049	0.019	[c]	. . .	0.0006	hot rolled
HH	Special High Grade[b]	[a]	0.0055	0.0015	0.0010	. . .	[d]	hot rolled

[a] By difference.
[b] ASTM slab zinc grade.
[c] Not determined; probably about 0.002%.
[d] Not determined; probably very low.

[2] The italic numbers in brackets refer to the list of references appended to this paper.

the hot-rolled strip with the 203.2-mm (8 in.) dimension parallel to the rolling direction.

Test Program

Triplicate preweighed panels 203.2 by 101.6 by 1.27 mm (8 by 4 by 0.050 in.) of two rolled zinc compositions were exposed to the atmosphere for time periods of 2, 7, and 20 years at four ASTM test sites [*4*]:

A—Kure Beach, N. C., 24.38-m lot (80-ft lot)—East Coast marine. This site is located on the Cape Fear Peninsula, 17 miles southeast of Wilmington, N. C., and is 24.38 m (80 ft) from the Atlantic Ocean. The panels face east southeast parallel to the ocean. The saltwater spray falls directly on the test panels.

B—Newark, N. J. (New York area)—moderately severe industrial. Specimens face south southwest at an elevation of 3.35 m (11 ft). The area is surrounded by chemical plants and oil refineries.

C—Point Reyes, Calif.—West Coast marine. The site is located 588.3 m (1930 ft) from the ocean behind low hills covered with salt grass and bushes. Panels face west toward the Pacific Ocean. The atmosphere is characterized by salt spray and condensation from westerly winds and dense fogs. Specimens are wet most of the winter and in the summer the area is very dry by day with frequent, heavy fogs at night.

D—State College, Pa. (University Park)—rural. The site is located one mile north of State College, Pa., at an elevation of 358.1 m (1175 ft). The specimens face southeast. There is very little industrial contamination.

All panels were insulated from the test racks at each location and were exposed at an inclined angle of 30 deg from the horizontal.

Information on the duration of exposure at the four test sites is presented in Table 2. The time of exposure varied slightly for the 20-year exposures. It is to be noted that two different sets of panels were exposed at Point Reyes, Calif., because of vandalism in the fall of 1962 after about 4 years' exposure. A second set of panels was installed at this location on 12 June 1964. The second set of panels for both alloys comprised reserve panels taken from the same rolled materials as the original panels and held in storage at ASTM headquarters. This means that data for Point Reyes are available only for exposure periods of 2, 7, and 15 years and that the exposure time periods for 7- and 15-year panels do not overlap those of 2-year panels. Around 1972, the panels exposed at Newark were moved several miles to another location at Kearny, N. J.

To remove corrosion products after exposure, specimens were chemically cleaned, according to methods reported elsewhere [*5*], and weighed. Weight losses due to corrosion were calculated from specimen weights prior to and

TABLE 2—*Test sites and exposure periods.*

Exposure Site	Site Code	Date Exposed	Date Removed			Days Exposed			
			2 Years	7 Years	20 Years	2 Years	7 Years	20 Years	15 Years
Kure Beach, N. C. (80-ft site)[a]	A	11/22/58	11/21/60	11/22/65	11/22/78	730 2 years	2557 7 years	7305 20 years	
Newark, N. J.[b]	B	10/31/58	11/ 3/60	11/1/65	6/21/79	734 2.01 years	2558 7 years	7538 20.65 years	
Point Reyes, Calif.	C	6/11/58 6/12/64	6/ 6/60	6/6/71	5/16/79	726 1.99 years	2550 6.99 years		5452 14.94 years
State College, Pa. (University Park)	D	11/ 6/58	11/10/60	10/18/65	4/12/79	735 2.01 years	2538 6.95 years	7462 20.44 years	

[a] Feet × 0.3048 = metres.
[b] Panels transferred from Newark to Kearny, N. J. site in about 1972.

after exposure. Two standard ASTM tension test specimens were then machined from each panel and the ultimate tensile strengths (based on the original thicknesses) and elongations were determined. A schematic drawing of an exposure panel showing the position of the tension test specimens is given in a previous publication [3]. Similar tension test data were also obtained on triplicate test specimens cut from each of duplicate initial and storage panels that served as controls. The storage panels, wrapped in waterproof paper and wax coated, were kept by The New Jersey Zinc Co. in a constant-temperature room controlled at 25 ± 1°C. All tension tests on zinc were run at 6.35 mm/min (0.25 in/min.) head speed with the stress parallel to the rolling direction.

Pit depth measurements were made on the center section of each exposed panel after removal of the tension test specimens. A calibrated focus microscope was used to determine the four deepest pits in each panel.

Results

Table 3 lists all the original and derived data or the several evaluation methods used to appraise the two rolled zinc alloys after 20 years' exposure. The data from Point Reyes are for only 15 years' exposure.

Corrosion Rates—Weight Loss

The corrosion rates determined by weight loss measurements for the two zinc alloys exposed 2, 7, and 20 years are shown graphically in Fig. 1. As a result of vandalism at the Point Reyes site (C) in the fall of 1962, replacement panels had to be exposed in June 1964; these may influence the corrosion results for the 7- and 15-year periods relative to the 2-year exposures.

In general, the addition of copper to zinc (Alloy 62) has little effect on the corrosion rate with the possible exception of the Kure Beach and Point Reyes locations. At Kure Beach, the difference in corrosion rate between Alloy 61 and Alloy 62 increases with increasing exposure time with the copper-containing Alloy 62 displaying the higher rate. A significantly higher corrosion rate for Alloy 62 is found after 2 years at Point Reyes, but this difference decreases and tends to be negligible after 7 and 15 years. These results indicate that copper has a slight accelerating effect on zinc corrosion in the marine environment. The higher corrosion rate produced by copper in zinc is not unexpected since zinc is electronegative to most of its metal impurities and alloying elements, to hydrogen, and to most surface contaminants. In marine environments airborne salts may deposit on the panel surfaces and combine with moisture to form electrolytes with low resistivity. Electrochemical cells can then form between zinc and copper, which results in accelerated galvanic corrosion of the anodic zinc.

The corrosion rates at three of the test sites fluctuate with exposure time. Site A (East Coast marine) shows the highest corrosion rate after 2 years:

TABLE 3—*Twenty-year data for rolled zinc alloys in 1957 test program.*

Metal	Density, g/cc	Site	Nos.	Exposure Time, days	Weight Change		Corrosion Rate		Pit Depth, mils					Ultimate Tensile Strength, ksi		Elongation in 2 in., %	
									4 Deepest			Maximum					
					g	mg/dm²	mdd[a]	mpy[b]	Sky	Ground	Avg	Sky	Ground	Control	Exposed	Control	Exposed
Alloy 61 (High Grade zinc)	7.13	Kure Beach, NC (80 ft) (A)	49–50	7305	13.10	3121	0.427	0.085	9.61	6.77[c]	8.19	10.47	8.11	19.5	17.65	64	39
			51–52		14.73	3544	0.485	0.097	7.41	7.62	7.52	7.87	10.04		18.0		43.5
			53–54		16.07	3830	0.524	0.105	8.86	9.01[d]	8.94	10.24	9.01		17.45		40
		Newark, N. J.[e] (B)	55–56	7538	21.50	5141	0.682	0.137	2.37	4.88	3.63	3.62	5.51		17.8		55
			57–58		22.93	5467	0.725	0.146	4.49	5.33	4.91	5.16	6.61		17.65		49
			59–60		22.70	5449	0.723	0.145	3.91	6.51	5.21	4.25	10.83		17.75		33
		Point Reyes, Calif. (C)	61–62	5452	2.64	631	0.116	0.023	3.37	3.18	3.26	4.02	3.43		19.55		48
			63–64		0.62	148	0.027	0.005	3.70	2.85	3.28	5.12	3.94		20.05		54.5
			65–66		4.97	1187	0.218	0.044	3.69	3.51	3.59	4.21	3.81		19.65		56.5
		State College, Pa. (D)	67–68	7462	6.89	1633	0.219	0.044	2.58	3.35	2.97	2.80	4.45		19.15		52.5
			69–70		7.31	1747	0.234	0.047	3.90	3.55	3.73	5.12	4.65		19.25		56.5
			71–72		7.62	1817	0.243	0.049	3.03	3.60	3.32	3.58	4.41		19.1		57
Alloy 62 (1Cu-Zn)	7.18	Kure Beach, N. C. (80 ft) (A)	49–50	7305	20.47	4858	0.665	0.134	13.79	6.56	10.18	18.31	8.39	22.8	20.35	52	27.5
			51–52		21.62	5120	0.701	0.141	14.51	3.37	8.94	17.12	4.17		20.25		25.5
			53–54		20.21	4786	0.655	0.132	13.03	7.07	10.05	15.51	10.40		20.85		26
		Newark, N. J.[e] (B)	55–56	7538	24.89	5884	0.780	0.157	6.74	9.29	8.02	8.35	11.38		21.05		43
			57–58		23.84	5657	0.751	0.151	6.96	7.06	7.01	7.28	8.35		21.35		43.5
			59–60		24.21	5725	0.759	0.153	5.99	9.18	7.58	7.28	10.62		20.95		45
		Point Reyes, Calif. (C)	61–62	5452	3.43	812	0.149	0.030	2.11	2.62	2.37	2.91	3.23		22.2		47
			63–64		4.34	1082	0.189	0.038	2.64	2.77	2.71	3.19	2.95		22.4		50.5
			65–66		2.83	670	0.123	0.025	2.07	3.21	2.64	2.44	4.41		23.1		47.5
		State College, Pa. (D)	67–68	7462	8.16	1932	0.259	0.052	4.07	4.83	4.45	4.84	4.92		21.95		46.5
			69–70		8.63	2043	0.273	0.055	3.76	4.50	4.13	4.06	5.08		22		50.5
			71–72		8.58	2027	0.272	0.055	3.91	4.28	4.10	4.09	4.61		21.4		45.4

[a] mdd = milligrams per square decimetres per day.
[b] mpy = mils per year.
[c] Two pits.
[d] Single pit.
[e] Panels moved from Newark to Kearny, N. J., site in about 1972.
Conversion factors: feet × 0.3048 = metres.
mpy × 25.4 = μm/year.
mils × 25.4 = μm/year.
ksi × 6.9 = MPa.

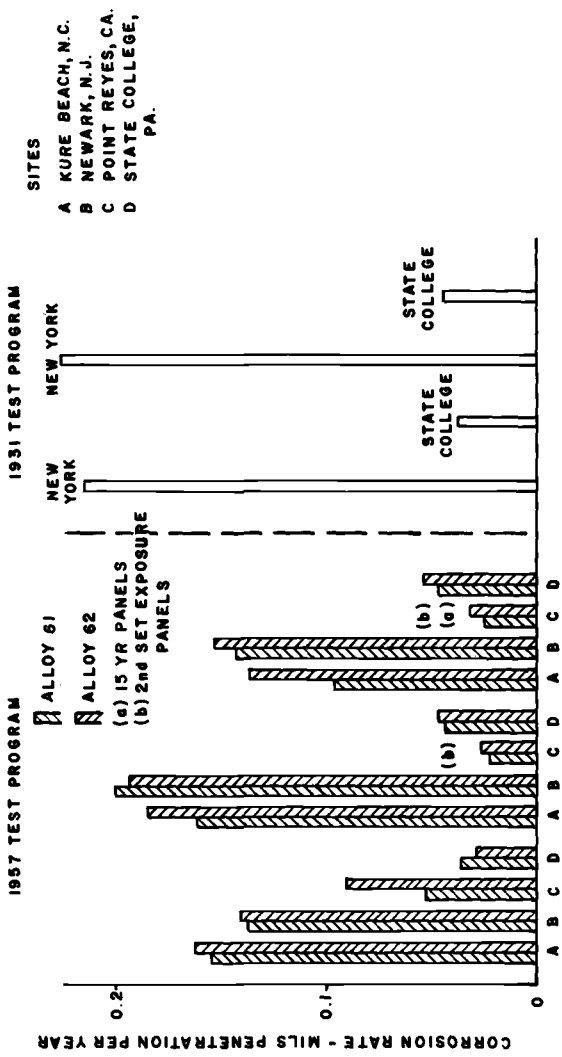

FIG. 1—*Corrosion rates of Alloy 61 (High Grade zinc) and Alloy 62 (1Cu-Zn) at various sites for various exposure times. Comparable data from 1931 test program included (mils by 25.4 = μm/year).*

3.94 to 4.14 μm/year (0.155 to 0.163 mils/year), whereas Site B (industrial) is most corrosive at 7 years: 4.90 to 5.08 μm/year (0.193 to 0.200 mils/year), and 20 years: 3.63 to 3.89 μm/year (0.143 to 0.153 mils/year). As expected, the lowest corrosion rate is displayed by the rural atmosphere (Site D) for the 2-year exposure time: 0.711 to 0.904 μm/year (0.028 to 0.0356 mils/year), but the West Coast marine (Site C) holds this position at 7 years: 0.559 to 0.660 μm/year (0.022 to 0.026 mils/year). Since 20-year data are not available for Site C, a comparison cannot be made with Site D for this exposure time. For the Kure Beach (East Coast marine) and Newark (industrial) sites the corrosion rate shows an apparent maximum at 7 years, while an apparent minimum in corrosion rate at Point Reyes occurs at 7 years, which illustrates the variability of atmospheric corrosivity at these locations. As pointed out earlier, the fact that panels at Point Reyes were exposed on two different dates 6 years apart may have influenced the corrosion rates observed after 2 years compared with those after 7 and 15 years.

Past short-term exposure studies [*6,7,8*] have shown that marine test sites can differ considerably in their corrosivity and that corrosivity at a given site can vary from year to year. Factors such as time of wetness of the corroding metal panels, panel temperature, and atmospheric sulfur dioxide and atmospheric chloride content can alter corrosion rates in a marine environment. At the 24.38-m (80 ft) lot at Kure Beach test panels are subjected to direct salt spray so that the atmosphere will contain higher concentrations of chloride than lots that are farther away from the ocean, as is the case for Point Reyes. A combination of salt spray and little rain, or widely dispersed periods of rain, can cause a considerable increase in corrosion as occurred at Kure Beach after 7 years. At the industrial Newark/Kearny sites the high, variable corrosion rate is probably due in large part to the acidity of the moisture caused by the sulfur dioxide content in the atmosphere produced by chemical plants and oil refineries in the area. The decrease in corrosivity at the Newark site in recent years may be due to a reduction in sulfur dioxide activity produced by installation of industrial pollution control systems.

Only at the rural State College site does the corrosion rate increase slightly and consistently with increasing exposure time. A similar increase in corrosion rates with time for High Grade Zinc was observed for industrial (New York) and rural (State College) areas in the 1931 program as shown in Fig. 1. The corrosivity of the New York site in the 1931 program is higher than that for the Newark site in the 1957 program. The lower corrosivity at the Newark/Kearny sites may be due to site location or an actual reduction in industrial pollution due to pollution control measures taken in the New York area in recent years. The data for rural State College indicate that the corrosivity at this site has been gradually increasing over the years. This increase in corrosion rate is not unusual since there has been population and industrial growth in the State College area over the past 50 years, which probably means higher levels of sulfur dioxide in the atmosphere.

It is to be noted that the 1931 panels were exposed vertically while the 1957 panels were exposed 30 deg from horizontal. The good agreement between the two sets of results indicates that panel exposure angle has no great effect on overall corrosion rate based on these limited data. However, panels exposed at 30 deg to the horizontal tend to develop a rougher surface texture under corrosive attack, as is discussed in the next section.

Corrosion Effects—Pitting

Zinc panels exposed in the 1931 test program were found to corrode smoothly and to be free of pits, except for the marine site at La Jolla, Calif., where surface roughening occurred. In the 1957 program, pitting and roughening of the zinc panel surfaces occurred. This difference in behavior is thought to have been caused by the fact that the 1931 panels were mounted vertically and the 1957 panels were mounted 30 deg from horizontal. On the latter sloping panels contaminants can deposit and adhere more readily and moisture will drain less rapidly than on vertically mounted panels.

Photographs at ×11 1/2 magnification of the skyward and groundward surfaces of Alloy 61 (High Grade) and Alloy 62 (1Cu-Zn) panels exposed for 20 years with surface corrosion products removed are shown in Figs. 2 to 5. The Point Reyes panels were exposed for only 15 years. Similar data were presented previously for these materials after 7 years of exposure at Kure Beach, Newark, and State College [*3*]. The surfaces of the panels of the copper-bearing alloy appear darker in the photographs because of a black film of redeposited copper from the cleaning operation. The differences between the copper-bearing and copper-free zinc alloys are accentuated at these magnifications, being only slight on visual observation.

The appearances of the surfaces of the panels exposed for 7 [*3*] and 20 years are not greatly different for the various exposure sites. The pits observed on the panels of Alloy 61 and Alloy 62 exposed 20 years at Kure Beach appear deeper, but their numbers, diameters, and distribution are similar to the 7-year panels. The degree of surface roughening of Alloy 62 at the Newark and State College sites is more pronounced for the longer exposure time on both the skyward and groundward surfaces. The 15-year corroded panels at Point Reyes show the least general surface roughness among all the panels, although some pitting on both surfaces is clearly visible.

Photographs of polished cross sections of the 20-year panels at ×4 1/2 magnification showing pit depth and shape and general surface roughness caused by corrosion are given in Figs. 6 and 7. Pitting tended to be more distinct on panels of the copper-containing alloy due to local galvanic cells set up between zinc and the more noble zinc-copper epsilon phase precipitated from solid solution as particles, predominantly at grain boundaries. The High Grade zinc panels displayed more of a tendency to develop general surface roughness comprised of hills and valleys or large craters. Valleys were consid-

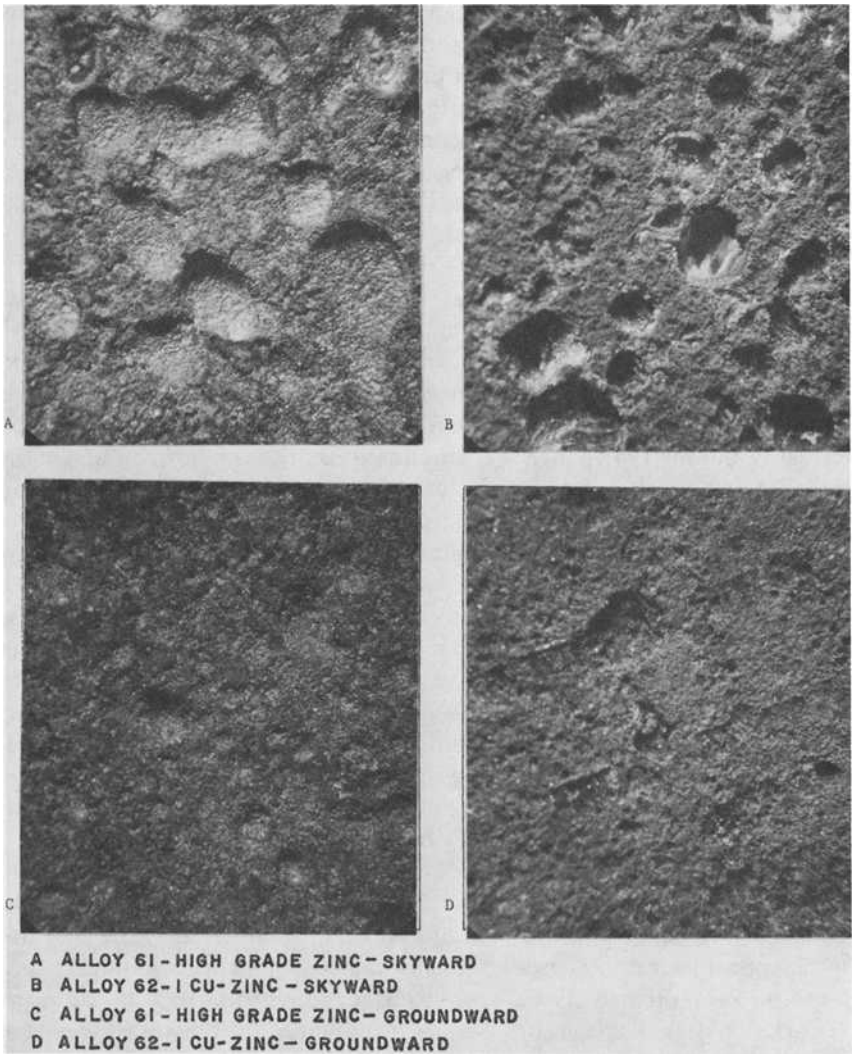

FIG. 2—*Photographs of the surfaces of 20-year panels from Kure Beach with corrosion products removed* (×11 1/2).

ered as pits in making pit depth measurements. Pit depth data for the various panels are given in Fig. 8. The four deepest pits on each of triplicate panels were averaged to obtain the values shown. Pit depths of Alloy 61 and Alloy 62 are compared for both skyward and groundward surfaces.

It can be seen from the photographs that a greater number of pits are present on the skyward surfaces of the panels than on the groundward surfaces. The pit depth data (Fig. 8) show that deeper pits tend to develop on the

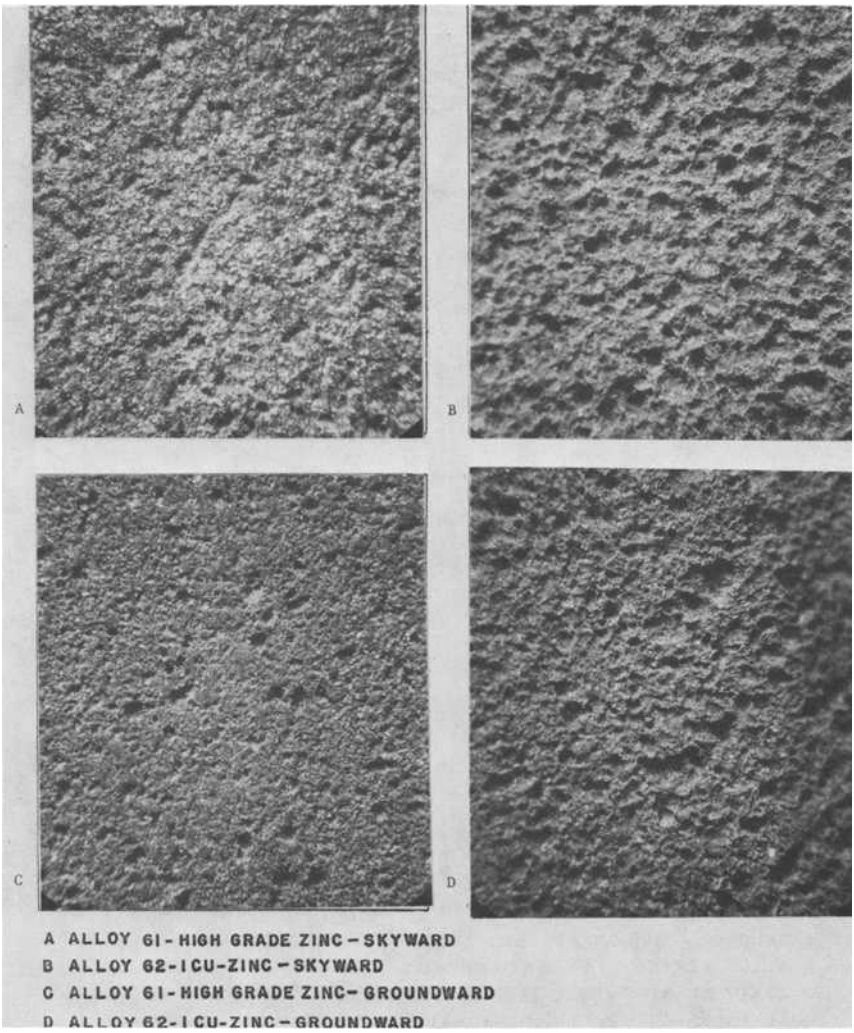

FIG. 3—*Photographs of the surfaces of 20-year panels from Newark with corrosion products removed* (×11 1/2).

copper-containing zinc alloy panels. This is particularly true for the panels exposed at the Kure Beach and Newark sites. With the exception of these same sites, pit depths on the skyward and groundward surfaces are not significantly different. The greatest pit-depths are obtained at Kure Beach for the zinc-copper alloy on the skyward surface and the greatest increase in pit depth on increasing exposure time from 7 to 20 years occurs at this location. Pit depths developed on panels at State College and Point Reyes appear to be

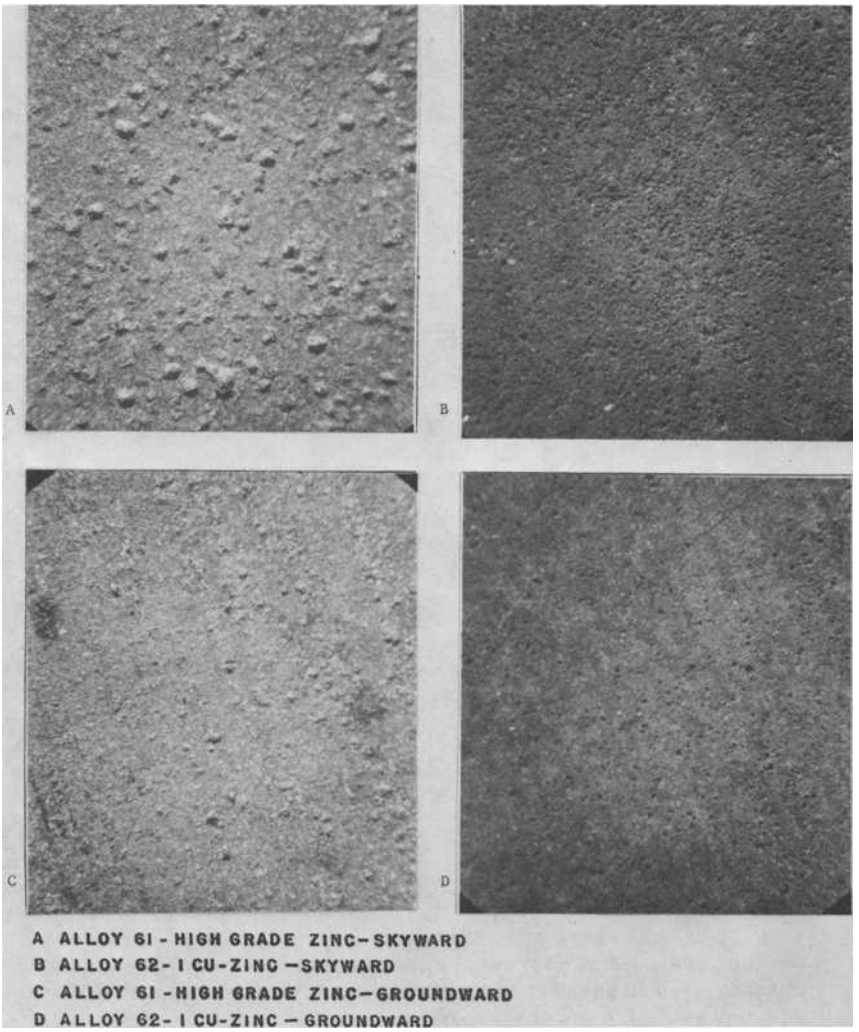

FIG. 4—*Photographs of the surfaces of 15-year panels from Point Reyes with corrosion products removed (×11 1/2).*

quite similar and show no marked differences due to alloy composition. It should be noted that the data for Point Reyes are only for 15-year exposure. While pit depths tend to increase with time at all the exposure sites, the rate of increase tends to diminish with time except possibly in the marine environments.

The relationship between average total penetration of a panel by general corrosion and by pitting corrosion can be seen from the pit-depth/total-

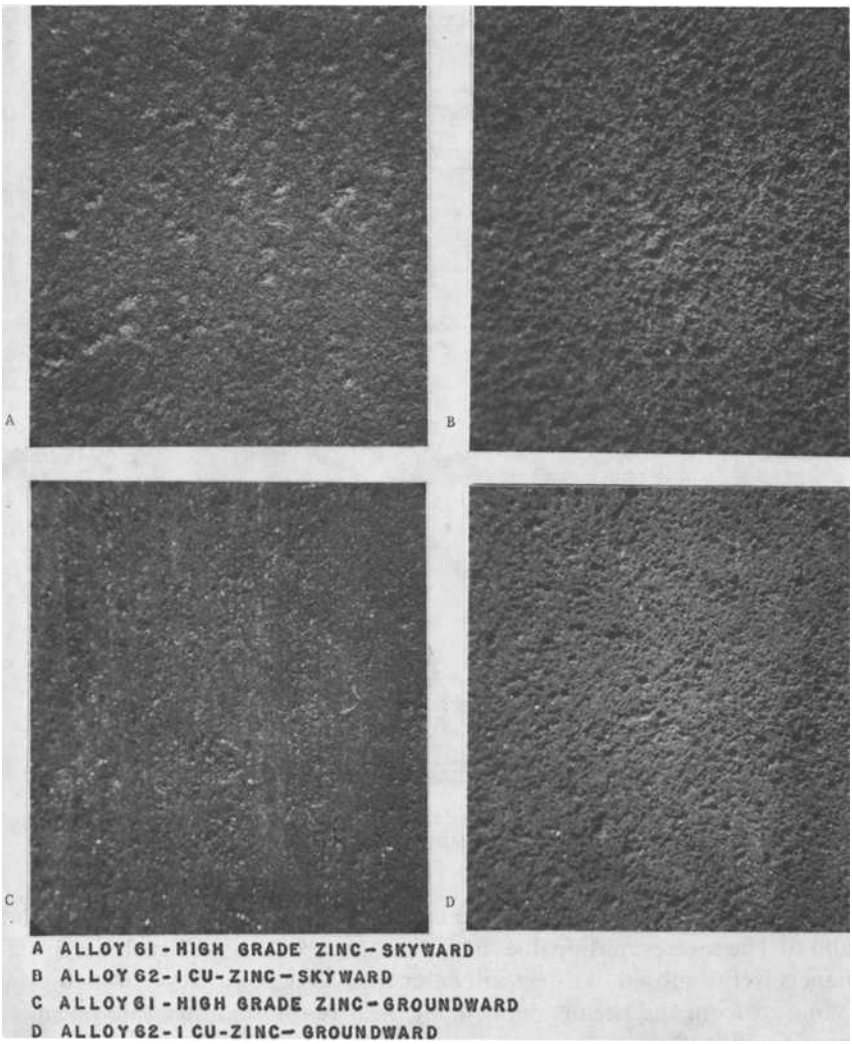

FIG. 5—*Photographs of the surfaces of 20-year panels from State College with corrosion products removed* (×11 1/2).

penetration ratios given in Table 4. Pit depths used are those for the skyward side. Total penetration values are calculated by multiplying the corrosion rate in mils per year by the years of exposure.

For the Newark and State College sites the ratio is the highest after 2 years and tends to decrease at the longer exposure times. The lowest ratios for Alloy 61 and Alloy 62 are observed at the Newark site after 20 years, where the overall corrosion rates are the highest. At the marine sites, Kure Beach

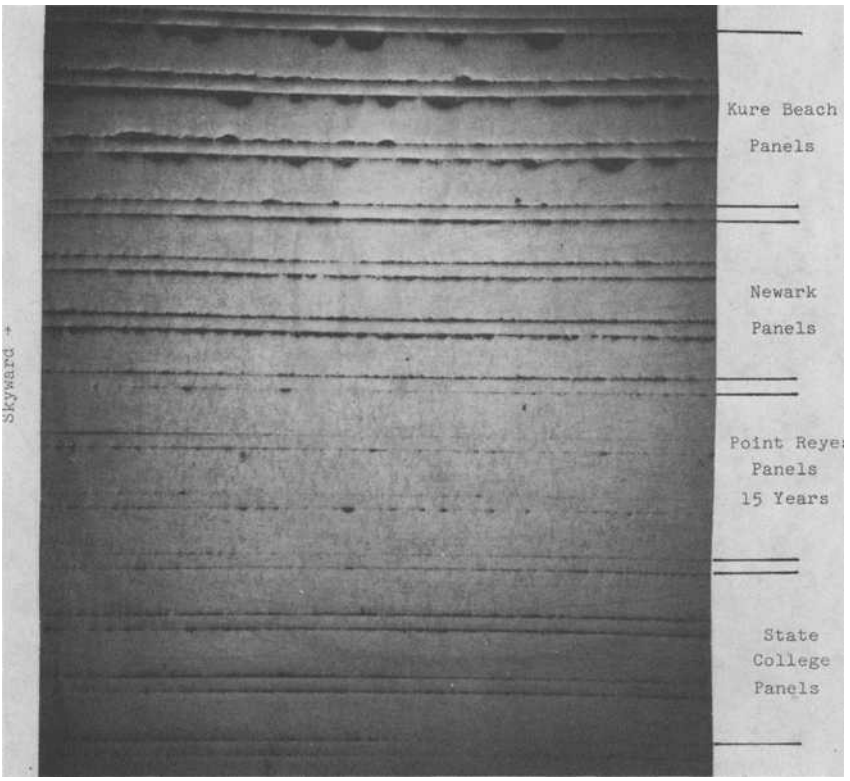

FIG. 6—*Cross sections of 20-year exposed panels of Alloy 61 with corrosion products removed (×4 1/2). Thin zinc spacers separate the test specimens.*

and Point Reyes, the ratio is found to fluctuate with exposure time for both alloys. The severest pitting does occur at the seacoast Kure Beach site, where panels were exposed to direct saltwater spray. At Point Reyes, which is far removed from the ocean, the content of airborne seawater salts seems to have a minor effect on the overall corrosion of zinc, but pitting appears to be significant.

Some of the factors, in addition to pit geometry and alloy composition, that might play a role in pit growth characteristics in the various environments include filling of pits with corrosion products, pH of moisture entering the pit, electrical conductivity of moisture entering the pit due to contained salts, and rate of drying in the pit relative to general panel surface. The higher conductivity of electrolytes entering the pits at marine locations like Kure Beach and Point Reyes probably makes a major contribution to the general pitting process and accentuates the effect of copper in zinc on pitting.

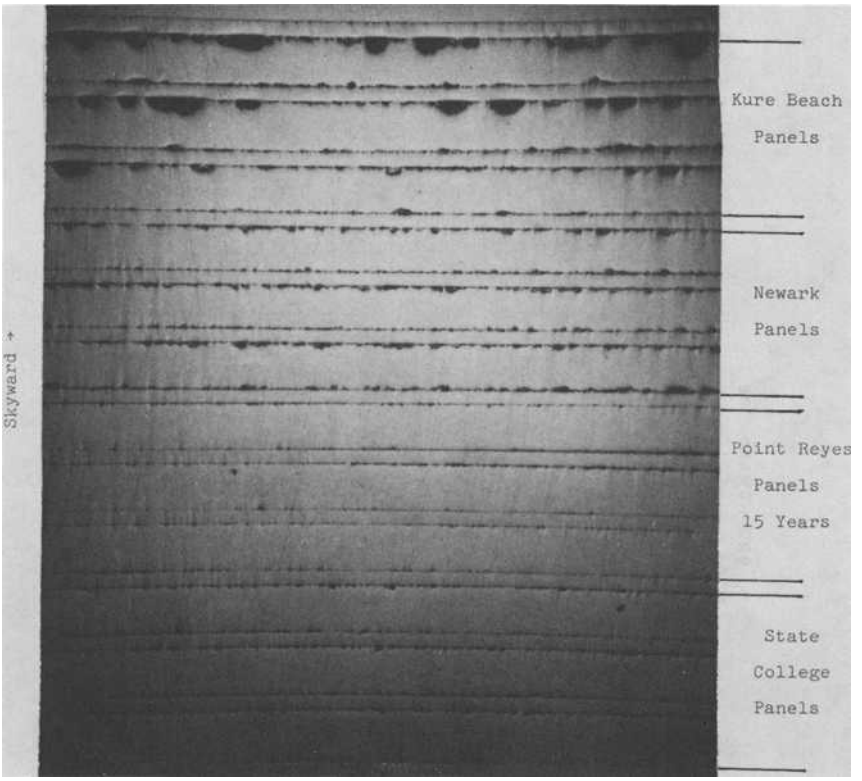

FIG. 7—*Cross sections of 20-year exposed panels of Alloy 62 with corrosion products removed (×4 1/2). Thin zinc spacers separate the test specimens.*

From a practical standpoint, perforation of zinc by pitting is most likely to occur in marine environments. Zinc containing copper would be more prone to perforation-type failure than unalloyed zinc.

Mechanical Property Changes

Strength and ductility data obtained on original, stored, and corroded panels of Alloys 61 and 62 to determine if these properties can be correlated with corrosion rates are given in Figs. 9 to 16.

Tensile Strength

Tensile strength data for Alloys 61 and 62 are given in Figs. 9 and 10, respectively. The stored specimens of Alloy 61 show minor fluctuations in strength as a function of storage time due to aging, amounting to a total change in tensile strength relative to that of the original panel of 3.45 MPa

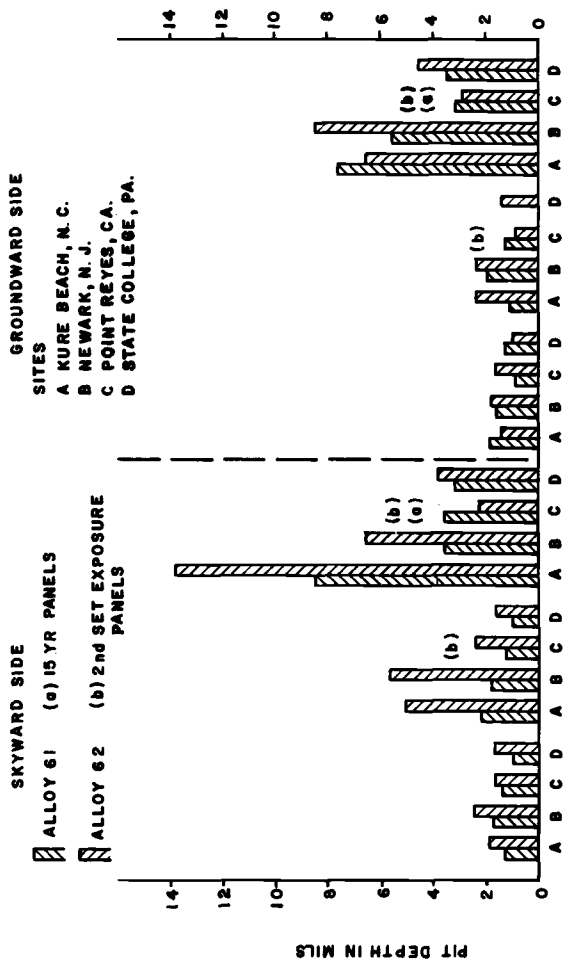

FIG. 8—*Pit depth data for Alloys 61 and 62 for various exposure times at four exposure sites (mils by 25.4 = μm/year).*

TABLE 4—*Relationship between average total penetration and pit depth.*

Location	Metal	Total Penetration, mils[a]			Pit Depth,[b] mils			Pit Depth/Total Penetration Ratio		
		2 Years	7 Years	20 Years	2 Years	7 Years	20 Years	2 Years	7 Years	20 Years
Kure Beach, N. C.	Alloy 61	0.310	1.127	1.92	1.29	2.25	8.66	4.27	2.00	4.51
(80 ft site)	Alloy 62	0.327	1.295	2.72	1.86	5.10	13.78	5.60	3.94	5.07
Newark, N. J.[d]	Alloy 61	0.274	1.400	2.86	1.69	1.79	3.59	6.18	1.28	1.26
	Alloy 62	0.282	1.351	3.06	2.50	5.69	6.56	8.90	4.21	2.14
Point Reyes, Calif.	Alloy 61	0.106	0.154	0.36[c]	1.42	1.25	3.59[c]	13.40	8.11	9.97[c]
	Alloy 62	0.182	0.179	0.465[c]	1.69	2.42	2.27[c]	9.30	13.52	4.88[c]
State College,	Alloy 61	0.071	0.304	0.92	1.04	0.94	3.17	14.45	3.09	3.45
University Park, Pa.	Alloy 62	0.056	0.324	1.08	1.56	1.63	3.91	27.90	5.03	3.62

[a] Mils × 25.4 = μm.
[b] Skyward side.
[c] Removed after 15 years.
[d] Panels moved to Kearny, N. J. site in about 1972.

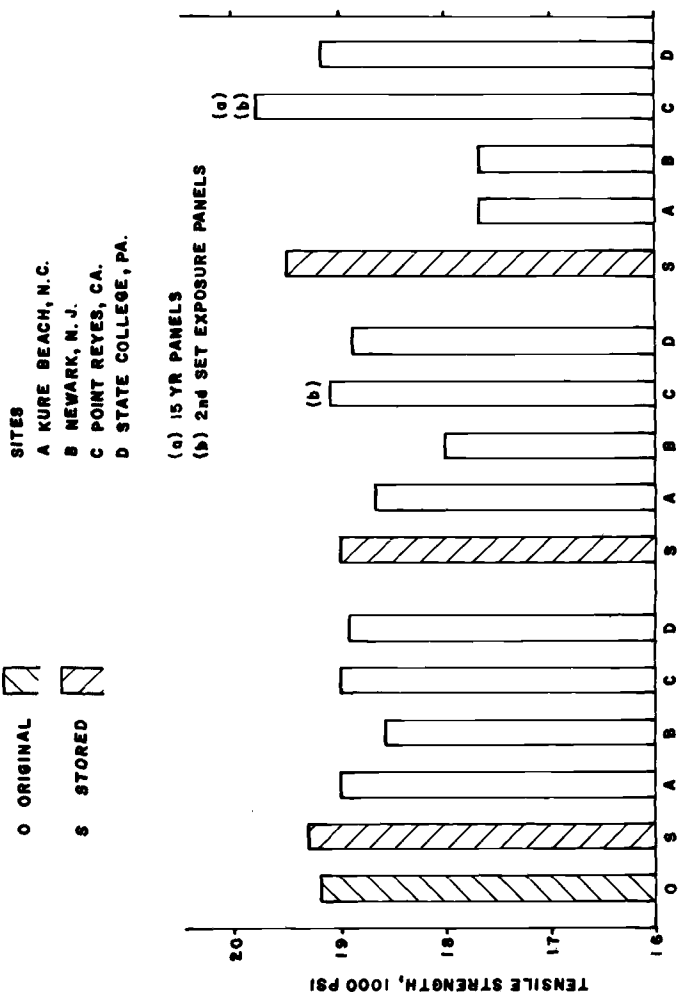

FIG. 9—*Tensile strength of Alloy 61 after various times at four test sites (psi by 0.0069 = MPa).*

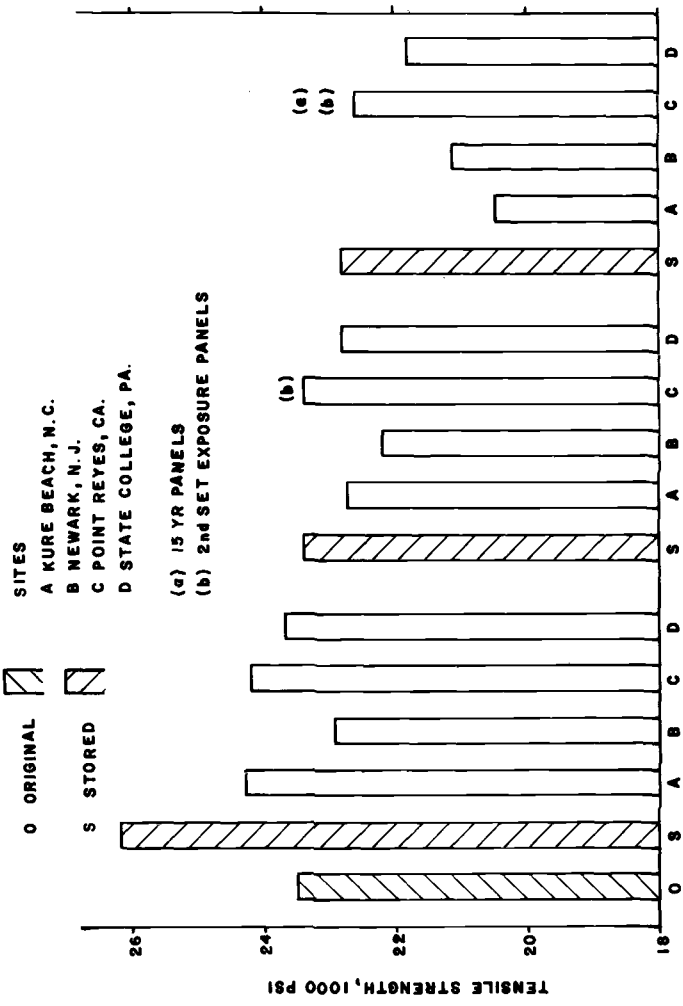

FIG. 10—*Tensile strength of Alloy 62 after various exposure times at four test sites (psi by 0.0069 = MPa).*

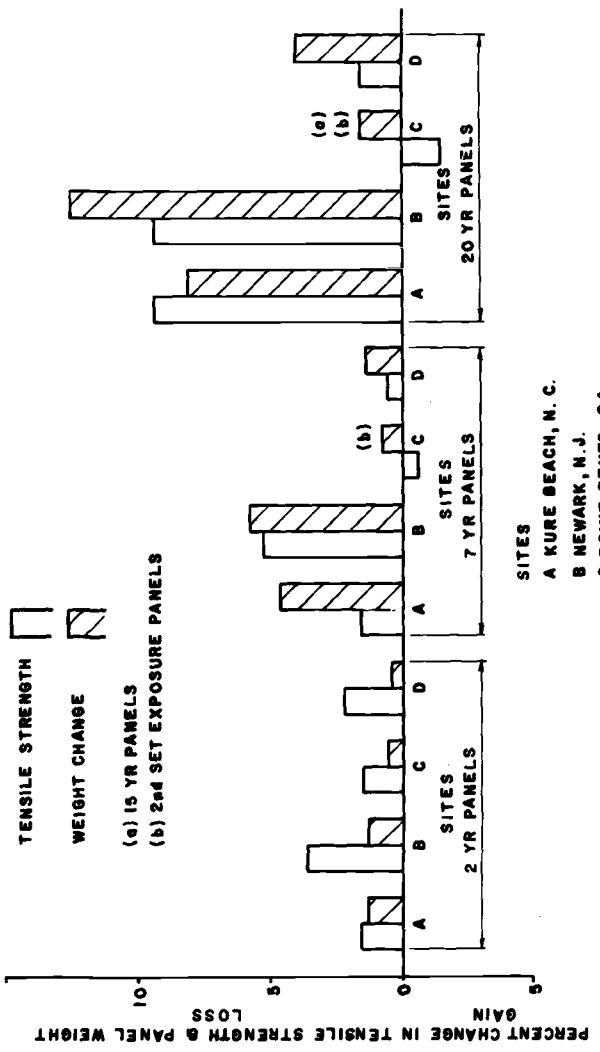

FIG. 11—*Comparison of percent change in tensile strength and weight for exposed panels of Alloy 61.*

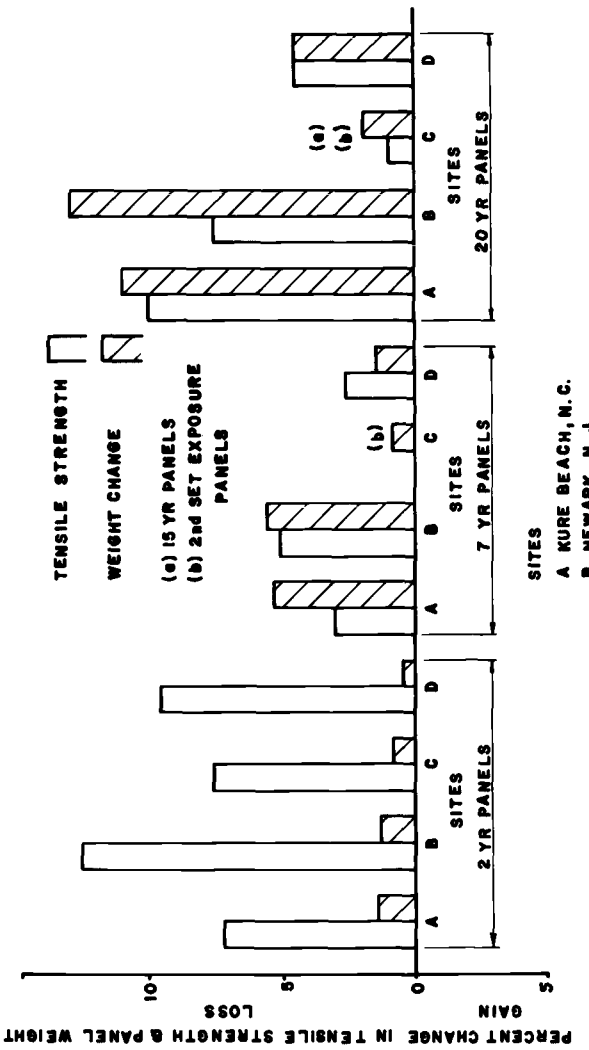

FIG. 12—*Comparison of percent change in tensile strength and weight for exposed panels of Alloy 62.*

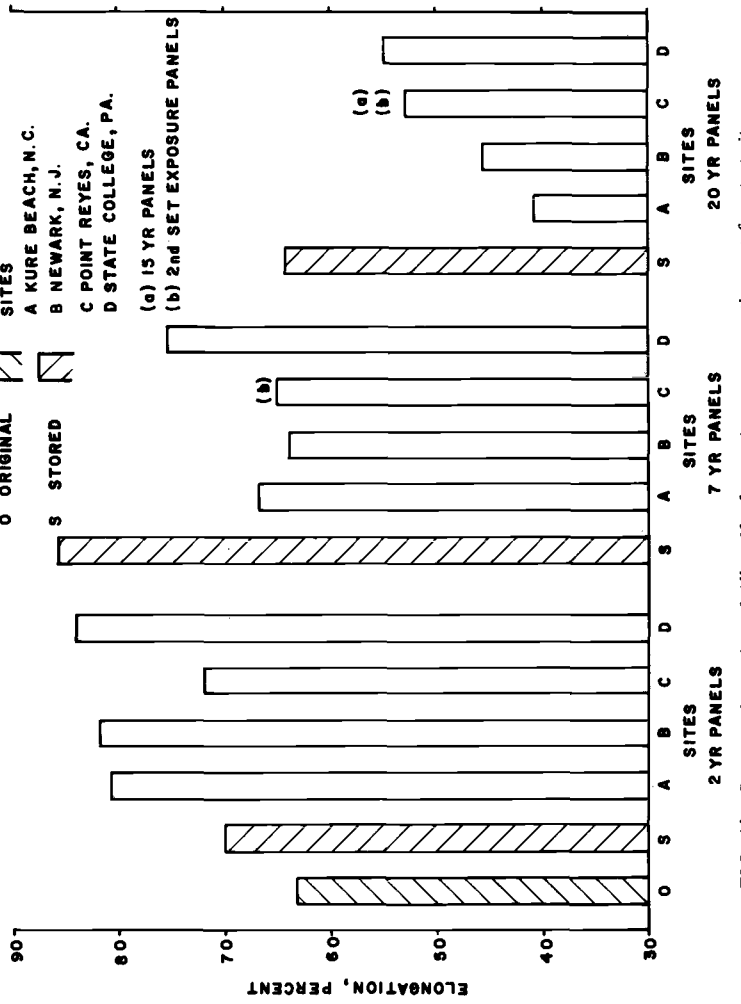

FIG. 13—*Percent elongation of Alloy 61 after various exposure times at four test sites.*

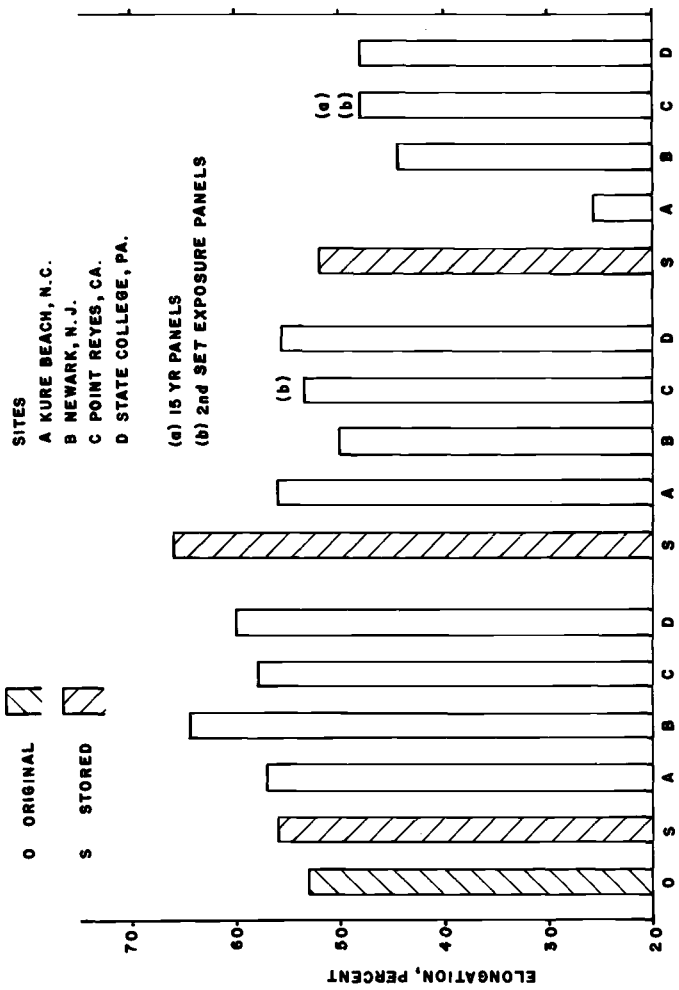

FIG. 14—*Percent elongation of Alloy 62 after various exposure times at four test sites.*

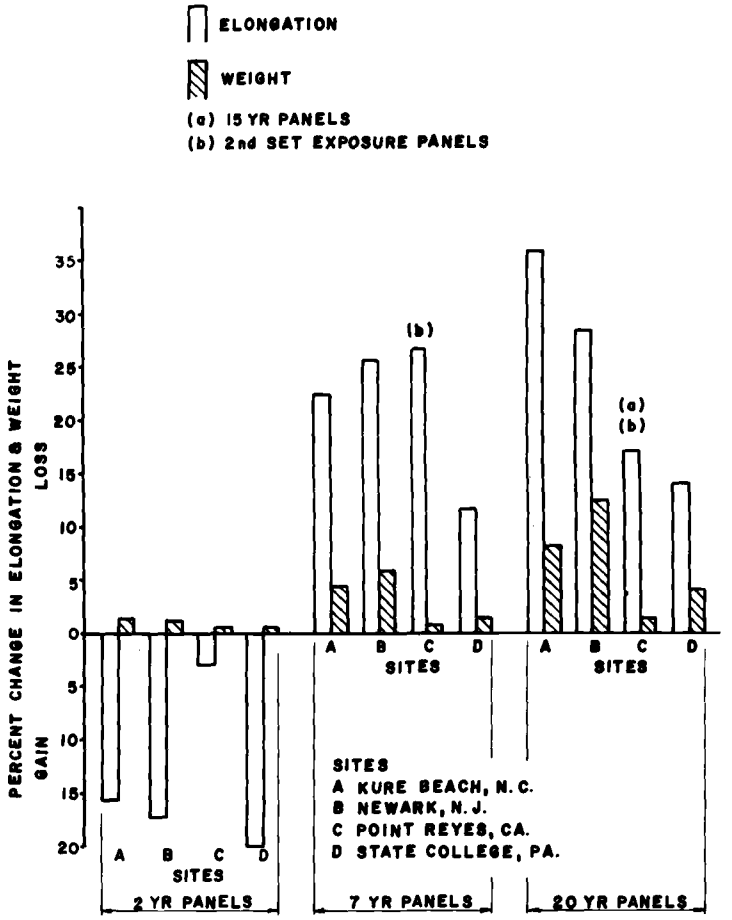

FIG. 15—*Comparison of percent change in elongation and weight for exposed panels of Alloy 61.*

(500 psi) (2.6 percent). Among the exposed specimens, only those at the Kure Beach and Newark sites show a significant loss in strength with increasing exposure time. Heat from a grass fire at the Newark lot prior to the removal of the 2-year panels may have altered the strength of the zinc panels. The 7- and 15-year panels exposed at Point Reyes display higher strengths than the 7- and 20-year stored panels, probably as a result of different time and temperature aging histories. The former materials represent a second set of panels which were previously stored 5 years indoors before exposure outdoors at Point Reyes.

The stored panels of Alloy 62 which contain copper (Fig. 10) show a large increase in strength of about 11.5 percent over that of the original control material after 2 years, followed by a decrease at longer exposure times. The total change in tensile strength for stored panels due to aging amounts to

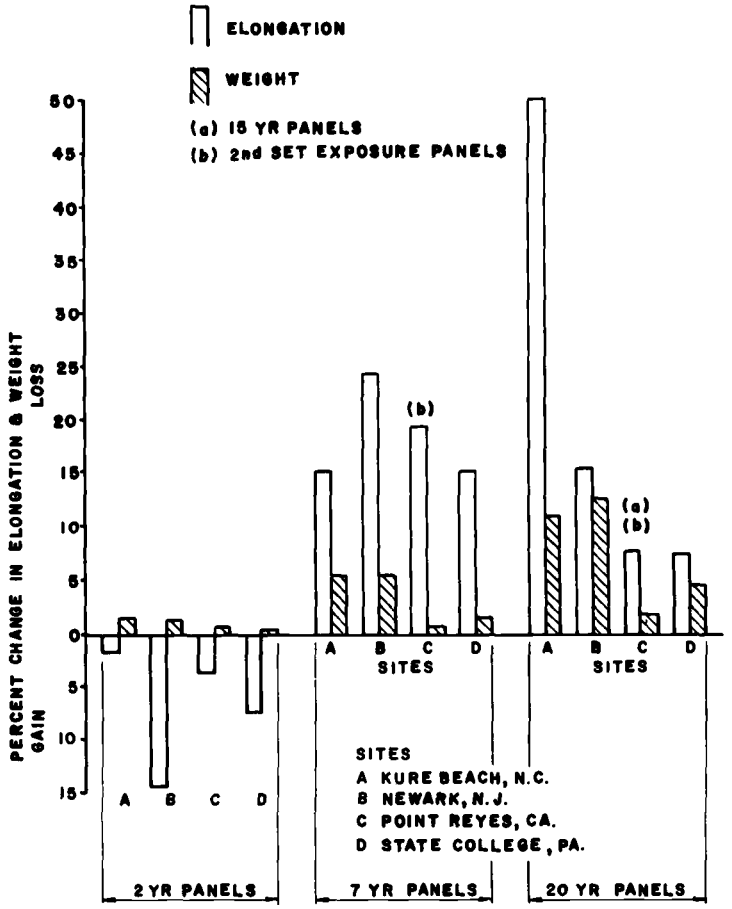

FIG. 16—*Comparison of percent change in elongation and weight for exposed panels of Alloy 62.*

23.46 MPa (3400 psi) (14.5 percent). Except for the Point Reyes site for 7- and 15-year exposure times, all corroded panels show a noticeable loss in tensile strength compared with the stored panels, as was the case for Alloy 61.

If the changes in strength of the corroded panels are caused only by uniform loss in section thickness (loss in weight), then the percent loss in tensile strength should be equal to the percent loss in weight. If corrosion is nonuniform or pitting occurs, the percent loss in strength should be somewhat greater than the percent loss in weight. As discussed in the foregoing, aging in zinc can produce both positive and negative changes in strength.

Data for the percent change in tensile strength are compared with percent weight loss for Alloy 61 in Fig. 11 and for Alloy 62 in Fig. 12. The tensile strengths of the stored panels were used as the base to calculate the percent change in strength for the exposed panels. The poorest agreement between

strength and weight loss is obtained at the shortest exposure of 2 years for both alloys with Alloy 62 showing the greatest difference because it undergoes the largest strength changes on aging. The correlation between strength and weight changes improves at the longer 7- and 20-year exposure times because weight loss values are increasing and strength changes due to aging tend to become smaller, but discrepancies between the two parameters still exist. As previously mentioned, aging in the 7- and 15-year corroded Alloy 61 panels at Point Reyes is responsible for the gains in tensile strength observed. Even for the 20-year corroded panels at Kure Beach and Newark which tend to have the deeper pits, the percent loss in tensile strength is less than percent loss in weight due to corrosion, indicating that aging and other effects besides corrosion are influencing the tensile strengths of the zinc alloys.

Besides aging, another factor which may account for some of the lack of agreement between strength and weight loss values is the precision with which these measurements can be made. The range of standard deviations for tensile strength for Alloy 61 are from 0.55 to 2.57 MPa (81 to 373 psi) and for Alloy 62 from 2.37 to 6.39 MPa (343 to 926 psi) for the 20-year exposures. These deviations represent from 0.5 to 4 percent of the measured tensile strengths and, therefore, can contribute to the magnitude of the observed differences. For instance, the range in the percent change in weight obtained in the 1957 program for corroded panels of Alloys 61 and 62 exposed for 2, 7, and 20 years are 0.23 to 1.31, 0.66 to 5.84 and 1.51 to 12.87, respectively. In particular, the percent changes in weight for panels exposed for 2 years are quite small.

The results on changes in tensile strength and weight loss show that apparent good correlation is achieved in some cases and poor correlation in others. The major factor responsible for observed differences appears to be the inability to ascertain how much of the measured changes in tensile strength are due to corrosion and how much to aging changes within the metal itself. The storage set procedure employed in the 1957 test program does not provide a reproduction of the thermal history experienced by the exposed specimens. A solution to this difficult problem is needed if this method of evaluating corrosion results for zinc is to be truly useful.

The maximum loss in tensile strength after 20 years' exposure is only about 10 percent for the Kure Beach site. From a practical point of view, this change in strength is of negligible importance and is proportional to the loss in cross-sectional thickness.

Tensile Elongation

Elongation results for Alloy 61 are shown in Fig. 13 and for Alloy 62 in Fig. 14. The elongations for stored panels of both alloys are equal to or higher than those of the original panels for all three exposure times as a re-

sult of aging. The highest elongations for the stored panels are obtained after 7 years, being 23 percent over the original panel for Alloy 61 and 13.2 percent for Alloy 62. For the 2-year exposure, the exposed panels of both alloys display higher elongations than the stored panels. This difference in elongations is probably due to the fact that the exposed panels are subjected to higher temperatures on direct exposure to the sun in summer weather than stored panels, which results in more rapid aging. After 7- and 20-year exposure times, the exposed panels show, as expected, elongations below those of stored panels. The lowest elongations recorded for both alloys occur for panels exposed at Kure Beach (41 percent for Alloy 61 and 26 percent for Alloy 62). These panels have the deepest corrosion pits, which may be at least partially responsible for their lower ductility.

A comparison of the percent changes in elongation and weight loss for Alloys 61 and 62 is given in Figs. 15 and 16, respectively. The differences are greater than those found for tensile strength. The 2-year specimens for both alloys show a gain in percent elongation. At the 7- and 20-year exposure times, the loss in percent elongation far exceeds the percent loss in weight for both alloys at all the exposure sites. The standard deviation for elongation measurements for Alloy 61 ranged from 2.71 to 13 percent and for Alloy 62 from 1.86 to 2.58 percent, which would account for only a small fraction of the observed differences. It is not possible to assess what portion of the percent loss in elongation is due to corrosion and what portion is due to aging, as is the case for tensile strength. Based especially on the large differences between elongation and weight loss obtained for 20-year panels exposed at Kure Beach, it appears that pitting has a more adverse effect on elongation than on tensile strength.

From a practical standpoint, however, both zinc alloys still possess a high degree of ductility after 20 years' exposure even at Kure Beach, where the elongation is 26 percent for Alloy 62 and 41 percent for Alloy 61.

Conclusions

Based on the corrosion data gathered in the 1931 program for 10- and 20-year exposures and in the 1957 program for 2, 7, and 20 years' exposures, the following conclusions on the corrosion of zinc can be drawn:

1. The 1957 test program results confirm those of the 1931 program in that the weight loss method is the most reliable way of determining corrosion rates for rolled zinc.
2. Exposing test panels vertically and at 30 deg from the horizontal gives similar total corrosion rates in rural and industrial environments.
3. The vertically mounted panels in the 1931 program and the panels mounted 30 deg from the horizontal in the 1957 program showed different surface corrosion patterns. Vertically mounted panels tended to show a

smooth, uniform attack. Sloping panels exhibited a roughened surface texture.

4. Adding copper to rolled zinc does not change the average rate of corrosion except in a severe marine environment where panels are in direct contact with the salt spray. Under these conditions the copper-containing zinc shows higher corrosion rates than unalloyed zinc.

5. Copper-bearing zinc is more likely to develop distinct pits during corrosive attack than unalloyed due to localized galvanic action. Marked pitting on the skyward surface occurred only at Kure Beach test site, which is close to the ocean. The maximum net change in tensile strength of about 10 percent occurred at this site after 20 years, which is comparable to the change in section thickness.

6. The highest corrosion rates were obtained in direct salt spray marine and industrial atmospheres. Much lower and similar corrosion rates are found in a rural atmosphere and in a seacoast atmosphere not in direct contact with salt spray.

7. Corrosion rates at Kure Beach (severe marine) and at Newark (industrial) were variable and the highest after 7 years. The rural State College location produced a gradual increase in corrosion rate with increasing exposure time. Increased air pollution is considered to be responsible. Point Reyes (marine) showed low corrosion rates at 7 and 15 years after a much higher rate at 2 years.

8. A good correlation between corrosion rates determined by weight loss and by tension test data was not obtained in the 1957 program because it was not possible to compensate for aging changes in the metal.

References

[1] Anderson, E. A. in *Atmospheric Exposure Tests on Non-Ferrous Metals, ASTM STP 67,* American Society for Testing and Materials, 1946, p. 2.

[2] Anderson, E. A. in *Atmospheric Corrosion of Non-Ferrous Metals, ASTM STP 175,* American Society for Testing and Materials, 1955, p. 126.

[3] Dunbar, S. R. in *Metal Corrosion in the Atmosphere, ASTM STP 435,* American Society for Testing and Materials, 1967, p. 308.

[4] Report of Advisory Committee on Corrosion, *Proceedings,* American Society for Testing and Materials, Vol. 58, 1958, pp. 229–238.

[5] Committee B-3 Reports, *Proceedings,* American Society for Testing and Materials, Vol. 62, 1962, p. 216.

[6] Guttman, H. and Sereda, P. J. in *Metal Corrosion in the Atmosphere, ASTM STP 435,* American Society for Testing and Materials, 1967, p. 326.

[7] Report of Committee G-1, Subcommittee IV, Section 1, Task Force on the Calibration of Atmospheric Corrosivity, *Metal Corrosion in the Atmosphere, ASTM STP 435,* American Society for Testing and Materials, 1967, p. 360.

[8] Anderson, E. A., *Corrosion,* Vol. 15, 1959, pp. 409–412.

D. E. Tonini[1]

Atmospheric Corrosion Test Results for Metallic-Coated Steel Panels Exposed in 1960

REFERENCE: Tonini, D. E., **"Atmospheric Corrosion Test Results for Metallic-Coated Steel Panels Exposed in 1960,"** *Atmospheric Corrosion of Metals, ASTM STP 767,* S. W. Dean, Jr., and E. C. Rhea, Eds., American Society for Testing and Materials, 1982, pp. 163–185.

ABSTRACT: Results of an ASTM-sponsored 20-year exposure of corrugated metallic-coated steel panels at five locations in the United States are reported. A total of 19 panels was placed at each exposure site, including at least one specimen from each of six types of continuous galvanizing lines in use when the test was initiated, five sheets galvanized using equipment similar to that used to prepare specimens for a similar test series initiated in 1926, one panel coated with pure aluminum, one panel coated with an aluminum-silicon alloy, and one panel coated with terne metal.

The analysis of the galvanized coatings data suggests the presence of nonlinear effects in the performance of the coatings. However, it was not possible to establish whether these effects were the result of nonlinearities in the coating performance itself or if they were the consequence of uncontrollable external factors which occurred during the exposure period.

The aluminized sheets were found to be essentially without failure at all test locations. In general, coating degradation beyond minor pinholing was not found.

The terne-coated sheets evidenced early rusting at all except the most aggressive of the test sites. Despite nearly total coating depletion, none of the test sheets have perforated.

KEY WORDS: aluminized coatings, ASTM atmospheric test sites, atmospheric performance, corrosion, hot dip galvanized coatings, industrial atmospheres, metallic coatings, rural atmospheres, terne coatings

An atmospheric corrosion test program for 710 by 910-mm (28 by 36 in.) corrugated metallic-coated steel panels was initiated at five locations during September 1960. A total of 19 panels was placed at each exposure site, including at least one specimen from each of six types of continuous galvanizing lines then in use, five sheets galvanized in equipment (pots) similar to those used for preparation of panels for a similar test series initiated in 1926, one panel coated with pure aluminum, one panel coated with an aluminum-silicon alloy, and one panel coated with terne metal (lead-tin alloy).

[1] Manager, Technical Services, American Hot Dip Galvanizers Association, Inc., Washington, D.C. 20005.

Although the formal objectives set for these tests are not clearly defined in the annual reports of ASTM Subcommittee A.05.14, reference to existing minutes and correspondence of A.05.14 generated during the test planning phase of the program reveals that the principal objective of the test was to address the need for universally accepted data to show that the coated sheet product from continuous galvanizing lines was equivalent in terms of service life to that of the older single-sheet pot galvanizing process [*1,2*].[2]

Inclusion of aluminum-coated sheets in the test matrix was apparently agreed upon to provide a comparative evaluation between the galvanized coatings and the then relatively new aluminum-coated sheets [*3*]. As it turned out, of the two aluminum coating lines then operating in the United States, one manufacturer produced an aluminum-silicon coating and the other a plain aluminized coating. There was no suggestion that an explicit test objective existed to evaluate the differences between aluminized and aluminized-with-silicon coatings. However, such an objective was stated for the G.01.04 Subcommittee on Atmospheric Corrosion test initiated in 1970 [*4*].

These panels have been inspected annually by ASTM Subcommittee A.05.14 on Sheet Tests. Reports of their inspections are contained in ASTM *Proceedings* as a part of the A-5 Committee on Corrosion of Iron and Steel annual reports from 1960 through 1979. The A-5 committee was renamed the Committee on Metallic Coated Iron and Steel Products in 1967 when Committee G-1 on Corrosion of Metals was organized. Subcommittee A.05.14 has retained responsibility for inspecting and reporting the condition of the panels in this test series and will do so until the tests are completed or terminated.

Experimental Program

Preparation of Test Specimens

The coating weights in Table 1 are those for the individual specimens exposed at each site. These coating weights, quoted in the Annual ASTM *Proceedings* reports for Committee A-5, are averages for the weight of coating determined from a 5.1-cm-wide (2 in.) strip sheared before corrugating from each end of the test panel. The pure aluminum-coated sheets averaged 424 g/m^2 (1.39 oz/ft^2) of coating; the aluminum-silicon, 281 g/m^2 (0.92 oz/ft^2); and the terne-coated sheet, which was of the type known in the trade as 40 pounds per double base box (dbb), had 400 g/m^2 (1.31 oz/ft^2) of coating (35 lb per dbb).

Although the minutes of the A.05.14 meeting which approved the 1960 tests (see Ref *1*) stated that coating weights were to be determined only on the skyward-exposed surface of the test specimens, subsequent correspond-

[2] The italic numbers in brackets refer to the list of references appended to this paper.

TABLE 1—*Identification and weights of coating on sheets in test of metallic-coated steels.*

Code	Coating Type	Ounces Per Square Foot[a]				
		State College	Newark	Kure Beach	Point Keyes	Brazos River
AP1	pot[b]	1.05	1.02	1.03	1.02	1.00
EP1	pot	1.38	1.41	1.39	1.40	1.40
RP1	pot	1.06	1.06	1.06	1.05	1.03
JP2	pot[b]	2.43	2.42	2.39	2.37	2.40
PP2	pot	2.25	2.24	2.21	2.27	2.28
CL1	line[c]	1.17	1.19	1.16	1.14	1.18
GL1	line	1.21	1.21	1.21	1.21	1.20
IL1	line	1.18	1.20	1.20	1.18	1.18
LL1	line	1.05	1.06	1.01	0.99	1.00
OL1	line	1.06	1.06	1.06	1.07	1.05
BL2	line[c]	2.06	1.98	1.86	2.03	2.17
HL2	line	2.12	2.12	2.12	2.13	2.14
ML2	line	2.92	3.00	3.09	3.06	3.02
NL2	line	1.82	1.83	1.88	1.92	1.94
SA1	Al-Si[d]	0.91	0.91	0.93	0.92	0.90
TA1	Al[e]	1.38	1.39	1.38	1.39	1.42
UT4	Terne[f]	1.28	1.31	1.31	1.29	1.34

[a] One ounce of zinc coating (galvanized) per square foot of surface equals 305.2 grams per square metre and corresponds to a coating thickness of 0.0017 in., which equals 0.141 micrometres (μm).

[b] Individually dipped in conventional galvanizing pots.

[c] Continuous galvanizing line.

[d] Aluminum-silicon coated sheets.

[e] Pure aluminum coated sheets.

[f] Terne-alloy coated sheets.

ence [5] as well as laboratory reports strongly indicate that skyward coating weights were not used. Rather, total coating weight, both sides, obtained by strip and weigh procedures defined by the ASTM Tests for Weight of Coating on Zinc-Coated (Galvanized) Iron or Steel Articles (A90-69) (1978) (Alternate Method 1:1 HCl) and (A 428-68T) (1978) the ASTM Test for Weight of Coating on Aluminum-Coated Iron or Steel Articles are cited throughout the tests. There are no records of "top to bottom" or "front to back" measurements being made. Therefore, there has been no way to determine the uniformity and distribution of the coating on the test panels during the analysis of the 20-year data set. There are no records of coating thickness measurements before or during the test. All inspection evaluations have been for skyward side only.

Also, it should be noted that the coating weights of the aluminum-coated panels exposed in the 1960 tests are substantially higher than those commercially available today and any conclusions drawn from these tests should be interpreted accordingly. Furthermore, for equivalent weights with zinc and

aluminum coatings, one ounce per square foot of aluminum coating equals 2.65 times the thickness of a one-ounce-per-square-foot zinc coating. Therefore, some care should be exercised in comparing zinc and aluminum coatings based on weight per unit area alone.

The following organizations supplied test panels for the 1960 tests:

ARMCO
Bethlehem Steel Corp.
Continental Steel Corp.
Follensbee Steel Corp.
Granite City Steel Corp.
J & L Steel Corp.
U.S. Steel Corp.
Weirton Steel Co.
Wheeling Steel Corp.

The panels were mounted from three holes, 9.5 mm (3/8 in.) diameter, punched 76.2 mm (3 in.) from each horizontal edge. Four of the corrugated test panels were attached to a frame made of stainless steel channel using machine screws, washers, and brass nuts. To prevent any question of corrosion caused by bimetallic couples, all metal pieces were electrically insulated from the test panels with trifluoroethylene washers and bushings (Figs. 1 and 2).

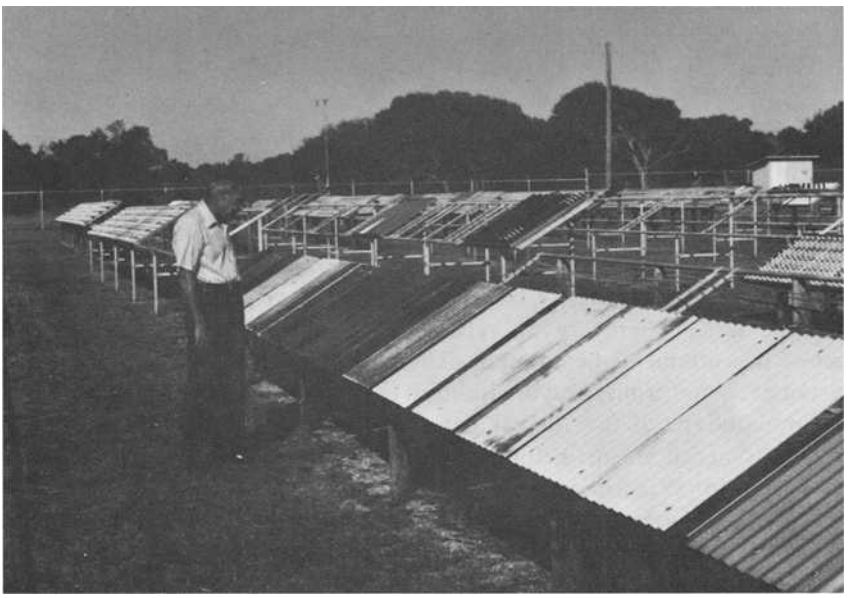

FIG. 1—*Atmosphere exposure test rack.*

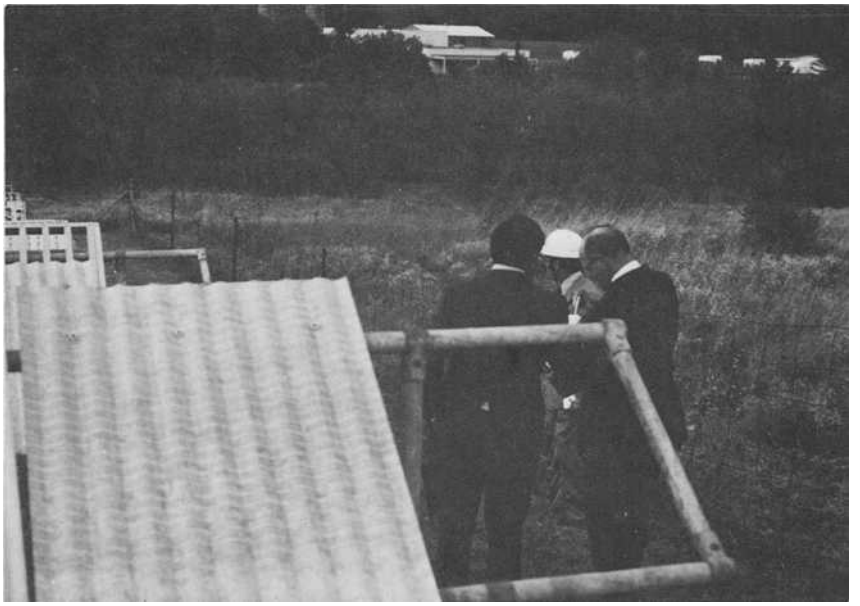

FIG. 2—*Closeup of test rack.*

Exposure Sites

The exposure locations for the 1960 test series were as follows:

LOCATION	ENVIRONMENT	ABBREVIATION
State College, Pa.	Rural	SC
Newark/Kearny, N.J.	Industrial	NK
Kure Beach, N.C.	Marine [244 m (800 ft) from surf]	KB
Point Reyes, Calif.	Marine [588 m (1930 ft) from surf]	PR
Brazos River, Tex.	Marine [1189 m (3900 ft) from surf]	BR

Because of differences in the direction of the prevailing winds and distance from seawater it was predicted that the corrosivities of the three marine sites would differ to a considerable extent [*6*].

The aggressivity of the State College and Kure Beach sites toward steel and zinc was given in an appendix to the 1959 Report of Committee B-3 [*7*]. The Newark site was only a few miles from the Kearny, N.J. location discussed in that report. In 1970, the Newark exposure site was moved to the vicinity of the Kearny generating plant of the New Jersey Public Service Electricity and Gas Company (PSEG) from the U.S. Steel facility in Newark

where the exposure test originated. Independent studies by U.S. Steel referred to in the Subcommittee A.05.14 report cited earlier showed that Newark had about the same corrosivity as did Kearny (see Ref *6*).

The relative corrosivities referred to by the Committee B-3 report during one exposure compared with those of State College were:

Location	Zinc Exposed	Steel Exposed
State College, Pa.	1.0	1.0
Kure Beach [244 m (800 ft) lot], N.C.	1.7	1.9
Point Reyes, Calif.	1.8	1.8
Kearny, N.J.	2.6	3.3

From these relative values, it was felt that an estimate of the relative life of galvanized coatings could be made from the corrosivity indexes developed by Committee B-3. A correlation between Committee B-3 corrosivity ratings and actual performance observed during 20 years of exposure is given later in Table 9.

Exposure Results

Coating Variable Effects, Zinc

The most significant coating variable for galvanized coatings is coating weight, usually expressed in grams per square metre (gm^2) or ounces per square foot (oz/ft^2) and, alternatively, in coating thickness in micrometres (μm) or thousandths of an inch ($1\ oz/ft^2 = 0.0017$ in. $= 1.7$ mils $= 43\ \mu m$). A typical sequence for galvanized coating appearance changes as a function of time was as follows:

Symbol	Description
G	Continuous zinc surface covered with corrosion products of zinc
A	Zinc-iron alloy visible
Y	Yellow corrosion products of alloy
phr	Pinhole rust
TrR	Trace, base metal rust
R	Base metal rust (0.1 to 100 percent)
P	Perforation of specimen

Visual evaluation ratings of the zinc-coated exposure specimens for each test site for 20 years of exposure are presented in Tables 2–6.

Coating Variable Effects, Aluminum

The coating variable which eventually will be investigated by this test program was the effect of silicon on the atmospheric performance of hot-dip

TABLE 2—*State College.*

Year Inspected		63	64	65	66	67	68	69	70	71	72	73	74	75	76	77	78	79
Years Exposed		1.6	2.6	4.7	5.8	6.7	7.6	8.6	9.7	10.6	11.6	12.6	13.6	14.6	15.69	16.69	17.78	18.8
Code	Avg Coating Weight oz/ft²																	
RP	1.05	G	TrA	1A	10A	3Y	10Y	12Y	0.2	4	15	30	50	80	92	94	94	97
EP	1.38	G	G	TrA	0.2A	0.5A	TrY	TrY	TrY	TrY	TrR	1	1	1	3	8	30	. . .
AP	1.06	G	G	TrA	15A	6Y	15Y	25Y	30Y	TrR	5	15	20	40	55	55	88	95
JP	2.43	G	G	TrA	TrA	TrA	TrA	TrA	TrA	TrA	TrA	TrY	TrR	TrR	TrR	TrR	TrR	Cl III phr
PP	2.25	G	G	G	G	G	TrA	TrA	TrA	TrA	TrA	TrA	TrR	TrR	TrR	TrR	TrR	Cl III phr
CL	1.17	G	G	G	G	G	G	G	G.	TrA	TrY	TrR	2	10	25	35	60	75
GL	1.21	G	G	G	G	G	G	G	G	G	TrA	0.2	1	5	15	33	45	75
IL	1.18	G	G	G	G	G	TrA	1A	TrY	TrY	1Y	0.1	0.5	1.5	5	30	45	50
LL	1.05	G	G	TrA	0.1A	0.1A	TrY	TrY	TrR	0.1	1	4	7	10	12	45	65	73
OL	1.06	G	G	TrA	0.1A	0.2A	1A	TrY	TrR	1	5	12	25	50	70	75	80	85
QL	1.16	G	G	G	G	TrA	TrA	TrA	TrA	TrA	TrA	TrA	TrR	2	3	20	40	55
KL	2.51	G	G	G	G	G	G	G	G	G	G	G	G	G	TrA	TrA	TrA	TrA
HL	2.06	G	G	G	G	G	G	G	G	G	G	G	G	G	TrA	TrA	TrR	0.2
BL	2.12	G	G	G	G	G	G	G	G	G	TrA	TrA	TrA	TrR	TrR	TrR	0.5	0.5
ML	2.92	G	G	G	G	G	G	G	G	G	TrA	TrA	TrA	TrA	TrA	TrA	TrA	TrA
NL	1.82	G	G	G	G	G	G	G	G	TrA	TrA	TrA	TrA	TrR	TrR	0.1	0.2	3
SA	0.91	35 phr	50 phr	25 phr	25 phr	30 phr	40 phr	60 phr	60 phr	60 phr	60 phr	Cl II phr	Cl II phr	Cl II phr	Cl II phr	Cl II phr	Cl II phr	Cl II phr
TA	1.38	Tr edge stain service	Tr edge stain	edge stain	NC	NC	NC	NC	NC	NC	NC	NC	NC	NC	NC	NC	NC	Cl II phr
UT	1.28	phr	50	80	80	80	85	90	55	60	60	70	85	90	90	90	100	100

1 oz/ft² = 305.2 g/m².
A Zinc-iron alloy visible.
G Continuous zinc surface covered with corrosion products of zinc.
E Surface of coating etched.
Tr Trace.
Y Yellow corrosion products of alloy.
R Base metal rust.
phr Pinhole rust spots, surrounded by brown stain.
Phr Ratings:
Class I, 1–10 phr
Class II, 11–100 phr
Class III, 101–1000 phr
( ) Year in which panel was reported as 100% R.

TABLE 3—*Newark/Kearny.*

Year Inspected		63	64	65	66	67	68	69	70	71	72	73	74	75	76	77	78	79
Years Exposed		2.1	3.1	4.7	5.8	6.7	7.6	8.6	9.7	10.6	11.6	12.6	13.6	14.6	15.69	16.69	17.78	18.80
Code	Avg Coating Weight, oz/ft^2																	
RP	1.02	2Y	TrR	20	70	98	100	100(7.65)	100(7.65)	100(7.65)	100(7.65)	100(7.65)	100(7.65)	100(7.65)	100(7.65)	100(7.65)	100(7.65)	100(7.65)
EP	1.41	8A	8Y	10Y	1	25	95	99.9	99.9	100(10.6)	100(10.6)	100(10.60)	100(10.60)	100(10.60)	100(10.60)	100(10.60)	100(10.60)	100(10.60)
AP	1.06	TrY	35Y	5	85	100	100(6.67)	100(6.67)	100(6.67)	100(6.67)	100(6.67)	100(6.67)	100(6.67)	100(6.67)	100(6.67)	100(6.67)	100(6.67)	100(6.67)
JP	2.42	G	TrA	TrA	TrY	1Y	0.2	3	15	30	40	80	95	96	99	99.9	99.9	100
PP	2.24	25A	25A	30A	1Y	5Y	1	3	20	50	80	98	99.5	100(14.58)	100(14.58)	100(14.58)	100(14.58)	100(14.58)
CL	1.19	G	G	3	20	85	100	100(7.65)	100(7.65)	100(7.65)	100(7.65)	100(7.65)	100(7.65)	100(7.65)	100(7.65)	100(7.65)	100(7.65)	100(7.65)
GL	1.21	G	G	TrR	20	90	99	100	100(8.63)	100(8.63)	100(8.63)	100(8.63)	100(8.63)	100(8.63)	100(8.63)	100(8.63)	100(8.63)	100(8.6)
IL	1.20	G	TrA	5Y	2	80	100	100(7.65)	100(7.65)	100(7.65)	100(7.65)	100(7.65)	100(7.65)	100(7.65)	100(7.65)	100(7.65)	100(7.65)	100(7.65)
LL	1.06	G	TrR	6	15	75	100	100(7.65)	100(7.65)	100(7.65)	100(7.65)	100(7.65)	100(7.65)	100(7.65)	100(7.65) 15.61	100(7.65) 15.61	100(7.65) 15.61	100(7.65) 15.61
OL	1.06	TrY	TrR	15	85	90	99	100	100(7.65)	100(7.65)	100(7.65)	100(7.65)	100(7.65)	100(7.65)	100(7.65)	100(7.65)	100(7.65)	100(7.65)
QL	1.15	G	G	2Y	10	85	100	100(7.65)	100(8.63)	100(8.63)	100(8.63)	100(8.63)	100(8.63)	100(8.63)	100(8.63)	100(8.63)	100(8.63)	100(8.63)
KL	2.41	G	G	G	G	G	TrR	TrR	1	2	5	7	10	12	15	15	30	60
HL	1.98	G	G	TrA	TrY	0.5	8	30	70	97	99.5	99.5	100(13.65)	100(13.65)	100(13.65)	100(13.65)	100(13.65)	100(13.65)
BL	2.12	G	G	TrA	TrY	0.5	5	10	35	60	75	95	99.5	99.8	99.8	99.9	100	100(17.78)
ML	3.00	G	G	TrA	TrY	TrY	TrR	TrR	0.5	3	7	10	20	25	35	60	65	88
NL	1.83	G	G	TrA	0.1Y	2	30	35	80	99	99.9	99.9	100(13.65)	100(13.65)	100(13.65)	100(13.65)	100(13.65)	100(13.65)
SA	0.92	TrY	6Y	6Y	6Y	...	...	...	...	...	1 phr	Cl I phr	Cl I phr	Cl I phr	Cl I phr	Cl I phr	Cl I phr	NC
TA	1.39	OK	OK	OK	NC	...	...	...	NC	...	NC	NC	NC	NC	NC	NC	NC	NC
UT	1.31	Slt phr	TrR	TrR	TrR	0.5	0.5	1	1	3	5	7	10	10	10	10	10	Cl III phr

1 oz/ft^2 = 305.2 g/m^2.

A Zinc-iron alloy visible.
G Continuous zinc surface covered with corrosion products of zinc.
E Surface of coating etched.
Tr Trace.
Y Yellow corrosion products of alloy.
R Base metal rust.
phr Pinhole rust spots, surrounded by brown stain.
Phr Ratings:
Class I, 1–10 phr
Class II, 11–100 phr
Class III, 101–1000 phr
( ) Year in which panel was reported as 100% R.

TABLE 4—*Kure Beach.*

Year Inspected		63	64	65	66	67	68	69	70	71	72	73	74	75	76	77	78	79
Year Exposed		1.9	2.7	4.7	5.7	7.0	7.7	8.6	9.7	10.8	11.7	12.7	13.7	14.7	15.71	16.71	18.03	19.0
Code	Avg Coating Weight, oz/ft^2																	
RP	1.03	TrA	2A	4A	TrY	5Y	8Y	10Y	TrR	1	5	30	40	50	70	98	98.5	99.5
EP	1.39	G	G	G	TrA	TrY	TrY	TrY	TrY	TrR	1	3	5	7	10	80	83	92
AP	1.06	...	G	G	0.1Y	7Y	10Y	12Y	12Y	TrR	3	20	40	50	60	98	98.5	99
JP	2.39	...	G	G	G	G	G	G	G	TrY	TrR	0.1	0.2	0.3	1	30	30	35
PP	2.21	...	G	G	G	G	G	G	G	TrY	TrY	TrR	0.1	0.2	0.3	10	11	13
CL	1.16	...	G	G	G	G	G	G	TrY	0.5Y	0.5	1	2	5	10	60	70	75
GL	1.21	...	G	G	G	G	G	G	TrY	0.5Y	0.5	1.5	3	5	12	70	96	98
IL	1.20	...	G	G	G	G	TrY	TrY	1Y	30Y	1	10	20	25	35	95	98	99.9
LL	1.01	...	G	G	TrY	TrY	TrY	0.5Y	TrR	TrR	0.5	2	12	20	40	90	94	97
OL	1.06	...	TrA	TrA	TrY	0.5Y	2Y	3Y	1	5	15	50	75	80	85	95	96	97
QL	1.15	...	G	G	G	G	G	G	G	TrY	TrY	TrR	0.1	0.3	0.5	40	45	65
KL	2.32	...	G	G	G	G	G	G	G	G	G	TrA	TrA	TrA	TrR	TrR	TrR	Cl I phr
HL	1.86	...	G	G	G	G	G	G	G	G	G	TrA	TrA	TrR	0.1	1	6	10
BL	2.12	...	G	G	G	G	G	G	G	G	TrY	TrR	TrR	0.1	0.5	3	8	15
ML	3.09	...	G	G	G	G	G	G	G	G	G	TrA	TrA	TrA	TrA	TrA	TrR	Cl II phr
NL	1.88	G	G	G	G	G	G	G	G	G	G	TrA	TrA	TrA	TrR	TrR	3	7
SA	0.93	OK	OK	E	E	E	E	E	E	E	E	E	E	E	E,NC	E,NC	E,NC	E/NC
TA	1.38	OK	OK	E	E	E	E	E	E	E	E	E	E	E	E,NC	E,NC	E,NC	E/NC
UT	1.31	Sev. phr	10	60	TrR	5	40	50	50	90	95	99	99.5	99.9	99.9	99.9	99.9	100

1 oz/ft^2 ≈ 305.2 g/m^2.

A Zinc-iron alloy visible.

G Continuous zinc surface covered with corrosion products of zinc.

E Surface of coating etched.

Tr Trace.

Y Yellow corrosion products of alloy.

R Base metal rust.

phr Pinhole rust spots, surrounded by brown stain.

Phr Ratings:

Class I, 1–10 phr

Class II, 11–100 phr

Class III, 101–1000 phr

( ) Year in which panel was reported as 100% R.

TABLE 5—*Point Reyes.*

Year Inspected		63	64	65	66	67	68	69	70	71	72	73	74	75	76	77	78	79
Years Exposed		2.0	3.0	5.0	6.1	7.1	7.7	9.1	10.0	11.1	11.8	13.0	14.0	15.2	16.04	17.82	18.87	19.1
Code	Avg Coating Weight, oz/ft²																	
RP	1.02	TrA	TrA	2A	2A	3A	3A	5A	5A	5A	5A	TrY	TrY	TrR	5	5	23	34
EP	1.40	G	G	G	G	G	G	TrA	TrA	TrA	TrA	TrY	TrY	TrR	1	1	7	7
AP	1.05	...	G	TrA	TrA	TrA	TrA	TrA	TrA	TrA	TrA	TrA	TrA	TrR	0.5	0.5	4	4
JP	2.37	...	G	G	G	G	G	G	G	G	G	G	G	G	G	G	G	G
PP	2.27	...	G	G	G	G	G	G	G	5Y	G	G	G	G	G	G	G	TrY
CL	1.14	...	G	G	G	G	G	G	G	5Y	TrY	TrR	TrR	TrR	0.5	0.5	1	1
GL	1.21	...	G	G	G	G	G	G	G	5Y	TrY	TrR	TrR	TrR	TrR	TrR	0.5	0.5
IL	1.18	...	G	G	G	G	G	G	G	5Y	G	TrY	TrR	TrR	1	1	12	24
LL	0.99	...	G	G	G	G	G	TrA	TrA	TrY	TrR	TrR	0.1 14.10	0.2 14.10	0.5 14.10	0.5 14.10	2	2
OL	1.07	...	G	TrA	TrA	TrA	TrA	TrA	TrA	TrY	TrA	TrA	TrR	TrR	2	2	20	5
QL	1.15	...	G	G	G	TrA	TrA	TrA	TrA	TrY	TrA	TrA	TrA	TrA	TrA	TrA	TrR	TrR
KL	2.43	...	G	G	G	TrA	TrA	TrA	TrA	TrY	G	G	G	G	G	G	A	TrA
HL	2.03	...	G	G	G	TrA	TrA	TrA	TrA	TrY	G	G	G	TrY	G	G	A	TrR
BL	2.13	...	G	G	G	G	G	TrA	TrA	TrY	G	G	G	TrA	TrY	TrY	TrY	TrY
ML	3.06	...	G	G	G	G	G	TrA	TrA	TrY	TrR	TrR	TrR	TrR	TrR	TrR	TrR	TrR
NL	1.92	G	TrA	TrA	TrA	TrA	TrA	TrA	TrA	TrY	TrA	TrY	TrY	TrY	TrY	TrY	TrR	TrR
SA	0.92	OK	OK	OK	NC	Tr phr	Tr phr	Tr phr	Tr phr	Tr phr	10 100	Cl II phr	Cl II phr	Cl II phr	E Cl II phr	E Cl II phr	E Cl II phr	E Cl II phr
TA	1.39	OK	OK	OK	NC	Tr phr	Tr phr	E	E 3 phr	E Tr phr	E 10 phr	E Cl I phr	E Cl I phr	E Cl I phr	E Cl II phr	E Cl I phr	E Cl I phr	E Cl I phr
UT	1.29	15% phr	5	50	75	1	1	5	100	100	100	100(9.1)	100(9.1)	100(9.1)	100(9.1)	100(9.1)	100(9.1)	100(9.1)

1 oz/ft² ≈ 305.2 g/m².

A Zinc-iron alloy visible.
G Continuous zinc surface covered with corrosion products of zinc.
E Surface of coating etched.
Tr Trace.
Y Yellow corrosion products of alloy.
R Base metal rust.
phr Pinhole rust spots, surrounded by brown stain.
Phr Ratings:
Class I, 1–10 phr
Class II, 11–100 phr
Class III, 101–1000 phr
( ) Year in which panel was reported as 100% R.

Year Inspected		63	64	65	66	67	68	69	70	71	72	73	74	75	76	77	78	79
Years Exposed		2.0	3.0	5.0	6.0	7.0	7.89	9.0	10.0	11.0	12.2	13.0	14.0	15.2	16.04	...	18.13	19.1
Code	Avg Coating Weight, oz/ft^2																	
RP	1.01	0.1A	0.2A	0.3A	0.4A	0.5A	TrY	TrY	TrY	1Y	TrR	0.1	0.5	1	1	...	3.5	30
EP	1.40	G	G	G	G	G	G	G	G	G	G	G	G	G	G	...	TrR	5
AP	1.03	G	G	TrA	TrA	TrA	0.5Y	1Y	2Y	5Y	10Y	TrR	TrR	TrR	0.5	...	1	60
JP	2.40	G	G	G	TrA	TrA	TrA	TrA	G	G	G	G	G	G	G	...	TrY	Cl I phr
PP	2.28	G	G	G	TrA	TrA	TrA	TrA	G	G	G	G	G	G	G	...	G	G
CL	1.18	G	G	G	G	TrA	G	G	G	G	G	G	G	G	0.2	...	2	3
GL	1.20	G	G	G	G	TrA	G	G	G	G	G	G	G	TrR	0.2	...	25	75
IL	1.18	G	G	G	G	TrA	G	G	G	G	G	G	TrR	TrR	10	...	17	75
LL	1.00	G	G	TrA	TrA	TrA	TrY	TrY	TrY	TrY	1Y	0.5	2	5	30	...	30	80
OL	1.05	G	G	TrA	TrA	TrA	TrA	TrY	1Y	3Y	5Y	3	10	15	TrR	...	70	85
QL	1.11	G	G	G	G	TrA	G	G	G	G	G	G	G	G	. . .	...	1	10
KL	2.47	G	G	G	G	TrA	G	G	G	G	G	G	G	G	G	...	G	G
HL	2.17	G	G	G	G	TrA	G	G	G	G	G	G	G	G	G	...	G	0.1
BL	2.14	G	G	G	TrA	TrA	TrA	TrA	TrA	TrA	TrA	TrA	TrA	TrA	TrA	...	TrA	0.1
ML	3.02	G	G	G	TrA	G	G	G	G	G	G	G	G	G	G	...	G	TrR
NL	1.94	G	G	G	TrA	TrA	TrA	TrA	TrA	TrA	TrA	TrA	TrA	TrA	TrA	...	TrA	TrA
SA	0.90	OK	Tr phr	Tr phr	Tr phr	Tr phr	Tr phr	Tr phr	Tr phr	Tr phr	Tr phr	Cl I phr	E Cl II phr	E CL II phr 15.2	E TrR	...	TrR	TrR
TA	1.42	12 phr	Tr phr	Tr phr	Tr phr	0.1 phr	0.1 phr	0.1 phr	0.1 phr	0.1 phr	0.1 phr	Cl I phr	E CL II phr	E CL II phr	E TrR	...	TrR	TrR
UT	1.34	50 phr	70	85	85 (R&RS)	5	5	6	100	100	100	100	100	100(10.0)	100(10.0)	...	100(10.0)	100(10.0)

1 oz/ft^2 = 305.2 g/m^2.

A Zinc-iron alloy visible.
G Continuous zinc surface covered with corrosion products of zinc.
E Surface of coating etched.
Tr Trace.
Y Yellow corrosion products of alloy.
R Base metal rust.
phr Pinhole rust spots, surrounded by brown stain.

Phr Ratings:
Class I, 1–10 phr
Class II, 11–100 phr
Class III, 101–1000 phr

( ) Year in which panel was reported as 100% R.

aluminum coatings applied over a steel substrate. However, the test objectives apparently were not established with this in mind as a major objective.

A typical sequence for visual evaluation of hot-dip aluminized steel coatings as observed in these tests was as follows:

SYMBOL	DESCRIPTION
TrY	Trace alloy corrosion products (silicon bearing only)
E	Surface of coating etched
phr	Pinhole rust (1 to 100 pits/sheet)
TrR	Trace base metal rust

Visual evaluation ratings of the hot-dip aluminized specimens (Codes SA, TA) for each test site are presented in Tables 2–6.

Coating Variable Effects, Terne Plate

Terne plate is a lead-tin alloy hot dip applied to steel. The atmospheric performance characteristics of terne plate have not been studied as fully as hot-dip aluminum or zinc coatings. Unlike the hot-dip galvanized coatings, terne plate almost immediately showed extensive red rust at four of five test sites; however, this condition was least severe for the panel exposed at the Newark/Kearny industrial test site.

A typical sequence for visual evaluation of terne plate coatings was as follows:

SYMBOL	DESCRIPTION
phr	Pinhole rust (slight to severe)
TrR	Trace base metal rust
R	Base metal rust (100 percent)

Visual evaluation ratings for the terne plate specimen (UT) for each test site are presented in Tables 2–6.

Atmospheric Exposure Variables

It is believed that the atmospheric variables (pollutant concentrations) were not time-dependent during the test period with the possible exceptions of the Newark/Kearny and Kure Beach sites.

As previously noted, the Newark test lot was physically moved from a U.S. Steel site adjacent to the Newark Air Terminal to the PSEG Kearny generating station. Any difference in atmospheric conditions between these two sites was most probably insignificant. However, it is believed by some that the general corrosivity of the Newark area may have been reduced at least during the 1970–1980 period of the test.

Although there may be other data to support the point that corrosivity at Newark/Kearny site has been reduced in recent years, in purely relative terms (based on average coating weight) it appears to have remained the same for

this test *in comparison with* State College. It should be noted here that the comparison for the 1960 test series with the B-3 indexes was based on time to "first rust." First rust conditions were, without exception, noted within ten years for all the exposed specimens at Newark/Kearny. It was not possible to determine whether significant changes in corrosivity at Newark/Kearny occurred from 1970 to 1980 although a possibility exists that this was the case.

At the Kure Beach test lot (the only ASTM atmospheric site which is instrumented and monitored for corrosiveness), Baker and Lee [*8*] have reported that the aggressiveness of the 25-m (80 ft) lot has decreased by approximately 50 percent in recent years. However, exposure conditions at the 250-m (800 ft) lot where the A.05.14 panels were exposed have remained essentially constant since 1949.

Discussion

Data Presentation, Galvanized Panels

The exposure site corrosivity data for the A-5/B-3 comparison of test site atmospheric aggressiveness were computed based upon weighted average coating weights and mean time to first rust within the designated coating classes defined in Table 7. From this, the relative test site corrosivity in Table 9 was computed from the data summary presented in Table 8. In addition, another calculation using the same data base was made to compute a service

TABLE 7—*Grouping of panels by coating weight.*

Classification	Avg Coating Weight (oz/ft^2)[a]	Code
Very light	1.02	LL
	1.03	AP
	1.05	RP
	1.06	OL
Light	1.15	QL
	1.17	CL
	1.19	IL
	1.21	GL
Light medium	1.4	EP
Heavy medium	1.8	NL
Light heavy	2.02	BL
	2.13	HL
	2.25	PP
	2.40	JP
	2.43	KL
Heavy	3.02	ML

[a] One ounce of zinc coating (galvanized) per square foot of surface equals 305.2 grams per square metre and corresponds to a coating thickness of 0.0017 in., which equals 0.141 micrometres (9 μm).

TABLE 8—*Galvanized panels: time to first rust (years).*

As Reported						
Identification Coating Weight, oz/ft^2	Code	Test Site				
		SC	NK	KB	PR	BR
1.05	RP	9.7	3.1	10.8	15.2	13.0
1.40	EP	12.6	5.8	11.7	16.04	18.1
1.03	AP	10.6	3.1	10.8	16.04	16.04
2.40	JP	...	7.6	12.7	20.0	...
2.25	PP	...	7.6	13.7	20.0	...
1.17	CL	13.6	4.7	11.7	16.04	16.04
1.21	GL	12.6	4.7	11.7	18.87	15.2
1.19	IL	12.6	5.8	11.7	16.04	15.2
1.02	LL	10.6	3.1	11.7	14.0	13.0
1.06	OL	10.6	3.1	9.7	15.2	13.0
1.15	QL	14.6	4.7	13.7	20.0	18.13
2.43	KL	...	9.7	...	...	...
2.13	HL	18.8	6.7	15.7	...	19.1
2.02	BL	17.78	6.7	14.7	...	19.1
3.02	ML	...	9.7	...	...	...
1.88	NL	16.69	6.7	16.7	...	...

parameter expressed in years of service (to first rust) per ounce of coating on the top side of the sheet only, Table 10.

As already noted, inspection results for each of the test sites are tabulated in Tables 2 through 6. A summary of time to first rust by exposure location for each panel is given in Table 8. Regression lines for the data in Table 8 were computed for each test location using an algorithm suggested by Quiram et al [*9*] programmed to a Texas Instruments T159/PC200 calculator system. Figures 3–7 plot the regression lines for the average coating weight of all galvanized sheets at a given exposure location against time to first rust for each of the exposure sites in the test.

Once the panels had reached a first rust condition, a record was made of the coating degradation process. The progression of the coating degradation is clearly evident in the annual inspection reports of the sheets. An example

TABLE 9—*Comparison of atmospheric test site relative corrosivity: A-5 (1980) and B-3 (1959).*

Test Site Location	B-3	A-5
State College, Pa.	1.0	1.0
Kure Beach, N.C.	1.7	1.1
Point Reyes, Calif.	1.8	0.7
Brazos River, Tex.	...	0.7
Newark/Kearney, N.J.	2.6	2.7

TABLE 10—*Years to time of first rust per ounce of galvanized coating, top of sheet.*

Estimated Top Coating Weight[a]	ID		SC	NK	KB	PR	BR
0.53	RP	pot	18.3	5.8	20.4	28.7	24.5
0.70	EP		18.0	4.4	16.7	22.9	25.9
0.52	AP		20.4	6.0	20.8	30.8	30.8
1.20	JP		...	6.3	10.6	16.7	...
1.13	PP		...	6.7	12.1	17.7	...
0.59	CL	line	23.1	8.0	19.9	27.2	27.2
0.61	GL		20.7	7.7	19.2	30.9	24.9
0.60	IL		21.0	9.7	19.5	26.7	25.3
0.51	LL		20.8	6.1	22.9	27.5	25.4
0.53	OL		20.0	5.8	18.3	28.7	24.5
0.58	QL		25.2	8.1	23.6	34.5	31.3
1.22	KL		...	8.0	...	...	...
1.07	HL		17.8	6.3	14.7	...	17.9
1.01	BL		17.6	6.6	14.6	...	18.9
1.51	ML		...	6.4	...	...	...
0.94	NL		17.8	7.1	17.8	...	...

[a] Coating weight distribution assumed equal on both sides of sheet.

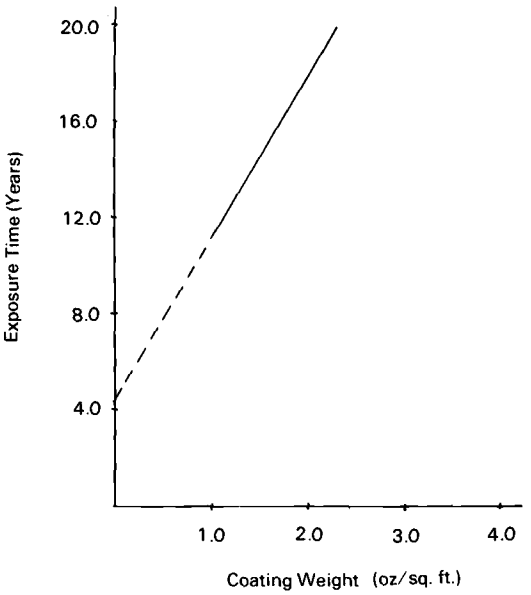

FIG. 3—*Time to first rust, galvanized panels at State College (1 oz/ft² = 305.2 g/m²).*

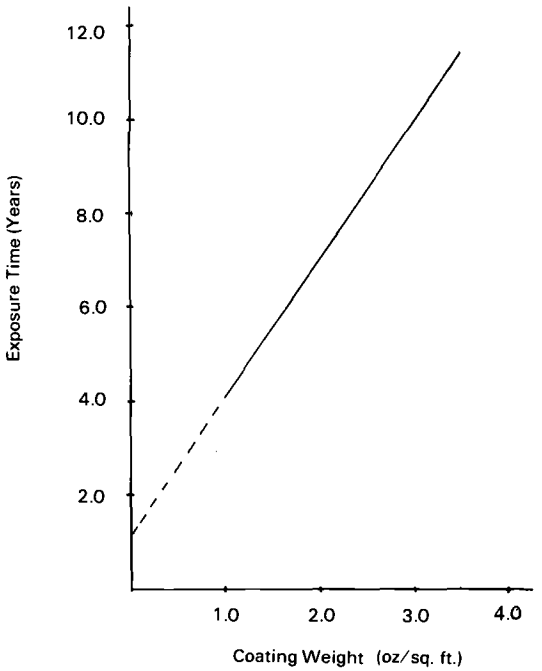

FIG. 4—*Time to first rust, galvanized panels at Newark/Kearny (1 oz/ft² = 305.2 g/m²).*

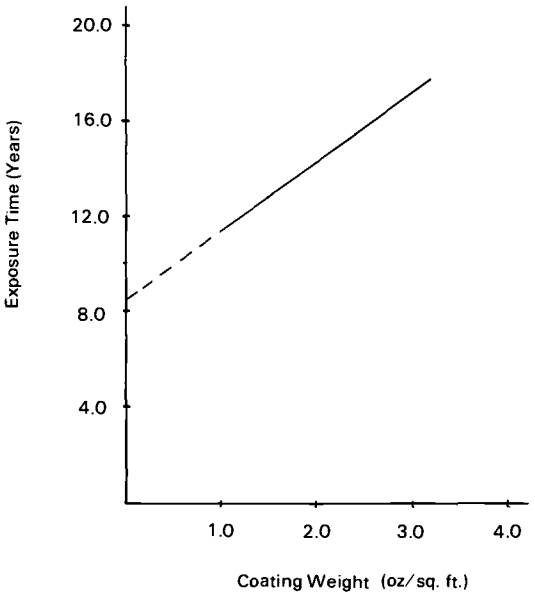

FIG. 5—*Time to first rust, galvanized panels at Kure Beach (1 oz/ft² = 305.2 g/m²).*

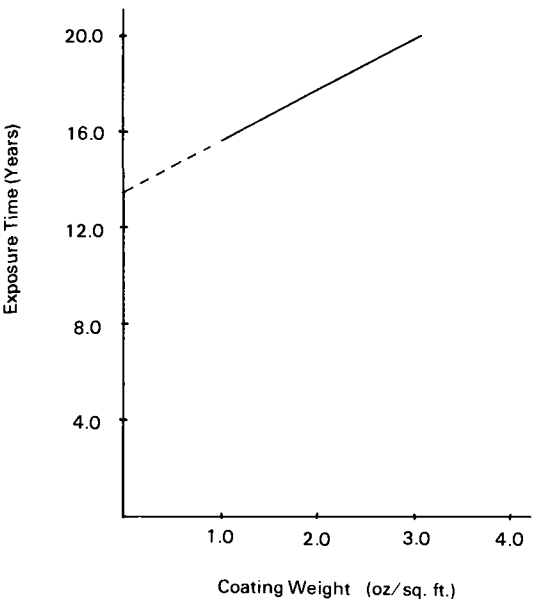

FIG. 6—*Time to first rust, galvanized panels at Point Reyes (1 oz/ft² = 305.2 g/m²).*

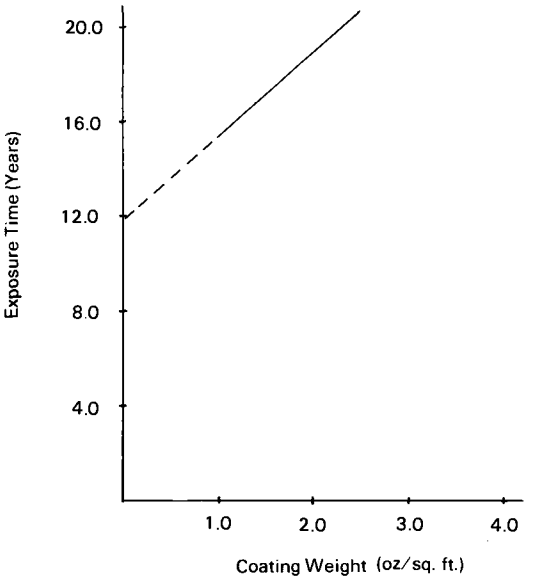

FIG. 7—*Time to first rust, galvanized panels at Brazos River (1 oz/ft² = 305.2 g/m²).*

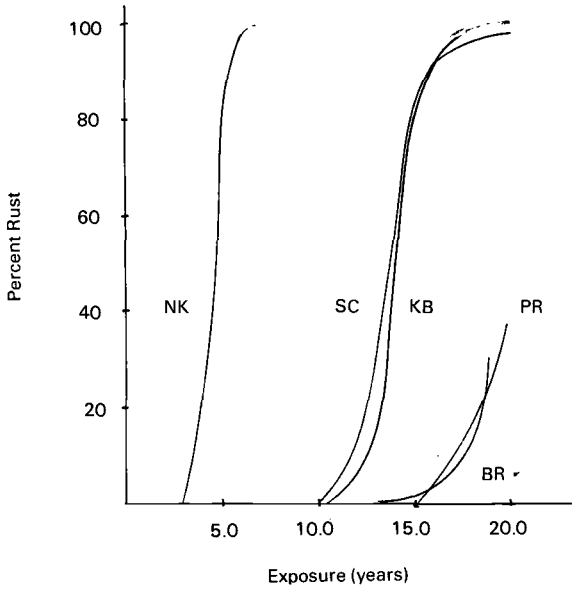

FIG. 8—*Curves showing coating depletion for panel RP [311 g/m² (1.02 oz/ft²)].*

of how the degree of rusting was related to time between first and total rust conditions is shown for panel RP [311 g/m² (1.02 oz/ft²)] in Fig. 8.

Data Analysis, Galvanized Panels

Examination of the performance for the galvanized line and galvanized pot specimens at each of the exposure locations shows that, on the average, the line-galvanized sheets performed somewhat better at all sites except Brazos River than did the pot-galvanized specimens on the basis of years per ounce to time of first rust, Table 8. However, when these average values were subjected to hypothesis tests using *t*-statistics at a 95 percent confidence level, the differences between the line and pot averages was not statistically significant.

For purposes of site corrosivity analysis, the specimens were classified by coating weights shown in Table 7. In establishing these coating classifications, coating weight was the primary consideration followed by "obvious" performance breakpoints such as for the "heavy-medium" class category.

When coating life (years/oz) in Table 10 is plotted against coating weights, a somewhat unexpected relationship is evident (Fig. 9). Although the coating life per ounce of coating appears to be relatively independent of coating weight at the Newark/Kearny location, the coating life appears to have a significant dependency upon the coating weight on the panels for the other exposure sites. This discovery would tend to confirm the preliminary conclusion that the failure of the regression lines to pass through the origin may be

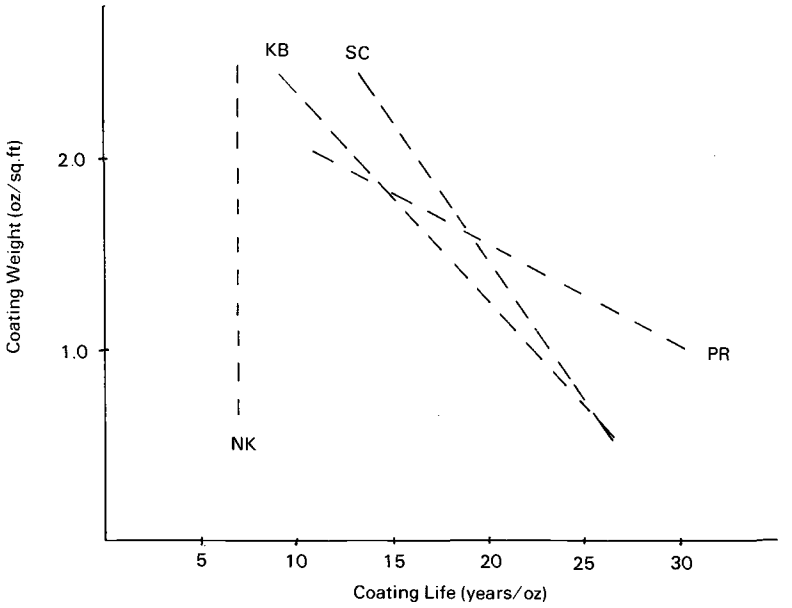

FIG. 9—*Relationship of coating life as a function of coating weight (1 oz = 28 g).*

attributable to as yet undetermined nonlinearities in the exposure program. On the other hand, one cannot completely rule out the possibility that there may be inherent nonlinearities in the performance of galvanized sheets. It does not appear that this result is affected by the type of coating on the panel, that is, line or pot.

One possible explanation for the apparent nonlinear behavior of the galvanized panels with respect to time to first rust as a function of coating weight may be that due to nonuniformities in coating thickness, the minimum coating thickness at which rust would first initiate does not increase at the same rate as that of average coating thickness. This hypothesis could possibly be checked by means of magnetic thickness gage surveys of unexposed control material. Regretably, such controls were not included in the test plan for this material. However, this explanation would not appear to account for the linear performance for coating life expectancy as a function of coating weight observed for the specimens at Newark/Kearny.

Furthermore, it should be noted that it has been demonstrated by Legault and Pearson [*10*] that galvanized sheets tend to corrode faster on skyward-oriented surfaces than on the earth-facing side of the sheet. Therefore, the sheet inspections of only sky-facing sides could also have affected the outcome of the results.

The regression lines in Figs. 3 through 7 do not extrapolate to the origin of the coordinate axes for the Brazos River, Point Reyes, and Kure Beach data

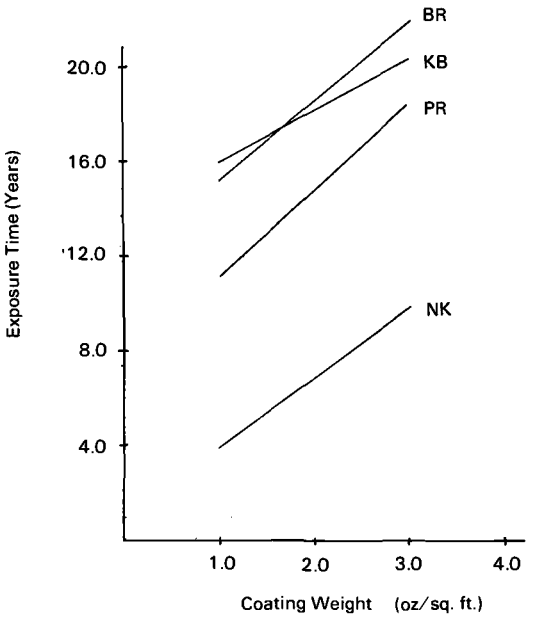

FIG. 10—*Comparison, time to first rust—BR, PR, KB with NK (1 oz/ft² = 305.2 g/m²).*

sets. Also, as can be seen in Fig. 10, the slopes of the regression lines for the Brazos River, Point Reyes, Kure Beach, and Newark/Kearny data are approximately the same. This suggests that these sites experienced a corrosion rate for the galvanized panels comparable to the industrial site at Newark/Kearny. The data argue against accepting that conclusion.

The failure of the regression line to pass through the origin for the Newark/Kearny data in Fig. 4 (where the exposure is essentially complete) may be the result of a lack of exposed specimens having less than one ounce per square foot of coating, performance nonlinearities, and experimental error. (It should be noted that failure of the regression line of the galvanized panels to pass through the origin is also evident in other analyses of ASTM atmospheric exposure data [*11*].)

The coating degradation curve in Fig. 8 appears to be well behaved and is consistent with that reported by others [*12*].

The anomalies in the behavior of the data probably are the consequence of one or a combination of (1) lack of data for the less-aggressive sites and (2) unevaluated nonlinearities in the corrosion performance of the test panels. These factors may be identified in the years yet remaining in the exposure program.

Data Analysis, Aluminized and Terne Panels

The performance of the aluminized sheets has been effectively without failure at all locations. This performance, including edges, has been so con-

sistently without reportable failure that coating degradation effects beyond minor pinholing cannot be measured even after 20 years of exposure.

The terne sheets very quickly showed significant rusting at all locations except Newark/Kearny, the most aggressive test site in the test. Despite this, the integrity of the sheets has been maintained without perforation.

Conclusions

Preliminary analysis of the 1960 exposure test program shows that the relative performance of the galvanized sheets was consistent with that from other similar tests, particularly for the State College and Newark/Kearny exposure sites.

Although, on the average, the line-galvanized sheets appeared to offer slightly better service before time to first rust, that apparent marginal improvement was not statistically significant. However, it is possible to conclude on the basis of the analysis that the sheet and pot-galvanized specimens performed in an equivalent manner when evaluated on a criterion of a year's service per ounce of coating.

The trends observed for the sheets placed at Kure Beach, Brazos River, and Point Reyes are not conclusive at this time. However, it appears that the corrosion rates at these locations may be found to be less aggressive than was anticipated when the tests were originated. Based on incomplete data, it appears that one or more of these test sites may be found to be less corrosive than the rural site at State College. A much more detailed study of microclimate changes at these locations since 1960 is indicated. Since the relative performance curves for State College and Newark do not appear to have changed significantly over the years, emphasis should be placed on changes in exposure conditions which may have taken at the marine exposure locations.

The apparent dependence at four of the five test sites of the years of rust-free performance per ounce of coating to coating weight deserves further study and analysis.

References

[1] "Minutes of Meeting of Subcommittee XIV of Committee A-5," American Society for Testing and Materials, 22 June 1959.

[2] Letter to C. M. Parker, American Iron and Steel Institute from C. P. Larrabee, Chairman, Subcommittee XIV, American Society for Testing and Materials, 6 July 1959.

[3] "Report of Meeting of Coated Sheets Subcommittee," Technical Committee on Sheet Steel, American Iron and Steel Institute, New York, 8 Oct. 1959.

[4] "Report of Committee G-1 on Corrosion of Metals," *Proceedings*, American Society for Testing and Materials, Vol. 70, 1970, pp. 410–411.

[5] Letter to O. B. Ellis, Armco Steel Corp., from D. W. Pettigrew, American Zinc Institute, New York, 25 Nov. 1960.

[6] *Proceedings*, American Society for Testing and Materials, Vol. 61, 1961, p. 137.

[7] *Proceedings*, American Society for Testing and Materials, Vol. 59, 1959, p. 200.

[8] Baker, E. A. and Lee, T. S., this publication, pp. 250–266.

[9] Quiram, J. F., Koperski, D. M. and Oliva, R. A., *Source Book for Programmable Calculators,* Texas Instruments, Inc., Dallas, Tex., 1978, pp. 4-24/4-31.
[10] Legault, R. A. and Pearson, V. P., *Atmospheric Factors Affecting the Corrosion of Engineering Metals, ASTM STP 646,* American Society for Testing and Materials, 1978, pp. 83-96.
[11] "Coating and Corrosion Costs of Highway Structural Steel," Report No. FHWA-RD-79-121, Federal Highway Administration, Washington, D.C. 1979, p. 92.
[12] *Proceedings,* American Society for Testing and Materials, Vol. 44, 1944, p. 93.

DISCUSSION

T. J. Summerson[1] *(written discussion)*—1. Were underside surfaces included in the evaluation?

2. With regard to the aluminized steel variables, how did the commercial purity compare with the aluminum-silicon coating?

3. Why did you state that the tests of aluminized steel are not to be considered a study of the aluminized steel product but only a comparison of the difference in composition between the two aluminum coating compositions?

D. E. Tonini (author's closure)—1. Evaluation of the bottom sides of the aluminum and aluminum-silicon coated sheets was not a formal part of the test program. Neither, for that matter, was the evaluation of the bottom sides of the galvanized sheets. However, rather severe degradation on the underside of the aluminum sheets has been observed. At the marine sites particularly, rather voluminous corrosion products are visible on the underside of the sheets.

2. There is a noticeable difference in the optical reflectivity between the aluminized and the aluminum-silicon coated test panels. However, there is no distinguishable difference in the coating performance.

3. I merely noted that there was not an explicitly stated test objective in the test documentation record to evaluate the difference in performance between the aluminized and aluminum-silicon coated test panels in the 1960 test series. Such an objective was clearly stated for the 1970 test series of these materials. This is not to say that such comparisons cannot legitimately be made for the 1960 tests if and when the coatings begin to deteriorate.

W. P. Ellis[2] *(written discussion)*—Have there been attempts to identify products of corrosion at the various test sites to characterize the nature of the aggressive atmospheric gases or particulates? Is this a valid concept?

D. E. Tonini—At the time the 1960 test series was initiated, characterization of atmospheres and an analytical appreciation of the effects of atmos-

[1] Kaiser Aluminum and Chemical Corp., Pleasanton, Calif.
[2] H. B. Fuller Co., Springhouse, Pa.

pheric contaminants upon the performance of metallic coatings were still largely in their infancy. Yet to come was the work of researchers such as Grossman, Guttman, Haynie et al, Sereda, and Shaw, among others, which has resulted in a much better appreciation of the effects of atmospheric and time-of-wetness parameters on the corrosion of metallic coatings.

Some corporate research groups are understood to have used corrosion product analysis to successfully characterize the nature of atmospheric exposure conditions. To my knowledge, these postmortem analyses are considered useful and valid indicators of overall exposure conditions. However, unless these analyses are made periodically, it may not be possible to place specific changes in atmospheric conditions on a time line.

There is considerable sentiment to provide basic instrumentation at the ASTM atmospheric test sites to measure sulfur dioxide contamination and time-of-wetness exposure conditions. Such information in the test data base would, in my opinion, greatly enhance the usefulness of the data we are collecting. The International Nickel Co. has kept such similar atmospheric records at its Kure Beach site for many years. This atmospheric data, coupled with corrosion product analysis, would be very valuable. I would support such an approach.

G. A. DiBari,[1] *G. Hawks,*[2] *and E. A. Baker*[3]

Corrosion Performance of Decorative Electrodeposited Nickel and Nickel-Iron Alloy Coatings

REFERENCE: DiBari, G. A., Hawks, G., and Baker, E. A., **"Corrosion Performance of Decorative Electrodeposited Nickel and Nickel-Iron Alloy Coatings,"** *Atmospheric Corrosion of Metals, ASTM STP 767,* S. W. Dean, Jr., and E. C. Rhea, Eds., American Society for Testing and Materials, 1982, pp. 186–213.

ABSTRACT: The corrosion performance of chromium-electroplated, decorative nickel and nickel-iron alloy electrodeposits has been studied in marine and industrial atmospheres and by means of copper-accelerated acetic acid-salt spray testing (CASS). Decorative nickel coatings, 15 and 30 μm thick, gave better overall corrosion performance than comparable decorative nickel-iron alloy coatings. Because of the rapid staining that occurs in marine and industrial atmospheres, nickel-iron alloy deposits are not suitable for decorative applications involving moderate and severe corrosion service. Decorative nickel-iron alloy deposits, 7.6 μm thick, appear suitable for mild corrosion service on the basis of CASS test results, but results were affected by iron content and type of electrodeposited chromium. The relatively good performance of thin alloy deposits accounts for established applications in mildly corrosive environments.

The performance of the decorative electrodeposited nickel coatings was influenced by the activity of bright nickel. Low-activity single-layer bright nickel (15 μm) performed better than high-activity bright nickel when used with microporous or microcracked chromium. High-activity double-layer nickel (30 μm) protected low-current-density areas of contoured steel panels better than low-activity double-layer nickel, either with microporous or microcracked chromium. Microporous chromium was more effective in this program; microcracked chromium was more effective in a previous study.

KEY WORDS: electrodeposits, coatings, nickel, nickel-iron, corrosion, atmospheric corrosion, atmospheric corrosion tests

Decorative electrodeposited nickel-iron alloy coatings are used commercially in combination with electrodeposited chromium to enhance the appearance of a diversity of products. To date, the applications of decorative nickel-iron alloy coatings have involved service in mildly corrosive envi-

[1] Senior program manager, The International Nickel Co., Inc., New York, N. Y. 10004.

[2] Senior research technician, Inco Research and Development Center, Inc., Suffern, N. Y. 10901.

[3] Senior research assistant, LaQue Center for Corrosion Technology, Inc., Wrightsville Beach, N. C. 28480.

ronments; for example, domestic appliances and tubular furniture. These applications appear to be well established. It has been suggested that decorative nickel-iron electrodeposits may be suitable for more severe service [*1,2*].[4] The corrosion performance of decorative nickel-iron alloy electrodeposits has been studied to determine whether the alloy deposits are suitable for moderate and severe service, in addition to their present satisfactory usage for mild exposures.

Historical Notes

The electrodeposition of nickel-iron alloys was described in the technical literature as early as 1871. Brenner suggests that the work on nickel-iron alloy plating between 1900 and 1930 was due to efforts to eliminate various defects in nickel deposits—high internal stress, exfoliation, staining, and microcracking—attributed to the presence of iron [*3*]. Marschak, Stepanow, and co-workers were probably the first to evaluate the corrosion resistance of nickel-iron alloy deposits. They concluded that corrosion resistance was not noteworthy and that resistance to corrosion was better in alloys containing more than 50 percent nickel than in those with less than 35 percent nickel. Raub, also, concluded that nickel-iron alloy coatings were of little value for protecting steel [*3*]. Wesley and Knapp studied the number of perforations occurring in electrodeposited nickel-iron alloy foils on exposure to an industrial atmosphere. Small amounts of iron, 3 and 7 percent, inhibited the tendency for perforations to occur in foils that were not chromium plated. Chromium-plated nickel-iron foils, however, had a greater tendency to perforate than chromium-plated nickel foils [*4*].

The first process for electrodepositing decorative nickel-iron alloys of good quality is the one described by Du Rose and Pine [*5*]. The addition of an organic sulfonate to control stress, and operation at low pH to control the incorporation of basic matter, undoubtedly made it possible to produce sound deposits. Deposits containing 30 to 40 percent iron were hard, tough, and ductile. Deposits containing 10 to 30 percent iron prevented the rusting of steel better than an equal thickness of nickel. Du Rose and Pine concluded that bright nickel-iron alloy deposits were not useful for decorative purposes because of rapid staining on atmospheric exposure, staining that could not be prevented by applying conventional electrodeposited chromium over bright nickel-iron alloy deposits.

Present Status

Two types of processes for electrodepositing nickel-iron alloy coatings are now in use commercially. One type uses a complexing agent to control the ferric-ferrous ratio and prevent precipitation of hydroxide. The other uses a reducing agent to prevent oxidation of ferrous to ferric and, hence, precipita-

[4] The italic numbers in brackets refer to the list of references appended to this paper.

tion of hydroxide. In most other respects, decorative nickel-iron processes are similar to bright nickel processes in that they use a combination of organic additives to control internal stress, brightness, and leveling of the deposits. Clauss reports that saccharin compounds are important in the alloy processes, but that it proved necessary to develop special additives to achieve satisfactory leveling characteristics [*1*].

The corrosion performance of chromium plated bright nickel-iron electrodeposits has been discussed [*1,6*]. Chessin, Seyb, and Walker suggest that, with the possible exception of deposits containing greater than 40 percent iron, decorative nickel-iron alloys compare favorably with single-layer bright nickel at thicknesses less than 12 μm. Clauss, Tremmel, and Klein arrive at a similar conclusion. They suggest, in addition, that by varying the degree of air agitation, a double-layer-type coating can be produced in the same electrolyte; that is, by stopping air agitation, the topmost layers will contain about half the amount of iron as do initial layers deposited with air agitation. It has been suggested that double-layer-type coatings combined with microporous chromium could conceivably be suitable for severe and very severe service [*1*].

Program Outline and Other Details

The experimental program involved the electrodeposition of decorative nickel and nickel-iron alloys on contoured, as well as some flat, steel panels. All panels were electroplated with chromium. Replicate panels were exposed to marine and industrial atmospheres and to copper-accelerated acetic acid-salt spray testing (CASS). The program outline, process details, panel preparation, exposure locations, and evaluation techniques are described in this section.

Program Outline

The program is outlined in Tables 1–3. The tables list the lot numbers and give the coating thicknesses and types of coatings applied to replicate panels in each lot.

The planning for the first part of the program, Table 1, was influenced by a survey of commercially plated parts made by Inco in 1976. Toaster shells, rotisserie oven shelves, and frypan covers were sectioned and examined metallographically and chemically. The average coating thicknesses on all parts surveyed was 7.9 $\pm$ 1.2 μm and the alloy coatings were deposited directly on steel. As a result, the first part of the program included deposits 7.6 μm thick deposited directly on steel panels. The type of chromium and iron content were varied to evaluate the influence of these two factors.

The second part of the program, Table 2, is designed to compare the corrosion performance of single-layer bright nickel 15 μm thick with that of sin-

TABLE 1—*Panels prepared to determine the influence of iron content and chromium type on CASS test performance of thin (7.6 μm) decorative nickel-iron alloy deposits on steel.*

Flat Panels			Contoured Panels		
Lot No.[a]	% Fe	Cr Type[b]	Lot No.	% Fe	Cr Type
1	0	R	2	0	R
3	0	MP	4	0	MP
5	15	R	6	15	R
7	15	MP	8	15	MP
9	25	R	10	25	R
11	25	MP	12	25	MP
13	33	R	14	33	R

[a] Three panels from each of the indicated lots were CASS tested.

[b] Microporosity (MP) in the chromium layer was induced by depositing a special nickel layer from Solution No. 6, Table 4, 2.5 μm thick, containing microscopic particles, prior to electroplating with chromium. R denotes low-porosity conventional chromium.

The low-activity nickel used in Lots 1–4 was deposited from Solution No. 5; for Lots 5–12, the nickel-iron coatings were prepared in Solution No. 1; Lots 13 and 14, from Solution No. 2, Table 4.

TABLE 2—*Panels prepared to compare the corrosion performance of single-layer bright nickel and nickel-iron alloy coatings.*

Coating Thickness, μm and Type[a]				
Lot No.	Bright Nickel	Bright Ni-Fe	Chromium Type	% Iron
15	15H		R	0
16	13H		MP	0
17	13H		MC	0
18	15L		R	0
19	13L		MP	0
20	13L		MC	0
21		15	R	20
22		13	MP	20
23		13	MC	20
24		15	R	25
25		15	MP	25
26		15	MC	25
27	15H		R	0
28		15	R	20
29		15	R	25

[a] High-activity bright nickel (H) corresponds to Solution 4; low-activity bright nickel (L), to Solution 5, Table 4. Deposits with 20% iron were prepared from Solution 1; those with 25% iron from Solution 2, Table 4. R, MP, and MC denote regular, microporous, and microcracked chromium, respectively. Microporosity was induced as described in Table 1. Microcracking was induced by depositing a special nickel layer from Solution 7, Table 4, 2.5 μm thick, prior to chromium plating.

TABLE 3—*Panels prepared to compare the corrosion performance of double-layer nickel and nickel-iron alloy coatings with different levels of iron in initial and topmost layers.*

	Coating Thickness, μm and Type[a]				
Lot No.	SBNi	Bright Nickel	Bright Ni-Fe	Chromium Type	% Iron, Top/Bottom
30	23	7.6H	. . .	R	. . .
31	23	5.1H	. . .	MP	. . .
32	23	5.1H	. . .	MC	. . .
33	23	7.6L	. . .	R	. . .
34	23	5.1L	. . .	MP	. . .
35	23	5.1L	. . .	MC	. . .
36	. . .	. . .	30	R	9/20
37	. . .	. . .	27.5	MP	9/20
38	. . .	. . .	27.5	MC	9/20
39	. . .	. . .	30	R	20/25
40	. . .	. . .	27.5	MP	20/25
41	. . .	. . .	27.5	MC	20/25

[a] The 9/20 nickel-iron deposits were prepared from Solution 1; the 20/25 deposits from Solution 2, Table 4. SBNi denotes semibright nickel (Solution 3, Table 4). The other symbols are the same as described in Tables 1 and 2.

gle-layer bright nickel-iron alloy deposits of the same thickness. Two types of bright nickel are included to provide continuity with previously published information [*7*]. The two types are designated high-activity, H, and low-activity, L, bright nickel. High-activity bright nickel consistently displays a corrosion potential in the CASS test electrolyte that is 20 to 30 mV more active than that of the low-activity bright nickel. In general, one would expect low-activity bright nickel to perform better on steel than high-activity bright nickel as a single-layer coating. The two types of bright nickel are deposited from two different processes available commercially and are typical of processes widely used in industry. Three types of chromium were included. Two different nickel-iron processes were used to prepare coatings with low, L, and high, H, iron contents.

Table 3 outlines the third part of the program. Double-layer nickel coatings (30 μm thick) plated with regular, microporous, and microcracked chromium, and double-layer-type nickel-iron alloy coatings (30 μm thick) plated with the same three types of chromium are included. The double-layer nickel coatings consist of semibright nickel combined with either high- or low-activity bright nickel. In the case of double-layer coatings, high-activity bright nickel performs significantly better than low-activity bright nickel [*7*]. The double-layer-type nickel-iron alloy coatings consist of a layer 23 μm thick deposited in the presence of air agitation, and 7.5 μm deposited without air agitation in Lots 36 and 39. The thickness of the layer deposited without air agitation was 4.5 μm to compensate for the 2.5-μm-thick special nickel deposit used to induce microporosity or microcracking of the chro-

mium in Lots 37, 38, 40, and 41. The percent iron in the top and bottom layers is given in Table 3 and depends on which process is used to deposit the alloys.

Process Details

The compositions of the electroplating solutions used to prepare the panels are given in Table 4, along with operating conditions. Proprietary additives were not identified and were used in concentrations recommended by the suppliers of the processes.

Panel Preparation

All panels were 10.2 by 15.4 cm contoured or flat steel panels. The contoured panel has been described in the literature [*8*]. The contoured panel results in nonuniformly thick deposits at various points on the surface. The nonuniformity of deposit thickness can be controlled and reproduced from panel to panel.

Panels were plated in groups of nine on a rack designed to assure good distribution of coating thickness. Eighteen panels for each of the lots listed in Tables 2 and 3 were prepared. Stainless steel control panels were first plated in nickel-iron solutions to produce foils which were used to measure and adjust the thickness of the coatings. After obtaining the desired thickness, the foils were sampled and analyzed for iron.

The cycle used for precleaning and treating the panels is given in Table 5.

Exposure Locations and Evaluation Techniques

The panels from the first part of the program were CASS-tested only. All CASS testing was done according to ASTM recommended procedures [Copper-Accelerated Acetic Acid-Salt Spray (Fog) Testing (CASS Test) (B 368-68)]. Five panels from each of the lots listed in Tables 2 and 3 were exposed in the industrial atmosphere of Kearny, N. J.; another five were exposed in the marine environment of Kure Beach, N. C.; three panels were CASS-tested.

Panel performance is evaluated by means of visual inspection, performance ratings are assigned, and the nature of the defects is described according to the rating system developed by ASTM Committee B-08 [Recommended Practice for Rating of Electroplated Panels Subjected to Atmospheric Exposure (B 537-70)]. In the ASTM system, two numbers are used, one to describe protection, the second to describe appearance. A rating of 10/10 indicates perfect protection and appearance. A rating of 0/0 indicates that more than 50 percent of the surface has been attacked. From practical experience a rating of 7/7 or lower indicates failure of the coating.

TABLE 4—*Compositions of electroplating solutions and operating conditions.*

Solution No. 1. Nickel-Iron (L)	15% Iron	25% Iron
$NiSO_4$ $6H_2O$ (g/l)	92.3	105.4
$NiCl_2$ $6H_2O$ (g/l)	64.3	57.8
H_3BO_3 (g/l)	41.4	43.5
Total iron (g/l)	2.5	3.5
Ferric (g/l)	0.66	0.52
Stabilizer (g/l)	20	20
Proprietary additives	. . .	. . .

Operating Conditions

pH: 3.2 (2.8–3.3)
Temperature: 60°C
Current density: 2–10 A/dm^2

2. Nickel-Iron (H)	25 and 33% Iron
$NiSO_4$ $6H_2O$ (g/l)	85
$NiCl_2$ $6H_2O$ (g/l)	135
H_3BO_3 (g/l)	49
Total iron (g/l)	9.7
Stabilizer (g/l)	4
Proprietary additives	. . .

Operating Conditions

pH: 3.8 (3.5–4.0)
Temperature: 57°C
Current density: 5 A/dm^2

3. Semibright Nickel (Coumarin Type)	
$NiSO_4$ $6H_2O$ (g/l)	322
$NiCl_2$ $6H_2O$ (g/l)	43
H_3BO_3 (g/l)	43
Wetting agent (ml/l)	0.20
Leveling agent (g/l)	1.1

Operating Conditions

Reduction product (g/l): 1.6
pH: 4.0–4.2
Temperature: 57°C
Agitation: Mild circulation
Current density: 5 A/dm^2

4. Bright Nickel/High Activity (H)	
$NiSO_4$ $6H_2O$ (g/l)	330
$NiCl_2$ $6H_2O$ (g/l)	56
H_3BO_3 (g/l)	46
Wetting agent (vol. %)	0.12
Proprietary additives	. . .

Operating Conditions

pH: 4.0–4.2
Temperature: 57°C
Agitation: Mild circulation
Current density: 5 A/dm^2

TABLE 4—(*Continued*)

Solution No.

5. Bright Nickel/Low Activity (L)

$NiSO_4$ $6H_2O$ (g/l)	342
$NiCl_2$ $6H_2O$ (g/l)	80
H_3BO_3 (g/l)	46
Proprietary additives	. . .

Operating Conditions

pH:	3.4–3.8
Temperature:	60°C
Agitation:	Filtered low-pressure air
Current density:	5 A/dm^2

6. Special Nickel to Induce Microporosity

$NiSO_4$ $6H_2O$ (g/l)	300
$NiCl_2$ $6H_2O$ (g/l)	60
Boric acid (g/l)	45
Microscopic particles (g/l)	49
Proprietary additives	. . .

Operating Conditions

pH:	3.0–4.0
Temperature:	60°C
Agitation:	Filtered low-pressure air
Current density:	4 A/dm^2

7. Special Nickel to Induce Microcracking

$NiCl_2$ $6H_2O$ (g/l)	240
Additives (g/l)	50
Proprietary additives	. . .

Operating Conditions

pH:	3.6–4.5
Temperature:	29°C
Agitation:	Filtered low-pressure air
Current density:	8 A/dm^2

8. Chromium Plating Solution

Chromic acid (g/l)	250
Sulfate ion (g/l)	2.5
Temperature	44°C
Current density	21.6 A/dm^2

Results and Discussion

The results are given in Figs. 1–16 and are discussed in the following in terms of the requirements and definitions in the Specification for Electrodeposited Coatings of Copper Plus Nickel Plus Chromium and Nickel Plus Chromium (B 456-79).

TABLE 5—*Cycle used for precleaning and treating steel panels for plating.*

1. Vapor degrease
2. Rack panels
3. Clean anodically in alkaline cleaning solution[a] for 2 min @ 60°C
4. Rinse in demineralized water
5. Acid dip in 1-1 hydrochloric acid for 1 min
6. Rinse in demineralized water
7. Anodic clean as in (3) but for 1 min
8. Rinse in demineralized water
9. Acid dip as in (5) but for 15 s
10. Rinse in demineralized water
11. Plate

[a] Proprietary cleaner.

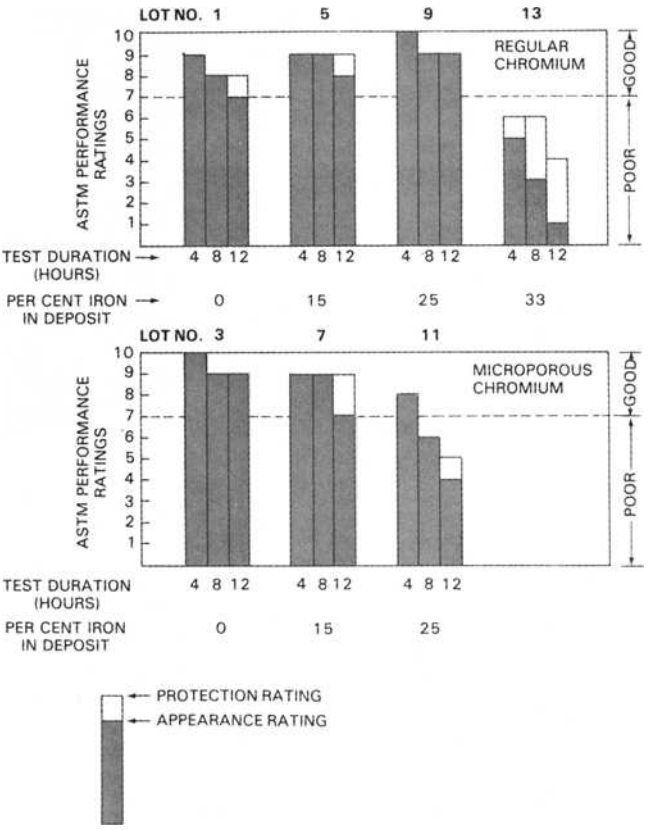

FIG. 1—*Influence of iron content and type of chromium on CASS test performance of thin (7.6 μm) decorative nickel-iron alloy deposits on steel.*

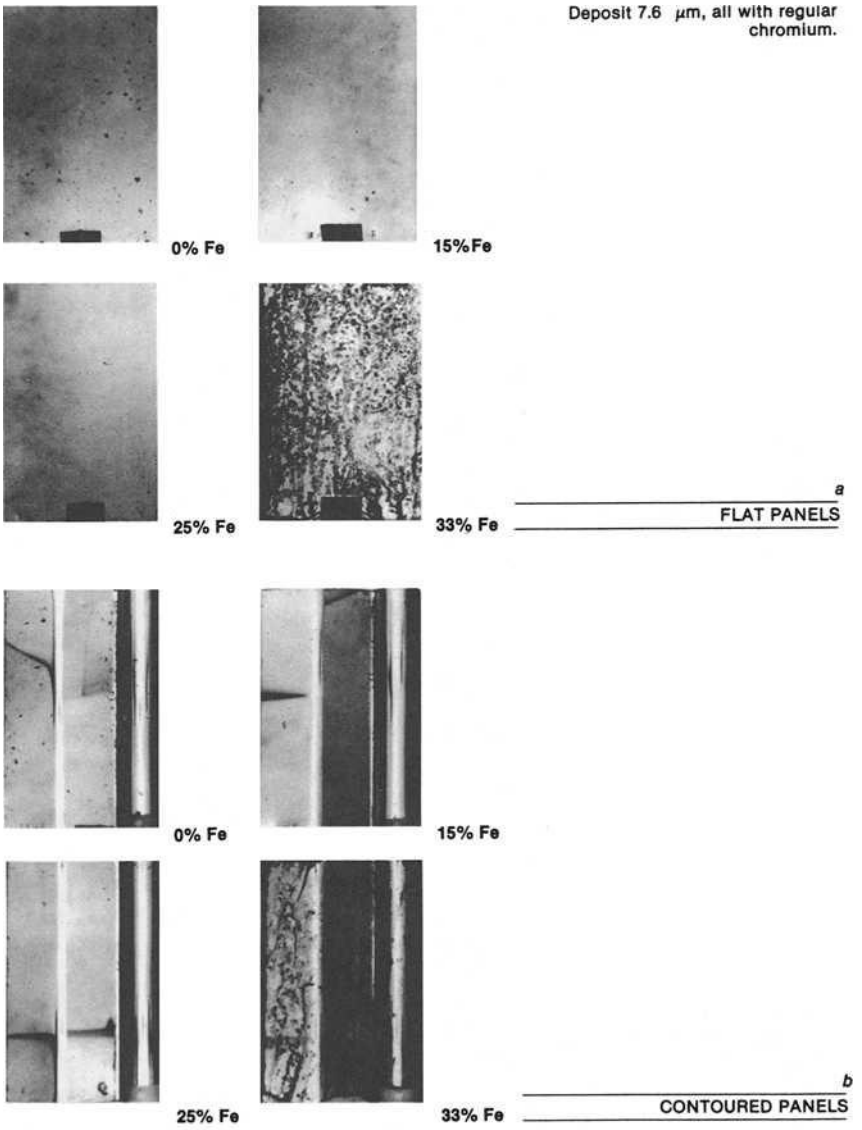

FIG. 2—*Effect of iron content on the appearance of nickel-iron alloy deposits after 8 h of CASS testing.*

Corrosion Performance of Thin (7.6 μm) Single-Layer Coatings

ASTM Method B 456-79 defines mild corrosion service as exposure indoors in normally warm dry atmospheres with the coating subject to minimum wear or abrasion. The minimum coating thickness on steel for mild service is 10 μm of single-layer bright nickel in combination with regular chromium. Test durations in CASS are not specified, but 8 h in acetic acid

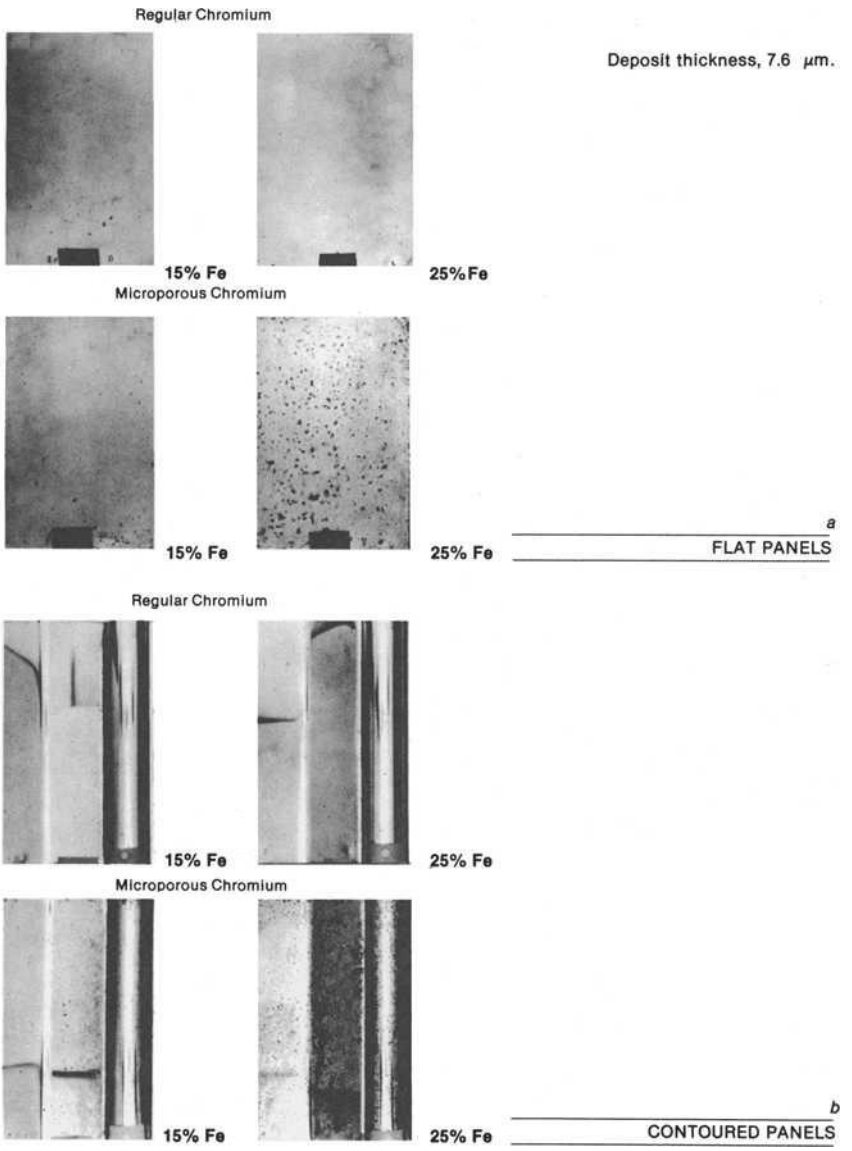

FIG. 3—*Effect of type of chromium on the appearance of nickel-iron alloy deposits with two levels of iron after 8 h of CASS testing.*

salt spray is suggested as a corrosion test suitable for mild corrosion service. Evidence of basis metal corrosion or blistering of the coating is cause for rejection. Coatings 7.6 μm thick are nonspecification coatings and are, thus, not covered by ASTM Method B 456-79. We decided to test these thin coatings for 4, 8, and 12 h in CASS.

Figure 1 gives ASTM ratings that illustrate the influence of iron content

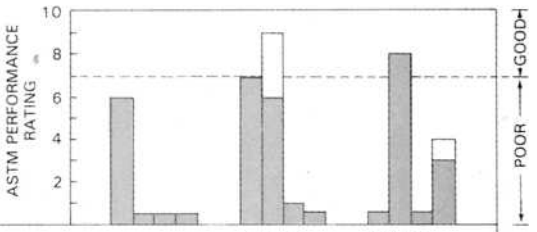

TYPE OF CHROMIUM	REGULAR	MICRO-POROUS	MICRO-CRACKED
TYPE OF NICKEL H = HIGH ACTIVITY L = LOW ACTIVITY	H L - -	H L - -	H L - -
PER CENT IRON IN DEPOSIT	0 0 2025	0 0 2025	0 0 2025
LOT NO.	15182124	16192225	17202326

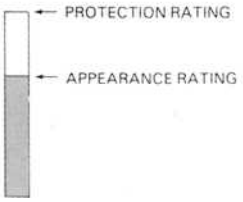

FIG. 4—*Influence of iron content, type of chromium, and nickel activity on 3-month performance in the marine atmosphere of SC-2-type coatings.* (*Coating thickness: 15 μm; coating type: single layer.*)

and type of chromium on the corrosion performance of flat panels. With regular chromium, the performance ratings of the nickel-iron alloys with up to 25 percent iron are better than or roughly the same as the ratings for bright nickel deposits. Above 25 percent iron, the decorative nickel-iron deposit is considerably poorer than the bright nickel deposit. Microporous chromium affected performance adversely when the deposit contained greater than 15 percent iron.

The effect of iron content and type of chromium on the appearance of flat and contoured panels after 8 h of CASS is shown in Figs. 2 and 3. The appearance of these panels shows the sharp distinction in performance between deposits containing 33 percent iron and deposits containing 0, 15, and 25 percent iron, and the adverse effect of microporous chromium at certain iron levels.

The results of the first part of the program suggest that the corrosion performance of thin decorative nickel-iron alloys depends on iron content and type of chromium. On the basis of CASS test results alone, thin nickel-iron alloy deposits appear suitable for mild corrosion service. The data given in

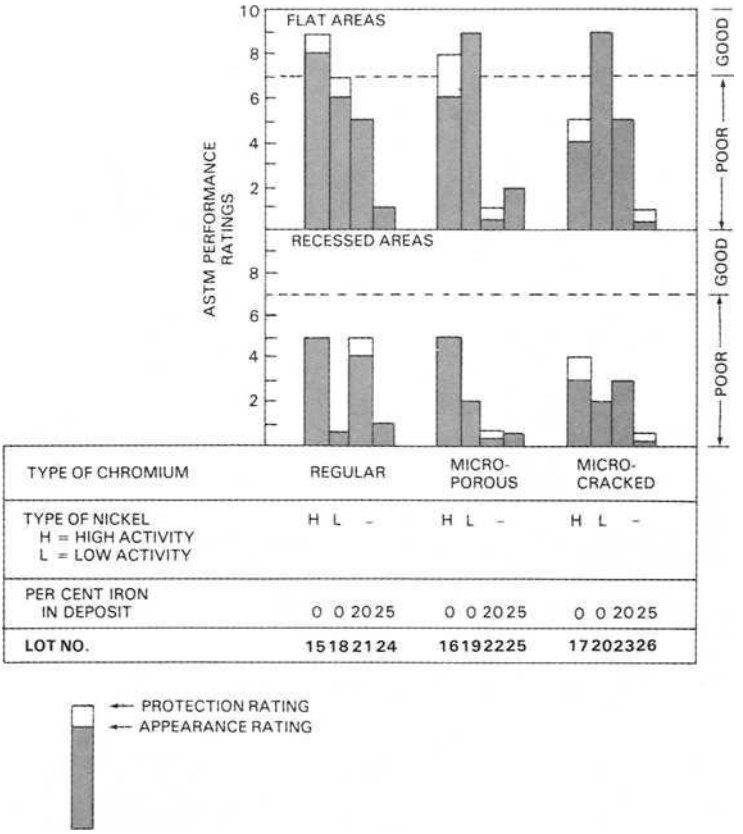

FIG. 5—*Influence of iron content, type of chromium, and nickel activity on 3-month performance in the industrial atmosphere of SC-2-type coatings. (Coating thickness: 15 μm; coating type: single layer.)*

the following indicate there is a lack of correlation between the performance of nickel-iron coatings in CASS and in marine and industrial atmospheres. Additional study of thin nickel-iron alloy deposits would be desirable.

Corrosion Performance of Single-Layer Coatings 15 μm Thick

Moderate corrosion service (SC-2) is defined as exposure indoors in places where condensation of moisture may occur as in kitchens and bathrooms. The minimum nickel thickness on steel for moderate service is 15 μm in combination with microporous or microcracked chromium. The recommended test duration in CASS is 4 h.

Figure 4 gives corrosion performance ratings for various deposits on contoured panels at the end of 3 months in the marine environment. The nickel deposits with regular chromium performed poorly and this probably ac-

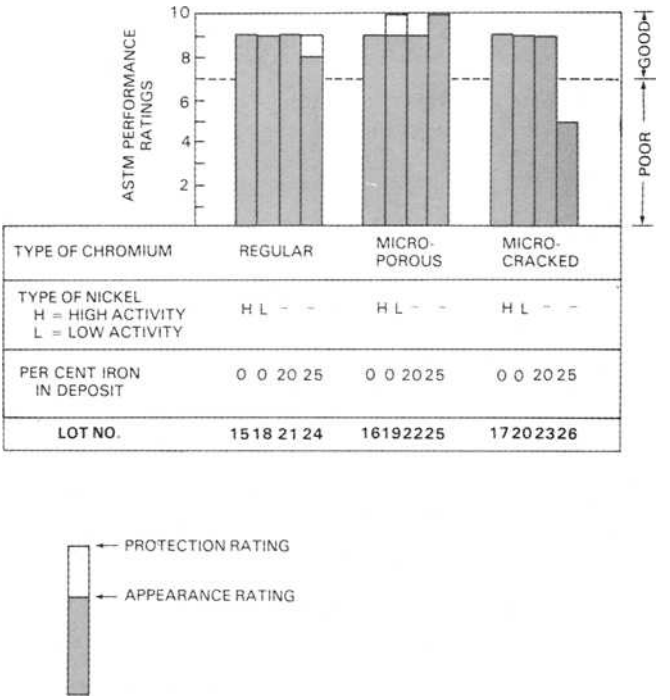

FIG. 6—*Influence of iron content, type of chromium, and nickel activity on 4-h CASS test performance of SC-2-type coatings on steel. (Coating thickness: 15 μm; coating type: single layer.)*

counts for the fact that ASTM Method B 456-79 recommends the use of 20 μm of single-layer bright nickel with regular chromium, not 15 μm as used in this program for comparison purposes. The nickel-iron alloys performed poorly with regular, microporous, or micro-cracked chromium. The low-activity bright nickel performed better than high-activity single-layer bright nickel with either microporous or microcracked chromium. The single-layer high-activity bright nickel failed with microcracked chromium. The ratings of the recessed areas of contoured panels were 0/0 for all deposits.

The results in the industrial environment are given in Fig. 5. Although protection and appearance ratings are better than in marine, similar trends are observed. The high-activity single-layer bright nickel is better than the low-activity bright nickel with regular chromium; the low-activity bright nickel is better than the high-activity bright nickel with microporous and microcracked chromium. The high-activity single-layer bright nickel with microcracked chromium, also, failed in the industrial environment. The decorative nickel-iron alloys did not give acceptable results irrespective of iron content or type of chromium.

The results of CASS testing the 15-μm-thick single layer coatings are given in Fig. 6. In contradiction to the results in the marine and industrial envi-

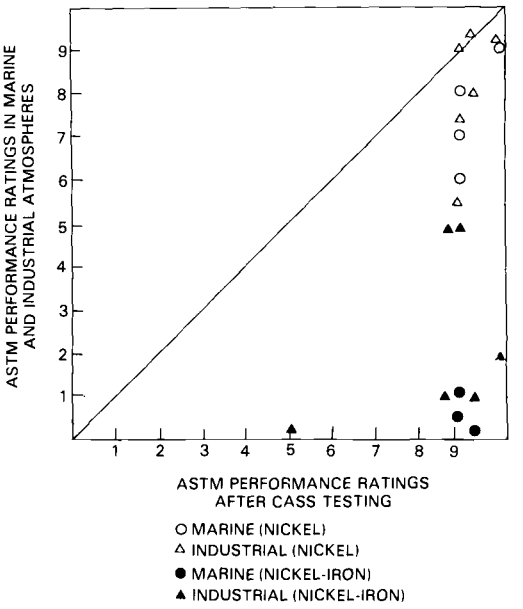

FIG. 7—*Correlation between 4-h CASS and 3 months in marine and industrial atmospheres.*

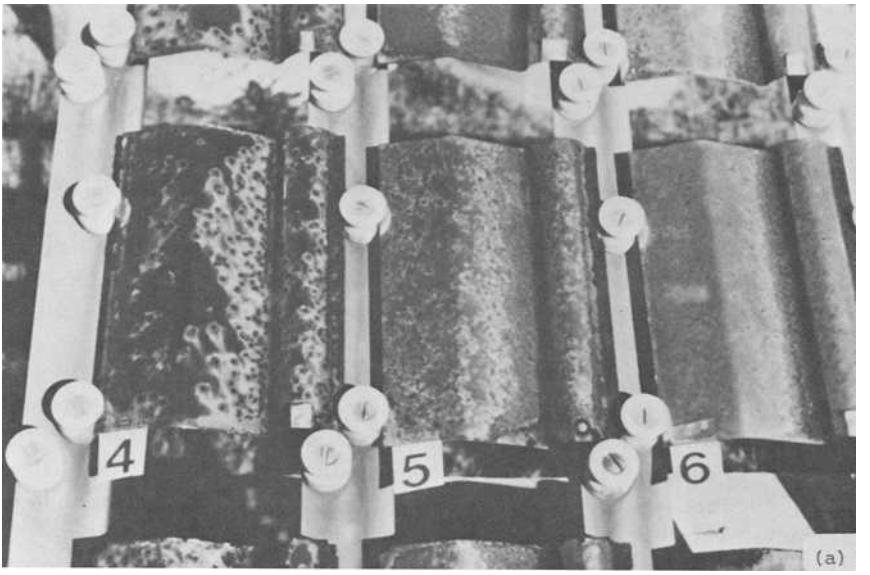

FIG. 8—*Appearance of single-layer bright nickel and nickel-iron alloy deposits 15 μm thick after 17 months in a marine atmosphere at Kure Beach, N. C.* (a) *High-activity bright nickel with* (left to right) *regular, microporous, and microcracked chromium.* (b) *Low-activity bright nickel with* (left to right) *microporous and microcracked chromium.* (c) *High-activity bright nickel* (left) *and bright nickel-iron with 25 percent iron* (right) *each plated with regular chromium.*

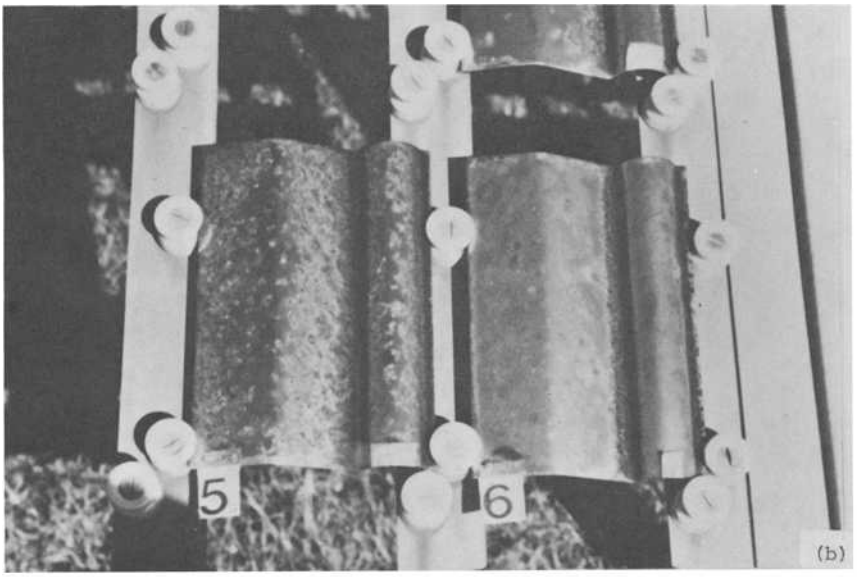

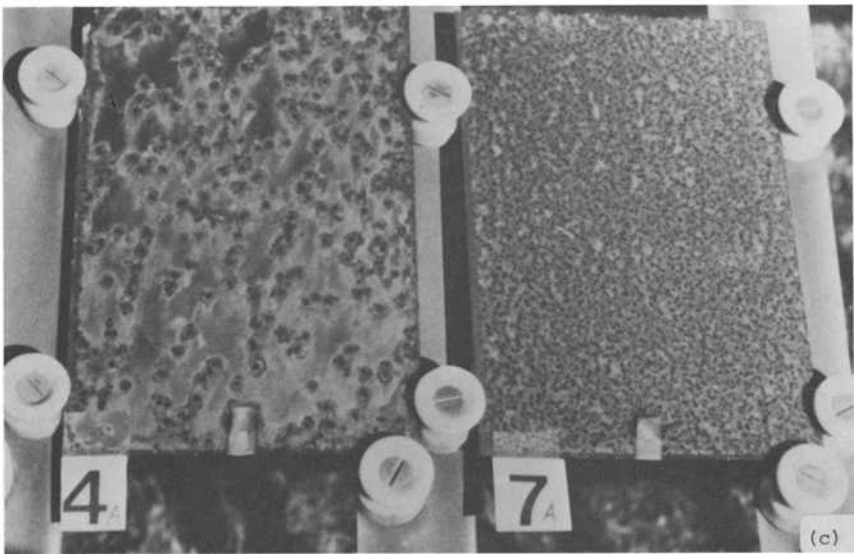

FIG. 8—*Continued.*

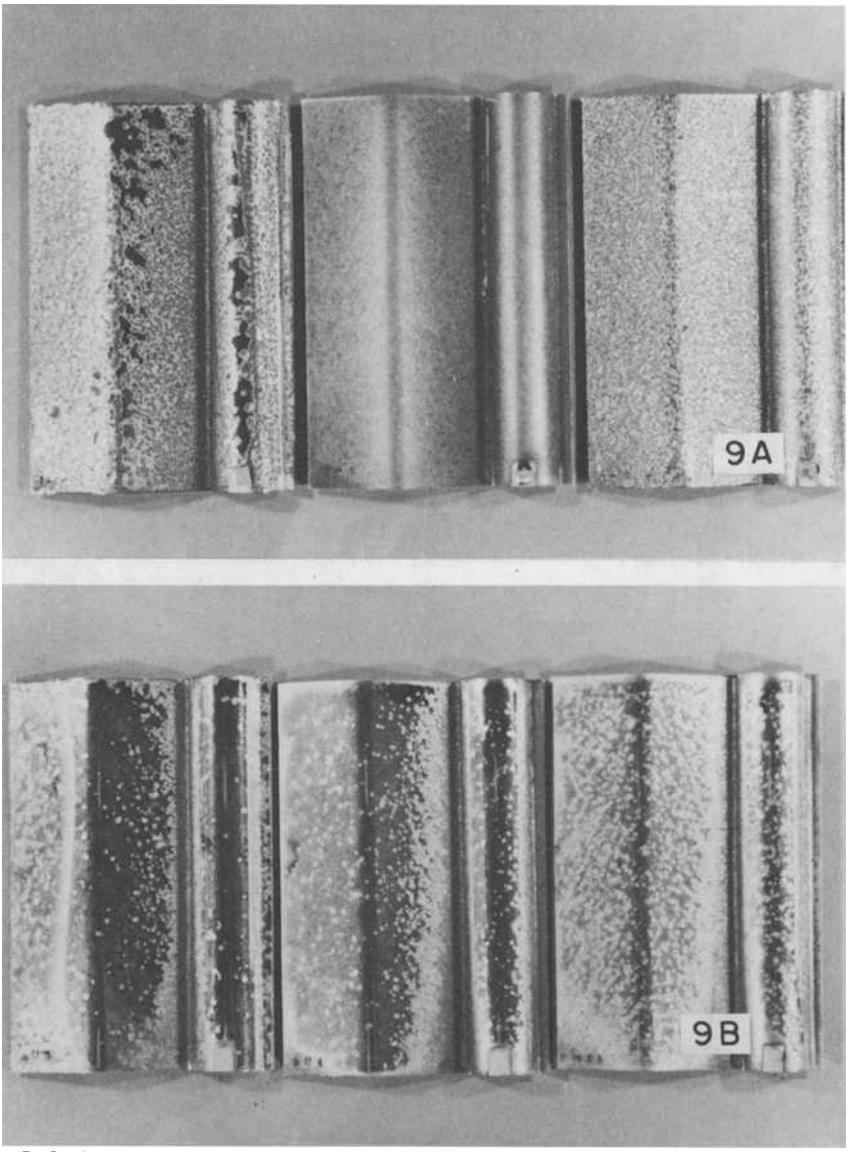

FIG. 9—*Appearance of single-layer bright nickel and nickel-iron alloy deposits 15 μm thick after 15 months in an industrial atmosphere at Kearny, N. J.* (a) *High-activity bright nickel.* (b) *Low-activity bright nickel.* (c) *Bright nickel-iron with 20 percent iron.* (d) *Bright nickel-iron with 25 percent iron. Subfigures:* (left to right) *regular, microporous, and microcracked chromium.*

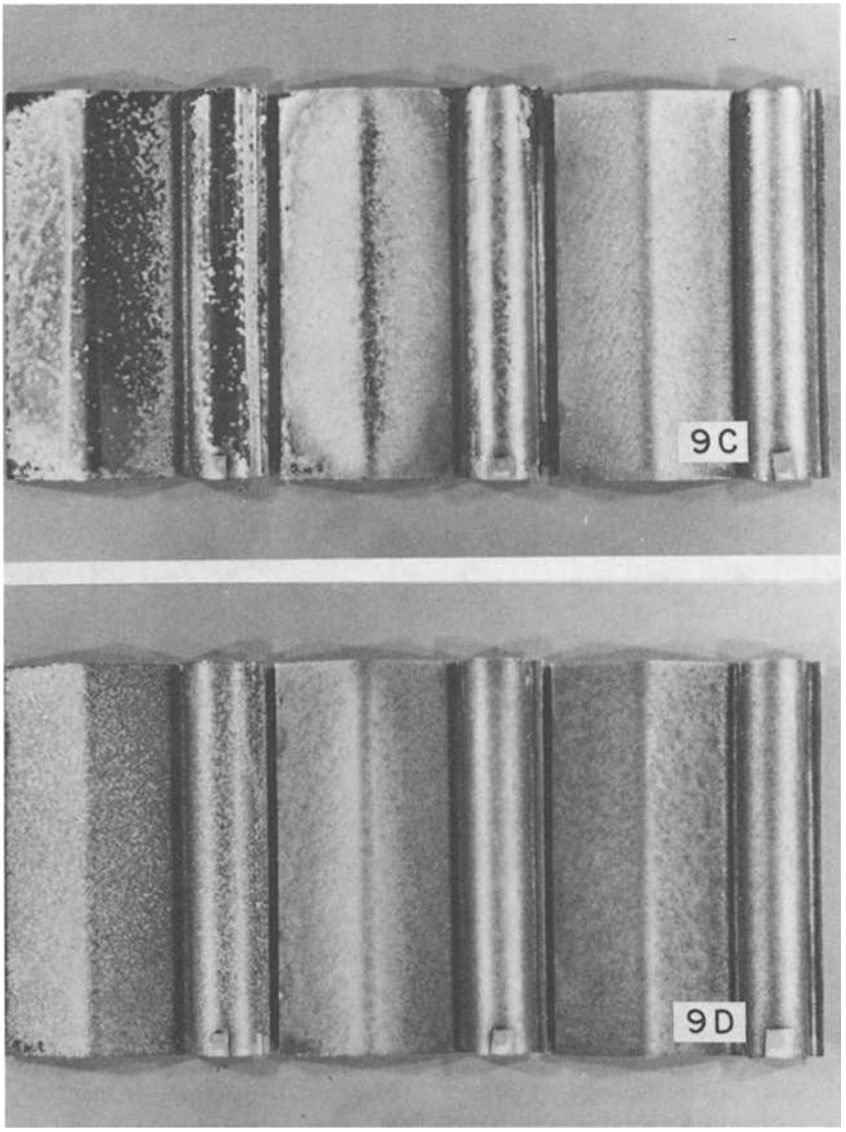

FIG. 9—*Continued.*

ronment, almost all the coating systems display performance ratings that are better than 7/7. The correlation between 4 h of CASS-testing and 3 months in marine or industrial atmospheres is shown in Fig. 7. The diagonal line represents perfect agreement. The greater the distance of a point from the diagonal, the less the agreement. The agreement between the 4-h CASS test

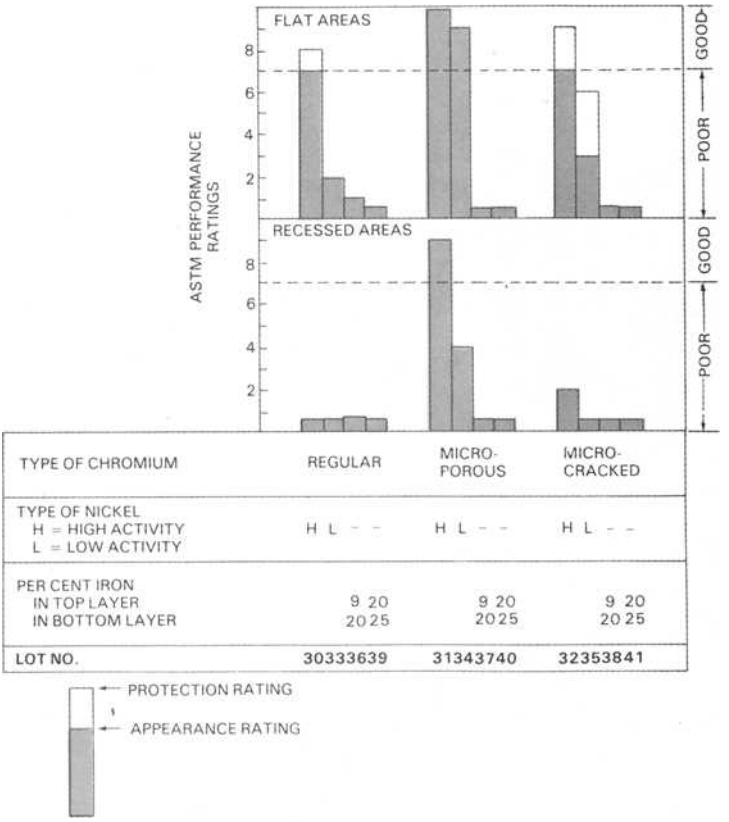

FIG. 10—*Influence of iron content, type of chromium, and nickel activity on 17-month performance in the marine atmosphere of SC-3-type coatings. (Coating thickness: 30 μm; coating type: double layer.)*

ratings and the 3-month exposure data is reasonably good for the bright nickel coatings, but decidedly poor for the nickel-iron alloy deposits. The CASS test predicts better performance for the nickel-iron alloys than is observed in marine and industrial atmospheres, indicating that a reduction in the correlation factor is required; that is, 4 h CASS is equivalent to 3 to 4 weeks of outdoor exposure for electrodeposited nickel-iron alloys.

The outdoor exposures of the panels plated with single-layer coatings 15 μm thick were continued for 17 months and 15 months in marine and industrial atmospheres, respectively. The appearance of the panels at the end of the exposures is shown in Figs. 8 and 9. The appearance illustrates the relative performance of the coating systems and the uniform corrosion pitting and rust staining observed with the nickel-iron alloy deposits.

In summary, the performance of single-layer bright nickel coatings 15 μm

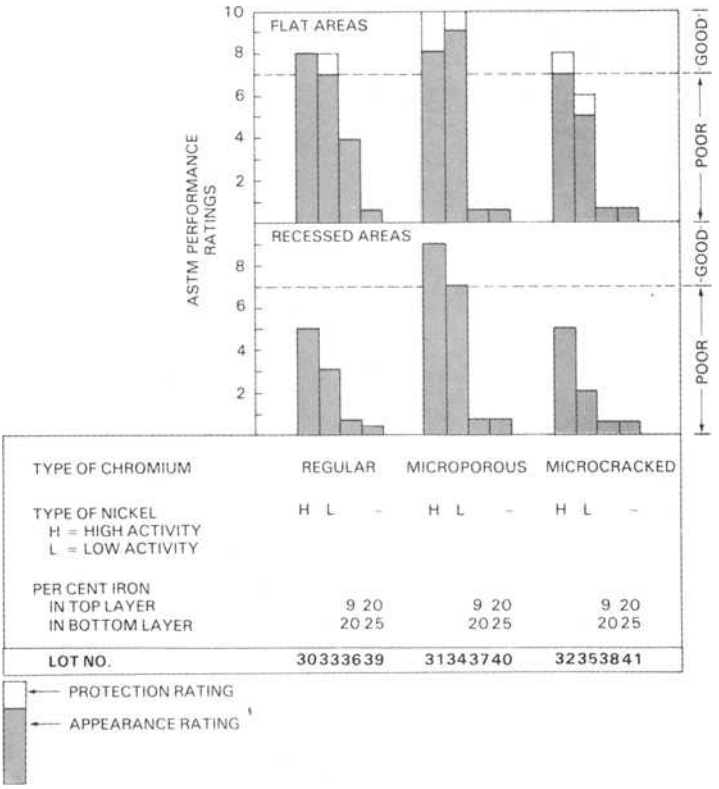

FIG. 11—*Influence of iron content, type of chromium, and nickel activity on 15-month performance in the industrial atmosphere of SC-3-type coatings. (Coating thickness: 30 μm; coating type: double layer.)*

thick is influenced by the activity of the bright nickel and the type of chromium. Low-activity single-layer bright nickel seems preferred when used with microcracked or microporous chromium. The high-activity bright nickel performs better with regular chromium. The nickel-iron alloy deposits do not give acceptable performance in marine and industrial environments. CASS test results do not correlate with results of outdoor exposure in the case of the decorative nickel-iron deposits.

Corrosion Performance of Double-Layer Coatings 30 μm Thick

Double-layer nickel coatings 30 μm thick electroplated with regular chromium are recommended for severe corrosion service (SC-3) in ASTM Method B 456-79. With microporous or microcracked chromium, double-layer nickel coatings 30 μm thick are suitable for very severe service (SC-4). Severe service involves exposure outdoors where coatings may be frequently

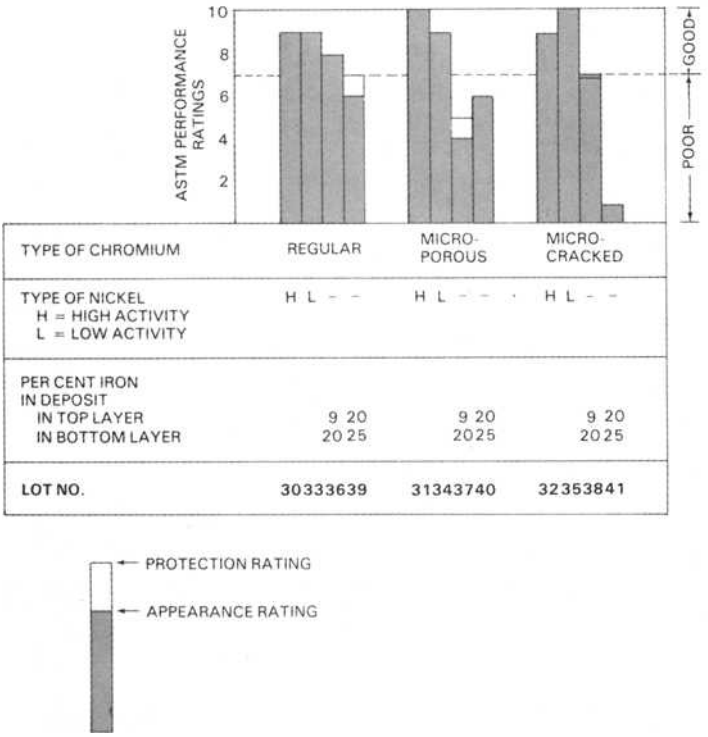

FIG. 12—*Influence of iron content, type of chromium, and nickel activity on 16-h CASS test performance of SC-3-type coatings on steel. (Coating thickness: 30 μm; coating type: double layer.)*

wet by rain, strong cleaners, and saline solutions. Very severe service involves outdoor exposures where damage to the coating from denting, scratching, and abrasion is likely to occur, as well as frequent wetting.

The minimum requirement for severe corrosion service is 16 h of CASS. For very severe service, the requirement is 22 h of CASS. The double-layer coatings listed in Table 3 were tested for 17 months in the marine atmosphere, 15 months in the industrial atmosphere, and for 16 h of CASS.

Corrosion performance data for double-layer nickel and nickel-iron alloy coatings after 17 months in the marine atmosphere are given in Fig. 10 for the flat and recessed areas of contoured steel panels. Corrosion performance was influenced by the type of chromium and the activity of the double-layer nickel. The high-activity double-layer nickel gave acceptable performance with regular chromium. The low-activity double-layer nickel and the double-layer-type nickel-iron alloy deposits performed poorly with regular chromium.

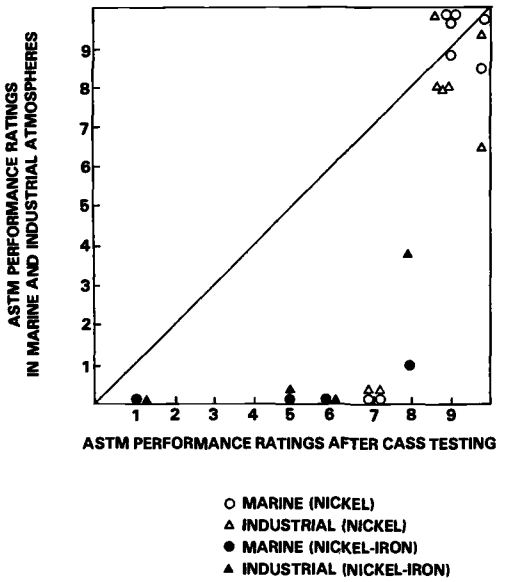

FIG. 13—*Correlation between 16-h CASS and 15 to 17 months in marine and industrial atmospheres.*

The use of microdiscontinuous chromium improved the performance of the double-layer nickel coatings. The best combination was the high-activity double-layer nickel coating with microporous chromium. The low-activity double-layer nickel with microcracked chromium did not perform well. The nickel-iron alloy coatings did not give acceptable performance in the marine environment irrespective of type of chromium.

The results in the industrial environment after 15 months of exposure are given in Fig. 11. Double-layer nickel coatings with microporous chromium performed better than similar coatings with microcracked chromium. The performance of the nickel-iron alloy coatings was not acceptable in the industrial environment.

The CASS test results for the double-layer coatings are given in Fig. 12, and the correlation between 16 h of CASS testing and 15 and 17 months in marine and industrial atmospheres is shown in Fig. 13. The correlation between results of CASS testing and outdoor exposure is good for double-layer nickel coatings, but poor for nickel-iron alloy coatings.

The appearance of the double-layer nickel and nickel-iron coatings after 17 months of marine and 15 months of industrial exposure is shown in Figs. 14 and 15, respectively. The relatively good performance of the double-layer nickel coatings is apparent.

The metallographic cross sections of decorative nickel-iron deposits 30

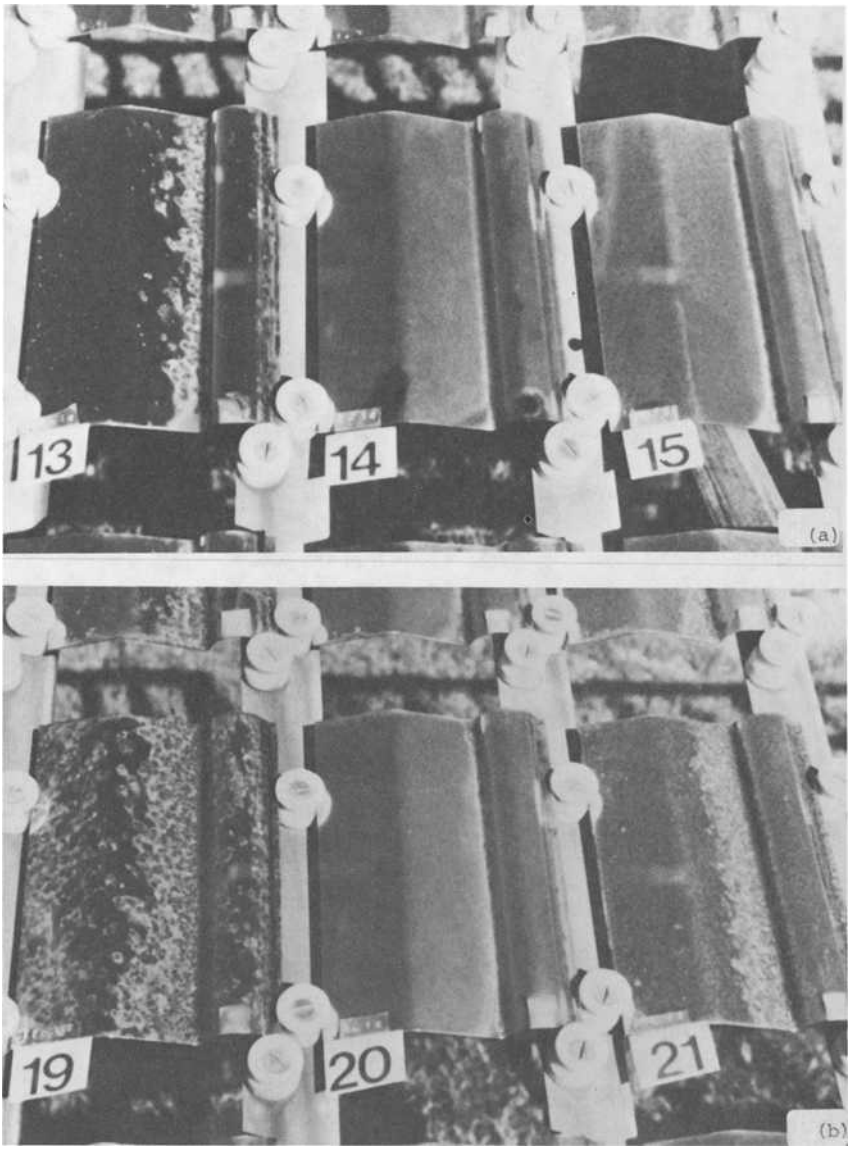

FIG. 14—*Appearance of double-layer nickel and nickel-iron deposits after 17 months in a marine atmosphere at Kure Beach, N. C.* (a) *High-activity double-layer nickel with* (left to right) *regular, microporous, and microcracked chromium.* (b) *Low-activity double-layer nickel with regular, microporous, and microcracked chromium.* (c) *Nickel-iron alloy deposits with 9 percent iron in top and 20 percent iron in bottom layer with* (left to right) *regular chromium and microporous chromium.* (d) *Nickel-iron alloy deposits with 20 and 25 percent iron in top and bottom layers, respectively, with microporous and microcracked chromium,* left to right.

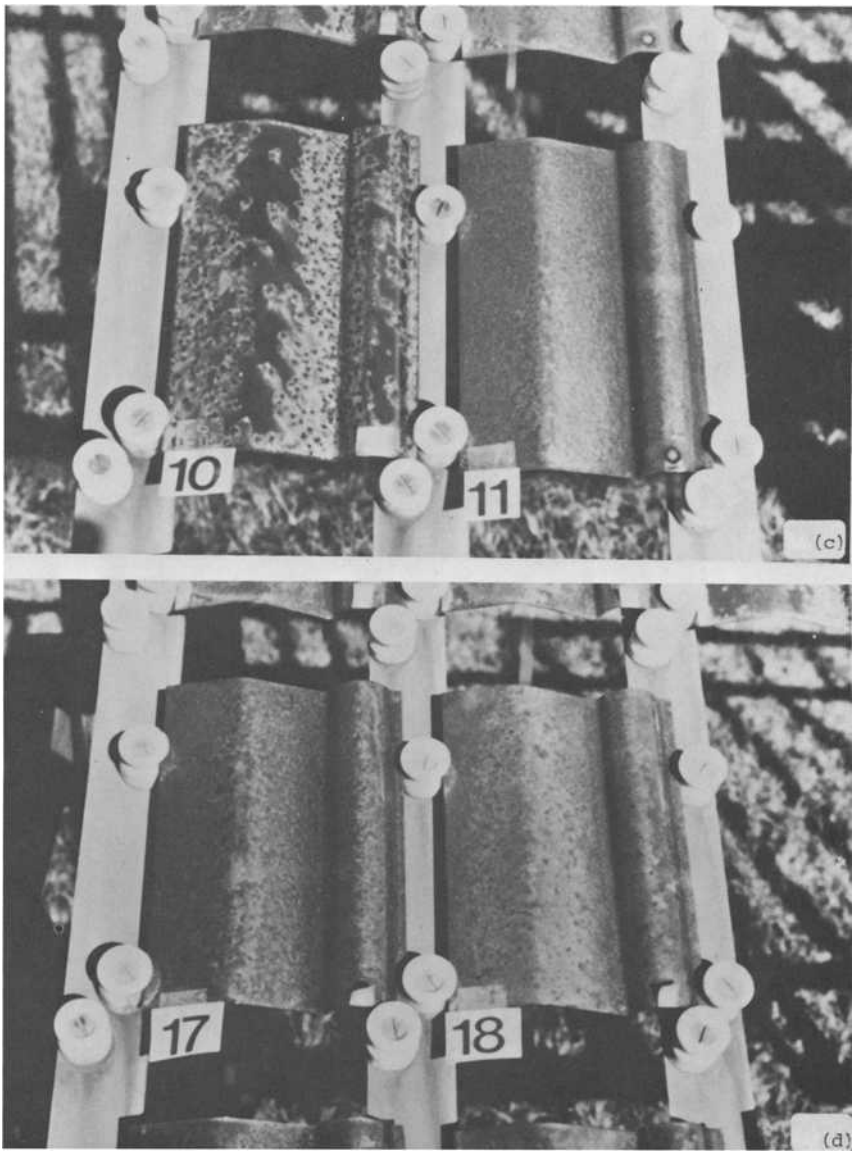

FIG. 14—*Continued.*

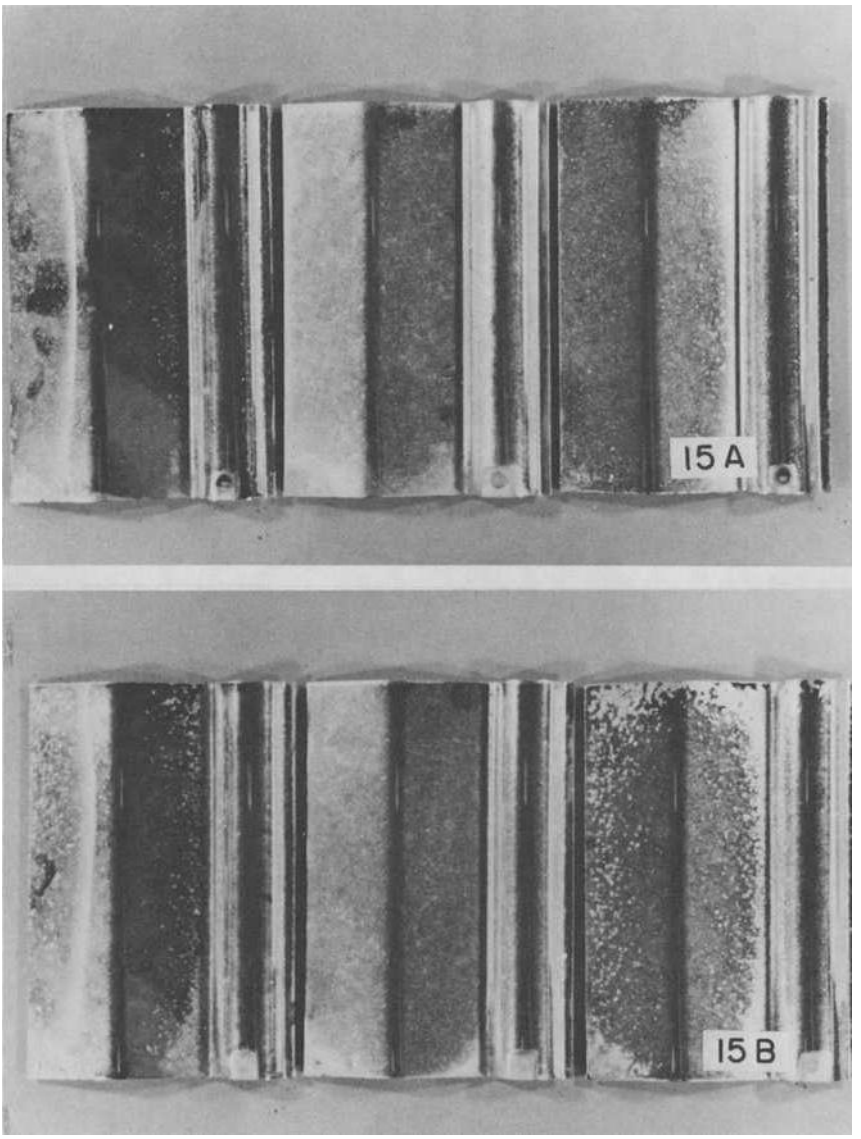

FIG. 15—*Appearance of double-layer nickel and nickel-iron deposits after 15 months in an industrial atmosphere at Kearny, N. J.* (a) *High-activity double-layer nickel.* (b) *Low-activity double-layer nickel.* (c) *Nickel-iron alloy deposits with 9 percent iron in top and 20 percent iron in bottom layer.* (d) *Nickel-iron alloy deposits with 20 percent iron in top and 25 percent iron in bottom layer. Subfigures:* (left to right) *regular, microporous, and microcracked chromium.*

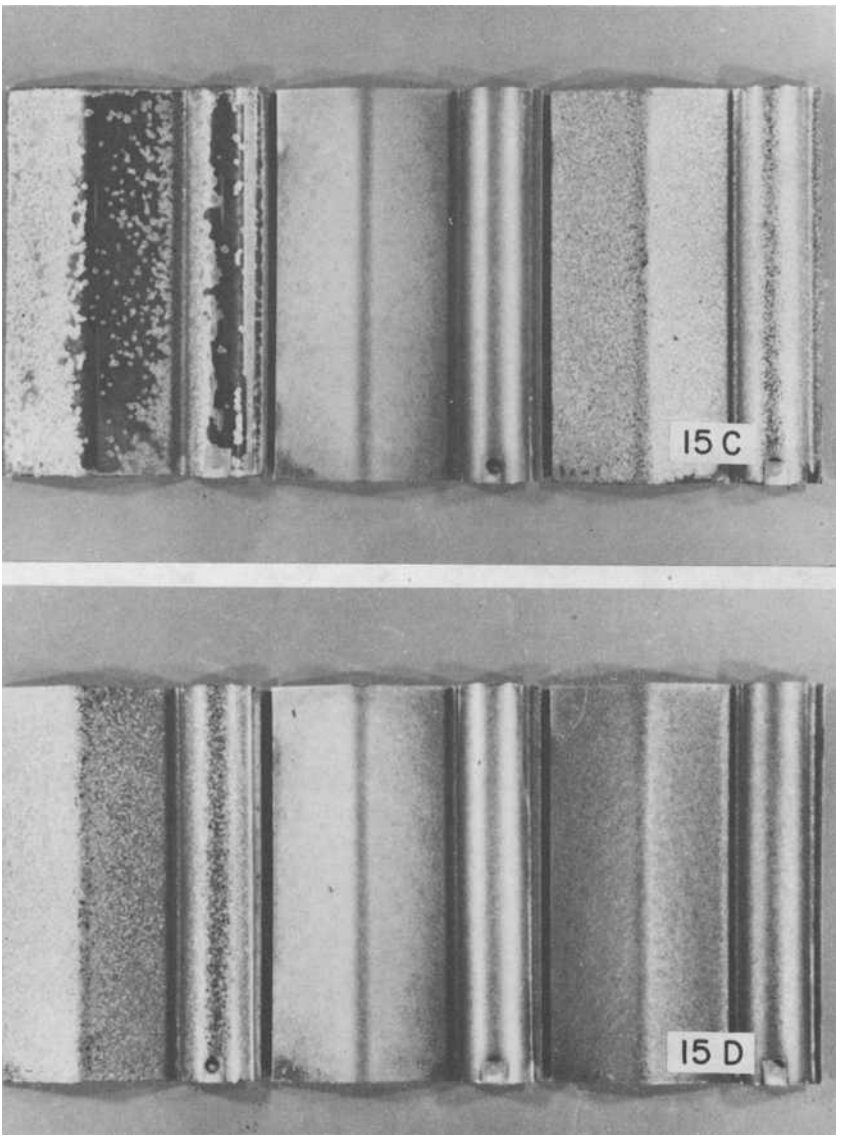

FIG. 15—*Continued.*

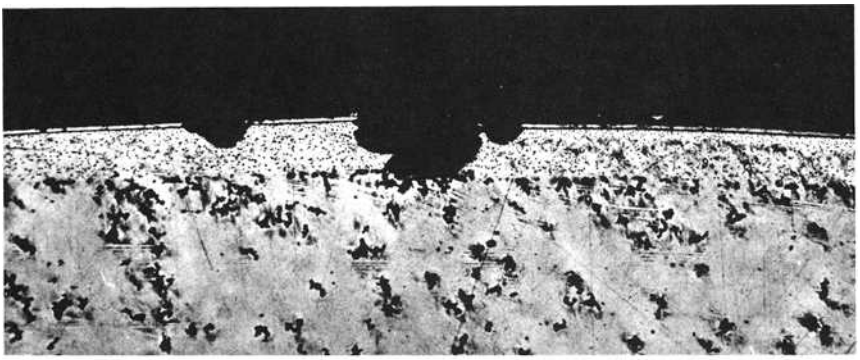

200X

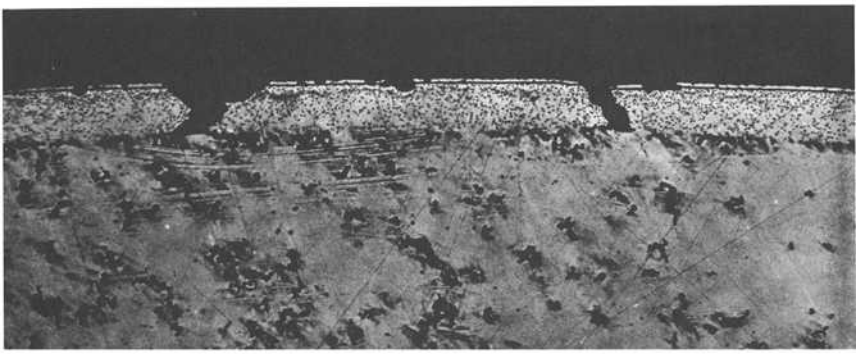

200X

FIG. 16—*Cross sections of chromium-electroplated double-layer-type nickel-iron deposits on steel after 15 months' exposure in the industrial environment.*

μm thick plated with microporous chromium, Fig. 16, show that a few pits penetrate to the substrate but that the majority are superficial in the 15-month industrial exposure.

Summary and Conclusions

The overall corrosion performance of single-layer bright nickel coatings 15 μm thick and double-layer nickel coatings 30 μm thick was consistently better than the performance of equivalent thicknesses of nickel-iron alloy coatings. The major defect of the latter was rapid staining in marine and industrial atmospheres. Metallographic examination of cross sections of the nickel-iron deposits showed less penetration to the substrate than expected from the appearance of the deposits. In the absence of a way to control superficial staining, however, the nickel-iron alloy coatings do not appear

suitable for decorative applications involving outdoor exposure. Thin coatings (7.6 μm) of either nickel or nickel-iron have been found satisfactory for mild interior service applications. The nickel-iron alloy coatings should be applied to articles intended for mild service until further development work offers a solution to the staining problems.

The work confirmed that high-activity double-layer nickel protects the low-current-density areas of contoured steel panels better than low-activity double-layer nickel, either with microporous or microcracked chromium. Microporous chromium was more effective in this program than microcracked chromium. In a previous study, microcracked chromium was better than microporous chromium [*8*]. In the case of single-layer coatings, low-activity bright nickel performed better than high-activity bright nickel when microporous or microcracked chromium was used.

References

[*1*] Clauss, R. J., Tremmel, R. A., and Klein, R. W., *Transactions of the Institute of Metal Finishing,* Vol. 53, 1975, p. 22.
[*2*] McMullen, W. H., *Metal Finishing Guidebook and Directory,* Metal and Plastics Publications, Inc., Hackensack, N. J., 1979, p. 294.
[*3*] Brenner, A., *Electrodeposition of Alloys,* Vol. 2, Academic Press, New York, 1963, Chapter 31.
[*4*] Wesley, W. A. and Knapp, B. B., *Transactions of the Institute of Metal Finishing,* Vol. 31, 1954, p. 267.
[*5*] Du Rose, A. H. and Pine, P. R. *Steel,* Vol. 114, No. 24, 1944, p. 124.
[*6*] Chessin, H., Seyb, E. J., and Walker, P. D., *Plating and Surface Finishing,* Vol. 63, No. 12, 1976, p. 32.
[*7*] DiBari, G. A., *Metal Finishing,* Vol. 75, No. 5, June 1977.
[*8*] DiBari, G. A., *Metal Finishing,* Vol. 75, No. 6, June 1977.

DISCUSSION

S. K. Coburn[1] (*written discussion*)—What metallographic technique is used to prepare the plated steel specimens for microscopic examination so that the film is not damaged?

G. A. DiBari, G. Hawks, and E. A. Baker (*authors' closure*)—The conventional procedure is to electrodeposit a thick metallic coating over the entire specimen, so as to completely envelope it. The surface of interest is exposed by sectioning the specimen appropriately. The metallic backing prevents damage and rounding of the coating during polishing. In our case, a large number of specimens were mounted side-by-side and encapsulated in plastic. This, also, helps protect the surface film. The conventional procedure is preferred when preparing plated specimens for thickness determinations by the microscopical method.

[1] U. S. Steel Corp., Pittsburgh, Pa.

R. J. Clauss[1]

Comments on the Corrosion Performance of Decorative Nickel-Iron Coatings

REFERENCE: Clauss, R. J., **"Comments on the Corrosion Performance of Decorative Nickel-Iron Coatings,"** *Atmospheric Corrosion of Metals, ASTM STP 767,* S. W. Dean, Jr., and E. C. Rhea, Eds., American Society for Testing and Materials, 1982, pp. 214–221.

ABSTRACT: The durability of decorative nickel-iron coatings in various types of exposure is discussed in detail. It has been determined that these coatings, as part of a specific multiple deposit system, perform acceptably for exterior automotive applications. It is necessary that a microdiscontinuous chromium be present in the composite coating to achieve optimum results and it is desirable to use a copper underlayer to the nickel-iron electrodeposits. Corrosion test results are also reported which establish that static tests cannot be relied upon to predict actual mobile service performance.

KEY WORDS: bright nickel-iron alloy, exterior automotive, static tests, mobile tests, duplex alloy coatings, microdiscontinuous chromium, copper underlayer deposits, multiple deposits, staining

Bright nickel-iron alloy coatings have been used commercially, as an alternative to bright nickel coatings, since 1973. During this time, they have found wide use in appliance, furniture, kitchenware, and a variety of other applications. Today it is estimated that the bright alloy deposit is used worldwide for about 10 percent of the market which has historically used bright nickel decorative coatings.

Initially the bright alloy deposits were used where its decorative features dominated the protective requirements. These were applications where bright nickel coatings plated with regular chromium served very satisfactorily. Gradually, over a period of several years, new developments and an understanding of the unique character of nickel-iron coatings have expanded its used to applications where a protective role is also vital. These alloy coatings are being used, for instance, on bicycle, lawnmower, and other exterior applications. More recently the nickel-iron deposit, in a well-defined coating system, has been used on specific original equipment manufactured (OEM)

[1] Manager, Research & Development, Udylite, Plating Systems Division, Hooker Chemical and Plastics Corp., Warren, Mich.

exterior automotive components in the United Kingdom. Consequently, with a growing recognition of its unique characteristics as well as its unusual economic advantages, nickel-iron decorative protective coatings have established a sizable and successful niche in the decorative area.

As discussed in our technical papers as early as 1973 [*1,2*],[2] the development of light, rust-colored film stain from corrosion of a bright nickel-iron alloy deposit can be a detrimental factor to retaining the decorative aspect of the coating [*3*]. It should be emphasized, however, that observations over a period of years have established that the stain which develops on static exposure, in either a marine or industrial location, does not necessarily have a direct relationship to the performance of commercially plated products. This will become evident in the data presented herein.

In reporting corrosion data in this paper, the procedure of the American Society for Testing and Materials (ASTM) has been used. This procedure, the ASTM Recommended Practice for Rating of Electroplated Panels Subjected to Atmospheric Exposure (B 537-70), uses a two-number system in which the first number denotes protection of the substrate and the second number is descriptive of appearance. A perfect specimen showing no deterioration is rated 10/10. Progressive degrees of failure are denoted by lower numbers. A rating below 7 for either protection or appearance is frequently considered unsatisfactory.

Static Testing

Since nickel-iron alloy deposits can develop stain as an inherent corrosive characteristic, the iron content of the coating plays a major role in determining the severity of the problem. Therefore, judgment on the iron content of the deposit should be exercised according to the application and service required. A 35 percent iron alloy, for instance, can be completely satisfactory for interior use while very severe applications may limit average iron content to the 20 to 25 percent alloy range.

The influence of iron content on corrosion stain was studied and typical results are given in Table 1. The Detroit test site was a severe industrial location and included a winter season in the exposure period. The data show that the severity of corrosion stain is directly related to the iron content of the alloy. Subsequent to this determination, which was made a number of years ago, new processes were developed to achieve improved performance.

A specific patented technique to assist in overcoming stain was developed to permit the successful use of these alloy deposits in severe outdoor applications. This process [*5*], a duplex system, allows two or more levels of iron content in the alloy deposit with the lowest iron content nearest the exposed surface. Successful use of this system requires a maximum iron content of about 15 percent in the final or outer deposit. The significant benefits of this

[2] The italic numbers in brackets refer to the list of references appended to this paper.

TABLE 1—*Influence of iron content on staining of bright nickel-iron coatings—ten months' static exposure at Detroit, Mich.*

Coating System	Deposit Thickness, μm
Copper	15
Bright nickel-iron	20
Nickel[a]	3.5
Microporous chromium	0.25
Iron content of nickel-iron, %	Appearance Rating
21	5
9	8

[a] Nickel deposit contains microfine inorganic particles to induce microporosity in the subsequent chromium deposit.

process are shown in the data reported in Table 2, where duplex layers of nickel-iron alloy were plated in two sequences. The first system shows the desired sequence with the lowest iron-content layer near the exposed surface, while the second system is plated with the higher iron content alloy nearer the exposed surface of the deposit. Exposure at Kure Beach, N. C., a severe marine environment, showed a dramatic reduction in stain when the alloy deposits were plated in the recommended sequence. These tests showed conclusively that lower concentrations of iron near the outer or exposed surface of the deposit have a dramatic effect on stain reduction.

Further, corrosion tests conducted over a period of several years established that a nickel overlay on the alloy deposit can contribute in two significant ways to the durability of alloy coatings systems: (1) Thin nickel deposits can induce microporosity or microcracking in subsequent chromium depos-

TABLE 2—*Corrosion ratings of duplex nickel-iron coatings on static exposure in a marine environment—eleven months' static exposure at Kure Beach, N. C.*

Coating System	Thickness, μm	Rating
Preferred duplex system		
copper	15	
bright nickel-iron (19.7 to 22.8% Fe)	15	10/9
bright nickel-iron (8.7 to 10.6% Fe)	5	
nickel[a]	3	
microporous chromium	0.4	
Control		
Copper	15	10/6
Bright nickel-iron (8.7 to 10.6% Fe)	15	
Bright nickel-iron (19.7 to 22.8% Fe)	5	
Nickel[a]	3	
Microporous chromium	0.4	

[a] Nickel deposit contains microfine inorganic particles to induce microporosity in the subsequent chromium deposit.

TABLE 3—*Influence of nickel overlay on staining of bright nickel-iron coatings—nine months' static exposure at Kure Beach, N. C.*

Coating System	Deposit Thickness, μm
Copper	15
Bright nickel-iron (29%)	25
Nickel[a]	variable
Microporous chromium	0.25
Nickel overlay thickness	Appearance Rating
2 μm	4
5	6

[a] Nickel deposit contains microfine inorganic particles to induce microporosity in the subsequent chromium deposit.

its and; (2) a thin nickel coating plated on top of the alloy will further suppress the appearance of stain. The contribution of microporous or microcracked chromium in increasing durability is well known and accepted by the entire electroplating industry. The use of the thin nickel overlay, as a stain suppressant, is a more recent innovation. The beneficial effect of such a layer is illustrated in Table 3. The single layer of bright nickel iron had a 29 percent iron content, which exceeds our recommendation for severe exposure. Nevertheless, increasing the thickness of the overlay increased the appearance rating from four to six. When the thicker nickel overlay is combined with controlled iron content by the two-layered approach, the total improvement is significant as demonstrated in the mobile test results described in this paper. While a 1 to 2 μm nickel thickness is adequate to achieve microdiscontinuity in the subsequent chromium layer, a nickel thickness of 3 or 4 μm is more effective in suppressing potential corrosion stain from the alloy.

Finally, it has been established in both static and mobile testing that the use of copper as an undercoat to alloy deposits can contribute significantly to substrate protection. Indeed, due to the greater potential difference between copper and nickel-iron alloys [*1*], the contribution of copper to substrate protection is greater with the decorative alloy than with an all-nickel coating. A static exposure test at the Kure Beach marine test site showed an improvement in protection rating from 5 to 10, or the absence of basis metal corrosion, when copper was used as an undercoat to bright nickel iron–microporous chromium systems [*2*]. This substantial improvement was observed after 19 months of service. As with nickel coatings, copper is always most effective as an undercoat to the alloy deposit when used in conjunction with microporous chromium deposits.

Mobile Testing

Mobile tests have been conducted with many different plating systems to determine the influence of the nickel-iron alloy deposit. Some of these tests

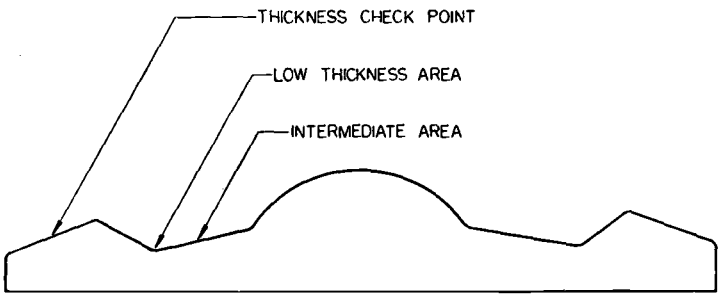

FIG. 1—*Hubcap cross section.*

have been conducted on steel hubcaps while others have been made on steel bumpers [*4*].

Over a period of years, hubcaps with a configuration shown in Fig. 1 have been used in mobile tests conducted in the Detroit, Mich. metropolitan area. Since Detroit is in the snow belt, the use of salt for deicing is quite extensive and the concentrated industrial development in this area results in high concentrations of sulfur dioxide. In essence, this is a very severe corrosion environment.

The test hubcaps have three distinct thickness levels of which two are far below recommended specifications for severe automotive exposure. Nonetheless, the test demonstrates the comparative performance of the nickel-iron alloy in a composite coating system with a typical all-nickel deposit which is currently used on automobiles. Table 4 details the thickness and type of deposit for each coating system at the checkpoint.

Figure 2 shows two typical hubcaps after one winter's exposure while Fig. 3 shows the same hubcaps after two years' exposure in Detroit [*4*]. Both the copper-nickel chromium coating and the copper-nickel iron-chromium deposits show similar failure in the low-thickness areas while both composite

TABLE 4—*Plated hubcap thickness levels.*

Rim (checkpoint) thickness	
copper	12 μm
nickel or nickel-iron	20 μm
Intermediate-thickness area	
copper	6 μm
nickel or nickel-iron	10 μm
Low-thickness area	
copper	4 μm
nickel or nickel-iron	6 μm

NOTES:
Chromium—microporous on all specimens.
Nickel deposit contains microfine inorganic particles to induce microporosity in the subsequent chromium deposit.

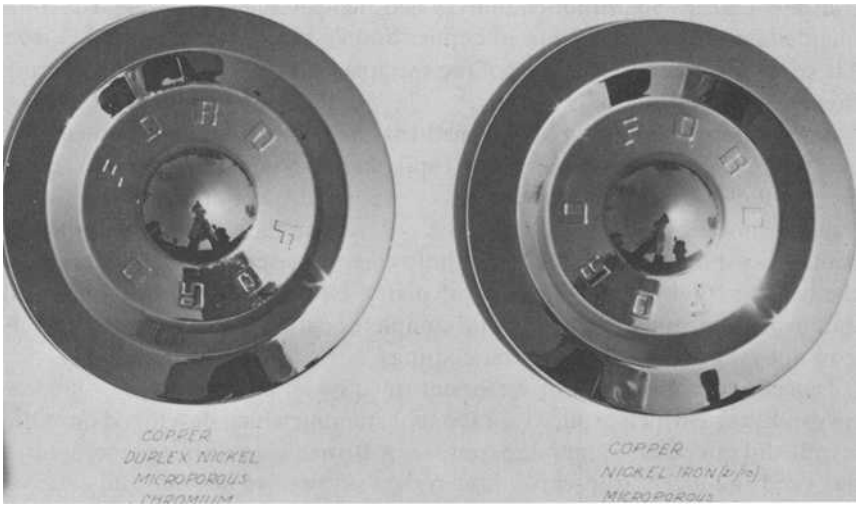

FIG. 2—*Typical hubcaps after one winter's mobile exposure in Detroit, Mich. The duplex nickel deposit was plated so that 60 percent of the total nickel deposit was sulfur-free semibright nickel with the remainder bright nickel. The duplex nickel-iron deposit had a 21 percent iron content in the lower layer and a 10 percent iron content in the outer or final layer. The lower layer comprised 70 percent of the total alloy deposit.*

FIG. 3—*Typical hubcaps after two winters' mobile exposure in Detroit, Mich.*

coatings performed without failure when deposit thickness was at recommended levels, that is, 12 μm of copper and 20 μm of nickel or nickel-iron These results are representative of the specimens exposed on four cars during the two-year test period.

These mobile test results confirmed that a decorative nickel-iron coating can perform quite satisfactorily in a total plating system that meets the criteria previously described for very severe exposure. It is important to observe that no staining developed during the two-year mobile testing even though routine washing of the car was the only cleaning used during the period of the test. Further extensive testing of plated bumpers in Detroit confirmed that protection and appearance of a complete coating which included nickel-iron alloy was equal to all-nickel coatings.

Indeed, our mobile results were confirmed by an independent test laboratory in Europe which explicitly noted that staining which developed on static testing did not occur in mobile exposure. A British automotive manufacturer has used the nickel iron-chromium system on regular interior and exterior production parts since 1977 with corrosion performance comparable to the nickel-chromium system previously used. While these results cannot be directly compared with U. S. exposure conditions, it should be noted that no problems with staining have been reported during the three years of service.

Summary

In summary, the protection of the substrate and the elimination or suppression of stain from the nickel-iron alloy can be accomplished provided the total coating system is designed for severe exposure conditions. A multiple coating system is recommended for the use of nickel-iron coatings only, as it is for nickel, when severe exposure applications are present.

An important conclusion of our work, which included static and mobile testing over a period of five years, is that static test results cannot be relied upon to predict actual service results. Further, simple bright nickel, iron–chromium deposits have been serving very satisfactorily in mildly corrosive applications for many years without any notable corrosion problems and as a completely acceptable alternative to bright nickel-chromium coatings.

References

[1] Clauss, R. J. and Tremmel, R. A., *Plating,* Vol. 60, 1973, pp. 803.
[2] Clauss, R. J., Tremmel, R. A., and Klein, R. W., *Transactions,* Institute of Metal Finishing, Vol. 53, 1975, p. 22.
[3] DiBori, G. A., Hawks, G., and Baker, E. A., this publication, pp. 186–213.
[4] Clauss, R. J. and Tremmel, R. A. in *Proceedings,* 9th World Congress on Metal Finishing, Interfinish, 1976.
[5] U. S. Patent 3,812,566, Patent Office, Washington, D. C.

DISCUSSION

S. K. Coburn[1] (*written discussion*)—Is the salt level applied to the streets of Detroit in the vicinity of 100 000 tons per year? Where do these figures come from?

R. J. Clauss (*author's closure*)—Information on the use of de-icing salt is furnished by the Department of Public Works of the City of Detroit. The amount cited is considered to be representative of an average winter. During a severe winter, usage of salt will exceed 100 000 tons.

J. P. Lyle[2] (*written discussion*)—What were the exposure times for the wheel covers and bumpers? What do you predict they will look like after ten years' exposure?

R. J. Clauss (*author's closure*)—The exposure of the wheel covers and bumpers varied from one to three winters on cars driven in the metropolitan Detroit area. I believe their performance will be at least comparable to all nickel coatings of equal thickness after an equivalent length of service in the same locality. Prediction of appearance after ten years is virtually impossible for any coating system since factors such as service location and owner maintenance have an overwhelming influence on performance.

[1] U. S. Steel Corp., Pittsburgh, Pa.
[2] Alcoa Corp., Alcoa Center, Pa.

Modeling, Characterization, and Correlations

D. Knotková-Čermáková[1] *and K. Bartoň*[1]

Corrosion Aggressivity of Atmospheres (Derivation and Classification)

REFERENCE: Knotková-Čermáková, D. and Bartoň, K., **"Corrosion Aggressivity of Atmospheres (Derivation and Classification),"** *Atmospheric Corrosion of Metals, ASTM STP 767,* S. W. Dean, Jr., and E. C. Rhea, Eds., American Society for Testing and Materials, 1982, pp. 225–249.

ABSTRACT: Corrosivity classification of the atmosphere is important for selecting optimal protective systems. This classification should be based on an understanding of the corrosion process together with reasonable engineering principles. By a critical analysis of the factors providing limits to the classification problem, several heretofore unresolved questions have been answered. These questions involve design factors, effects of different types of sheltering, fabrication effects, and the transformation of measured values to information which can be utilized technically. The Czechoslovakian system of standards covering this field is described and complemented by examples of specialized specifications for different industries. Questions for further research are proposed in order to further the classification efforts.

KEY WORDS: atmospheric corrosion, corrosivity classification, protective systems, steel

A large number of products and devices are used in the atmosphere and, as a result of the action of weather, deterioration occurs continually. For example, atmospheric corrosion causes the majority of the recorded economic losses attributed to corrosion. It is necessary to provide protection against atmospheric corrosion for many products so that the service life of these products, as measured by their appearance and reliability, is adequate.

The atmosphere is a very complex environment because it varies both with time and location. The real conditions which exist at the surface of a product or device result from the mutual action of natural and man-made components of the atmosphere together with the effects of material, design, and operation of the product or device. The interaction of these various factors is diagrammed schematically in Fig. 1.

It is desirable to characterize the atmosphere with regard to its corrosivity

[1] G. V. Akimov State Research Institute of Material Protection, Prague, Czechoslovakia (SVÚOM).

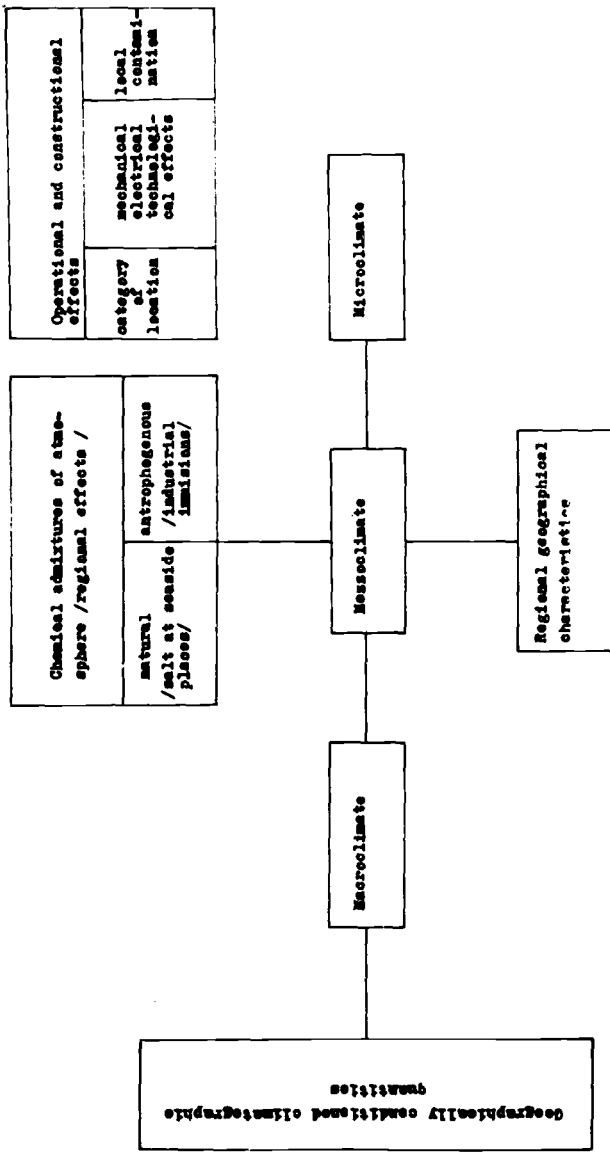

FIG. 1—*Interaction of factors affecting the atmosphere.*

so that a classification system may be developed. This approach is valuable to engineers and designers selecting systems for providing corrosion protection as well as to those concerned with the performance of products and devices exposed to the atmosphere. The term "corrosivity" (corrosion aggressivity) refers to the extent of degradation of the material, system, or product by the atmospheric environment. Corrosivity is evaluated by the influence of the various components of the atmosphere on the kinetics of the reactions causing damage. Therefore, it follows that the corrosivity of the atmosphere cannot be specified in general, but only for specific types of materials and protective systems. Thus, the description of the damaging properties of the atmosphere must contain those parameters and their combinations which have an important effect on the kinetics of corrosion of the material in question.

In order to develop a standard procedure for estimating the corrosivity of the atmosphere, it is necessary to have a suitable basis. Various methods of classifying the corrosivity of the atmosphere have been proposed. These methods treat the effects of the atmosphere in a generalized manner. However, the severity of a service exposure must be determined from knowledge of the actual conditions which the product sees. This paper presents a contribution to the effects to classify the corrosivity of the atmospheric environment by generalizing the effects of various components of the atmosphere. The goal of this work is to provide a technical basis to assist engineers both in assessing the life-time of products in the atmosphere and in determining the need for protective measures. Different possibilities for characterizing and classifying the corrosivity of atmospheres are presented.

Many years of research on atmospheric corrosion have provided a basis for characterizing and classifying the corrosivity of the atmospheres [*1–6*].[2] An understanding of the physical and chemical processes which occur during atmospheric corrosion has helped in formulating a kinetic model. A kinetic model, however, applies only to isolated periods of process. Figure 2 describes the results of laboratory experimental research on the influence of the degree of surface uptake of sulfur dioxide (SO_2), amount of water on the surface and temperature on the corrosion rate during periods of wetness [*22*]. Atmospheric corrosion is a discontinuous process and the frequency of active periods, their duration, and kinetics are controlled by the stochastically changing properties of the environment [*7–11*]. Therefore, the use of kinetic models based on chemical principles for describing the long-term process is rather limited. However, the results of empirical tests in atmospheres of varying severity can be utilized in the development of a mathematical model [*12–16*]. The classification of corrosivity for normal materials of construction should be based on theoretical knowledge, but it also should employ easily attainable parameters for describing the corrosivity.

[2] The italic numbers in brackets refer to the list of references appended to this paper.

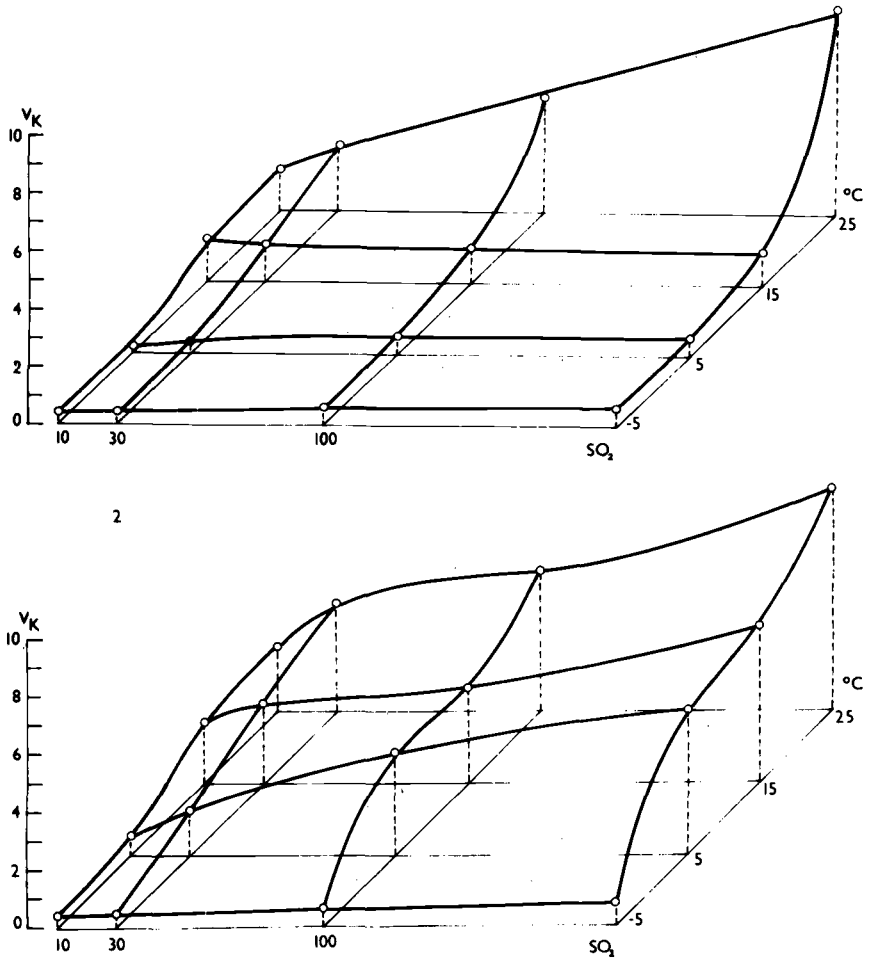

FIG. 2—*Dependence of steel corrosion rate* ($\mu g \cdot cm^{-2} \cdot h^{-1}$) *on* SO_2 *uptake* (10,30,100,200 mg · $m^{-2} \cdot d^{-1}$) *and temperature* (*−50°C, 5°C, 15°C, 25°C*) *at different relative humidities* (*1: 75 percent, 2: 85 percent, 3: 95 percent, 4: 100 percent, 5: 100 percent with about 200-μm-thick surface electrolyte layer*).

In order to meet these objectives, we have considered a system where the corrosivity of the atmosphere can be characterized by readily measured meteorological parameters and chemical components of the atmosphere. In this way, with the help of quantitative data, it is possible to define pertinent classes of corrosivity. A standard which classifies corrosivity should be as general as possible. One approach is to determine the effects of the conditions according to their occurrence, that is, according to characteristic properties of strictly defined types of atmospheres. The classification based on the relation of conditions to the kinetics of particular corrosion processes is

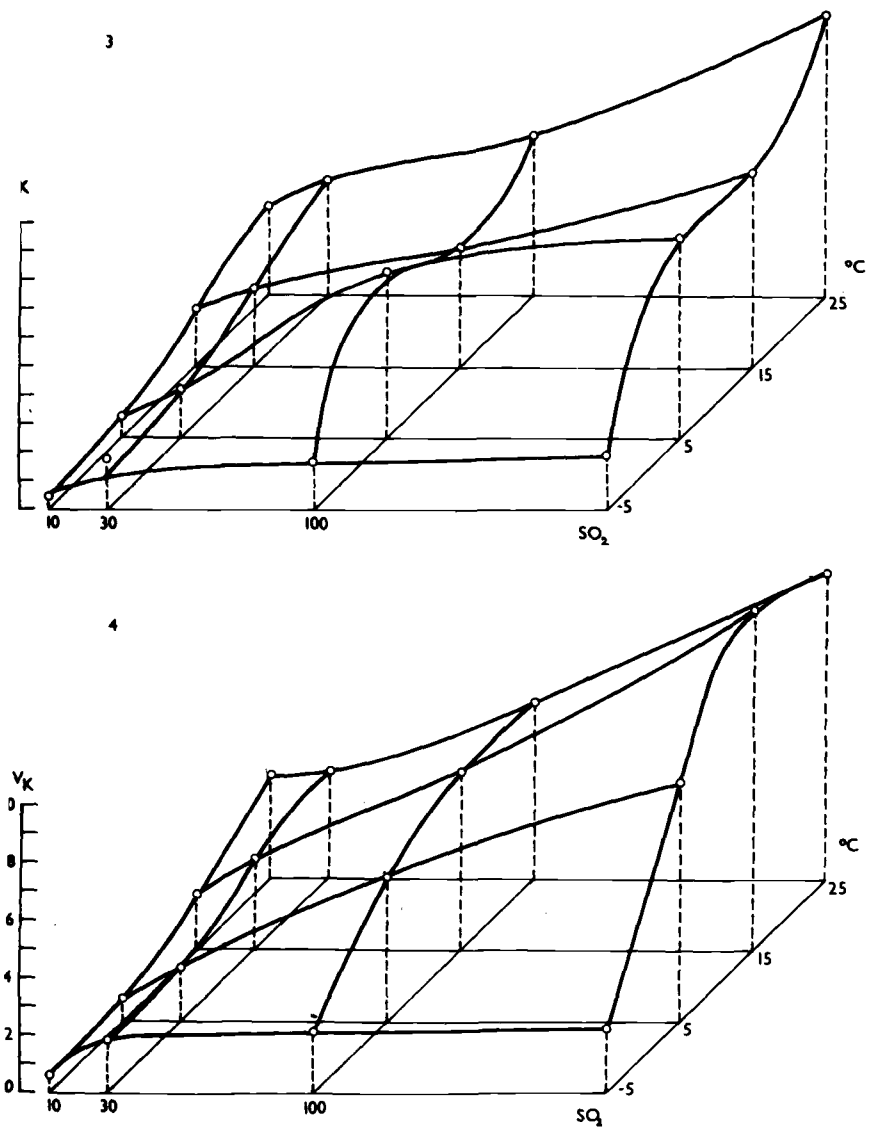

FIG. 2—*Continued.*

more complicated, but it is also more accurate, at least in theory. A combination of both approaches was used for developing the Commission for Mutual Economic Aid (CMEA) as well as the Czechoslovakian State Standard.

The quantitative characterization of service conditions should be based on data measured and published by the official meteorological and air pollution

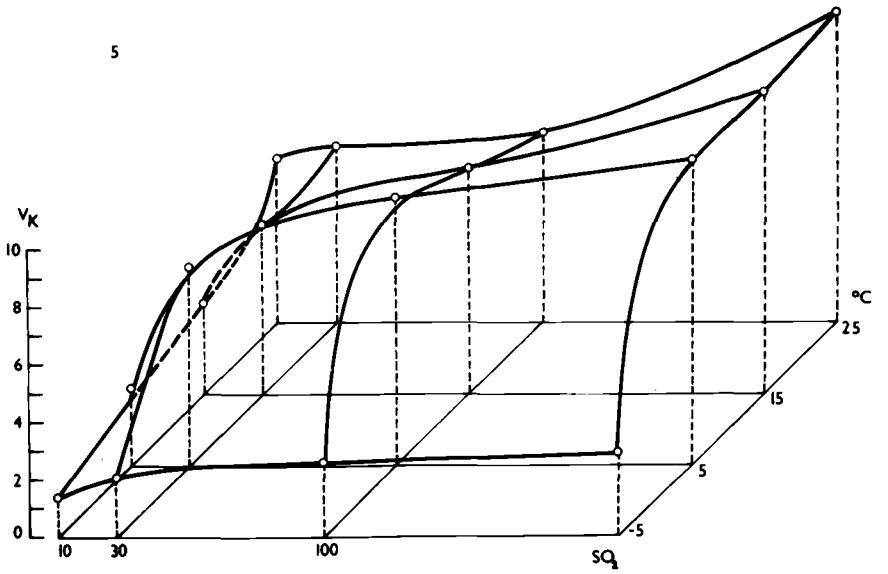

FIG. 2—*Continued.*

service. However, these published data are applicable only to outdoor atmospheric environments. It is obvious that corrosivity estimates should be applicable to all types of service conditions which structures and devices are subject to. Many products are used in sheltered spaces or in hidden areas in buildings, vessels, packages, etc. In these cases, it is desirable to characterize the environment by means of direct measurements of a decisive factor or an indication of the occurrence of a situation critical for the occurrence of corrosion. Another approach is to use a short-term test and extrapolate the results according to generally accepted procedures based on knowledge of the atmospheric corrosion of metals. Short-term measurements of corrosion as well as longer-term measurements are particularly important when the conditions for corrosion of the materials employed are specifically affected by the type of service.

Classification by its nature assumes a generalization of the results. A critical analysis of the results and the generalizations involved, based on the theory of atmospheric corrosion, leads to a number of limitations on the generalization and problems in its use. There is a significant difference in our understanding between corrosion in a boldly exposed configuration as opposed to what occurs in shielded areas. The limitations here follow because it is not possible to generalize the effects of configuration as well as the effects of operation and manufacture. The effects of extreme degrees of atmospheric pollution and specific pollutants also create problems. An additional limitation is caused by nonuniform corrosion due to specific factors of the design etc.

Our attempts to characterize the actual atmospheric environment with respect to its corrosivity and then to develop a standard classification system forced us to develop some experimental results on the question of the limitations. We have assumed that atmospheric corrosion is a discontinuous process in these environments. The corrosion rate depends both upon the properties of the metal surface, either bare or with a layer of corrosion products, and upon the properties and duration of the existence of the surface electrolyte. Our previous work [*17*] was based on the assumption that the surface corroded when it was wet and wetness occurred when the relative humidity of the atmosphere exceeded 80 percent and the temperature was above 0°C. This model is significantly poorer in predicting corrosion in sheltered and indoor microclimates than in the open air. Thus, for these categories of location, it is necessary to develop better techniques of estimating the time of wetness and also of following systematic differences in the levels of pollution which occur due to the accumulation of materials on unwashed surfaces.

Using systematic experiments, we have followed a wide group of climatic and atmospheric component variables in strictly defined types of atmosphere for all three categories of location (boldly exposed outdoor, sheltered outdoor, and interior, such as warehouse or vessel). At the same time, we have measured directly the frequency and duration of surface wetting, and followed the corrosion process as related to certain physical characteristics of the corroding body (temperature and mass).

Examples

Some of the results of this study [*18*] which have not been completely analyzed are presented in Table 1. The mean value of the measurements on four plain carbon steel specimens is presented. The specimens were prepared for

TABLE 1—*Mass losses of plain carbon steel for different categories of location at one locality.*

Location Category	Exposure Time, Months	Weight Loss (g/m^2) for the Mass of the Specimen		
		0.2 kg	2 kg	20 kg
Outdoor atmosphere	1	25.3	. . .	. . .
	3	93.4	192.3	172.8
	6	252.6	303.2	262.2
	12	448.8	488.5	452.8
Shed	1	3.2	. . .	10.0
	3	36.3	35.0	53.6
	6	72.3	75.6	103.6
	12	149.4	153.0	186.5
Store	1	few rust points		
	3	numerous rust points		
	6	points and areas of rust 1.5		
	12	2.7	2.6	3.5

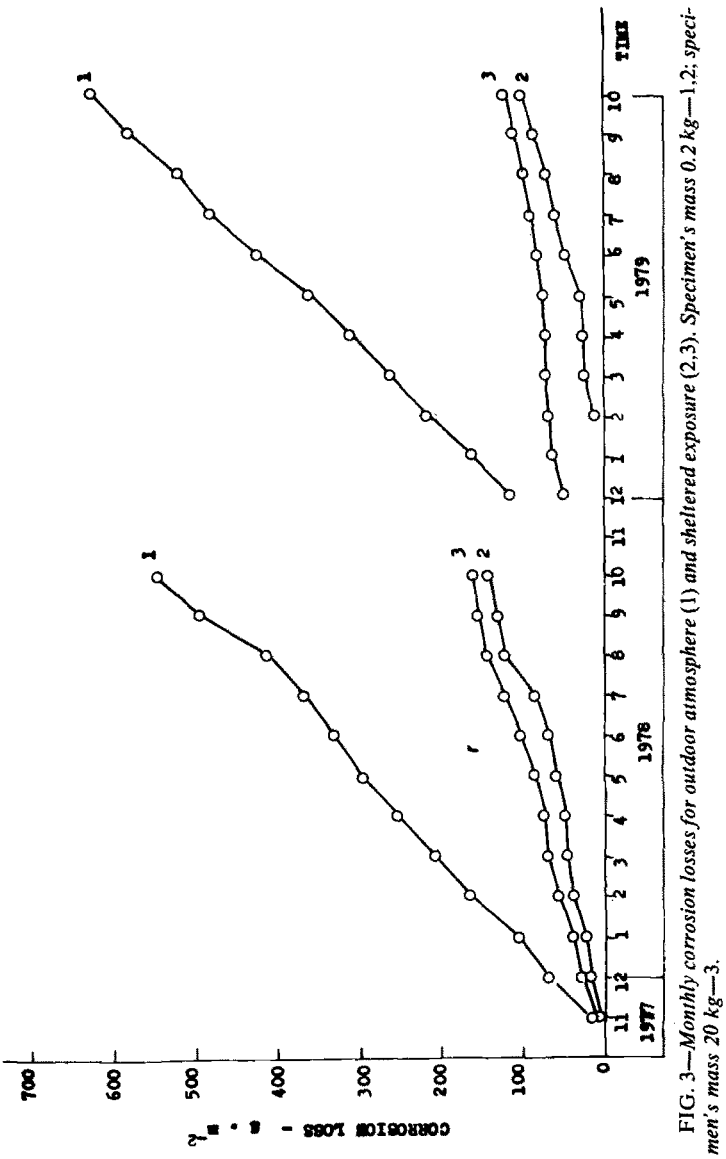

FIG. 3—*Monthly corrosion losses for outdoor atmosphere* (1) *and sheltered exposure* (2,3). *Specimen's mass 0.2 kg*—1,2; *specimen's mass 20 kg*—3.

ABLE 2—*Temperature-humidity characteristics summarized with respect to sampling intervals.*

Sampling After Month	Summarized Time of Wetness					
	I			II		
	OA	S	ST	OA	S	ST
3	140	384	135	48	80	4
6	354	720	304	138	175	4
12	1233	1814	725	489	438	11

NOTE:
OA = outdoor atmosphere.
S = shed.
ST = store.
I = for relative humidity $\geq 80\%$ at $t > 0°C$.
II = for relative humidity $\geq 90\%$ at $t > 0°C$.
The table contains numbers derived from thermohygrograph records as readings in 2-h intervals frequency.

exposure by a fine sandblast. In the case of the larger mass exposures, the specimens were fastened to steel cylinders. Monthly corrosion losses are shown in Fig. 3 for the outdoor and sheltered exposures only because in the interior "store" location there were only local points of corrosion after one month of exposure. Table 2 gives the temperature and humidity variations which occurred at all three testing sites. Plots of the SO_2 levels are shown in Fig. 4. An index of aggressivity calculated as the product of the humidity and

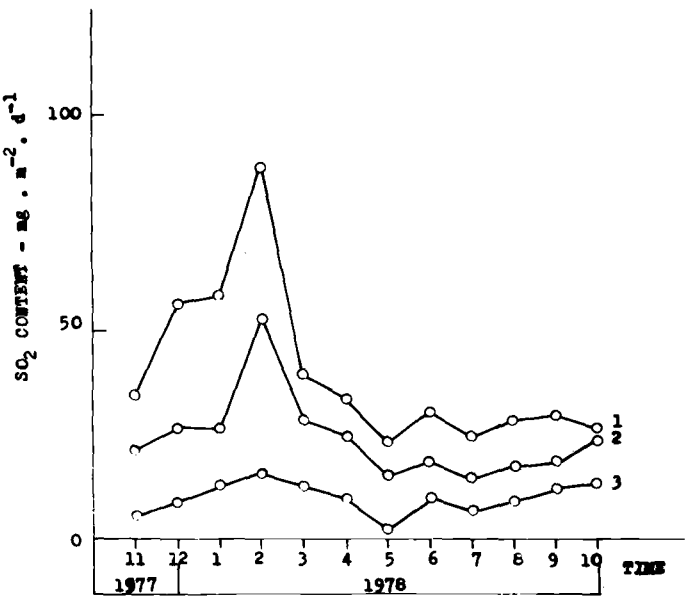

FIG. 4—*Pollution with* SO_2 ($mg \cdot m^{-2} \cdot d^{-1}$) *for outdoor* (1), *sheltered* (2) *and indoor* (3) *exposure.*

moistening data and SO_2 level is plotted in Fig. 5. The aggressivity index is based on the time-of-wetness defined either by direct measurement using the Czechoslovak detecting system [*23*] or by the number of hours when the relative humidity exceeds 80 percent and the temperature is above 0°C as taken from both temperature and humidity records. These results clearly show that it is necessary to study in more detail the mechanism and kinetics of the corrosion of metals in sheltered and partially sheltered locations.

The diverse corrosion effects caused by design factors etc., together with different possibilities of numerical corrosivity definitions, show that the general term "corrosivity" even if it is quantitatively defined has to be transformed for the use for specific product-classes. This is particularly important regarding structures and devices because the service lives of such products are always determined by the effect of the corrosive attack on the function of the product. If the effects of operation, for example, specific type of contamination, and heating are disregarded, there are still design features which create different conditions of wetting and also for the stimulation of the corrosion process. This is demonstrated by some data measured on large and articulated surfaces of a steel facade building wall. The facade walls are constructed of formed sheets of low-alloy steel of the Cor-Ten type. Wetness was measured with a Czechoslovakian measuring system employing inert conductivity detectors [*23*]. Our results are given in Table 3.

Significant differences in times-of-wetness were found between the bottom and top of the same 12-m-high facade wall. Even larger differences were observed in the time-of-wetness between the outside and inside surfaces of the sheet and also in the vicinity of structural elements which tend to retain debris, particularly rust falling off the wall. This is shown in Table 4.

These results demonstrate that it is possible to derive the aggressivity for a standard corroding surface or possibly for a simple product. For more complicated cases, however, even in the usual types of atmosphere, it is necessary to have specific experience or experimental data on the behavior of materials in the type of location where it is used. We assume that, in the future, empirical relations will be formulated for this purpose.

Microclimates which have specific or extreme effects due to the service conditons represent a special group of atmospheric environments. To get a better picture of these conditions, we carried out a 7-year testing program in 40 different microclimates of the textile, metallurgical, and chemical production industries. The data on the temperature and humidity were processed by a digital computer and arranged in classes according to the mean values, extremes, and depression of the dew point. These results, together with the extent of corrosion of steel, zinc, aluminum, and copper alloys, indicate clearly the specific character of the corrosivity of these microclimates compared with the general atmosphere. A partial listing of these results is presented in Table 5. Since these environments cannot be classified into a general system, we have proposed [*19*] a procedure for rapid experimental determination of the corrosivity of microclimates.

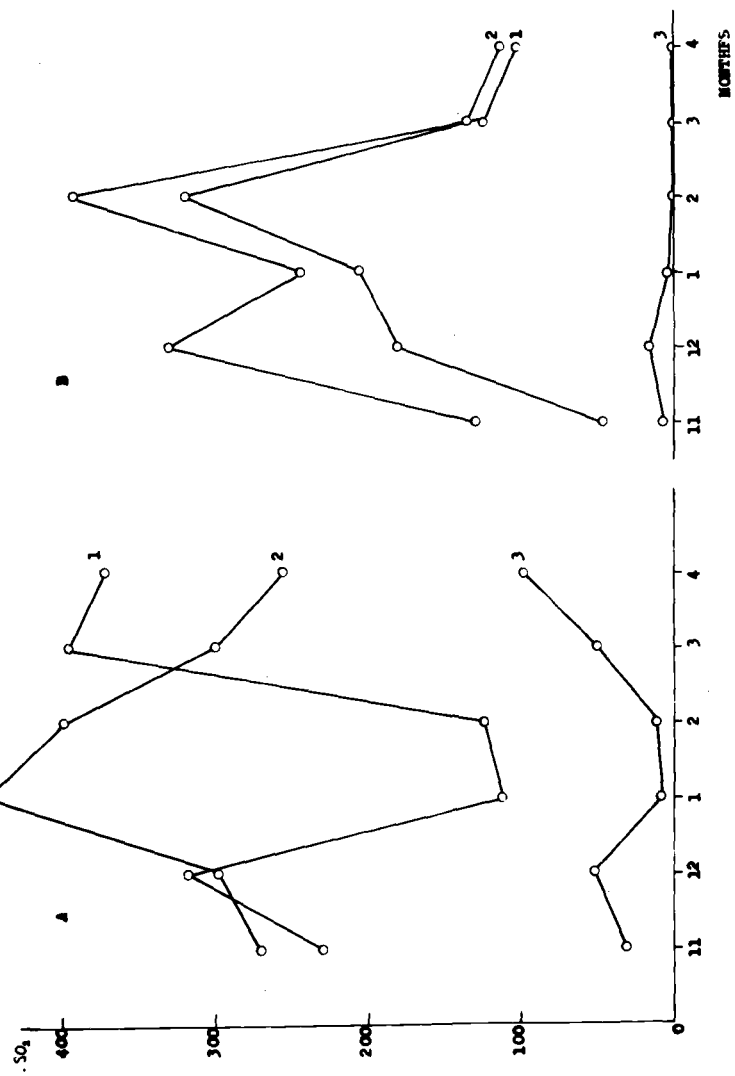

FIG. 5—*Indices of aggressivity (product of time of wetness and pollution with SO_2). A: τ measured directly by detecting system; B: τ derived from thermohygrographic records ($\sum$ h relative humidity $\geq$ 80 percent at $t > 0$°C). 1—outdoor atmosphere; 2—shed; 3—store.*

TABLE 3—*Moistening of the facade steel surface (orientation effect).*

Site Measured		Months (Beginning with January)										
		1	2	3	4	5	6	7	8	9	10	11
Reference specimen[a]	τ (h)	318	127	212.5	274	120	164	191.5	110.5	176	227.5	192
	[c]	5	9	12.5	45	30	37	63	36	24	13	14
	[b] days	17	13	18	30	31	30	28	31	17	23	16
Top outer side of mantle of building—south	τ (h)	245	96	67.5	127	45.5	21.5	105	136.5	153	209.5	158
	[c]	16	5	9	16	6	6	14	18.5	16	13	5.5
	[b] days	17	13	18	30	31	30	28	31	17	23	16
Top outer side of mantle of building—north	τ (h)	361	238	422	720	744	720	672	744	408	552	384
	[c]	9	5					not recorded				
	[b] days	17	13	18	30	31	30	28	31	17	23	16

[a] Reference specimen is situated at the terrace on usual stand (45 deg, south) for atmospheric tests at the same height as the other detectors.
[b] Number of days in the month for which the measurement is performed.
[c] Frequency of wetting periods.

TABLE 4—*Wetting of the steel surface of the facade (effect of the design arrangement).*

Period / Levels		Internal Area of the Facade Non-affected by Structural Arrangements Height, 2 m		Internal Area of the Facade at the Structural Element Height, 1 m		Internal Area 10 cm Above Bottom Edge (Effect of the Rust Fallout)		External Area of the Facade at a Height of 12 m	
		h	% of Total Time	h	% of Total Time	h	% of Total Time	h	% of Total Time
December 1975									
Level	*a*	323	43	466.5	62	525	70	481	64
Level	*b*	262.5	35.2	384.5	51.5	438	58.8	413	55.7
Level	*c*	165.5	22.2	207	27.8	248	33.3	286	38.7
Frequency	*n*	9		15		12		15	
January 1976									
Level	*a*	462.5	62	446	60	663	89	inlets	
Level	*b*	272	36.5	263	35.3	463	62	damaged	
Level	*c*	242	32	241	32	312	42	by wind	
Frequency	*n*	35		35		16			

NOTE: Level *a*—detection in a range of 0.01 to 0.25 V—includes the period of starting and drying; Level *b*—detection above 0.25 V; Level *c*—presence of liquid phase on the indicator surface; Frequency *n*—recorded according to the level *c*.

TABLE 5—*Corrosion in the microclimates with specific effects.*

Name of Locality	Contamination (mg/m^2 d)			Corrosion (g/m^2) in Three Years			
	SO_2	Cl	Others	Steel	Zinc	Copper	Aluminum
Store of acids	86.9	141	NO_x, HCl	1269	729	397	396
Store of salt	23.1	346	fallout	1081	1052	171	69
Chlorine liquefying	30.3	578.1	NaCl	3467	772	1762	478
Ammonia synthesis	25.7	39.7	NH_3	1058	154	85	45
Electrolysis	11.0	314		1585	68	. . .	188
Pickling Plant I	84.1	116.4		635	215	148	105
Pickling Plant II	136.0	3.9		236	25	9	5.6
Drawing plant	135.2	5.3		15	2	22	increment
Carding room	6.7	4.4	different	0.3	0.9	0.26	increment
Dyehouse	18.8	4.6	compounds	891	49	33	13

Classification Systems of Present Standards and Possibilities for Improving Their Quality

Various formulations of the corrosivity of the atmosphere which have narrower or broader validity and with different characteristics have been given in standards, for example, UNI 3564-65 PN-71/H-04651, GOST 9.039-74, and TGL 18704. At this time, one standard, ST SEV 991-78, "Corrosion of Metals, Classification of the Corrosion Aggressivity of Atmospheres," may be used to classify the corrosivity. This standard is unique because it includes levels of contamination from industrial activity above the basic natural atmospheres contaminated with SO_2 and sodium chloride occurring in various regions. In writing this standard, we considered knowledge about the effect of contamination with SO_2 or sodium chloride on the kinetics and mechanism of atmospheric corrosion when choosing the limits of the classes. An analysis of the levels and frequency of occurrence of these contaminants based on data published for the world was also used. The result is a standardized characterization of atmospheres of the industrial type, that is, contaminated with SO_2, atmospheres typical of shoreline and marine applications, that is, containing sodium chloride, and mixed types.

In the Czechoslovakian system of standards (see Fig. 6) the first step is to obtain the "climatic resistance" effect. This term expresses the ability of a product to operate under climatic conditions different from "normal," for example, in moist or dry tropical climates, or in arctic climates. The Czechoslovakian standard, CSN 03 8206+/ST SEV 458-77, "Dividing the Earth's Surface into Climatic Regions for Technical Purposes," is the basis for this step. This standard defines the values of the climatic effects of temperature and humidity. It divides the world into regions as follows:

Very cold	EF
Cold	F

Moderate	N
Tropic moist	TH
Tropic dry	TA
Moderately cold sea	H
Tropic sea	MT

The next step for obtaining a more precise prediction of the effects of climate on materials is concerned with the location of the surface and the contamination of the atmosphere. The method is described in CSN 03 8805[+]/ST SEV 460-77, "Types of the Climatic Performance of Products." Four types of location are described:

1. Boldly exposed in the atmosphere.
2. Under shed with limited exposure to precipitation and sun radiation.
3. In enclosed spaces, but with ventilation and without artificial control of climatic conditions.
4. In enclosed spaces with artificial control of climatic conditions.

This document also introduces the term "type of atmosphere," which is determined by the presence of gaseous, liquid, and solid components which have a deteriorating effect on materials. The types of atmosphere vary from clean environments to urban and industrial atmospheres, marine atmospheres, and combinations of industrial and marine. Data on the overall climatic region of service, together with the type of location and type of atmosphere, are combined to give the rating of "type of climatic performance" with relevant remarks. For example, a TH 34 rating refers to a tropical moist

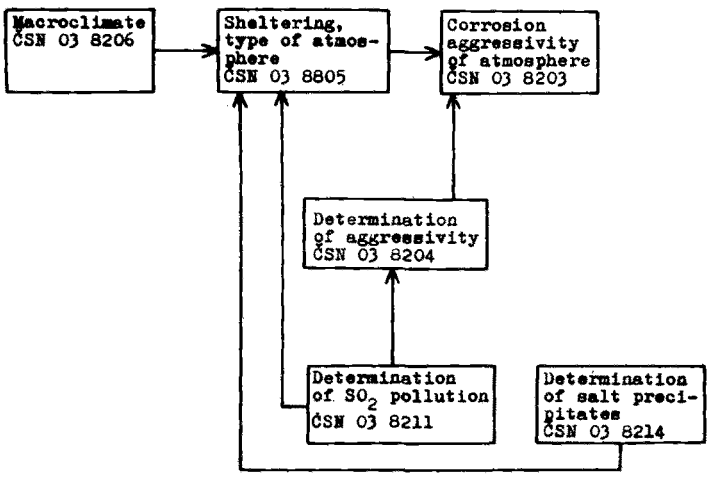

FIG. 6—*Relations of Czechoslovak standards deriving the corrosivity of atmospheres.*

climate with exposure in a non-air-conditioned building in an area adjacent to the sea.

More specific information is provided in the document CSN 03 8203+/ST SEV 991-78, "Classification of the Corrosion Aggressivity of the Atmosphere." This standard identifies five degrees of corrosivity of the atmosphere, based on the corrosion rates of engineering metals in atmospheres with various levels of contamination and in different locations. Another Czechoslovakian standard, CN S 03 8204, "Determination of the Corrosion Aggressivity of Atmospheres for Metals and Metallic Coatings," presents two experimental and one empirical calculational method for determining the corrosivity of atmospheres. The experimental methods are based on exposure tests.

The first method is a classic long-term exposure with periodic removals of steel specimens. The second method is a simplified approach based on the empirical relationship between the initial corrosion rate and its long-term course. Twelve data values on sequential one-month mass loss measurements of steel specimens are summed to give a total mass loss for the interval and then these sums are treated using a linear regression analysis to obtain a least-squares best-fit line for loss of mass with time. The slope of this regression line is designated as the initial corrosion rate: This initial corrosion rate is converted to a steady-state rate of corrosion by multiplying it by an empirical constant. This steady-state rate of corrosion then serves as the criterion for classifying the environment with regard to its corrosivity. This method assumes the stochastic nature of the corrosion process with the corrosion rate being determined by the time-of-wetness and the amount of atmospheric pollution. This standard also gives procedures for treating the relevant climatic and atmospheric analysis data.

It is apparent that these different approaches to measuring and treating data give different results. There are also different ways of using these classifications. However, the corrosion processes which occur in atmospheric exposures are a result of the interaction of condensed moisture on the corroding surface with certain types of pollutants in the atmosphere.

When considering the corrosive action of the atmosphere with regard to various factors including contamination effects, the following areas need more thorough investigation.

1. Effect of the category of location of the surface in question with respect to the effect of climate and contamination.
2. Measurement of both gaseous and solid contaminants, including aerosols in the atmosphere, both in terms of methods of measurements and the applicability of these results in the field of corrosion.
3. More detailed knowledge on the applicability of different systems for measuring the time-of-wetness or of directly measuring the corrosivity.
4. More results of studies on the corrosion behavior of metals and metals

with protective coatings in different types of atmospheres where there have been significant changes in the corrosivity of the atmosphere with time.

5. Studies of the possibility of using the results of corrosion experiments with standard specimens together with simple calculational models for estimating the corrosivity of the atmosphere.

Some examples of research which offers more information on these subjects have already been described. The following example is provided to show how standard meteorological data can be used to develop a corrosivity classification.

The character of the variation of temperature and humidity for the territory of Czechoslovakia (C.S.S.R.) was obtained by a statistical treatment of a 25-year series of hourly values of temperature and relative humidity for 11 representative meteorological stations during the period from 1949 to 1973. In choosing the stations, an effort was made to obtain coverage both in elevation and geographic location within the country. Based on these data, the time-of-wetness was calculated using the previously mentioned criteria and the results of these calculations are given in Table 6. These results then serve as a basis for a standardized approach for the effect of temperature and humidity on atmospheric corrosion in Czechoslovakia [*20*].

The use of the parameters, time of wetness, τ, and contamination, x, to describe the corrosivity of an atmosphere for use by engineers or designers is often limited by the availability of the data. It is not always possible to obtain direct measurements of the time-of-wetness by means of electrochemical or other detectors, or to have measurements of the contamination present by the adsorption method. Meteorological data, however, are more generally available, that is, data on humidity and temperature as well as results of continuous or periodic measurements of the environmental contamination. It is possible to convert these values to the parameters used to characterize atmospheric corrosivity with sufficient accuracy [*21*] for our purposes. In this study we have defined time-of-wetness as the time when the relative humidity is equal to or greater than 80 percent at temperatures above 0°C. This is an empirical definition of time-of-wetness, but it is supported by laboratory studies [*24*] which show that the corrosion rate is negligible when either the temperature or relative humidity is below these limits. If a sufficient quantity of temperature and humidity data is available, the time-of-wetness may be calculated easily with the aid of a digital computer.

Even average monthly relative humidity values and temperatures can be converted to the values of τ with sufficient precision based on the calculations performed on the data for a number of C.S.S.R. localities. Analyses of these data has lead to the empirical relationship:

$$\frac{\tau}{H} = A_1 T + A_2 T^2 + A_3 T^3 \qquad (1)$$

TABLE 6—*Number of hours with relative humidity of the air equal to or larger than 80% at the temperature above 0°C in months.*

City	Month (Beginning with January)												R/year[a]
	I	II	III	IV	V	VI	VII	VIII	IX	X	XI	XII	
Prague	162.8	209.8	230.8	259.0	305.2	292.8	301.1	316.4	371.0	456.4	433.1	267.2	3605.7
České Budějovice	133.3	175.0	229.4	273.6	331.3	344.3	347.9	380.3	412.7	448.0	411.4	222.9	3710.0
Liberec	164.1	214.4	224.0	303.8	360.6	347.3	378.1	390.0	423.2	461.0	435.2	271.7	3973.2
Hradec Králové	204.1	242.0	239.2	268.3	312.6	310.3	342.5	350.4	387.8	449.2	451.1	320.1	3877.7
Brno	171.2	220.2	211.6	216.6	257.1	273.3	296.0	302.1	334.1	408.4	428.2	268.0	3386.7
Červená	211.2	238.4	237.6	241.3	288.4	301.2	309.3	322.1	343.4	402.5	444.8	328.5	3668.8
Hurbanovo	148.0	187.4	239.6	276.0	338.3	346.2	358.4	388.5	416.4	434.2	423.0	256.2	3812.1
Sliač	140.0	205.4	229.5	228.9	258.5	284.5	292.4	318.4	362.3	420.7	439.2	258.7	3438.5
Poprad	65.1	114.1	170.6	273.2	322.9	324.2	333.5	328.6	392.6	463.3	380.6	148.1	3316.9
Košice	83.0	110.0	154.8	260.1	326.9	348.8	357.4	375.0	370.6	344.5	314.8	156.9	3202.9

[a] Hours with indicated humidity and temperature per year.

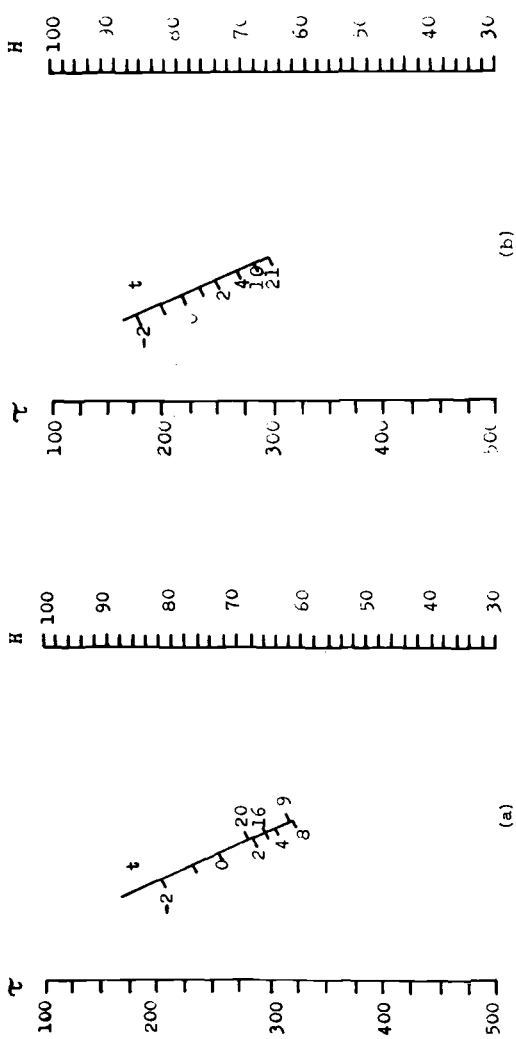

FIG. 7—*Nomographs for the estimation of probable monthly hours of surface wetting* (τ) *from mean monthly temperature* (t) *and relative humidity* (h): (a) *January–July;* (b) *August–December.*

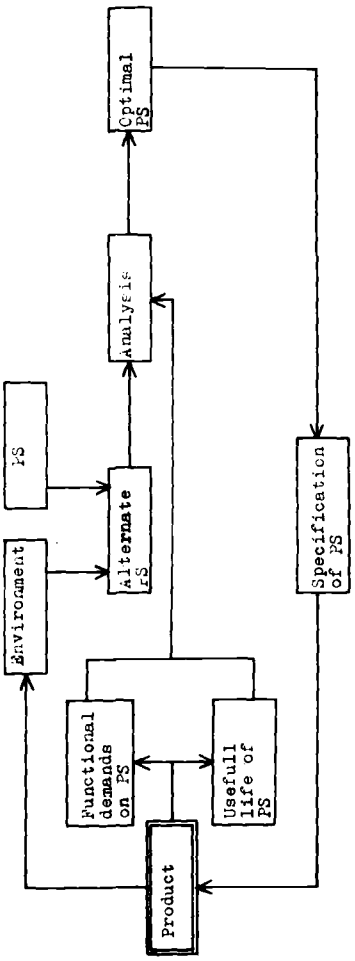

FIG. 8—*Schematic description of deriving rational protective systems (PS).*

where

τ = monthly time of wetness, h,
H = mean relative humidity computed for the month, %, and
T = mean temperature for the month, °C.

Nomagraphs for solution of this equation are given in Fig. 7.

It is apparent that the relationship between τ, H, and T is valid only for a limited geographical region and, thus, the estimate of the time-of-wetness shown in Fig. 7 (*a* and *b*) is limited to the outdoor atmosphere in Czechoslovakia.

It is also possible to derive an empirical relationship between the average sulfur dioxide content of the atmosphere expressed as mg m^{-3} and the data on accumulated adsorption on an alkaline surface expressed, for example, in mg $m^{-2}d^{-1}$ [ST SEV 991-78 "Corrosion of Metals, Classification of the Corrosivity of Atmospheres"].

Application of Corrosivity Classification

The main purpose of a corrosivity classification system is to permit the selection of an economically optimum corrosion protection system on structures and devices used in the atmosphere. The system of selecting optimal corrosion protection measures is outlined in general terms in the block diagram shown in Fig. 8. The classification of the atmospheric corrosivity carried out for the most general level is only of limited value as an input for a specific case. The classification of the atmospheric corrosivity into five degrees is the starting point for determining the quality requirements for the protective system which will be employed.

Several subdivisions of the corrosivity classification have been developed for Czechoslovakia. These subdivisions are important as part of specifica-

TABLE 7—*Definition of the degrees of the corrosion aggressivity of the atmosphere in the car industry.*

Degree of the Aggressivity	Characteristics
3	surfaces of parts for prevalent time of the operation and storage of cars quite separated from the outdoor atmosphere
4	surfaces of a part exposed to the direct action of the atmosphere (or covered only against the action of precipitations); however, covered against contamination from the road
5	surfaces of parts exposed to the direct effect of the atmosphere or contamination from the road or both and errosive action of solid particles

NOTE: The general classification system excludes corrosivity categories 1 and 2 for motor cars.

tions for products providing the selection principles, manufacturing requirements, and quality-control provisions. For example, the classification system which has been developed for the Czechoslovakian automotive industry is presented in Table 7.

The corrosivity classifications associated with the use of structural steel in buildings and structures are presented in Table 8 as another example. Recommended protection systems for various degrees of corrosivity (aggressivity) are provided in Table 9. In this table there are recommendations for the

TABLE 8—*Definition of the degrees of the aggressivity of atmospheres acting on steel structure.*

Aggressivity Degree		Characteristics
1	*a*	indoor environment with a low rate and time of duration of surface wetting of the steel structure; for example, in heated buildings
	b	inner spaces of hermetically enclosed parts of steel structures
2	*a*	environment of indoor rooms with a higher occurrence and time of duration of surface wetting of the steel construction; for example, in nonheated buildings; degree of pollution with $SO_2 \leqq 60$ mg·m^{-2}·d^{-1}
	b	environment of inner spaces of non-hermetically closed parts of steel structures equipped with openings for water outlet and with natural or artificial (also periodic) ventilation; degree of contamination with $SO_2 \leqq 60$ mg·m^{-2}·d^{-1}
3	*a*	outdoor environment with the action of precipitations; contamination with $SO_2 \leqq 60$ mg·m^{-2}·d^{-1}
	b	as under *a*, with partial protection about the action of precipitations
	c	environment of indoor rooms with a higher occurrence and time of duration of the surface wetting of the steel structure (for example, indoor rooms hermetically nonenclosed parts of the structure with openings for condensed water outlet); however, nonventilated, environment of insufficiently ventilated under-roof spaces; contamination with $SO_2 \leqq 60$ mg·m^{-2}·d^{-1}
4	*a*	outdoor environment with the action of precipitations; contamination with $SO_2 < 60, 120 >$ mg·m^{-2}·d^{-1}
	b	as under *a*, with a partial limitation of the direct action of precipitations
	c	outdoor or indoor environment with long-term or steady surface moistening of the steel structure contamination with $SO_2 \geqq 60$ mg·m^{-2}·d^{-1}
5	*a*	outdoor environment with the action of precipitations or with particularly limited action or both; contamination with $SO_2 > 120$ mg·m^{-2}·d^{-1}
	b	outdoor or indoor environment with long-term or continuous surface wetting of the steel structure; contamination with $SO_2 > 60$ mg·m^{-2}·d^{-1}
	c	environment of the degrees of the aggressivity of Nos. 3 and 4 with contamination of the structure surface by aggressive solid or liquid operation media

TABLE 9—*Recommended protecting systems for steel structures* (x = *recommended*).

Protection Systems	Technical Service Time of the Structure (Years)	Degree of the Atmosphere Aggressivity				
		1	2	3	4	5
O—structural steel	5	x	x	x		
without coating	10	x	x	x		
	30	x	x			
	50	x	x			
I—low-alloy steel	5					
	10			x	x	
	30			x	x	
	50			x	x	
II A—painting (120 μm)	5	x	x	x	x	
on hand-prepared	10	x	x			
surface	30	x	x			
	50					
II B—painting (120 μm)	5					
on blasted surface	10	x	x	x	x	
	30	x	x	x		
	50	x	x			
III—hot-dip galvanization	5					
	10		x	x	x	
	30		x	x		
	50		x	x		
IV—hand flame spraying	5					
of Al (150 to 200 μm)	10					
or Zn (120 to 150 μm)	30			x	x	
	50			x	x	
V A—automatic arc—	5					
spraying of Al (80 μm)	10					x
+ painting	30	x	x	x	x	x
	50	x	x	x	x	x
V B—hand hot spraying	5					
of Al (150 to 200 μm)	10					
or Zn (120 to 150 μm)	30					x
+ painting	50					x
V C—hot-dip galvaniza-	5					
tion + painting	10					
	30					x
	50					x

corrosion protection measures depending upon the corrosivity classification. The corrosion protection measures are as follows, with the least protection listed first:

Nonalloyed structural steel without protection,
Weathering low-alloy steel,

Standard paint coating, (120-μm dry film thickness) over minimal-quality surface preparation,
Paint coating (120-μm dry film thickness) over blasted surface,
Hot-dip galvanizing,
Flame spray with aluminum (150-μm thickness) or zinc (100-μm), and
Electrometallization with aluminum (80 μm) with two- or three-layer paint coating.

These recommendations are presented according to the requirements for service life of the structure and therefore have a basis for economic optimization of the system, including maintenance costs.

Similar refinements of the general classification system have been prepared or already exist for other industries, for example, railway transportation and ship production. Special applications of the classification system are possible for specific regions. In the case of the North Bohemian industrial complex studied in detail, we have developed a map showing the distribution of corrosion aggressivity [*25*].

Conclusion

The classification of corrosivity of the atmosphere represents an engineering system based on the results of theoretical studies of the kinetics and mechanism of atmospheric corrosion, together with an extensive data set on the climate and contamination present. The engineering value of this approach is to have a system for selecting the economic optimum corrosion-prevention measures for products using available data. The work on developing standard technical documents of this kind has been carried out for more than 20 years in the Czechoslovakian State Research Institute of Material Protection. This Institute has led in the development of corrosivity classification and, as a result, has provided input to the Commission for Standardization of the CMEA. In addition, the Institute has been the Secretariat of the International Organization for Standardization (ISO)/TC 156/WG4—Classification of the Environment with Respect to Corrosivity. We hope that this ISO working group will be a basis for closer international cooperation in this field. Classified corrosivity as an input category for optimation of protective measures for different technical equipments may in the future serve for increasing the economy of anticorrosion.

References

[*1*] Vernon, W. H. J., *Transactions of the Faraday Society*, Vol. 23, 1927, p. 162; Vol. 27, 1931 p. 264; and Vol. 29, 1933, p. 35.
[*2*] Tomashov, N. D., *Theory of Corrosion and Protection of Metals*, Macmillan, New York 1966.
[*3*] Rosenfeld, J. L., *The Atmospheric Corrosion of Metals*, Izd. Acad. Nauk S.S.S.R., Mos cow, 1966.

[4] Berukshtis, G. K. and Klark, G. B., "Corrosion Resistance of Metals and Metallic Coatings in Atmospheric Conditions," *Nauka,* Moscow, 1971.
[5] Schikorr, G., *Werkstoffe und Korrosion,* Vol. 15, 1964, p. 457.
[5a] Sydberger, T., "Influence of Sulphur Pollution on the Atmospheric Corrosion of Steel," Dissertation, Chalmers University of Technology, Göteborg, Sweden, 1976.
[5b] Ericsson, R., "Influence of Different Factors on the Atmospheric Corrosion of Steel," Dissertation, Chalmers University of Technology, Göteborg, Sweden, 1979.
[7] Michailovskij, J. N. et al, *Zashchita Metallov,* Vol. 7, 1971, p. 534.
[8] Bartoň, K., "Protection Against Atmospheric Corrosion," *Theories and Methods,* Wiley London, 1976.
[9] Sereda, P. J. in *Corrosion in Natural Environments, ASTM STP 558,* American Society for Testing and Materials, 1974, p. 7.
[10] Strekalov, P. V. and Michailovskiy, J. N., *Zashchita Metallov,* Vol. 8, 1972, p. 573.
[11] Michailovskiy, J. N., Sergeeva, E. I., and Sanko, V. A., *Zashchita Metallov,* Vol. 12, 1976, p. 105.
[2a] Legault, R. A. and Pearson, V. P. in *Proceedings,* Corrosion '77, National Association of Corrosion Engineers, 1977, Paper No. 133.
[2b] Legault, R. A., Mori, S., and Leckie, H. P., *Corrosion,* Vol. 29, No. 5, May 1973.
[2c] Legault, R. A. and Preban, A. G., *Corrosion,* Vol. 31, No. 4, April 1975, p. 117.
[13] Schwenk, W. and Ternes, H., *Stahl und Eisen,* Vol. 88, 1968, p. 318.
[4a] Haynie, F. H. and Upham, J. B. in *Corrosion in Natural Environments, ASTM STP 558,* American Society for Testing and Materials, 1974, p. 33.
[4b] Haynie, F. H. in *Abstracts,* The Electrochemical Society Fall Meeting, Pittsburgh, Pa., 15–20 Oct. 1978, p. 116.
[15] Haagenrud, S. E. in *Abstracts,* The Electrochemical Society Fall Meeting, 15–20 Oct., 1978, p. 114. Pittsburgh, Pa.
[16] Knotková, D. and Boschek, B., *Corrosion in Natural Environments, ASTM STP 558,* American Society for Testing and Materials, 1974, p. 52.
[17a] Bartoň, K., Knotková, D., Beránek, E., and Hladùvka, J., *Corrosion and Material Protection,* Vol. 20, No. 5, 1976, p. 82.
[17b] Bartoň, K. and Černý, M. in *Proceedings,* 2nd International Symposium on Atmospheric Corrosion Prognosis, Kutaisi, U.S.S.R., Nov. 1978.
[18] Knotková, D., Marek, V., and Jirovský, I. in *Proceedings,* 2nd International Symposium on Atmospheric Corrosion Prognosis, Kutaisi, U.S.S.R., Nov. 1978.
[19] Knotková, D. and Köhler, W., *Korrosion (ZKS),* Vol. 10, 1979, p. 243.
[20] Knotková, D., Coufal, L., Moidl, J., and Vlčková, J. in *Proceedings,* 5th International Symposium on Enviroeffect, Liblice, C.S.S.R., Vol. 3, May 1978, p. 129.
[21] Bartoň, K., Knotková, D., and Spanilý, J. in *Proceedings,* 2nd CMEA Congress on Corrosion of Metals, Prague, C.S.S.R., Vol. 6, 1975, p. 1561.
[22] Bartoň, K., Bartoňová, S., and Beránek, E., *Werkstoffe und Korrosion,* Vol. 25, 1974, p. 659.
[23] Jirovský, I., Knotková, D., Kokoška, I., and Průšek, J. in *Proceedings,* ECS Symposium on Atmospheric Corrosion, Florida, 1980.
[24] Bartoň, K., Bartoňová, S., and Beránek, E., *Werkstoffe und Korrosion,* Vol. 29, 1978, p. 199.
[25] Knotková, D. et al in *Proceedings,* 5th International ENVIROEFFECT Symposium, Liblice, C.S.S.R., 1978, p. 129.

E. A. Baker[1] *and T. S. Lee*[1]

Calibration of Atmospheric Corrosion Test Sites

REFERENCE: Baker, E. A. and Lee, T. S., "**Calibration of Atmospheric Corrosion Test Sites,**" *Atmospheric Corrosion of Metals, ASTM STP 767*, S. W. Dean, Jr., and E. C. Rhea, Eds., American Society for Testing and Materials, 1982, pp. 250–266.

ABSTRACT: Inherent in the ability to accurately assess the performance of a material exposed in the atmosphere is an understanding of the relative corrosivity of that environment. The most reliable of present test methods for ranking materials' corrosion behavior have necessarily utilized long-term exposures to the natural environment in question. Given the variable nature of many atmospheric factors, it becomes important to determine the relative stability in the corrosivity of an atmospheric exposure site. Only in this way can the desired credence be given to atmospheric corrosion data generated for a variety of materials over an extended duration.

A review is provided of the major factors which must be considered in establishing a program to monitor and calibrate an atmospheric test site. These factors include both environmental assessments and corrosion evaluations. Consideration is given to the specific environmental parameters which could be monitored as well as experimental procedures which affect the atmospheric corrosion behavior of materials.

KEY WORDS: atmospheric corrosion, marine environment, calibration tests, environmental monitoring, steel, iron, zinc

Over the years, considerable attention has been devoted to the weathering of materials. Observations of materials corrosion performance in the atmosphere have ranged from those made on existing structures to carefully designed experimental programs with the specific intent of characterizing the behavior of a given material. The programs have included both accelerated tests and exposures in natural environments.

Artificially simulating a natural environment which is universal for all materials has proven difficult. This was demonstrated by May and Alexander [*1*][2] in a series of tests with iron and zinc exposed to a variety of saline sprays (Figs. 1 and 2). None of the three simulations consistently reproduced the behavior exhibited by the materials under natural marine atmospheric conditions. This observation is not altogether surprising when one considers

[1] Senior research technologist and Marine Corrosion Section manager, respectively, LaQue Center for Corrosion Technology, Inc., Wrightsville Beach, N. C.

[2] The italic numbers in brackets refer to the list of references appended to this paper.

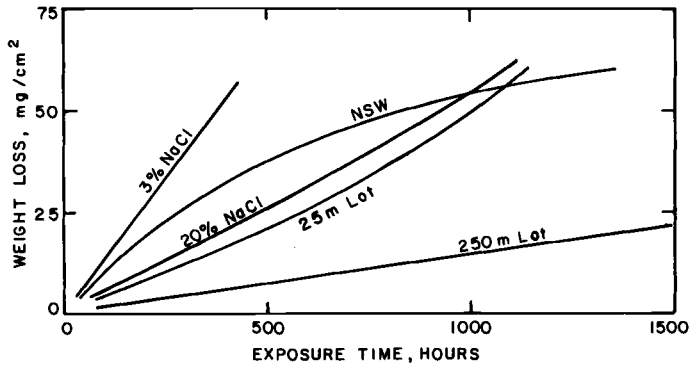

FIG. 1—*Comparative behavior of iron exposed in the marine atmosphere (25 and 250 m from the ocean) and in sprays of natural seawater, and 3 and 20 percent sodium chloride.*

the number of factors which can influence the corrosion behavior of a material and the variable nature of these factors in natural environments.

As the controlling factors in the atmospheric corrosion of materials become better defined, the ability to conduct viable short-term accelerated tests will be enhanced. While research continues in this direction, however, characterization of materials performance primarily continues through controlled exposures in natural environments.

A number of atmospheric test sites exist where natural exposures can be conducted for extended time periods. These sites are often categorized as being typical of marine, rural, or industrial environments. Within each of these categories, a wide range of behavior can be exhibited by a given material. This behavior can be related to the variations in the environmental characteristics and to variations in the experimental techniques employed at the various sites. Some consistency is achieved through the application of standard experimental practices such as the American National Standards

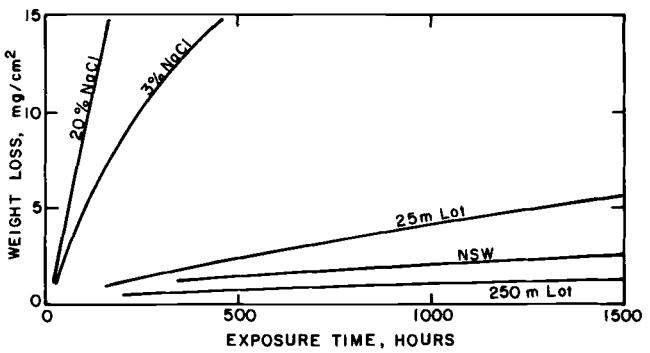

FIG. 2—*Comparative behavior of zinc exposed in the marine atmosphere (25 and 250 m from the ocean) and in sprays of natural seawater, and 3 and 20 percent sodium chloride.*

Institute/American Society for Testing and Materials (ANSI/ASTM) Recommended Practice for Conducting Atmospheric Corrosion Tests on Metals (G 50-76). However, the corrosivity of these environments is generally assumed to be constant unless specific programs exist on a continuing basis to monitor this factor.

Several tests have been conducted which have established the relative corrosivities of various locations for some finite period [*2–5*]. Recognizing the need to provide continuity in defining relative corrosiveness, ASTM has established Task Group G01.04.01.01, Calibrating the Corrosiveness of Atmospheric Test Sites.

It is the objective of this task group to develop a standard recommended practice by which tests can be conducted to calibrate an atmospheric corrosion test site and define its corrosiveness on a continuing basis. Some of the factors which will be considered in the development of this standard are reviewed in this paper.

Environmental Assessments

A variety of environmental variables can influence atmospheric corrosion. These will vary depending upon the nature of the test site (for example, chlorides in a marine environment, sulfur dioxide in an industrial environment), but some of the more significant variables include temperature, sunlight, wind, moisture, and contaminants.

Temperature

Correlations between the temperature of metal surfaces and corrosion have been presented by Guttman and Sereda [*4*]. The influence of temperature does not necessarily represent the prime controlling factor in a corrosion process but is related to other critical factors. Among these are the presence of moisture and the extent of sunlight. An analysis of the Guttman and Sereda data by Grossman [*6*] provided some insight into the accelerating effect of temperature during periods of wetness of the metal surface. Among the temperatures which can be measured are the ambient air temperature, dew-point temperature, test panel surface temperature, and a black-box temperature.

Sunlight

The extent of sunlight at an atmospheric test site will influence not only the degree of wetness on a specimen surface but will also affect the performance of coatings and some nonmetallics. The duration and intensity of ultraviolet and solar radiation are variables which can be monitored as shown in Table 1, which summarizes the solar radiation during 1978 at Kure Beach, N. C.

TABLE 1—*Typical solar radiation monitored at Kure Beach, N. C.*

Month	Solar Radiation	
	Duration Radiation, h	Intensity of Radiation, cal/cm^2
January	318	7355
February	312	8310
March	374	11902
April	381	13697
May	320	14500
June	400	15500
July	414	14461
August	386	14275
September	337	10073
October	334	10315
November	281	4870
December	288	5695

Wind

The intensity and direction of prevailing winds can affect corrosion by influencing both the surface conditions on a test specimen and the type of atmospheric environment which may prevail at a given test site. Grossman [*6*] reviewed the influence of increased wind intensity on surface-to-air heat transfer and the resultant increase in the relative humidity required to achieve condensation on a test specimen surface. The direction of prevailing winds can influence factors such as the quantities of chloride transported from the sea at a marine site or quantities of sulfur dioxide from industrial sites. Figure 3 shows the distribution of prevailing winds over the period of one year at Kure Beach, N. C. The series of wind roses shows that the majority of the winds off the ocean [northeast (NE) to southeast (SE)] were during the spring and fall months.

Moisture

Previous researchers [*4,6*] have examined the correlations between atmospheric corrosion and extent of moisture (which acts as the electrolyte for the corrosion process) on the specimen surface. A variety of techniques has been employed to measure the time-of-wetness on a specimen surface. However, some difficulty has been encountered in establishing specific designs which consistently measure wetness as a level which can be directly correlated with corrosion rates. Progress is being made toward the development of a standard recommended practice for conducting these measurements in ASTM G1.04.

Not only is the time-of-wetness important but, also, the nature of the wet-

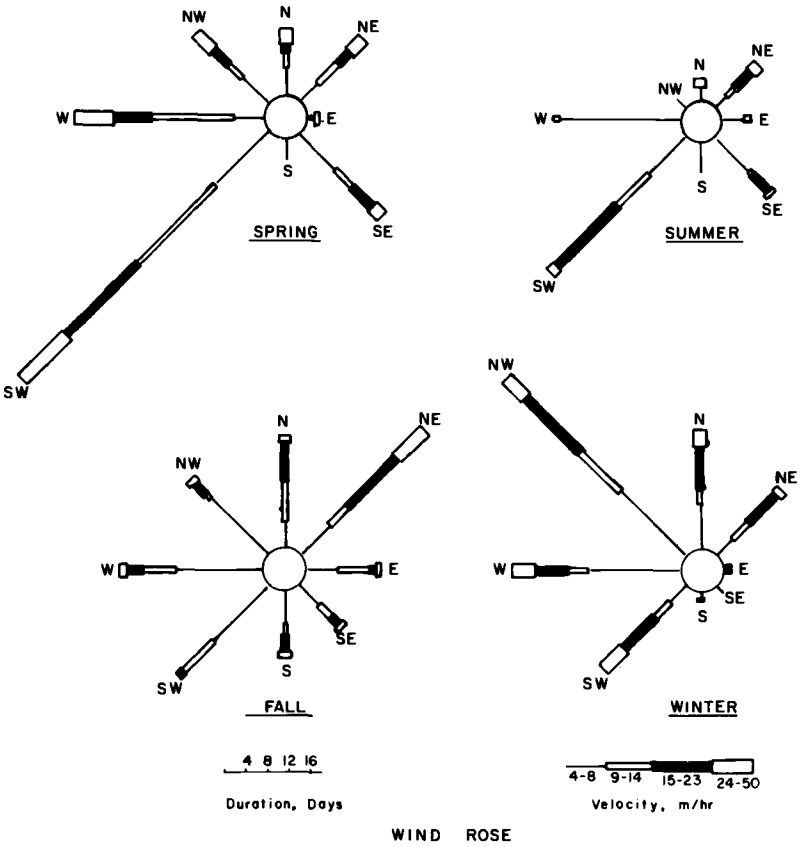

FIG. 3—*Seasonal distribution of wind direction and intensity at Kure Beach, N. C.*

ness is critical. In the case of a marine environment, moisture in the form of dew or sea spray will be more corrosive than a greater amount of moisture in the form of rainfall. In the case of industrial environments, however, the presence of an acid precipitation from sulfur dioxide in the atmosphere may prove very corrosive.

Contaminants

Two factors which are considered the prime corrosive agents for marine and industrial environments are the chloride and sulfur dioxide contents, respectively. The use of a "wet candle" technique [*7*] for chloride and sulfation plates [*8*] for sulfur dioxide offers a simple means of monitoring these variables. While the measured quantities represent an average in the atmosphere rather than an exact quantity on the specimen surface, it can often provide insight into the long-term corrosiveness of a test site.

Corrosion Evaluations

All materials exposed in the atmosphere do not respond to the same environmental factors in a common fashion. For example, it is recognized that the hygroscopic properties of the corrosion products will have a direct influence on the conditions under which the material can be considered wet and, therefore, the period during which the material will corrode [*9*]. Therefore, while it is difficult to extrapolate results on one material to another, it is practical to consider only one or two materials in establishing a series of corrosion evaluations designed to calibrate atmospheric corrosiveness. The nature of these materials must be such that they are relatively sensitive to changes in the environment. In this way, periodic assessment of the corrosion behavior will be indicative of the corrosivity of the environment.

The experimental techniques utilized in a calibration test must take into account those factors which are critical to the reproducibility and objectivity of the data. These include, but are not limited to, specimen preparation and orientation and time and duration of exposure.

Material Selection

As mentioned previously, the selection of a material for calibration tests is critical. The material must respond to environmental changes yet yield somewhat reproducible behavior under nominally equivalent exposure conditions. In selecting a material, a sufficient quantity of a controlled chemistry must be obtained to avoid variations in performance based on alloy composition. This is particularly important when the effect of small changes of copper content in iron is considered as shown in Fig. 4 [*3*].

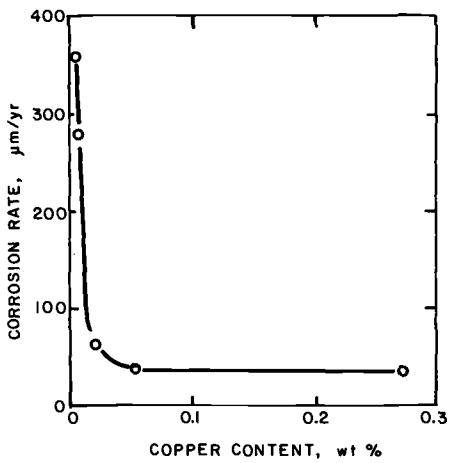

FIG. 4—*Effect of copper content on corrosion of iron in a marine atmosphere after 1.5 years' exposure.*

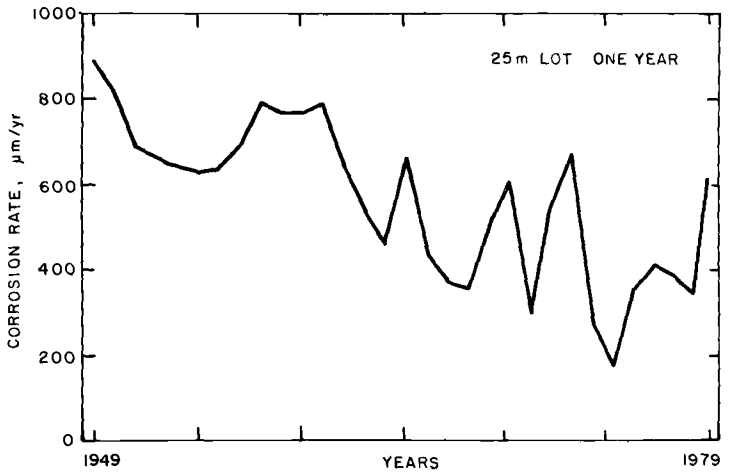

FIG. 5—*Corrosion rate of iron calibration specimens exposed vertically in the 25-m atmospheric lot at Kure Beach for one year, over the period 1949 to 1979.*

Most programs designed to evaluate relative corrosivities of atmospheres have utilized iron or steel, zinc, or copper test specimens. The use of calibration specimens can be traced to the early work of Hudson [*2*], who in 1943 established a ranking of environments based on exposures of iron specimens. The 50 by 100-mm specimens were exposed vertically for a period of one year and had the following nominal composition:

C	0.02 weight percent	S	0.044 weight percent
Mn	0.05	Cu	0.066
Si	0.008	Ni	0.054
P	0.013	Cr	0.001

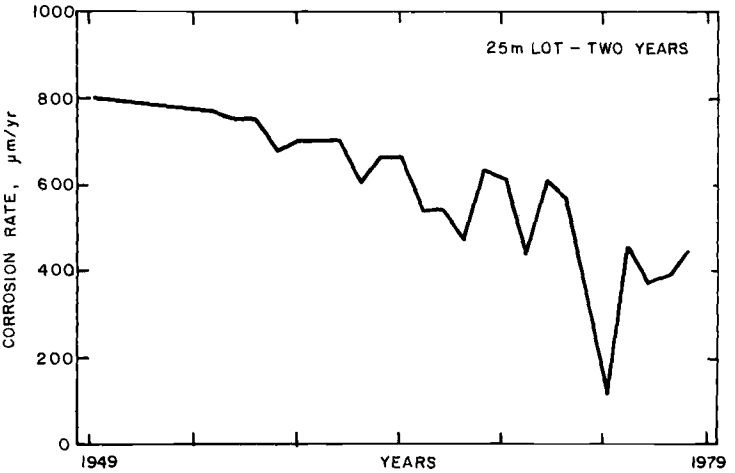

FIG. 6—*Corrosion rate of iron calibration specimens exposed vertically in the 25-m atmospheri lot at Kure Beach for two years, over the period 1949 to 1979.*

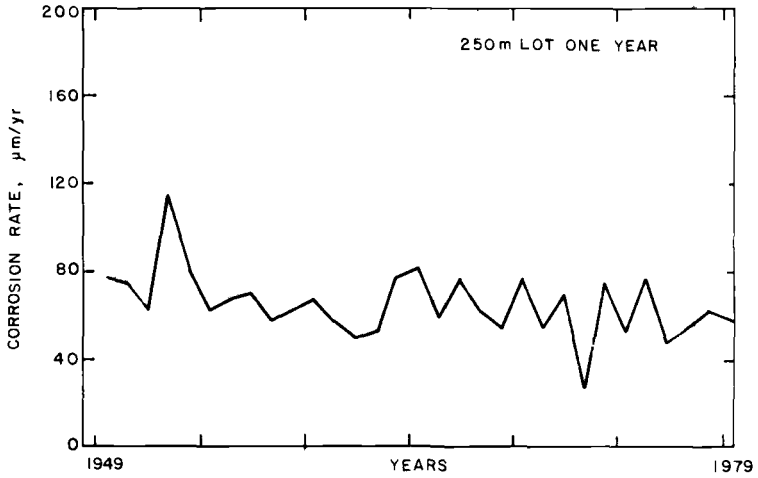

FIG. 7—*Corrosion rate of iron calibration specimens exposed vertically in the 250-m atmospheric lot at Kure Beach for one year, over the period 1949 to 1979.*

The exposure of this type of calibration specimen has continued in at least one site—Kure Beach, N. C. Figures 5–9 show corrosion rates measured annually, since 1949, for iron specimens exposed for one and two years in the 25-m atmospheric lot and for one, two, and four years in the 250-m atmospheric lot.

Specimen Orientation

As just indicated, the continuing calibration program at Kure Beach involves vertical exposures of specimens. This procedure is subject to greater

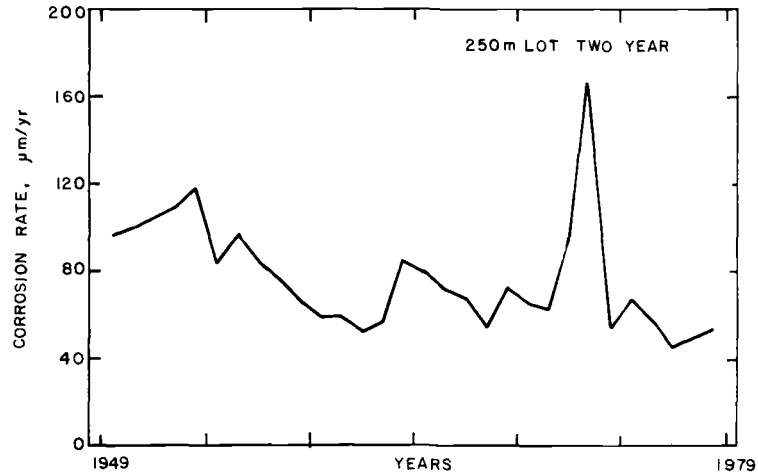

FIG. 8—*Corrosion rate of iron calibration specimens exposed vertically in the 250-m atmospheric lot at Kure Beach for two years, over the period 1949 to 1979.*

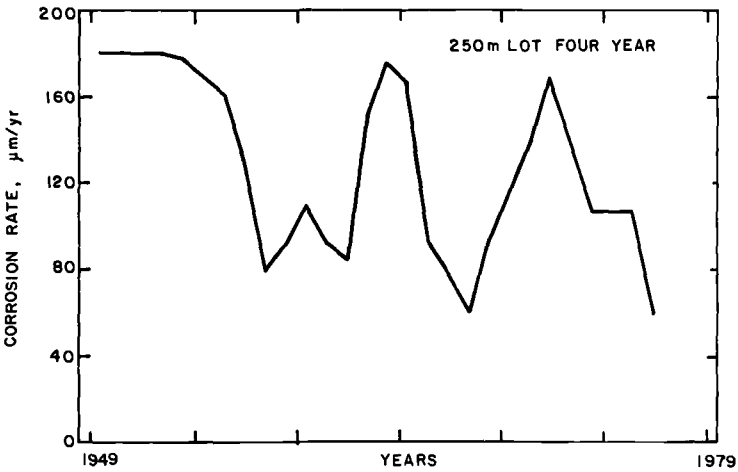

FIG. 9—*Corrosion rate of iron calibration specimens exposed vertically in the 250-m atmospheric lot at Kure Beach for four years, over the period 1949 to 1979.*

experimental sensitivity than is the standard 30-deg-angle exposure recommended in ASTM Method G 50-76. LaQue [*3*] reported the greater severity of corrosion of vertical specimens compared with specimens at 30 deg, as shown in Table 2. This was attributed to the formation of a less protective and nonuniform corrosion product in the vertical exposures. This can be seen in Fig. 10, which shows specimens exposed vertically and at 30 deg for one year at the 25-m Kure Beach atmospheric lot. An analysis of the thickness loss on the specimens (Table 3) indicates that the vertically exposed specimens exhibited not only the greater average thickness loss but also a greater degree of scatter. Recent tests in the less-severe environments of the 250-m Kure Beach atmospheric lot and a rural and industrial site have shown less difference between corrosion rates as a function of specimen orientation (Figs. 11 and 12).

Some variation in extent of attack is observed between the opposite surfaces when specimens are exposed vertically. This is particularly evident in a

TABLE 2—*Comparison of atmospheric corrosion rates of steel exposed vertically and at 30 deg from horizontal after one year.*

Location	Ratio of Corrosion Rate Vertical/30°
Kearny, N. J.	1.25
Vandergrift, Pa.	1.26
South Bend, Pa.	1.20
25-m Kure Beach lot	1.41
250-m Kure Beach lot	1.25

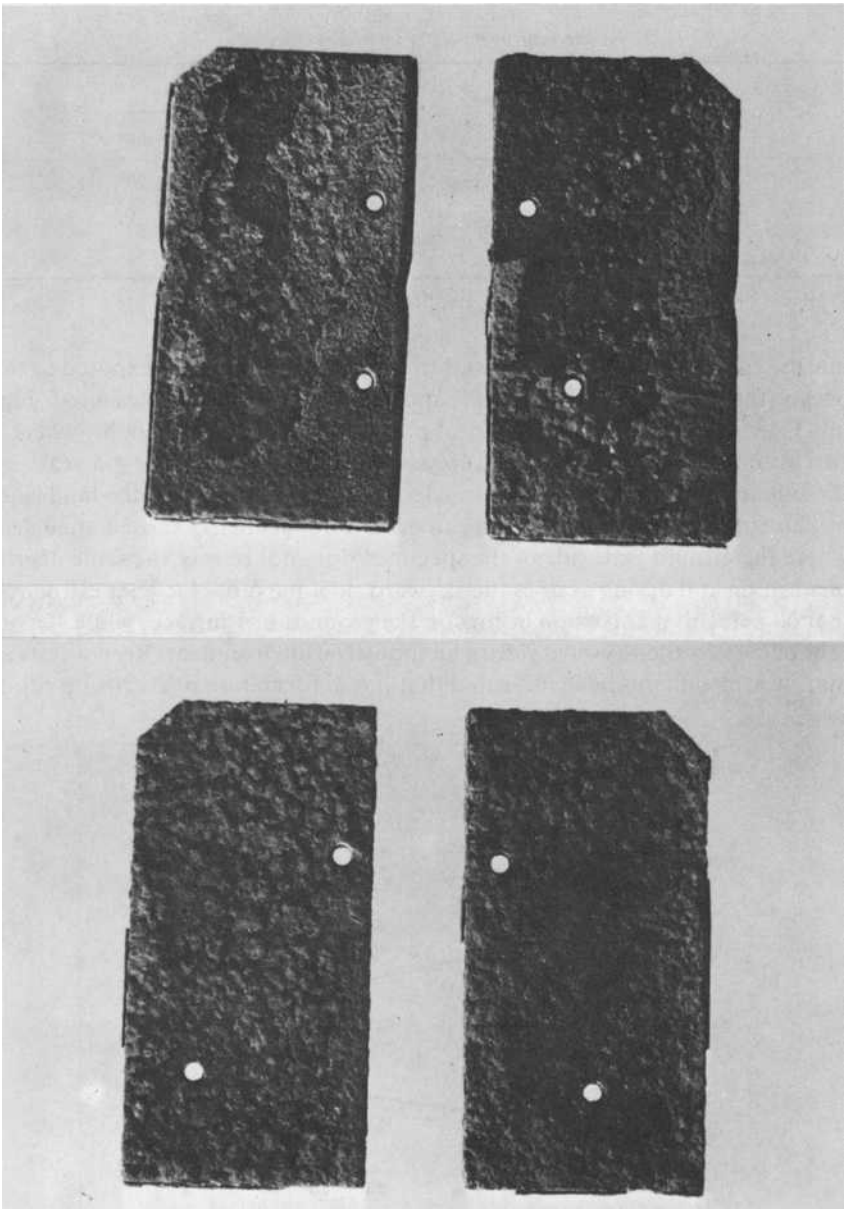

FIG. 10—*Appearance of iron specimens after one-year exposure in the 25-m atmospheric lot at Kure Beach.* Top: *vertical exposure, ocean side* (left) *and land side* (right). Bottom: *30-deg exposure, skyward* (left) *and groundward side* (right).

TABLE 3—*Comparison of thickness loss variability for iron specimens exposed for one year in the 25-m lot at Kure Beach.*

Exposure Condition	Thickness Loss,[a] mm	
	Avg	Range
Vertical	1.07 ± 0.34	1.23
Vertical	1.24 ± 0.39	1.25
30 deg	0.44 ± 0.22	0.93
30 deg	0.55 ± 0.22	0.95

[a] Based on 25 measurements within a specified grid.

marine environment, where a vast difference between the side exposed to the ocean (that is, salt spray and sand) and the landward side is measured. Figure 13 shows the appearance of steel pipe specimens in the 25-m lot where a corrosion rate greater than 850 μm/year can be estimated after 4.5 years on the side facing the ocean, with a rate less than 150 μm/year on the land side.

This side-to-side variation also can occur on specimens exposed at 30 deg, where the groundward side of the specimen does not receive the same degree of washing and drying as does the skyward side. Larrabee [*10*] has estimated that 60 percent of corrosion occurs on the groundward surfaces while 40 percent occurs on the skyward side in an industrial environment. Recent tests in marine atmospheres have indicated that initial formation of corrosion prod-

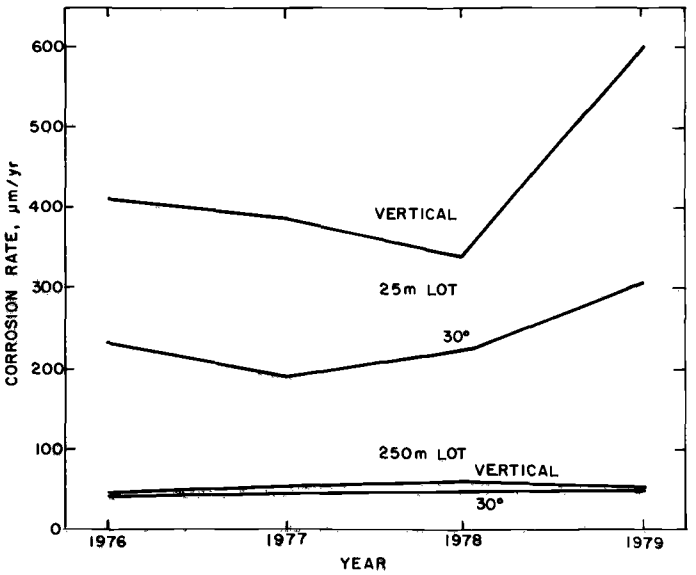

FIG. 11—*Comparison of corrosion rates in the 25-m and 250-m atmospheric lots at Kure Beach for iron specimens exposed vertically and at 30 deg from horizontal for one year.*

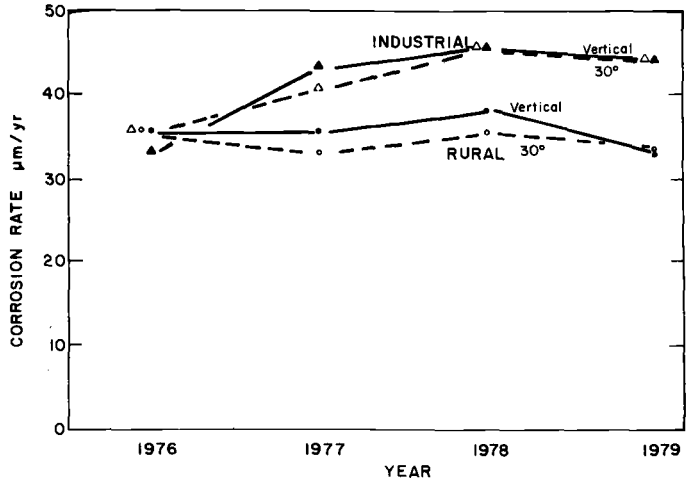

FIG. 12—*Comparison of corrosion rates in rural and industrial environments for iron specimens exposed vertically and at 30 deg from horizontal for one year.*

ucts occurs at slightly different rates on the groundward and skyward sides of steel specimens. However, after 6 months' duration, the corrosion rate difference between the two sides was negligible (Fig. 14). The slightly higher initial rates on the skyward side can most likely be attributed to the errosive effects of sand and perhaps a greater degree of wetness from salt spray.

A final consideration in the specimen orientation is the elevation and direction of exposure of the specimen. As shown previously, the directional effects in a marine location can be significant. Again, ASTM G 50 provides guidance in selecting a consistent direction of exposure to maintain appropriate conditions for reference purposes.

While a minimum exposure height of approximately 75 cm above ground is recommended in ASTM G 50, no specific maximum height is recommended. For calibration purposes, the elevation of the specimens must be kept constant. LaQue [*11*] has shown this to be particularly important for steels in marine environments. Figure 15 shows corrosion rates as a function of elevation of specimens above sea level. The maximum observed on these graphs has been related to a zone of maximum chloride in the atmosphere as it is swept upward by the prevailing winds from the sea. The corrosivity of a marine site may therefore be influenced to a great extent by factors which affect this maximum chloride path.

Chloride levels in both the 25-m and 250-m Kure Beach lots have been monitored (wet-candle technique) at a fixed height aboveground of 150 cm since 1962. The average annual levels are shown in Fig. 16. While the chloride level in the 250-m lot has remained relatively constant, it has shown a continuing decline in the 25-m lot. This appears to be related to the steadily

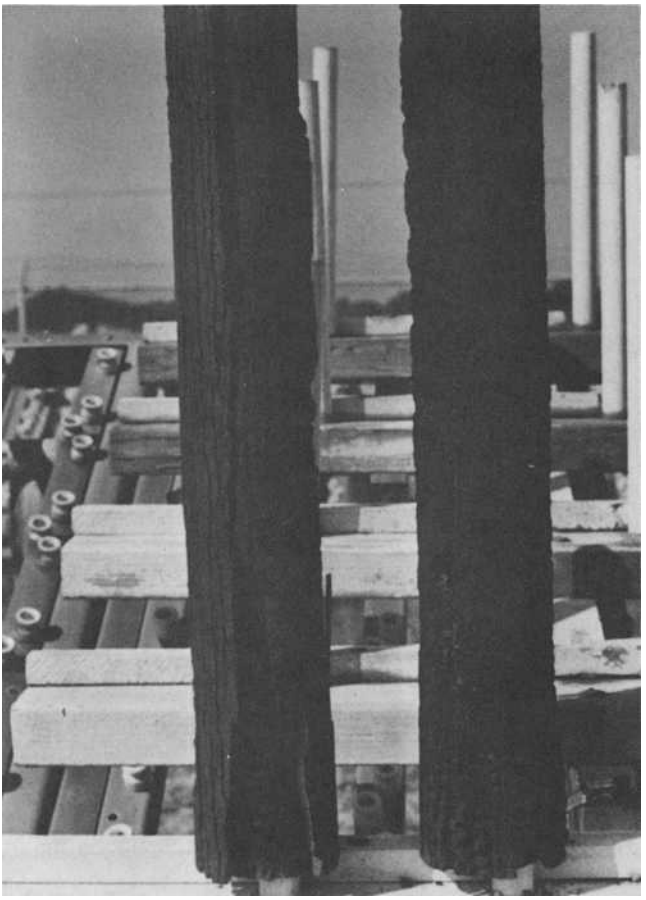

FIG. 13—*Appearance of steel pipe after 4.5 years' exposure in the 25-m lot at Kure Beach:* (left) *ocean side,* (right) *land side.*

increasing size of the sand dunes between the 25-m lot and the ocean. This in turn would tend to have the effect of shifting the maximum chloride content in the atmosphere to a somewhat higher elevation and thereby reduce the corrosiveness of the 25-m lot. This has been observed in the decreasing corrosion rates of control specimens of iron in the 25-m lot and the relatively constant rates observed in the 250-m lot (Figs. 5–9).

Exposure Time

The two time factors which would be expected to influence calibration tests are the time of exposure and the total duration of test. The time of ex-

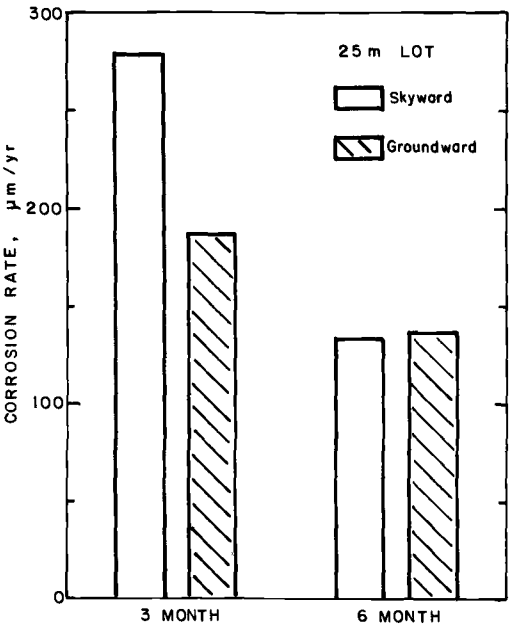

FIG. 14—*Comparative corrosion rates of skyward and groundward sides of iron specimens exposed for 3 and 6 months in the 25-m atmospheric test lot at Kure Beach.*

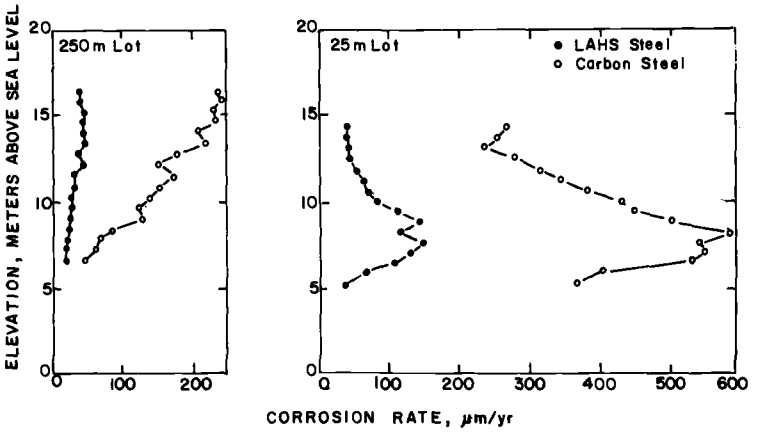

FIG. 15—*Effect of elevation above sea level on the marine atmospheric corrosion behavior (26 months' exposure) of carbon steel and low-alloy high-strength steel.*

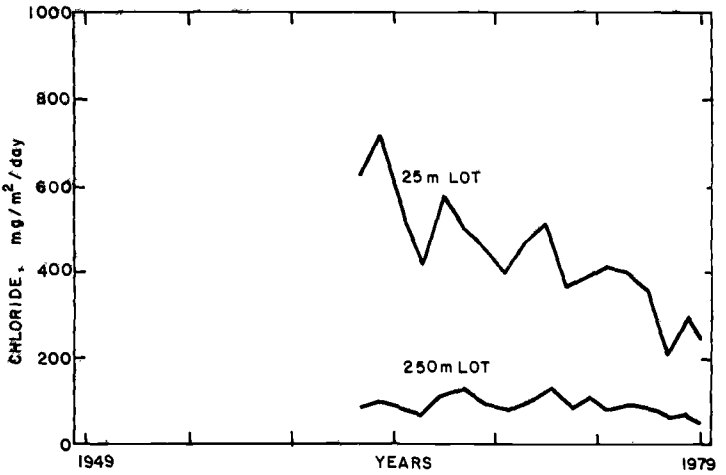

FIG. 16—*Average annual chloride levels in the 25-m and 250-m atmospheric test lots at Kure Beach.*

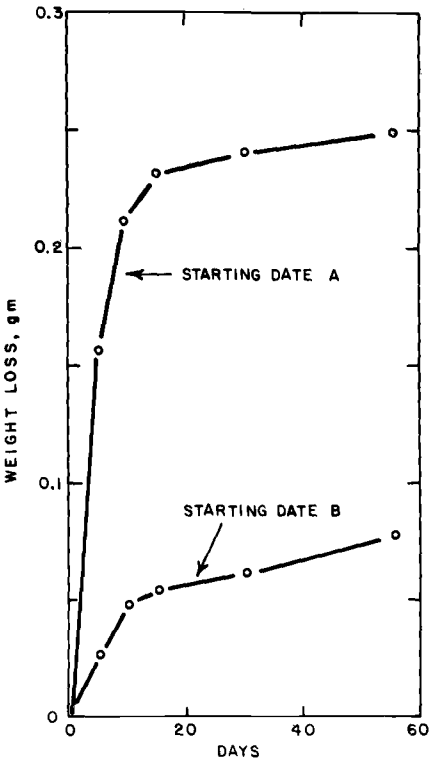

FIG. 17—*Weight loss versus time for specimens of zinc started in test on different dates.*

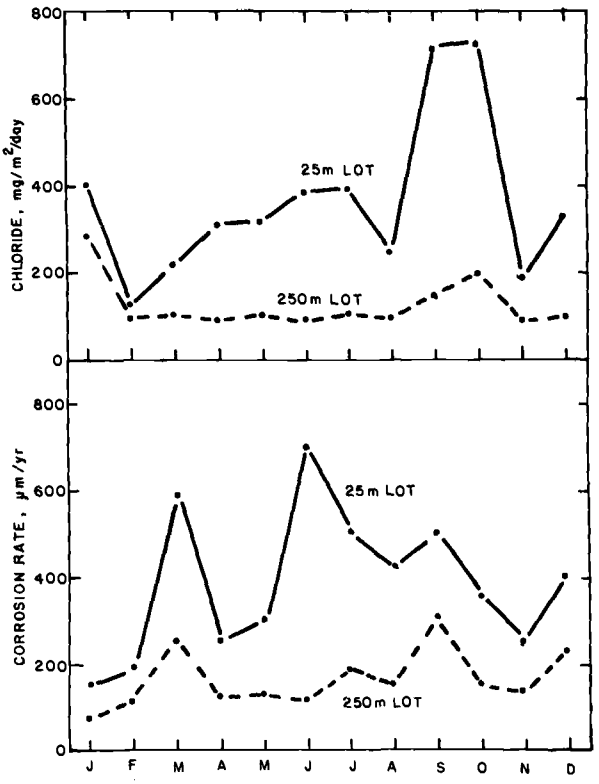

FIG. 18—*Comparison of corrosion rate of steel specimens exposed for one month at Kure Beach, N. C. over a one-year period with atmospheric chloride content.*

posure is critical in that the prevailing environmental conditions during the initial stages of corrosion can have a profound influence on the long-term corrosion behavior. This is particularly true for zinc, as was observed by Ellis [*12*]; see Fig. 17. Similar effects have been shown for steel and iron [*12,13*], but the degree of variation does not seem to be quite as severe or necessarily as protracted as with zinc.

Figure 18 shows short-term data for carbon steel exposed in the atmospheric test lots at Kure Beach over the period of one year. While the corrosion rate data do not directly correlate with the chloride measurements, other unmeasured factors, such as time-of-wetness, would have influenced these rates. Guttman and Sereda [*4*] showed good correlation between the prevailing environmental conditions monitored (time-of-wetness, sulfur dioxide, temperature) and the corrosion rates of steel, copper, and zinc during the first month of exposure at several locations. In some cases, these correlations existed for longer-term exposures also.

Given the practical limitations of the number of specimens which can be

exposed, care must be exercised in exposing calibration specimens at nominally the same time each year while closely monitoring the environmental conditions during the early days of exposure. Exposure duration should be sufficiently long to allow some averaging effects of environmental conditions, but, as with the case of zinc specimens, consideration should be given to exposures during at least two times of the year when environmental conditions typically are at extremes. Care should then be exercised in attempting to extrapolate these calibration data to the performance of materials exposed at other times of the year.

Conclusions

A variety of factors must be considered in establishing a program of monitoring and calibrating the corrosivity of an atmospheric test site. Monitoring of critical environmental parameters such as temperature, sunlight, wind, moisture, and contaminants can prove important in establishing an understanding of observed corrosion behavior. A series of corrosion tests on one or two materials, which are sufficiently sensitive to environmental changes, is also critical in establishing corrosivity. These corrosion tests must be conducted under controlled experimental conditions to minimize variations due to procedural details such as specimen orientation and time of exposure.

References

[1] May, T. P. and Alexander, A. L. in *Proceeding,* American Society For Testing and Materials, Vol. 50, 1950, p. 1131.
[2] Hudson, J. C., *Journal of the British Iron and Steel Institute,* Vol. 148, 1943, p. 161.
[3] LaQue, F. L. in *Proceedings,* American Society for Testing and Materials, Vol. 51, 1951, p. 495.
[4] Guttman, H. and Sereda, P. J. in *Metal Corrosion in the Atmosphere, ASTM STP 435,* American Society for Testing and Materials, 1968, p. 326.
[5] Coburn, S. K. et al in *Metal Corrosion in the Atmosphere, ASTM STP 435,* American Society for Testing and Materials, 1968, p. 360.
[6] Grossman, P. R. in *Atmospheric Factors Affecting the Corrosion of Engineering Metals, ASTM STP 646,* American Society for Testing and Materials, 1978, p. 5.
[7] Foran, M. R. et al, *Chemistry in Canada,* Vol. 10, 1958, p. 33.
[8] Huey, N. A., *Journal of the Air Pollution Control Association,* Vol. 18, 1968, p. 610.
[9] Vernon, W. H. J., *Transactions of the Faraday Society,* Vol. 19, 1924, p. 886.
[10] Larrabee, C. P., *Transactions of the Electrochemical Society,* Vol. 85, 1944, p. 297.
[11] LaQue, F. L., *Marine Corrosion,* Wiley, New York, 1975, p. 103.
[12] Ellis, O. B. in *Proceedings,* American Society for Testing and Materials, Vol. 49, 1949, p. 152.
[13] Dearden, J., *Journal of the Iron and Steel Institute,* Vol. 159, 1948, p. 241.

P. J. Sereda,[1] *S. G. Croll,*[1] *and H. F. Slade*[1]

Measurement of the Time-of-Wetness by Moisture Sensors and Their Calibration

REFERENCE: Sereda, P. J., Croll, S. G., and Slade, H. F., **"Measurement of the Time-of-Wetness by Moisture Sensors and Their Calibration,"** *Atmospheric Corrosion of Metals, ASTM STP 767,* S. W. Dean, Jr., and E. C. Rhea, Eds., American Society for Testing and Materials, 1982, pp. 267–285.

ABSTRACT: A 1-year program involving several laboratories located in different climatic zones has afforded an opportunity to evaluate the response of miniature moisture sensors (developed at the National Research Council of Canada) to surface moisture on panels exposed to the atmosphere. It has shown that when these moisture sensors are placed on the surface of metal or plastic panels they respond to moisture conditions at the surface or more precisely, at the sensor surface, and that such moisture conditions result from interaction of the total environment with the material as well as with the ambient relative humidity conditions.

KEY WORDS: corrosion, metals, atmosphere, measurement, time-of-wetness, moisture sensors, calibration, sensor potential, ambient relative humidity, temperature

Time-of-wetness was first measured by Sereda with a sensor consisting of a platinum foil strip on a zinc panel [*1–3*].[2] The period during which the potential generated by this galvanic cell exceeds 0.2 V was defined as the time-of-wetness, which served as the time base for the expression of the rate of corrosion in terms of MDD_w (milligrams/square decimetre/day of wetness). Subsequent work has demonstrated the significance of this factor and its correlation with rate of corrosion [*4–7*]. In the early work [*1–3*] it was observed that the potential measured by the cell varied in the range 0 to 1 V, apparently due to changing conditions of exposure. Whether the level of potential correlated, however, with certain ambient conditions such as relative humidity was not resolved.

Some success has been achieved by other workers in measuring integrated current using a sensor involving a galvanic or electrolytic cell and correlating

[1] National Research Council of Canada, Division of Building Research, Ottawa, Ont., Canada.

[2] The italic numbers in brackets refer to the list of references appended to this paper.

this with the rate of corrosion [*8–14*]. Although the monitoring of current levels above a certain value can be used as a measure of the time-of-wetness of such sensors, they are not appropriate, because of their large size, for monitoring surface moisture on exposed specimens of various materials or elements of buildings.

A new miniature moisture sensor has been developed. It monitors the presence of surface moisture in conjunction with atmospheric corrosion testing. Because of its possible usefulness, Subcommittee G01.04 on Weather of ASTM Committee G-01 on Corrosion of Metals organized a round-robin test series to evaluate its performance and to attempt its calibration in the range of 75 to 100 percent ambient relative humidity. This paper reports the results of the round-robin and the additional work carried out at the National Research Council of Canada (NRCC) Laboratories.

Experimental

The new moisture sensor was developed by NRCC in conjunction with Bell Northern Research Laboratories. It consists of a cell of alternate electrodes of zinc and gold or copper and gold on a glass-reinforced polyester (GRP) base 1.5 mm thick (Fig. 1*a*); the overall size is 20 by 25 mm. It was mounted on both galvanized metal and plastic bases 100 by 150 mm (Fig. 1*b*).

Temperature of the metal and plastic bases and that of the sensor was measured with 30-gage copper-constantan thermocouples embedded in the surface (Fig. 2). The mounted sensors were placed on a corrosion rack (Fig. 3).

At the Ottawa site, potential levels from the zinc/gold (Zn/Au) or copper/gold (Cu/Au) sensors and temperatures, including the ambient and dew-point temperatures (dew cells located in a Stevenson screen; see Fig. 3), were recorded every 10 min on magnetic tape.

One set of sensors having Zn/Au electrodes was distributed to a number of participating laboratories to extend the evaluation program to different climates. As various unforeseen difficulties arose, however, only two of the original six laboratories have been able to supply completed data. These are included in the present paper, along with extensive data collected at the NRCC laboratory.

Analyses of the data included determination of the frequency distributions of ambient relative humidity and the potential levels from Zn/Au and Cu/Au sensors mounted on metal and plastic panels. The distribution of surface temperature, the difference between surface temperature and ambient temperature, and surface temperature (metal or plastic) and sensor temperature were obtained for the periods when the potential from the Zn/Au cell exceeded 0.1 V and that from the Cu/Au cell exceeded 0.01 V. For the purpose of this paper these limits define the time-of-wetness. Data were collected at the Ottawa site for 1 1/2 years, and as they were reasonably

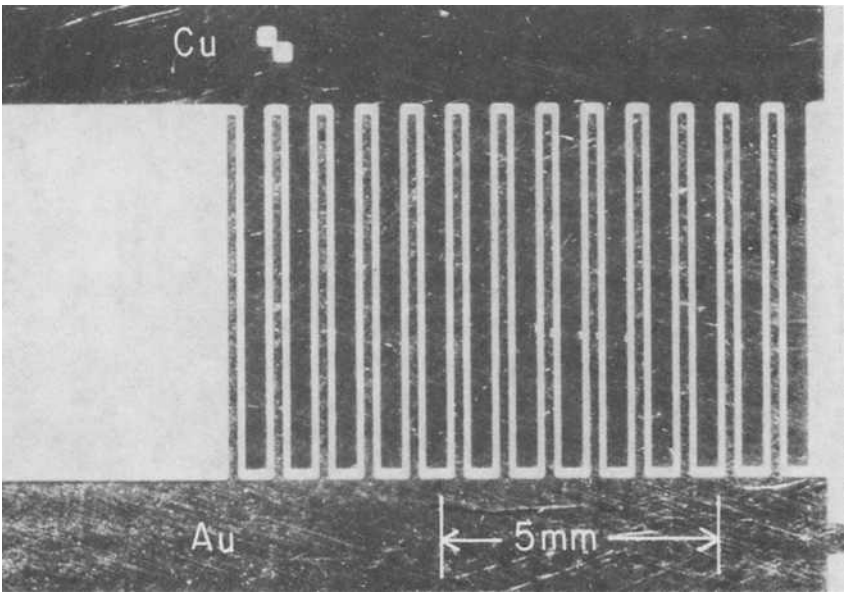

FIG. 1*a*—*Moisture sensor.*

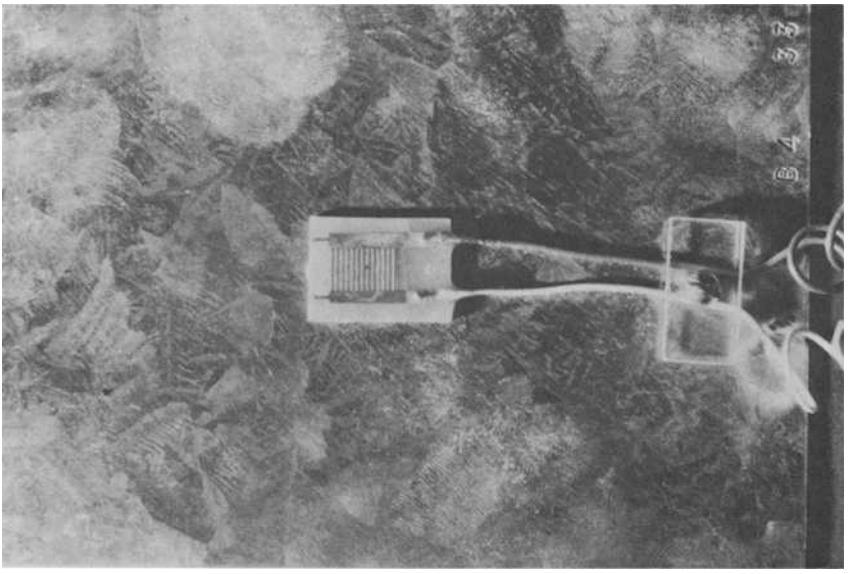

FIG. 1*b*—*Sensor mounted on metal base.*

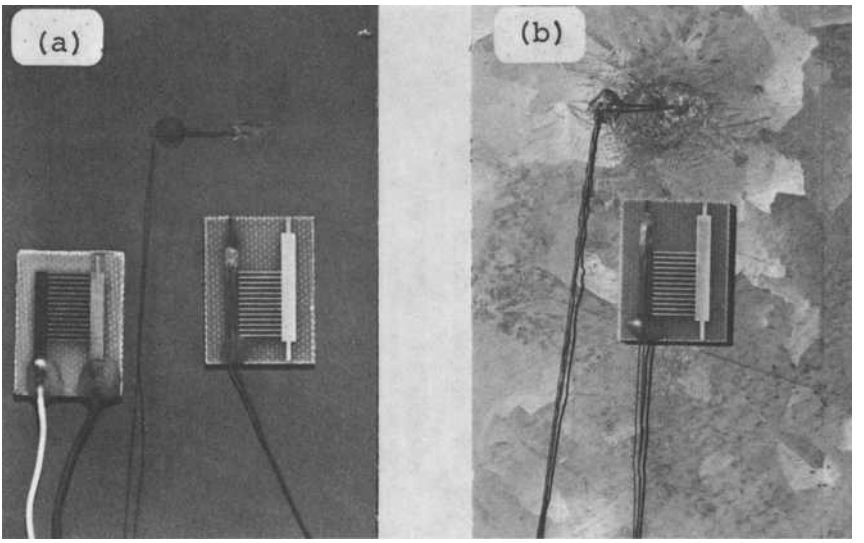

FIG. 2—*Thermocouples mounted on specimens and on sensors:* (a) *on plastic specimen;* (b) *on metal specimen.*

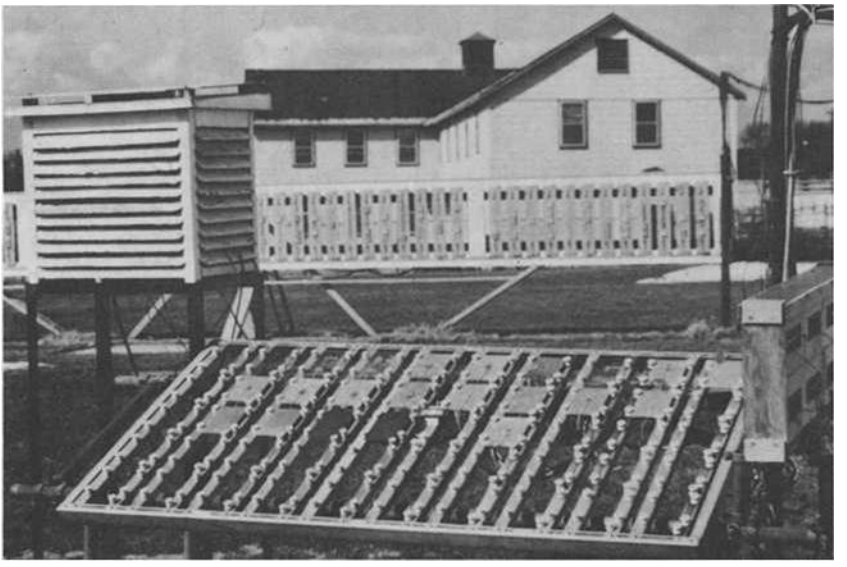

FIG. 3—*Exposure station at Ottawa.*

reproducible for comparable months of each year, only typical results are presented in this paper. Representative results reported by other participating laboratories are given to indicate the influence of different climatic conditions.

Results and Discussion

Characteristic Results for Periods of Rain, Snow, Dew, and Hoarfrost

Figure 4 presents typical data collected for a period of rainfall that occurred on 14 Sept. 1979. The ambient and sensor surface temperatures were very similar, the relative humidity was 100 percent during most of the period, and the potential recorded by the Zn/Au cell was steady at about 0.8 V and that by the Cu/Au cell was initially about 0.05 V and tended to decrease with the time-of-wetness, a characteristic of this type of cell. The increase in voltage is more rapid than the decay at the termination of rain because of the persistence of surface moisture.

Figure 5, showing a typical record of snowfall, has some similarity to Fig.

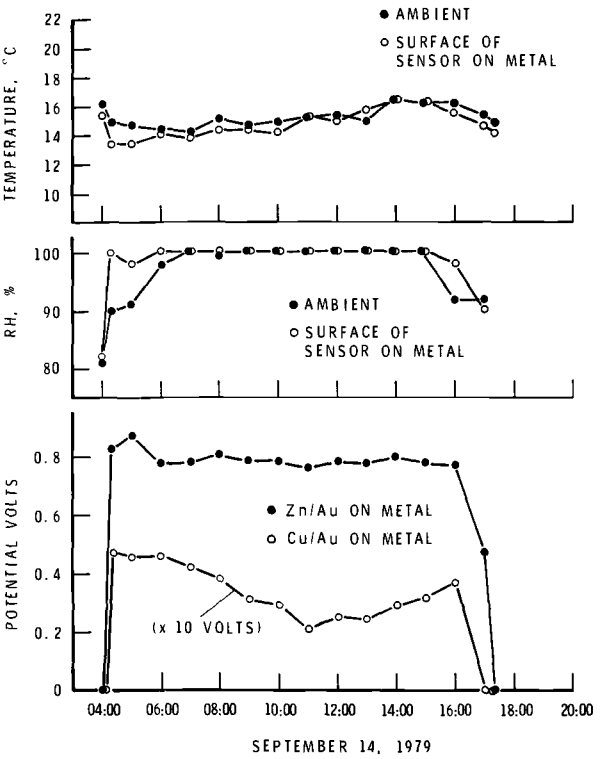

FIG. 4—*Record for interval of rainfall (20 mm), Ottawa.*

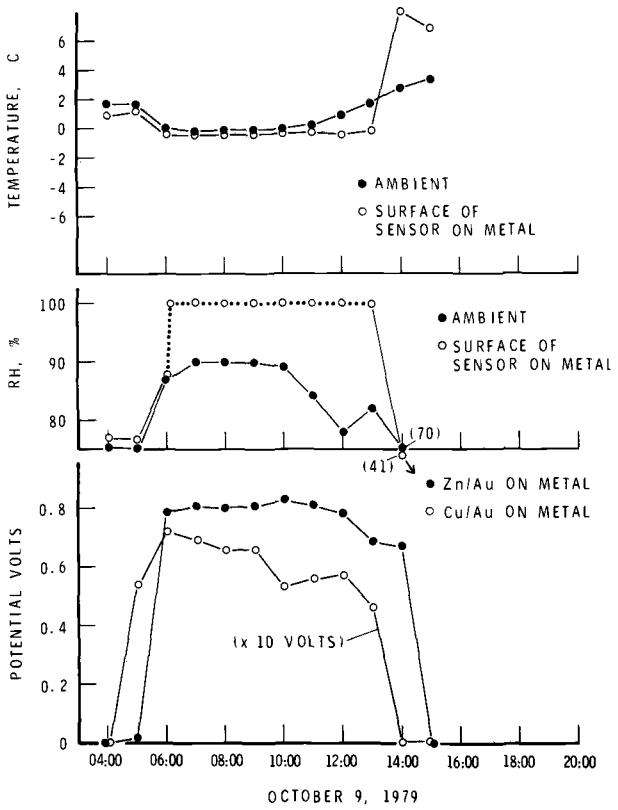

FIG. 5—*Record for interval of wet snowfall (20.4 mm of rain equivalent), Ottawa.*

4 for rainfall in having essentially equal ambient and surface temperatures. The ambient relative humidity was about 90 percent, but the surface relative humidity was assumed to be 100 percent because snow lay on its surface, probably creating a local condition of saturation under the snow cover. When the temperature rose, the snow melted and surface relative humidity was definitely 100 percent. The potentials on both Zn/Au and Cu/Au cells reached initially high values and remained fairly steady, in agreement with the assumed condition of saturation, although there was again a tendency for potential from Cu/Au cells to decrease.

Figure 6 is a typical record for a period of dew formation when the ambient temperature was falling slowly and the surface temperature continuously about 2 deg lower, in contrast with conditions during rainfall or snowfall. Consequently, the surface relative humidity was 100 percent, while the ambient relative humidity varied between 90 and 97.5 percent. Under these conditions the surface temperature is below the dew-point temperature and water vapor condenses on the surface. This represents a nonequilibrium

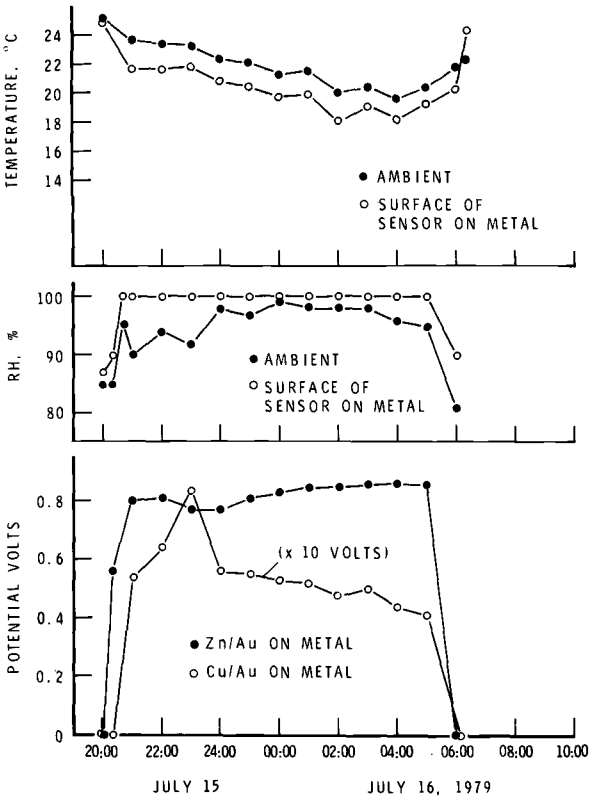

FIG. 6—*Record for interval of dew, Ottawa.*

state. Under these conditions the potential generated by the Zn/Au cell was fairly steady at about 0.8 V. The Cu/Au cell reached a high value of 0.085 V at the beginning but decreased with time to 0.04 V. In the period of dew formation a potential was recorded during most of the interval.

The results obtained for a period of hoarfrost formation are similar to those for dew formation, as shown in Fig. 7. The surface temperature was generally 2 deg C lower than the ambient temperature, but the ambient temperature decreased from −10 to −18°C. Under these conditions the relative humidity at the surface reaches 100 percent and water condenses (as hoarfrost), although the ambient relative humidity is in the range of 85 to 95 percent. During this interval, the potential recorded by the Zn/Au cell rose rapidly to a value of 0.45 V, decreasing to a value of 0.1 V in 14 h, and the Cu/Au cell recorded initially 0.095 V, decreasing to 0.025 in the same period. Under these conditions the Cu/Au cell started at nearly its highest possible potential (roughly one tenth of that produced by the Zn/Au cell). This is in contrast with what appears to happen at temperatures above freezing when

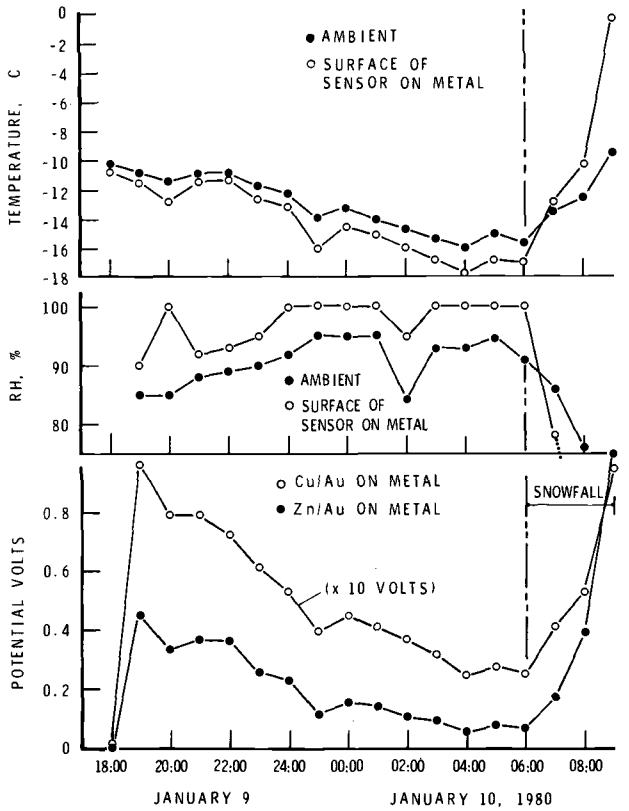

FIG. 7—*Record for interval of hoarfrost, Ottawa.*

dew is forming and the Zn/Au cell is relatively more sensitive (Fig. 6). This, however, has no significant effect on the measured time-of-wetness, as will be shown.

The results in Fig. 7 and those shown in Table 1 confirm that both Zn/Au and Cu/Au cells will develop a potential whether their temperature is above or below freezing, that is, 0°C. In Table 1 it is evident that for the winter months in Ottawa over 80 percent of the time-of-wetness occurred at temperatures below 0°C. For the month of February 1979 about 5 percent of the recorded time-of-wetness occurred at or below a temperature of −30°C. These observations confirm earlier findings [*15*] that films of water or solution on the surface do not freeze as bulk water does, but continue to serve as an electrolyte for the galvanic cell.

In general, the surface temperature is lower than the ambient temperature for an average of 83 percent of the time, but for plastic panels this value is 95 percent (Table 1). The temperature of the surface of metal panels was 2 to 4 deg C lower than the ambient temperature for an average of 13.2 percent of

TABLE 1—*Record of temperatures during time-of-wetness at Ottawa.*

Year and Month	Panel Sensor[a]	% T-O-W[b]	Lowest Temperature, °C, for <5% T-O-W	% T-O-W for Interval Below 0°C	Lowest Δt °C (Panel-Air) During T-O-W	% T-O-W for Interval in Previous Column	% T-O-W for $\Delta t < 0$°C[c]
1978							
Sept.	P-Cu/Au	36.1	−2	2.5	−2 to −4	35.4	93.8
Sept.	M-Cu/Au	28.3	0	1.7	−2 to −4	15.3	86.8
Sept.	M-Zn/Au	30.5	0	1.6	−2 to −4	14.6	85.3
Nov.	P-Cu/Au	22.4	−8	38.3	−4 to −6	2.3	93.3
Nov.	M-Cu/Au	14.7	−4	19.5	−2 to −4	15.7	88.8
Nov.	M-Zn/Au	13.2	−4	15.0	−2 to −4	14.1	91.0
1979							
Jan.	P-Cu/Au	25.0	−16	88.0	−2 to −4	5.8	76.8
Jan.	M-Cu/Au	21.9	−14	84.6	−2 to −4	2.9	73.1
Jan.	M-Zn/Au	24.8	−10	87.5	−2 to −4	2.4	70.7
March	P-Cu/Au	38.2	−12	51.4	−4 to −6	4.3	89.2
March	M-Cu/Au	25.9	−12	45.6	−2 to −4	17.8	83.5
March	M-Zn/Au	20.4	−10	36.6	−2 to −4	16.6	82.2
May	P-Cu/Au	28.6	0	3.8	−4 to −6	0.8	96.6
May	M-Cu/Au	22.5	2	1.0	−2 to −4	8.9	89.6
May	M-Zn/Au	23.8	2	0.6	−2 to −4	8.3	88.2
July	P-Cu/Au	26.2	8	0	−4 to −6	4.6	97.3
July	M-Cu/Au	21.8	10	0	−2 to −4	22.6	91.2
July	M-Zn/Au	18.6	10	0	−2 to −4	23.1	90.6
Sept.	P-Cu/Au	31.1	−2	15.3	−4 to −6	11.2	96.9
Sept.	M-Cu/Au	16.5	−2	13.4	−2 to −4	36.9	88.0
Sept.	M-Zn/Au	23.7	−2	12.2	−2 to −4	37.4	89.0
Nov.	P-Cu/Au	38.2	−6	37.9	−4 to −6	0.9	92.6
Nov.	M-Cu/Au	33.9	−4	29.9	−2 to −4	2.2	79.3
Nov.	M-Zn/Au	29.6	−4	33.6	−2 to −4	3.8	85.7
1980							
Jan.	P-Cu/Au	31.2	−20	87.3	−4 to −6	2.6	78.0
Jan.	M-Cu/Au	25.5	−18	86.6	−2 to −4	4.7	84.1
Jan.	M-Zn/Au	16.8	−16	81.8	−2 to −4	3.6	70.8

[a] P = clear plastic; M = metal.
[b] T-O-W = time-of-wetness.
[c] $\Delta t < 0$°C = panel temperature lower than ambient.

TABLE 2—*Frequency distribution of levels of potential for individual sensors, July 1979, Ottawa, Ont.*

Zn/Au Sensors			Cu/Au Sensors		
Designation	0.1 V	0.2 V	Designation	0.01 V	0.02 V
B4-1	18.64[a]	17.76	CA-1	21.86	20.66
B4-4	21.03	19.99	CA-2	21.40	20.47
B4-11	20.10	18.98	CN-2	22.25	20.42
B4-24	19.76	19.14	. . .	. . .	. . .
Avg	19.88	18.97	Avg	21.84	20.52

[a] Percent time when a given potential in volts is exceeded.

the time. The temperature of the surface of the plastic panels was 4 to 6 deg C lower than ambient temperature for an average of 5.0 percent of the time.

Although there were variations in the time-of-wetness for any one month, as recorded by a single Cu/Au or Zn/Au cell on metal, the annual time-of-wetness for the period August 1978 to August 1979 was 21.92 percent for the Cu/Au sensor and 21.89 percent for the Zn/Au sensor. For the same period, the Cu/Au sensor on plastic gave a value of 28.93 percent. To illustrate the

TABLE 3—*Monthly frequency distribution of levels of potential, using average values from 3 or 4 sensors (percent time when a given potential is exceeded).*

	Zn/Au Sensors		Cu/Au Sensors	
Month	0.1 V	0.2 V	0.01 V	0.02 V
1978				
Aug.	19.07	18.12	19.50	18.25
Sept.	29.82	29.13	27.63	26.12
Oct.	20.81	19.84	20.43	18.41
Nov.	13.82	13.15	15.96	13.70
Dec.	35.60	23.06	19.77	13.96
1979				
Jan.	25.12	18.27	21.05	14.36
Feb.	15.77	13.77	21.95	17.52
March	20.85	19.27	29.20	25.64
April	20.92	20.11	22.47	20.57
May	25.39	24.79	23.70	22.75
June	22.38	21.75	23.28	21.99
July	19.88	18.97	21.84	20.52
Aug.	28.91	27.91	30.16	28.97
Sept.	25.56	24.86	26.32	25.16
Oct.	38.27	35.06	35.80	32.58
Nov.	33.60	31.00	34.16	26.17
Dec.	28.33	25.73	25.94	19.56
Avg	24.94	22.63	24.65	21.54

reproducibility of individual sensors, data are presented from four sensors using Zn/Au cells and three sensors using Cu/Au cells (Table 2). The variation between sensors was not large, and good agreement was obtained between the two sets even on a monthly basis.

Table 3 lists the average monthly values (as percent time a given potential level is exceeded) from three or four sensors. These results show that potential levels of 0.1 or 0.2 V for Zn/Au cells and 0.01 or 0.02 V for Cu/Au cells can be used to indicate the time-of-wetness with an agreement of better than 10 percent. The variation between the two types of cells at 0.1 and 0.01 V or 0.2 and 0.02 V is between 1 and 5 percent for a period of 17 months.

Distribution of Ambient Relative Humidity, Potentials Measured by Moisture Sensors, and Resulting Correlation

The current program was designed to determine whether a simple relation exists between the potential generated by the sensors and ambient relative humidity. This assumes that the surface temperature is not too different from the ambient temperature, and that a certain pseudo-equilibrium exists between ambient and surface conditions. These assumptions are based on previous work in which it was observed that the percent time during which the potential from a platinum foil on zinc plate sensor exceeded 0.2 V corresponded to percent time during which the ambient relative humidity was above a critical value depending on site (in the range of 80 to 89 percent) [*3–16*].

Some results obtained from exposure sites in Ottawa, Ont., Thousand Oaks, Calif., and Cleveland, Ohio, as part of the round-robin test, are presented in Figs. 8 to 12. Each figure comprises three graphs coordinated to show the distribution of ambient relative humidity, distribution of measured potential, and the resulting correlation of potential with relative humidity. Figures 8 and 9 include data for both Zn/Au and Cu/Au cells. The characteristic distribution curves for potential are somewhat different for conditions above freezing (Fig. 8 for July) and conditions below freezing (Fig. 9 for January). These curves are also different for sensors mounted on plastic panels and metal panels.

The correlation curves for potential versus relative humidity are different for each month and for each type of panel. Attempts to obtain a single relation were not successful. The records from Thousand Oaks, Calif., for June and August (Fig. 10) and for October, November, and December (Fig. 11) and those from Cleveland, Ohio, for January, April, and June (Fig. 12) demonstrate how the monthly changes in ambient relative humidity conditions influence the distribution of potential generated by the Zn/Au sensor mounted on metal panels. These are major changes that greatly influence the apparent correlation of potential versus relative humidity. In Cleveland the sensor indicated a potential for the month of June at an ambient relative

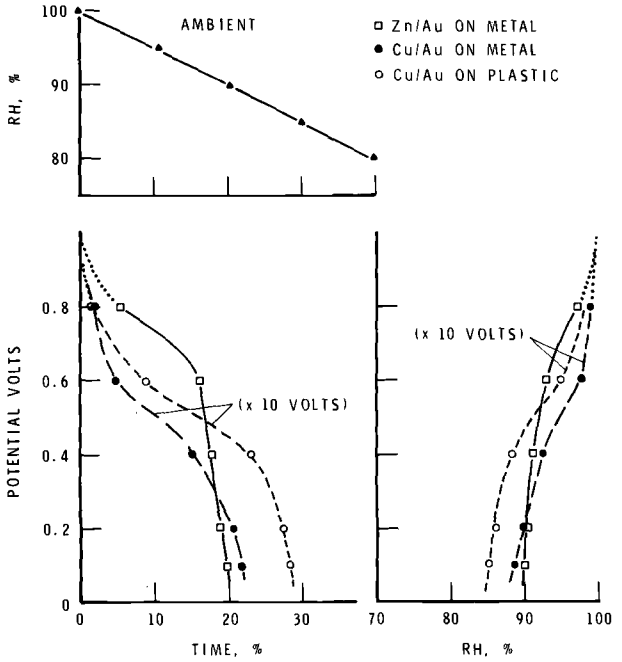

FIG. 8—*Record for July 1979, Ottawa.*

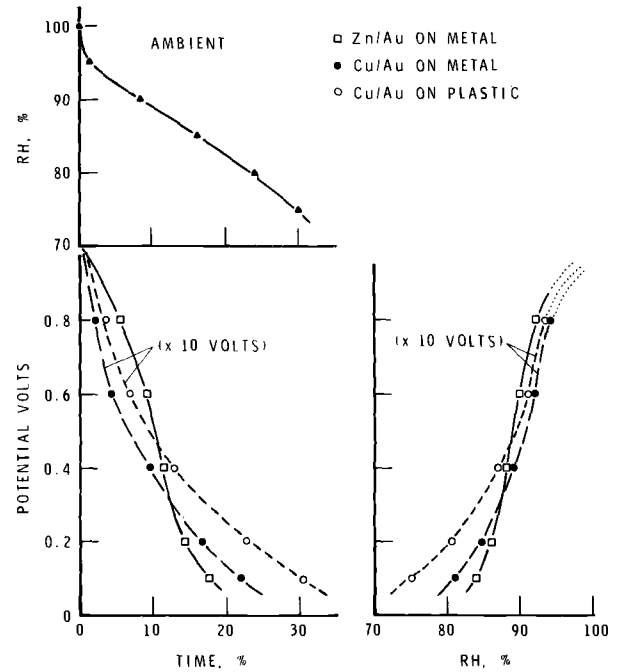

FIG. 9—*Record for January 1980, Ottawa.*

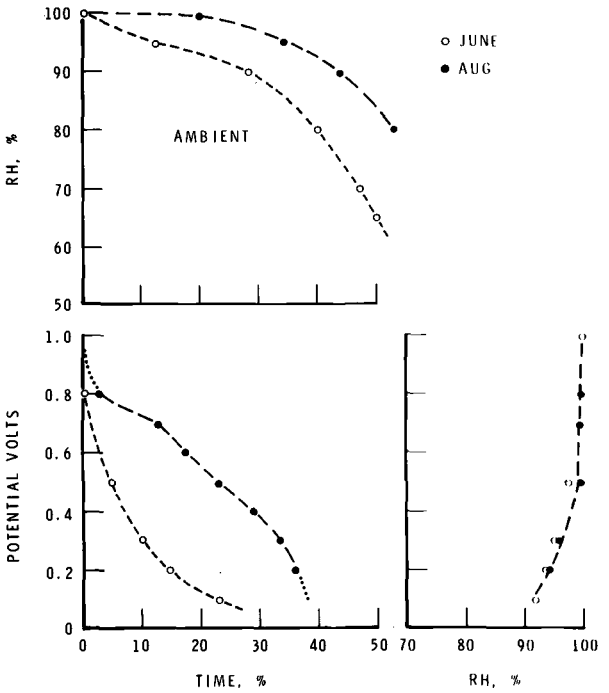

FIG. 10—*Record for June and August, Rockwell International Science Center, Thousand Oaks, Calif.*

humidity below 70 percent, whereas in January it indicated a potential only when the ambient relative humidity was over 95 percent (Fig. 12). A similar result was obtained for November in Thousand Oaks, Calif. (Fig. 11).

The explanation of these results can be found in the distribution of relative humidity for each month. In January in Cleveland the relative humidity was above 97 percent for 40 percent of the time, and in November in Thousand Oaks it was above 95 percent for 30 percent of the time. Under such conditions the surface temperature would be nearly the same as the ambient, as shown in Figs. 4 and 5. Atmospheric conditions for the month of June in Cleveland dictated that the ambient relative humidity was above 80 percent only 5 percent of the time, as may be seen in Fig. 12. Under such dry conditions it is expected that most of the potential recorded represented periods of dew formation (Fig. 6), when the surface temperature is lower than ambient by as much as 2 deg (this is often below the dew-point), representing non-equilibrium conditions resulting in condensation. Thus a potential was recorded although the ambient relative humidity was below 70 percent. The two correlations of potential versus relative humidity for the months of January and June in Cleveland represent the two extreme atmospheric conditions encountered in this program. Otherwise, the conditions were intermediate, with a mixture of periods of high ambient humidity (for example,

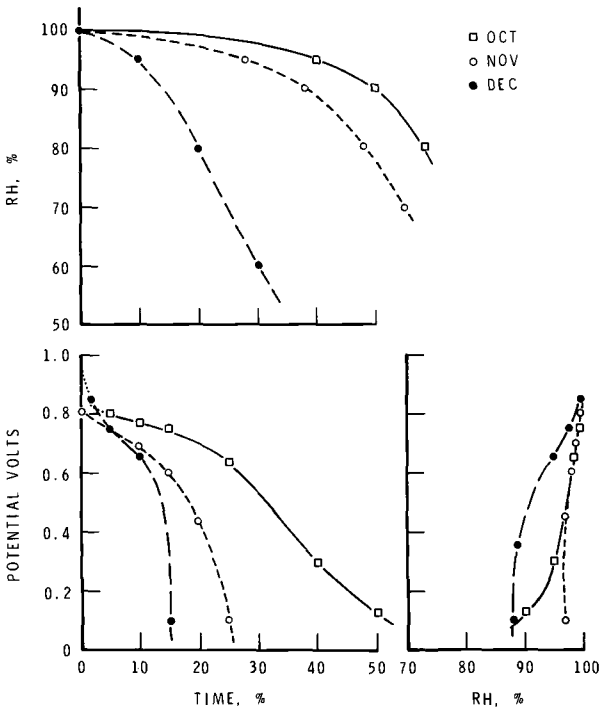

FIG. 11—*Record for October (1–18), November, and December 1978, Rockwell International Science Center, Thousand Oaks, Calif.*

during rainfall) and conditions of surface condensation during lower levels of ambient relative humidity owing to surface temperatures lower than ambient temperatures.

Surface Temperature of Base Panel and That of Sensor

It is clear that surface temperature relative to ambient is a very important parameter in determining time-of-wetness. Temperature differences between sensor and base are given in Table 4. The temperature of the sensor was, on the average, higher by 0 to 0.5 deg C for 13 percent of the time on a metal base and lower by 0 to 0.5 deg C about 84 percent of the time. For this reason, condensation usually occurs first on the sensor. The temperatures plotted in Figs. 4 to 7 are those for the sensor since they are more directly related to the recorded time-of-wetness. This could not be done for all the data given in Table 1 because the thermocouples were installed on the sensors only during the latter part of the program.

When a sensor was mounted on a plastic base, the sensor temperature was lower by 0 to 0.5 deg C with respect to the temperature of the base for 57 percent of the time and higher for 43 percent of the time. This was so because the thermal characteristics of the sensor are similar to those of the plastic base on which it was mounted, and the net gain or loss of heat for the system

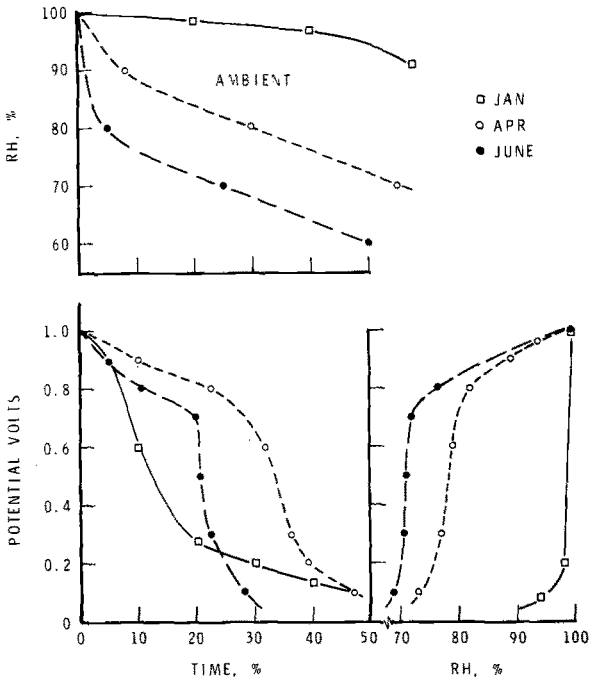

FIG. 12—*Record for January, April, and June 1979, Republic Steel Research Center, Cleveland, Ohio.*

was nearly equal. This is in contrast with the case where the sensor is mounted on a metal plate, as discussed earlier. It is desirable that the sensor not disturb the thermal regime of the surface, an objective that can be approached when the sensor is very thin. New sensors are now made only 0.1 mm thick and should respond quickly to surface temperature changes, decreasing to a minimum any temperature difference between sensor and base.

Conclusions

1. New miniature sensors provide a reasonable indication of surface wetness; sensors using Zn/Au and those using Cu/Au cells are equally effective.
2. Temperature of an exposed surface may be different from that of air; if it is lower, condensation can occur when the relative humidity of the air is not at saturation. The temperature difference depends on the character of the surface and the weather conditions.
3. The time-of-wetness of a surface will vary not only from one locality to another and from one month or year to another, but also with type, size and orientation of specimen exposed to a given atmosphere.
4. When sensors are used to indicate surface conditions, they must be small and thin to minimize temperature difference.
5. There is no unique relation between the potential developed by these sensors and ambient relative humidity.

TABLE 4—*Percent time when value of temperature difference between sensor and base is in range denoted.*

	Zn/Au Sensor on Metal Base		Cu/Au Sensor on Metal Base		Cu/Au Sensor on Plastic Base	
1979	0 to +0.5°C	0 to −0.5°C	0 to +0.5°C	0 to −0.5°C	0 to +0.5°C	0 to −0.5°C
June	13.7	86.0	14.4	85.1	37.9[a]	45.0
July	12.7	86.7	11.0	88.8	35.4	50.2
Aug.	10.4	88.5	10.5	88.2	27.2	60.2
Sept.	21.8	70.9	23.1	71.5	33.9	49.4
Oct.	9.6	89.3	10.0	88.7	21.4	70.6
Nov.	15.3	82.1	18.7	77.7	23.3	66.5
Dec.	14.7	84.0	15.8	83.3	23.2	62.1
1980						
Jan.	12.8	82.8	7.1	89.7	29.5	58.0
Feb.	9.0	89.7	8.4	87.6	40.8	48.4
Avg	13.3	84.4	13.2	84.5	30.3	56.7

[a] The remainder of time the difference was greater than +0.5°C.

Acknowledgment

The authors wish to acknowledge, with thanks, the contribution of F. C Livermore and B. K. MacLaurin of Bell Northern Research Laboratories in the development and fabrication of the sensors. Credit is due to Rockwell International Science Center, Thousand Oaks, Calif., especially F. Mansfeld, and to Republic Steel Research Center, Cleveland, Ohio, especially Edward C. Rhea (now with Reynolds Metals), for participating in the ASTM round-robin and for collecting and analyzing the data included.

This paper is a contribution from the Division of Building Research, National Research Council of Canada, and is published with the approval of the director of the Division.

References

[*1*] Sereda, P. J., American Society for Testing and Materials Bulletin No. 228, Feb. 1958, pp. 53–55.

[*2*] Sereda, P. J., American Society for Testing and Materials Bulletin No. 238, May 1959, pp. 61–63.

[*3*] Sereda, P. J., American Society for Testing and Materials Bulletin No. 246, May 1960, pp. 47–48.

[*4*] Sereda, P. J., *Industrial and Engineering Chemistry,* Vol. 52, No. 2, Feb. 1960, pp. 157–160.

[*5*] Guttman, H. and Sereda, P. J. in *Metal Corrosion in the Atmosphere, ASTM STP 435,* American Society for Testing and Materials, 1968, pp. 326–359.

[*6*] Guttman, H. in *Metal Corrosion in the Atmosphere, ASTM STP 435,* American Society for Testing and Materials, 1968, pp. 223–239.

[*7*] Haynie, F. H. in *Durability of Building Materials and Components, ASTM STP 691,* American Society for Testing and Materials, 1980, pp. 157–179.

[*8*] Tomashov, H. D., Berukshtis, G. K., and Lokotilov, A. A., *Zavodskaia Laboratoriia,* Vol. 22, 1956, pp. 345–349.

[*9*] Kucera, V. and Mattsson, E. in *Corrosion in Natural Environments, ASTM STP 558,* American Society for Testing and Materials, 1974, pp. 239–260.

[*10*] Kucera, V. and Mattsson, E. in *Proceedings,* Seventh Scandinavian Corrosion Congress (7 NKM), Trondheim, Norway, May 1975, pp. 202–217.

[*11*] Kucera, V. and Collin, M. in *Proceedings,* European Congress on Metallic Corrosion, London, Sept. 1977, pp. 189–196.

[*12*] Mansfeld, F. and Kenkel, J. V., *Corrosion Science,* Vol. 16, 1976, pp. 111–122.

[*13*] Mansfeld, F. and Kenkel, J. V. in *Proceedings,* Corrosion/77, The International Corrosion Forum, San Francisco, Calif., March 1977, Paper No. 134.

[*14*] Hagenrud, S. in *Extended Abstracts of the 154th Electrochemical Society Meeting,* The Electrochemical Society Inc., Princeton, N. J., Vol. 78-2, 1978, pp. 327–328.

[*15*] Strekalov, P. V., Mikhailovoskii, Yu N., and Donilova, M. W., *Protection of Metals,* Vol. 14, No. 3, May–June 1978, pp. 195–199.

[*16*] Sereda, P. J. in *Corrosion in Natural Environments, ASTM STP 558,* American Society for Testing and Materials, 1974, pp. 7–22.

DISCUSSION

S. C. Byrne[1] (*written discussion*)—The time-of-wetness gage should be drastically affected by hydroscopic or other properties of corrosion products which, in turn, should be affected by atmospheric composition. Has any work been planned to further define the role of atmospheric composition in determining time-of-wetness?

P. J. Sereda (*authors' closure*)—The time-of-wetness, as defined by a minimum level of potential (representing the current generated by the galvanic cell) is affected by surface contaminants resulting from deposition of atmospheric pollutants on the sensor. However, the surfaces where corrosion is being monitored are also exposed to the same contaminants, which, in turn, affect the deposition of films of moisture to foster the process of corrosion. Work is needed to measure the microenvironment at corroding surfaces.

F. Mansfeld[2] (*written discussion*)—1. The difference in the response of your sensor and our ACMs could be related to the different sensitivity of the device. You measure the voltage drop across a very large resistor which is due to galvanic current flow. However, this voltage drop separates the two electrodes and you cannot measure the maximum galvanic current which one would measure with a zero resistance ammeter.

2. Another reason for different sensitivity is that the gold electrode in your sensor does not form corrosion products which would condense moisture and lead to current flow. The zinc electrode could be wet, while the noble electrode (Pt/Au) is still dry.

3. Despite the fact that different designs of time-of-wetness t_w sensors measure different t_w-values at a given test site, do you think that one could use a sensor of constant design to compare different test sites?

P. J. Sereda (*authors' closure*)—1. The statement is true, but what is significant is to have adequate sensitivity to detect films of moisture which correspond to or foster practical rates of corrosion.

2. This paper presents results showing that sensors detect condensing films of water because the surface temperature is often below the ambient and at or below the dew point. Under these conditions, corrosion products are not required to condense water on any surface. Furthermore, it is not the corrosion products only, but more likely the deposited contaminants from the atmosphere (ions of Cl^-, $SO_4^=$, etc.) deposited on all surfaces which would depress the vapor pressure of water and form solutions below 100 percent relative humidity that contribute to galvanic current, and are detected as the time-of-wetness.

[1] Alcoa Laboratories, Alcoa Center, Pa.
[2] Rockwell International Science Center, Thousand Oaks, Calif.

3. Conclusions 3 and 5 of the text are an answer to this question. Whatever sensor is used, provided it is small enough to respond to ambient temperature changes in the same way as a given specimen surface, it will give different values for the time-of-wetness for different type, size, and orientation of specimens exposed to a given atmosphere. In other words, there is not a unique value of the time-of-wetness for a given site; thus comparison of the time-of-wetness of different sites is valid only for identical specimens exposed in the same way at the different sites. Recent work by our institute has shown that two identical plastic specimens exposed side by side, one oriented vertically and the other horizontally, recorded the time-of-wetness (using our miniature sensors described in the paper) in the ratio of 1 : 1.7.

F. H. Haynie[1]

Evaluation of the Effects of Microclimate Differences on Corrosion

REFERENCE: Haynie, F. H., **"Evaluation of the Effects of Microclimate Differences on Corrosion,"** *Atmospheric Corrosion of Metals, ASTM STP 767,* S. W. Dean, Jr., and E. C. Rhea, Eds., American Society for Testing and Materials, 1982, pp. 286–308.

ABSTRACT: Analytical and statistical analyses of data obtained from a contracted exposure study performed by Rockwell International in St. Louis, Mo. reveal that many microclimate differences can account for observed differences in corrosion behavior within a geographic region. Data from Mansfeld's Atmospheric Corrosion Monitors (ACM's) were evaluated with data from the Regional Air Monitoring System (RAMS). Relative humidity, temperature, wind speed, and levels of total sulfur gases such as sulfur dioxide and oxides of nitrogen were found to be statistically significant variables. Problems of covariance were avoided by partitioning the large data set into subsets.

Relative humidity was found to be the most important but least accurate variable. Because it is seldom measured at exposure sites, an equation was developed to relate site-to-site relative humidity differences to temperature differences. With average relative humidity and another empirical equation, time-of-wetness can be estimated. The results are in good agreement with time-of-wetness from the ACM's.

KEY WORDS: atmospheric corrosion, climate, pollution, measurement, statistical analysis, zinc, steel, wind speed, temperature, relative humidity, time-of-wetness, sulfur dioxide, nitrogen oxide

In 1974 the Environmental Protection Agency (EPA), through Rockwell International as a prime contractor, established a Regional Air Monitoring System (RAMS) to develop and validate regional air quality simulation models. This 25-station network in the St. Louis, Mo. area was one of the most sophisticated of its type. Data from continuous gaseous air pollution monitors and meteorological sensors were recorded in a central computer. Considerable effort was devoted to assuring the quality of the data [*1*].[2]

Other types of studies were done in the St. Louis area to take advantage of this unique system. Among them was a study of the effects of pollutants on materials [*2*]. Materials were exposed for periods of from 3 to 30 months and were evaluated for cumulative damage after exposure. The establishment

[1] Rockwell International Science Center, Creve Coeur, Mo.

[2] The italic numbers in brackets refer to the list of references appended to this paper.

of relationships between damage and environmental conditions was limited to multiple regression of the damage values with long-term averages of the RAMS data [*2*].

Although long-term averages of collected data have a much higher probability of being closer to a true mean than do individual values or short-term averages, there are disadvantages in using them to analyze for functional relationships. There can be bias in validation procedures that preclude certain types of suspect data. More important, the number and range of values are drastically reduced.

In 1976, continuous Atmospheric Corrosion Monitors (ACM's) were placed at four sites and the data from these devices were continuously recorded in the central computer. These monitors were galvanic cells of copper/zinc and copper/steel as described by Mansfeld [*3*]. The output from the instrumentation to the computer was a voltage proportional to the logarithm of the measured cell current. For the fall of 1976, a period when the RAMS data were considered to be most valid, a data tape of hourly averages of the ACM outputs was created. These values are proportional to the geometric mean of the cell current. Hourly averages of the continuously monitored RAMS data that have been subjected to several stages of validation are on file. Combining these data creates a file of over 2000 sets having a much wider range of values than do long-term averages.

This paper analyzes this set of data to associate corrosion behavior with observed microclimate differences at the four sites and the changes in microclimates with time.

Validation and Treatment of Data Types

Multiple-regression analysis techniques are based on the assumptions that "independent" variables are fixed and not covariant. In essence, the values upon which the dependent variables are regressed are assumed to be error-free and not related to each other. In the real world of meteorological and pollution data, neither of these assumptions is true. Thus, it is prudent to analyze each data type independently to determine the relative magnitude and causes of error, then analyze for covariance before multiple-regression analysis is performed. Also, the recorded data for each type need to be converted to units that make scientific as well as mathematical sense in a statistical relationship.

There are three basic types of data in this set: (1) ACM response, (2) meteorological data, and (3) gaseous pollution data. Each of these types will be discussed separately.

ACM Response

ACM's consisting of galvanic cells of alternating plates of copper and zinc separated by sheets of plastic insulators were exposed to the atmosphere at Sites 103 and 106 within the urban area of St. Louis. When an electrolyte

bridges the exposed plate edges, the galvanic potential between the copper and zinc creates a current. The amount of current is a function of the amount and type of electrolyte on the surface, as well as other factors.

Similar ACM's of copper and steel were exposed at Sites 112 and 122. Site 112 is within the beltline of St. Louis but up prevailing wind from the center of the city. Site 122 is approximately 40 km north of center city.

The instrumentation at each site was such that a logarithmic conversion of the current produced a 1-V change in output for each decade change in current. With a positive 2-V offset to prevent the recording of negative numbers, the output of the instrumentation at μA current was 2 V (Fig. 1).

Figure 1 shows histograms of the recorded data for the four sites. At each site there appears to be a bimodal distribution of values: one large mode at the low end for a dry surface, and the other small one at the high end for a com-

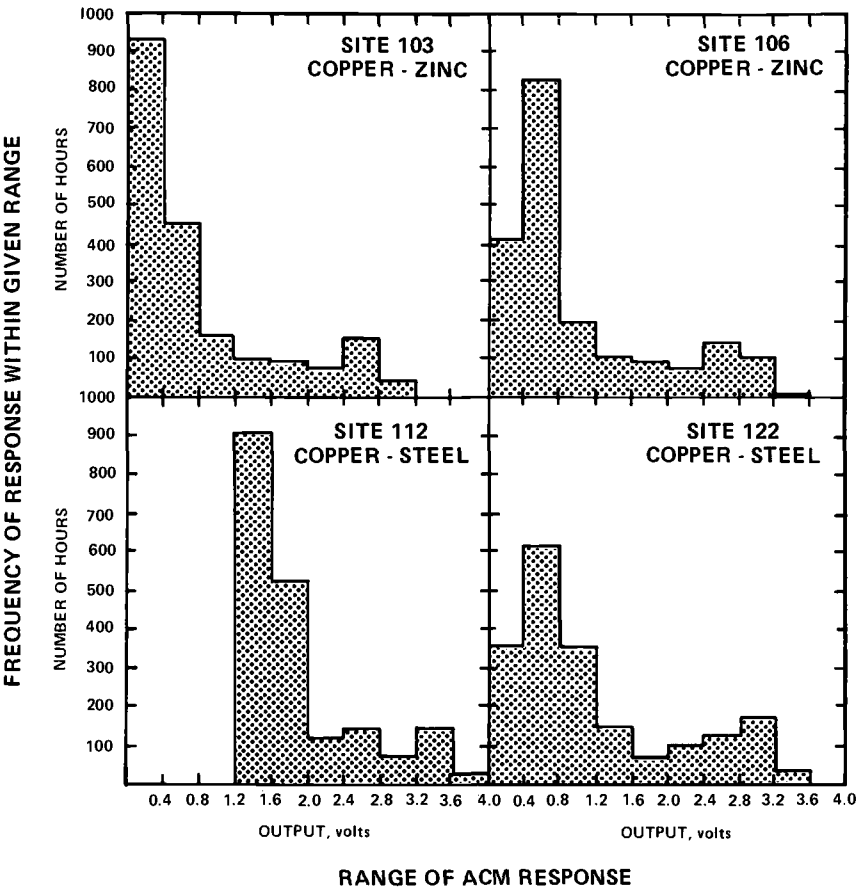

FIG. 1—*Distributions of Atmospheric Corrosion Monitor response at four sites. (One volt equals one decade of galvanic current—from 0.01 μA to 100 μA for 4 V.)*

pletely wet surface. The current measured when the surface of the ACM is dry is due to the background current of the ACM amplifiers. The current at the high end is the result of galvanic corrosion. In between the two modes, the current measures corrosion related to the moisture on the ACM surface.

The background current has a much higher value at Site 112 than for the other three sites. The values of the upper modes that are associated with corrosion are more comparable between sites and types of ACM's. Because corrosion is the parameter to be studied, the background current must be subtracted from the total current to get corrosion currents.

The most obvious response of the ACM's is to changes in relative humidity. When the ambient relative humidity is low and not changing, the measured current should be the background current. The mass and geometry of the ACM's are such that the response may lead or lag ambient changes. For example, moisture collected on the surface takes time to evaporate after there has been a lowering of the ambient relative humidity. It is, thus, possible to have the surface wet with a corrosion current being generated at the same time that the ambient relative humidity is relatively low. In addition, as will be discussed later, the determination of relative humidity is subject to considerable error.

Three different techniques were used to calculate background current: (1) average of values around the lower mode, (2) average of values occurring at relative humidities below 40 percent, and (3) the zero intercept of a linear regression of current on relative humidities below 50 percent. A conversion of these data to equivalent corrosion rates for zinc and steel was made using the following factors: (1) exposed areas of zinc and steel, respectively, of 4.3 and 3.5 cm^2, and (2) respective conversion factors (from electrochemical equivalence) of 14.96 and 11.62 μm/year for each $\mu A/cm^2$ measured on zinc and steel. The converted results are presented in Table 1.

With the exception of Site 112, all of the values are small and relatively consistent. Even Site 112 is small when compared with upper-mode values.

The regression intercepts were taken as background current to calculate a baseline for zero corrosion. The measured current above these values was converted to corrosion rates for each hour at each site. In Table 2, averages of these data for the entire exposure period are compared with corrosion rates calculated from weight loss data for weathering steel and galvanized steel

TABLE 1—*Background current as corrosion rate, μm/year.*

Site	Mode Avg	Avg Below 40 RH	RH Regression Intercept
103	0.073	0.077	0.056
106	0.087	0.097	0.080
112	1.084	1.403	1.518
122	0.082	0.082	0.051

TABLE 2—*Comparison of calculated corrosion rates.*

		Corrosion Rates, μm/year		
			Weight Loss	
Site	Metal	ACM	Mean	Standard Deviation
103	zinc	2.146	0.655	0.028
106	zinc	3.236	0.738	0.014
112	steel	10.992	3.607	0.541
122	steel	5.221	7.852	0.767

over the same period [*2*]. These values are consistent considering the differences between materials and geometry of specimens.

ACM response has been used to estimate time-of-wetness. Because the response is a continuum of values between two modes rather than two values, time-of-wetness must be defined with respect to some value in between the two modes. The surface is considered wet when the selected value is exceeded. The value should be high enough so as not to be influenced by error in the background or leakage current, yet low enough to account for most of the corrosion. Table 3 shows how percentages of corrosion and time above a stated value of corrosion rate vary with that value for the four sites. At Site 103, for example, 91.1 percent of the corrosion occurs when the corrosion rate exceeds 0.5 μm/year. That corrosion rate is exceeded only 23.5 percent of the time. Below a corrosion rate of 1.5 μm/year the percentage of time increases disproportional to the increases in percentages of corrosion. This is an indication of the distribution of values around the background current mode. Above a corrosion rate of 1.5 μm/year, values are not appreciably affected by variations in background current and the ACM's are considered to be wet. Based on regressions of data in Table 3, best estimates of the percentage of time the surfaces of the ACM's were wet are presented in Table 4.

These data in Table 4 show that not only is the difference between steel and zinc ACM's highly significant, but also that the differences between sites are statistically significant. These results are indicative of environmental differences and differences in hygroscopicity of corrosion products on the surfaces formed at different test sites.

Meteorological Data

Of several types of meteorological data recorded at each site, three are believed to significantly affect the corrosion rate at any given time. These three are (1) wind speed, (2) temperature, and (3) dew point.

Wind Speed—Wind speed was measured at the top of 30-m towers at each of the four sites. The materials including the ACM's were exposed at approximately 3 m from the ground. The flux of reactants to the ACM surface is

TABLE 3—*Percent of corrosion and time when stated corrosion rate is exceeded.*

Corrosion Rate, μm/year	Site 103		Site 106		Site 112		Site 122	
	Corrosion	Time	Corrosion	Time	Corrosion	Time	Corrosion	Time
0.5	91.1	23.5	94.5	25.9	99.8	34.2	96.8	31.2
1.0	89.8	19.9	93.6	21.9	99.4	29.3	96.1	26.3
1.5	88.5	17.7	92.9	20.0	99.1	26.9	95.5	23.9
2.0	87.5	16.4	92.1	18.4	99.0	25.8	95.2	22.9
2.5	86.1	15.1	91.4	17.4	98.8	24.9	94.9	22.2
3.0	84.9	14.2	90.7	16.8	98.5	23.8	94.6	21.6

TABLE 4—*Percent of time when wet.*

Site	ACM	Best Estimate	Standard Deviation
103	cu/zn	18.42	0.29
106	cu/zn	20.69	0.40
112	cu/steel	28.21	0.54
122	cu/steel	25.33	0.61

controlled by turbulent diffusion. The magnitude of eddy diffusion is related to the wind shear at the ACM surface. The wind shear at the ACM is a function of the wind speed at the level of the ACM, which in turn is a function of the wind speed at 30 m.

From theoretical considerations [*4*] it is assumed that wind velocity variation with height from the ground and distance from the ACM obeys the relationship

$$v^+ = 3.8 + \frac{1}{3.6} \ln S^+ \tag{1}$$

where

$$v^+ = \frac{v}{v^*} \text{ and } S^+ = \frac{v^* S}{\nu}$$

and

v = wind velocity,
v^* = "friction velocity" = $\sqrt{\tau/\rho}$,
S = height,
ν = kinematic viscosity,
τ = shear, and
ρ = density.

Based on an analogy between mass and momentum transfer in turbulent flow [*5*], the deposition velocity may be expressed as

$$u = \frac{v^{*2}}{v} \tag{2}$$

where

u = deposition velocity,
v = wind speed near ACM, and
v^* = friction velocity near ACM.

With Eq 1, the wind velocity at a height of 30 m, and a kinematic viscosity for air of 0.15 cm^2/s, the friction velocity can be determined and subsequently the wind speed near the ACM. Assuming a distance of 10 cm from the ACM,

the friction velocity near the specimen and the deposition velocity can be calculated.

The form of the equation requires a trial-and-error solution. This was done for a range of wind speed values and the results were fitted to the following empirical equation

$$u = 0.3025\ [v - 0.1875v^{0.9275}]^{0.754} \tag{3}$$

where u is the deposition velocity in centimetres per second and v the wind speed at a height of 30 m in metres per second. Deposition velocity (u) is possibly an important factor affecting corrosion rate because pollutant flux is equal to the deposition velocity times the pollutant concentration.

Calculated values of u using Eq 3 and the RAMS data for wind speed range between 0.12 and 1.4 cm/s with most values between 0.3 and 1.0 cm/s. The averages of deposition velocity ranged from 0.504 cm/s at Site 122 to 0.787 cm/s at Site 103. These theoretically calculated values are consistent with experimentally determined values for gaseous pollutants [*6*].

Temperature—The ambient temperature data were most likely the most reliable of any of the measured variables. The instrumentation accuracy was ±0.05 deg C and, based on comparisons of the number of missing hourly averages after validation, the temperature instruments were the most reliable of all the instruments used at the RAMS sites. The fraction of valid hourly averages ranged from 0.9848 at Site 122 to 0.9995 at Site 103.

The data consist of minute averages of 120 half-second data readings. These minute averages were transmitted to the central computer for validation, storage, and hourly averaging.

Temperature affects corrosion rate through changes in kinetics and through changes in relative humidity which alter time-of-wetness. The effect on kinetics is expected to have an Arrhenius behavior and for that reason the temperature values were inverted using the relationship

$$E = \frac{1000}{T + 273.16} \tag{4}$$

where E is desired temperature parameter and T the hourly average temperature in degrees Celsius. The logarithm of the corrosion rate is expected to be linearly related to the negative of this parameter.

Dew Point—While the temperature data were the best of the RAMS data, the dew-point data were probably the worst. The claimed accuracy of the instrument was ±1 deg C. The instruments were very unreliable because of the accumulation of contaminants and moisture on the mirror used to sense dew formation. An attempt was made to eliminate this problem by drastically reducing the operating and sampling time. The instruments were operated for 5 min out of each 1/2 h. Thus, hourly averages consist of no more than averages of two sets of 5-min averages.

The validation procedure, although conceptually sound, created a highly

undesirable bias in the hourly averages. Data were rejected if the dew point exceeded the temperature by more than 1 deg C. This behavior is most likely to occur when the relative humidity is near its maximum. Thus, rejecting these data unrealistically lowers the average dew point. The percent of hourly average data thus validated is 85, 87, 85, and 98, for Sites 103, 106, 112, and 122, respectively.

Relative humidity as a proxy for time-of-wetness is the most important variable affecting atmospheric corrosion. In order to properly evaluate the effects of any other variables, the effects of relative humidity must be understood.

An empirical relationship for relative humidity as a function of temperature and dew point was obtained by curve-fitting table data [*7*]. The relationship is

$$RH = 100\ e^{-[6.32(T-D)/(80+T)]} \tag{5}$$

where

RH = relative humidity,
T = temperature, °C, and
D = dew point, °C.

Over the range of values observed in this study, Eq 5 gives the relative humidity within ±1 percent, which is probably lost in the error caused by the use of inaccurate dew-point data.

This equation and the hourly average data for temperature and dew point were used to calculate hourly average relative humidity. If the dew point exceeded the temperature or data were missing, the relative humidity was assumed to be 100 and flagged. For flagged relative humidities, the averages of relative humidities at the other three sites were calculated. If the average was equal to or greater than 85, the value was kept at 100. If the average was less than 85, the average replaced the 100. This procedure (1) gives values for missing data, (2) counteracts bias from the validation process, and (3) tends to normalize the data. It probably creates a lot of hourly averages of 100 which actually are within the range of 95 to 100.

Figure 2 is a comparison of the results between sites and with data from the National Weather Service Office at the St. Louis International Airport during the same period of exposure. The airport data are single observations at 3-h intervals. The number of observations is multiplied by three for comparison. Also shown is the number of hours at RH = 100 percent.

The behavior below 60 percent is relatively consistent. With the exception of Site 122 the hours at 100 percent are consistent. Site 122 had the least missing data and the highest number of values within the range of 95 to 100 percent. Other variations from site to site may be real or caused by dew-point error.

An analysis of variance of the relative humidity data showed that the vari-

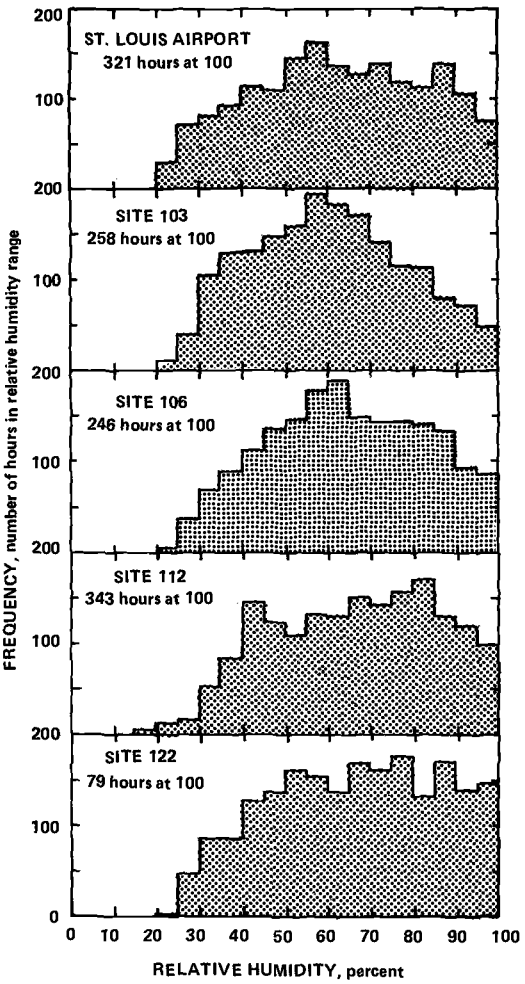

FIG. 2—*Comparison of relative humidity distributions in St. Louis.*

ables of site, day, and hour were all highly significant in increasing order. This type of behavior is expected and tends to validate the data.

In estimating time-of-wetness it is useful to know the fraction of time that some critical relative humidity is exceeded. Table 5 presents this type of data for the four sites and the airport. Also given are linear regression coefficients for each set of data.

These results and the percent-of-time-when-wet values from Table 4 can be used to estimate critical relative humidities. The respective critical relative humidities thus calculated for Sites 103, 106, 112, and 122, are 90, 91, 89, and 85. The overall best estimate of the standard deviation on each value is 0.8.

TABLE 5—*Percent of time stated relative humidity was equaled or exceeded.*

	Site				
RH	Airport	103	106	112	122
100	15.6	12.2	11.6	16.2	3.7
95	19.0	14.6	15.8	20.9	10.7
90	24.1	18.0	20.4	26.5	17.3
85	30.1	21.8	26.8	32.6	25.4
80	35.6	27.2	33.4	40.7	31.6
Intercept	116.86 ± 5.05	85.72 ± 5.72	119.88 ± 5.94	136.64 ± 6.58	144.64 ± 2.61
Slope	−1.02 ± 0.06	−0.74 ± 0.06	−1.09 ± 0.07	−1.21 ± 0.07	−1.41 ± 0.03

The only site that is significantly different from the others is Site 122. The critical relative humidities for the copper/steel ACM's at Sites 112 and 122 should be the same. This observed behavior and the significant difference in the number of hours at 100 percent relative humidity indicate that the upper end of the distribution at Site 122 is biased low.

The data in Tables 4 and 5 have a common variable, which is the percent of time a stated value is equaled or exceeded. Thus, any selected critical corrosion rate can be related to a critical relative humidity. Linear regressions were obtained for each site and comparisons were made for statistical differences. Sites 103, 106, and 112 were not statistically different but Site 122 was different from the others. This is demonstrated in Fig. 3, which shows that the 95 percent confidence limits on the true means of critical relative humidities mutually exclude the two regression lines. It appears that calculated relative humidities in the critical range at Site 122 are biased low by more than 5 percent.

Over 99 percent of the variability in the relative humidity frequency distributions for all sites shown in Fig. 2 can be explained by the empirical relationship

$$f = e^{-4.6[100\text{-}RH_{avg}/RH_{avg}][RH/100]^3} \tag{6}$$

where f is the fraction of time that relative humidity equals or exceeds the stated value and RH_{avg} is the average relative humidity.

This equation can be used to estimate the fraction of time a surface is wet if the critical relative humidity and the average relative humidity are known. Conversely, the average relative humidity can be estimated if the fraction of time when wet and critical relative humidity, as represented by RH in Eq 6, are known. Table 6 is a comparison of values calculated from data in Table 4 assuming a critical relative humidity of 90 percent with average of calculated data shown in Fig. 2.

Within the same air mass, one would expect the average relative humidity to be inversely related to average temperature from site to site in a functional

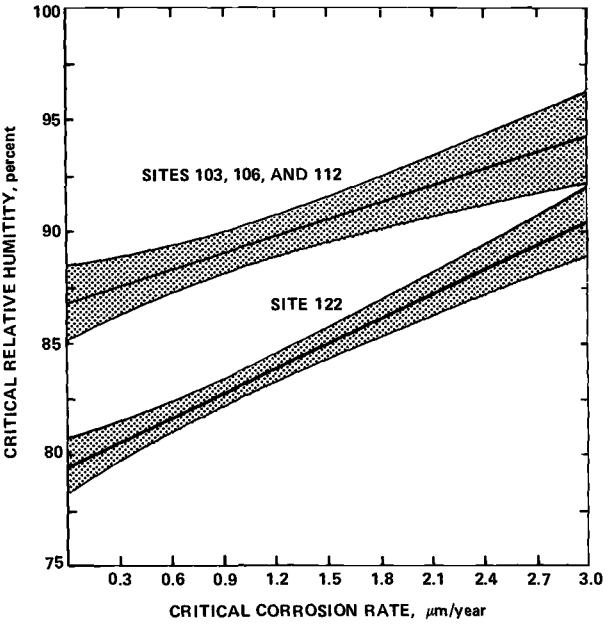

FIG. 3—*Comparison of critical relationships for assumed wetness.*

relationship similar to Eq 5. Some moisture may be gained or lost as the temperature changes, so the change in dew point will not be as large as the temperature change. Thus, the change in the temperature/dew-point spread will only be a fraction of the temperature difference.

Based on the airport average values of relative humidity (68.38), temperature (9.52°C), and dew point (2.92°C), the constant in Eq 5 is −5.05 rather than −6.32 as it is for the point-in-time relationship. As an approximation, the change in the average temperature/dew-point difference from site to site is assumed to be one third of the average temperature change from site to site. The average temperatures at Sites 103, 106, 112, and 122 were, respectively, 10.45, 10.89, 10.67, and 8.31°C. These values, the airport data, and the fol-

TABLE 6—*Comparison of average relative humidities using different methods.*

Site	From Dew-Point Data	From Fraction of Time When Wet[a]
Airport	68.38	. . .
103	65.38	66.47
106	68.78	68.04
112	71.76	72.60
122	67.65	70.95

[a] Assumed to be wet when corrosion rate of 1.5 μm/year was exceeded.

lowing expression derived from Eq 5 can be used to estimate average relative humidities at each site

$$RH_i = RH_0 e^{-5.05[80-2T_0+3D_0][T_i-T_0]/3(80+T_i)(80+T_0)} \quad (7)$$

where

RH_i = average relative humidity at site with missing dew-point data,
RH_0 = average relative humidity at site with dew-point data,
T_i = average temperature at site with missing dew-point data,
T_0 = average temperature at site with dew-point data, and
D_0 = average dew point.

The average relative humidities thus estimated for Sites 103, 106, 112, and 122 are, respectively; 67.46, 67.04, 67.25, and 69.62. From Eq 6 the respective fractions of time when wet are 0.198, 0.192, 0.195, and 0.231. With the exception of Site 112, these estimates are in good agreement with the data from Table 4. The respective percentage errors are 7.7, 7.2, 30.9, and 8.8 with a median of 7.7. This compares favorably with an average two-standard deviations on the data in Table 4 of 3.9 percent.

Pollution Data

With the exception of Site 112, the following gaseous pollutants were continually measured and recorded: O_3, NO, NO_2, CO, CH_4, SO_2, H_2S, total nitrogen oxides, total hydrocarbons, and total sulfur-containing gases. Site 112 did not measure SO_2 and H_2S but did measure the others. All of the data were expressed in parts per million. Details on instrument accuracy, calibration procedures, and data validation are given in Ref *1*.

Among several validation procedures was a correction for data with values below the lower detectable limit for each instrument. The measured value was replaced by one half of the lower detectable limit. Values were quite often in this range. This procedure excludes many values caused by low-side instrument error while keeping the high-side values, thus tending to bias long-term low-level averages toward the high side.

From the results of previous experiments and theoretical considerations, there is no reason to believe that hydrocarbons significantly affect corrosion rate. With both hydrocarbons and oxides of nitrogen primarily emissions from mobile sources, they are expected to be highly covariant. Other groups of pollutants are covariant, for example, NO, NO_2, and total oxides of nitrogen. Three of the pollutant measurements were selected for detailed analysis: O_3, total nitrogen oxides, and total sulfur. The last two can serve as proxies for their related compounds.

The hourly average ppm-values for these gases were converted to micrograms per cubic metre ($\mu g/m^3$) using the perfect gas law, assuming one atmosphere pressure and the average temperature during each measurement. Total nitrogen oxides were expressed as nitrogen dioxide and total sulfur as sulfur dioxide.

The lower detectable limit for each of these instruments was 0.005 ppm. Many hourly average values were recorded as 0.0025 ppm, especially for ozone and total sulfur. This converts to less than 10 $\mu g/m^3$. When long-term averages are around 30 $\mu g/m^3$, however, these low-level values become a significant part of the average.

The ACM's can respond only to the pollutants that reach their surfaces. For that reason pollutant flux should be a more important factor than pollutant concentration. Each of the pollutant concentration values was multiplied by the deposition velocity calculated from wind speed to give values for flux. The resulting averages for the total exposure time are given in Table 7.

Both NO_2 and SO_2 can react with zinc to form soluble products. The flux values in Table 7 can be multiplied by 0.0314 and 0.045 for NO_2 and SO_2 stoichiometric reactions, respectively, to calculate equivalent zinc corrosion rates that can possibly be caused by these pollutants. For NO_2 at Sites 103 and 106 the rates are 2.25 and 2.53 μm/year, respectively. Similarly for SO_2 the respective values are 1.26 and 1.23 μm/year. In total these corrosion rates exceed the average corrosion rates calculated from weight loss data or from the ACM responses. This suggests that not all of the pollutants that can reach the zinc surface react to form a soluble product. The formation of a sulfate is thermodynamically favored over the formation of a nitrate. When the SO_2 level is low and the NO_2 level high, however, the less-favored reaction can occur.

For a subset of data where relative humidity was equal to or greater than 95 and the ACM's corrosion rate was equal to or greater than 3 μm/year (surfaces most probably wet), the average flux of SO_2 was considerably lower than for the total time. The total possible contribution of SO_2 was considerably lower than for the total time. The total possible contribution of SO_2 and NO_2 pollutants during the periods of wetness was 2.95 μm/year for zinc. This value is considerably smaller than the average corrosion rate of 13.83 μm/year that was measured with the ACM's during the same periods. It is possible, thus, that some of the pollutant that is absorbed during dry periods reacts with the surface when it is wet.

Analysis of Relationships

The obvious relationship between ACM response and relative humidity is evidenced by Fig. 4. Both the timing of peaks and their magnitudes are shown to be related. This strong effect and the magnitude of error in the relative humidity make analysis for the possible effects of other variables difficult. The technique of multiple-regression analysis assumes that the independent variables are fixed (error-free) and are independent of each other (not covariant). Relative humidity was the least accurate of the "independent" variables. Thus, its error can mask the possible effects of other variables.

The use of a correlation matrix can reveal the problem of covariance between "independent" variables. A matrix for data at the four sites is given in Table 8.

TABLE 7—*Averages for pollutants at each site.*

Site	O_3		NO_2		SO_2	
	Concentration, $\mu g/m^3$	Flux, $\frac{cm}{s} \cdot \frac{\mu g}{m^3}$	Concentration, $\mu g/m^3$	Flux, $\frac{cm}{s} \cdot \frac{\mu g}{m^3}$	Concentration, $\mu g/m^3$	Flux, $\frac{cm}{s} \cdot \frac{\mu g}{m^3}$
103	41.9	34.3	115.5	71.8	34.4	28.0
106	31.9	21.0	148.3	80.6	48.7	27.4
112	30.4	20.3	136.9	65.3	17.8	10.3
122	51.2	28.6	28.0	15.1	47.1	23.9

NOTE: Flux is the product of deposition velocity (u), cm/s, and concentration, $\mu g/m^3$. Multiply by 31.5 to get $\mu g/cm^2$ year.

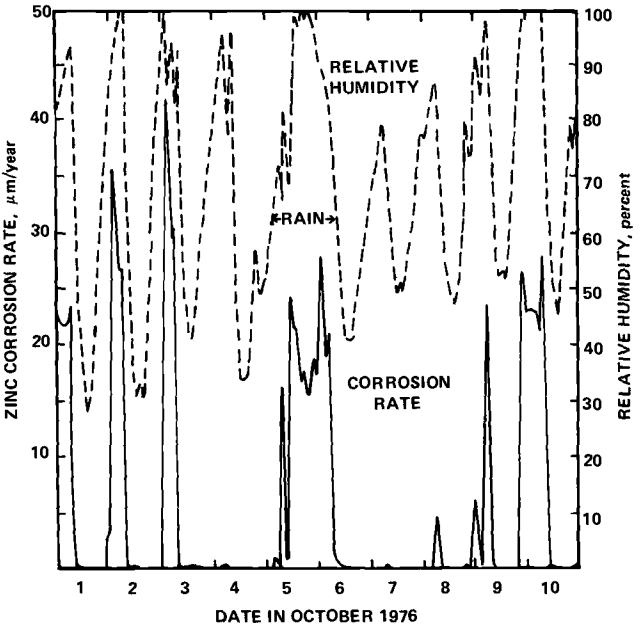

FIG. 4—*Atmospheric Corrosion Monitor response at Site 106.*

Only the temperature factor (E) and SO_2 concentration correlation coefficient were not included at this level of significance. As expected, relative humidity is the variable most significantly correlated with the logarithm of corrosion rate. It in turn is significantly correlated with all the other variables. Multiple-regression analysis of such data can produce equations with statistically significant coefficients. The magnitudes of those coefficients, however, may have little relationship to cause and effect.

Table 9 gives the results of multiple-regression analysis of zinc and steel ACM sets of data.

TABLE 8—*Correlation matrix of variables for four sites.*

Variable	Correlation Coefficients for Variable Pairs Which Exceed 0.999 Probability of Significance					
	RH	E	u	SO_2	NO_2	O_3
LnC	0.72	0.07	−0.21	−0.10	0.12	−0.23
RH	. . .	0.36	−0.20	−0.06	0.16	−0.36
E	. . .	. . .	−0.12	. . .	0.07	−0.40
U	. . .	. . .	. . .	−0.10	−0.27	0.34
SO_2	. . .	. . .	. . .	. . .	0.08	−0.05
NO_2	. . .	. . .	. . .	. . .	. . .	−0.28

NOTE: C = corrosion rate, μm/year; other terms defined in text.

TABLE 9—*Multiple-regression analysis results for logarithm of corrosion rate.*

	Independent Variable	RH	E	$u \cdot SO_2$	$u \cdot NO_2$	Constant
Zinc	coefficient	0.1000	−5.460	−0.00150	0.00493	9.9242
$N = 2974$						
	standard					
$R^2 = 0.560$	deviation	0.0017	0.323	0.00056	0.00051	
$F = 943.7$	F	3462.2	286.0	7.0	93.5	. . .
Steel	coefficient	0.0951	−6.299	−0.01307		15.3703
$N = 2074$						
	standard					
$R^2 = 0.606$	deviation	0.0018	0.364	0.00203		
$F = 1061.8$	F	2736.6	299.3	41.4		. . .

With the exception of the SO_2 flux, the signs for the coefficients are as expected. The negative covariance between relative humidity and SO_2 concentration may be causing the negatively significant coefficient for the SO_2 flux. The actual values for the coefficients for relative humidity and E are probably higher than the foregoing results because of their counteracting nature and their strong covariance.

When the surface of the ACM is completely wet, the ambient relative humidity should have no effect on the corrosion rate. It was assumed that when the corrosion rate was equal to or greater than 3.0 μm/year and the ambient relative humidity was equal to or greater than 95 percent, the surfaces should be completely wet. Table 10 gives the correlation matrices and results of multiple-regression analysis of these subsets of data.

The signs for the temperature factor coefficients and the NO_2 flux are as expected. The unexpected negative sign for the deposition velocity (μ) effect and the negative correlation between u and NO_2 for the zinc ACM data indicate that the deposition velocity is acting as a proxy for the NO_2. Comparing the magnitudes of the temperature factor coefficients with those of Table 9 shows that for zinc the value is lower and for steel it is higher. It was expected to be higher in both cases because the effect of relative humidity was not present to counteract it.

The correlation between temperature factor and SO_2 in the case of the zinc data could explain the observed lack of statistical significance for pollutants. The temperature factor has a negative effect, which may be partially offset by a positive SO_2 effect and a positive NO_2 effect. For the steel data the covariance between the temperature factor and NO_2 can reduce the magnitude of both coefficients.

The data were further restricted to the range of temperature factors where $3.46 \leq E \leq 3.50$ to see if the pollutant effects were significant. Corrosion rate rather than the logarithm of the corrosion rate was taken as the dependent variable. Even with this restriction there was still a strong correlation between

TABLE 10—*Results of analysis of wet surface data.*

Zinc ACM's

	Correlation Coefficient Matrix for Variable Pairs[a]					Regression Equation			
	E	u	SO_2	NO_2	O_3	Variable	Coefficient	Standard Deviation	F
LnC	−0.38	−0.21	. . .	. . .	. . .	Constant	15.0778		
E	. . .	. . .	0.23	0.32	. . .	E	−3.428	0.495	48.0
u	. . .	. . .	. . .	−0.48	. . .	u	−0.4658	0.1115	17.4
SO_2	. . .	. . .	. . .	0.21	. . .	$N = 277$, $R^2 = 0.1869$, $F = 31.5$			
NO_2	. . .	. . .	. . .	. . .	. . .				

Steel ACM's

	E	u	SO_2	NO_2	O_3	Variable	Coefficient	Standard Deviation	F
LnC	−0.48	. . .	−0.18	. . .	. . .	Constant	35.6164		
E	. . .	. . .	. . .	0.19	. . .	E	−9.134	0.836	119.4
u	. . .	. . .	−0.27	−0.30	. . .	$u \cdot NO_2$	0.00246	0.0008	9.5
SO_2	. . .	. . .	. . .	−0.19	0.21	$N = 375$, $R^2 = 0.249$, $F = 61.0$			
NO_2	. . .	. . .	. . .	. . .	−0.3				

[a] Significant at 0.999 probability.

the temperature factor and O_3 for the steel data, with a positive correlation between O_3 and SO_2. This resulted in significant negative coefficients for SO_2 and O_3 flux. Table 11 is a correlation matrix for the zinc ACM subset. The zinc corrosion rate is significantly correlated with SO_2 and NO_2 concentrations and fluxes. The coefficients for fluxes are higher than for concentrations. The temperature factor correlates only with NO_2 concentration and not with NO_2 flux.

Regression analysis results are given in Table 12. Both of the coefficients in Table 12 are higher but not significantly different from coefficients predicted from stoichiometric reactions: 0.045 for $u \cdot SO_2$ and 0.0314 for $u \cdot NO_2$. This is possibly caused by the absorption of some of the pollutants reaching the surface when it is dry and then reacting when it is wet. Another possibility is that the total concentration of these pollutants in the atmosphere was higher than was measured by the instruments that measure only gases.

From Table 7, the average fluxes at the zinc ACM sites during the total exposure

$$(27.7 \frac{\text{cm}}{\text{s}} \cdot \frac{\mu\text{g}}{\text{m}^3} \text{ for } u \cdot SO_2 \text{ and } 76.2 \frac{\text{cm}}{\text{s}} \cdot \frac{\mu\text{g}}{\text{m}^3} \text{ for } u \cdot NO_2)$$

are considerably higher than the mean fluxes (Table 12) during the periods of wetness and restricted range of temperatures. The pollutants don't just disappear during periods of high relative humidity. They are absorbed into condensed moisture in the atmosphere as well as on surfaces. Some may be catalyzed in solution to sulfuric and nitric acid. The pollutants, though still in the atmosphere, can no longer be measured as a gas. The unmeasured pollutants still can contribute to corrosion by being delivered to the surfaces by the flux of moisture particles.

If it is assumed that the actual fluxes of pollutants during periods of wetness were higher than measured by the ratio of the total time average to the average during periods of wetness, the calculated damage coefficients are lower: 0.052 for $u \cdot SO_2$ and 0.054 for $u \cdot NO_2$. These values are quite close to the theoretically predicted coefficients for stoichiometric reactions.

While a previous study [*5*] provided evidence for the stoichiometric reac-

TABLE 11—*Correlation matrix for zinc ACM's within restricted temperature range when wet.*

	Correlation Coefficient[a]/Number of Sets							
	E	u	SO_2	NO_2	O_3	$u \cdot SO_2$	$u \cdot NO_2$	$u \cdot O_3$
C	. . .	. . .	0.18/98	0.28/99		0.27/98	0.37	. . .
E	. . .	. . .	. . .	0.21/99		. . .	. . .	. . .
u	. . .	. . .	. . .	−0.46/97		. . .	. . .	. . .
$u \cdot NO_2$	. . .	. . .	. . .	. . .	. . .	. . .	. . .	−0.27/87

[a] Significant at 0.95 probability level; fluxes include u in term.

TABLE 12—*Regression analysis of zinc ACM subset of data.*

Variable	Constant	$u \cdot SO_2$	$u \cdot NO_2$	$N = 77$
Mean	μm/year	$10.6 \frac{cm}{s} \cdot \frac{\mu g}{m^3}$	$60.3 \frac{cm}{s} \cdot \frac{\mu g}{m^3}$	
Coefficient	14.14	0.13	0.06	$R^2 = 0.1766$
Standard deviation	. . .	±0.076	±0.02	$F = 7.936$
F	. . .	3.2	12.3	

tion of SO_2 with zinc, this is the first evidence for NO_2 in the atmosphere reacting with zinc. Previous data sets were too small to partition into meaningful-size subsets that eliminate covariance of "independent" variables. Even with this large data set it was not possible to eliminate the covariance between temperature and pollutants at the steel ASM sites. Thus, the coefficient for the temperature effect includes by proxy the effects of pollutants.

A technique of fixing the coefficients as determined in the absence of covariance, and calculating the coefficient for the remaining variable for data sets where that variable was covariant with the others, was used to determine an overall relationship for the zinc/copper ACM's. This was a two-step process involving increasingly larger data sets. First, a temperature factor coefficient and intercept were calculated on those data where the corrosion rate equaled or exceeded 3 μm/year and the relative humidity equaled or exceeded 95 percent. Second, a coefficient for the effect of relative humidity was calculated using the complete data set. It was assumed that the maximum amount of corrosion occurs at 100 percent relative humidity and follows the functional form

$$C = Cm\, e^{-B(100\text{-}RH)/RH} \tag{8}$$

where C is the corrosion rate and Cm the maximum corrosion rate (function of temperature and pollution level). Based on the results of this technique and stoichiometric reactions with pollutants, the best estimates of coefficients produce the relationship

$$Co = [0.045\, u \cdot SO_4 + 0.0314\, u \cdot NO_2 + e^{17.133-4.237E}]e^{-5.4(100\text{-}RH)/RH} \tag{9}$$

where Co is the best estimate of the corrosion rate μm/year for specific conditions of pollutants, temperature, and relative humidity.

This equation can explain approximately 43 percent of the observed variability in the zinc corrosion response. Relative humidity accounts for 35.1 percent, temperature 6.6 percent, and the pollutants only 1.3 percent of the total variability. The standard deviation on Co is 5.5 μm/year. Because conditions at the surface of the ACM lead or lag ambient conditions and the ambient relative humidity values have considerable error, a much better fit is not expected. For example, at average levels of pollutants and temperature,

an error of 5 percent relative humidity can cause an error in Co of around +2.8 μm/year. At the higher observed temperatures the same error in relative humidity can cause a +7.9-μm/year error in the estimated corrosion rate.

Coupling the zinc to copper accelerates the corrosion of the zinc. Only the constant (17.133) in the temperature exponential term is involved in this effect. From the data in Tables 2 and 4 the constant for uncoupled zinc was calculated to be 12.897. Thus, an equation for the instantaneus corrosion rate of zinc as a function of pollutants, relative humidity, and temperature is

$$Co = [0.045\ u \cdot SO_2 + 0.0314\ u \cdot NO_2 + e^{12.897-4.237E}]e^{-5.4(100-RH)/RH} \quad (10)$$

When the surface is fully wet at a temperature of 11°C and an NO_2 flux of 36 ($cm/s \cdot \mu g/m^3$), the equation simplifies to

$$Co = 1.264 + 0.045\ u \cdot SO_2 \quad (11)$$

This equation is very close to the results of a regression of weight loss data for small galvanized specimens exposed at the average conditions of 11°C and 36 ($cm/s \cdot \mu g/m^3$) for NO_2 flux [5]

$$\frac{C_z}{tw} = 2.32 + 0.049\ u \cdot SO_2 \quad (12)$$

where C_z is the corrosion in micrometres and tw the time-of-wetness in years.

The covariance between the pollutants and the temperature factor makes it impossible to calculate meaningful pollution coefficients for the steel/copper ACM's exposed at Sites 112 and 122. The temperature factor effect includes by proxy the effects of the pollutants. The best estimate of a relationship for the steel ACM's is

$$Co_s = e^{33.585-8.778E-6.89(100-RH)/RH} \quad (13)$$

TABLE 13—*Mean and standard deviations of pollutant variables.*[a]

Variable	Units	Mean	Standard Deviation
Deposition Velocity u	$\frac{cm}{s}$	0.5399	0.1968
SO_2	$\frac{\mu g}{m^3}$	36.61	33.29
NO_2	$\frac{\mu g}{m^3}$	61.44	121.53
O_3	$\frac{\mu g}{m^3}$	44.01	38.25
$u \cdot SO_2$	$\frac{cm}{s} \cdot \frac{\mu g}{m^3}$	18.90	19.13
$u \cdot NO_2$	$\frac{cm}{s} \cdot \frac{\mu g}{m^3}$	29.23	51.23
$u \cdot O_3$	$\frac{cm}{s} \cdot \frac{\mu g}{m^3}$	25.54	25.65

[a] Based on 2074 sets of data from Sites 112 and 122.

where Co_s is the best estimate of the instantaneous corrosion rate for steel in μm/year at particular values of E and relative humidity.

The constants 33.585 and −8.778 include the effects of pollutants as well as temperature at these two sites. The equation is not applicable to other locations if the pollution levels are not similar. As a point of reference, Table 13 gives the means and standard deviations for the variables that could be affecting the corrosion rate.

Summary and Conclusions

The Atmospheric Corrosion Monitors developed and used by Mansfeld and co-workers can be used to indicate the magnitude of corrosivity as well as time-of-wetness. The response of the ACM's to changes in ambient conditions, however, is affected by their geometry. Couples mounted on a very thin substrate should respond faster to such changes. Over long averaging times the errors caused by leads and lags in response will tend to compensate each other and reduce the total error. Total time-of-wetness measured by this device should be representative of the time-of-wetness on most metal surfaces.

A galvanic current equivalent to a corrosion rate equal to or greater than 1.5 μm/year appears to be a good criterion for assuming that the ACM surface is wet. This value corresponds to a critical relative humidity of approximately 90 percent. From 88 to 99 percent of the corrosion measured at the four sites occurred when values met this criterion.

Corrosion rates are strongly dependent on relative humidity; however, relative humidity is one of the least accurate environmental measurements. It is seldom measured where materials are exposed, yet microclimate differences can be significant between sites that are within a few hundred metres from each other. Because temperature and relative humidity are related to each other within the same air mass, an unknown relative humidity can be estimated from temperature differences and a relative humidity at a different site. With average relative humidity, time-of-wetness can be estimated.

In the real world, environmental factors are strongly covariant and subject to error. The unquestioned use of multiple-regression analysis of such data to explain corrosion behavior can be misleading. A large data set collected in St. Louis allowed partitioning into subsets that eliminated covariance. Through this process it was determined that the flux to the surface of total oxides of nitrogen (expressed as NO_2) as well as the flux to the surface of total sulfur (as SO_2) contributed significantly to the corrosion response of zinc/copper ACM's. This is the first time an NO_2 effect has been observed in a field experiment.

Covariance of pollutant fluxes with temperature made it impossible to delineate pollutant effects on the steel/zinc ACM's. For both the zinc and the steel ACM's, temperature and relative humidity affected corrosion rate in increasing order of significance. With relative humidity the most important

factor, and being most in error, the empirical expressions relating corrosion rate to environmental factors are as good as one can expect. The resulting expression for zinc corrosion agrees well with expressions derived from other data.

Acknowledgments

The ACM data used in this paper were collected as a part of an EPA contract directed by Dr. Florian Mansfeld of the Rockwell International Science Center. I gratefully acknowledge this work and Dr. Mansfeld's help in making it possible to calculate corrosion rates from recorded responses of ACM's.

Mr. William Deland of Computer Sciences Corp. spent many hours in programming so that the data could be analyzed as they were. It required much more than creating a data file to be analyzed by standard statistical programs. The procedures that were finally used evolved as work proceeded, based in part on trial and error of theoretical considerations. Without Mr. Deland's ability and patience I would not have been able to complete this work.

References

[*1*] Hern, D. H. and Taterka, M. H., *Regional Air Monitoring System Flow and Procedures Manual*, Report for EPA Contract DU-68-02-2093 by Rockwell International, Creve Coeur, Mo., Aug. 1977.

[*2*] Mansfeld, F., "Regional Air Pollution Study—Effects of Airborne Sulfur Pollutants on Materials," EPA-600/4-80-007, Environmental Protection Agency, Jan. 1980.

[*3*] Mansfeld, F. and Kenkel, J. V., *Corrosion*, Vol. 33, No. 1, Jan. 1977, p. 13.

[*4*] Bird, R. P., Stewart, W. E., and Lightfoot, E. N., *Transport Phenomena*, Wiley, New York, 1962, p. 162.

[*5*] Haynie, F. H. in *Durability of Building Materials and Components, ASTM STP 691*, American Society for Testing and Materials, 1980, p. 157.

[*6*] Owers, M. J. and Powell, A. W., *Atmospheric Environment*, Vol. 8, 1974, p. 63.

[*7*] Lange, N. A., *Handbook of Chemistry*, McGraw-Hill, New York, 1956, p. 1414.

F. Mansfeld,[1] *S. Tsai,*[1] *S. Jeanjaquet,*[1] *E. Meyer,*[1]
K. Fertig,[1] *and C. Ogden*[2]

Reproducibility of Electrochemical Measurements of Atmospheric Corrosion Phenomena

REFERENCE: Mansfeld, F., Tsai, S., Jeanjaquet, S., Meyer, E., Fertig, K., and Ogden, C., **"Reproducibility of Electrochemical Measurements of Atmospheric Corrosion Phenomena,"** *Atmospheric Corrosion of Metals, ASTM STP 767,* S. W. Dean, Jr., and E. C. Rhea, Eds., American Society for Testing and Materials, 1982, pp. 309–338.

ABSTRACT: A brief discussion is given of recent efforts to use electrochemical techniques for monitoring of atmospheric corrosion phenomena. Problems existing with the interpretation of time-of-wetness measurements are identified, and the finding that electrochemical sensors in their present design and application determine only fractions of the true corrosion rate is discussed. In order to resolve some of these difficulties, a statistically designed experiment is being carried out to evaluate the reproducibility of electrochemical measurements of atmospheric corrosion phenomena and to determine the effects of sensor design on time-of-wetness and cell efficiency. Results are presented for the first phase of this project, in which 15 atmospheric corrosion monitors (ACM) of the copper/steel and 15 ACM's of the steel/steel type, have been fabricated with steel and copper from three different heats. These ACM's have been tested in triplicate runs by exposure to aqueous 1-mM sodium chloride at a relative humidity of 45 percent until the surface had dried out, followed by additional exposure to either a moist air environment at three levels of relative humidity (65, 80 and 95 percent) or a sodium dioxide (SO_2) test at three levels of $SO_2 \approx 0$, 0.2, and 1.1 ppm. During each test, steel plates from each heat were exposed to determine weight loss data. At present, only the drying-out data have been analyzed by statistical methods. It has been found both from electrochemical and weight loss data that the heat of the steel plays an important role, with one heat corroding at a higher rate than the other two which have equal corrosion rates. No differences were found between the five sensors of one heat. Additional factors that influence the measurement are day-to-day variations of the environment in the test chamber and to some extent the position of the ACM's in the test chamber. By comparing the electrochemical and weight loss data, a cell efficiency of about 20 percent was found for copper/steel and about 7 percent for steel/steel. This low cell factor is considered to be due mainly to local cell action on individual plates and to uncompensated ohmic drop in the electrolyte.

The copper/steel and steel/steel ACM's are being exposed on the Rockwell International Science Center roof for an aging period of three months, after which another series of laboratory tests will be conducted.

[1] Group manager, senior staff associate, senior technical specialist, and members of technical staff, respectively, Rockwell International Science Center, 1049 Camino Dos Rios, Thousand Oaks, Calif. 91360.

[2] Member of technical staff, Rockwell International Electronics Research Center, 1049 Camino Dos Rios, Thousand Oaks, Calif. 91360.

KEY WORDS: atmospheric corrosion, electrochemical sensors, statistical analysis, time-of-wetness, cell efficiency, weight loss data

Atmospheric corrosion behavior has traditionally been evaluated by weight loss measurements in exposure tests over long time periods with the purpose of comparing the corrosion resistance of different materials at a given test site or evaluating the relative corrosivity of different test sites, or both. Electrochemical methods have found wider use only more recently in studies designed to determine parameters such as the time-of-wetness, t_w, or instantaneous corrosion rates. For mechanistic studies of atmospheric corrosion, electrochemical measurements are extremely important because they provide continuous records of corrosion behavior which can be compared with continuous records of air quality parameters taken at the same test site. Using an appropriate model for the atmospheric corrosion process and statistical procedures, attempts can be made to establish correlations between material properties and environmental factors that describe the observed corrosion behavior. Electrochemical corrosion monitoring devices (ECMD's) used for these purposes include Sereda's sensors for t_w measurements [*1*],[3] galvanic types such as copper/steel or copper/zinc as used by Kucera [*2*], Voigt [*3*], Mansfeld [*4–6*], and others, and the two-electrode type which is used with an applied electromotive force (emf) [*2,7,8*]. A review of the different approaches and the results obtained with ECMD's has been given elsewhere [*9*]. Generally speaking, it can be stated that Sereda's sensors can be used for t_w determinations only, and that there is only an arbitrary criterion for determining when the sensor surface is wet. The galvanic sensors record the corrosion rate of the anodic material (steel, zinc, etc.) in the couple since for diffusion control of the cathodic process the measured galvanic current I_g is equal to the corrosion current $I_{corr}{}^A$ of the freely corroding anode [*5*]. Despite the fact that the dissolution rate of the anodic material is accelerated by coupling to the cathode, the unique property of the galvanic current measurements remains that

$$I_g = I_{corr}{}^A \tag{1}$$

The corrections which are normally necessary to convert the measured I_g data into dissolution rates are not necessary, since one is interested only in the corrosion rate of the anode material.

Two-electrode-type ECMD's can be used on the basis of the polarization resistance technique. A constant emf ΔE applied to two electrodes of the same material causes a current flow, ΔI, which determines I_{corr} [*10*]

$$I_{corr} = \frac{2B}{\Delta E}\,\Delta I = k\Delta I \tag{2}$$

[3] The italic numbers in brackets refer to the list of references appended to this paper.

where B depends on the Tafel slopes. It has to be considered that ΔE has to be kept small enough to ensure that the basic assumptions of the Stern–Geary method are met. In Kucera's approach [*2,7*], where $\Delta E = 100$ mV, Eq 2 does not apply for calculation of I_{corr}. The principal problem with the use of Eq 2 is that the Tafel slopes usually cannot be measured at the same time as ΔI. This introduces a certain error in the constant, k, as discussed elsewhere [*10*]. Additional errors can be introduced by experimental problems. An important source of error is the occurrence of uncompensated ohmic drop due to low-conductivity surface electrolytes, which reduces the value of ΔE "seen" by the ECMD and causes a lower current flow ΔI than corresponds to the applied ΔE.

While the application of electrochemical techniques to atmospheric corrosion studies in recent years has led to a better understanding of some basic phenomena and has provided additional tools for corrosion monitoring and control, a few problems with the use of ECMD's have been noted recently [*7–9*]. The present interpretation of t_w measurements is unsatisfactory, since no sound definition seems to exist on which t_w can be based. As an example, Fig. 1 shows t_w data taken on the Rockwell International Science Center roof over a 3-year period using copper/steel atmospheric corrosion monitors (ACM's). For most of the time, t_w was taken as the time for which I_g exceeded the background current of the ACM amplifier (0.02 μA). Starting in June 1978, t_w was redefined as the time for which $I_g \geqslant 0.05$ μA ($\approx$0.01 μA/cm^2) (t'_w in Fig. 1). Also shown in Fig. 1 for the same location is the time t_{80} for which relative humidity exceeded 80 percent. This is considered the "critical rela-

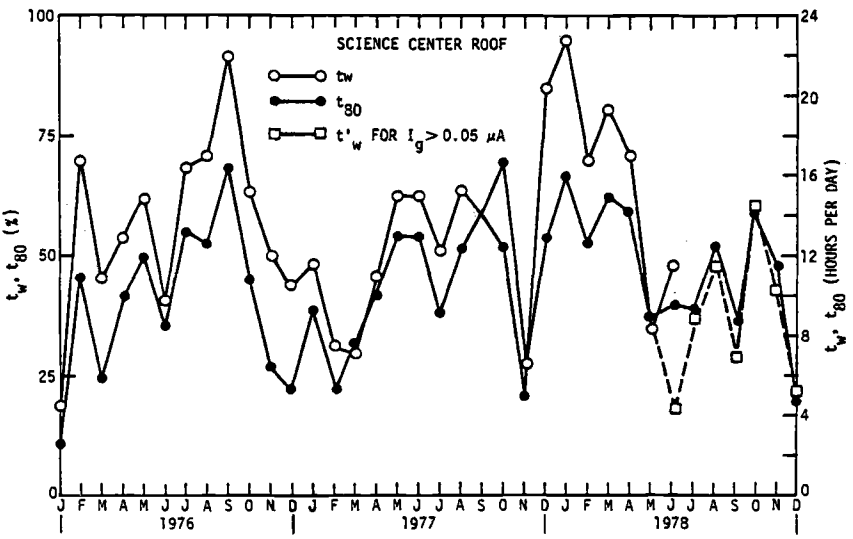

FIG. 1—*Time-of-wetness* t_w *and time for RH* $\geqslant$ *80 percent* (t_{80}) *for a 3-year period on the Science Center roof.*

tive humidity" for steel. In most cases, $t_w > t_{80}$, which suggests that t_w, in its present definition, relates to a relative humidity value that is lower than 80 percent. The t'_w data correspond more closely to t_{80} data except for June 1978. Further discussion is necessary concerning the definition of t_w. Since the corrosion current can have wide fluctuations during the wetness periods, it might be necessary to define t_w as the time for which a certain corrosion rate, for example, 1 μm/year, is exceeded, which would correspond to about 0.09 $\mu A/cm^2$ for steel and 0.07 $\mu A/cm^2$ for zinc. This approach would reduce the t_w data in Fig. 1 considerably, but also illustrates that a problem exists at present with the definition of t_w.

The observations by Kucera [*7*] in outdoor exposure and by Mansfeld and Tsai [*8*] in laboratory experiments, which have shown that ECMD's measure only fractions of the true corrosion rate of a metal under atmospheric corrosion conditions, suggest that a more serious problem exists. Table 1 gives the data obtained by Mansfeld and Tsai, who carried out weight loss experiments and electrochemical measurements with copper/steel and steel/steel ACM's under identical conditions [*8*]. Steel plates (5 by 5 cm) and ACM's were covered with a 0.5-mm-thick layer of 0.01 N aqueous solution of sodium sulfate (Na_2SO_4) and allowed to dry at fixed relative humidities (RH). The weight loss data have been converted into charge density data, Q (Cb/cm^2), for comparison with the integrated galvanic current data, Q_g, for copper/steel and the corresponding data for steel/steel sensors at $\Delta E = 30$ mV (Q_{30}). For the latter ACM's, it has been assumed that the cathodic reaction is under diffusion control ($b_c \to \infty$) and that $b_a = 60$ mV, which for $\Delta E = 30$ mV leads to $k = 1.75$ (Eq. 2). It can be seen that the electrochemical measurements underestimate the corrosion loss since $Q_i/Q_{WL} < 1$ (i = g or 30). However, close agreement is found for the two types of sensors with average ratios, $Q_g/Q_{WL} = 0.20$ and $Q_{30}/Q_{WL} = 0.175$, which can be considered to represent the ACM efficiency or cell factor. Kucera [*7*] has reported similar values of the cell factor from exposure tests in Sweden.

TABLE 1—*Comparison of weight loss and ACM data obtained in 0.01-N Na_2SO_4/air* (Q *in* Cb/cm^2).

Test Condition	Q_{WL}	Q_g	Q_g/Q_{WL}	Q_{30}[a]	Q_{30}/Q_{WL}
RH, %			Steel		
30	1.90	0.320	0.17	0.366	0.19
45	2.75	0.433	0.16	0.483	0.18
60	3.62	0.954	0.26	0.604	0.17
75	6.49	1.254	0.19	1.027	0.16
90	n.d.	3.252	. . .	1.306	. . .
			0.20		0.175

[a] For $k = 1.75$ (Eq 2).

In order to evaluate in more detail the factors that determine the reproducibility of electrochemical corrosion sensors, the cell efficiency and the time-of-wetness, a statistically designed experiment is being carried out. Preliminary results are reported in the following.

Experimental Approach

The purpose of the experiment is to evaluate whether electrochemical sensors can provide statistically consistent measurements which can be correlated with weight loss data. For this purpose sensors were fabricated from different heats of the same material and tested under different conditions of humidity and pollution. In this context it was not so important that test conditions were chosen which duplicate exactly conditions in outdoor exposure as long as all sensors were tested exactly in the same manner.

Fifteen ACM's, each of the copper/steel and steel/steel types, have been constructed as described earlier [*4–6,8,9*], using three different heats of 4130 steel and OFHC copper (for details see Table 2). In this way, for each type of ACM there are three groups of five sensors, each prepared from identical materials (same heats of steel and copper, respectively). In order to evaluate the reproducibility of the electrochemical measurements, a test sequence has been defined arbitrarily which includes the drying-out phase, the importance of which has been demonstrated earlier [*6,8,9*], and variations of relative humidity or sulfur dioxide (SO_2) levels. The ACM surfaces were precondi-

TABLE 2—*Materials used in fabrication of ACM's.*

Group	Steel	Copper
B. Manufacturer/ supplier	Jones & Laughlin	Anaconda
Type	E-4130A	OFHC
Specification	MIL-S-18729C	
Heat	31994	
Thickness (in.)	0.025	0.020
C. Manufacturer/ supplier	Interlake	MacKellar Materials Co. (Mill No. 1)
Type	E-4130A	CDA Alloy 101
Specification	MIL-S-18729C	. . .
Heat	B-1851	. . .
Thickness (in.)	0.025	0.020
D. Manufacturer/ supplier	Interlake	Citco, New Haven Operations
Type	E-4130A	CDA Alloy 101
Specification	MIL-S-18729C	. . .
Heat	B-2928	. . .
Thickness (in.)	0.025	0.020

NOTE: 1 in. = 25.4 mm.

tioned after polishing by drying under a layer of 1-mM aqueous solution of sodium chloride. This solution was chosen because it had been found in preliminary experiments that ACM surfaces pretreated in this manner gave a response to RH = 65 percent which was in a range which could be reliably measured with the existing equipment. Weight loss specimens which were pretreated in the same manner were exposed in each test for correlation with the electrochemical data. Each test was repeated three times, starting with freshly polished ACM's. After this first round of testing, the 30 ACM's were placed on the Science Center roof for a 3-month period. After this time a second round of tests will be carried out in order to evaluate the effects of corrosion product formation and aging on the reproducibility of ACM data. After another 6-month exposure period, the reproducibility of the ACM data will be tested again. Some of the results obtained to date are discussed in the following.

Preparation of ACM's and Weight Loss Specimens

The ACM's were wet-polished with 600-grit silicon carbide paper and dried quickly under a nitrogen stream. This procedure has been found to produce the least amount of organic contamination. The ACM's were then checked by measuring the electrical resistance between the two pairs of plates. If the resistance was below 10 MΩ, the surface was wiped with a clean paper towel to remove metallic particles or the surface was repolished.

In order to obtain weight loss data for determination of the "cell factor" and evaluation of the reproducibility of weight loss measurements, plates (5 by 5 cm) of 4130 steel were polished as described earlier and one side was coated with Turco Mask. Two plates each of the three heats of steel are used for each experiment, using the same pretreatment in 1-mM sodium chloride (NaCl).

Measurement System

The electrochemical measurements are performed in a glass tube (1.2 m long, 15 cm inside diameter) which is closed at both ends, under controlled conditions of relative humidity and SO_2 concentration. The 15 ACM's are mounted on a support plate and connected to their individual amplifier system, which is directly below the support plate. The ACM's are arranged in statistical distributions of heat (B, C, D) and sensor number (1–5). Figure 2 is a photograph of the ACM arrangement in the glass tube. At both ends of the support plate, three weight loss specimens each were positioned. Wet air is fed into the tube from both ends at a flow rate of 4 litres/min, using a plastic tube that has holes drilled into it at intervals which were considered to produce a uniform relative humidity distribution in the tube. The desired relative humidity value and SO_2 concentration are produced in a mixing system which has been described earlier [*4–6*]. The air exits at both ends of the

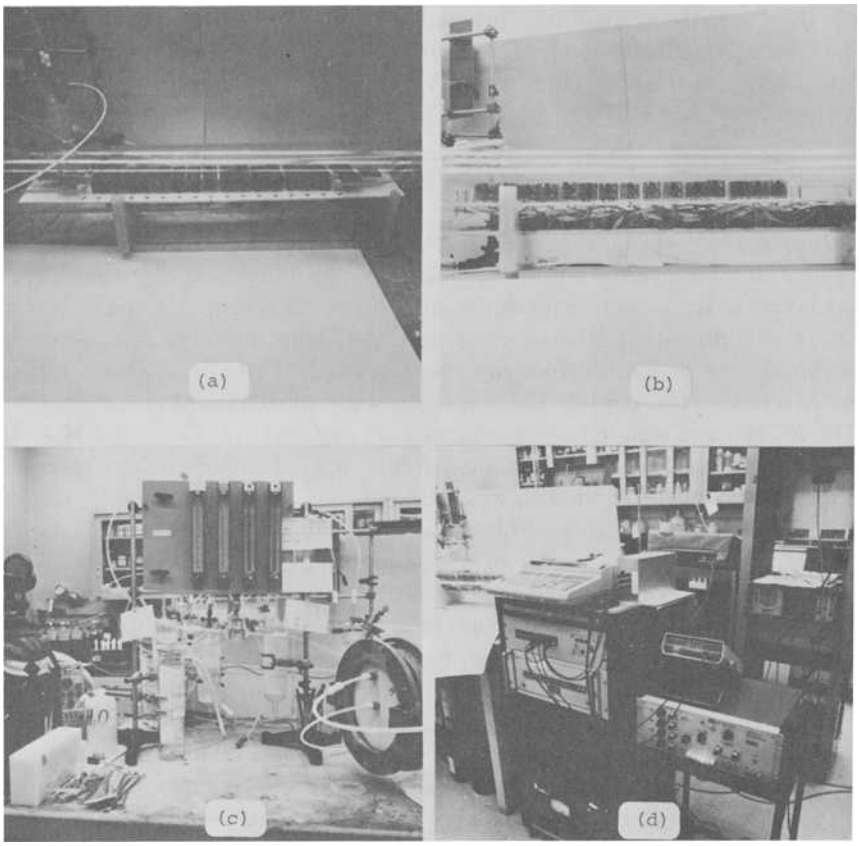

FIG. 2—*Experimental arrangement:* (a,b) *glass tube with ACM's and weight loss specimens;* (c) *gas mixing system and end plate of tube;* (d) *computer, multiprogrammer, function generator for* $\Delta E = \pm 30$ *mV, and digital voltmeter.*

tube and is fed into a test chamber for monitoring of the flow rate, relative humidity, and SO_2 concentration.

After checking the performance of the 15 amplifier systems and the ACM's by applying a fixed voltage and measuring the corresponding current flow, a 0.5-mm layer of aqueous 1-mM NaCl was placed on the ACM's and the weight loss specimens. After checking the initial current flow, the support plate was placed in the tube and both ends were closed. After setting relative humidity to 45 percent, the run was started.

The details of the measuring process for ACM data are given in the Appendix. Current measurements were taken every 50 s. The galvanic current for copper/steel cells or the current flow at ±30-mV applied voltage for steel/steel cells is recorded sequentially for each of the 15 cells (five times per cell in a 5-s period) using a Hewlett-Packard (HP) multiprogrammer HP 6940B. Control and timing is provided by an HP computer 9825S on which

the data are stored for futher processing and analysis. After each run, the data are plotted using an HP plotter 9872B for a first evaluation followed by integration for the different test intervals using a computer program written for this purpose.

Test Sequence

Drying Tests—In all experiments, the ACM surfaces were conditioned by drying under a layer of 1-mM NaCl to provide an identical corrosion product layer for the subsequent relative humidity or SO_2 tests. Drying is carried out in an ambient air atmosphere at RH = 45 percent and usually occurred within 3 to 6 h. The current-time curve is measured continuously for all ACM's during this period. The run was usually started in the late afternoon. The ACM's and weight loss specimens were exposed in the tube at RH = 45 percent until the following morning. After drying, all amplifiers were rezeroed and the next phase of the run was initiated.

Relative Humidity Tests—Following drying at RH = 45 percent, relative humidity was increased to 65, 80 and 95 percent for 2 h each. A YS191 dewpoint hygrometer monitored the relative humidity of the air coming out of the test tube to determine the actual relative humidity value in the tube during the test. After this 6-h period, the experiment was terminated. Weight loss data were measured for the steel plates and statistical analyses were performed for the ACM data.

SO_2-Tests—Following drying at RH = 45 percent, relative humidity was set to 95 percent for 2 h. After this time, 0.2-ppm SO_2 was added to the wet air for 2 h followed by 2 h at 1.1-ppm SO_2. These concentrations have been measured at the outlet of the test tube, using a Meloy Labs Sulfur Gas Analyzer, since it was observed that a large amount of the SO_2 which was introduced into the test tube was lost by reaction, adsorption, etc. After the 6-h test, weight loss data were measured and statistical analyses performed for the ACM data.

Experimental Results

Time Dependence of ACM Response

Typical examples for the experimental results in the form of current-time curves are shown for copper/steel and steel/steel drying at RH = 45 percent (Figs. 3 and 4), exposed to increasing relative humidity (Figs. 5 and 6), or increasing SO_2 concentration (Figs. 7 and 8).

The drying data for the four copper/steel ACM's (Fig. 3) show a steady increase of the galvanic current while the electrolyte layers become thinner. This increase becomes more pronounced when the electrolyte is almost completely dried. A sharp drop to very low currents occurs during the final stages

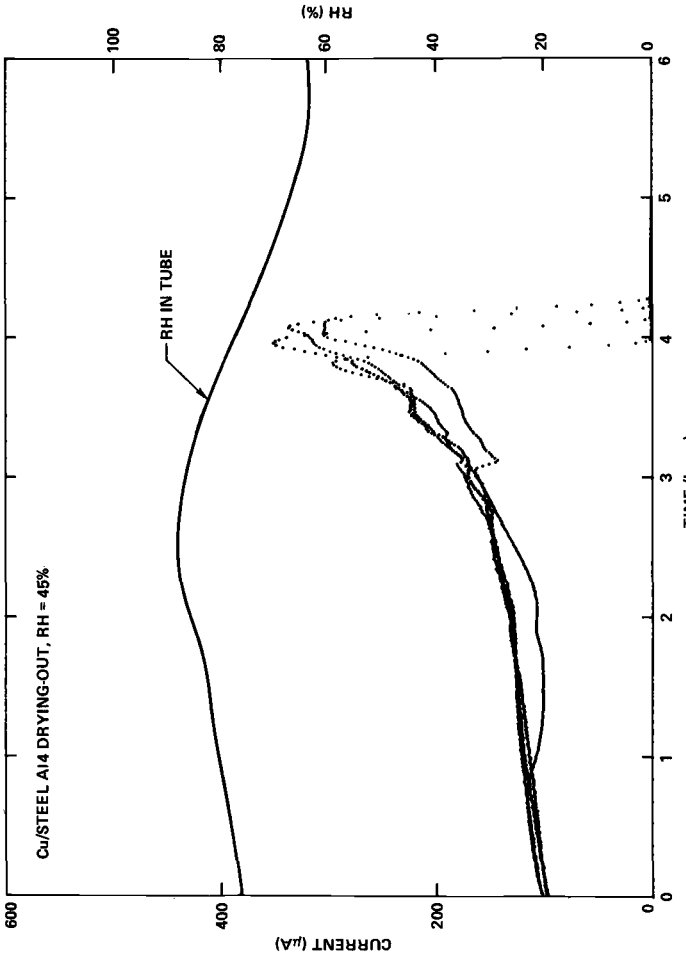

FIG. 3—*Experimental results for copper/steel drying at RH = 45 percent.*

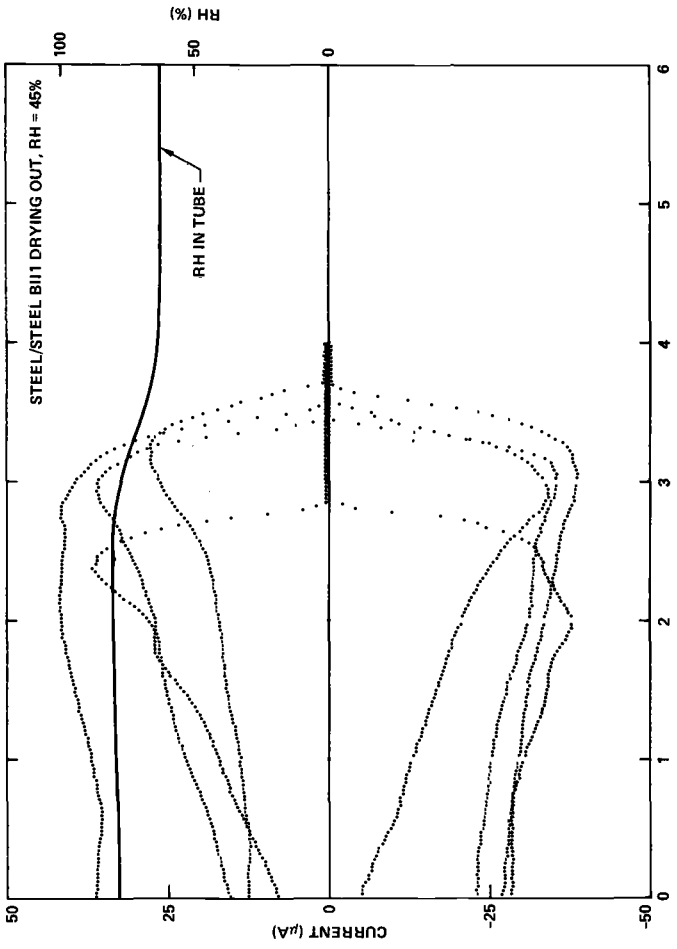

FIG. 4—*Experimental results for steel/steel drying at RH = 45 percent.*

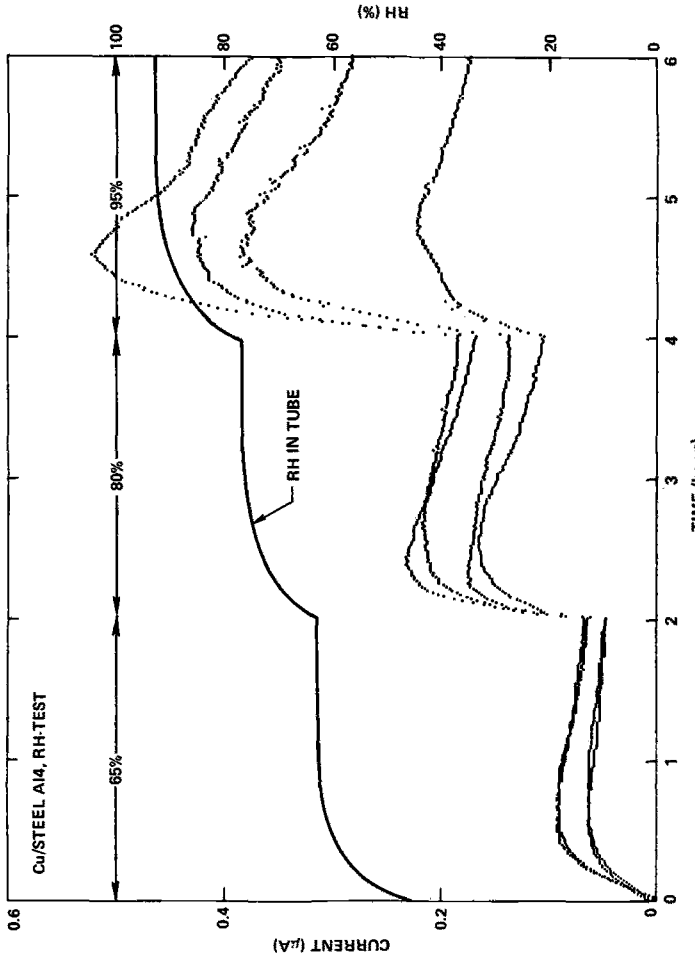

FIG. 5—*Experimental results for copper/steel exposed to RH = 65, 80, and 95 percent for 2 h each.*

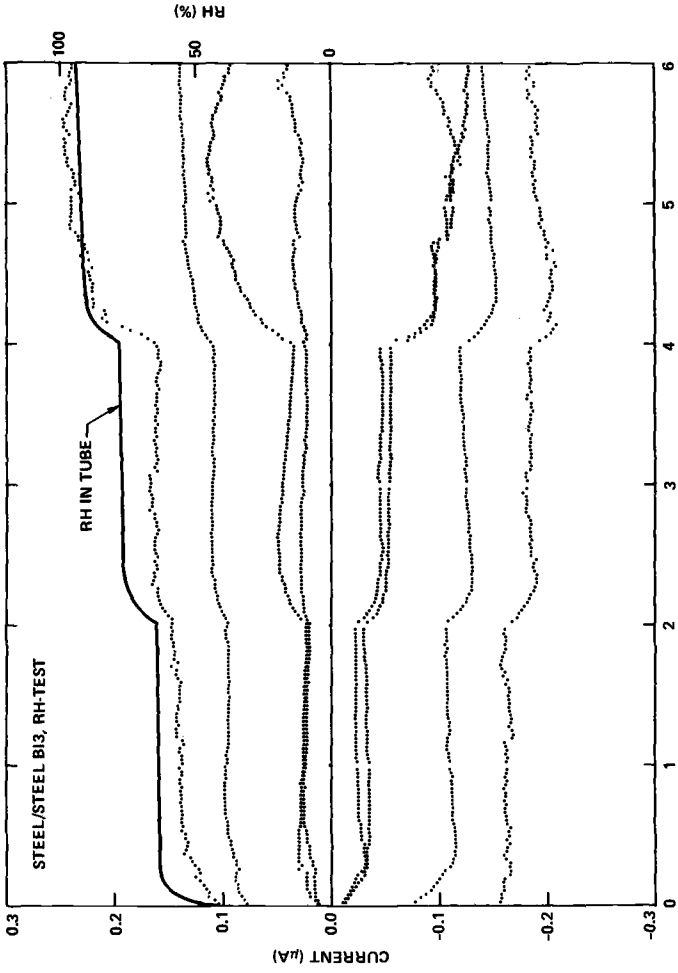

FIG. 6—*Experimental results for steel/steel exposed to RH = 65, 80, and 95 percent for 2 h each.*

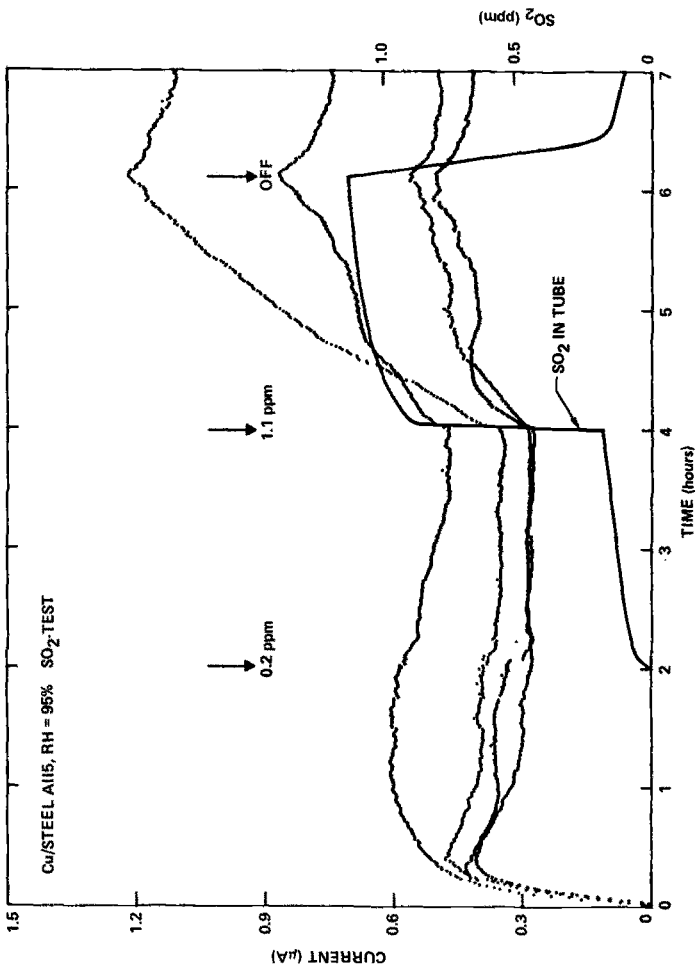

FIG. 7—*Experimental results for copper/steel exposed to SO_2 concentration of ≈0, 0.2, and 1.1 ppm for 2 h each.*

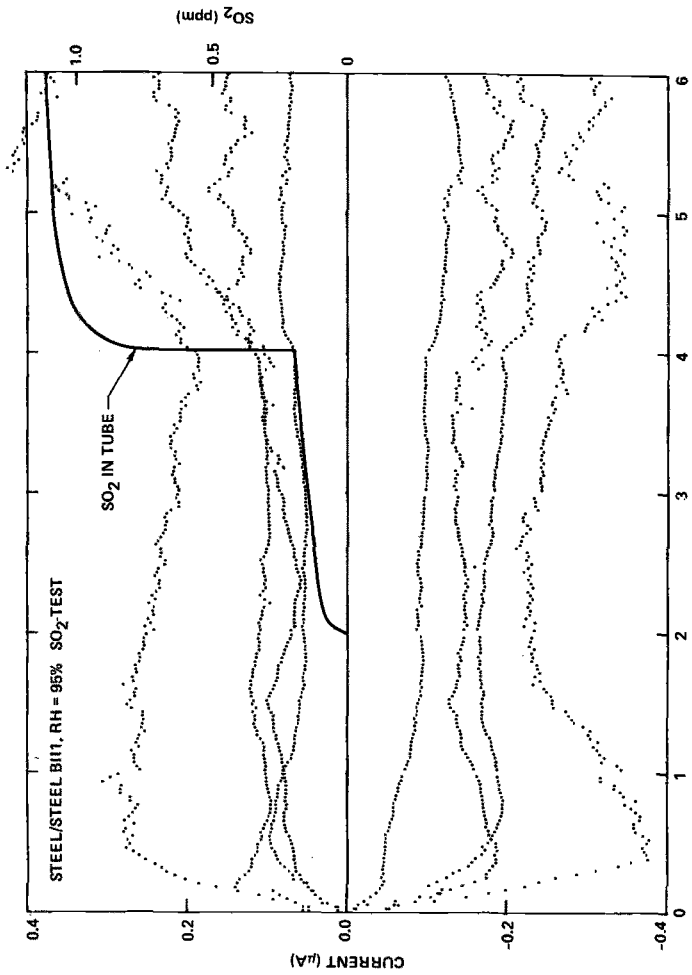

FIG. 8—*Experimental results for steel/steel exposed to SO_2 concentration of ≈0, 0.2, and 1.1 ppm for 2 h each.*

of evaporation, indicating that the corrosion reaction has stopped or become very slow due to a lack of electrolyte. For the four ACM's in Fig. 3, very close agreement is found for the current-time traces. Drying occurred between 4.0 and 4.3 h. The maximum current, I_{max}, was between 300 and 350 μA.

The relative humidity at the output of the tube stayed very high, despite setting the relative humidity control to 45 percent at a flow rate of 4 litres/min, which is probably due to the relatively large amount of electrolyte (about 15 ml) on the ACM's and weight loss specimens. For the example in Fig. 3, relative humidity reached a maximum of 88 percent after $2\frac{1}{2}$ h and was at 65 percent after 6 h when, according to the electrochemical data, the ACM surfaces were dry.

The current-time behavior during drying of the steel/steel ACM's is shown in Fig. 4. A potential of ± 30 mV was applied to the ACMs with polarity reversal after 50 s, which leads to alternating negative and positive currents as shown in Fig. 4. In general, an increase of current with time was observed and was more pronounced toward the end of the experiment. Close agreement in the times at which the specimens dried is found for three of the four ACM's in Fig. 4 which represent the first four specimens on one end of the support plate.

Relative humidity stayed close to 80 percent during the time that a current flow was observed; it then decreased to about 65 percent and was still 63 percent after 6 h. A steady value of RH = 45 percent was reached only after 14 h.

The response of four copper/steel ACMs, coated with the corrosion-produced layer which was formed during the drying test, is shown in Fig. 5 for the relative humidity sequence of 65-80-95 percent for 2 h each. When relative humidity was increased from 45 to 65 percent, the current increased immediately and then slowly decreased. When relative humidity was increased again to 80 and to 95 percent, the ACM's behaved similarly. The spread of the current for the four ACM's at the end of the test reached a factor close to two.

The relative humidity took about 1 h to reach the desired values. For all three relative humidity levels, the final values were a few percent too low. It is not entirely clear whether this result is real or an instrumental artifact.

The response of four steel/steel ACM's to varying levels of relative humidity is shown in Fig. 6. The current follows rapidly a relative humidity change. It takes about 1/2 h at RH = 65 percent and 1 h at 80 and 95 percent until the relative humidity at the output of the tube reaches the value that was set at the flowmeter of the mixing system. As shown in Fig. 6, fairly large differences of the current between the ACM's are observed.

As shown in Fig. 7 for copper/steel there was an initial increase of the current when relative humidity was increased from 45 to 95 percent followed by a slow decrease. When 0.2-ppm SO_2 was added to the wet air, this decrease slowed down or stopped in most cases. The SO_2 concentration at the output of the tube (Fig. 7) increased slowly and reached about 0.18 ppm at the end

of 2 h. An increase to 1.1 ppm produced an immediate increase of the current, showing that there is a definite effect of SO_2 at higher concentrations (and high relative humidity) on corrosion of steel. The ambient SO_2 concentration reached 1.09 ppm after 1 h and 1.13 ppm after 2 h. When the SO_2 was turned off, an immediate decrease of the current was observed; however, in most cases, the current measured when the SO_2 level returned to 0.2 ppm again remained higher than after 4 h at the initial SO_2 level of 0.2 ppm.

The corresponding data for steel/steel ACM's are given in Fig. 8, which also shows the SO_2 concentration at the exit of the tube. In some cases, a slight increase of the ACM current can be observed when the SO_2 concentration was increased to 0.2 ppm. A larger effect was observed for 1.1 ppm. It is interesting to note that significant scatter occurred for most steel/steel ACM's at 1.1 ppm which was not observed at the lower SO_2 concentration.

Summary of Experimental Data

A detailed statistical analysis of the experimental data will be performed in the final phases of this project. For the first evaluation of the results obtained until now, a summary is given in the following figures which contain the time, t_{dry}, at which the current dropped to very low values and the surface was assumed to be dry, and the maximum current, I_{max}, recorded during the experiment. For the relative humidity and SO_2 tests, the current I_2 after each 2-h period is recorded. For the statistical analysis the t_{dry} data and the amount of electricity Q flowing in each time segment will be used.

An example of data obtained during drying of copper/steel is given in Fig. 9. The data are plotted for the 15 positions along the axis of the tube. It was sometimes observed that the t_{dry} data were somewhat higher at the ends of

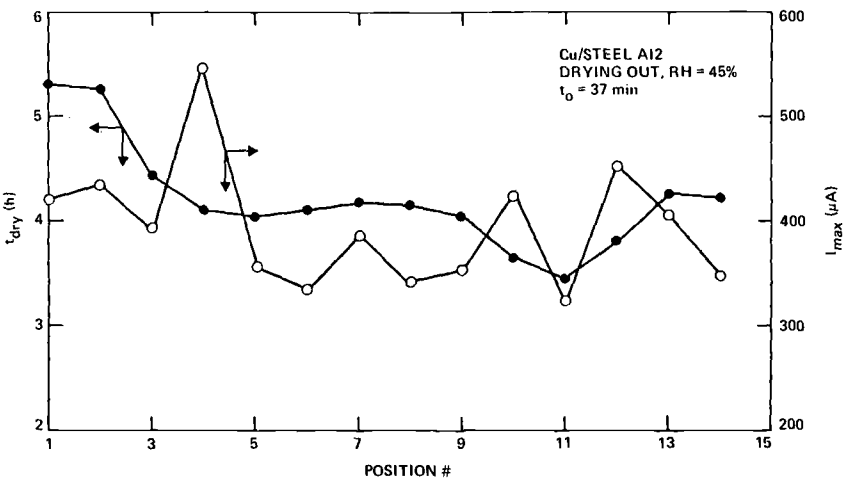

FIG. 9—*Time to drying* t_{dry} *and maximum current* I_{max} *for copper/steel.*

the tube, perhaps because the local humidity at these locations was higher due to the presence of the weight loss specimens (see Fig. 2). These were covered with more electrolyte (1.3 ml/specimen) than the ACM's (0.5 ml/ACM) because of their larger area. The average t_{dry} was about 4 h. The I_{max} data seem to show more scatter than the t_{dry}-values. The amplifier for the ACM at Position 15 stopped functioning during the test, but was repaired before the following relative humidity test.

A certain time elapses between application of the electrolyte and start of the experiment when the ACM's are placed in the test tube and all connections are made. This time is designated as t_o and has to be added to t_{dry}.

The corresponding results for steel/steel are given in Fig. 10, which contains t_{dry} and the maximum values for I^+ and I^- corresponding to the applied voltage of ±30 mV. The average value of t_{dry} was about 3.3 h. For the statistical analysis, the average values $I_{max} = 1/2(I^+ + |I^-|)$ are used for each ACM.

Examples for the relative humidity tests are given in Fig. 11 (copper/steel) and Fig. 12 (steel/steel). An increase from RH = 65 to 80 percent produced only a small effect on I_2 because of the gradual decay of the current during the 2-h test (Figs. 3 and 4). A much larger effect was observed when relative humidity was set to 95 percent. These results confirm the earlier results [*4–6*] which suggested an exponential increase of I_g with relative humidity. The results for the SO_2 tests are given in Fig. 13 (copper/steel) and Fig. 14 (steel/steel). Due to the tendency for a gradual current decay at RH = 95 percent in the absence of SO_2, which continues more or less at 0.2-ppm SO_2, most data points for 0.2 ppm are below those determined in the absence of SO_2. As discussed in the preceding, a much larger effect is observed for 1.1 ppm.

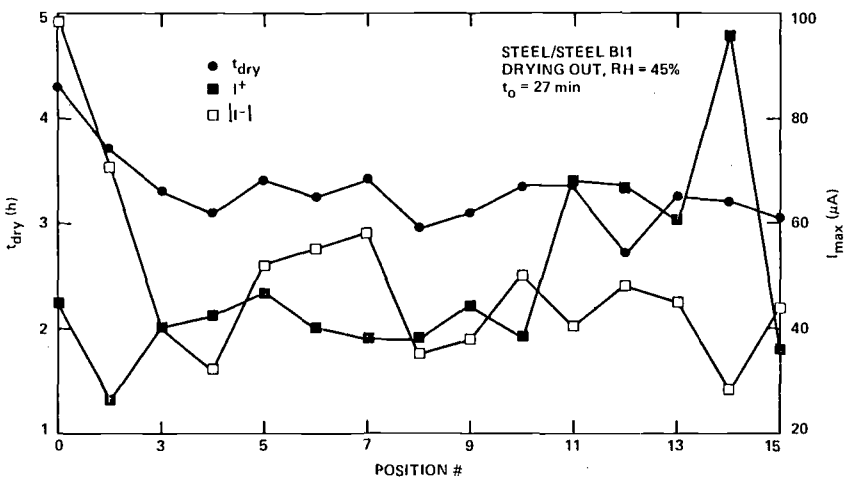

FIG. 10—*Time to drying* t_{dry} *and maximum current* I_{max} *for steel/steel.*

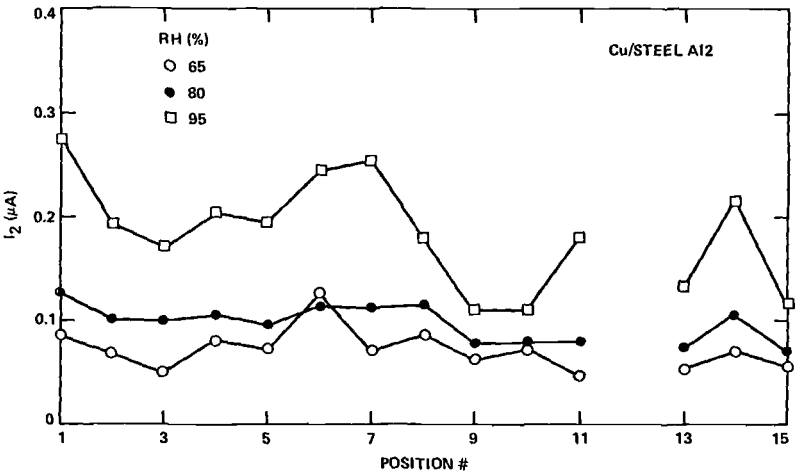

FIG. 11—*Current at the end of each 2-h period at RH = 65, 80, and 95 percent (copper/steel).*

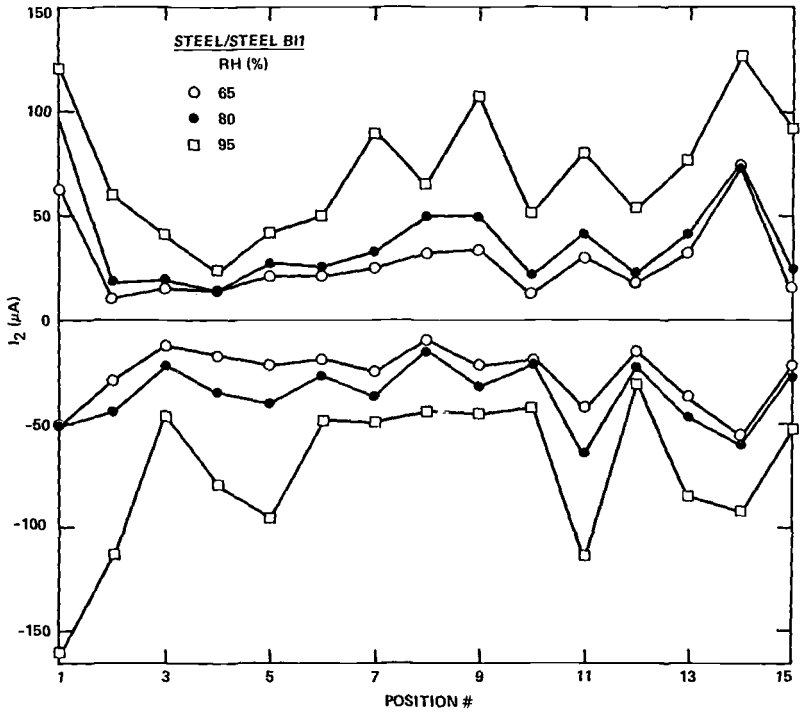

FIG. 12—*Current at the end of each 2-h period at RH = 65, 80, and 95 percent (copper/steel).*

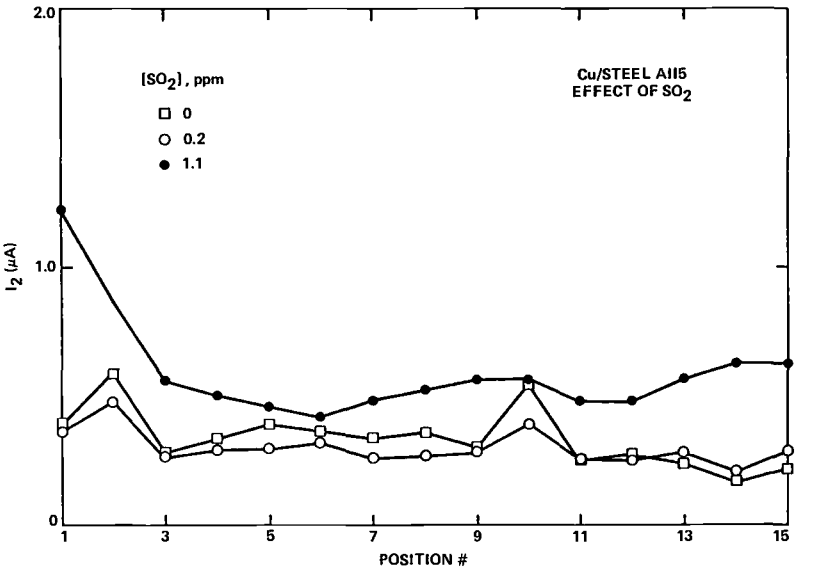

FIG. 13—*Current at the end of each 2-h period at ≈0, 0.2, and 1.1-ppm SO_2 (copper/steel).*

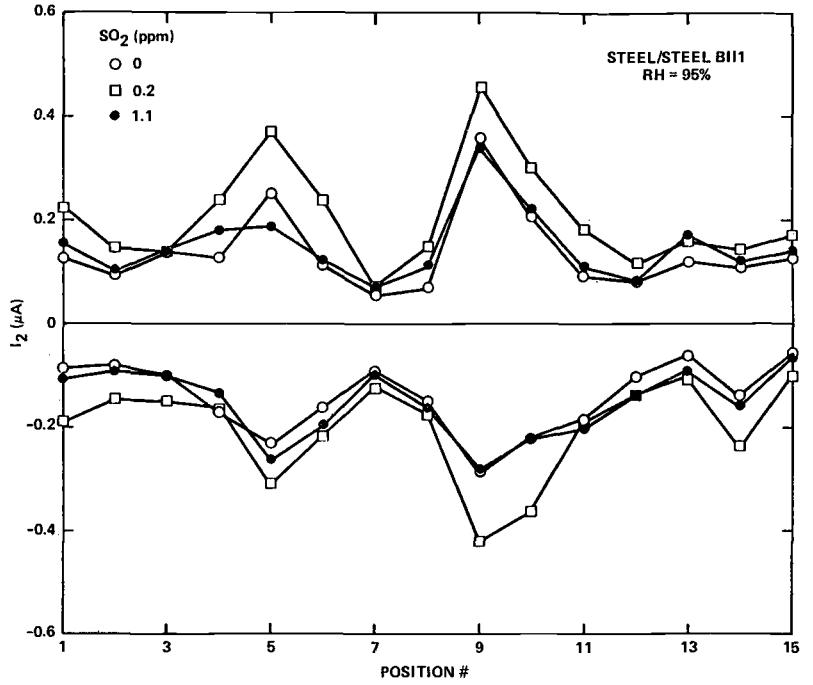

FIG. 14—*Current at the end of each 2-h period at ≈0, 0.2, and 1.1 ppm SO_2 (steel/steel).*

TABLE 3—*Average values of* t_{dry}, I_{max} *and* Q *for drying of copper/steel ACM's.* (A_{steel} = 4.30 cm^2).

Code	t_{dry}, h	I_{max}, μA	Q, mCb
AI1	5.58 ± 0.44	570 ± 82	3798 ± 460
AI2	4.56 ± 0.59	421 ± 52	3015 ± 298
AI4	4.64 ± 0.49	305 ± 46	2302 ± 264
AI5	4.19 ± 0.45	296 ± 48	2422 ± 341
AII3	4.80 ± 0.47	334 ± 57	2606 ± 167
AII4	5.70 ± 0.42	337 ± 34	3641 ± 246
AII5	4.56 ± 0.31	308 ± 58	2333 ± 294
Mean	4.97	367	2874
SD	0.48	98	627
V	0.20	8354	336848

Discussion

Until now, integration of the current-time curves and statistical analysis of these data in terms of the effects of heat, sensor, position, and time has been done only for the drying data. A summary of the experimental data is given in Tables 3–9, followed by the results of the statistical analysis.

In Tables 3 and 4, average values are given for t_{dry}, I_{max}, and Q for each set of measurements with copper/steel (Table 3) and steel/steel (Table 4) ACM's. Also listed in these two tables are the mean (M), standard deviation (SD) and variance (V) for all measurements carried out for copper/steel and steel/steel ACM's. The drying time, t_{dry}, is longer for copper/steel than for steel/steel. This effect, which could be due to the larger amount of NaCl solution on the larger surface area of the copper/steel ACM's (Table 3, 4), is being studied at present for ACM's with varying numbers and thicknesses of plates. The Q-values for steel/steel have to be multiplied by the k-factor in Eq 2 in order to obtain the amount of electricity corresponding to the corrosion loss during the drying-out period.

TABLE 4—*Average values of* t_{dry} *and* Q *for drying of steel/steel ACM's* (A_{steel} = 2.15 cm^2 × 2).

Code	t_{dry}, h	Q, mCb
BI1	3.74 ± 0.36	350 ± 60
BI2	3.39 ± 0.31	294 ± 64
BI3	3.17 ± 0.24	265 ± 39
BII1	3.69 ± 0.29	327 ± 42
BII2	3.44 ± 0.29	273 ± 86
BII3	3.40 ± 0.23	295 ± 37
Mean	3.47	301
SD	0.21	32
V	0.037	874

TABLE 5—*Average values of* t_{dry}, I_{max} *and* Q *for drying of copper/steel ACM's (three different heats: B, C, D).*

Code	Heat B			Heat C			Heat D		
	t_{dry}, h	I_{max}, μA	Q, mCb	t_{dry}, h	I_{max}, μA	Q, mCb	t_{dry}, h	I_{max}, μA	Q, mCb
AI1	5.06 ± 0.58	595 ± 85	4267 ± 394	5.00 ± 0.52	573 ± 37	3780 ± 608	4.81 ± 0.19	528 ± 72	3347 ± 340
AI2	4.50 ± 0.69	435 ± 66	3340 ± 620	3.80 ± 0.46	425 ± 60	2949 ± 732	3.64 ± 0.35	407 ± 38	2755 ± 334
AI4	4.31 ± 0.58	351 ± 25	2594 ± 512	4.01 ± 0.43	265 ± 25	2080 ± 258	4.17 ± 0.52	300 ± 38	2231 ± 375
AI5	4.63 ± 0.62	350 ± 27	2795 ± 176	4.45 ± 0.41	279 ± 34	2347 ± 283	4.30 ± 0.30	261 ± 25	2125 ± 186
AII3	4.44 ± 0.61	398 ± 54	2787 ± 314	4.31 ± 0.21	303 ± 20	2457 ± 147	4.52 ± 0.57	301 ± 20	2574 ± 309
AII4	5.20 ± 0.57	399 ± 23	3881 ± 393	5.10 ± 0.24	365 ± 22	3389 ± 272	5.38 ± 0.43	350 ± 37	3653 ± 368
AII5	4.28 ± 0.18	354 ± 50	2671 ± 205	3.94 ± 0.41	295 ± 54	2197 ± 252	4.12 ± 0.23	276 ± 48	2132 ± 322
Mean	4.36	411	3191	4.37	358	2743	4.42	346	2688
SD	0.36	87	659	0.51	110	647	0.56	94	608
V	0.11	6473	371845	0.23	10378	358774	0.17	7590	316849

TABLE 6—*Average values of* t_{dry} *and* Q_{avg} *for drying of steel/steel ACM's.*

	Heat B		Heat C		Heat D	
Code	t_{dry}, h	Q, mCb	t_{dry}, h	Q, mCb	t_{dry}, h	Q, mCb
BI1	3.50 ± 0.45	395 ± 85	3.12 ± 0.29	328 ± 26	3.26 ± 0.28	327 ± 27
BI2	3.00 ± 0.46	322 ± 95	2.73 ± 0.25	279 ± 48	2.89 ± 0.12	280 ± 40
BI3	2.79 ± 0.17	298 ± 34	2.64 ± 0.17	255 ± 13	2.59 ± 0.34	243 ± 43
BII1	3.46 ± 0.16	365 ± 38	3.05 ± 0.27	293 ± 22	3.36 ± 0.30	303 ± 26
BII2	3.18 ± 0.25	324 ± 35	3.21 ± 0.39	287 ± 46	3.12 ± 0.32	264 ± 19
BII3	2.93 ± 0.20	321 ± 36	2.74 ± 0.22	272 ± 22	2.94 ± 0.24	292 ± 38
Mean	3.14	338	2.92	286	3.03	285
SD	0.29	36	0.24	25	0.28	30
V	0.07	1052	0.05	503	0.07	728

In Tables 5 and 6 the average values for each test have been listed again, but have been calculated separately for each heat. I_{max} and Q are higher for Heat *B* than for the other two heats which appear equal. The t_{dry} results, on the other hand, are similar for all three heats. The weight loss data in Tables 7 and 8 are listed separately for the relative humidity and the SO_2 tests. However, an analysis of the electrochemical data shows that by far the highest corrosion occurs in the preceding drying phase and, as can be seen from the two tables, the weight loss data for the two tests are very similar. Heats C and D behave very similarly, while Heat B corrodes at a higher rate. The reason for this result is not known; however, it is an important result that the small differences in corrosion rate were detected at a statistically significant level.

A summary of the mean t_{dry} and charge density Q' data for the three heats of copper/steel and steel/steel ACM's is given in Table 9. Although the data

TABLE 7—*Weight loss data for 4130 steel, RH tests* (Δm *in mg*).

Code	Heat B	Heat C	Heat D
AI1	25.3	24.0	23.0
	39.7	25.2	26.5
AI2	29.3	29.8	27.6
	23.7	23.3	25.7
AI4	37.0	26.2	24.4
	41.0	20.8	29.4
BI1	29.9	26.7	18.2
	24.7	23.8	25.6
BI2	37.2	28.8	25.8
	22.8	26.7	28.3
BI3	28.2	18.9	23.9
	28.5	25.5	25.3
Mean	30.6	25.0	25.3
SD	6.4	3.1	2.9

TABLE 8—*Weight loss data for 4130 steel, SO_2 tests (Δm in mg).*

Code	Heat B	Heat C	Heat D
AI13	34.4	24.1	28.1
	39.9	31.4	30.7
AI14	37.1	28.7	27.3
	25.7	30.2	25.7
AI15	37.2	25.3	26.6
	33.8	24.7	26.3
BI11	40.2	26.5	23.7
	37.9	20.0	22.6
BI12	26.5	22.9	21.5
	28.8	29.5	21.1
BI13	31.5	22.4	23.7
	34.6	19.4	26.2
Mean	34.0	25.4	25.3
SD	4.9	3.9	2.8

are consistent between heats for t_{dry}, there is an indication that the electrolyte layer dries faster for steel/steel than for copper/steel ACM's. This is probably due to the presence of more electrolyte on the copper/steel ACM, which has a total of 20 plates compared with 10 plates for steel/steel. Experiments are now being carried out with ACM's that have different numbers of plates and different plate thicknesses in order to determine the effect of ACM design on reproducibility of ACM data, time-of-wetness, and the cell factor.

Since the relative humidity and SO_2 tests add only very little to the Q'-values, a cell factor can be calculated from the data in Table 9 after converting the weight loss per unit area into charge densities, using Faraday's law. For copper/steel a cell factor of about 18 percent is found, which is in re-

TABLE 9—*Summary of drying data for copper/steel and steel/steel sensors.*

	Heat B		Heat C		Heat D	
	t_{dry}, h	Q_{avg}, mCb/cm^2	t_{dry}, h	Q'_{avg}, mCb/cm^2	t_{dry}, h	Q'_{avg}, mCb/cm^2
Copper/steel	4.6	742	4.4	638	4.4	625
Steel/steel	3.1	157 (275)[a]	2.9	133 (233)	3.0	133 (233)
Weight loss (mg/cm^2)						
RH test		1.8 (4070)[b]		0.96 (3310)		0.97 (3345)
SO_2 test		1.31 (4520)		0.98 (3380)		0.97 (3345)

[a] $Q^T = \frac{2B}{\Delta E} Q'_{avg} = 1.75\ Q'_{avg}$.

[b] 1 mg/cm^2 = 3.45 Cb/cm^2.

markable agreement with the value of 20 percent determined earlier for drying under 0.01-N Na_2SO_4 at relative humidity values between 30 and 75 percent (Table 1). On the other hand, the cell factor for steel/steel is only about 7 percent which is much lower than the average value in Table 1. One reason for this much lower cell factor might be the lower conductivity of the 1-mM NaCl used in the present experiments. This would lead to a lower effective $\Delta E_{\text{eff}} = \Delta E - \eta_\Omega$, where η_Ω is the uncompensated ohmic drop in the solution. Alternating current impedance measurements are being carried out to determine whether this source of error is important. The most likely explanation for the low cell factor is corrosion on individual plates without electrolytic connection to neighboring plates and consequently without current flow in the measuring circuit.

Statistical Analysis

The experiments were designed to test the null hypothesis that the sensing devices provide statistically consistent measurements. This will imply that the comparison of corrosion data obtained at several different sites will not be statistically confounded with the differences among the sensors used at the sites. In order to test this hypothesis, factorial designs consisting of four factors were used. These factors were steel distributor or heat, days during which the experiments were run, position or relative location of the sensors in the test chamber, and sensors. The steel used in the fabrication of the sensors was bought from three different distributors, which were not selected "at random" but were selected so that the steel used would be representative of three different sources. Hence, distributor or heat was a fixed effect in the model for the design. Similarly, the days during which the experiments were run were not selected at random, but were consecutive. The relative locations of the sensors in the test chamber were selected and rotated each day, so that every sensor occupied all of the positions that were expected to affect the results of the experiment. Therefore, days and relative position were considered fixed effects in the model. Finally, the sensors were considered to be a random sample from the total population of all possible sensors that might have been fabricated from the heats of steel and copper that were used in the experiment.

Since it is physically very unlikely that either the effect of relative position or sensor interacts with the day-to-day effect, the measure of these interactions was considered experimental error. Replications were impossible because of the nature of an observation, and hence a direct estimate of the error could not be made.

Five sensors were fabricated from the material from each distributor. This required sensors to be analyzed as "nested" factors within distributor. Since only one position could be represented by any one sensor on a given day, it

was possible to measure either the effect of relative position or sensor, but not both, for a given analysis configuration. Therefore two different models were hypothesized and tested. The first model can be expressed as

$$y_{ijkl} = \mu + \alpha_i + \beta_j + \alpha\beta_{ij} + \gamma_{k(i)} + \beta\gamma_{jk(i)} + \epsilon_{l(ijkl)} \tag{3}$$

where

y_{ijkl} = observation on the jth day using the kth sensor fabricated from the steel of the ith distributor,
μ = an overall mean effect,
α_i = effect of different heats,
β_j = day-to-day effect,
$\alpha\beta_{ij}$ = interaction effect of heat with day,
$\gamma_{k(i)}$ = effect of different sensors fabricated from the same heat,
$\beta\gamma_{jk(i)}$ = interaction effect of day with sensor, the measure of which is considered due only to experimental error, and
$\epsilon_{l(ijkl)}$ = independent experimental error that is, for every observation, normally distributed with mean zero and common variance. As explained in the preceding, it is not directly measurable.

The hypotheses tested were

$$\begin{aligned} H_A &= \text{all } \alpha_i &&= 0 \\ H_B &= \text{all } \beta_j &&= 0 \\ H_{AB} &= \text{all } \alpha\beta_{ij} &&= 0 \\ H_C &= \text{all } \gamma_{k(i)} &&= 0 \\ H_{BC} &= \text{all } \beta\gamma_{jk(i)} &&= 0 \end{aligned}$$

To test, in other words, if the different levels of each of the main factors (heat, days, and sensors) and interaction factors have the same effect. Using analysis of variances for nested factorial designs, Hypotheses H_A and H_B were both rejected with well over 99 percent confidence, which means that there is a significant heat and day-to-day effect. The day-to-day effect cannot be the result of different surface activities after polishing since there was no difference between the five sensors in one heat. It is more likely that the local humidity changed from day to day, causing the observed effect. The hypotheses H_{AB}, H_C, and H_{BC} could not be rejected even for a significance level of 0.25. These results were found for both the copper/steel and steel/steel ACM's.

Since the sensors were not found to be significantly different, the second model was hypothesized in order to test the null hypothesis of no effect due to the relative position of the sensors in the test chamber. The model

$$y_{ijkl} = \mu + \alpha_i + \beta_j + \alpha\beta_{ij} + \eta_k + \alpha\eta_{ik} + \beta\eta_{jk} + \alpha\beta\eta_{ijk} + \epsilon_{l(ijk)}$$

is the same as the first model except that the relative position effect, η_k, is not nested within the distributor and, hence, its interaction with the other two

main effects can be estimated. Specifically, y_{ijkl}, μ, α_i, β_j, $\alpha\beta_{ij}$, and $\epsilon_{l(ijk)}$ are the same as in the previous model, whereas

η_k = effect of different positions in the test chamber,
$\alpha\eta_{ik}$ = interaction effect of heat with position,
$\beta\eta_{ik}$ = interaction effect of day with position, and
$\alpha\beta\eta_{ijk}$ = interaction effect of heat, day, and position. The measure of this interaction is considered due to experimental error only.

The mean sums of squares for the interaction effects $\beta\gamma_{jk(i)}$ in the first model and $\alpha\beta\eta_{ijk}$ in the second model were found to be nearly equal, thus providing support for the assumption that both are estimates of experimental error. The hypotheses tested were

$$H_D\text{: all } \eta_k = 0$$
$$H_{AD}\text{: all } \alpha\eta_{ik} = 0$$
$$H_{BD}\text{: all } \beta\eta_{jk} = 0$$

Again, using analysis of variances of the hypothesis, H_D was rejected with well over 99 percent confidence, which means that the position of the sensor in the tube affects its output. This is probably due to higher local humidity because of the presence of the larger amounts of electrolyte on the weight loss specimens at the ends of the tube. The interaction effects could not be rejected at a significance level of 0.25. These results were exactly the same for the copper/steel and the steel/steel ACM's.

In conjunction with each experiment to test sensor homogeneity, a factorial experiment was designed and conducted simultaneously to measure actual weight loss due to corrosion in the test chamber. These weight loss experiments included the three factors of steel heat, chamber position (left- or right-hand side of the test chamber), and day. Analyses of variance for each of these experiments were in agreement with the electrochemical experiments discussed earlier which showed that the difference between heats is statistically significant with more than 99 percent confidence. However, the data from these experiments did not provide sufficient evidence to indicate a significant difference between the right- and left-hand positions, or among the days during which the experiments were run.

These results clearly indicate that the heat of the steel from which these sensors are fabricated is quite important. Any further testing must also include day-to-day variation and chamber location as significant factors. However, given that the sensors are fabricated with steel from a single uniform heat, they can be expected to provide statistically consistent measurements.

Summary

1. Problems with present definitions of the time-of-wetness have been discussed. Results obtained in the authors' laboratory and by other investi-

gators have shown that electrochemical sensors measure only a fraction of the atmospheric corrosion rate.

2. In order to evaluate the factors which determine the reproducibility of electrochemical corrosion sensors, the cell factor, and the time-of-wetness, a statistically designed experiment is being carried out. Preliminary results are being reported.

3. Fifteen sensors of the copper/steel and steel/steel type, respectively, have been assembled using three different heats of 4130 steel and copper. These sensors are being tested in triplicate runs by exposing all 15 sensors at the same time in a test tube in a fixed test sequence which includes variations of relative humidity and SO_2 concentrations. Weight loss specimens are exposed at the same time under identical conditions for correlation with the electrochemical data.

4. The results of a statistical analysis of the current-time curves during the initial drying period under a thin layer of an aqueous 1-mM NaCl solution show that the heat of the steel plays an important role. No differences in corrosion behavior were found for the five sensors of a given heat. Day-to-day variations due to differences of the local environment in the test chamber and to some extent the position of the sensor in the chamber can also affect the results.

5. By comparing the electrochemical and the weight loss data, a cell efficiency of about 20 percent was found for copper/steel and about 7 percent for steel/steel. These low cell factors are considered to be due to local cell action on the individual plate of a sensor without current flow in the external measuring circuit, and to the low conductivity of the test electrolyte.

6. The sensors will be tested again after a 3-month and a 6-month aging period in outdoor exposure.

Acknowledgment

This material is based upon work supported by the National Science Foundation under Grant No. DMR-7923965.

APPENDIX

Design of Measurement System for Reproducibility Studies

A measurement system has been designed which uses a multiprogrammer and a minicomputer to perform these tests as shown in Figs. 15 and 16. The current measurement is somewhat different for copper/steel and steel/steel ACM's.

For copper/steel ACM's the galvanic current flowing between the dissimilar plates in the presence of electrolyte is measured as shown in Fig. 15. A current follower keeps the dissimilar metals at the same potential and measures the current continuously (zero resistance ammeter). This current is recorded sequentially for each of the 15 cells by closure of the relay R_i using the analog-to-digital (A/D) converter of the Hewlett-Packard 6940B multiprogrammer. The mean of five measurements taken in

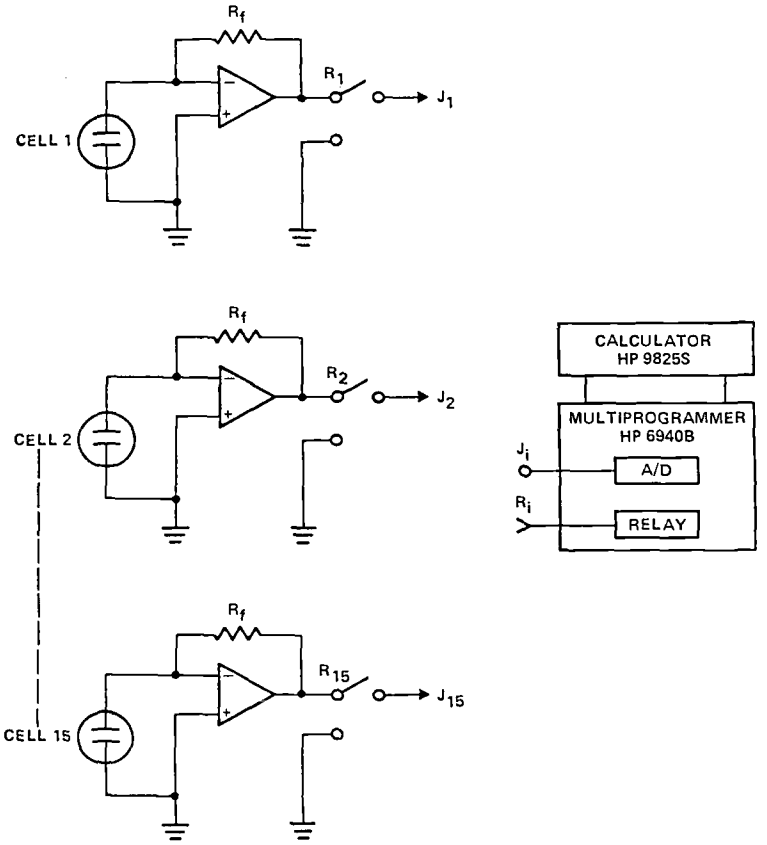

FIG. 15—*Galvanic current measurement of copper/steel ACM.*

a 5-s period is recorded every 50 s for each sensor. Control and timing are provided by the HP9825S computer on which the data are stored for further processing and display.

For steel/steel ACM's the polarization resistance is determined by applying an emf of ±30 mV, the polarity of which is changed every 50 s. A PAR 175 universal programmer is used to apply the potential square wave (Fig. 16). Switching and measurement of the current are performed as discussed for the copper/steel ACM's except that the five current measurements which are averaged are always taken between 38 and 43 s of each 50-s potential pulse.

References

[*1a*] Sereda, P. J., American Society for Testing and Materials Bulletin No. 246, May 1960, p. 47.

[*1b*] Sereda, P. J., *Industrial and Engineering Chemistry,* Vol. 52, No. 2, 1965, p. 157.

[*1c*] Sereda, P. J. in *Corrosion in Natural Environments, ASTM STP 558,* American Society for Testing and Materials, 1974, p. 7.

[*2*] Kucera, V. and Mattsson, E. in *Corrosion in Natural Environments, ASTM STP 558,* American Society for Testing and Materials, 1974, pp. 239–260.

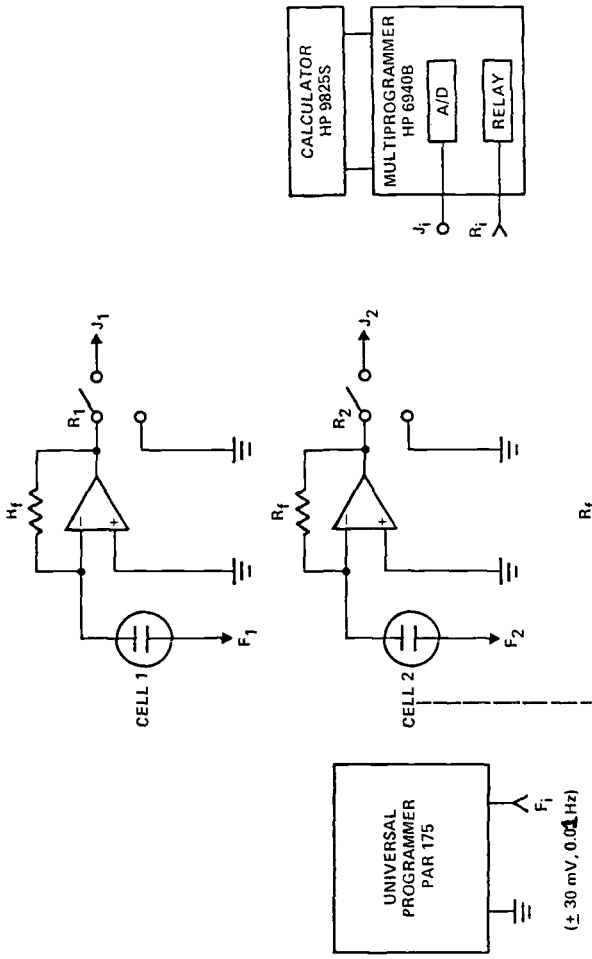

FIG. 16—*Current measurement for steel/steel ACM with ±30-mV potential applied.*

[3] Voigt, C., *Korrosion,* Vol. 10, No. 3, 1979, p. 179.
[4] Mansfeld, F. and Kenkel, J. V., *Corrosion Science,* Vol. 16, 1976, p. 111.
[5] Mansfeld, F. and Kenkel, J. V., *Corrosion,* Vol. 33, 1977, p. 13.
[6] Mansfeld, F., *Werkstoffe und Korrosion,* Vol. 30, 1979, p. 38.
[7] Kucera, V. and Collins, M. in *Proceedings,* Sixth European Congress on Metallic Corrosion, Society of Chemical Industries, London, 1977, p. 189.
[8] Mansfeld, F. and Tsai, S., "Laboratory Studies of Atmospheric Corrosion," *Corrosion Science,* Vol. 20, 1980, p. 853.
[9] Mansfeld, F. in *Electrochemical Corrosion Testing, ASTM STP 727,* American Society for Testing and Materials, 1981, p. 215.
[10] Mansfeld, F. in *Advances in Corrosion Science and Technology,* Plenum Press, New York, Vol. 6, 1976, p. 163.

DISCUSSION

S. C. Byrne[1] *(written discussion)*—The time-of-wetness gage should be drastically affected by the hydroscopic or other properties of corrosion products which, in turn, should be affected by atmospheric composition. Has any work been planned to further define the role of atmospheric composition in determining time-of-wetness?

F. Mansfeld et al (authors' closure)—The question of the effects of the chemical nature of corrosion products on atmospheric corrosion behavior has been addressed in an earlier paper (Ref *5* of text). Different chlorides and sulfates were added to synthetic rust and it was shown that the response of an ACM depended strongly on the nature of the additives. It was pointed out that the strong involvement of the corrosion products, the chemical nature of which is determined by the composition of the atmosphere, is one of the characteristic features of atmospheric corrosion.

[1] Alcoa Laboratories, Alcoa Center, Pa.

A. A. Bragard[1] *and H. E. Bonnarens*[1]

Prediction at Long Terms of the Atmospheric Corrosion of Structural Steels from Short-Term Experimental Data*

REFERENCE: Bragard, A. A. and Bonnarens, H. E., **"Prediction at Long Terms of the Atmospheric Corrosion of Structural Steels from Short-Term Experimental Data,"** *Atmospheric Corrosion of Metals, ASTM STP 767*, S. W. Dean, Jr., and E. C. Rhea, Eds., American Society for Testing and Materials, 1982, pp. 339–358.

ABSTRACT: Two experimental laws expressing the relationship between the weight losses and the time of exposure allow a fair assessment of the corrosion evolution of steels in numerous sites. The simultaneous existence of these two laws implies intercorrelation between the coefficients of the empirical equations.

The effects of the climatic and pollution factors on these coefficients are discussed.

It is suggested to represent the corrosiveness of a test site toward a steel grade by the one-year weight loss and the further evolution of corrosion as a function of this weight loss and the relative humidity of the site.

KEY WORDS: structural steels, atmospheric corrosion field tests, weather factors, corrosion site calibration, corrosion laws, long-term predictions

Results of numerous exposure programs in atmospheric test sites to study the uniform corrosion of steels have been reported. Unfortunately, most of the reports do not provide information on the climatic and pollution conditions during the exposure period. Very often, local atmospheric conditions are described in general terms or even are related to a rough classification of typical environments such as rural, urban, industrial, or marine.

A few studies, however, have attempted to correlate the factors which influence atmospheric corrosion with the performance of steels. Although pertinent information has been drawn from the data collected, it appears that the many factors involved need to be better defined. Indeed, to the best of our knowledge, there is no relationship between the corrosion of a given steel

* Research sponsored by the Commission of the European Communities (ECSC) and the Institut pour l'encouragement de la Recherche Scientifique dans l'Industrie et l'Agriculture (I.R.S.I.A.), Belgium.

[1] Head and chemical engineer, respectively, "Utilization of Steel" Department, Centre de Recherches Metallurgiques (C.R.M.) Liége, Belgium.

grade and the environmental conditions accurate enough to reliably predict the behavior of the same steel in locations other than those where it was actually exposed, on the basis of the climatic and pollution factors only.

Studies of this type do provide, however, useful information on the ways of characterizing the exposure sites, on the corrosion behavior of steels, and on the prediction of long-term behavior from short-term data.

The purpose of this paper is to present the method available and the conclusions that can be drawn in this field.

Evolution of Corrosion

The need to establish relationships between corrosion weight losses and exposure time is obvious, not only in order to predict the performance of a steel from field data, but also to assess the effects of environmental factors on materials.

It is generally observed that the atmospheric corrosion of steel follows a power formula of the type

$$p = k\, t^n$$

where

p = weight loss, g/dm^2,
t = exposure time, years, and
k and n = constants.

The values of both k and n vary with steel grade and with site of exposure.

This law, proposed previously by several authors, gives a fair representation of the corrosion phenomena in many sites. Using this law it is theoretically possible to predict long-term behavior of a steel from short-term experimental data. The degree of confidence that can be placed in the extrapolation will depend upon the validity of the law for the steel considered.

To illustrate the reliability of the prediction by means of this method, we will use data from a long-term program carried out at three sites in Belgium. These are located at

1. Liège: This site is open on the roof of a six-story building. The prevailing winds come from the direction of a large steel plant.
2. Ostende I: This site is on a dike at the seashore. Prevailing winds are from offshore and often there is considerable salt mist and fog.
3. Ostende II: This site is close to Ostende I, and located 250 m from the seaside. It is protected from the sea by a 15-m-high dune.

The atmosphere of Liège is polluted by sulfur dioxide (SO_2), but chlorides are absent. Ostende I and II are typical marine sites. The airborne sulfur pollution at both sites is lower than that of Liège, although not negligible. The

chloride pollution is quite important and shows a marked seasonal variation in levels. A typical example of the reduction in monthly airborne chloride levels (wet-candle determination) with distance from the sea in the Ostende district is plotted on a log-linear scale in Fig. 1. There is a marked month-to-month variation in levels, mainly near the coast.

From a joint program with the aim to "calibrate" the different levels of corrosiveness of steels that could be observed at a network of 18 European sites, it appeared that the corrosion at Ostende I was always the greatest (three steels; 1, 2, 3, 4, and 5 years' exposure), and that Liège could be considered as an industrial site situated in the average of the corrosivity scale [*1*].[2]

A total of 24 different steels was exposed at each site for a period of 10 years. The chemical analyses are given in Table 1.

For each steel, values of k and n were calculated from the data of weight losses at 1, 2, 3, and 4 years' exposure. The two parameters were then used to predict the weight loss at 10 years. The predicted and actual 10-year values for weight losses are given in Table 2.

For Liège and Ostende II, the calculated values are generally underestimated. For Liège, however, the predicted and actual values are very close,

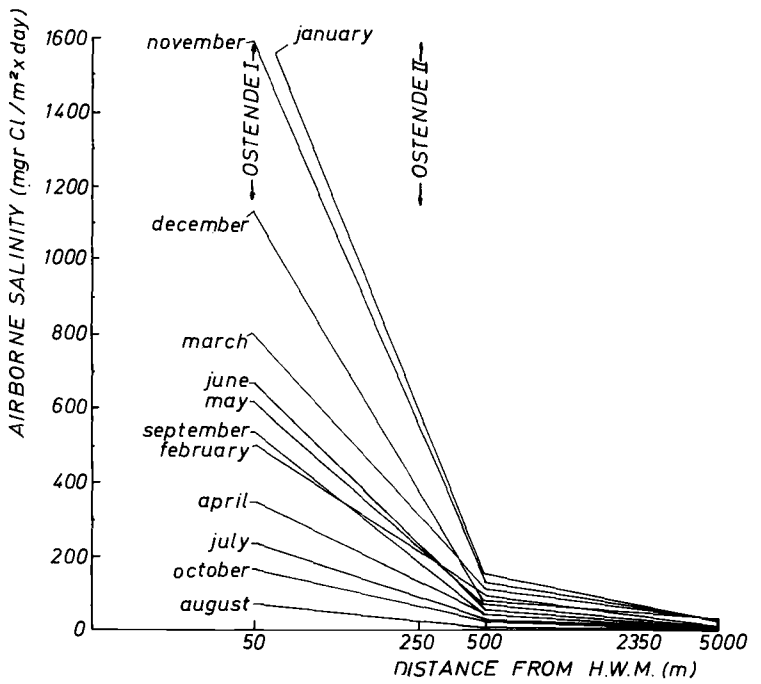

FIG. 1—*Salinity versus distance, Ostende district (year 1975).*

[2] The italic numbers in brackets refer to the list of references appended to this paper.

TABLE 1—*Chemical analyses of steels.*

Steel	C, 10^{-3}%	Si, 10^{-3}%	Mn, 10^{-3}%	P, 10^{-3}%	S, 10^{-3}%	Cu, 10^{-3}%	Al, 10^{-3}%	N_2 Total 10^{-4}%	Ni, 10^{-3}%	Sn, 10^{-3}%	V, 10^{-3}%	Cr, 10^{-3}%	Mo, 10^{-3}%
1	173	61	510	43	39	147	20	252	52	17	6	15	7
2	50	8	374	69	71	16	8	130	36	3	6	19	5
3	127	7	818	54	36	18	9	85	41	3	7	28	6
4	109	118	686	25	36	375	47	58	32	4	9	10	8
5	122	9	515	34	42	245	8	56	34	6	10	21	6
6	168	30	797	43	43	392	9	112	11	5	9	24	4
7	42	20	280	20	13	23	3	24	40	4	3	5	1
8	42	20	240	25	12	460	3	20	37	5	3	4	1
9	74	385	254	86	15	375	3	55	207	6	4	721	4
10	100	515	400	112	42	440	3	94	535	11	10	950	5
11	246	36	1395	15	21	230	3	43	30	4	2	21	4
12	120	24	690	11	23	260	2	62	46	4	31	13	6
13	205	tr.	464	10	28	18	3	44	13	4	3	28	3
14	170	54	506	10	26	180	8	61	40	6	3	28	7
15	120	60	425	113	26	605	5	61	614	10	2	36	11
16	70	390	365	85	25	410	23	132	46	6	3	638	3
17	91	325	378	100	20	340	23	159	48	5	4	572	2
18	120	254	868	71	12	21	43	142	38	3	4	309	3
19	120	282	882	55	11	22	49	148	39	4	4	308	2
20	220	6	812	61	41	19	2	115	46	5	6	17	2
21	90	232	880	50	31	235	54	97	43	6	3	17	5
22	210	27	778	42	31	220	2	97	45	6	3	11	2
23	153	172	1230	35	28	279	76	117	47	4	2	341	3
24	155	386	1330	38	28	28	111	135	45	3	3	19	2

TABLE 2—*Experimental and calculated 10-year weight losses.*

Steel	Liège			Ostende I			Ostende II		
	Experimental	Calculated	Experimental / Calculated	Experimental	Calculated	Experimental / Calculated	Experimental	Calculated	Experimental / Calculated
1	13.8	13.5	1.02	31.8	32.6	0.98	33.9	28.9	1.17
2	32.2	31.6	1.02	. . .	191.7	. . .	. . .	69.6	. . .
3	26.4	25.0	1.06	70.5	59.6	1.18	57.6	35.3	1.63
4	16.8	16.2	1.04	34.2	44.2	0.77	28.4	22.0	1.29
5	17.0	16.7	1.02	32.8	33.7	0.97	34.8	33.0	1.05
6	15.6	14.8	1.05	28.0	32.7	0.86	29.1	26.7	1.09
7	27.5	27.7	0.99	. . .	156.3	. . .	. . .	81.0	. . .
8	18.3	17.5	1.05	41.9	115.1	0.36	36.3	37.6	0.97
9	8.1	8.6	0.94	65.3	45.3	1.44	21.8	20.0	1.09
10	7.2	7.6	0.95	39.1	24.4	1.60	20.3	17.4	1.17
11	16.3	16.0	1.02	33.2	28.6	1.16	26.5	23.2	1.14
12	15.9	14.9	1.07	53.9	29.1	1.85	29.9	29.4	1.02
13	23.7	22.3	1.06	. . .	250.0	. . .	. . .	115.6	. . .
14	16.2	15.1	1.07	36.8	38.8	0.95	36.3	30.4	1.19
15	10.8	11.2	0.96	20.2	18.1	1.12	22.6	20.3	1.11
16	8.5	8.5	1.00	63.5	60.7	1.05	25.0	24.0	1.04
17	8.8	9.6	0.92	46.9	39.1	1.20	23.1	22.7	1.02
18	15.9	15.2	1.05	52.3	37.3	1.40	24.6	23.9	1.03
19	16.1	15.4	1.05	49.4	47.4	1.04	28.7	27.4	1.05
20	25.3	21.4	1.18	78.4	93.5	0.84	57.2	47.3	1.21
21	16.5	15.4	1.07	31.9	26.4	1.21	30.5	23.7	1.29
22	16.6	16.1	1.03	29.4	28.9	1.02	33.7	29.2	1.15
23	15.5	12.8	1.21	45.0	36.5	1.23	20.4	18.4	1.11
24	19.6	19.1	1.03	33.5	30.4	1.10	29.9	22.5	1.33

while for Ostende II the agreement is poorer. For Ostende I, the calculated values are nearly always misleading.

Similar attempts made for other sites show that the law $p = kt^n$ is valid in numerous cases, as far as deviations of ± 10 percent or even ± 20 percent are allowed. Consequently, although data at long terms obtained by extrapolation should be used with caution, it is tempting to use the law to provide some information on further performance.

Another experimental relationship has been observed between the weight losses of several steels in a given site, for example, between the weight losses at, say, 1 year and weight losses at longer terms.

Examples of the relationship at Liège are given in Fig. 2 for the 24 steels of Table 1. A straight-line graph is obtained in each case.

For the sake of generalization and in order to make easier the interpretation of this law, it is best to express the relationship in the logarithmic form

$$\log p_y = a \log p_x + b$$

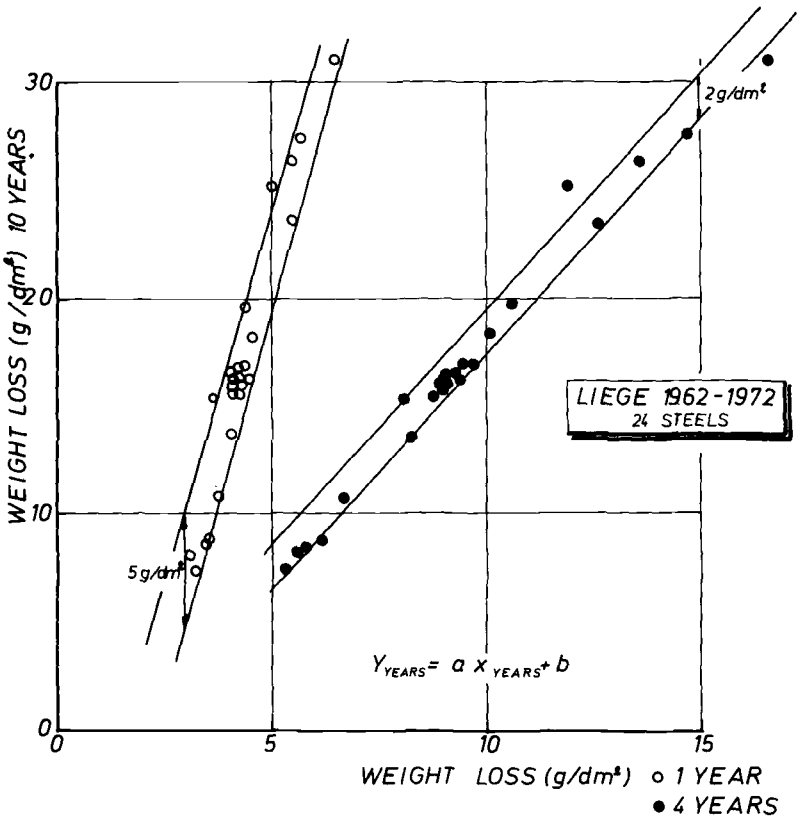

FIG. 2—*Relationship between short-term and long-term exposure periods (linear–linear), Liège.*

where p_y is the weight loss after y years and p_x the weight loss after x years. The dimensionless coefficients a and b depend upon the site and the periods x and y.

Figure 3 presents the data of Fig. 2 in bilogarithmic coordinates. The best fit is again a straight line.

A survey of the data reported in the literature suggests that similar relationships do exist in various locations. We have selected some of them. In May 1941, test specimens from a large group of low-alloy steels were exposed at three locations in the United States [2], namely

1. Kure Beach, N. C.—marine site at 240 m from the ocean, up to 15.5 years (Fig. 4).
2. Block Island, R. I.—marine site on a bluff overlooking the ocean, up to 17.1 years (Fig. 5).
3. Bayonne, N. J.—industrial location, up to 18.1 years (Fig. 6).

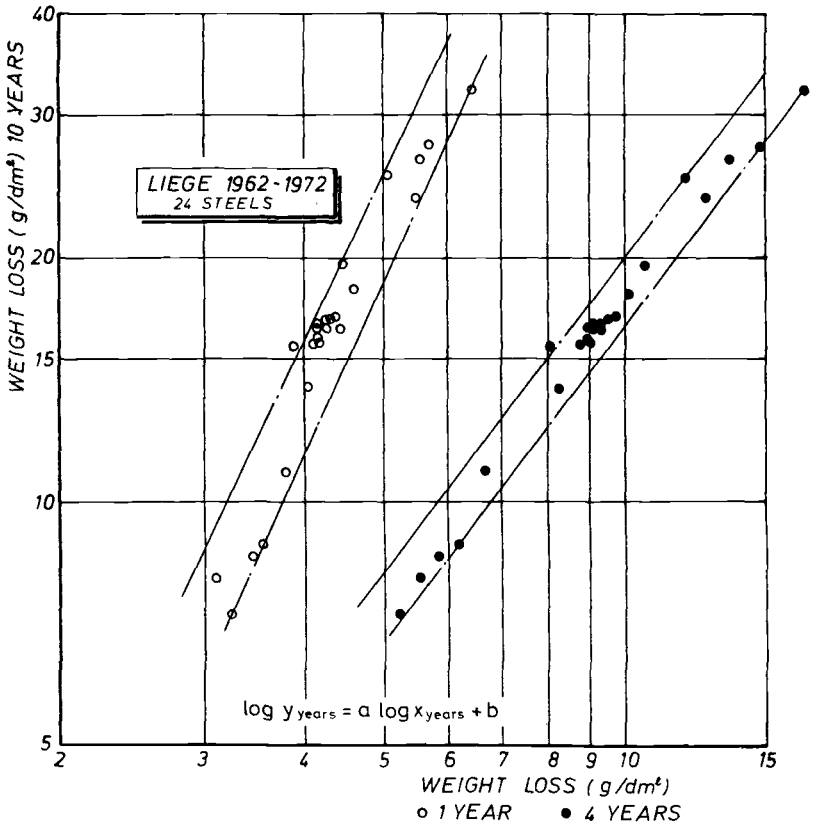

FIG. 3—*Relationship between short-term and long-term exposure periods (log–log), Liège.*

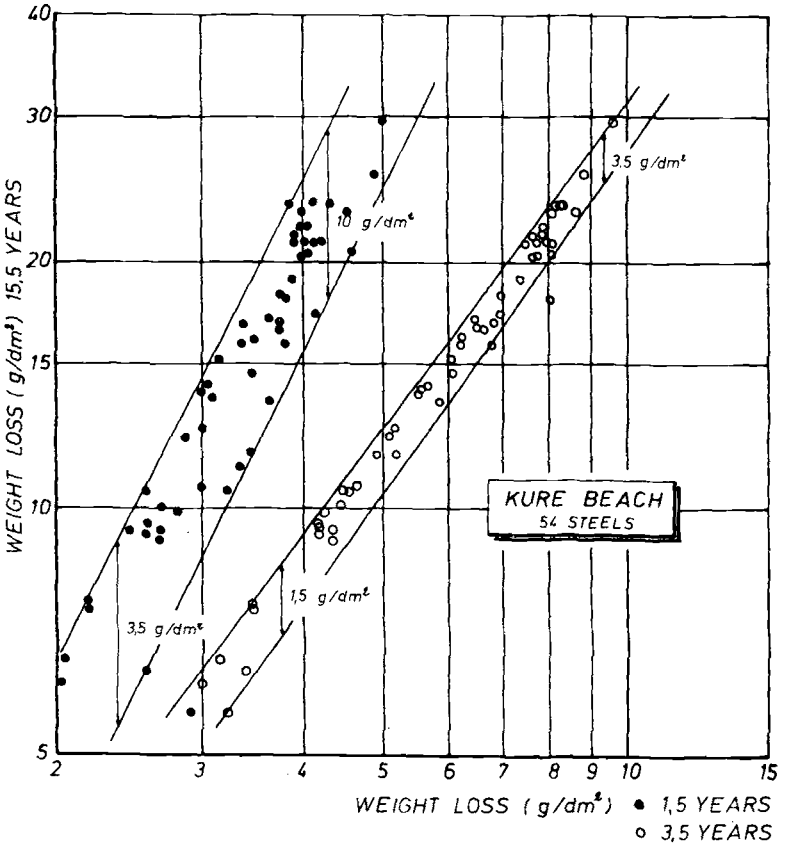

FIG. 4—*Relationship between short-term and long-term exposure periods, Kure Beach.*

In Japan, exposure tests of eight structural steels were carried out over a period of five years, starting in April 1961, at seven locations [*3*]. The sites were chosen as follows:

industrial area: Tokyo, Kawasaki
subtropical zone: Makurazaki
high-humidity area: Wajima
inland national standard weather: Takayama
cold weather district: Obihiro
seashore area: Omaezaki

Figure 7 shows the relationship between 1 and 5 years. Although the five last sites have quite different atmospheres, a single relationship is observed.

At Panama, a study of 10 structural steels was started in the late 1950's at

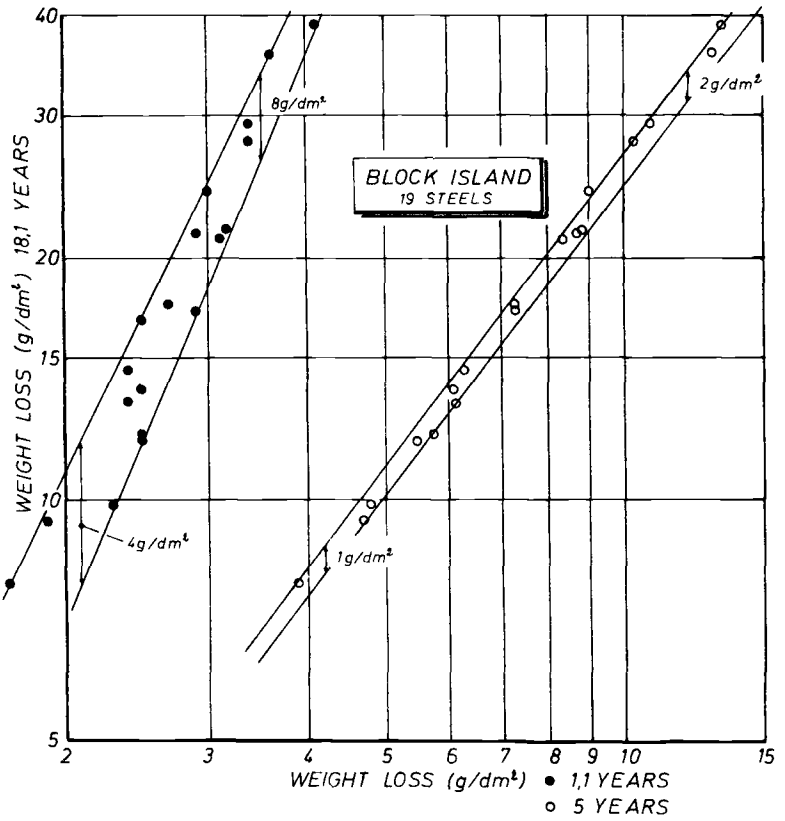

FIG. 5—*Relationship between short-term and long-term exposure periods, Block Island.*

two sites and lasted 16 years [*4*]. The two sites were located on opposite sides of the Isthmus of Panama:

1. A marine site on the Caribbean seashore, 17 m above sea level. Prevailing winds were from the sea.
2. An inland site, 8 km from the Pacific Ocean. The prevailing wind was from the land.

Figure 8 shows the relationships that can be drawn for the two sites.

Figure 9 is quite interesting because it is related to three steel grades (normal steel, copper steel, weathering steel) that were exposed in the United States at or near seven city areas and in seven rural sites within each area, during 64 months [*5*].

Plotting the available data (New Orleans city and San Francisco rural exposures were discontinued), we have found that the straight-line graphs of

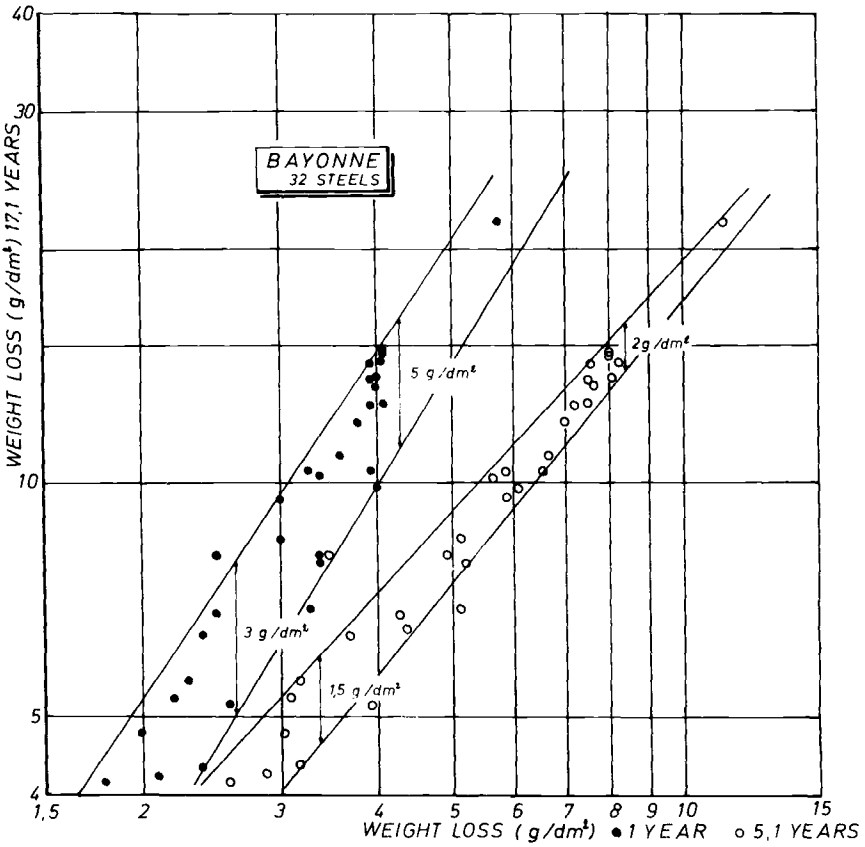

FIG. 6—*Relationship between short-term and long-term exposure periods, Bayonne.*

eight sites (including rural and urban sites) are gathered in quite a narrow band (Fig. 9*a*). For the remaining 4 sites, the straight lines are situated on either side of the aforementioned band (Fig. 9*b*).

All the plots of Figs. 2 to 9 show definitely that empirical relationships can be developed between the corrosion losses at different exposure times.

In order to compare the sites among themselves, we have established for each of them the relationship (4 years—10 years). We have first verified that all the data obey the law $p = kt^n$ for the exposure period. The weight losses at 4 years were then obtained by interpolation. Those at 10 years were interpolated or extrapolated, as the case may be. Extrapolation was needed for the Japanese sites and the 8 U. S. sites of the narrow band of Fig. 9*a*.

A plot of the results is given in Fig. 10. It is noteworthy that the slopes of the lines for the various sites are the very same.

It must be stressed that the steels of the different tests were not strictly the

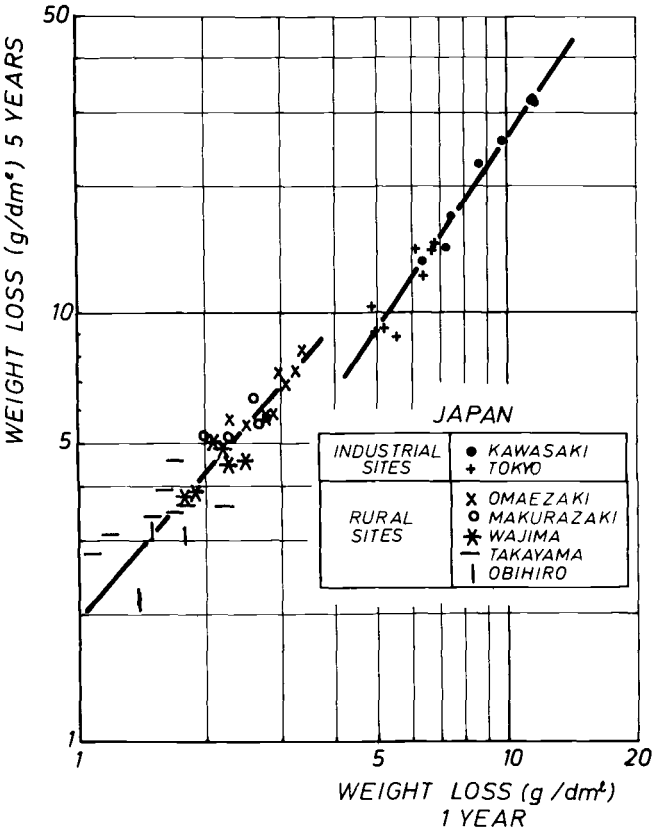

FIG. 7—*Relationship between short-term and long-term exposure periods, Japan.*

same, and that the specimen dimensions varied from country to country. Earlier studies have indicated that the specimen size may influence the assessment of the corrosion rates. In addition, at a given site, the conditions in the early stages of exposure have an influence on the subsequent corrosion rate. Indeed, in several European sites, including Liège, the weight losses of specimen put out initially in winter were always higher than those put out in summer. The differences could still exist after some years.

To get an idea of the influence of specimen size and of season, at the starting date we have compared, in Fig. 11, the corrosion losses of specimen of two different sizes, exposed either in winter or in summer. This comparison is limited to four steel grades (two weathering steels, a mild steel, and a microalloyed steel) exposed at Liège. It can be seen in Fig. 11 that the straight lines are sliding in a parallel direction, and that a single relationship could be considered, despite the differences in conditions of each series of data.

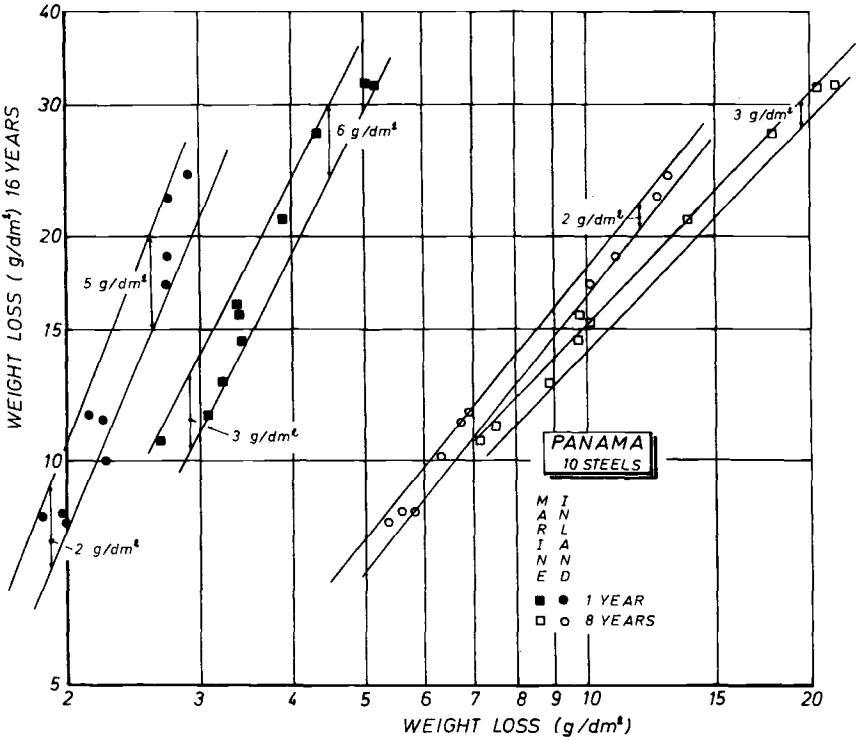

FIG. 8—*Relationship between short-term and long-term exposure periods, Panama.*

It may be concluded that where empirical relationships $\log p_y = a \log p_x + b$ are fair enough, we have a mean to predict reliably the corrosion losses of a new steel at long terms, provided the weight loss after one or a few years is experimentally determined.

Assessment of the Corrosiveness of Exposure Sites

The simultaneous existence of the two laws we have just discussed—the first one describing the corrosion behavior of a particular steel over a period of time and the second one characterizing the site and the exposure periods—implies that the coefficients of these laws are interrelated. Indeed, for a given steel in a particular site, it can be stated that

1.

$$p_x = k\, x^n \quad \text{and} \quad p_y = k\, y^n$$

or

$$\log p_x = \log k + n \log x \quad \text{and} \quad \log p_y = \log k + n \log y$$

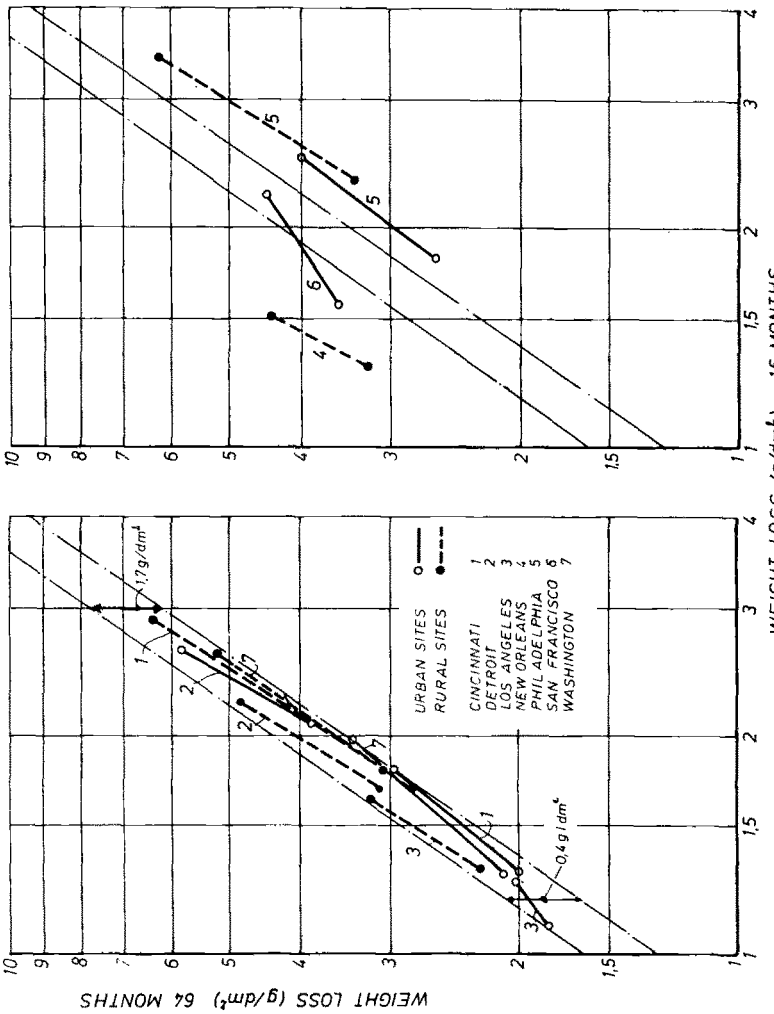

FIG. 9—*Relationship between short-term and long-term exposure periods, United States.*

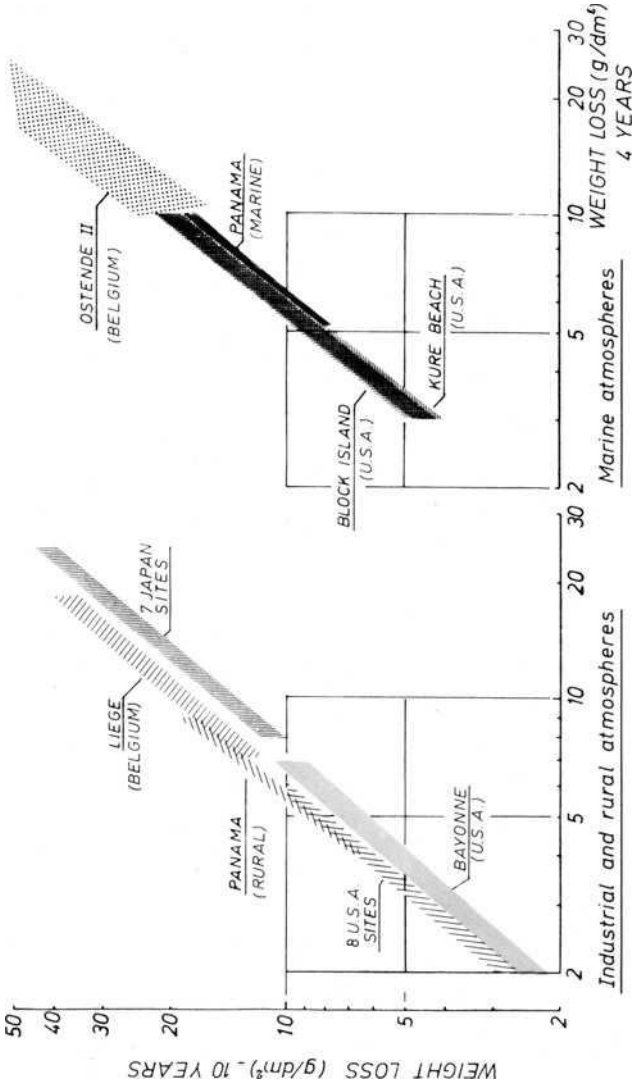

FIG. 10—*Relationship between 4 years' and 10 years' exposure periods, all sites.*

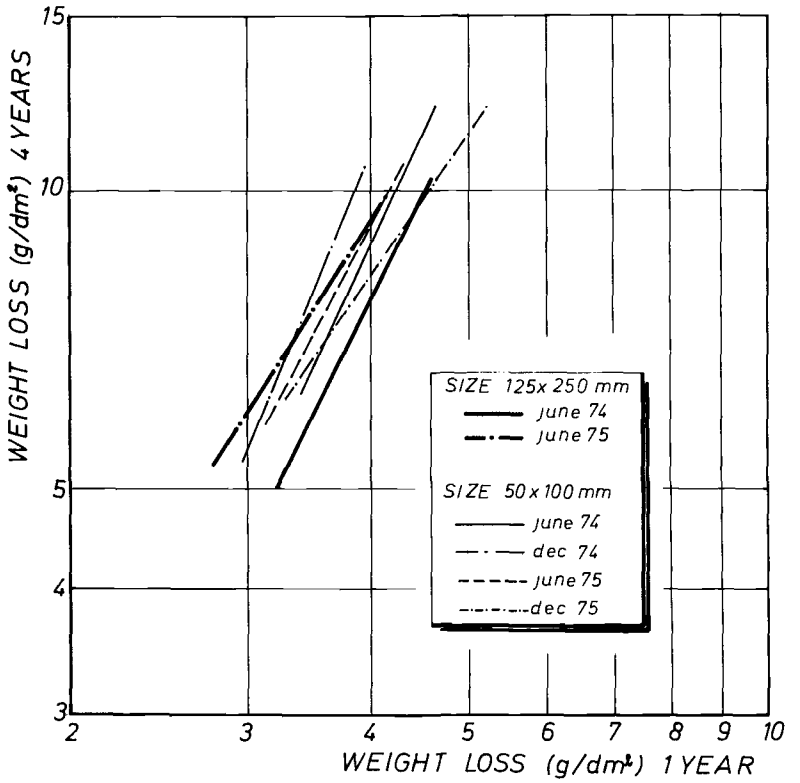

FIG. 11—*Influence of specimen size and season of exposure on weight losses.*

2.

$$\log p_y = a \log p_x + b$$

It follows that

$$\log k = \frac{n\,(a \log x - \log y) + b}{1 - a}$$

This relationship must be simultaneously satisfied for different periods x and y and for different steels. Consequently we must have

$$\log k = n\,A + B$$

where the coefficients A and B are dependent only on the site.

According to this last equation, A and B would allow us to characterize the corrosion agressivity of the site for a large group of steel grades, while k and n would not be independent. Hence, in order to assess the influence of the environmental conditions, two ways are open—using, on the one hand, A and B, and on the other hand, k and n.

The first way, using A and B, implies first that the behavior of a sufficiently large number of steel grades should be known in a wide range of environments in order to calculate A and B for each site. Besides, the climatic and pollution factors should be measured at each site, using the same procedure, for a sufficiently long period. Finally, relationships between these factors and the parameters A and B should be sought.

Due to the paucity of the published data available, it is not possible to investigate the capabilities of this method.

Thanks to the results of a collective program that was jointly carried out by six European laboratories, we will now show that the second way, that is, based on k and n, can actually be used successfully. For this research, four of the usual structural steels, namely, Fe 37, Fe 52, Fe 37,[3] Fe 52,[3] (microalloy steel),[3] and two weathering steels,[3] were exposed at 12 sites throughout the European Community [6]. Specimen were removed after 1, 2, 3, and 4 years' exposure, respectively. During the whole program, climatic and pollution factors were monitored in the immediate vicinity of the specimen exposed. Among them, the most significant factors that could be correlated to the weight losses due to corrosion are:

1. Monthly average of daily maximum temperatures,
2. Number of hours per month in which the relative humidity exceeded 80 percent,
3. Monthly airborne sulfur pollution (determined by the ASTM Method for Evaluation of Total Sulfation in Atmosphere by the Lead Peroxide Candle [D 2010-65 (1967)].
4. Monthly airborne chloride pollution (determined by the wet-candle method: wick dipping in a solution of glycerol water).

The use of candles for SO_2 an Cl^- determination is an easy and cheap way for the simultaneous supervision of several sites during long periods of time. Generally a cyclic variation of these factors is observed.

Special problems arose in the interpretation of some data collected in marine sites and sometimes in continental sites where the airborne chloride could be enhanced in case of stormy weather.

Indeed, it was observed that in exceptional climatic conditions, which occurred one or three times during the 4 years of exposure, according to the site, the chloride levels were some 7 to 20 times greater than the highest value registered in the remaining period. In a particular site, a monthly amount accounted for more than half the total that was measured during the four years. In addition, when such extreme chloride levels were observed, abnormal SO_3 levels were also found. It should be noted that in flat countries the influence of a storm can persist to some extent quite far inland.

[3] According to Euronorm 25.

The difficulty in the interpretation is that such deviations are not reflected on the corrosion rate or on the rust analysis, at least for specimens having been exposed for one year before the storm. If the protective action of the rust layer is not yet sufficient, however, it means that if the storm occurs a few months after the beginning of exposure, the corrosion rates could be affected. Thus, it seems that some data have to be properly corrected in order to avoid an excessive influence on the averages. Such corrections unavoidably involve subjective decisions.

The climatic conditions during the first months of exposure also deserve mention. It appeared that they have a strong influence on the weight losses after one year, thus on the k-coefficient. This particular influence must be taken into account when attempts are made to correlate k with the climatic conditions.

This is clearly illustrated by Fig. 12, which shows data observed at two industrial sites (Düsseldorf and Liège) and one rural site (Eupen) where one-year weight losses of two steel grades are plotted against the mean daily SO_3-values observed during the six first months of exposure. Specimens were exposed yearly in summer and in winter.

One single relationship is found for Fe 37 steel. For the weathering steel, there are two relationships according to the season at the time of exposure. In this case, if we assume that the corrosion reactions are temperature-dependent and follow the Arrhenius theory, one single relationship is also obtained.

Now if we analyze the data of the 12 sites, the same trend is observed but with an increased scatter even when taking into account the chloride pollution. The degrees of correlation are not improved when considering annual averages instead of those of the six first months.

It may be concluded that it is difficult to predict reliably the corrosion behavior of a steel solely from the climatic and pollution factors.

A different approach was then adopted, based on the following two observations:

1. The main factors affecting corrosion in a given site have a yearly evolution which is reasonably similar from year to year except in marine sites, where a few stormy months can affect the salinity measurements by giving some odd levels.
2. The concentrations of Cl^- and SO_4^{--} in the rusts of the same specimen vary little over time.

The rusting of a specimen during the first year is influenced by all the climatic factors, and consequently the weight loss after the first year (which corresponds to k) is a fair measurement of the corrosiveness of a site atmosphere.

On the other hand, once the rust layer is formed, it may be assumed that

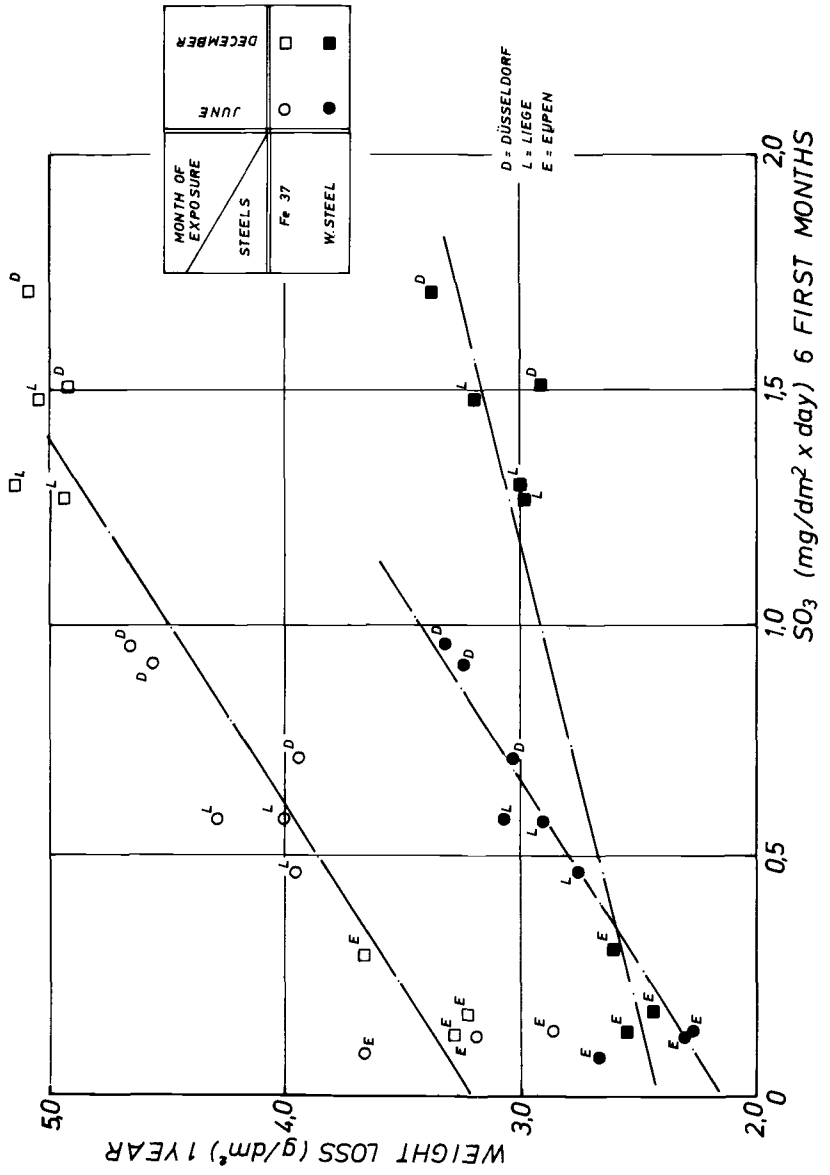

FIG. 12—*Relationship between SO_3 pollution and weight loss.*

TABLE 3—*Computation of* n *as a function* P_1 *and humidity* (H).

				r	σ_r
Fe 37	$n = -0.04361$	$P_1 + 0.810\ 10^{-3}$	$H + 0.523$	0.973	0.039
Fe 52	$n = -0.00094$	$P_1 + 1.253\ 10^{-3}$	$H + 0.085$	0.967	0.034
Weathering I	$n = -0.09513$	$P_1 + 1.294\ 10^{-3}$	$H + 0.241$	0.975	0.041
Weathering II	$n = -0.07986$	$P_1 + 1.158\ 10^{-3}$	$H + 0.317$	0.941	0.060

NOTES:
P_1 = one year's weight loss.
H = number of hours per month in which the relative humidity exceeded 80%.

its further evolution (thus coefficient n) will be related mainly to its moisture content and thus will be promoted by the action of high humidity. For this reason an attempt was made to assess n as a function of the monthly number of hours in which the relative humidity exceeded 80 percent (H).

For the four structural steels and from the results at the eight sites where humidity of the atmosphere was monitored, empirical equations were developed. The best relationship had the form $n = a P_1 + b H + c$, thus also taking into account P_1, the weight loss after one year. These equations are given in Table 3, together with the correlation coefficients (r) and the residual standard deviations (σ_r).

The low values of σ_r indicate that the agreement between observed n-values and those calculated from the empirical equations is generally good.

To visualize the influence of the discrepancies between calculated and actual values of n on the prediction of corrosion rates, weight losses at four years were computed for the 32 cases (4 steels, 8 sites), using the formula $p = kt^n$, with k taken as the one-year weight loss. The ratio between calculated and measured values of weight losses was never outside the range 1.10 to 0.90. It was in the range 1.05 to 0.95 twenty-five times.

Prospects for Long-Term Predictions of Atmospheric Corrosion Losses from Short-Term Experimental Data

Analysis of the results examined in this study shows that the following prospects are open for forecasting the durability of steels:

In a particular site where the behavior of several steels was assessed on long periods, one wishes to predict the behavior of a new steel grade.

If for the measured steels the relationship $\log p_y = a \log p_x + b$ is observed, it is sufficient to determine the weight loss of the new steel after x years ($x > 1$) to predict its evolution after y years.

The behavior of a particular steel is known in several representative sites, and one wishes to predict its behavior in a new site.

The steel is exposed in the new site during one year and the value of the

weight loss obtained taken as k. In the new site, the humidity is measured during the same period. On the other hand, using the data from the other sites, one computes for the particular steel the equation giving n as a function of k and humidity. This equation is used to calculate n in the new site.

References

[1] Songa, T. in *Proceedings*, Commission of the European Communities Symposium on Steel, Part 1, Luxembourg, 18–21 Nov. 1975, pp. 202–205 and p. 231.

[2] Copson, H. R. in *Proceedings*, American Society for Testing and Materials, Vol. 60, 1960, pp. 650–660.

[3] Horikawa, K. et al, *Nippon Kokan Technical Report Overseas,* Tokyo, May 1968, pp. 51–58.

[4] Southwell, C. R., Bultman, J. D., and Alexander, A. L., *Materials Performance*, Vol. 15, July 1976, pp. 9–26.

[5] Haynie, F. H. and Upham, J. B., *Materials Protection and Performance*, Vol. 10, Nov. 1971, pp. 18–21.

[6] "Recherche Collective sur la Corrosion Atmosphérique des Aciers. Rapport de Synthèse et d'Exploitation de l'Ensemble des Résultats," Commission of the European Communities Sponsored Research Project 6210/92, Publication EUR 7400 FR.

S. C. Byrne[1] *and A. C. Miller*[1]

Effect of Atmospheric Pollutant Gases on the Formation of Corrosive Condensate on Aluminum

REFERENCE: Byrne, S. C. and Miller, A. C., **"Effect of Atmospheric Pollutant Gases on the Formation of Corrosive Condensate on Aluminum,"** *Atmospheric Corrosion of Metals, ASTM STP 767*, S. W. Dean, Jr., and E. C. Rhea, Eds., American Society for Testing and Materials, 1982, pp. 359–373.

ABSTRACT: As part of a program to develop predictive methods to estimate the long-term durability of aluminum parts, a methodology was developed to calculate the chemical composition of condensates formed on aluminum exposed to polluted air.

In this study, it is proposed that the maximum concentrations of ionic species in a condensate must be limited by the equilibrium condition established between the dissolved ions and the gases from which they formed.

KEY WORDS: atmosphere, corrosion, pollutants, aluminum, acid gases, equilibrium, thermodynamics

Alcoa Laboratories has, over the years, collected a great deal of information on atmospheric corrosion for the purpose of correlating these data with data from laboratory corrosion tests. These studies as well as examinations of failed parts from field service have indicated that improved methods to predict field service life of aluminum alloys are necessary.

An illustration of this need is typified by the differences observed when one compares stress-corrosion cracking (SCC) data, based on percent survival versus stress, for 7XXX alloys exposed at Alcoa's Vernon Works (near Los Angeles) with data from exposures at the Point Judith, R. I. seacoast [*1,2*].[2,3] The Vernon environment appears to be the more severe environment for SCC of 7XXX alloys. On the other hand, when one compares the same type of data for 2XXX alloys, the severity of environment is reversed; that is, the Point Judith exposure is the more aggressive. Stress-corrosion data from accelerated laboratory tests show similar reversals, especially when one tries

[1] Staff engineer and senior scientist, respectively, Alcoa Laboratories, Alcoa Center, Pa. 15069.

[2] The italic numbers in brackets refer to the list of references appended to this paper.

[3] References *1* and *2* deal with variations in environment affecting SCC.

to correlate these data with field exposures. It has long been known that some accelerated tests correlate better with data from specific outdoor exposure stations than do data from other tests, and, further, that the degree of correlation is highly dependent on the alloy [*3*].

Clearly, a test method to predict the field service performance of a material should take into account not only the specific material (composition, structure, etc.) involved, but should consider the chemical environment and the physical conditions (such as temperature or mechanical loading) to which the material will be subjected during service. Because this requires a very broad approach, an extensive study was designed to allow the development of methods to predict service life under conditions of static or dynamic loading and in the atmospheric conditions found in today's major population centers. In recent years, however, man-made pollutant gases such as sulfur dioxide (SO_2), nitrogen oxides, hydrocarbons from incomplete combustion, and ozone have been of increasing concern as to their effect on metallic corrosion. Although many complex reactions can take place between these gases and the natural atmospheric gases in the presence of sunlight, the products of these reactions exist for a rather short time relative to the time frame involved for most corrosion processes. Additionally, unpublished work by Kozarek at Alcoa Laboratories has shown that various gas mixtures of N_2, O_2, water (H_2O), SO_2, hydrochloric acid (HCl), and the nitrogen oxides represented by NO_2 have the most corrosive effect on aluminum alloys. In this program, the effect of soiling and accumulations of corrosion products were not considered, because such effects are difficult, if not impossible, to quantify at this time. It is possible, however, to determine the reaction products formed from these gas mixtures and make quantitative estimates of their relative amounts.

The purpose of the experimental part of this program was twofold:

1. to determine if a laboratory-simulated atmosphere containing N_2, O_2, SO_2, HCl, NO_2, and H_2O produces the same corrosion on aluminum as outdoor atmospheric exposure, and
2. to determine if the chemical species produced by such gas mixtures are those expected from thermodynamic considerations.

Procedure

To accomplish the first experimental objectives, some 99.99Al (annealed, 1.6-mm sheet) specimens were prepared by diamond polishing and ultrasonic cleaning in methanol (CP grade). Specimens then were exposed at Alcoa's Vernon Works near Los Angeles, at Alcoa Technical Center near Pittsburgh, Pa., and in the laboratory apparatus, shown in Fig. 1, designed to expose the specimen to gas mixtures producing a simulated polluted atmos-

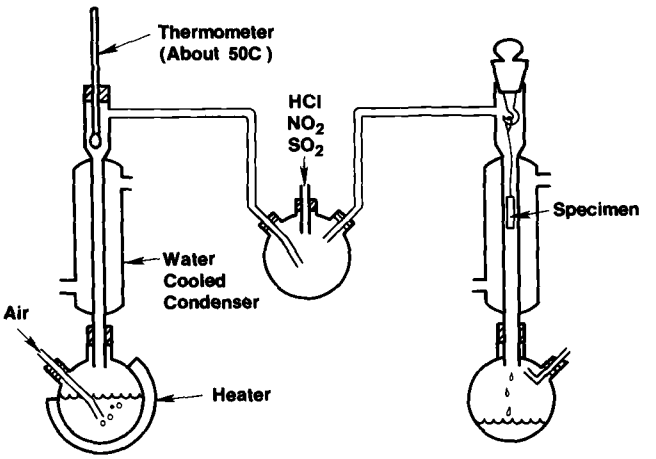

FIG. 1—*Glass apparatus for exposing specimens to wet or dry atmospheres. The pollutant gases were mixed with water-saturated air (about 50°C) and introduced into the specimen chamber (about 30°C), producing a wet "fog" over the specimen.*

phere. The apparatus was capable of producing dry or humid conditions. The atmospheric exposures were 1 to 4 weeks; the laboratory exposures were for 6 to 24 h because it was found, after some experimenting, that these exposure times produced dense adherent corrosion product films ideal for surface analysis. The compositions of the various gas mixtures used in the laboratory experiments are given in Table 1.

After exposure, the surfaces of the specimens were analyzed by ion scattering spectroscopy (ISS) and secondary ion mass spectroscopy (SIMS). Auger spectra were also obtained for some of the specimens.

The second objective, the experimental determination of what chemical species would be present in the condensate formed from the gas mixtures, was accomplished by collecting the condensed phase produced in the laboratory experiment. The dissolved ionic species were identified using ion chromatography.

TABLE 1—*Composition of gas mixtures used in surface analysis experiments: partial pressures, atmospheres (50°C).*

HCl	NO_2	SO_2	O_2	N_2	H_2O
7.6×10^{-4}	. . .	. . .	0.18	0.70	0.12
7.6×10^{-4}	. . .	. . .	0.21	0.79	. . .
. . .	7.6×10^{-4}	. . .	0.18	0.70	0.12
. . .	7.6×10^{-4}	. . .	0.21	0.79	. . .
. . .	. . .	7.6×10^{-4}	0.18	0.70	0.12
. . .	. . .	7.6×10^{-4}	0.21	0.79	. . .

Results

Surface Analysis

The surface analysis data indicated that the reaction products formed on the aluminum surfaces were aluminum oxide and its hydrates. The thickness of the atmospherically formed oxide-hydrates correlated with NO_X levels and these thicker oxides were more heavily hydrated; again, this appeared to correlate with higher atmospheric NO_X concentrations. Surface analyses of specimens exposed in laboratory-simulated environments indicated that, first, humid conditions were necessary to effect the surface changes noted on the outdoor exposures and, second, thick highly hydrated films were produced by exposure to wet NO_2.

The results of the surface analyses can be subdivided into three general classifications: (1) surface composition, (2) oxide thickness, and (3) the degree of hydration of the surface oxide.

Surface Composition—Data from all of the analytical techniques were used to deduce the qualitative surface composition of the specimens. Aside from oxygen and aluminum, the following elements were identified on the surfaces of all the specimens: carbon, fluorine, sodium, magnesium, sulfur, chlorine, potassium, calcium, and iron. Except for the cases noted in the following, the concentrations of the surface impurities were estimated to be less than 1 atomic percent and were within the levels normally accepted as residual contamination from cleaning and handling. There was no systematic surface enrichment of sulfur or chlorine on the surfaces exposed to either wet or dry HCl and SO_2 gases, nor was there any evidence that stable nitrogen compounds existed on the surface at the time of analysis. The surface compositions determined by each of the three methods were in excellent qualitative agreement.

One of the exceptions to the low levels of surface contamination was that quantities of sodium, potassium, and calcium were observed on the specimens exposed to wet NO_2 gas. These impurities probably were leached from the glass walls of the reaction vessel by the acidic atmosphere, which subsequently condensed on the specimen. This result is not surprising because it is known that many glasses show surface segregation of alkaline and alkaline-earth metals that can be removed by acid etching. The contaminant layer on the specimens was about 1 nm thick and actually covered less than 25 percent of the outer surface.

The specimens exposed at Alcoa's Vernon Works in Los Angeles were found to have surface concentrations of sodium and chlorine larger than those found on the other specimens. The most likely source of these elements is airborne salt particles that deposited on the surface. The quantity of salt on the surface did not change appreciably between the 1-week and 3-week exposure specimens.

Another element found on the surfaces of both the laboratory-prepared

specimens and the atmospheric specimens was fluorine. Surface concentrations have been observed to range from nearly undetectable quantities (by Auger spectroscopy) to an estimated 20 to 40 percent surface coverage, in the form of AlF_3.

Three of the four atmospheric exposure specimens showed high and approximately equal levels of fluorine. Surprisingly, the 4-week Alcoa Technical Center (ATC) exposure showed several times less fluorine than the 1-week ATC exposure specimen. There was also a large variation between the concentrations found on the laboratory-prepared specimens.

Examination of all of the surface analysis data, however, indicates that there is no correlation between the overall characteristics of the surface films and the quantity of surface fluorine. To a first approximation, it appears that a fluoridated surface layer does not strongly affect the gas-solid or condensate-solid reactions.

Oxide Thickness—The surface oxide thicknesses on the laboratory and outdoor exposure specimens were obtained by depth probing with ISS; the results are summarized in Fig. 2. From the chart, it can be noted that laboratory exposures with the dry gases and with wet HCl and wet SO_2 had little or no effect on the oxide thickness. For the laboratory specimens, the exception was wet NO_2. After a 6-h exposure to wet NO_2, the oxide layer had increased in thickness by about 50 percent. After 24 h the oxide layer was about four times thicker than the base oxide. These results seem to indicate that for the three pollutant species tested, the condensate formed from wet NO_2 reacts most actively with the aluminum surface.

The difference between the oxide thickness on the Vernon and ATC exposure specimens was also evident. After one week's exposure at ATC, there was little change in oxide thickness from the base oxide; after one week at Vernon, the oxide thickness had doubled. The difference in the rate of oxide formation is corroborated by a comparison of the 4-week exposure at Alcoa Center (ATC) with the 3-week exposure at Vernon. This agreement between the wet NO_2 laboratory exposure and Vernon exposure is not surprising when one considers the high NO_2 levels reported at Vernon [*4*]. The important result is that wet NO_2 exposure correlates with increased oxide thickness both in laboratory tests and outdoor exposure.

Further information about the oxide layers can be obtained from Fig. 3, obtained from the ISS data. For a uniform layer, the ratio of the aluminum signal to the oxygen signal (Al/O) remains quite constant. As the ion beam sputters through the oxide and into the metal, the aluminum signal grows and the oxygen signal decays, causing the Al/O ratio to increase as a function of sputter time. Thus, the peak height inflection in the Al/O peak height ratio serves to indicate the location of the base of the oxide layer. In addition, the rate at which the Al/O ratio grows is a measure of the "roughness" of the oxide-metal interface. Well-defined surface layers yield sharp inflection points; diffuse interfaces yield the type of curve shown by the 24-h wet

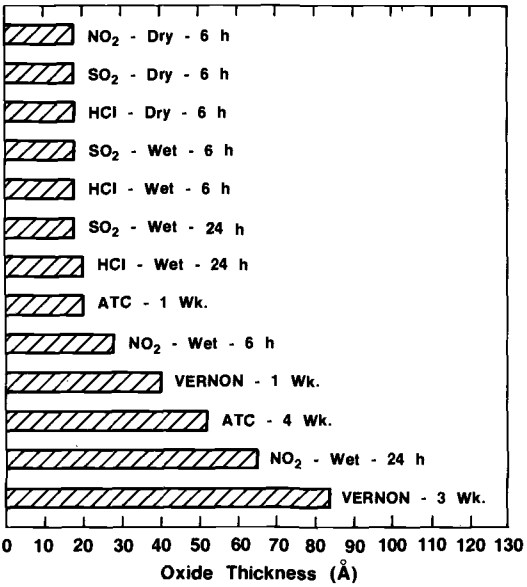

FIG. 2—*Comparison of oxide thicknesses for laboratory and atmospheric exposure specimens. Oxide thickness developed on the 99.99 percent aluminum specimens was determined by depth probing with the ISS. (ATC = Alcoa Technical Center, Alcoa Center, Pa., near Pittsburgh; Vernon = Los Angeles.)*

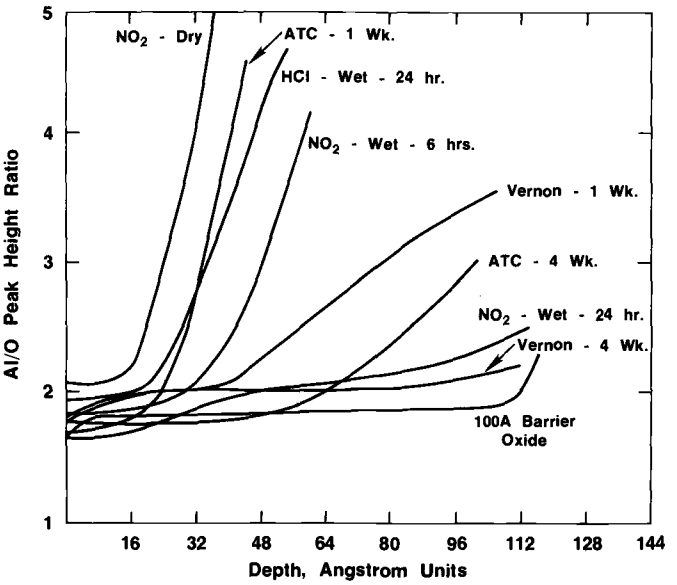

FIG. 3—*ISS spectra for selected oxide films. The Al/O peak height ratio was used to determine the location of the base metal-oxide interface. Barrier oxides were formed by boric acid anodizing.*

NO_2 exposure curve in Fig. 3. The wet NO_2, ATC, and Vernon exposure specimens showed a trend toward more poorly defined oxide-to-metal interfaces as the oxide layer thickened. This suggested that the oxide growth rate was nonuniform, that the surface was becoming rougher, or that the profile resulted from both of these factors, another similarity between the wet NO_2 laboratory experiment and real-world atmospheric exposure.

Surface Hydration—Examination of the molecular fragments in the SIMS spectra provides clues about the chemical nature of a surface. Two species of particular interest in the study of aluminum oxides are the AlO and AlOH mass fragments at Masses 43 and 44. Though not strictly quantitative, plots of the ratios of the AlOH to AlO peak heights as a function of sputter time are informative. In Fig. 4, the curves for Al $(OH)_3$ and the barrier oxide represent the wet (as hydrated) and the dry extremes, respectively. It can be seen from Fig. 4 that the wet NO_2 and the longer-term atmospheric exposure specimens tended to have AlOH/AlO values that were greater than those for aluminum hydroxide, implying those specimens were highly hydrated. Though not shown, the same data were obtained for all the other specimens, that is, the dry NO_2, HCl, and SO_2 exposures. The AlOH/AlO curves for these specimens tended to fall between the curves for the 1-week ATC exposure and barrier oxide, which implies that these oxides were relatively dry. Differences noted in the SIMS data at short sputter times reflect surface moisture, which, in turn, is dependent on the conditions the specimen was

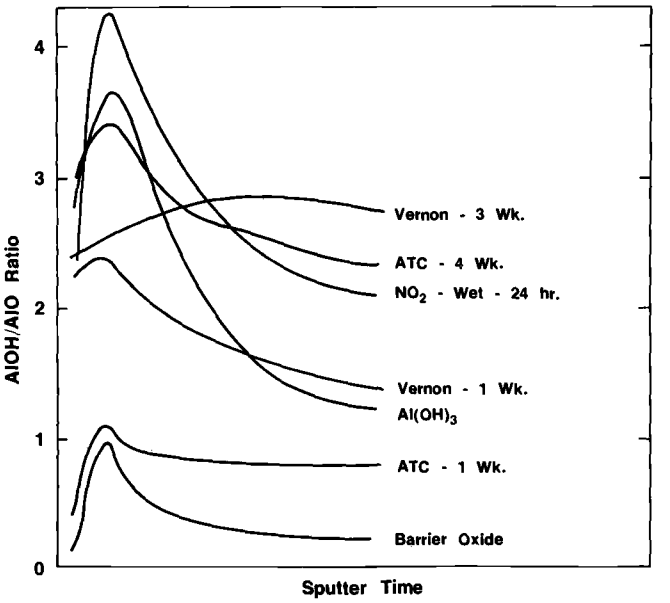

FIG. 4—*SIMS spectra for some oxide films. The more-hydrated oxides appeared to be formed in the atmospheres containing nitrates.*

subjected to after exposure but before it was inserted in the vacuum chamber. In addition, a high outgassing was noted for the heavily hydrated wet NO_2 specimens, implying that the surfaces of these oxides are quite unstable and desorb water easily.

Ion Chromatography

The ion chromatography data identified simple oxyacid anions and chlorides as the principal dissolved anions. If the condensed phase was collected from an aluminum surface, the ionic species were the anions Cl^-, NO_3^-, NO_2^-, $SO_4^=$, and $SO_3^=$. The cationic species were Al^{+3} and H^+. If no aluminum was in the system, that is, if the condensate was collected from glass, the anions were Cl^-, NO_3^-, NO_2^-, and $SO_4^=$, and the cation was H^+.

Thermodynamic Calculations

Because the experimental results showed that the pollutant gases considered in the laboratory produced the same oxide surface as that noted on aluminum exposed to the outdoor atmosphere and that the reaction products of these gases were acid anions, it was necessary to consider, first, which reactions, yielding these anions as products, are thermodynamically feasible, and, second, if the relative amounts of the products of these reactions can be calculated using thermodynamic data and gas solubilities, given the initial concentrations of the atmospheric pollutants.

As a basis for the thermodynamic calculations, it was assumed that an equilibrium between the atmospheric gases and the ionic species in the condensed phase on the metal surface was a limiting condition. This assumption was justified by an examination of data published by Mansfeld [*5*] and by similar work done at Alcoa Laboratories.

Mansfeld [*5*] found that when a metal corrodes in the atmosphere, the corrosion current varies with the time-of-wetness. Similar (unpublished) data, obtained at Alcoa Laboratories by Wagner and English, show that the maximum corrosion rate is achieved at very select times during the wet-dry cycle; in this instance, the maximum corrosion rate and, hence, the maximum concentrations of ionic species, occurs when moisture first begins to condense on the metal surface. As condensation continues, the solution becomes more dilute because water condensation now occurs at a higher rate than initially, producing a solution containing more water relative to dissolved gases. At some time later in the wet cycle, corrosion should proceed very slowly indeed, because one would expect to reach a point where rapidly condensing water is actually cleaning the metal surface. One can speculate that the situation reached later in the wet cycle is rare for atmospheric exposures, that is, actual cleaning of a metal surface by condensing water occurs a relatively small number of hours during the year, while the initial stage of moisture condensation, typified by "dew," may be present for a substantial

fraction of the year. Further, because metal exposed in the atmosphere usually accumulates a substantial soil layer, "washing" would take a perhaps unrealistically long period of condensation time to occur.

Wagner and English also observed that a second maximum in the current versus time-of-wetness curve occurs during the "dry" cycle. At the beginning of this cycle, water on the metal begins to evaporate and the concentration of the dissolved ionic species formed in the "wet" cycle increases. In this instance, one would expect the maximum to occur at, or just before, the point at which the last traces of moisture are removed. Again, the situation in the atmosphere may be much more severe than in the laboratory because of the hydroscopic nature of the soil deposit (the metal is probably never completely dry) and because, with time, the concentration of dissolved solids formed by soil and corrosion products interacting with anions by solution of atmospheric pollutants would tend to increase. In any case, *the maximum concentrations of ionic species in a condensate must be limited by the equilibrium condition established between the dissolved ions and the gases from which they formed.*

The argument used to select the particular most-probable chemical reactions was an elementary thermodynamic one, based on the Gibb's free-energy change for chemical mass transfer. For a chemical reaction

$$\alpha A + \beta B + \cdots = \gamma C + \delta D + \cdots \tag{1}$$

where α moles of A react with β moles of B to produce γ moles of C and δ moles of D

$$\Delta G = \Delta G^0 + RT \ln \frac{a_C^{\gamma} \cdot a_D^{\delta} \cdots}{a_A^{\alpha} \cdot a_B^{\beta}} \tag{2}$$

where

ΔG = Gibb's free-energy change,
ΔG^0 = standard free energy of formation,
R = ideal gas constant (1.987 cal/mol-°C),
T = absolute temperature (Kelvin), and
a = activity of α moles of reactant A, etc.

Because the change in the Gibb's free energy during a chemical reaction is a measure of the total energy released or used up when the reaction is taking place, the term "chemical potential" denoted by the symbol μ, is used when referring to the Gibb's free-energy change, ΔG, for a chemical reaction.

In order to Use Eq 2, two types of data must be located. First, ΔG^0 or μ^0, for the reaction in question must be calculated. For the purpose of this investigation, values of standard free energies of formation and solution were calculated using data from the International Critical Tables [*6*] or from *Oxidation Potentials* by Latimer [*7*].

The second type of data needed are activity coefficients for use in the cal-

culations of the activity terms by the equation

$$a = \gamma' C$$

where γ' is the activity coefficient in units consistent with C and C is the concentration (in molar or molal units). In the case of a gas the activity is called the fugacity, f, and is given by

$$f = \gamma' P$$

where P is the pressure in atmospheres and γ' the activity coefficient in units consistent with P.

By calculating μ for various reactions, one can find out if a reaction is thermodynamically possible or, if the reactants are in equilibrium with the products, one can calculate the equilibrium constant, K, and from that calculate the concentration of the products if the reactants and their concentrations are known. For equilibrium, $\mu = 0$, so Eq 2 becomes

$$\mu^0 = RT \ln K \tag{3}$$

Table 2 gives the list of reactants, products, and intermediates found by using the Chemical Equilibrium Package (CEP)[4] computer program [*9*]. Using these chemical species, the reactions in Table 3 were constructed and the μ^0-values calculated. The data were then used to calculate equilibrium constants for all of the possible reactions (also given in Table 3).

With knowledge of the equilibrium constants, equations relating the concentrations of ionic species in solution to the partial pressures of the pollu-

TABLE 2—*Reactants, product, and intermediates considered.*

H_2O (*l, v*)	SO_2 (*g*)
H^+	HSO_4^-
NO_3^-	$SO_4^=$
NO_2^-	O_2 (*g*)
NO (*g*)	N_2 (*g*)
NO_2 (*g*) (or N_2O_4)	
HNO_2 (*ag*)	
HClO (*aq*)	
ClO^-	
Cl_2 (*aq*)	
HCl (*g*)	
Cl^-	

NOTES:
g = gas.
l = liquid.
aq = dissolved in water.

[4] The Chemical Equilibrium Package is a series of computer programs and a large data base of thermochemical data that permit interactive thermal calculations to be performed on chemical systems. Of particular use in this program is the SOLGASMIX program, which permits calculations on gas-aqueous solution equilibria.

TABLE 3—*Reactions, equilibrium constants, and standard potentials.*

Only Cl^-, NO_3^-, $SO_4^=$ and very small amounts of NO_2^- were found. Thus, reactions that give these products through suitable intermediates are:

(1) $2\ NO_2\ (g) + H_2O\ (l) = HNO_2\ (aq) + HNO_3\ (aq)$	$K_1 = 2.41 \times 10^5$	$\mu^0 = -7.34$ kcal
(2) $3\ HNO_2\ (aq) = 2\ NO\ (g) + HNO_3\ (aq) + H_2O\ (l)$	$K_2 = 2.3 \times 10^2$	$\mu^0 = -3.22$ kcal
(3) $HNO_2\ (aq) = H^+ + NO_2$	$K_3 = 4.5 \times 10^{-4}$	$\mu^0 = +4.56$ kcal
(4) $2\ NO\ (g) + O_2\ (g) = 2\ NO_2\ (g)$	$K_4 = 1.65 \times 10^{12}$	$\mu^0 = -16.66$ kcal
(5) $4\ HCl\ (g) + O_2\ (g) = 2\ Cl_2\ (aq) + 2\ H_2O\ (l)$	$K_5 = 8.57 \times 10^{13}$	$\mu^0 = -19.00$ kcal
(6) $Cl_2\ (aq) + H_2O\ (l) = HClO\ (aq) + HCl\ (aq)$	$K_6 = 4.38 \times 10^{-4}$	$\mu^0 = +4.58$ kcal
(7) $HClO\ (aq) = H^+ + ClO^-$	$K_7 = 3.2 \times 10^{-8}$	$\mu^0 = +10.22$ kcal
(8) $2\ SO_2\ (g) + 2\ NO\ (g) + 2\ H_2O\ (g) = 2\ H_2SO_4\ (aq) + N_2\ (q)$	$K_8 = 10^{102}$	$\mu^0 = -139$ kcal
(9) $2\ SO_2\ (g) + O_2\ (g) + 2\ H_2O\ (g) = 2\ H_2SO_4\ (aq)$	$K_9 = 10^{72}$	$\mu^0 = -98$ kcal
(10) $HSO_4^-\ (aq) = H^+ + SO_4^=$	$K_{10} = 1.26 \times 10^{-2}$	$\mu^0 = +2.6$ kcal
(11) $4\ SO_2\ (g) + 2\ NO_2\ (g) + 4\ H_2O\ (g) = 4\ H_2SO_4\ (aq) + N_2\ (g)$	$K_{11} = 10^{161}$	$\mu^0 = -220$ kcal
(12) $8\ HCl\ (g) + 2\ NO_2\ (g) = 4\ Cl_2\ (aq) + N_2\ (g) + 4\ H_2O\ (l)$	$K_{12} = 10^{106}$	$\mu^0 = -63$ kcal

NOTES:
g = gas.
l = liquid.
aq = dissolved in water.

tant gases were derived using Eq 3. The equilibrium equations were then solved simultaneously for the concentration of the product ion in question in terms of the partial pressures of the reactant gases.

The procedure used to solve the equations took two factors into account. First, reactions that go to completion are limited by the solubility of the gas in water. For example, all of the SO_2 in water will become sulfuric acid; therefore, the final concentration of $SO_4^=$ in the condensed phase will depend on the $HSO_4^-/SO_4^=$ equilibrium and on the solubility of $SO_2(g)$ in water [*10–13*].[5] Second, the gases were allowed to inter-react; for example, NO_2 was allowed to react with SO_2 to form N_2 and H_2SO_4 as well as to react with water and O_2 to form nitric and nitrous acids. An interactive computer program was written to solve the equations.

Discussion

There are no reliable quantitative data with which to test the calculations at this time. An attempt was made to calculate the condensate composition on a glass plate for the nonequilibrium experiments performed in the atmospheric test chamber previously used for the time-of-wetness studies conducted by Wagner and English, because ion chromatography data were available for condensates in these tests. Although there was considerable scatter in the anion analyses of the condensed phase from these experiments, the data on condensate composition calculated by the equilibrium equations appeared to correlate suprisingly well (Table 4) for Cl^- and $SO_4^=$ but poorly for NO_3^- and NO_2^-. Because the nitrogen oxide anion calculations were consistently several orders of magnitude higher than the analytical data, it was thought that a reaction was taking place between the NO_2 and some material in the chamber or that some of the NO_2 was being chemically adsorbed on the chamber material. The same conclusion had been proposed by Wagner and English because they could not find an empirical relationship between the NO_2 pressure and the amounts of nitrates and nitrites in their condensates.

A second exercise, calculating the expected condensate composition for several locations in the United States, produced some interesting results. Environmental Protection Agency data for pollutant concentrations found in these areas (Table 5) were used to determine if significant differences in condensate composition would be expected. The results, shown in Fig. 5, show that Los Angeles data produced a condensate high in nitrates. In the three-dimensional plot, Point Judith and ATC condensates lie on the side of a dividing plane where the equilibrium model predicts that no significant nitrates will appear in the condensate. On the other hand, the Los Angeles condensate is well into the nitrate region and Chicago (not shown for clarity) is on the nitrate side of the plane just in front of Point Judith.

[5] References *10–13* were sources of information used to calculate fugacities and gas solubilities for CEP and the interactive program.

TABLE 4—*Comparison of nonequilibrium measurements with equilibrium calculations for gas mixtures in atmospheric chamber.*

Cl^- Ion (moles/litre) Run	Measured	Calculated	PHCl, atm
1	4.3×10^{-4}	4.6×10^{-4}	7.6×10^{-6}
2	9.9×10^{-5}	10×10^{-4}	4.1×10^{-6}
3	2.2×10^{-4}	8.6×10^{-4}	10.5×10^{-6}
4	5×10^{-4}	18×10^{-4}	15.4×10^{-6}
$SO_4^=$ Ion (moles/litre)			PSO_2, atm
1	40×10^{-5}	6.8×10^{-5}	7.6×10^{-6}
2	9×10^{-5}	4.1×10^{-5}	4.1×10^{-6}
3	20×10^{-5}	8.8×10^{-5}	10.5×10^{-6}
4	14.6×10^{-5}	12.4×10^{-5}	15.9×10^{-6}
NO_3^- Ion (moles/litre)			PNO_2, atm
1	4.6×10^{-4}	2.7×10^{-2}	7.6×10^{-6}
2	1×10^{-4}	1.5×10^{-2}	4.1×10^{-6}
3	7.0×10^{-4}	4×10^{-2}	10.5×10^{-6}
4	9×10^{-4}	6×10^{-2}	15.4×10^{-6}
NO_2^- Ion (moles/litre)			PNO_2, atm
1	3×10^{-6}	8.8×10^{-3}	7.6×10^{-6}
2	2×10^{-4}	4.8×10^{-3}	4.1×10^{-6}
3	3×10^{-5}	13×10^{-3}	10.5×10^{-6}
4	4.8×10^{-5}	20×10^{-3}	15.4×10^{-6}

By examining Fig. 5, one can visualize how the various locations can change (with respect to nitrates) if the pollutant concentrations change. The dividing plane is fixed by the stoichiometry of the reactions in Table 3; since the value of chloride assumed for ATC is probably too high, a lower value would probably shift the ATC point closer to the x–z plane, just into the nitrate region. Similarly, the Point Judith location may be shifted farther into the no-nitrate region if the airborne chloride is increased. Note, however, that while rather small changes in SO_2 or HCl content may shift locations like ATC and Point Judith back and forth across the dividing plane, it would take a very large increase in HCl and SO_2 to shift the Los Angeles point into the no-nitrate region.

TABLE 5—*Air pollutant concentrations for several locations.*

Pollutant Gas	Concentrations, $\mu g/m^3$			
	Point Judith	ATC[b]	Los Angeles	Chicago
SO_2	14	54	25	27
NO_2	26	53	135	57
HCl[a]	50	50	50	50

[a] Data from Barton [*13*].
[b] ATC = Alcoa Technical Center.

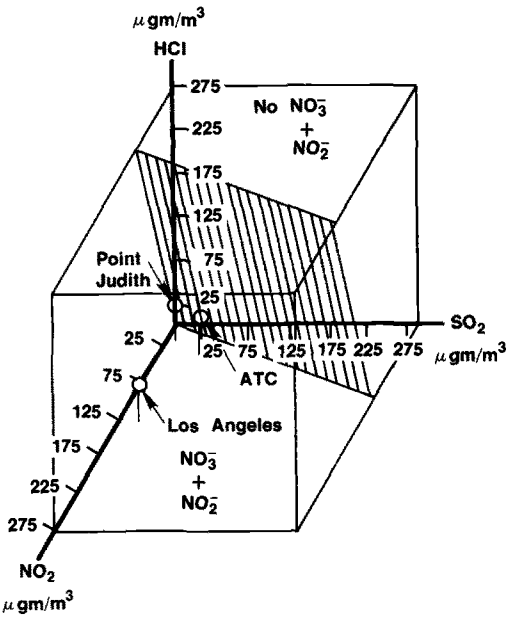

FIG. 5—*Expected condensate compositions for three locations. Point Judith and ATC (Pittsburgh) atmosphere points are located in a region in back of a dividing plane where condensates with no nitrates form. Chicago is located on the nitrate side of the plane, just in front of Point Judith.*

Conclusions

The equilibrium model for condensate compositions, that is, that the maximum concentrations of ionic species in a condensate must be limited by the equilibrium condition established between the dissolved ions and the gases from which they form, appears to delineate differences between condensates formed in several polluted atmospheres. The major difference is the result of a region where nitrates can coexist with other pollutants. The differences in condensate composition found may help in explaining the reversal of corrosion test data noted at the beginning of the paper.

The model accurately predicts the ionic species present in acid-gas atmospheres, namely, sulfuric, nitric, and hydrochloric acids. It is believed that the methodology developed can be used to determine test electrolyte composition as a function of air composition so that further electrochemical and kinetic studies into the durability of aluminum alloys can be made.

References

[*1*] Lifka, B. W., *Aluminum*, Vol. 53, 1977, pp. 750–752.

[*2*] Sprowls, D. O. and Brown, R. H. in *Proceedings*, International Conference of Fundamental Aspects of Stress-Corrosion Cracking, The Ohio State University, Columbus, Ohio, 11–15 Sept. 1967, National Association of Corrosion Engineers, 1969.

[3] Craig, H. L., Sprowls, D. O., and Piper, D. E. in *Stress-Corrosion Cracking in High Strength Steels and in Titanium and Aluminum Alloys*, B. F. Brown, Ed., Naval Research Laboratory, 1972, Chapter 10.
[4] "National Air Quality, Monitoring and Emissions Trends Report 1977," Environmental Protection Agency, EPA-450/2-78-052, Dec. 1978.
[5] Mansfeld, F. and Kenkel, J. V., *Corrosion Science*, Vol. 16, 1976, p. 111.
[6] *International Critical Tables*, Vol. 7.
[7] Latimer, W. M., *Oxidation Potentials*, 2nd ed., Prentice-Hall, New York, 1952.
[8] Giauque, W. F. and Wiebe, R., *Journal of the American Chemical Society*, Vol. 50, 1928, p. 116; see also "JANAF Thermochemical Tables."
[9] Eriksson, G. and Rosen, E., *Chemica Scripta*, Vol. 4, 1973, p. 193.
[10] Wilson, G. L. and Miles, F. D., *Transactions of the Faraday Society*, Vol. 36, 1940, p. 345.
[11] Rabe, A. E. and Harris, J. F., *Journal of Chemical and Engineering Data*, Vol. 8, No. 3, 1963, p. 333.
[12] Linke and Siedell, *The Solubility of Inorganic and Metal-Organic Compounds*, American Chemical Society, Washington, D. C., 1958.
[13] Barton, Karel, *Protection Against Atmospheric Corrosion—Theories and Methods*, Wiley, New York, 1976.

M. Khobaib,[1] *F. C. Chang,*[1] *E. E. Keppler,*[1] *and C. T. Lynch*[2]

Accelerated Atmospheric-Corrosion Testing

REFERENCE: Khobaib, M., Chang, F. C., Keppler, E. E., and Lynch, C. T., **"Accelerated Atmospheric-Corrosion Testing,"** *Atmospheric Corrosion of Metals, ASTM STP 767,* S. W. Dean, Jr., and E. C. Rhea, Eds., American Society for Testing and Materials, 1982, pp. 374–394.

ABSTRACT: No accurate methods are known for accelerated testing of corrosion which yield reliable results for predicting the service life of aircraft components and materials which degrade or fail due to environmental attack. In an effort to provide the basis for development of realistic accelerated corrosion tests, research is being conducted in controlled atmospheres on the localized environmental enhancement of crack-growth rates of aerospace alloys. Corrosion-fatigue and rising-load experiments have been conducted using accelerating pollutants such as sulfur dioxide (SO_2) and ambient air to 100 percent relative humidity air in a specially designed atmospheric chamber. Initial results indicate that realistic environmental enhancement of crack-growth rates can be employed to develop accelerated tests which can be related to actual in-service degradation. For materials with high stress-corrosion susceptibility, the threshold for crack growth (K_{Iscc}) was estimated to be 45 to 46 MPa $\sqrt{m}$ for 4340 steel at a 1440-MPa yield strength level, as compared to 49 to 52 MPa $\sqrt{m}$ as determined by means of rising-load test and 44 to 46 MPa $\sqrt{m}$ by fracture analysis in 1000-ppm SO_2 at 80 percent relative humidity. Thus, a rapid and reproducible method for K_{Iscc} determination appears feasible.

KEY WORDS: accelerated corrosion testing, realistic environments, crack growth, localized environmental enhancement, rising-load testing, low-cycle corrosion fatigue

Over the past four years a considerable number of studies have been conducted within the Air Force and at the National Bureau of Standards (NBS) regarding the total cost of corrosion prevention and control for aircraft. The inescapable conclusion is that total corrosion costs in terms of life-cycle management and maintenance of aircraft represent an intolerable burden to the Air Force in maintaining force effectiveness at a reasonable cost to the taxpayer. In a 1978 NBS report [*1*][3] the total corrosion cost was calculated to be $70 billion nationally. For the Air Force the direct cost of corrosion

[1] Systems Research Laboratories, Inc., 2800 Indian Ripple Road, Dayton, Ohio 45440. Co-author Chang is now with the Army Materials and Mechanics Research Center, Watertown, Mass.

[2] Air Force Wright Aeronatical Laboratories, Wright-Patterson Air Force Base, Ohio 45433.

[3] The italic numbers in brackets refer to the list of references appended to this paper.

maintenance in the field and at the depot level has been estimated to be $750 million, and the total corrosion cost including facilities is estimated to be in excess of one billion dollars. During the 1975 and 1977 Air Force Office of Scientific Research-Air Force Materials Laboratory (AFOSR-AFML) Corrosion Workshops, improved accelerated tests were cited as being a major area of need requiring further research [*2,3*]. One of the major problems in effectively reducing aircraft-corrosion maintenance costs has been the inability of the research community to develop realistic corrosion tests which give meaningful results in a reasonable length of time. There are no accurate methods for accelerated testing for corrosion which yield reliable results for predicting the service life of aircraft components and materials which degrade or fail due to environmental attack. Current alternatives involve the use of gross tests such as saltwater immersion which yield relative corrosivity values that have no quantitative relation to service life or outdoor atmospheric exposure tests which require experiments of three to five years or longer and are specific to one local environment.

A program has been initiated to provide the basis for the development of realistic accelerated tests which can be used to predict the long-range corrosion behavior of materials under actual service conditions. Test environments are based upon reasonable variations in the concentration of accelerating pollutants, humidity, and temperature, using primary and secondary air-quality standards to establish concentration base levels for accelerating pollutants such as sulfur dioxide. Controlled atmospheric experiments are being conducted for general corrosion and for localized environmental enhancement of crack-growth rates. Crack-growth studies include low-cycle corrosion-fatigue, rising-load, and constant-slow-strain-rate tests. Initial results are reported in this paper for 4340 steel and 7075-T651 aluminum alloys under rising-load and low-cycle fatigue. Results of several corrosion studies in a controlled atmosphere will be compared later to results for general corrosion of test panels at outdoor sites located in corrosive and relatively benign atmospheres.

The state of the art in accelerated-corrosion testing methods as described in the ASTM Book of Standards and approved by the National Association of Corrosion Engineers (NACE) involves the aforementioned use of gross tests such as salt fog and alternate salt-immersion tests with their lack of quantitative values for corrosivity or relative corrosivity with respect to service experience. Atmospheric outdoor tests where panels are exposed to various environments require a time scale which precludes rapid materials-selection decisions or paint-protection-measures evaluations. These tests are specific to limited environments and seldom take into account stress factors which may accelerate the localized corrosion and enhance crack growth, leading to premature failure. Cyclic loading is, of course, also precluded. Establishing realistic test environments requires, at a minimum, a reasonable selection of atmospheric environmental variables coupled with stress factors

which aerospace components are expected to experience. The selection of appropriate air-quality standards is difficult and should be based upon knowledge of ambient-air pollutant levels and experimental work to determine the relative importance of these pollutants. The effects of sulfur dioxide (SO_2) on high-strength steels (as discussed in this paper) and nitrogen dioxide (NO_2) on high-strength aluminum alloys (to be reported in a subsequent paper) must be related to the interaction of these gases with water vapor and airborne particulates and to causal factors. In this paper, the design and layout of the experimental apparatus for simulating the environment and the initial results obtained in environmentally acceleratd crack-growth studies conducted on high-strength steels and aluminum alloys are given. Experiments have been conducted in dry and humid air and then in more aggressive environments containing a mixture of SO_2 and humid air. Rising-load tests have been used to determine the apparent K_{Iscc} for 4340 steels in such an environment. Fractographic analysis has been employed to correlate the results and the types of failure that have occurred. Initial results have been obtained on 7075-T651 aluminum and 4340 steel.

Experimental

A 50.8-mm-thick plate of 4340 steel of aircraft quality was used. The high-strength Al-7075-T651 alloy used was obtained from Rockwell International in the form of 76.2-mm-thick plate. Research-grade SO_2 and NO_2 and reagent-grade sodium chloride (NaCl) were employed. Distilled water was used throughout the experiments. The critical stress-intensity factor, K_{Ic}, the threshold stress intensity for stress-corrosion cracking, K_{Iscc}, and crack-growth data were obtained using compact-tension plane-strain fracture-toughness specimens as shown in Fig. 1. Both steel and aluminum specimens were machined in the short-transverse (ST) orientation. The high-strength 4340 steel was heat-treated to yield strengths of 1275 and 1440 MPa.

Fracture-Toughness Testing

The compact-tension specimens were precracked to 2.54 mm by fatigue-cracking the specimens according to ASTM specifications. Two specimens from each heat treatment were loaded monotonically to failure (in ambient air—average relative humidity (RH) $\approx$ 50 percent in laboratory air) to determine the stress intensity at fracture, K_{Ic}.

Accelerated K_{Iscc} Testing

The apparent threshold for sustained-load stress-corrosion cracking, K_{Iscc}, in humid air and in different mixtures of humid air and SO_2 was estimated using the accelerated rising-load procedure [*4*]. The testing technique utilized was identical to the procedure used for K_{Ic} fracture-toughness testing

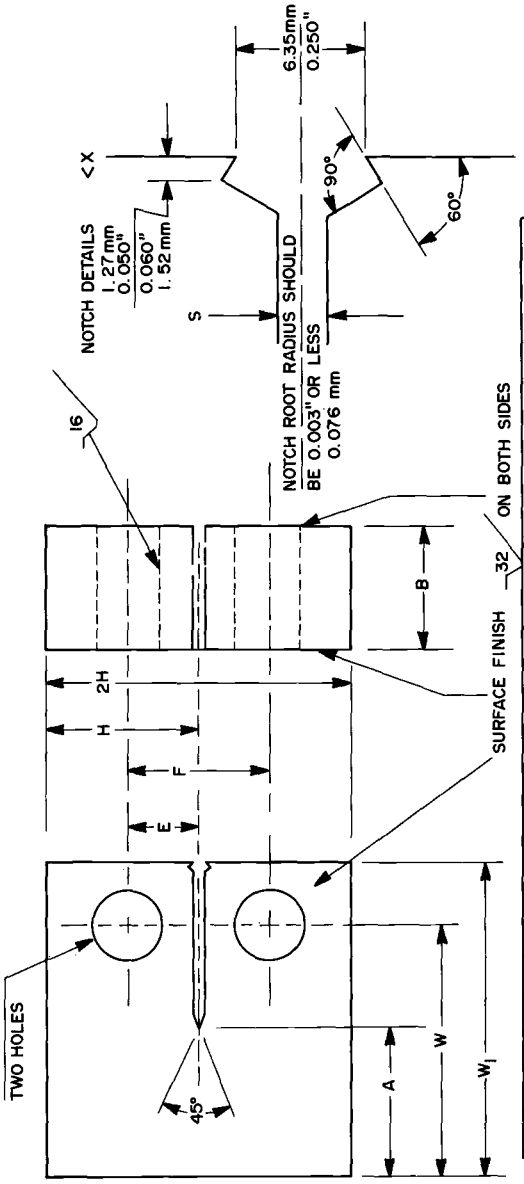

MATERIAL	B	A	W	W_1	S	E	F	H	D
ALUMINUM	25.4mm	29.2mm	50.8mm	63.5mm	2.36mm	13.97mm	27.94mm	30.48mm	12.7mm
STEEL	19.05mm	22.22mm	38.10mm	47.62mm	1.90mm	10.46mm	20.95mm	22.86mm	9.52mm

FIG. 1—*Compact-tension specimen.*

TABLE 1—*Apparent K_{Iscc}-values obtained by rising-load tests.*

Specimen No.	Environment	Loading Rate, N/min	Apparent K_{Iscc},[a] MPa$\sqrt{m}$	Yield Strength, MPa
2B	1000-ppm SO_2 + 80% RH	22	55	1440
3B	1000-ppm SO_2 + 80% RH	88	49	1440
10A	1000-ppm SO_2 + 80% RH	22	72	1240
23A	1000-ppm SO_2 + 100% RH	22	70	1240
29A	80% RH	22	78	1240
15A	50% RH	22	78	1240

[a] These values are approximate.

[ASTM Test for Plane-Strain Fracture Toughness of Metallic Materials (E 399-72)], except that a slower rate of loading was employed and the specimen was exposed to the environment while being loaded. These tests were conducted with standard 19.05-mm-thick compact-tension specimens. The specimens were precracked to crack lengths of 2.54 mm at stress intensities below 15 MPa $\sqrt{m}$ ($R = 0.1$ and $f = 0.1$ Hz). A special environmental chamber (to be described in detail later) was used to maintain and control the constituents of the specific environments required for the tests. The specimens were loaded in air, in 80 percent relative humidity, in 1000-ppm SO_2 at RH = 80 percent, and in 1000-ppm SO_2 at RH = 100 percent, at fixed loading rates corresponding to 22 and 88 N/min. K_{Iscc}-values were estimated from the load-displacement record, using the 5 percent secant offset procedure similar to that used for the K_{Ic} testing. The results are given in Table 1.

The Environmental Chamber

The environmental chamber and the gas-train assembly are shown in Fig. 2. The chamber is made of 316 stainless steel while the grips, pull rods, and pins are made of 17-4 PH steel, which exhibits good resistance to wet SO_2 and wet NO_2 environments. It is a leakproof system with bellows and other attachments to attain high vacuum. The temperature inside can be controlled from 0 to 538°C. The unit is installed in a closed-loop Materials Testing System (MTS) machine for conducting mechanical tests in realistic environments.

The test atmospheres were supplied through the gas train, which consists of a gas mixing and delivery system. High-purity bottled gases (SO_2 and dry air in this case) were metered by Matheson Flowmeters 601 and 603 and then mixed in the mixing tube. The concentration of SO_2 in the chamber is routinely measured by calibrated Gastec analyzer tubes. Special gas-sampling outlets are provided in the chamber. The relative humidity inside the chamber is controlled by means of a BMA dry and wet bulb hygrometer. The water vapor is added in the form of steam by boiling distilled water in a flask main-

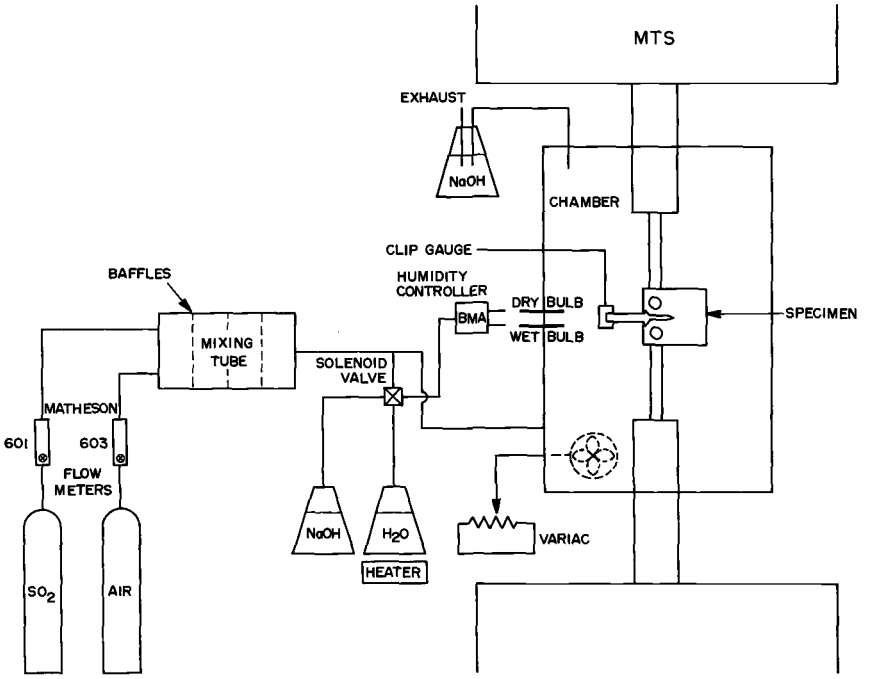

FIG. 2—*Gas train and environmental chamber.*

tained at a constant temperature. The steam flow is controlled by the output voltage of the BMA controller, which monitors the opening and closing of the solenoid valve on the steam line. The steam is injected into the gas mixture prior to its entry into the chamber in order to obtain the required mixture of SO_2 and relative humidity air.

Gas pressures used in all the tests have been slightly above atmospheric to provide positive flow through the environmental chamber. The gas inlet and outlet are positioned specifically to minimize the channeling effect. The gas is circulated inside the chamber by means of a circulating fan (placed inside the chamber) to maintain a uniform environment throughout the chamber. Negligible condensation occurred during these tests except in the case of RH = 100 percent. The fatigue-crack-propagation data discussed in the next section were obtained using compact-tension plane-strain fracture-toughness specimens (Fig. 1). Tests were conducted in the controlled atmosphere inside the environmental chamber as described. The inert dry nitrogen was used as a control, while the RH = 80 percent air, 1000-ppm SO_2 and RH = 80 percent, and 1000-ppm SO_2 and RH = 100 percent were used as representative aggressive environments for stress corrosion and environmentally accelerated corrosion fatigue.

Corrosion-Fatigue Crack Growth

All tests were conducted at room temperature using a 100-kN Materials Testing System (MTS) machine. The crack length was monitored through crack-opening-displacement (COD) measurements during fatigue testing. To determine the crack length from COD data, compliance measurements were carried out for both high-strength steels and aluminum alloys. Tests were conducted in air, and crack lengths were determined using optical and COD measurements simultaneously on the MTS machine. The COD was measured by a double-cantilever displacement gage prepared in accordance with the ASTM Method E 399-72. The displacement gage was calibrated to measure COD from 0 to 1.25 mm ± 0.0125 mm using a System Research Laboratories (SRL) developed strain-gage amplifier. The COD was recorded as a function of cycles.

A sinusoidal tension-tension waveform was employed for all fatigue-crack-growth-rate tests. Most of the tests were conducted at an R-ratio (K_{min}/K_{max}) of 0.6 and a frequency of 0.1 Hz. The slow frequency and high R-ratio were utilized to facilitate the observation of environmental effects. Limited tests were conducted at frequencies of 0.25 and 0.5 Hz also. All specimens were initially precracked according to ASTM E 399-72 on the same MTS machine on which the corrosion-fatigue tests were conducted.

No significant differences were found in the COD/load and crack length/load curves. The crack length, a, was calculated from the analytical compliance relationship [*5*]

$$a/W = 1.001 - 4.6695\ U + 18.460\ U^2 - 236.82\ U^3 + 1214.94\ U^4 - 2143.6\ U^5$$

where

$$U = \frac{1}{\sqrt{\dfrac{EB(\mathrm{COD}_{max} - \mathrm{COD}_{min})}{P_{max} - P_{min}}} + 1}$$

where E is the Young's modulus and P the stress. W and B are the dimensions indicated in Fig. 1. The stress-intensity values were calculated from [*5*]

$$K = \frac{P}{BW^{1/2}} \times \frac{(2 + a/w)0.886 + 4.64(a/w) - 13.32(a/w)^2 + 14.72(a/w)^3 - 5.6(a/w)^4}{(1 - a/w)^{3/2}}$$

where B and W are the dimensions indicated in Fig. 1 such that B and $a > 2.5\ (K_{Ic}/\mathrm{YS})^2$, with K_{Ic} being the fracture toughness and YS the tensile yield strength. The crack-length-versus-number-of-cycles data were converted to fatigue-crack-growth rates (da/dN) using a computer program [*5*].

Seven to eleven data points were fitted to a second-order polynomial, and the derivative (*da/dN*) was then obtained for the middle data point. This process was then repeated over the range of data.

All fractured surfaces were examined visually and then by light microscopy. The specimens were then ultrasonically cleaned in acetone, deionized water, and methyl alcohol. The light-microscopic observation was followed by scanning electron microscopy (SEM) for detailed examination of the fractured surfaces.

Results and Discussion

Crack Propagation

The fatigue-crack-propagation behavior of many ferrous and nonferrous alloys can be schematically represented as in Fig. 3 [*6*]. The rate of crack growth depends strongly upon K at K-levels approaching K_c or K_{Ic} at the high end and at levels approaching an apparent threshold at the low end, with an intermediate region that depends upon some power of K or ΔK. The upper end corresponds to the onset of unstable fracture, while the lower end corresponds to the fatigue "threshold" ΔK_{th} [*7,8*] which appears to be related to the metallurgical structure [*9*].

The environment-enhanced fatigue-crack-growth response of high-strength metals may be broadly characterized in terms of three general patterns of behavior [*10*], as illustrated schematically in Fig. 4. The first type of behavior represents those material-environment systems where fatigue-crack-growth rates are enhanced by the presence of an aggressive environment through a

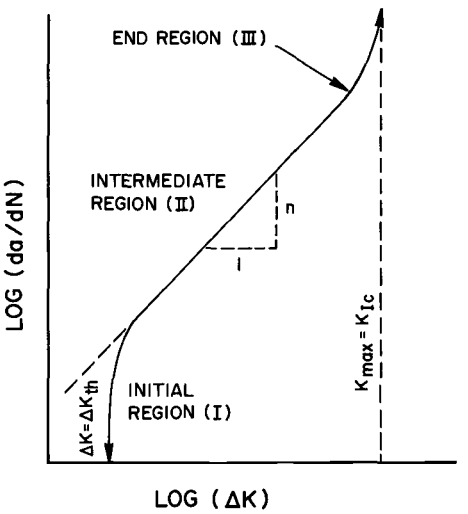

FIG. 3—*Schematic diagram of fatigue-crack-growth rate behavior.*

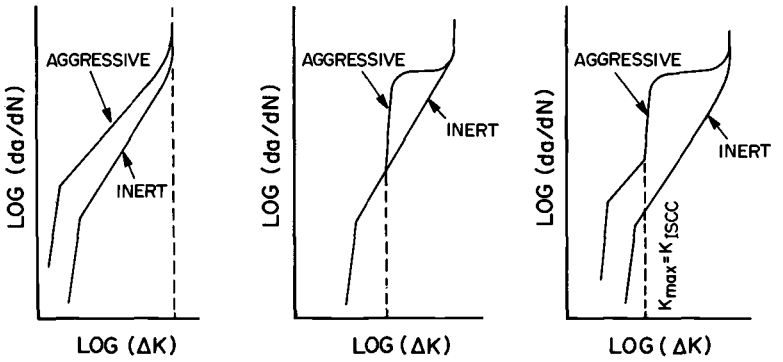

a) TRUE CORROSION FATIGUE (TCF) b) STRESS CORROSION FATIGUE (SCF) c) SCF ON TCF

FIG. 4—*Types of fatigue-crack-growth behavior.*

synergistic action of corrosion and cyclic loading. This is "below K_{Iscc}" behavior [*11–13*] and applies to materials which are not susceptible to stress corrosion where $K_{Iscc} > K_{Ic}$. This behavior is classified as true corrosion fatigue. The second type of behavior is representative of those systems where there is a substantial environment-enhanced sustained-load crack-growth component [*14,15*], which occurs whenever the stress intensity in the cycle is above K_{Iscc}. This behavior is classified as stress-corrosion fatigue. The most common type of behavior pertains to material/environment systems which exhibit stress-corrosion fatigue above K_{Iscc} and also true corrosion fatigue at all stress-intensity levels. Such behavior lies between the two extremes and is shown in Fig. 4*c*.

Crack-Growth Behavior of Al 7075-T651

The accelerated atmospheric effects resulting from the variation of the relative humidity upon observed crack-growth rates were investigated. The low-cycle corrosion-fatigue data are expressed in terms of crack-growth rate da/dN as a function of the stress-intensity-factor range ΔK. The dependence of crack-growth rate upon the humidity level in air for Al 7075-T651 is shown in Fig. 5. At high levels of humidity such as RH = 80 percent, the crack-growth rates were substantially increased as compared to those in dry air ($\leq$ RH = 5 percent). The immersion results for crack growth in aqueous solutions are shown for the sake of comparison. While increasing relative humidity also increases the crack-growth rates, the change in crack-growth rate from gaseous environment to total-immersion aqueous environment is much more significant. This rate is also less realistic for estimating corrosion reactions except where standing water is present. Similar results on several aluminum alloys have been obtained by other workers [*16–23*]. The com-

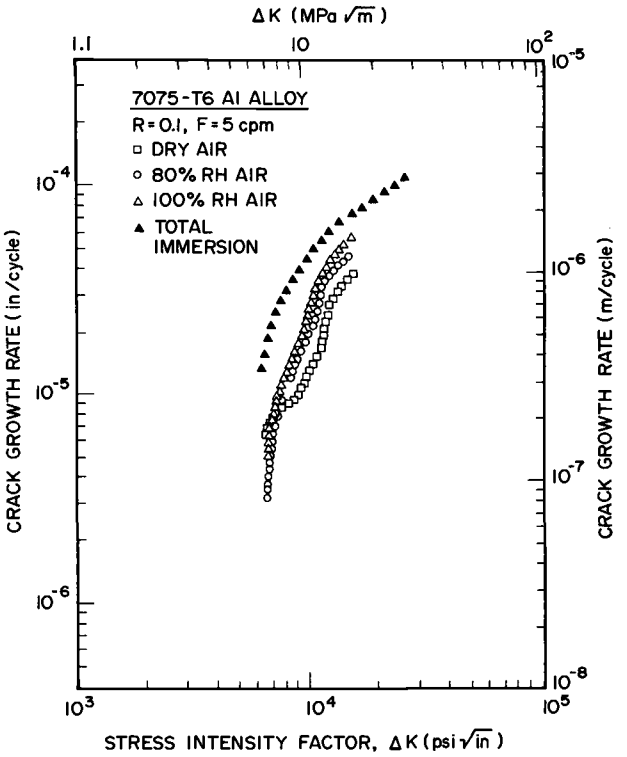

FIG. 5—*Crack-growth-rate data obtained for Al 7075-T651, tested at various relative humidity levels.*

monly accepted explanation of crack-growth acceleration due to a high level of humidity is the pressure mechanism of hydrogen embrittlement suggested by Broom and Nicholson [*19*] which requires a water-metal surface reaction and proposes that the increase in the rate of fatigue-crack growth results from the synergistic action of a mechanical process—fatigue, which creates a sufficient amount of fresh surface—and the chemical reaction of water vapor with the resulting fresh surface.

Crack-Growth Behavior of 4340 Steel

Figure 6 represents the crack-growth-rate data on 4340 steel with a yield strength of 1345 MPa obtained at three levels of humidity. In all these tests a frequency of 0.1 Hz and a load ratio R of 0.1 were used. While the shapes of the three curves are similar, noticeable differences exist in the crack-growth rates at high K-levels. Note that although the differences in crack-growth rates (at different humidity levels) are small, very definite differences are present. The differences found are reproducible within an experimental error

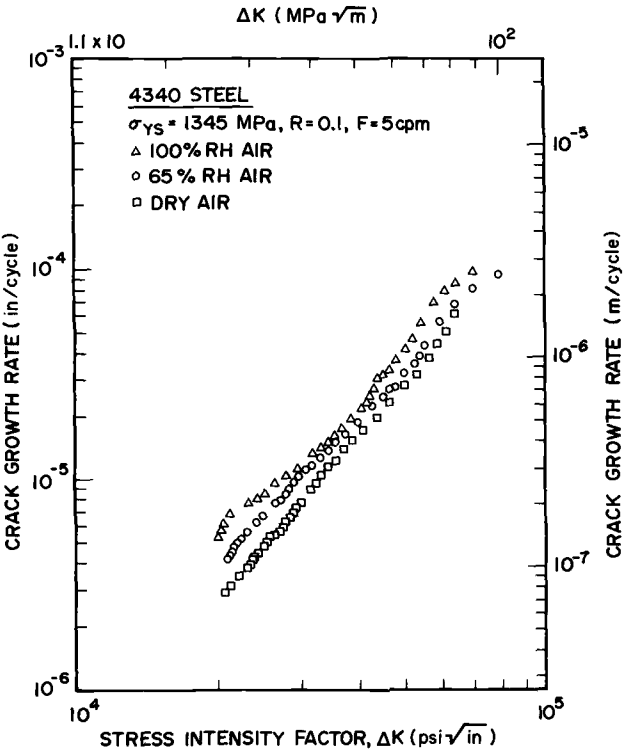

FIG. 6—*Crack-growth-rate data obtained for 4340 steel (1345 MPa), tested at various relative humidity levels.*

TABLE 2—*Specimen life in cycles.*

4340 Steel	1335 MPa	
Specimen No.	RH	N_f(cycle)
1	dry air ≤5%	60 174
2	65%	40 593
3	100%	33 864
Al 7075-T651		
Specimen No.	RH	N_f(cycle)
1	dry air ≤5%	40 347
2	80%	26 950
3	100%	41 005

of *da/dN* less than the $\Delta da/dN$ values. Similar differences in crack-growth rates were observed for 7075-T651 aluminum. These differences become more pronounced when one considers data on cycles to failure. These data are shown in Table 2 for both Al 7075-T651 and 4340 steel. Similar increases in crack-growth rates of high-strength 4340 steel due to water vapor were observed under both sustained and cyclic loading by Lynch and other workers [*24–30*]. Dahlberg [*31*] has demonstrated more distinct differences in the crack-growth rates of 4340 steel tested at different humidity levels when an R-ratio of 0.8 was used. However, the differences in crack-growth rates with increasing humidity levels were similar to those obtained in the present investigation where smaller *R* ratios were used.

Although several mechanisms have been suggested for hydrogen embrittlement [*32–35*] (such as the decohesion model [*34*] and the pressure model [*35*]), no single theory gives a complete description of the problem. For high-strength steels, however, in "hydrogen-producing" atmospheres [for example, hydrogen (H_2), water (H_2O), hydrogen sulfide (H_2S)], decohesion theories are widely accepted [*15,35–38*] (for monotonic and cyclic loading). Also, the general concensus is that the presence of water vapor in the atmosphere enhances crack-growth rates for both high-strength aluminum and steel alloys.

Crack Propagation of 4340 Steel in Humid SO_2

High-strength 4340 steel at yield strengths of 1240 and 1440 MPa were tested at a load ratio of 0.6 and a frequency of 0.1 Hz. The atmospheres were ambient air, dry nitrogen, air with RH = 80 percent, and 1000-ppm SO_2 in air with RH = 80 percent air. The crack-growth results for 1240-MPa steel are shown in Fig. 7, while Fig. 8 shows the *da/dN*-versus-ΔK plot for 1440-MPa steel. A comparison of these two figures shows that there is a greater enhancement in the crack-growth rates for 1440-MPa steel compared with 1240-MPa steel due to the SO_2 environment. These data indicate a "bump" (abrupt change in the slope in the intermediate region) of the *da/dN*-versus-ΔK plot obtained for 1440-MPa steel tested in the 1000 ppm SO_2 and RH = 80 percent environment. A similar "bump" is obtained for 1240-MPa in this same environment. The ambient air and RH = 80 percent plots, however, follow the normal trend [*6*]. This difference in the nature of the plot (or appearance of the "bump") is expected when the *K*-level exceeds the K_{Iscc}-value for the metal-environment system. In general, this follows the trend of Fig. 4*c*, which is most significant because the extrapolation from this slope change to the abscissa of the plot produces the K_{Iscc}-value as shown in Fig. 4*c*. Accordingly, the K_{Iscc}-values have been obtained from Figs. 7 and 8 and are 55 and 46 MPa $\sqrt{m}$ for 1240- and 1440-MPa steels, respectively. The accuracy of this estimate has been further verified by the rising-load method and fractographic observations. The K_{Iscc}-value obtained for 1440-MPa steel by such extrapolation is in very close agreement with the K_{Iscc}-values obtained

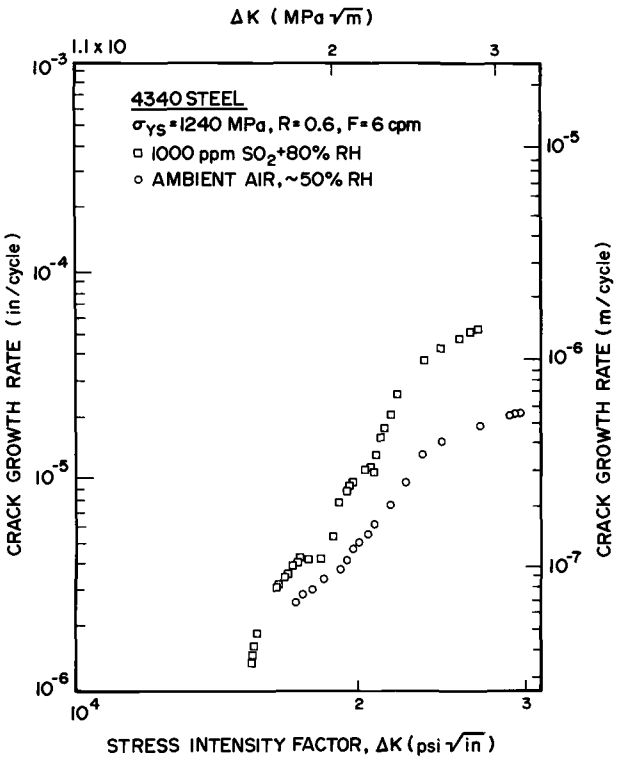

FIG. 7—*Crack-growth-rate data obtained for 4340 steel (1240 MPa), tested in 1000-ppm SO_2 at RH = 80 percent environment.*

from the other observations. The high value of K_{Iscc} obtained for 1240-MPa steel could not be supported by either rising-load or fractographic observations. Such high values of K_{Iscc} obtained by extrapolation of *da/dN*-versus-ΔK curves have been reported previously [*39*]. However, the K_{Iscc} value obtained by such extrapolation for 1440-MPa steel is quite consistent and accurate. The validity of this extrapolation is supported by the results of Austen and Walter [*40*] on high-strength 835M30 steel in a 3.5NaCl environment and the results we have obtained on 4340 steel in 3.5NaCl solution. However, the high value of K_{Iscc} obtained for 1240-MPa steel requires further studies in several environments. A more detailed investigation of the nature of the *da/dN*-versus-ΔK plot is required when there is a very small difference in K_{Iscc} and K_c-values for the metal-environment system. In this case 1240-MPa steel is not so susceptible as 1440-MPa steel to hydrogen-assisted stress-corrosion cracking in the environment/conditions of the test, and the results apparently are intermediate between the first two cases of the schematic presentation of Fig. 4. In such a case, further detailed study of frequency/

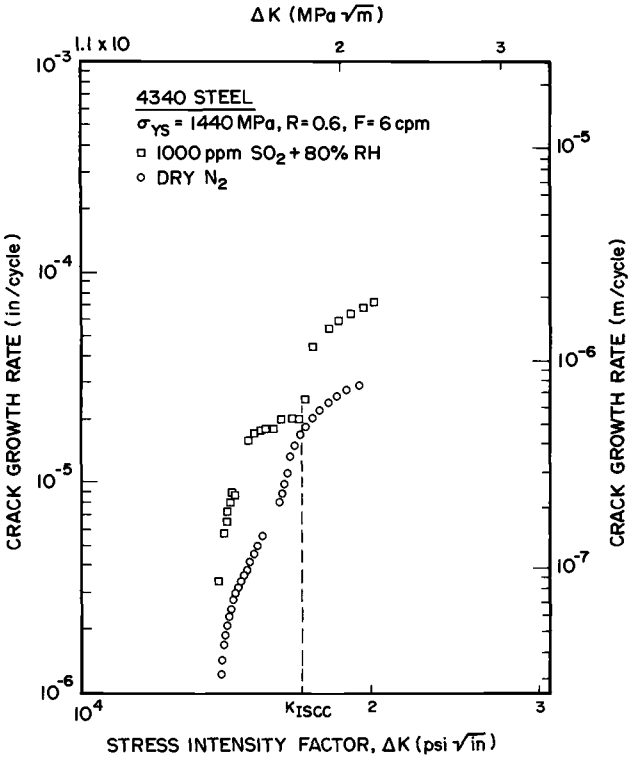

FIG. 8—*Crack-growth-rate data obtained for 4340 steel (1440 MPa), tested in 1000-ppm SO_2 at RH = 80 percent environment.*

load/R-ratio effects may be necessary to improve the determination of K_{Iscc} by extrapolation.

Rising-Load K_{Iscc} Tests

The approximate values of K_{Iscc} obtained for 1240- and 1440-MPa steels in various environments are given in Table 1. Only two loading rates of 22 and 88 N/min were used. The values quoted in Table 1 must be taken as the higher-limit estimates because of the rapid K-rates utilized and the limited nature of the test procedure. More experiments at slower rates should improve the approximation of K_{Iscc}-values.

Fractographic Analyses

Fractographic analyses of the fracture surfaces of the specimens were conducted to provide further information concerning the crack-tip mechanism in corrosion fatigue of 4340 steels at different K-levels in humid SO_2 envi-

ronments. Figure 9 shows fractographs taken from the surface of a 1240-MPa steel specimen tested in 1000-ppm SO_2 + RH = 80 percent. These fractographs indicate that at low values of K, 40.5 MPa $\sqrt{m}$, the surface features are very ductile (Fig. 9*a*). At higher values of K, there is little evidence of intergranular fracture. The fracture is mainly transgranular and ductile in nature. No substantial component of intergranular fracture could be found, even in the fracture zone corresponding to high values of K, ≈57.5 MPa $\sqrt{m}$ (near the fast fracture) (Fig. 9*b*). Different fracture-surface characteristics were obtained for 1440-MPa steel corrosion fatigued in 1000-ppm SO_2 + RH = 80 percent. Figure 10*a* shows the ductile nature of failure at low K-values of 35 to 36 MPa $\sqrt{m}$, while Fig. 10*b* shows the mixed mode of failure, corresponding to a K value of ≈40 MPa $\sqrt{m}$.

Figure 10*c* is a typical fractograph obtained in the fracture zone corresponding to a K-value of ≈46 MPa $\sqrt{m}$. The entire fractured surface was scanned several times, and a definite intergranular failure mechanism was observed over the entire cross section when the K-value exceeded 45 to 46 MPa $\sqrt{m}$. The value of K_{Iscc} was approximated by careful measurement of the crack length and found to be ≈46 MPa $\sqrt{m}$, which is in agreement with the K_{Iscc}-value obtained from the da/dN-versus-ΔK plot; this value falls within good approximation of the value obtained by the rising-load method.

Figure 11 shows the fractographs obtained from the fractured surface of 1240-MPa steel tested in dry N_2. The fractured surfaces (Fig. 11*a*) are characteristic of ductile failure, containing dimple rupture. In Fig. 11*b* the dimples can be more clearly seen at higher magnification.

Conclusions

The presence of water vapor in the atmosphere accelerates the crack-growth rates of high-strength steel and aluminum alloys. Crack-growth rates increase with increasing relative humidity, with the effect being more pronounced in steel at a yield strength of 1440 MPa as compared to 1240 MPa.

There is a significant increase in crack-growth rates (and corresponding decrease in cycles to failure) for high-strength alloys in full immersion in aqueous solutions as compared to an air atmosphere of 100 percent relative humidity.

Corrosion-fatigue crack-growth rates increase from ambient air to air with RH = 80 percent to RH = 80 percent + 1000-ppm SO_2. This is true for all alloys with the effects being more pronounced in the 1440-MPa steel than in the 1240-MPa steel.

The value of K_{Iscc} can be extrapolated from the corrosion-fatigue curve, provided the conditions of load, frequency, and R-ratio are optimized. The results of rising-load corrosion-fatigue extrapolation and fractography experiments are in excellent agreement for the 1440-MPa steel. Thus, a rapid determination of K_{Iscc} is provided for susceptible alloys.

FIG. 9a—*Fracture surface of 1240-MPa steel, tested in 1000-ppm SO_2 + RH = 80 percent environment at 40.5 MPa $\sqrt{m}$ (×1100).*

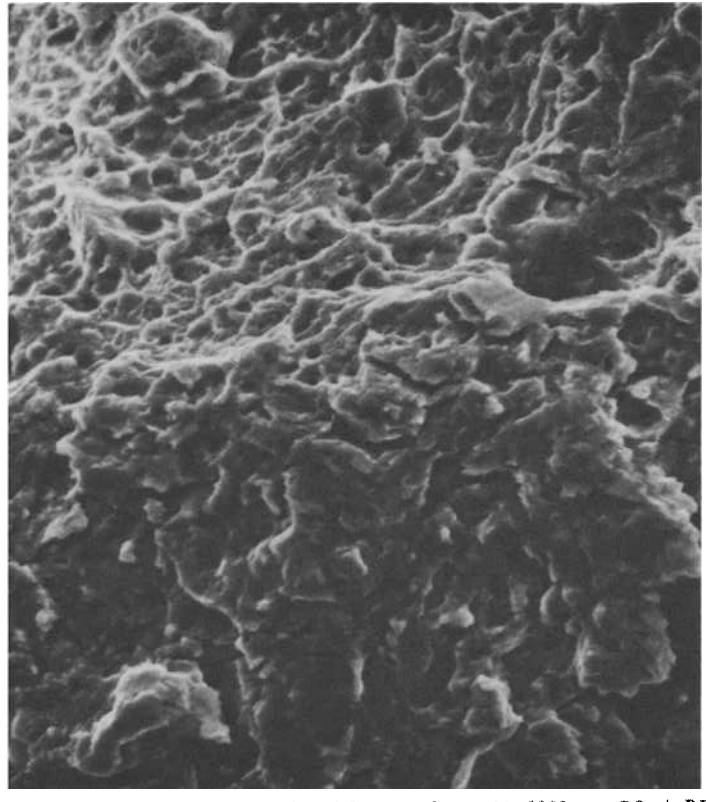

FIG. 9b—*Fracture surface of 1240-MPa steel, tested in 1000-ppm SO_2 + RH = 80 percent environment at 57.5 MPa $\sqrt{m}$ (×3500).*

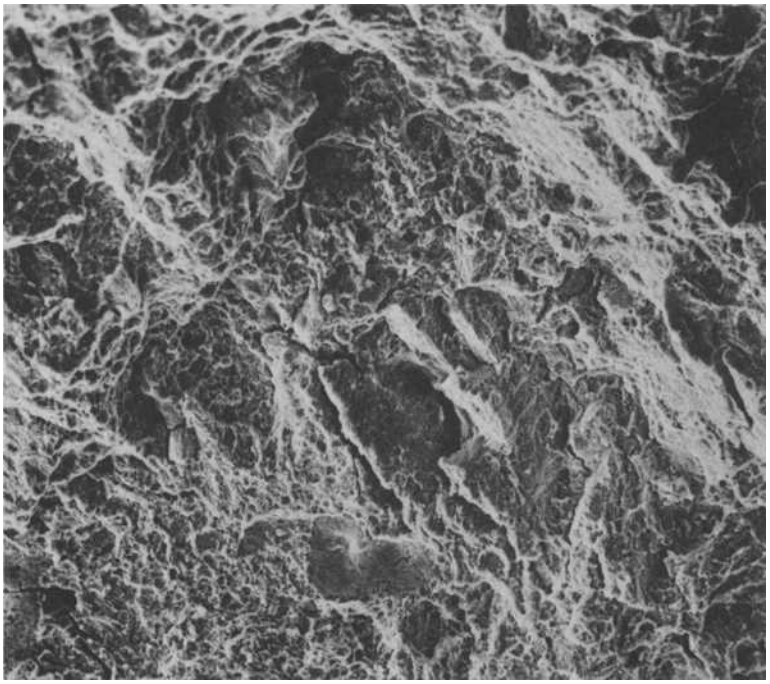

FIG. 10*a*—*Ductile morphology obtained for 1440-MPa steel, resulting from test in 1000-ppm* SO_2 + *RH = 80 percent environment in the range 35 to 36 MPa* $\sqrt{m}$ (×600).

FIG. 10*b*—*Mixed-mode fracture obtained for 1440-MPa steel, resulting from testing in 1000-ppm* SO_2 + *RH = 80 percent environment at 40 MPa* $\sqrt{m}$ (×*1100*).

FIG. 10*c*—*Intergranular and brittle failure obtained for 1440-MPa steel, resulting from test in 1000-ppm* SO_2 + *RH = 80 percent environment in the range 45 to 46 MPa* $\sqrt{m}$ (×*1100*).

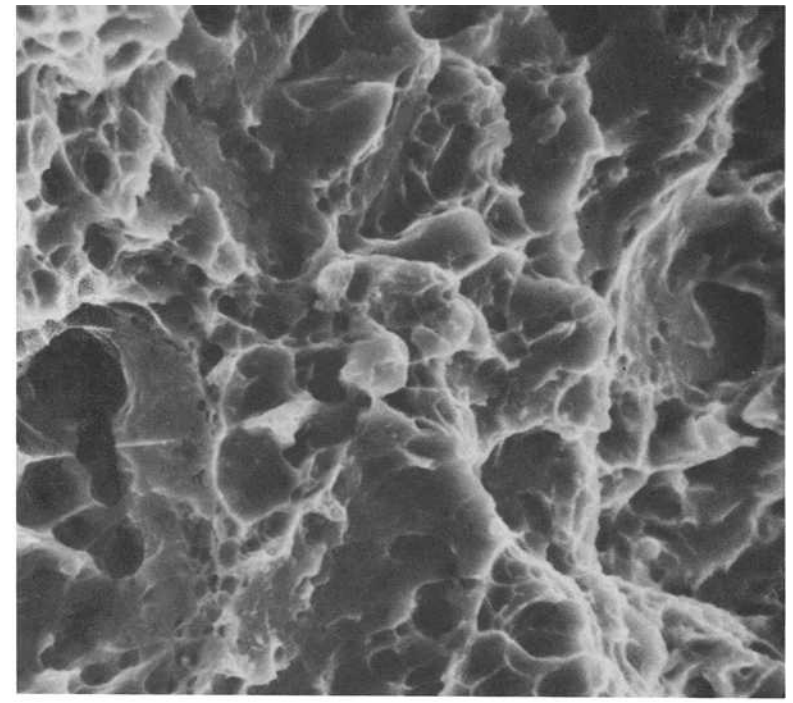

FIG. 11b—*Higher magnification of Fig. 11a showing dimple rupture* (×5000).

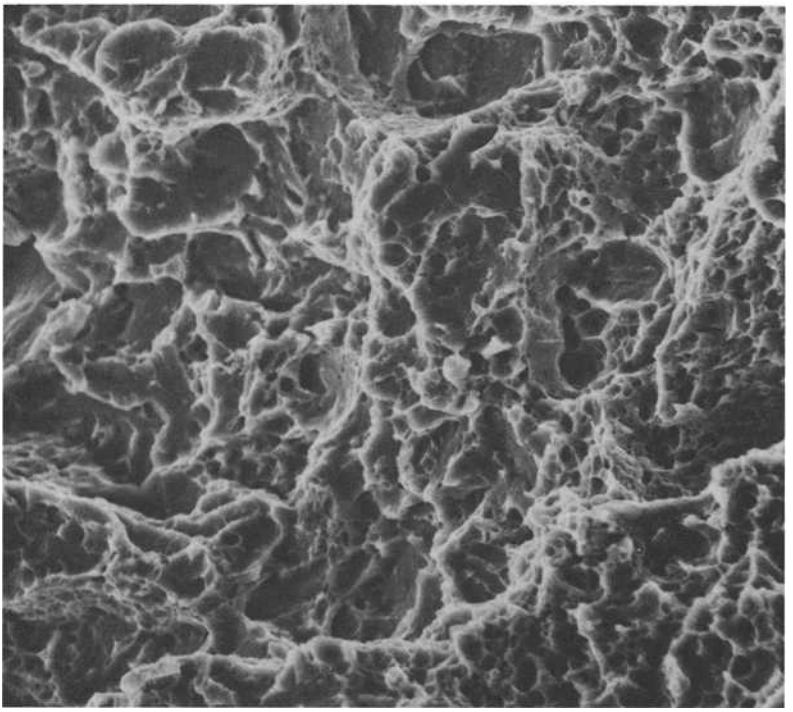

FIG. 11a—*Ductile morphology resulting from test conducted in dry nitrogen* (×2200).

Acknowledgments

The authors express their thanks to F. M. Thornton for reducing the experimental data and to M. B. Strope for assisting in the fractographic analysis.

References

[1] Bennett, L. H., Kruger, J., Parker, R. L., Passaglia, E., Reimann, C., Ruff, A. W., and Yakowitz, H., *Economic Effects of Metallic Corrosion in the United States,* Parts I and II, NBS Special Publication 511-1,2, U.S. Department of Commerce, National Bureau of Standards, Washington, D.C., May 1978.

[2] *Proceedings,* AFOSR/AFML Corrosion Workshop, AFML-TR-77-175, M. Hoch and J. Gwinn, Eds., Air Force Materials Laboratory, Wright-Patterson Air Force Base, Ohio, 1975.

[3] *Proceedings,* AFOSR/AFML Workshop on Corrosion of Aircraft, E. D. Verink, Jr., Ed., St. Augustine, Fla., 13–15 Sept. 1977, The University of Florida, Gainsville, 1977.

[4] Clark, W. G. and Landes, J. D. in *Stress Corrosion—New Approaches, ASTM STP 610,* American Society for Testing and Materials, 1976, p. 108.

[5] Ashbaugh, N. E., Technical Report AFML-TR-79-4127, Air Force Materials Laboratory, Wright-Patterson Air Force Base, Ohio, Sept. 1979.

[6] *Stress Corrosion Cracking in High Strength Steels and in Titanium and Aluminum Alloys,* B. F. Brown, Ed., U.S. Government Printing Office, Washington, D.C., 1972.

[7] Paris, P. C., *MTS Closed Loop Magazine,* Vol. 2, No. 5, 1970.

[8] Bucci, R. J., Clark, W. G., Jr., and Paris, P. C. in *Stress Analysis and Growth of Cracks, ASTM STP 513,* American Society for Testing and Materials, 1972, p. 177.

[9] McMillan, J. A. and Wei, R. P., *Metallurgical Transactions,* Vol. 1, 1970, p. 1741.

[10] McEvily, A. J. and Wei, R. P. in *Proceedings,* International Conference on Corrosion Fatigue—Chemistry, Mechanics and Microstructures, Storrs, Conn., 1972, National Association of Corrosion Engineers, 1972, p. 381.

[11] Barsom, J. M., *Engineering Fracture Mechanics,* Vol. 3, 1971, p. 15.

[12] Gallagher, J. P., *Journal of Materials,* Vol. 6, 1971, p. 941.

[13] Gallagher, J. P. and Wei, R. P. in *Proceedings,* International Conference on Corrosion Fatigue—Chemistry, Mechanics and Microstructures, Storrs, Conn., 1972, National Association of Corrosion Engineers, 1972, p. 409.

[14] Wei, R. P., *Journal of Engineering Fracture Mechanics,* Vol. 1, 1970, p. 633.

[15] Wei, R. P. and Landes, J. D. in *Materials Research and Standards,* American Society for Testing and Materials, Vol. 9, July 1969, p. 25.

[16] Wadsworth, N. J., Nicholson, A., and Hutchins, J., *Philosophical Magazine,* Vol. 3, 1958, p. 1154.

[17] Broom, T. and Nicholson, A., *Journal of the Institute of Metals,* Vol. 89, 1960/1961, p. 183.

[18] Bradshaw, F. J. and Wheeler, C., *Applied Materials Research,* Vol. 5, 1966, p. 112.

[19] Hartman, A., *International Journal of Fracture Mechanics,* Vol. 4, 1965, p. 167.

[20] Wei, R. P., *International Journal of Fracture Mechanics,* Vol. 4, 1968, p. 159.

[21] Wei, R. P. and Landes, J. D., *International Journal of Fracture Mechanics,* Vol. 5, 1969, p. 69.

[22] Hartman, A. and Schijve, J., *Engineering Fracture Mechanics,* Vol. 1, 1970, p. 615.

[23] Wei, R. P. et al, "Fracture Mechanics and Surface Studies of Fatigue Crack Growth in Al Alloys," Report No. 9, IFSM-79-98, Lehigh University, Bethlehem, Pa., Contract No. N00014-75-C-0543, April 1979.

[24] Lynch, C. T., Vahldiek, F. W., and Thornton, F. W. in *Proceedings,* 1978 Tri-Service Conference on Corrosion, New Orleans, 4–6 Oct. 1978.

[25] Che-Yu Li, P. M., Talda, P. M., and Wei, R. P., *International Journal of Fracture Mechanics,* Vol. 3, 1967, p. 29.

[26] Johnson, H. H. and Willner, A. M., *Applied Materials Research, Vol. 4, 1965, p. 34.*

[27] Hancock, G. G. and Johnson, H. H., *Transactions,* Metallurgical Society of the American Institute of Mining, Metallurgical and Petroleum Engineers, April 1966.

[28] Hanna, G. L., Troiano, A. R., and Steigerwald, E. A., *Transactions,* American Society for Metals, Vol. 57, 1968, p. 658.
[29] van der Sluys, W. A., *Transactions,* American Society of Mechanical Engineers, Vol. 89D, 1967, p. 28.
[30] Gallagher, J. P., "Environmentally Assisted Fatigue Crack Growth Rates in SAE 4340 Steel," Ph.D. Dissertation, Department of Theoretical and Applied Mechanics, University of Illinois, Urbana, Ill., 1968.
[31] Dahlberg, E. P., *Transactions,* American Society for Metals, Vol. 58, 1965, p. 46.
[32] Johnson, H. H. and Paris, P. C., *Engineering Fracture Mechanics, Vol. 1, 1968, p. 3.*
[33] Johnson, H. H. in *Proceedings,* Conference on the Fundamental Aspects of Stress Corrosion Cracking, Ohio State University, Columbus, Ohio, 1967.
[34] Oriani, R. A. and Josephic, P. H., *Acta Metallurgica,* Vol. 22, 1974, p. 1065.
[35] Zappfe, C. and Sims, C., *Transactions,* American Institute of Mining, Metallurgical and Petroleum Engineers, Vol. 145, 1941, p. 225.
[36] Thompson, A. W. and Bernstein, I. M. in *Advances in Corrosion Science and Technology,* R. W. Staehle and M. G. Fontana, Eds., Plenum Press, New York, Vol. 7, 1971.
[37] Austen, I. M. and McIntyre, P., *Metal Science,* Vol. 13, 1979, p. 420.
[38] Ritchie, R. O., Castrocedeno, M. H., Zackay, V. F., and Parker, E. R., *Metallurgical Transactions, A.,* Vol. 9A, 1978, p. 35.
[39] Ritchie, R. O., Suresh, S., and Toplosky, J., Fatigue and Plasticity Lab Report No. FPL/R/80/1030, Contract No. DE-AC02-79ER10389, A000, Massachusetts Institute of Technology, Cambridge, Mass., Jan. 1980.
[40] Austen, I. M. and Walter, E. F. in *Proceedings,* International Conference on the Effect of Environment on Fatigue, Institute of Mechanical Engineers, London, 1977, pp. 1–10.

Summary

Summary

Atmospheric corrosion has been studied actively for more than 80 years by materials scientists and engineers. In spite of this extensive work, a number of significant questions remain. The papers in this publication have been divided into two general categories: (1) outdoor exposure results, and (2) modeling, characterization and correlations. Although the classification of papers into categories such as this is necessarily arbitrary, it is hoped that this division will be helpful to readers in approaching the subject matter. The summaries below are presented in the order they appear in the text.

Outdoor Corrosion Results

Knotková, Vlčková, and Honzák have described the research program carried out at the State Research Institute for Materials Protection in Czechoslovakia to develop weathering steels for structural applications. The first part of their study provides detailed information on the corrosion behavior of weathering steels as a function of pollution level. In this work standardized exposure conditions were employed, and the results were presented in a generalized format. Then the atmospheric corrosion of weathering steels in actual structural configurations including a demonstration building was studied. They also presented a comparison of costs of weathering steels to painted steels in structural applications. This paper is unique in that a wide range of information from basic atmospheric corrosion rate data to engineering application problems is presented.

Townsend and Zocolla have considered a specific but important atmospheric corrosion problem: comparing the atmospheric corrosion resistance of steels in order to comply with ASTM A 588, the weathering steel specification. This specification defines the atmospheric corrosion resistance of weathering steels as approximately twice that of carbon structural steel with copper. The corrosion resistance of steels with copper is also defined as approximately twice that of carbon structural steel without copper. Since the corrosion resistance of steel alloys varies strongly with exposure time, it is not clear how to make the comparisons required by A 588. The first step in the solution Townsend and Zocolla proposed was to generate quantitative expressions for the mass loss versus time behavior of the three steels by applying the linear relationship

$$\log C = B \log t + \log A$$

where C is the corrosion mass loss, t is the exposure time, and A and B are constants. Secondly, for the purpose of complying with A 588, the authors propose that the comparison of steel corrosion resistance be based on the ratio of times required to achieve a particular loss of thickness, readily calcu-

lated from the mass loss-time equations. Although the thickness loss is selected arbitrarily, the proposed value of 250 μm (0.01 in.) appears to be justified by a number of considerations.

Copper alloys are usually thought to have excellent atmospheric corrosion resistance. However, newer alloys and more demanding applications have required more detailed data and understanding of the atmospheric behavior of these materials. Castillo and Popplewell have presented an interesting update to earlier publications from their laboratory on the atmospheric corrosion resistance of copper alloys. Although most of the results cover only four years of exposure, their approach is important and useful in terms of understanding the engineering performance of copper alloys. Their program included 24 copper alloys with 8 new compositions. The emphasis of the program on both mechanical properties and atmospheric stress corrosion cracking resistance reflects the shift of use of copper alloys from architectural and marine applications to electrical and electronic applications. Their results on both long-term and short-term stress corrosion cracking susceptibility of a variety of copper alloys indicate that high zinc levels are very detrimental in industrial atmospheres and that ammonia may not be an important cause in atmospheric stress cracking of brasses, that is, season cracking. Their results on the poor performance of manganese containing alloys and the indication of possible stress corrosion cracking problems of nickel silvers in marine atmospheres are also significant. This paper, together with the following two papers on copper alloys in the atmospheres, constitutes an important contribution to our understanding of the behavior of this alloy system.

Holm and Mattsson have reported the corrosion behavior of 36 copper alloys including coppers, brasses, and bronzes in either sheet or rod form. These materials were evaluated in rural, marine, and urban atmospheres in Sweden. The evaluations included appearance evaluation, corrosion product analyses, mass loss measurement, depth of penetration, change in tensile properties and in the higher zinc brasses, degree of dezincification. This paper provides an excellent comprehensive study of the performance of copper alloys over a range of atmospheres and for significant time intervals.

A similar study of copper alloys behavior after extended atmospheric exposure is provided by Costas. This paper was included in this compilation as a conclusion of the ASTM 1957 B-3 Atmospheric Exposure Program. Sixteen copper alloys completed this program and were evaluated for mass loss, pitting, tensile properties, corrosion product analysis, and metallographic examination. The results were similar to previous studies in which these alloys showed relatively low corrosion rates in the atmosphere (between 0.2 and 2.3 μm per year) with the industrial site showing the most severe attack. Dezincification was noted only in the 30 percent zinc alloy, and intergranular attack was noted only in the aluminum bronze alloy (CDA 642).

To evaluate dry cooling for use in electric power plants, Battelle's Pacific Northwest Laboratory has conducted a large-scale study of U.S. air-cooled

industrial equipment and of European dry-cooled power stations. Aluminum fins are used widely in air-cooled heat exchangers, and Wheeler, Johnson, and May summarize the air-side aluminum corrosion data obtained from surveys and laboratory studies. Aluminum fins were generally resistant to corrosion in locations described as rural-dry, rural-wet, and also industrial-dry. Instances of severe corrosion have occurred at a few humid, marine, and industrial sites. At these sites, the principal factors influencing corrosion appeared to be the presence of contaminants and the amount of time the equipment was off line. Corrosion was minimized when the operating temperatures were above the dew point. It was reported that galvanized steel air-cooled equipment also operated without substantial corrosion at most locations.

Showak and Dunbar also presented the results from the ASTM 1957 B-3 Atmospheric Exposure Program. Two zinc alloys, high grade and 1 percent copper, were tested in four locations including rural, marine, and industrial atmospheres for 20 years. The panels were evaluated for mass loss, pit depth, and change in mechanical properties. In general, the results of this exposure confirmed the earlier 1931 program results, that is, atmospheric rates between 1 and 3 μm/year (0.05 and 0.1 mils per year). The copper bearing alloy had slightly higher atmospheric corrosion rates in the most severe marine and industrial atmospheres. However, the copper bearing alloy was more prone to pitting. Tensile test results were not useful because natural aging of the alloys tended to obscure corrosion effects. This paper should be of particular interest to those following the 1976 exposure program and those concerned with using zinc as a reference material in atmospheric exposures.

Tonini has reported the results of a 1960 exposure test program carried out on coated steel panels by ASTM Subcommittee A05.14. The purpose of the program was to document the equivalent performance of sheet from continuous galvanizing lines and that from the older pot galvanizing process. When the two coatings were compared on the basis of years to first rust per ounce of coating, no significant differences were found. However, several anomalies were found in the results which indicate that the atmospheric corrosion of galvanized coatings is still not clearly understood. For example, when coating life, defined in terms of years to first rust per ounce of coating, was plotted against coating weight, coating life depended significantly on coating weight except at the Newark/Kearney site. In addition, plots of time to first rust versus coating weight did not pass through the origin; it is noted that this behavior has been seen in other analyses of ASTM atmospheric data.

DiBari, Hawks, and Baker have sought to determine if the corrosion resistance of electrodeposited nickel-iron alloy coatings could be increased beyond that required for the usual decorative applications. The performance of nickel and nickel-iron coatings, therefore, was compared at three thickness levels in atmospheric exposures and also in the copper-accelerated acetic acid-salt spray (CASS) test. The thinnest coatings (8 μm) of both types appeared

to be equally suitable for applications in mildly corrosive service. With 15 and 30 μm coatings, the nickel coatings outperformed the nickel-iron alloy coatings in both the marine and industrial atmospheres. Since the major defect of the nickel-iron alloy coatings was rapid rust staining in the atmosphere, it appeared that these coatings should continue to be used in only mild corrosion service until a remedy was developed.

This view was opposed by Clauss to cited evidence indicating static test results could not be relied upon to predict actual service results for items such as hubcaps. In particular, it was reported the staining of nickel-iron alloy coatings which developed in static exposures was not found in mobile tests.

Modeling, Characterizations, and Correlations

It is often necessary to determine the behavior of materials in atmospheric exposures when there is not sufficient time to carry out a long term exposure program in a variety of different types of atmospheres. Accordingly, a number of different approaches have been attempted to better understand atmospheric corrosion. Knotková and Barton of the State Research Institute of Material Protection in Prague, Czechoslovakia, have reported their system for classifying the corrosivity of atmospheres. Their system incorporates meteorological and climatic measurements and air pollution monitoring measurements with standard panel test results. Their system includes boldly exposed outdoor exposures with sheltered outdoor and interior exposures such as warehouse or vessel applications. They have also identified problem atmospheres such as those associated with textile, metallurgical, and chemical processing plants. The resulting system should be very helpful to designers charged with specifying protective measures against atmospheric corrosion.

Several efforts have been made in the past to determine the relative corrosiveness of atmospheric test site locations. Since then, much has been learned about the role of pollutants and meteorological factors, but there is much still to learn. Therefore, ASTM has established Task Group G01.04.01.01, entitled Calibrating the Corrosiveness of Atmospheric Test Sites. The objective of the task group is to develop a recommended practice by which tests can be conducted to calibrate the corrosivity of an atmospheric corrosion test site on a continuing basis. Baker and Lee have reviewed some of the factors which are being considered in developing this standard, and they present some rather interesting results which have been acquired over the years in related studies.

The concept of time of wetness as a parameter of atmospheric corrosion rate has been under study for many years. Earlier work indicated the importance of this factor, but problems with measuring devices have prevented the widespread acceptance of this approach. Sereda organized a task group within ASTM G-1 Subcommittee G01.04 on Atmospheric Corrosion to develop a standard for measuring time of wetness. The paper on measurement of time

of wetness by moisture sensors by Sereda, Croll, and Slade reports the results of this effort. A new miniature sensor based on printed circuit technology was developed for this study. A round robin test was set up with six laboratories participating initially, but only two were able to complete the program. Based on this work, the authors concluded that the new miniature sensors based on either zinc-gold or copper-gold were equally effective. These sensors did not give a unique relationship between relative humidity and potential, but they were effective at detecting condensed moisture on the surface in question. The results of this study provide a basis for further work in standardizing the moisture sensor approach to measuring time of wetness.

Haynie has skillfully analyzed data from an EPA corrosion study conducted in the St. Louis area for an extended period. In this first-of-its-kind study, air pollution, meteorological, and corrosion data were continuously recorded at four exposure sites by a central computer. The corrosion data were the galvanic currents from copper/zinc and copper/steel atmospheric corrosion monitors (ACM's as described by Mansfeld). Based on regressions of the percent time corrosion rates exceeded minimum values, time of wetness values were calculated. The values for the zinc and steel ACM's were significantly different, as were differences between the four sites. These data indicated environmental differences within the geographic region. Relative humidity, temperature, windspeed, and SO_2 and NO_2 levels were found to be significant variables. Relative humidity was found to be the most important variable affecting corrosion rates. Critical relative humidities calculated for the four sites were 90, 91, 89, and 85; the latter value was believed to be too low. Also a good criterion for defining the time when the ACM surface was wet was a galvanic current equivalent to a corrosion rate equal to or greater than 1.5 μm/year. The need for such a definition is discussed by Mansfeld in his following paper.

The application of electrochemical techniques to atmospheric corrosion has increased in recent years, but Mansfeld et al have indicated certain problems with electrochemical monitoring devices. For example, the interpretation of time of wetness measurements is not clear, since no sound definition exists on which the time of wetness can be based. Also, a more serious problem is that electrochemical monitoring devices measure only fractions of the true corrosion rate. To evaluate in more detail the factors that determine the reproducibility of electrochemical corrosion sensors, cell efficiencies, and the time of wetness, a statistically designed experiment was carried out. Among the more significant results reported were the low efficiencies found for copper/steel and steel/steel cells, that is, about 20 percent and 7 percent, respectively. These low efficiencies were attributed to local cell action and the low conductivity of the electrolyte. Evaluation of the results of the completed experiment will undoubtedly increase our understanding in this important area.

Bragard and Bonnarens in their paper have contributed significantly to

our knowledge of the mass loss versus time behavior of steels being tested in the atmosphere. Initially, they use the data from 24 steels at three sites to test the validity of the equation

$$p = kt^n$$

where p is corrosion loss, t is exposure time, and k and n are constants. It should be noted that this expression is equivalent to that used by Townsend and Zocolla. In this realistic test, more than 75 percent of the observed and calculated values were within 20 percent. Another linear mass loss versus time relationship for steels at a specific site was developed, that is, the expression

$$\log p_x = a \log p_y + b$$

where p_x and p_y are the corrosion losses after x and y years and a and b are constants. When the four year and ten year weight losses of a large number of steels from a wide variety of sites were plotted (Fig. 10), the surprising result was that the slopes, that is, "a" values, for all the sites were the same. The reasons for this result are not clear, but the relationship offers another means of predicting long-term losses from short-term ones. In assessing the corrosiveness of test sites, the authors suggest that the first year weight loss is a reasonable measure of test site corrosiveness toward a steel. Empirical expressions were developed for calculating n as a function of first year weight loss and test site relative humidity; the results correlated well with observed values. These results should be useful in reducing the work and time required for the atmospheric testing of steels.

Byrne and Miller have attempted to develop a better understanding of the atmospheric corrosion of aluminum alloys. They noted that the severity of corrosion of aluminum alloys did not always correspond to the level of pollution in the atmosphere, and in particular there were some unusually corrosive conditions in the Los Angeles area. They carried out some laboratory experiments in which high purity aluminum specimens were exposed to controlled atmospheres in which either nitrogen oxides, NOX, sulfur oxides, SOX, or hydrogen chloride was present. The resulting aluminum oxides were measured for thickness and degree of hydration. They found that in particular nitrogen oxides plus moisture cause accelerated corrosion of aluminum alloys. In analyzing the results of the natural atmospheric exposures, they observed that NOX would react with SOX to produce nitrogen and sulfuric acid. Thus, atmospheres with excess SOX should be less corrosive to aluminum alloys than those with excess NOX. Some results from natural atmospheres were provided to support this conclusion. This paper should be particularly interesting to those concerned with the effects of pollutants on metals in the atmosphere.

The development of accelerated corrosion tests is an important facet of atmospheric corrosion research. Accelerated tests must reproduce faithfully

the behavior of materials in natural atmospheres in order to be useful. Khobaib, Chang, Keppler, and Lynch have attempted to use modern fracture analyses approaches in low-cycle fatigue and rising-load tests to estimate the critical stress intensity to initiate stress corrosion cracking in high strength aluminum (AA 7075-T651) and steel (AISI 4340) alloys. They have carried out their tests in both dry and moist gaseous environments. In the case of the 4340 steels, tests were also carried out with specimens of different yield strength and in moist atmospheres containing 1000-ppm SO_2. Their results indicate that these techniques reveal the tendency of high-strength alloys, that is, 4340 at 1440 MPa yield stress, to stress corrosion crack whether tested in cyclic loading or rising load. Confirmation of stress corrosion cracking during the cyclic loading tests was obtained by fractography. In addition, it was found that these techniques are sensitive to variations in atmospheric conditions which increase susceptibility to stress corrosion cracking, such as total immersion of the 7075 aluminum alloy in water. These results are particularly important to these studying the fracture susceptibility of high-strength materials in aircraft and military applications.

Conclusion

This compilation of papers provides a good cross section of the state of the art in atmospheric corrosion testing. There is an even balance between exposure test results and attempts to develop models, correlations and accelerated tests for atmospheric corrosion. This compilation is particularly interesting because of the international scope of the papers and the wide range of materials and subjects covered. It is our hope that the decade of the 1980's have as much progress in atmospheric corrosion work as in previous decades.

S. W. Dean, Jr.
Air Products and Chemicals, Inc., Allentown, Pa. 18105; editor.

E. C. Rhea
Reynolds Metals Co., Richmond, Va. 23261; editor.

Index

S

Z